PEDOGENESIS ON THE SEFTON COASTAL DUNES, NW ENGLAND

JENNIFER ANNE MILLINGTON
BSc (Liverpool Hope University College) MSc (University of Liverpool)

A thesis submitted in partial fulfilment of the
requirements of the University of Wolverhampton
for the degree of Doctor of Philosophy

August 2010

Signature J.A. Millington

Date 27/08/2010

"And so castles made of sand fall in the sea, eventually"

J. Hendrix (1967).

This thesis is dedicated to Mum and Dad who, although are no longer here, are the real influence behind this research. My thoughts and ideas are inspired from their own outlook on life, as they took great pride in encouraging me to take an interest in nature and the world around me. They taught me not to take things for granted and to want to achieve the most I can through not letting a moment or opportunity pass.

ABSTRACT

Pedogenesis on the Sefton coastal dunes

By Jennifer Anne Millington

This work examines the use of pedo-properties to identify dune soil system responses to environmental change on the Sefton coast, based on the development of conceptual pedogenic models. Previous environmental change and shoreline dynamics are determined through O.S. maps and aerial photographs, while present day processes are investigated through a dune-toe photographic survey and seasonal monitoring by fixed point photography. Topsoil (0-5 cm) physico-chemical characteristics are presented in a series of baseline GIS maps, displaying spatial pedo-property variation across the dune landscape. Combined with vegetation data, topsoil analysis identifies 10 distinct pedo-environments. Physico-chemical characteristics of associated National Soil Resources Institute (NSRI) soil profile classifications and an exposed stratigraphic section are presented graphically in a proposed sequence of development.

Topsoil and soil profile samples are analysed for soil pH, soil organic matter (SOM) content, particle size, geochemical composition and mineral magnetism. Significant differences ($p < 0.05$) are apparent for the suite of topsoil characteristics collated, indicating discrete dune environments are influenced by specific soil properties. Distinct down-profile variations in soil characteristics are also apparent between dune environments, highlighting pedological dynamism. Multivariate Factor analysis groups bare sand and mobile dune communities into 'frontal dunes' and fixed dune community, pasture, scrub, deciduous woodland and coniferous plantations into 'hind dunes', separating these topsoil environments from heath and slack communities. Factor analysis also identifies linkages between pedo-characteristics within soil profile horizons, suggesting pedogenesis on the Sefton dunes initiates as raw sand, progressing to sand-pararendzinas through leaching of nutrients. Desalinization and decalcification processes lead to brown earth development, followed by increased acidicification, subsequently, resulting in micro-podzol formation. Groundwater gley soils are associated with dune slacks, where drainage is inhibited and anaerobic conditions prevail. Analysis of buried soils suggests such pedo-environment formations are cyclic, responding to phases of shoreline regression/transgression, dune activity and stabilization.

Conceptual models are designed to graphically demonstrate pedogenesis under both erosion and deposition regimes on the Sefton coast. Regression equations and correlation coefficients between pedo-properties and distance from mean high water are used as a proxy for soil age, which represent lateral soil maturity from the unstable frontal dunes to the stable hind dunes inland. The models simulate formation and process of the full array of soil properties, accounting for geomorphological impacts and anthropogenic influences. This has great implications for dune managers by raising awareness of pedogenesis as an integral part of nature and associated habitats, which could be incorporated in future shoreline management plans (SMPs).

Acknowledgements

This research is part-funded by Sefton Metropolitan Borough Council (SMBC) and part by the University of Wolverhampton, to whom I am most grateful for this opportunity. I would like to thank all of my supervisory team; Dr Colin Booth, Professor Michael Fullen, Professor Ian Trueman, Professor Annie Worsley and Dr Nigel Richardson for their expert advice, help and guidance. Also, thanks to Graham Lymbery, Coastal Defence at SMBC, for providing additional supervision, local knowledge, literature, and emergency transport in bad weather! I would also like to thank everyone who provided me with technical support during this research, especially David Luckhurst for his invaluable knowledge of computing and GIS, and David Townrow for hours of XRF analysis.

I gratefully acknowledge all personnel and organisations involved in this research, particularly; Peter Gahan and Paul Wisse, SMBC; Alice Kimpton and Michael Downey, Natural England; and Andrew Brockbank, National Trust, for permitting fieldwork and for taking the time to personally meet for discussions. I would also like to thank Dr Selvakumar, India Agricultural Institute, for providing carbon and nitrogen analyses on my samples.

I owe a debt of thanks to Simon for his continuous support and hours of laughter. If it was not for his hard work and willingness in the field, I would most certainly still be digging soil profiles now! Thanks also to my sister Carol for her company and putting up with shoes full of sand during numerous photographic surveys (usually involving 'chippy lunch' bribery!). Although, I'm still not entirely sure if I have convinced her that soils are not boring!

Finally, I would like to thank all my friends and family for their encouragement and support. In particular, Jeni P for days of dedicated fieldwork and camping, Woolly for the best packed rucksack, Becky and Mozza for help with data entry, Liz for advice and fieldwork, and Miles for saving my laptop from disaster. Each has contributed towards making my research as enjoyable and relatively stress-free as possible.


Y617 KYA

CONTENTS

CHAPTER 9: Conclusions

List of appendices

List of Figures

Chapter 1

Chapter 2

Chapter 3

Chapter 4

Chapter 5

Chapter 6

Chapter 7

Chapter 8

List of Tables

Chapter 1

Chapter 2

Chapter 3

Chapter 4

Chapter 5

Chapter 7

Chapter 8

CHAPTER 1

Introduction, research aims and literature review

Chapter 1 introduces the rational for this investigation, preceded by a detailed description of the overall aims and objectives. A brief introduction to coastal dune geomorphological formation and classifications is given. This is followed by discussion of existing global interests in the possible effects that changes in sea level may have on such coastal environments during this century. The Sefton Coast and its context within north-west Europe are presented, followed by consideration of the role of pedogenic processes in such dynamic coastal dune environments. An outline of the need for researching the potential for using soil characteristics and pedogenic patterns to predict coastal environmental change during this century is presented.

1.1 Introduction to the research

Soft coastal landscapes, including beaches, sand dunes and mudflats, represent fast-responding and mobile geomorphic systems that are highly sensitive to environmental change (Hansom, 2001). Climate change, rising sea-level and their effects on sand dune systems are currently under scientific debate (e.g. Hulme *et al.,* 2002; Evans *et al.,* 2004; Orford and Pethick, 2006), as responses are expected to be dynamic and variable, anticipating land encroachment, raised groundwater and migration of ecological zones. IPCC (2007) predictions indicate a eustatic sea level rise of 49-55 cm by the year 2100. Pre-anthropogenic influenced coastal environments survived advances in sea level by migrating landwards, a process that is almost impossible today, often due to artificial sea defences and residential development (Woodroffe, 2002). Prevention of natural landward migration is termed 'coastal squeeze' and is often applied to situations where coastal margins are squeezed between fixed landward boundaries (artificial or otherwise) and rising sea levels, resulting in a direct loss of habitat (Doody, 2001). Therefore, information on sand dune system responses to coastal change is vital for nature conservation and protection of residential areas.

According to the final 'England Biodiversity Strategy Report' to DEFRA (Mitchell *et al.,* 2007), one of the underpinning requirements for biodiversity management is data for understanding ecosystem, habitat and species response to climate change. This is emphasized further by Orford and Pethick (2006), who outlined the lack of research into likely future habitat responses to physical shoreline changes, therefore, requiring fresh approaches to conceptual modelling of coastal habitats.

Pedogenesis is an integral part of natural ecosystems; therefore, the role of soils is critical to establishing cause and effect (Mitchell *et al.,* 2007; van den Ancker and Jungerius, 2007). Buried soil profiles contain remnants of phases of previous landscape stability and instability, along with information concerning development trends and timescales (Jungerius, 1989; Wilson, 1992). To predict dune system response to the effects of sea level fluctuations, a greater understanding of both past and present pedo-dynamic behaviour is essential.

Therefore, this research investigates sand dune pedogenic responses to environmental change based on the Sefton coastal dunes (Figure 1.1). The Sefton coast was chosen for detailed investigation for the following reasons:

1. The sand dunes form the largest dune system in England and the fourth largest in Britain (Radcliffe, 1977). Due to its rare dune habitats and species, it is also one of the most important areas for nature conservation in Europe.
2. Cycles of dune activity, separated by periods of stability and soil formation, have occurred over the last 1000 years (Tooley, 1978; 1982; Pye, 1990; Pye and Neal, 1993), providing an opportunity to investigate pedogenic responses to coastal change.
3. The front at Formby Point is eroding rapidly, with concerning implications for coastal zone management (Houston, 1989) and combating the effects of 'coastal squeeze' between the coastal margin and dunes fixed by conifer planting.

1.1.1 Aims and objectives of the research

Through identification and analysis of dune soil systems on the Sefton coastal dunes, the following research aims aim to establish pedogenic responses to environmental change:

- Analysis of existing Habitat Directive classification data aims to define dune environments as an indication of varying soil type. Different vegetation types prefer different soil characteristics, such as alkaline or acidic conditions, chemistry and texture (Fullen and Catt, 2004). Eventually, the soils will also provide nourishment back to vegetation characteristics. These spatial patterns of vegetation-type distributions can be mapped using a Geographical Information System (GIS), which can then be investigated for soil properties.
- Characterization of the physico-chemical properties of contemporary topsoil samples, for each of the dune vegetation habitat environments, will identify associations between vegetation-type and soil characteristics. Spatial and temporal topsoil distributions can be mapped using GIS, to identify pedogenic succession processes with increasing distance inland. Groupings and separations between influencing soil properties will determine distinct pedo-environments.
- The potential to associate classified soil profiles to each of the defined vegetation/pedo-environments will further enhance predicted soil evolutionary trends, especially in response to environmental change. As this has not been conducted on the Sefton coast before, clarification of profile horizons and soil processes in operation within them will provide indications of future pedogenic scenarios.
- Considerations of the effects of diverse shoreline behaviour and dune dynamics on the soil system will be achieved through reconstruction of historic dune environments. Monitoring contemporary dune topography, coupled with historic reconstructions, will aid understanding of local coastal change rates.
- Based on topsoil characteristics, development of the first ever geomorphopedological (GMP) map of the entire Sefton dunes, aims to illustrate the spatial distribution of soil profile classifications. Highlighting whether differences in accretion and erosion/deposition regimes have an impact on pedogenic patterns and rates, will prove useful for dune management.

Figure 1.1 Location map of the Sefton coastal dunes, NW England (www.OpenStreetMap.org; Ordnance Survey, 2000, 1:50,000 (© Crown Copyright. All rights reserved Sefton Council Licence no 100018192)).

- Building pedogenic development models applicable to the Sefton coastal dunes, by considering localized coastal erosion/accretion patterns, will highlight the impact of geomorphic and anthropogenic influences on proposed pedogenic pathways within each coastal unit. These can be used to inform both local and international dune managers, on similar coasts and, possibly in any other young cyclic pedogenic systems.

1.2 Coastal sand dunes and their formation

Detailed explanations of coastal dune formation and succession are provided in the literature (e.g. Pethick, 1984; Bird, 2000; Smithson *et al*., 2002), however, a brief interpretation is given here and is represented in Figure 1.2. Pethick (1984) separated dunes from all other coastal landforms, by associating them with aeolian processes rather than water. Aeolian processes transport sand- or silt-size particles, producing coastal dunes both directly, through redistributing products of other processes, and indirectly, through wave generation. Many authors (e.g. Pethick, 1984; Tsoar, 2005; Anthony *et al.,* 2006) discussed coastal dune formation factors as effective onshore wind velocities and deflation of large supplies of uncohesive particles of sand, silt and clay. This is clarified by Goldsmith (1985), who described dunes as general sediment accumulation above high tide level, particularly where deposition occurs against obstacles, such as driftwood or vegetation. Backshore gradients are increased and a ridge is formed, impeding further landward transport of blown sand (Bird, 2000). In the absence of obstacles, sand would be dispersed as a thin layer across the hind land (Smithson *et al,* 2002). Dune development is supported by the availability of a wide sandy beach as a sediment source area and can be well developed where the tidal range is large, as on the Atlantic coasts of Britain (Short and Hesp, 1982), and coasts of Belgium, The Netherlands, Germany and Denmark (Bakker *et al.,* 1990). Dune systems remain mobile until sand supply ceases or stabilization by vegetation occurs.

1.2.1 Sand dune morphological classifications

Abundant sand dune varieties in deserts and on coasts, means there is no accepted classification that refers to all known dune types (Tsoar *et al.,* 2004). Some classifications are based on individual field experiences (e.g. Hunter *et al.,* 1983; Goldsmith, 1989; Sherman and Bauer, 1993), while others on global views (e.g. Pye and Tsoar, 1990; Livingstone and Warren, 1996). However, Tsoar *et al.* (2004) classified dunes into three distinct groups, according to directional variability of the winds: i) Migrating dunes, in which the entire dune body advances with little change in dimension; ii) Elongating dunes, in which the dune's length becomes extended with time; and iii) Accumulating dunes, in which the dunes have little or no net advance or elongation. The classifications in Figure 1.3 are representative of migrating coastal dune systems, incorporating communities derived from the European Union Habitats Directive (2007), as generally these are the dune systems of north-west European coastal environments.

1.2.2 Embryo dunes (Embryonic shifting dunes)

Sokolov (1881) described how interception of aeolian derived sand by an obstacle, will allow sand to remain on the windward side, ultimately forming a gentle slope. Jungerius (2008)

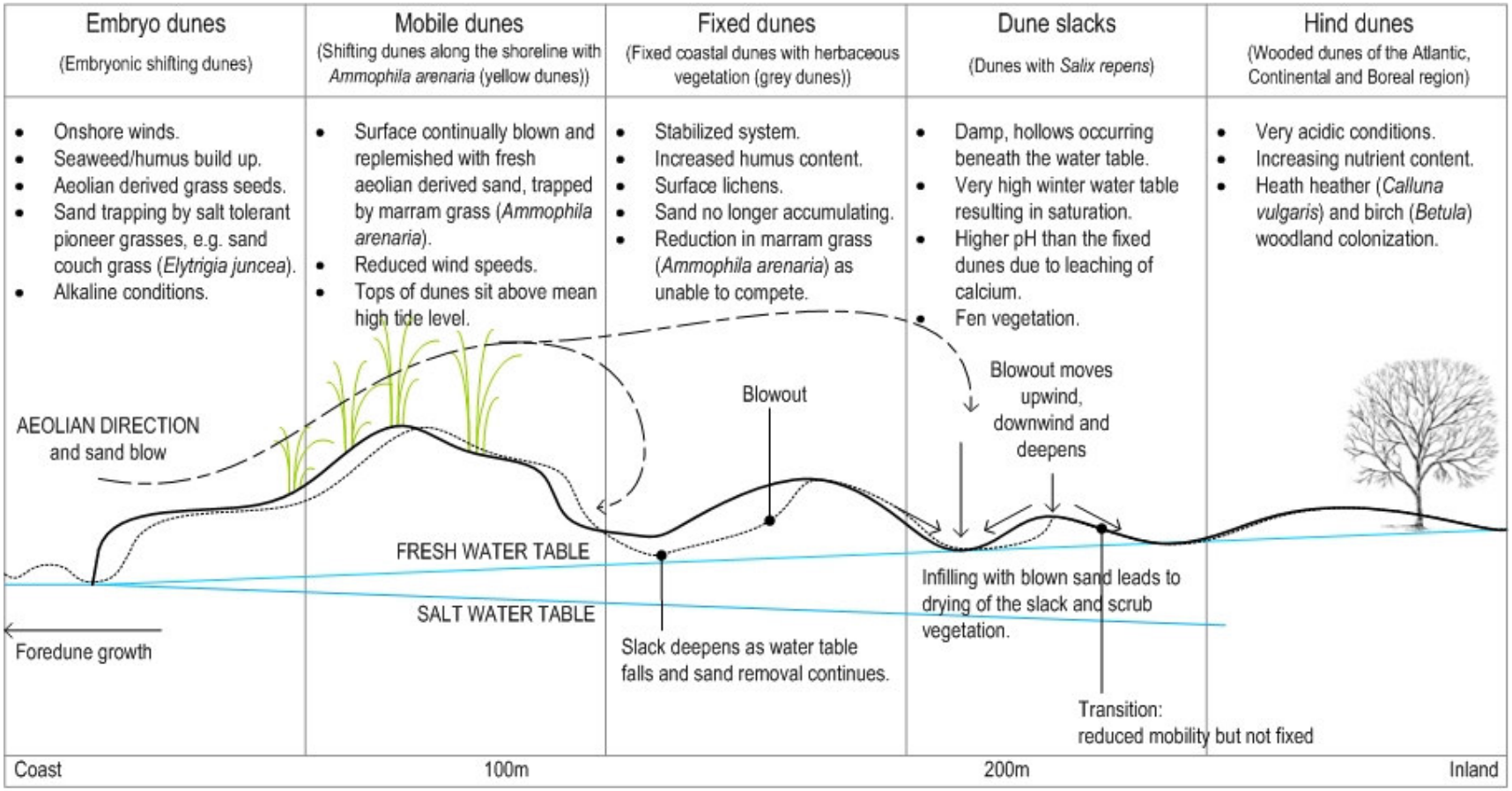

Figure 1.2 Idealized transect across a sand dune system (exaggerated vertical scale) identifying main dune geomorphological (solid line), dynamic processes (dashed line) and ecological characteristics (modified from various literature, e.g. Goldsmith, 1985; Houston, 1992; Bird, 2000; Smithson *et al*., 2002; Tsoar, 2005; Anthony *et al.,* 2006). Vegetation communities derived from the European Union Habitats Directive Interpretation Manual (2007) are expressed in brackets under the classifications chosen for this research.

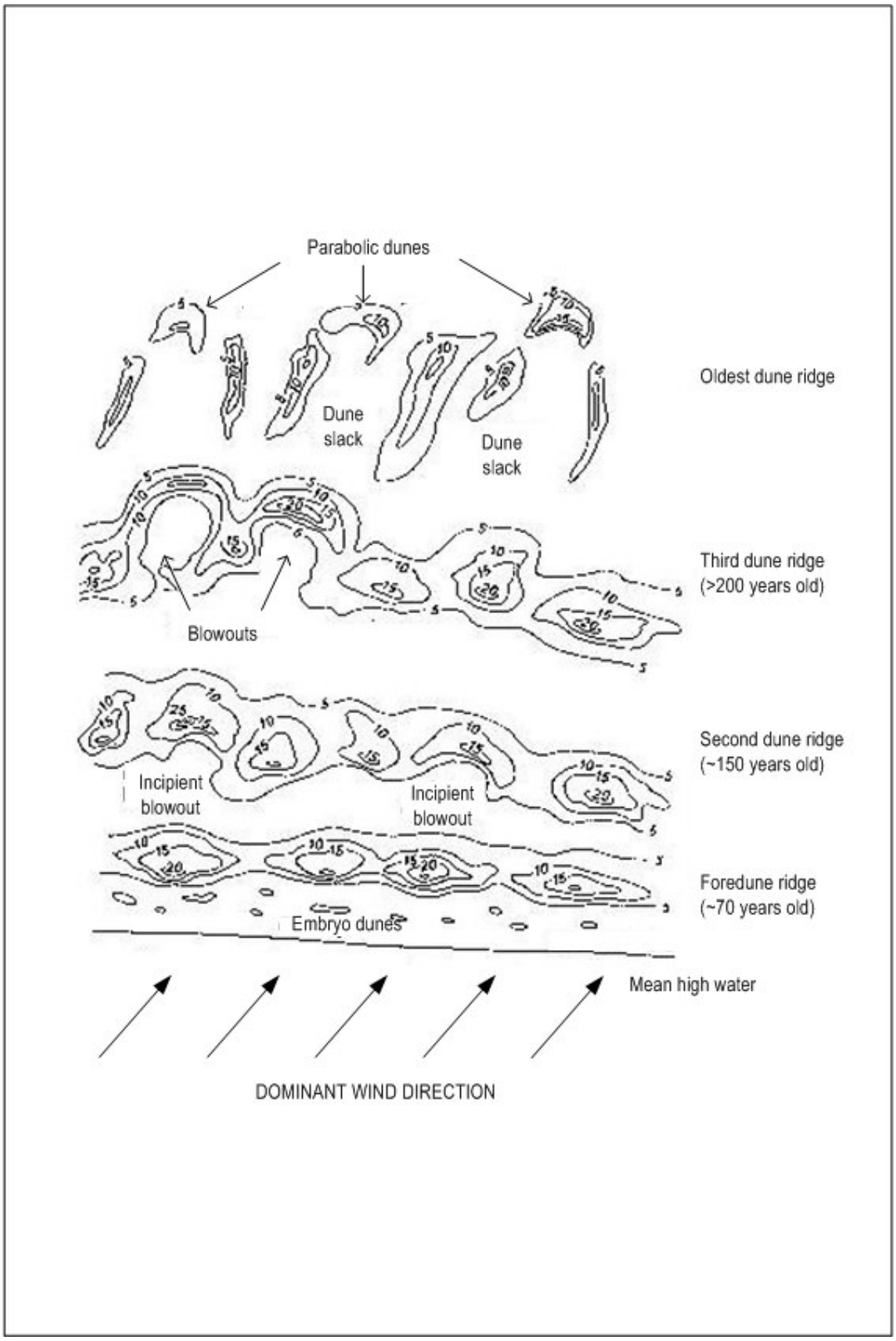
Parabolic dunes
Oldest dune ridge
Dune slack
Dune slack
Third dune ridge (>200 years old)
Blowouts
Second dune ridge (~150 years old)
Incipient blowout
Incipient blowout
Foredune ridge (~70 years old)
Embryo dunes
Mean high water
DOMINANT WIND DIRECTION

described these initial embryo developments as either shadow or obstacle dunes, becoming higher and wider as accretion continues and vegetation colonizes, but remain unconnected (Pethick, 1984) (Figure 1.3). Embryo dunes eventually connect to form a foredune, ~2 m high (Pethick, 1984). Embryo dunes play an important role in sediment beach/dune budgets, as described by Ranwell (1972), who suggested that an accreting foredune can be enhanced by up to 2 m of sand a year, but overwhelmed if sand is supplied too rapidly.

1.2.3 Mobile dunes (Shifting dunes with *Ammophila arenaria*)

Mobile dunes, or *yellow dunes* (Ellenberg, 1988), are described by Bird (2000) as a sediment barrier parallel to the high tide shoreline. A fully developed dune, landward of the foredunes, is sometimes classified as the first dune ridge (Pethick, 1984) (Figure 1.3). The concept of this barrier acting as a protector of the hindland from extreme storm conditions has been demonstrated by Woodroffe (2002) and Saye *et al.* (2005). While embryo dunes continue to grow, mobile dunes have generally reached maximum height and tend to migrate downwind when sand is blown from the steep windward face, up and over the ridge, to accumulate on the gentle leeward slope; i.e. dune 'roll over' (Houston, 1992). Time intervals between each mobile dune ridge have been estimated by Pethick (1984) to be 70-200 years.

1.2.4 Dune cliffs

Formation of a foredune cliff cut back by storm waves is a widespread occurrence. For example, Bird (2000) refered to a foredune that runs parallel to the high tide line on the north-east coast of Norfolk, in the vicinity of Sea Palling, that has revived after phases of severe erosion during storm surges in 1953. Further work by Lee (2008) related decreased beach levels with increased cliff recession rates along the North Norfolk and Suffolk coasts, UK. In southern Britain, dunes generally have cliffed seaward margins except where there has been local beach progradation, as at the northern part of Studland beach in Dorset (Saye *et al.,* 2005). Carter and Wilson (1990) noted that several dune ridges were added to Magilligan Point, Northern Ireland, between 1953 and 1983 during a phase when adjacent dune-fringed coasts were cut back. But progradation has not been sustained and these dunes are now cliffed.

1.2.5 Parallel dunes

Multiple dune ridges that have formed successively as foredunes behind a prograding sandy beach are classified as parallel dunes (e.g. Bird, 2000). Bird and Jones (1988) illustrated their formation as incipient dunes on the beach developing into new foredunes seaward of earlier dunes, which become parallel dune ridges separated by elongated unvegetated troughs called slacks (see Section 1.2.8). According to Pethick (1984), dune ridges range in height from 1-30 m, each representing stages in dune development.

1.2.6 Blowouts and parabolic dunes

Unstable dunes with limited vegetation have been described by Hesp and Thom (1990) as blowouts and parabolic dunes. Carter *et al.* (1990) further described blowouts as unvegetated or

sparsely vegetated hollows that have been excavated in vegetated mobile dunes by onshore winds with sand driven landward to form a looped ridge. A blowout that has extended its axial length to more than three times the mean width is termed a parabolic, or *U-dune* (Jungerius and van der Muelen, 1989; Gares, 1992; Bird, 2000) (Figure 1.3). Morkunaite and Cesnulevicius (2001) referred to particularly well developed parabolic dunes in Juodkrante, Lithuania, where the length exceeds 4 km and the width ranges between 200-300 m.

1.2.7 Transgressive dunes

In addition to blowouts and parabolic dunes, Hesp and Thom (1990) described broader transgressive mobile dunes to form either where aeolian derived sand has been retained by vegetation, or where previously vegetated dunes have been disrupted by numerous blowouts until they merge into an elongated dune. In Newborough Warren, north Wales, Ranwell (1972) identified three parallel transgressive sand ridges that have migrated inland, each backed by low-lying sandy terrain representing stages in plant succession. Carter *et al*. (1990) discussed how such low-lying plains can be formed by deflation of sand to the level of the water table.

1.2.8 Dune slacks (Dunes with *Salix repens*)

Hollows in dune topography, passing beneath the water table are classified as dune slacks, some of which may be intermittent, forming seasonally or when the water table rises (Bird, 2000). Ranwell (1959) described slacks as either wet, in which the water table never falls <1 m of ground level in any season, or dry, in which the water table in summer is 1-2 m below ground level. Slacks are usually round or oval in shape generated by wind action, and are excavated by deflation during dry conditions and when the area is devoid of vegetation (Gresswell, 1953). Infilling of slacks by blown or inwashed sand or by the formation of peat deposits may produce flat-floored enclosures, which are permanently stabilized dune topography until invasion of a migrating mobile dune from the seaward side (Gresswell, 1953; Houston, 1992; Bird, 2000).

1.2.9 Fixed coastal dunes with herbaceous vegetation and hind dunes

Dune stabilization by marram grass (*Ammophila arenaria*) results in fixed dune development, or *grey dunes* (due to the darker colour of incorporated organics) (Ellenberg, 1988); however, blowouts can still occur. Over time mobile dunes reduce to undulating low hummocks (Houston, 1992). Older, vegetated dunes are classified as hind or *brown dunes* (Ellenberg, 1988). These are divided into heath (decalcified fixed dunes with *Empetrum nigrum*), scrub (dunes with *Hippophae rhamnoides*) and woodland (wooded dunes of the Atlantic, Continental and Boreal region). An example of well-developed, deeply leached, heath-woodland colonized sand is described by Bird (1995) on the landward side of the South Haven peninsula in Dorset.

1.3 Effects of sea level on coastal dunes

Global postglacial sea level rise was initially compiled into one eustatic curve, until it became apparent that the pattern of sea level change differed from place to place (Fairbridge, 1961). As

a result, there is increasing worldwide interest in the effects that changes in sea level may have on coastal dune environments during this century (e.g. Van der Meulen, 1990; Carter, 1991; Pye and Neal, 1993). Particularly as sand dune systems are vital components of coastal flood defences, acting as mobile flood defence barriers capable of altering position and form in response to environmental change (Saye *et al.* 2005). Although it is widely accepted that sea level fluctuations determine levels of dune activity, different authors have contrasting views on precise roles. Interactions between relative sea level, affecting stability of coastal forms, and sediment abundance or deficit, resulting in either progradation sufficient to reverse transgression or erosion even when sea level is falling, is central to the functioning of the coastal system (Carter *et al.,* 1987). Some authors (e.g. Innes and Frank, 1988) related renewed sea level rise with coastal retreat and landward migration of dune deposits, whereas others (e.g. Tooley, 1978) equated dune migration with falling sea levels and greater intertidal exposures with increased sand supply.

1.3.1 Late Quaternary eustatic sea level fluctuations

Coastal dunes have formed over a variety of time scales. Older dune systems include aeolian deposits derived from coastal lowlands that emerged during low sea level phases of the Pleistocene. For example, Hesp and Thom (1990) related the major dune systems on the south-east coast of Australia to such emergence events. Bird (1998) discussed that despite Pleistocene coastal dunes being largely removed by glacial processes during the Last Glacial phase in north-west Europe, an old dune complex in south-west England overlies emerged Late Pleistocene shingle beaches.

1.3.2 Holocene eustatic sea level fluctuations

Most sand dune systems have developed during the mid to late Holocene from sand supplied to beaches from the sea floor as a result of the Late Quaternary marine transgression (Bird, 2000; Pye, 2001; Tsoar, 2005). Subsequent eustatic sea level has been relatively stable during the past 6000 years, apart from minor oscillations. In Britain, the Medieval Warm Period, ~AD 800-1300, followed by the Little Ice Age, ~AD 1350-1850 (Roberts, 1998), represents the principal climatic oscillation of the Late Holocene. Marine transgression altered sea level by ±1-2 m, carrying sediment shoreward to be abandoned as coastal dunes during subsequent regression (Roberts, 1998). This is evident along the North Sea coast of Northumberland, north-east England (Wilson *et al.,* 2001; Knight *et al.,* 2002). However, there is much debate in the literature as to whether these rapid rates of dune advance are the result of increased storminess and dune roll-back processes, or whether vegetation clearances destabilized the hind dunes.

1.3.3 Effects of future sea level rise

According to Bird (1985), sandy coasts across the globe have been retreating during the past century, as a response to eustatic sea level rise. Early calculations suggested that eustatic sea level would have risen 30-80 cm by the year 2000 (Wigley and Raper, 1993). However, recent Intergovernmental Panel on Climate Change (IPCC) (2007) predictions indicate a rise of 49-55

cm by the year 2100, resulting in extensive marine submergence of low-lying coastal areas. Pye (2001) stated that based on previous patterns, wind/wave dynamics will have a greater effect than rising sea level during this century.

Attempts have been made to predict the effects of sea level rise on coastlines (Tooley and Jelgersma, 1992; Warrick *et al*., 1993; Bird, 1993), but they remain speculative because of limited monitoring of recent and continuing changes, and the imprecision of available models (Pye, 1984; Christiansen and Bowman, 1986). Authors suggest that as coastal dune fringes become cliffed, initiation of blowouts will occurr, some of which may develop into large transgressive dunes (e.g. Pye and Bowman, 1984; Van der Muelen, 1990; Carter, 1991; Pye, 2001). Fluctuations in sea level and resulting shoreline position will also have an effect on dune groundwater levels, affecting base levels for deflation (Pye, 2001; van der Meulen, 1990; Noest, 1991).

1.4 Context of the Sefton Coast

The Sefton coastal dunes (Figure 1.1) borders the 32 km coast between Southport Pier (SD 325 182) and Crosby Lighthouse (SD 303 987), north-west England, between the Ribble and Mersey estuaries, respectively, thus forming a natural defence against marine flooding of low-lying land in west Lancashire and north Merseyside (Pye and Neal, 1993). This is a macrotidal environment, with a tidal range of 8.2 m at high spring tide and strong south-westerly to north-westerly winds (Lennon, 1963). The dunes comprise the western margin of an extensive, flat peat and mossland region, underlain by impermeable Downholland silt (Brodie, 1996). Doody (1991) stated that the dunes covered an area 17 km in length, 1.5 km wide and comprised 2109 ha. More recently, however, Burkmar (2008) supported the total area as 1961 ha, identified by the National Vegetation Classification (NVC) survey of the Sefton Coast, amounting to ~15% of the total dune habitat of England.

The Sefton dunes are of high conservation, amenity and recreational value. The Sefton Coast Management Scheme, established 1978, evolved into the Sefton Coast Partnership in 2000. Much of the dunes are designated internationally, nationally and locally important, including Sites of Special Scientific Interest (SSSIs), Special Areas of Conservation (SACs) and Special Protection Areas (SPAs), which are outcomes of the European Union, Habitats Directive, 1992, details of which are given in Sefton Borough Council (1995). Natural England, the National Trust and Sefton Borough Council manage much of the landscape, with clear objectives covering conservation, landscape maintenance and renewal, foreshore and woodland management, interpretation and monitoring (after the Coast Management Scheme Steering Group, 1983).

1.4.1 Sea level fluctuations on the Sefton coast

Historic variations in relative sea level on the west coast of England were examined by Picton (1849), who stated that during the Pleistocene the entire Lancashire district was covered by ice. When the ice retreated across Britain, the removal of the weight from the depressed land led to

slow isostatic adjustment of the land. The Sefton coast lies on the 'hinge-line' between isostatic uplift to the north and relative fall to the south, resulting in a seemingly stable relative sea level. This indicates that any rise or fall in sea level cannot be attributed to land movements. According to De Rance (1883), ice retreat across Lancashire revealed a vast plain with a coastline lying far west of the present day shore, near the present 20-fathom contour (36.5 m below current sea level). Figure 1.4 shows the geology of sedimentology of the Irish Sea.

Tooley (1974) initially proposed nine periods of marine transgression, but this was revised to five (Tooley, 1978), identified in coastal mossland sediments, designated as Downholland I-V. The earliest, ~8000 BP, is recorded at Formby where peat deposition gave way to estuarine silt accumulation, followed by the second, ~6500 BP, represented as a single stratigraphic unit at Downholland Moss (now ~4 km from the coast). This is confirmed by sediment analysis and radiocarbon dating (Pye and Neal, 1993), which suggests the Sefton dune complex developed from a large offshore sand bank that was in existence by 6800 BP. A further layer of silty-clay in the Downholland Moss stratigraphy represents the third transgressive event, at 5900 BP during the Flandrian transgression when major rivers flooded. Then the coastline migrated eastwards to the approximate position described by Hall and Folland (1967) as the present 10 m contour-line, ~7 km inland. Pollen analytical research carried out by Stoney (1988) on Formby Moss recorded sand intervals within peat of early post-Elm decline age, post-5000 BP, prior to its final burial by sand during the Flandrian III fall in sea level. This sand is likely to be the moderately mobile sandy substrate described in Figure 1.4. Tooley (1978) proposed the fourth transgression, between 4800 and 4545 BP, is recorded in sediments at the Alt Mouth (Travis, 1926; Tooley, 1982), Formby and Birkdale. The dune system became stabilized ~3800 BP due to renewed higher sea level and persisted until ~3000 BP when sea levels began to recede (Innes and Tooley, 1993). Tooley's (1978) final transgression is identified by a radiocarbon date of 2335 ±120 BP, obtained from a relic dune slack at Formby. However, this transgression phase is speculative and relies on the work of Jelgersma *et al.,* (1970) who identified dune slacks in The Netherlands to be closely related to this period.

The present erosional phase is identified as initiating in the early 20th Century. Present day monitoring of the north-west coast of England has highlighted changes over recent decades on account of the perceived 'Global Warming' phenomenon (Hulme *et al*., 2002; IPCC, 2007). For instance, Shackley *et al.* (1998) outlined a rise in sea level at Liverpool of ~6 cm during the last 50 years, followed by subsequent increased flooding of major rivers (Evans *et al*., 2004).

1.4.2 Morphological chronology of the Sefton coastal dunes

Geomorphologists first began to take an interest in the Sefton Coast during the late 19th and early 20th Centuries, when both Ainsdale and Freshfield dunes featured in the 1915 Survey of 'areas worthy of protection' carried out by the Society for the Promotion of Nature Reserves (Sheail, 1976). Reade (1871) identified a series of biogenic and minerogenic stratigraphic units in the coastal lowlands of south-west Lancashire, which suggests several phases of sea

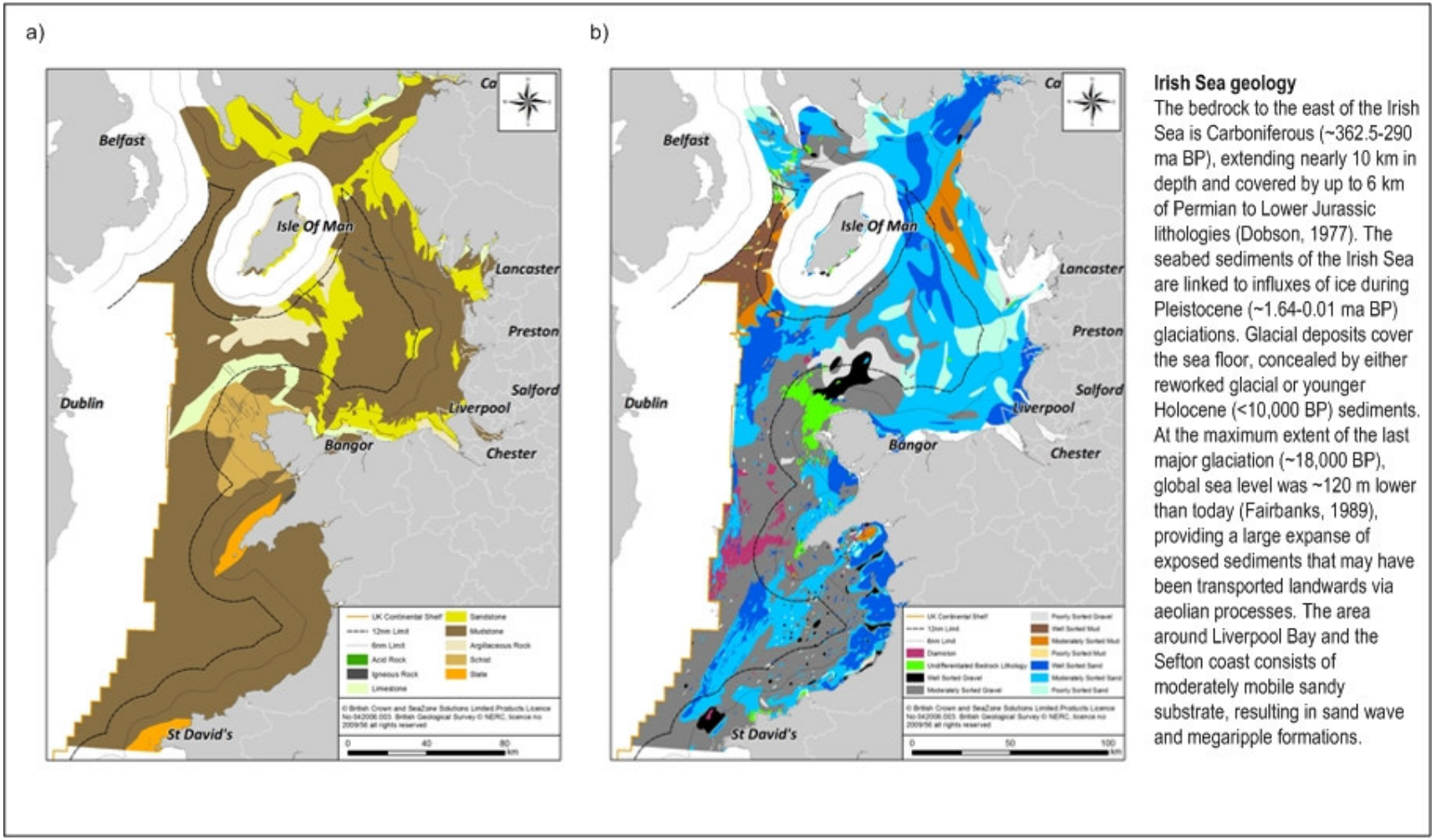

Figure 1.4 Maps of the Irish Sea showing distribution of a) bedrock and b) sediments (Irish Sea Conservation Zones, 2010)

regressions and transgressions. Further evidence concerning the origin of these unconsolidated deposits was provided by Rance (1869, 1872, 1877 and 1878) and Reade (1872, 1881a, 1881b, 1902 and 1908).

Gresswell (1953) produced a model of coastal evolution, by mapping coastal landforms and geomorphic features to suggest that the estuarine-marine silts and freshwater peats were replaced with blown sand. Although Gresswell's model has been the basis for much work on the coastal evolution of the north-west region, subsequent investigations have proved it to have significant flaws (Tooley, 1978). The Sefton coastal dunes were considered to have formed in response to the onshore movement of sand during the later Holocene (Gresswell, 1953). This is confirmed by Reade (1881a) who calculated the age of the dunes at 2580 years BP. However, Neal (1993) and Pye and Neal (1993) identified a series of peats and humic horizons within an aeolian sequence, the oldest of which can be dated to ~5100 ^{14}C years BP.

Despite arguments over the age of the oldest deposits, most authors (e.g. Tooley, 1982; 1990; Pye, 1990; Innes and Tooley, 1993) agree that the main phase of dune development occurred between 4500-2500 BP, corresponding with dunes of north-west Europe (e.g. Morkunaite and Cesnulevicius, 2001). Optical dates (Pye *et al.,* 1995) support radiocarbon evidence for a dune-forming period at Formby Point during the early to mid-Flandrian, ~3000 BP, before burial by estuarine silts during the later Flandrian transgression.

Tooley (1990), through published radiocarbon date analysis, identified a widespread phase of dune stability in north-west Scotland and Northern Ireland, between 2500-2000 BP. Tooley's (1978) identification of a dune slack soil (2335 ±120 BP) in the Sefton dunes at Formby, can be associated with this phase of dune stability. Pye (1990) reported a comparable date in the same dune slack peat horizon of 2510 ±120 BP. This soil is similar to that described by Wilson (1991) from Magilligan Point in Northern Ireland. Further descriptions of these periods of dune activity, separated by phases of dune stabilization and soil formation can be found in related literature (e.g. Neal, 1993; Pye and Neal, 1993, 1994; Pye *et al*., 1995; Neal and Roberts, 2000). Such patterns of dune development on the Sefton coast can be correlated with chronologies from The Netherlands (Jelgersma *et al.,* 1970), implying large scale climatic forcing of dune system evolution.

1.4.3 Present day coastline morphology

Pye (1990) highlighted the Sefton coast as a transition between open coast and estuarine regimes, influenced by processes both in the eastern Irish Sea (Wright *et al.,* 1971) and in the Ribble and Mersey estuaries (Plater *et al.,* 1993). Stratigraphic and sedimentological data (Pye and Neal, 1993) indicate that high dunes did not develop in the Formby dune complex until the 13th Century, when a major phase of coastal erosion was initiated during the Little Ice Age. Sand stabilization and foreshore reclamation measures carried-out 1850-1900 were highly effective and contributed to a seaward progradation of the entire Formby coastline (Pye and

Neal, 1993). Abandonment of these measures contributed to a return to shoreline erosion and a new phase of frontal dune instability, still in progress today.

Sediment dynamics at Formby Point have been studied in detail (Pye and Smith, 1988; Plater *et al.,* 1993; Pye and Neal, 1993, 1994; Brodie, 1996), concluding that the frontal dunes are eroding at a mean rate of 3 m/yr, and during single storm events 6-14 m (Pye, 1991). Pye and Neal (1993, 1994) described the factors that contributed to this onset of post-1900 erosion as, climatic change, effects of dredging and training wall construction in the Mersey and Ribble estuaries (Smith, 1982), abandonment of dune and foreshore management, and by an increase in recreational pressure, sand mining and military activities. Up to 220 m of accretion near Victoria Road, 1845-1906 (Gresswell, 1953; Turner, 1984; Pye and Neal, 1994), has been offset by ~400 m of erosion at Formby Point since then until the present day (Plater *et al.,* 1993). Saye *et al.* (2005) emphasized that the present shoreline at Formby Point lies almost in exactly the same position as during the late 18th Century, having advanced and retreated again by >300 m, evident in Turner's (1984) coastline map (Figure 1.5).

1.4.4 Contemporary geomorphology of the Sefton coastal dunes

According to the literature, several dune morphological types are identifiable in the modern Sefton system. Dunes between Birkdale and Ainsdale are parallel, with a suggested mean height of 9 m (Gresswell, 1953). On the seaward side, Neal (1993) described embryo dune formations becoming merged as grasses colonize. Salisbury (1925) estimated that it takes ~4 years for a coherent ridge to form separated from landward ridges by slacks. Edmondson *et al.* (2001) described these early stages of dune development as being followed by subsequent 'green beach' formation on the foreshore, initiated by colonization.

The eroding coast between Fisherman's Path (SD 280 098) and Lifeboat Road (SD 271 063) supports foredune ridge and sand sheet activity. Pye and Neal (1993) outlined maximum dune development occurring at Formby Point, where dunes reach 25 m above sea level and blown sand extends 4 km inland. Most of the inland dunes are stable, however, several blowouts and active transgressive dunes have been reported between Ainsdale and Southport and south of Formby Point (Pye, 1990; Pye and Neal, 1993; Paterson, 1997; Neal and Roberts, 2001; Saye *et al.* 2005).

Morphology of the Sefton dunes has been significantly altered by anthropogenic activities (Plater *et al.,* 1993). Figure 1.6 summarizes various anthropogenic impacts. Travis (1915) argued that marram grass (*Ammophila arenaria*) planting during the 18th Century encouraged the growth of the high frontal dunes at Formby, described by Pye and Neal (1993), in an otherwise flat dune topography landscape. Saye *et al.* (2005) suggested sand fencing on the upper beach at Ainsdale, Freshfield and north of the River Alt mouth, 1880-1914, caused the development of multiple parallel ridges. These dunes are described by Plater *et al.* (1993) as roughly parallel, 200 m wide ridges, separated by seasonally waterlogged slacks. However, Pye

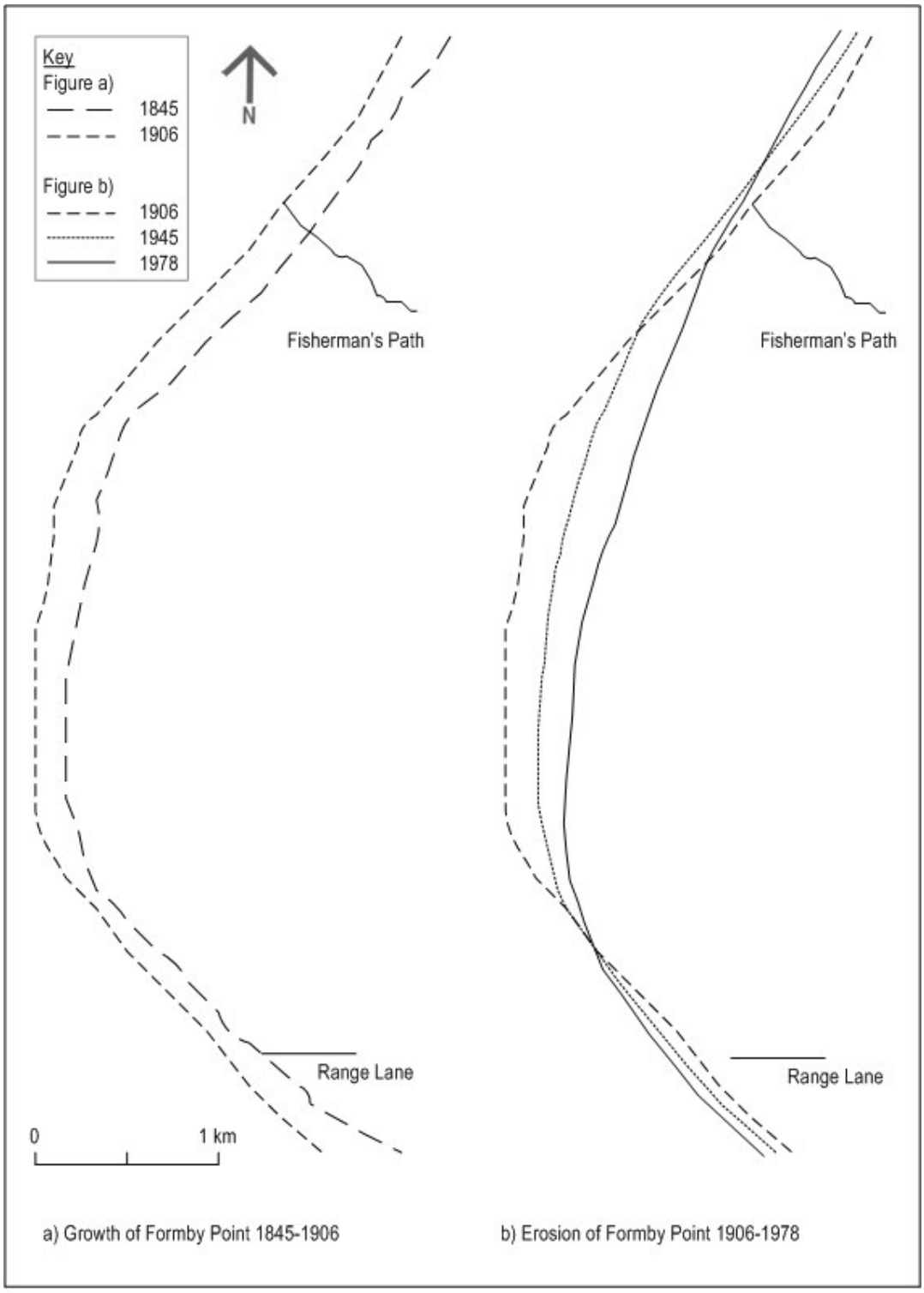

Figure 1.5 Growth of Formby Point showing: a) accretion under active management and b) subsequent erosion, based on O.S. map evidence (redrawn from Turner, 1984).

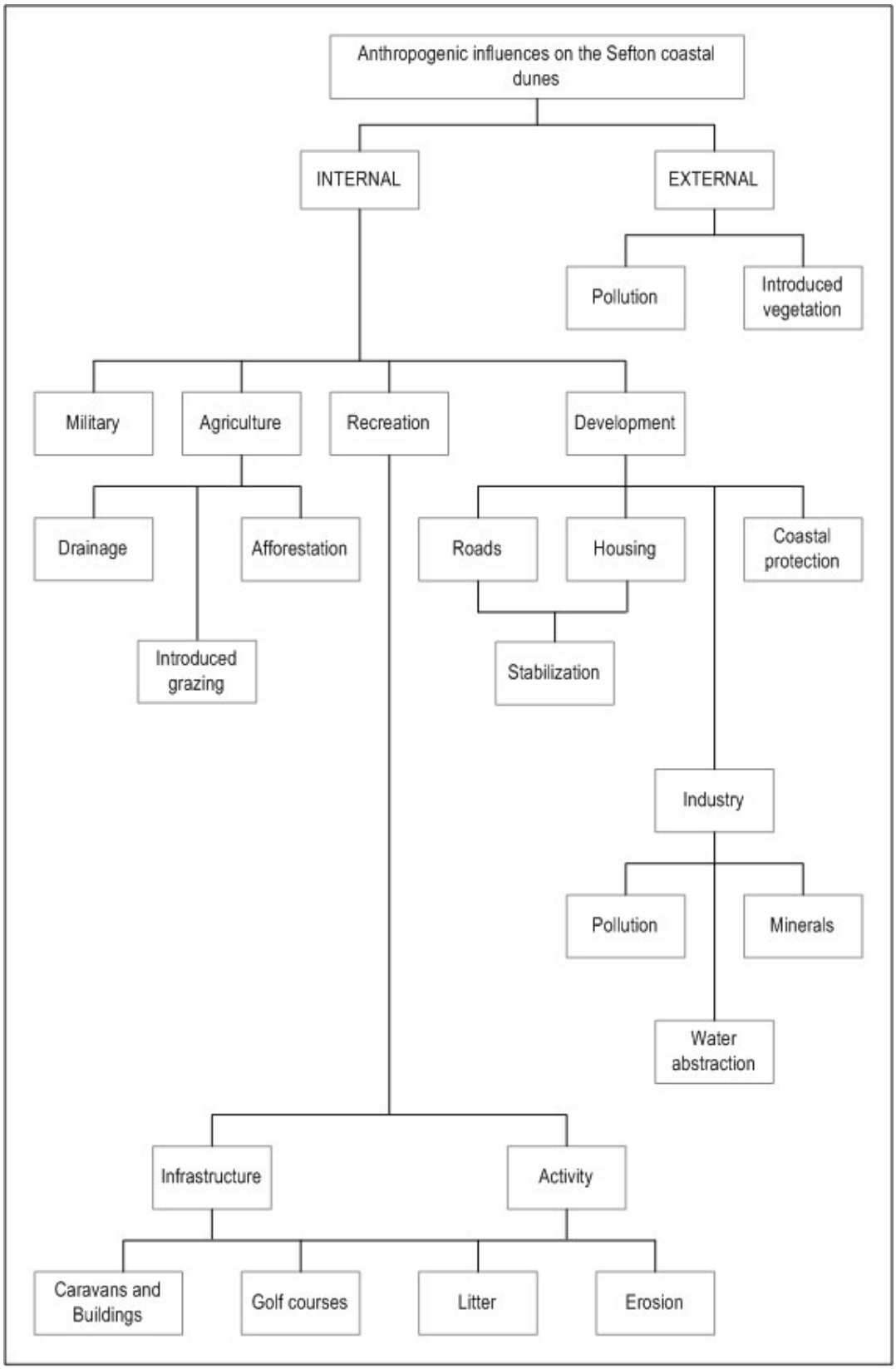

Figure 1.6 Summary of anthropogenic impacts and effects on the Sefton coastal dunes.

(1990) indicated erosion has truncated some of these ridges. Construction of the Coastal Road, in ~1923, meant levelling of some of the highest dunes (Gresswell, 1953) and detrimental effects on natural dune succession.

Landward of this parallel dune system an irregular zone of low hummocky dunes occurs, which Pye (1990) suggested formed pre-1800. Plater *et al.* (1993) associated several slacks within this system with natural blowouts, although true parabolic dunes are poorly developed. Much of the land beyond these dunes has been anthropogenically altered by levelling for building purposes and the construction of golf courses (Gresswell, 1953).

1.4.5 Dune vegetation and succession

Malloch (1989) outlined a sand dune vegetation zonation for Britain, but also noted that there is minimal detail of the vegetation found in the literature. A brief description has been given by Smithson *et al.* (2002) who summarized that the first deposition of embryo dunes was initiated by deposition of sand around pioneering plants. In the British Isles and Europe, marram grass (*Ammophila arenaria*) and sand couch grass (*Elytrigia juncea*) are common species that colonize bare sand with the ability to grow through and anchor frequent sand burial.

1.4.6 Dry dune vegetation succession on the Sefton coast

Salisbury (1925) discussed the soils and plants of successive dune ridges south of Woodvale. Edmondson *et al.* (1993), using existing NVC surveys, described lyme-grass (*Leymus arenarius*) occurring along the entire coastal foredunes, giving way to marram grass on the mobile parallel dune ridges, apart from the disturbed most northerly and southerly points (Figure 1.7). Successful growth of marram grass relies on constant supplies of fresh sand; therefore, colonies disperse on the landward side, giving way to other dune species (Gresswell, 1953). Pye (1990) referred to the leeward side of transgressive sand dune ridges at Sefton, as reverting from semi-fixed dunes back to marram grass (*Ammophila arenaria*) community type as a result of high sand accretion rates.

According to Edmondson *et al.* (1993), acidic grasslands and dune heaths occupy the eastern boundaries of the dune system where anthropogenic development has occurred, Freshfield (formerly a golf course) being one of the most extensive areas. Hall and Folland (1967) described this environment as being dominated by heather (*Calluna vulgaris*), indicative of the expected environment should grazing or management of the pastures cease.

Deciduous woodland exists on the coast but has not developed as a result of natural succession. Edmondson *et al.* (1993) mentioned a large area of alder (*Alnus glutinosa*) woodland in a slack area on Ainsdale NNR. This is not evident on the Ordnance Survey 1848 map, but is represented on the later edition of 1870. Although this stand was originally introduced, it is now spreading into an adjacent slack area by natural regeneration.

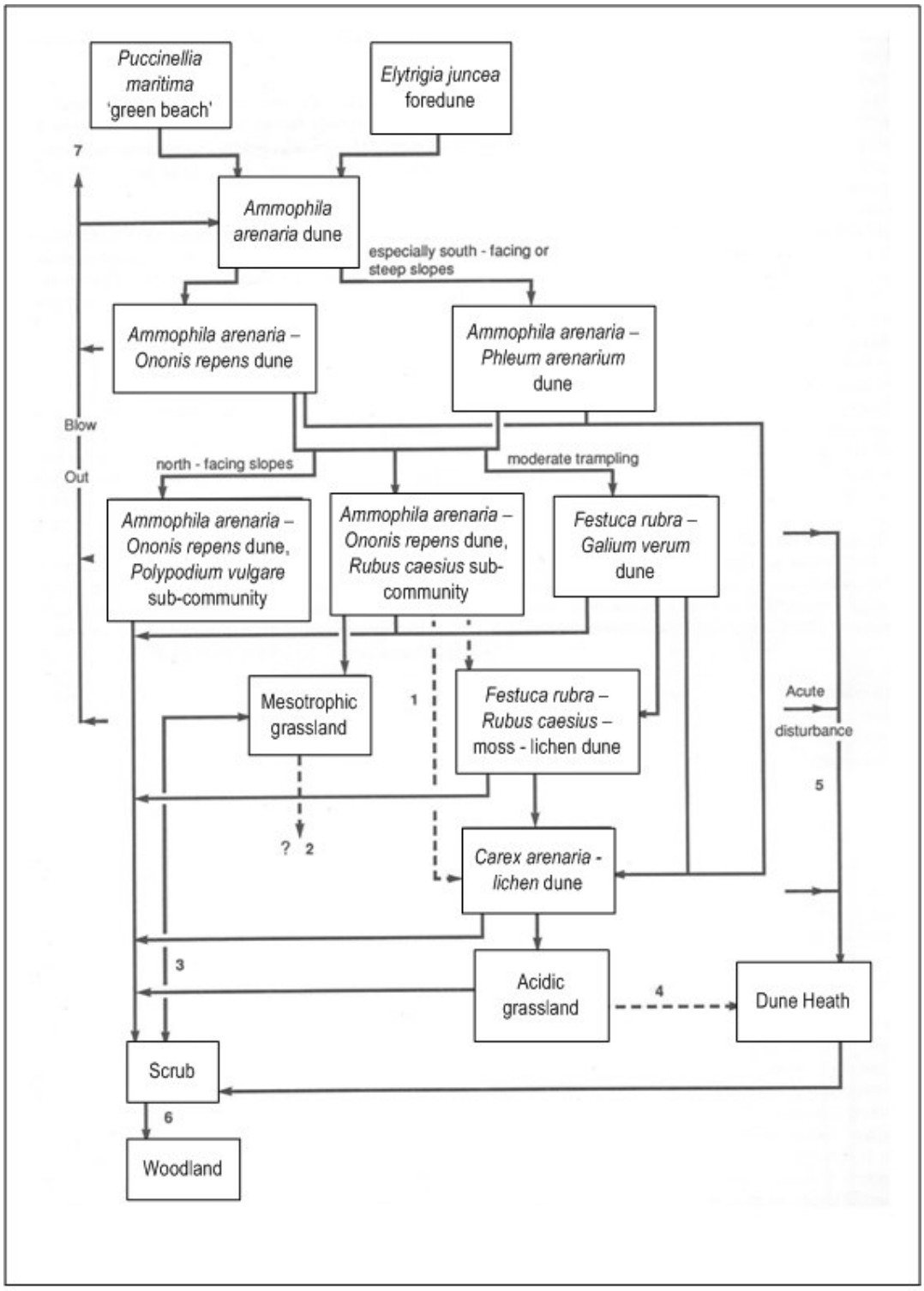

Figure 1.7 Proposed pathways for dry dune succession (from Edmondson *et al.*, 1993); 1) increased water retention may reduce leaching rates, 2) acidic communities are less likely, 3) nutrient enrichment causes mesotrophic grassland development, 4) landward ridges colonized by calcifugous grassland, with heath in lows, 5) heath occurs on disturbed land, 6) mature scrub is at woodland stage, and 7) secondary dune slacks formed by deflation to water table.

1.4.7 Dune slack vegetation

Slack vegetation on the Sefton coast was extensively reviewed by Smith (1978). Ranwell described 12 categories of dune slack vegetation, including recognized transitions between wet and dry slack areas, where fixed dunes have formed over slack environments. A table of his findings is given in Rhind *et al.* (2001). For example, creeping willow (*Salix repens*), which requires a good supply of water, is widespread on the Sefton semi-fixed and fixed dunes, comparable to findings of Rhind *et al.* (2001) on the Newborough dunes, Anglesey.

Payne (1983) also suggested a model for dune slack succession, based on trends towards increasingly dry conditions and the development of acidity and scrub, which is preceded by a model by Edmondson *et al.* (1993) with similar outcomes (Figure 1.8). Hall and Folland (1967) sampled two slacks, one considered dry and one wet, finding creeping willow (*Salix repens*) and early hair-grass (*Aira praecox*) dominant in both. Some variations do exist, however, as a result of slack age and hydrology, as the accumulation of sand and organic matter with age, combined with colonization, causes slack environments to become drier (Edmondson *et al.,* 1993; Jones, 1993).

Successional stages of creeping willow colonizing slack areas have been investigated, finding correlations between plant form and habitat (Blanchard, 1952; Rechinger, 1964; Jones, 1980; Barton, 1981; Meikle, 1984). Blanchard (1952) suggests duration of winter flooding is more significant in affecting growth of creeping willow than depth of submergence. This is confirmed by Payne (1983), who concluded that in wet slacks, creeping willow is tall and dominant.

1.4.7 Pine plantations

Typical sand dune landscapes often underlie forests established several decades ago for stabilization purposes (e.g. Chen *et al.,* 2005). In Ainsdale NNR, 120 ha of pinewood (*Pinus nigra*) planting took place from 1887 to the 1960s, the history and management of which has been described by several authors (e.g. Gresswell, 1953; MacDonald, 1954; Pethick, 2001; Simpson and Gee, 2001). Coniferous plantations are known to lead to modifications of the soil (e.g. Ovington, 1955; Challinor, 1968; James and Wharfe, 1989; Sturgess, 1992; 1993). Pine planting has also resulted in lowering of the water table (Gee, 1991) and, subsequent, drying of dune slacks, which Atkinson (1988) associated with loss of species diversity and increased birch invasion. This is comparable to the work of Hill and Wallace (1989), who concluded that the effects of afforestation on Newborough sand dunes, Anglesey, was stabilization of the dune morphology, lowering of the water table and considerable changes to floristic composition, due to shading, drought, nutrient competition and needle litter accumulation.

1.4.8 Attitudes towards dune management on the Sefton coast

Only recently have sand dunes been valued as a landscape worthy of preservation. Until the late 19th Century, dune environments were used for cultivation and grazing, overexploitation of which would reactivate sandblow (Greswell, 1953). Perceptions turned to controlling blown sand

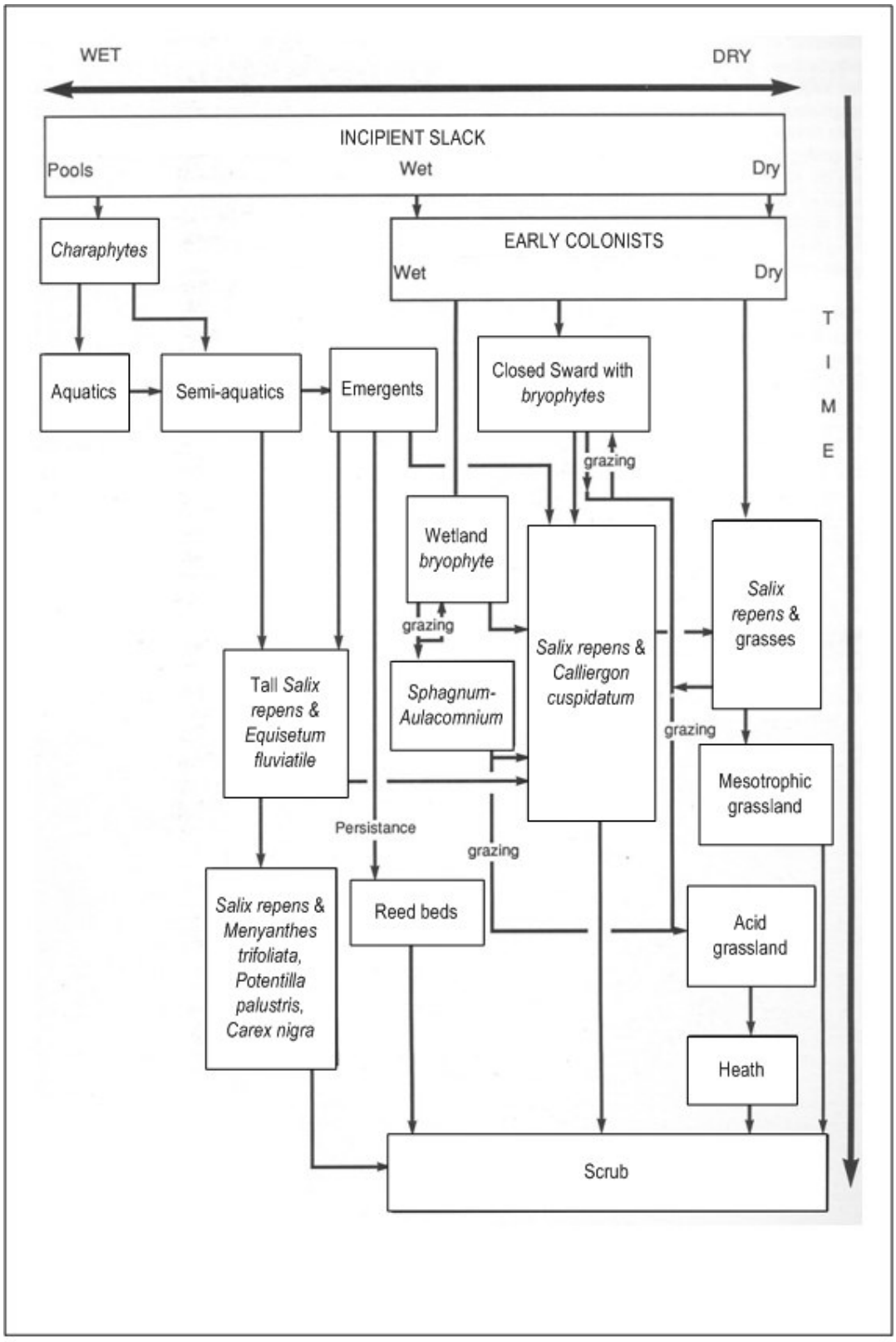

Figure 1.8 Proposed pathways for dune slack succession (after Edmondson *et al.*, 1993).

and halting sand drift, which led to stabilization techniques, including planting of conifers and scrub species such as sea buckthorn (*Hippophae rhamnoides*) (Wheeler *et al.,* 1993).

The pinewoods, along with associated introduced red squirrel (*Sciurus vulgaris*) community, are now locally accepted as a natural part of the Sefton landscape. However, excessive stabilization of the dunes has resulted in 'coastal squeeze' and loss of habitat can be observed where the landward position is fixed, i.e. afforested dunes, and erosion at the seaward margin is active (Pethick, 2001). Despite ongoing monitoring techniques and conservation practises, it is still not known how dune environment dynamics will respond to coastal change. The general consensus in the literature has been an emphasis on struggling against natural forces to reduce or prevent erosion by dune restoration projects (Payne, 1983), including thatching of timber and brushwood cuttings on the exposed sand surfaces (Beach Protection Authority, 1982) and marram planting (Hewett, 1970). Therefore, both natural and introduced, internationally-designated habitats that may be in danger of 'coastal squeeze' or disappearing altogether can be conserved and protected (Doody, 2001; Orford and Pethick, 2006).

Recently, however, a new attitude to dune management has evolved. Concerns that existing management approaches, which depend on orderly succession of habitats, are evident in the literature (e.g. Orford and Pethick, 2006). Pethick (2001) outlined that although sand dunes are not resistant to wave attack, they can be mobilized during storm events. The release of eroded sand onto the beach, which indirectly acts as a sea defence through dissipation of wave energy, is subsequently transported back to the dune as part of a beneficial cyclical process. The multi-barred intertidal beach acts as the natural coastal defence of the Sefton coast (Parker, 1975). Natural coastline re-orientation processes; i.e. erosion of Formby Point and accretion to the north and south (Gresswell, 1953; Turner, 1984; Plater *et al.,* 1993; Pye and Neal, 1994; Saye *et al.,* 2005), are seen as the coast maintaining its natural defence and prevention of this should not be attempted (Shoreline Management Plan, 1999).

Effects of 'coastal squeeze' can be overcome by abandoning stabilization techniques and allowing dune activity (Pethick, 2001). For example, clear-felling pine areas creates an extended fixed dune habitat that, if managed according to Shoreline Management Plan (1999) proposals (i.e. sand fences, matting, planting and access control) will eventually be 'squeezed' and habitats lost once again as the coastline retreats. In fact, sustaining habitats, despite natural processes of environmental change, has become extremely difficult in rapidly changing coastal systems (Natura, 2000). Instead, Pethick (2001) controversially recommended increasing grazing pressure and encouraging access to subsequently cause blowouts and development of parabolic dunes, with associated slacks, to maintain characteristics of a migrating dune landscape. While frontal dune erosion inevitably leads to loss of habitat area, Pye (2001) suggested it may also bring benefits in the form of geomorphological and ecological dynamism. This is supported by Orford and Pethick (2006), who suggested coastal managers may need to

consider 'coastal breakdown', segmentation and habitat reduction as the basis of 21st Century coastal evolution and planning.

1.5 The role of pedogenic processes in coastal dune management

Soils are an integral part of nature, and therefore soil diversity and soil responses should be taken into account when managing nature areas (van den Ancker and Jungerius, 2007). However, studies of dune soils in Britain have generally been neglected because of their limited agricultural value. On the Sefton coast, despite a small part previously used for growing asparagus (Hall and Folland, 1967; Lewis and Cowell, 2002) and some modern day afforestation (MacDonald, 1954; Simpson and Gee, 2001), the greater part is of little agricultural importance. However, research (e.g. Wilson, 1992) indicates dune soils may contain important information concerning development trends and timescales.

1.5.1 Introduction to pedogenesis and soil classifications

The definition of soil varies considerably depending on discipline, ranging from the environmental perspective that soil is a medium for plant growth (e.g. Lyon and Buckman, 1922), to a geologists idea that soil is a layer of weathered rock (e.g. Ramann, 1928). Generally, soil can be described as the upper layer of the earth's mantle and the product of complex interacting processes (Ragg *et al.,* 1984). Dokuchaev (1883) identified five soil-forming factors: parent material, biota, relief, climate and time, later revised by Jenny (1941) to determine that each of these factors are not forces but independent variables. From this, modern considerations define soil as an abiotic system, with biospheric functions, acting as a habitat, accumulator, source of substrates for organisms, a link between biological and geological cycles and a planetary membrane (Nikitin, 2001).

A soil profile is a vertical section through the soil, within which horizons are roughly parallel to the surface (Ragg *et al.,* 1984). These horizons differ in colour, texture, structure and soil organic matter (SOM) content (Smithson *et al.,* 2002), becoming differentiated by physical, chemical and biological processes (Ragg *et al.,* 1984). Letter symbols, reflecting genesis of the horizon, are given in Table 1.1, which has been modified from Hall and Folland's (1967) Memoirs of the Soil Survey of Great Britain, incorporating further horizon definitions classified by Green *et al*. (1993) for environmental soil research. A soil chronosequence is defined as a group of soils that are similar with respect to all soil forming factors except for time (Jenny, 1941). This approach has been applied in pedologic research to study development of soil properties, such as texture, structure, colour and chemical composition.

Bockheim *et al.* (2005) presented recognition of soil-forming events, such as eluviation and illuviation, resulting in the identification of seven processes, including podzolization, calcification, laterization, gleization, salinization, solonization and solodization. These differences led to the first soil classification, proposed by Dokuchaev (1883) after identifying the five soil-forming factors. However, each national system has evolved from this with different approaches,

Organic and organo-mineral surface horizons	
L	Undecomposed litter
F	Partially decomposed litter
H	Well-decomposed humus layer, low in mineral matter
A	Mixed, mineral-organic layer
Ah	Topsoil with a high organic matter content
Ap	Ploughed layer of cultivated soils
Ag	An A horizon with rusty mottling, subject to periodic waterlogging
Sub-surface horizons	
E	Eluvial horizons, depleted of clay and/or sesquioxides
Ea	Bleached (ash-like) horizon in podzolised soils
Eb	Brown (paler when dry), friable, weak-structured horizon depleted of clay (characteristic of *sols lessivés)*
B	Altered horizon by illuvial concentrations of materials denoted as; t (clay), h (humus) and f (iron) in podzols
Bs	Illuvial horizon enriched in iron and aluminium
Bf	Thin iron-enriched horizon indicating a ferric podzol
Bh	Illuvial organic-enriched horizon indicating a humus podzol
BhFe	Thin rusty red indurated pan, composed of iron oxide coatings on stones
Cu	Little altered horizon, except by gleying. Where two or more layers occur in the lower part of the profile, they are designated Cu1, Cu2, etc.
Cr	Horizon resting on rock
Bca Cca etc	Horizon containing appreciable amounts of redeposited (secondary) calcium carbonate
Bg Cg etc	Mottled (gleyed) horizons subject to waterlogging
A/C B/C etc	Horizons of transitional or intermediate character

Table 1.1 Soil horizon letter notations (modified from Hall and Folland's, 1967, Memoirs of the Soil Survey of Great Britain, incorporating further horizon definitions described by Green *et al.* (1993).

therefore, creating comparison problems (Fullen and Catt, 2004). Cruickshank (1972) reviewed the development of the US Soil Taxonomy. In 1974, the Food and Agriculture Organization/United Nations Educational, Scientific and Cultural Organization (FAO/UNESCO) developed a world soil classification system, dividing all of the world's soils into 26 Soil Units. However, the system used in this thesis will be the soil classification system of England and Wales, as described by Avery (1980), as it is more widely employed in north-west European studies (e.g. Jungerius and van der Meulen, 1988; Wilson, 1992; Fullen *et al.,* 1999). Soils that are representative of soils occurring on sand dune systems are characterized in Figure 1.9: FAO soil unit classifications are also incorporated.

1.5.2 Generalized pedogenesis on coastal dunes

The study of pedogenesis, or soil formation, on sand dunes has generally been neglected, probably due to the fact that dune soils are not productive from an agricultural perspective (Jungerius, 1989). Dune sand is widely known as being an inactive soil having few positive characteristics for flora (e.g. Tsoar, 2005). Particles are relatively coarse and pore spaces are large, therefore dune soils have high permeability and leaching rates prevail (Ampe and Langohr, 2003). In such environmental conditions, rooting depth, as well as profile development, is limited and a lack of cohesion between the grain particles results in high erodibility.

Soil scientists have recorded some general coastal pedogenic data, but the collection is limited. Sevink (1991) explained that interaction and alternation between geomorphological and biological processes accounts for complexity of soil patterns in dunes. Because of this, Jungerius and van der Meulen (1988) classified north-west European dunes into different zones based on their geomorphological stability, a description of which can be found in Jungerius (1990). This concept is applicable in coastal dunes elsewhere in Europe (e.g. Wilson, 1992; Fullen *et al.,* 1999). Ranwell (1972) records pedogenic trends on stabilized dunes simply as increases in SOM, paralleling decreases in pH and calcium carbonate ($CaCO_3$), with increasing age and usually distance inland.

Lammerts *et al.* (1992) recognized soil processes, especially pH fluctuations, to control the colonization and decline of vegetation, similar to Wilson's (1992) analysis of both ground and buried soils, on coastal dunes in Northern Ireland. Fullen *et al.* (1999) illustrated the possibility of examining pedogenesis and increasing acidity across the Ayres, northern coast of the Isle of Man, by means of a transect inland from recent coastal deposits at the beach, through to stabilized dunes. The soils were described as calcareous rendzina, shallow soils with high organic-matter content, the acidic condition of which can be related to both intense leaching and coniferous afforestation producing an acidic, needle litter topsoil. This is comparable to Ranwell's (1972) previous illustration of the spread of heath vegetation onto Holocene dunes on South Haven peninsula, Dorset, where leaching of carbonates and iron oxides occurred.

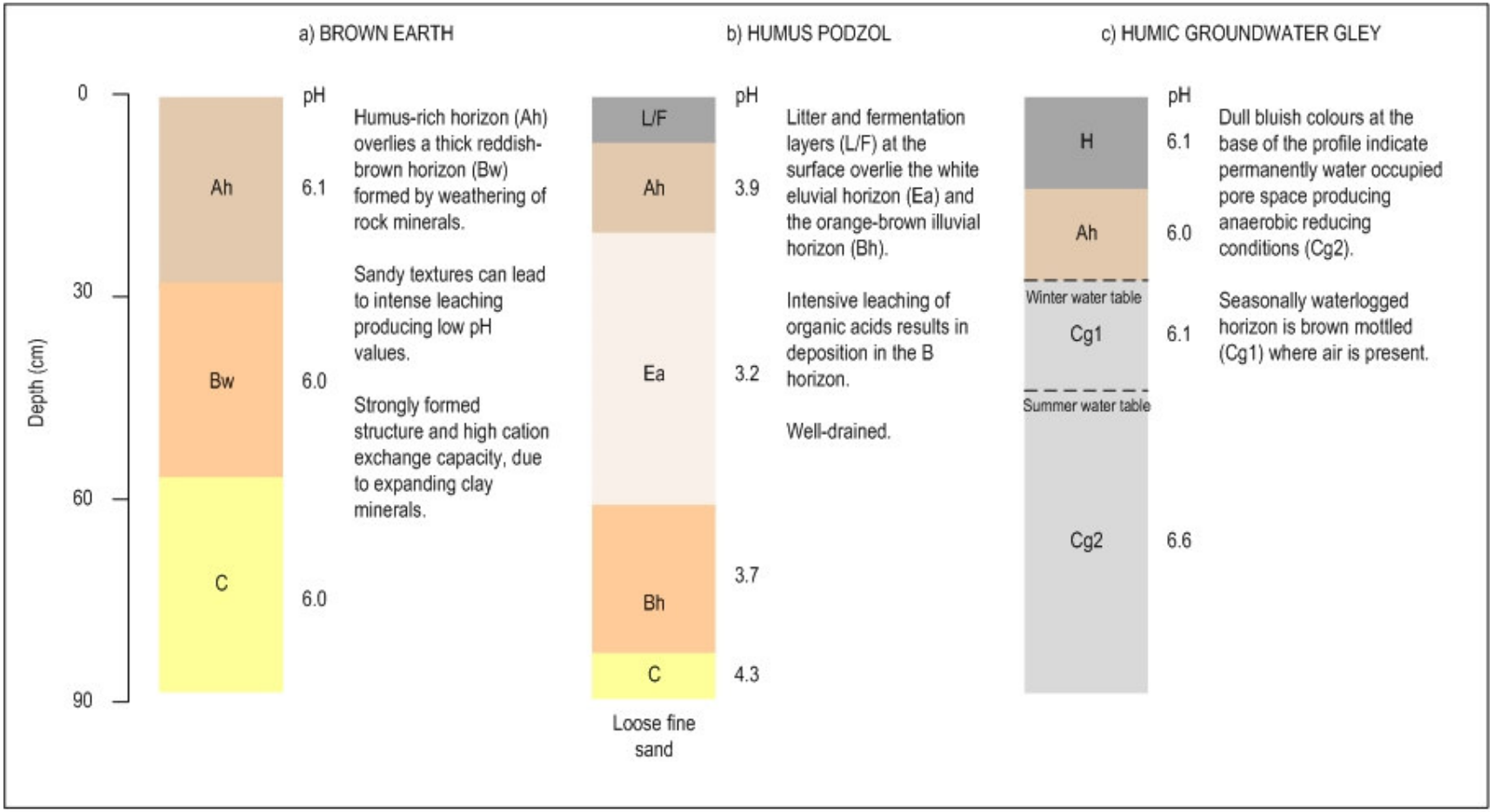

Figure 1.9 Idealized soil profile classifications of England and Wales representative of sand dune environments (after Avery, 1980) incorporating FAO soil unit classifications; a) brown earth (FAO: Cambisol); b) humus podzol (FAO: Humic Podzol); and c) humic groundwater gley (FAO: Stagnogley (gley caused by stagnation of drainage)) (redrawn from Smithson *et al.*, 2002).

1.5.3 Soils on the Sefton coast

Several dune soils were recognized on the Sefton coast by Hall and Folland (1967). These were skeletal soils on mobile dunes, pararendzinas on dunes stabilized by vegetation, groundwater gleys in slacks and micro-podzols beneath deep pine litter. However, the Soil Survey of England and Wales (Ragg *et al*., 1984) place the soils in the Sandwich Association (Figure 1.10; Tables 1.2, 1.3), comprising only terrestrial raw sands and sand-pararendzinas and have not differentiated them further (Mackney *et al.,* 1983; Beard *et al.,* 1987), although it was known that other soils did exist within this association (Jarvis *et al.,* 1984). Soils on decalcified dunes are of the Beckfoot series (Ragg *et al*., 1984) and soils in slacks are of the Formby series (Claydon and Hollis, 1984). The physico-chemical characteristics of the Sefton coastal soils were described by James (1985). James and Wharfe (1989) and James (1993) presented more detailed classifications, suggesting soil development initiates as terrestrial raw sand (Section 1.5.3.1), developing into sand-pararendzinas, interspersed with slack groundwater gleys, and finally acid sands or micro-podzols (Figure 1.11) from which a geomorphopedological map of Ainsdale NNR (Figure 1.12) precedes a pedogenic model (Figure 1.13).

1.5.3.1 Terrestrial raw sand on the Sefton coast

Terrestrial raw sand refers to freshly deposited sand, unaltered by pedogenic processes. Evident from James and Wharfe's (1989) soil map, this occurs on unstable seaward dune ridges or inland where erosion has been induced.

1.5.3.2 Sand-pararendzinas on the Sefton coast

Sand-pararendzinas, occurring on dune ridges and stable sands under continuous vegetation cover, are shallow A-C horizon sequences with high organic-matter content in the top few cm (refer to Figure 1.11). As pedogenic processes involve acidification and humus incorporation through faunal activity, the absence of earthworm species where SOM is <1% (Chamberlain and Butt, 2008) indicates the immaturity of these soils. Jones *et al.* (2004) found above-ground biomass in mobile and semi-fixed dunes to be positively related to atmospheric nitrogen inputs, due to increased cover of marram grass (*Ammophila arenaria*). The authors realized that this increased biomass may lead, in the long term, to increased soil organic matter (SOM) accumulation and, consequently, accelerated soil development. This was emphasized further by Johnson (1979).

Application of nutrients to established dune communities allowed Willis (1963) to demonstrate that in dune pastures on calcareous sand, phosphorus was an important growth-limiting nutrient. In such conditions pioneer grasses can become infected with vesicular-arbuscular (VA) mycorrhizal fungi, which is important for the early growth of plants such as marram grass (*Ammophila arenaria*) (e.g. Read, 1989; Sturgess, 1991). Wharfe (1984) and James and Wharfe (1989) analysed chemical elements in a non-afforested dune succession transect in Ainsdale NNR, indicating positive balances for sodium in terrestrial raw sand and sand-pararendzinas due to high input rates. The negative calcium and magnesium balances were the result of

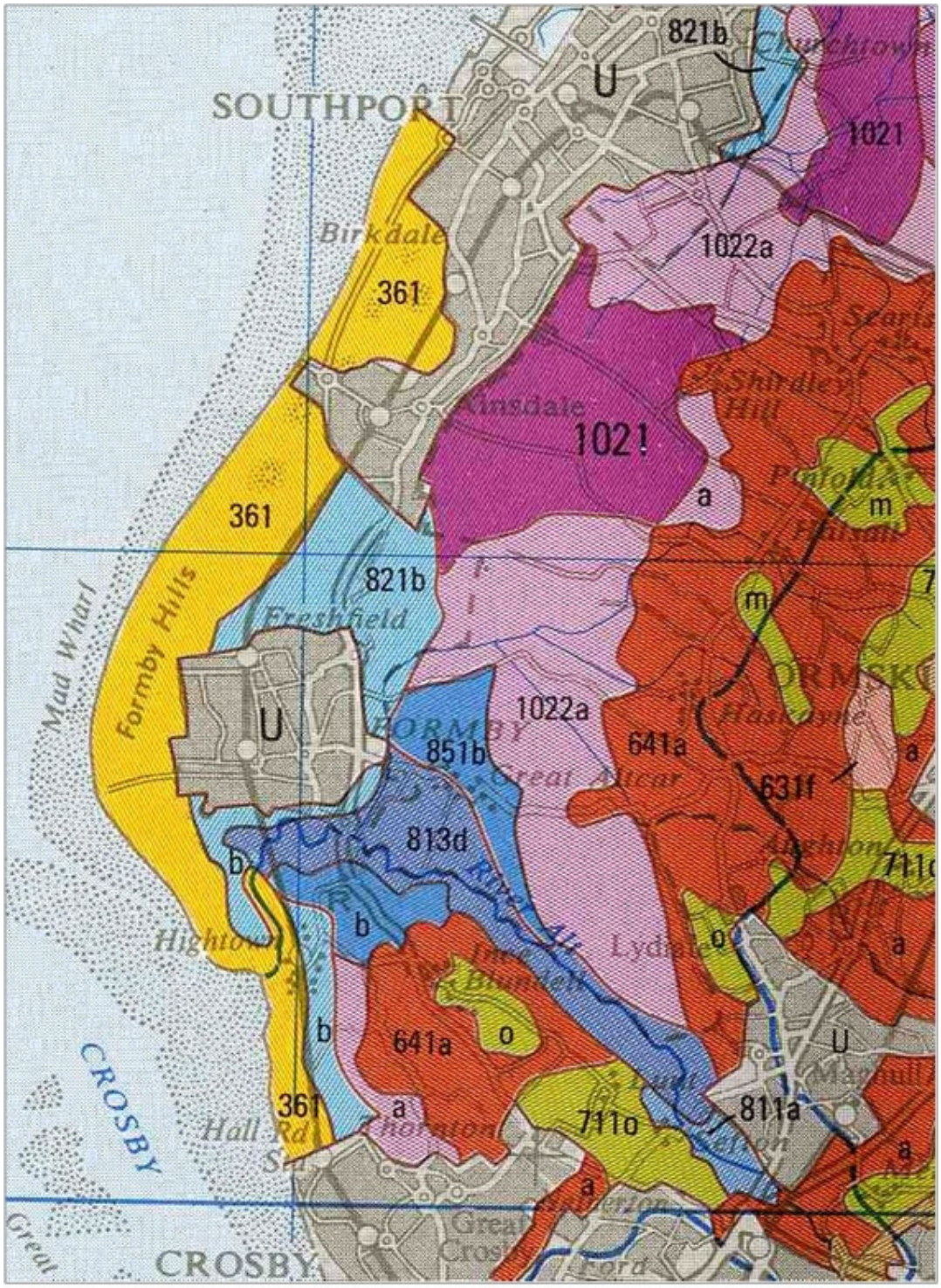

Figure 1.10 Representation of Sefton dune soils as symbol 361 on Soil Survey of England and Wales map (Mackney *et al.*, 1983) (for descriptions refer to Tables 1.2 and 1.3).

Table 1.2 Origin of symbol 361 according to the legend for the 1:250,000 Soil Association Map of England and Wales (modified from Mackney *et al.*, 1983)

Symbol	Classification	Description
3	Lithomorphic soil	Shallow soils in which the only significant pedogenic process has been the formation of an organic or organic-enriched mineral surface horizon. They are formed over bed-rock or little altered, soft unconsolidated material at or within 30 cm depth.
3.6	Sand-pararendzina	Soils formed in calcareous soft, unconsolidated sandy deposits other than alluvium.
3.61	Typical sand-pararendzina	(refer to Table 2.2)

Table 1.3 Description of symbol 361 according to the legend for the 1:250,000 Soil Association Map of England and Wales (modified from Mackney *et al.*, 1983)

Map symbol	Association	Sub-groups	Geology	Characteristics	Landuse	Area (km^2)
361	Sandwich	11 Raw sand 321 Beckfoot 821 Formby	Dune sand and marine shingle	Mainly deep well drained calcareous and non-calcareous sandy soils. Some sparsely vegetated unstable soils. Waterlogged soils in hollows locally. Shingle bars and spits locally extensive. Risk of wind erosion.	Sand dune and some wetland habitats; recreation; very limited agriculture and coniferous woodland; some gravel extraction in the South East Region.	343 (0.22% of the surveyed area of England and Wales).

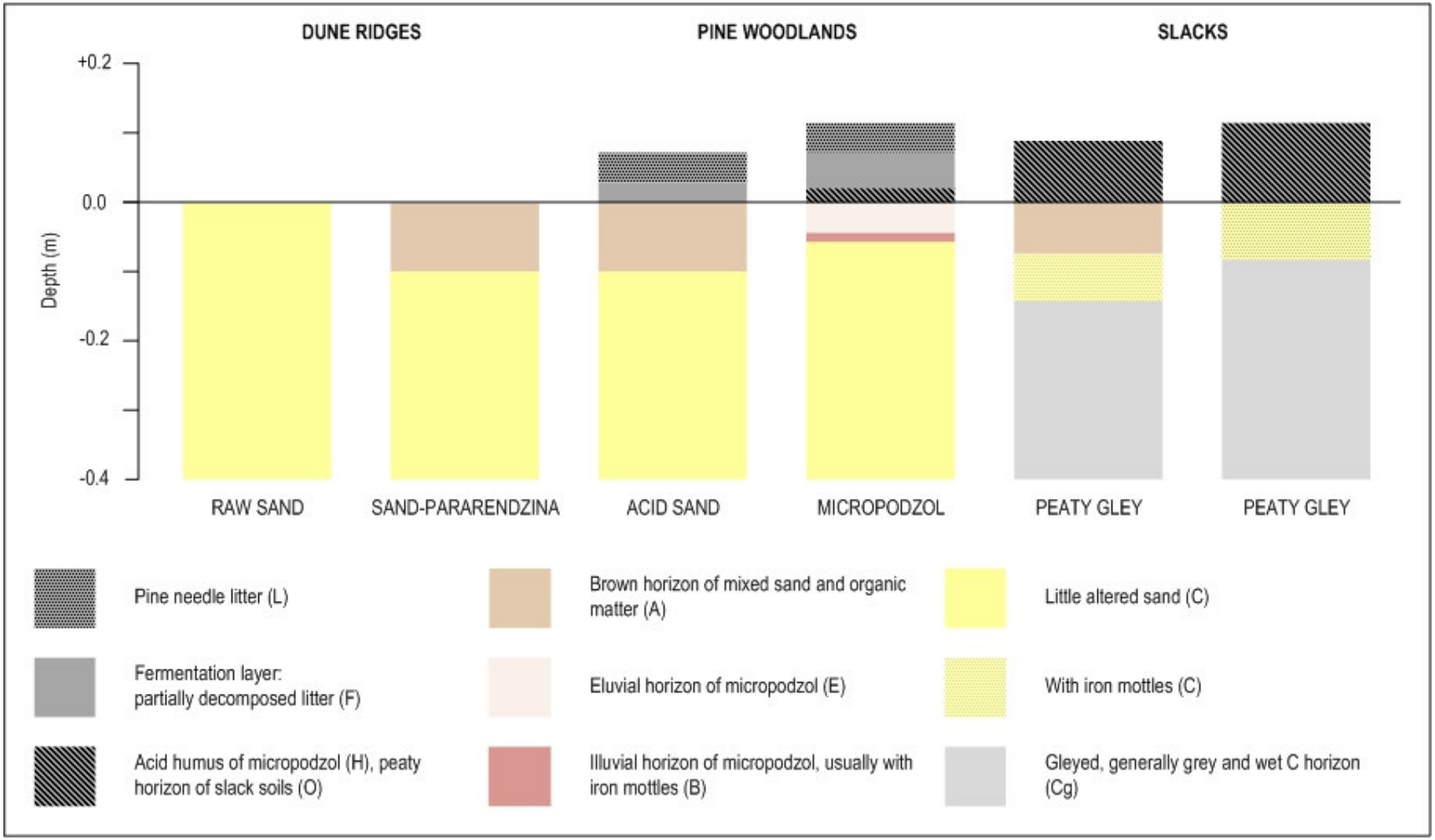

Figure 1.11 Soil classification and profile morphology of representative soil types from the modern Sefton dunes (redrawn from James, 1993).

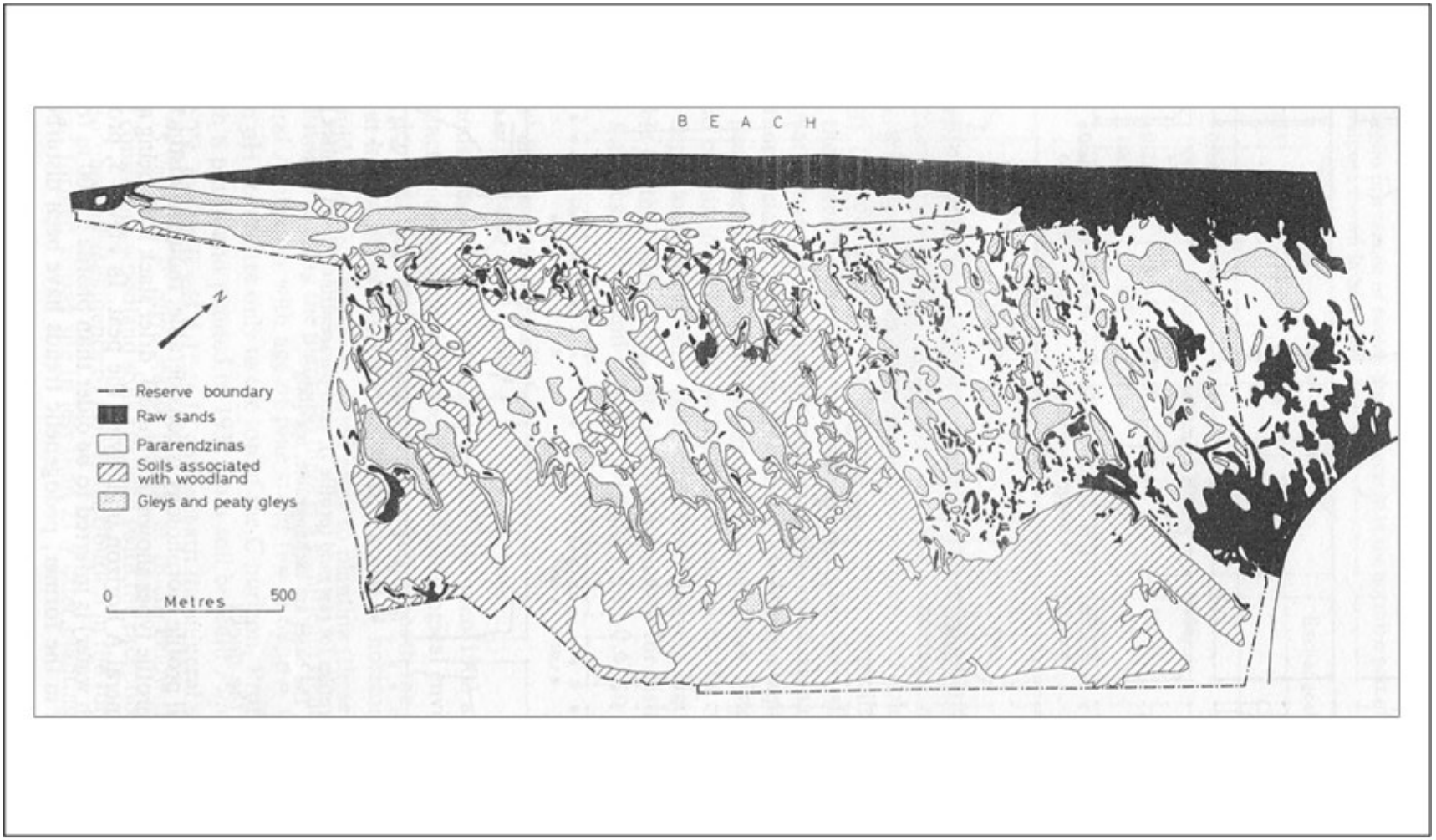

Figure 1.12 Soil map of Ainsdale NNR (after James and Wharfe, 1989).

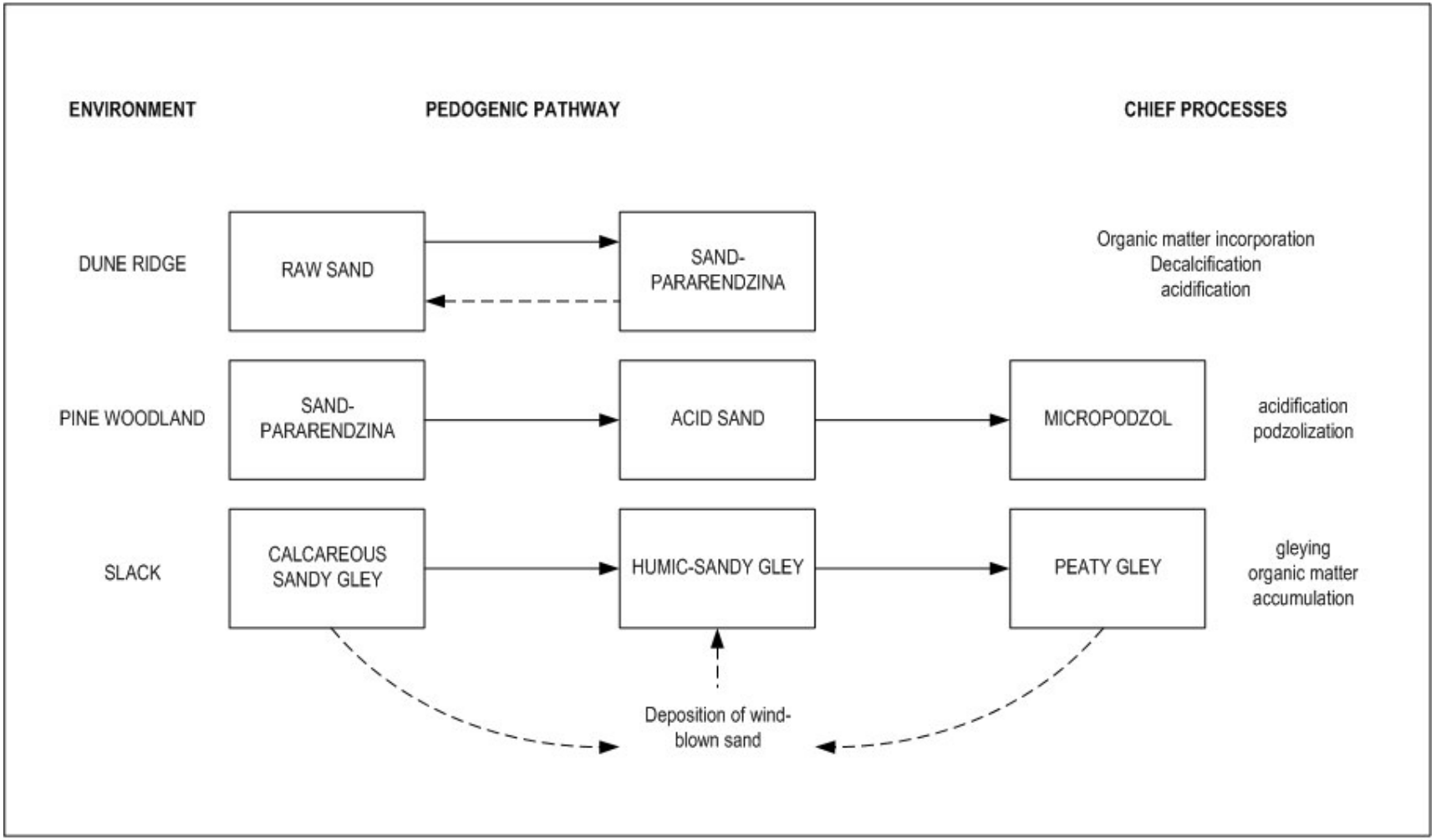

Figure 1.13 The chief soil-forming environments of the Ainsdale duneland (redrawn from James and Wharfe, 1989).

leaching from calcareous soils (James *et al.,* 1986), which is similar to work by Vestin *et al.* (2006), who identified higher content of exchangeable Ca and Mg in coastal soils with alkaline parent materials.

1.5.3.3 Groundwater gleys on the Sefton coast

Slack soils can be described as a distinct pedogenic sub-system (Neal, 1993), with an oxidized mineral horizon beneath surface organic material. According to Hall and Folland (1967) oxidizing conditions predominate in well-drained soils, but where water stagnates for periods of time, micro-organisms and plant roots use dissolved oxygen faster than it can be renewed. Bloomfield (1951) described how under such anaerobic conditions, ferric ions are reduced to the ferrous state, either by microbial action or by direct reaction with soluble products of plant decomposition. This process is known as gleying, resulting in development of grey-colours in contrast to characteristic browns and reds of ferric oxides formed in well drained soils.

Hall and Folland (1967) associated groundwater gley soils with complete or partial seasonal saturation of the profile from groundwater. Analysis of James and Wharfe's (1989) spatial soil map (Figure 1.12) demonstrates the importance of groundwater table depth on the spatial pattern of dune slack soil profile morphology and chemistry. According to Willis (1963), nitrogen is the primary limiting nutrient in dune slack soils, as accumulation of SOM leads to decreased pH, inhibiting nitrification, and ammonium becomes the major mineral nitrogen source to replace phosphorus as the key growth-limiting element. Here, plants such as creeping willow (*Salix repens*) produce a shrub layer enriched with litter, in which species interconnected by mycorrhiza can occur. Beltman *et al.* (1992) found differing vegetation types in separate slack environments could not be explained by nutrient sources, suggesting that binding processes to the soil must form the explanation. Hentschel *et al.* (2007) suggested that in spruce forest soils, leaching of inorganic nitrogen is constrained by the ability of SOM to retain water and that wetting intensity of the soil does not alter N or dissolved organic carbon concentrations.

1.5.3.4 Micro-podzols on the Sefton coast

Coniferous plantations on coastal dunes have caused widespread physico-chemical soil alterations throughout Britain (e.g. Ovington, 1950; 1951; Wright, 1955; 1956; Hall and Folland, 1967; James and Wharfe, 1989) and parts of Europe (Ampe and Langohr, 2003). On the Sefton coast, the microclimate and ecology of pinewoods create a different soil forming environment to that of open dunes. Deposition of an acidic needle litter, ≤2 cm thick, leads to acidification and bleaching of the E horizon and a rusty-mottled B horizon (James, 1993), resulting in micro-podzol formation (Figure 1.12). Micro-podzols have also been identified under dune heath at Freshfield (Kear, 1985).

1.5.3.5 Effects of deforestation on Sefton coastal soils

Pine removal began on the Sefton coast during the 1940s. Sturgess (1991) investigated effects of pinewood removal in Ainsdale NNR through soil profile analysis, concluding that SOM and

nitrogen contents in felled sites were similar to pararendzina values after 50 years. Reversions have also been effective in Northern Ireland (McBride and Wilson, 1991), where podzols have reverted back to brown calcareous soils as a result of agricultural activities.

Two more recent phases of pine removal were carried-out, initially in 1992, and during winter 1995-1996 (Figure 1.14). Sturgess (1992, 1993) outlined that afforested sand dunes, along with subsequent exclusion of vegetation, cannot be restored to diverse dune flora by clear-felling. However, Purdie (2002) disputed this through a soil pH survey in Ainsdale NNR, concluding that there were significant differences between restoration areas and pine woodland showing substantial soil pH changes since removal in 1991-1992 and 1995-1996. In addition, there was minimal pH difference between the restoration areas and the fixed dunes, highlighting that these areas were becoming open dune habitats. Authors (e.g. Hendrickson *et al.,* 1989; Pennock and Van Kessel, 1997; Bock and Van Rees, 2002) explain that these pH influences may be a result of more favourable soil moisture and temperature conditions for the growth of micro-organisms in felled environments. In these conditions, decomposition of resistant litter can be accelerated and immobilized cations can be released. Olsson *et al.* (2000) outlined that whole-tree harvesting can lead to decreased available reserves of soil-limiting nutrients. Merino *et al.* (2004) agreed, and in addition to the nutrient export with biomass, subsequent losses by leaching can increase significantly.

Fullen (1991, 1998) outlined that conversion of natural vegetation to other land use can decrease SOM, while the conversion back to natural vegetation can replenish SOM. Impacts of SOM enrichment on soil carbon dynamics have been documented (e.g. Hagedorn *et al.,* 2001), creating the potential to study soil carbon sequestration (e.g. Lal, 2003; Jankauskas *et al.,* 2005; Fullen *et al.,* 2006).

1.5.4 Timescales in soil development: comparisons between European coastlines

McBride and Wilson (1991) and Wilson (1992) have identified four stages in soil development on coastal dunes in the north of Ireland. Recently deposited calcareous dune sand, lacking pedological horizonation and low in organic matter represents stage 1. Hall and Folland (1967), along with Minton (1985), described these soils as so recently deposited that profile development consists of little more than the incorporation of small amounts of organic matter in the surface layer. Following vegetation colonization, these sediments may progress to stage 2 sand-pararendzinas, classified by Kubiena (1953), within 15 years at Ainsdale (James and Wharfe, 1989), 16 years at Magilligan Point, Northern Ireland (Wilson, 1992) and within 18 years on the Dutch island of Schiermonnikoog (Olff *et al.,* 1993). Soils eventually develop into brown calcareous sands, stage 3, within 75 years. However, Jarvis *et al.* (1984) identified sand-pararendzinas over 100-years old.

Stage 4 of Wilson's (1992) proposal is the onset of acidification and, subsequent, podzolisation, which Sevink (1991) described as being induced by lower temperatures, rapid leaching and

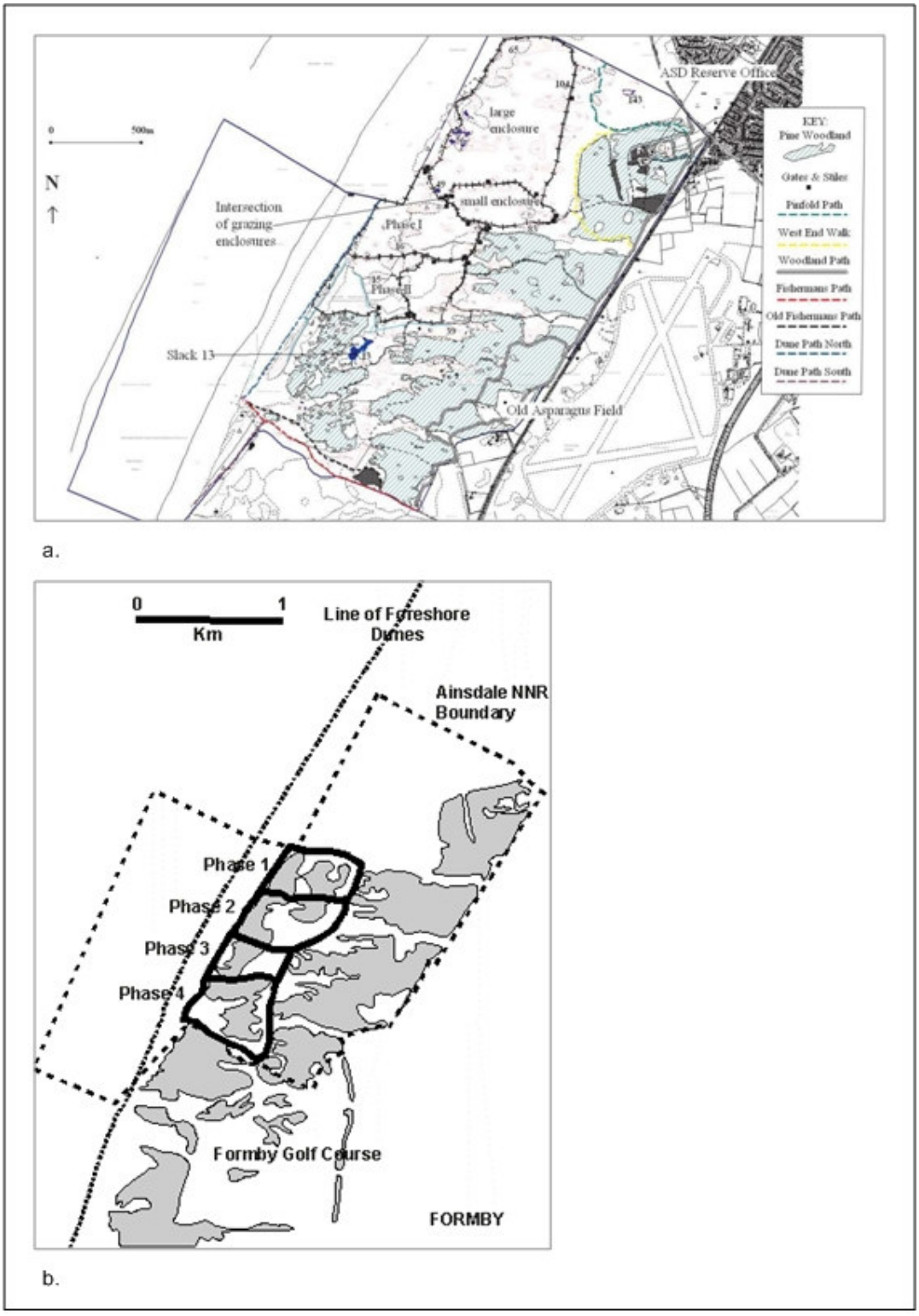

Figure 1.14 a) Ainsdale Sand Dunes NNR Wardening Map showing pine removal phase 1, conducted in summer 1992, and phase 2, conducted during winter 1995/96; b) map showing previous pine removal and forthcoming pine removal sites (both maps used with permission from Natural England).

lower litter decomposition rates. Wilson (1960) observed in the UK, under natural vegetation, distinct podzols could develop in calcareous dune sands within a century. This was proved by James and Wharfe (1989), where following pinewood planting in Ainsdale NNR, 1902-1960, sand-pararendzinas progressed to acid sands and then micropodzols within 20-90 years after afforestation. Moriarty (1978) claims the threshold for this in dune soils is pH ≤5.0 and reports the youngest podzolized pine soil at Ainsdale to have formed within 21-years. However, Sevink (1991) and Wilson (1992) both argued this process can take several centuries in The Netherlands and the north of Ireland, respectively, as evolution of these soils are dependent on the other forming factors (Jenny, 1941) and how they relate to each other. Rates of these processes are unknown in detail, as studies of relatively recent dune soils are limited.

1.5.5 Palaeosols in coastal dunes

Soils developed on past land surfaces are defined by Ruhe (1965) as palaeosols. Buried organic horizons on coastal dunes are evidence of once stable surfaces with vegetation, subsequently buried by windblown material, as discussed by Jungerius (1985). Comparisons of these palaeosols with present-day soils allow deductions to be made about environmental conditions at the time of their formation (Lowe and Walker, 1997). However, buried soils may be modified physically and chemically through recent soil forming processes post-burial (Choi, 2005), resulting in false palaeoenvironmental interpretations, termed pseudosoils. Olson and Nettleton (1998) identified the soil properties most affected as texture and porosity, and the content and distribution of carbonate and clay. For example, Kemp *et al*. (1994) described how diagenesis processes, such as compaction, or changing groundwater levels, can lead to alterations in soil composition. However, as demonstrated by Martini and Chesworth (1992), the distinct coloured horizons in sediment sequences, caused by mobilization and subsequent accumulation of iron and other elements during diagenesis, can make distinguishing true palaeosols and pseudosoils difficult.

Hart and Peterson (2006) provided a palaeoecological study in recent literature on sand dunes on the Oregon coast, where storm waves exposed Late Holocene forests on the beaches and in marine terraces, dated at 3.07 ±1.45 ka and 3.27 ±1.46 ka, respectively. The authors were able to develop conceptual models of coastal evolution, presented in Figures 1.15a-c. The concept of studying palaeosols is also applicable in coastal dunes throughout Europe and, usually, identifies dune soil profiles to show a sequence of buried parent material horizons, indicative of periods of deflation, alternating with buried organic horizons, indicative of former stable land surfaces (e.g. Wilson, 1992; Fullen *et al.,* 1999; Knight *et al.,* 2002; Millington *et al.,* 2008, 2009).

1.5.6 Vegetational history of the Sefton coastal dunes

Palaeosols often preserve pollen from the vegetation at the time of stability and soil formation. Identification and recording of such pollen, along with existing sea level and morphological chronology data (Section 1.4.2) provides evidence for environmental reconstruction. For

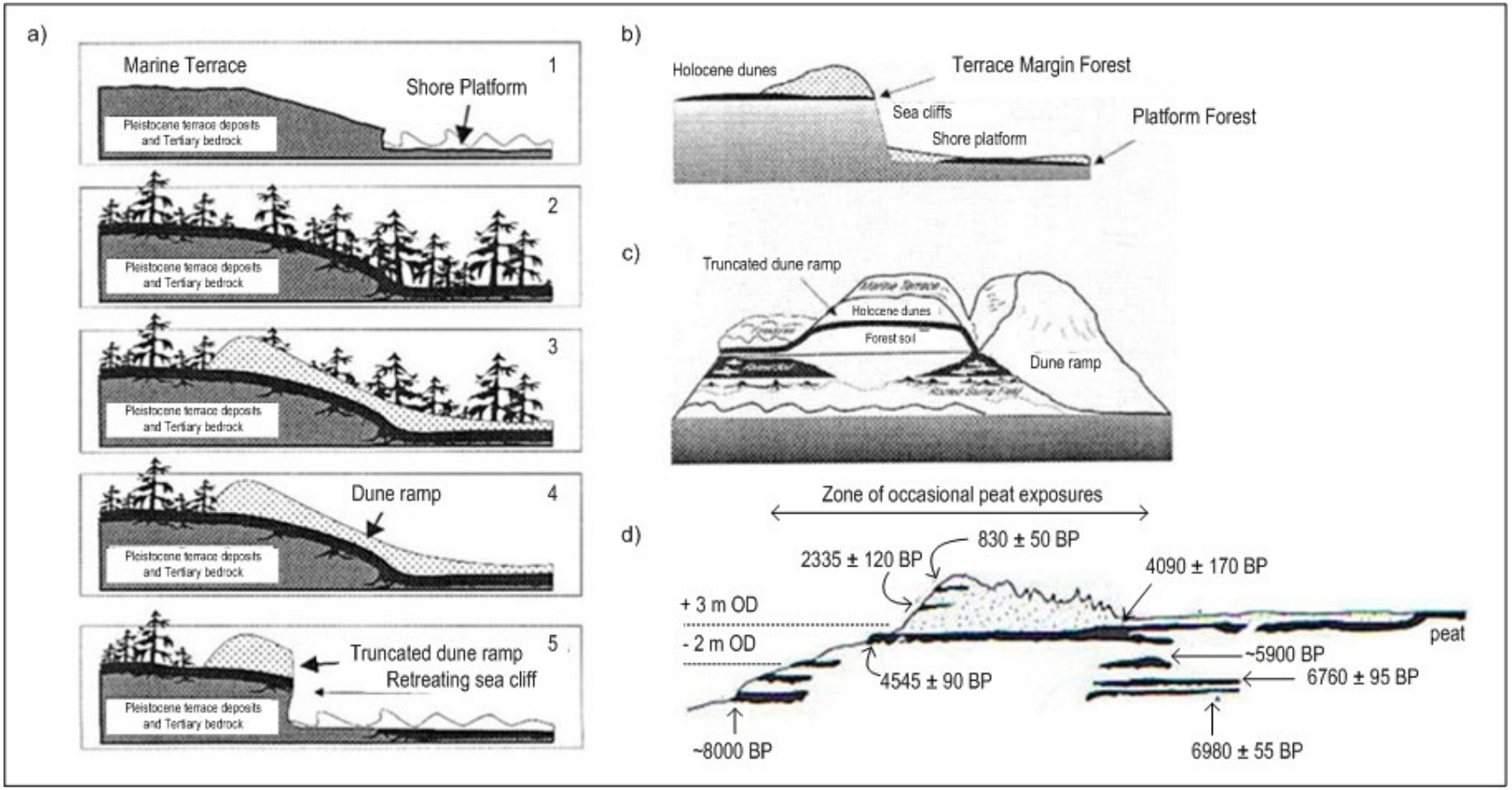

Figure 1.15 Conceptual models of buried soils: a) five stage model of Late Holocene evolution on the Oregon coast (after Hart and Peterson, 2006); 1) shore-cut platform, 2) marine regression and forest advance, 3) burial of forest, 4) preservation of soil on beaches and in marine terraces, and 5) erosion and exposure of buried soil; b) east-west cross section perpendicular to the Oregon coastline; c) block diagram facing the Oregon coast from offshore; and d) Historical schematic summary of dated peats and their locations on the Sefton coast (after Tooley, 1978).

example, Innes and Tooley (1993) noted pollen evidence of forest clearance and creation of open habitat, within peat beds on the Sefton coast, the burials of which are dated to 3200 ±60 BP and 2680 ±50 BP, suggesting intensive agricultural activity in the hind dune area at these times. Tooley (1978, 1990) dated a dune slack soil, located in the upper intertidal zone at Formby Foreshore, to 2335 ±120 BP (Figures 1.14d). A pollen diagram from Slack 100, Ainsdale NNR (O'Garra, 1976), contains herbs typical of dune slack associations, supported by a date of 2510 ±120 BP (Pye, 1990).

A later period of sand stability has been dated by Tooley (1978) to between 1795 ±240 BP and 1370 ±85 BP on the north shore of the Ribble Estuary, the pollen evidence from which is indicative of extensive forest clearance for agriculture. A final period of stability is dated by Tooley (1978) between 830 ±50 BP and 805 ±70 BP (Figure 1.15), which corresponds with organic horizons in the north Wirral dune system, 925 ±50 BP to 540 ±40 BP (Kenna, 1986), all of which contain typical dune slack flora pollen. Later stable periods, followed by renewed sand blowing and peat burial, are confirmed by Innes and Tooley (1993), through evidence of 18th Century peat overblown by sand on Formby Moss, possibly during the Little Ice Age.

1.6 Methods of recording coastal dynamics

Coasts, especially dunes, present a unique problem to scientists and engineers due to their dynamic nature. Therefore, identification and mapping of habitats is vital to providing baseline information for conservation management (Doody, 1989; Gibson and Looney, 1992; Kutiel *et al.,* 2000). Previous research involved in measuring coastal dune landscapes focused on using perpendicular transects to monitor temporal profile changes (e.g. Smith and Zarillo, 1990; Morton *et al,* 1993; Arens, 1997), but this approach fails to account for alongshore dynamics. A more extensive surveying approach uses a grid over the dune system to survey *x, y* and *z* points (e.g. Gares and Nordstrom, 1990). Maps, conveying concepts in the most easily understandable form (Calder *et al.,* 2008), can then be created. The critical step in creating maps from ground data is interpolation, or estimating the value, of the spaces where point data are not collected. Burrough and McDonnell (1998) stressed the importance of considering the assumptions made about spatial variations of data collection points and how results will be affected. A description of numerous land utilization surveys and vegetation surveys for the Sefton coast is given in Mackay (1993).

1.6.1 Geographical Information Systems (GIS)

GIS are computer-based technologies for digital geographical data, to capture, store, manipulate, analyse and display diverse sets of tabular, spatial and geo-referenced data (Burrough and McDonnell, 1998). GIS methodologies are popular for data acquisition and analysis, as they provide methods of combining layers of data relevant to the same spatial area (Aitkenhead and Aalders, 2007), and also carrying out statistical analyses (Anselin, 2000). The first operational GIS were developed by the Federal Department of Forestry and Rural Development in Ottawa, Ontario, Canada, to map soil information, agriculture, recreation,

wildlife, waterfowl, forestry and land use (Goodchild, 2000). This GIS supported a national coordinate system that spanned the continent, coded lines as 'arcs' and stored attribute information in separate files. Since then, GIS have been used in many environmental disciplines, such as land cover modelling and planning (e.g. Aspinall *et al.,* 1993), topographic and volumetric assessments (e.g. Andrews *et al.,* 2002), and mapping the nature and extent of soil erosion and landslides to create a soil database and pedological maps (Costantini *et al.,* 2007; Repe (2007), to name but a few.

GIS initially use created digital information, the most common method of which is digitization, where a hard copy map is transferred into a digital medium through the use of a computer-aided design (CAD) program, and geo-referencing capabilities. Another digitizing technique involves tracing geographic data (in the form of vector lines, points and polygons) directly on top of imported aerial (raster) imagery. These GIS technologies have been employed on the Sefton coast to map the sand dune vegetation resource. Two phases of survey and map development, covering 1970 ha, were conducted by Sefton Metropolitan Borough Council (SMBC), initially in 1988/89 and then April 2003-July 2004. The vegetation boundaries were mapped in the field and verified by aerial photographs prior to digitization in GIS.

1.6.2 Photographic analysis

Much of the UK landscape was photographed by the Royal Air Force as part of the Second World War efforts. However, the first oblique aerial photograph of the Sefton coast was taken in 1920 (Neal, 1993), and overhead aerial photography of dune environments in Europe has been ongoing for ~90 years (Jungerius, 1985), making it possible to trace both vegetation (Van Dorp *et al.,* 1985) and geomorphological developments (Robinson, 1989). Jungerius *et al.* (1981) and Jungerius and van der Meulen (1989) suggest aerial photographs are useful for investigating spatial and temporal patterns of blowouts; whereas blowout formation processes are best investigated with erosion pins. Aerial photography is important in medium-term monitoring practices (Jungerius, 1989), as it allows recognition of the development of landscape features within decades. For example, Bailey and Bristow (2004) successfully determined migration rates from three sets of aerial photographs for dunes at Aberffraw, north Wales. However, Skelsey *et al.* (2004) described how increasing supplies of raw satellite data and aerial photography are not being matched by our ability to analyse such information into useful formats. Therefore, approaches have been adopted to map proportions of sand and vegetation in slacks at the sub-pixel level. For example, Lucas *et al.* (2002) performed spectral unmixing of airborne imaging spectrometer (CASI) imagery using both a linear mixture model and fuzzy membership functions.

Fixed Point Photography (FPP), taking photographs from fixed points and angles, is a relatively new concept in landscape monitoring (e.g. Zier and Baker, 2006). FPP has been in operation at Ainsdale NNR since 1967 to record vegetation change (Wheeler *et al,* 1993). Similar photography surveys are being used to record changes in physical features including

vegetation, such as the Crummay *et al.* (2001) work on Penhale Sands, Cornwall. Fullen and Moore (1999) successfully monitored dynamics of the Morfa Dyffryn dunes, mid-Wales, as a 10 year fixed point photography case study, which is continuing as on ongoing survey (Millington *et al.,* 2008).

1.7 Soil properties

Physico-chemical soil properties depend on parent material composition, weathering reactions and pedogenic processes, leading to either heterogeneous or consistent regional pedo-patterns (Sandren and Thompson, 1990). There are many standard measurements of physico-chemical soil properties, with reference to the International Soil Reference and Information Centre (ISRIC) (van Reeuwijk, 2002) and soil survey laboratory methods handbook (Avery and Bascomb, 1982), including soil acidity (e.g. Purdie, 2002), particle size analysis (e.g. Booth, 2002; Booth *et al.,* 2003; Pye and Blott, 2004b; Saye and Pye, 2006), percentage SOM lost on ignition (e.g. Jankauskas *et al.,* 2005; 2006; Fullen and Booth, 2006), X-ray fluorescence (XRF) spectroscopy (e.g. James and Wharfe, 1989; Olsson *et al.,* 2000; Saye and Pye, 2006; Chen *et al.,* 2008), cation analysis (e.g. James *et al.,* 1986) and total soil carbon and nitrogen (e.g. Jones *et al.,* 2004; Kundu *et al.,* 2007; Guo *et al.,* 2008; McKinley *et al.,* 2008; Ordóñez *et al.,* 2008).

1.7.1 Applied mineral magnetism in soil science

Advancement of laboratory technologies and procedures has enabled pedological application of mineral magnetic techniques to expand extensively during the last few decades (Dearing, 1985; Maher, 1986; Dearing *et al*., 1996; Maher *et al*., 2002). The magnetic phenomenon is further described by Smith (1999), a brief outline of which is in Appendix 1.1.

As soil magnetism is controlled by environmental effects (Pope, 2000), it can be dealt with as any other soil property; e.g. assessing the role of Jenny's (1941) soil forming factors. However, compared with traditional analytical methods, Walden *et al*. (1996) concluded mineral magnetic analyses provided a rapid, non-destructive and inexpensive tool that is sensitive to low detection levels (Thompson and Oldfield, 1986; Walden *et al*., 1999; Maher and Thompson, 1999). Rocks, sediment and, subsequently, soil exhibit some form of magnetic behaviour (Dearing, 1999; Smith, 1999) and, therefore, magnetic properties can be used to characterize (e.g. Maher, 1986; Maher and Thompson, 1999; Kapička *et al.,* 2003; Booth *et al*., 2005, 2006), discriminate (e.g. Dearing *et al*., 1996; Chittleborough *et al.,* 1998; de Jong *et al.,* 2000; Booth *et al*., 2005, 2006; Fialová *et al.,* 2005), identify pedogenic processes (e.g. Fine *et al.,* 1989; Sandgren and Thompson, 1990; Thompson, 1990; Rivas *et al.,* 2006), for relative dating (e.g. Pope, 2000) and for monitoring and modelling environmental change (e.g. Dearing *et al.,* 1995; Crockford and Willett, 2001).

Soil processes can either enhance or reduce concentrations of magnetic minerals. For example, production of new 'secondary' minerals of ultrafine ferromagnetic magnetite (explanation in

Appendix 1.1) is sustained by fermentation processes (Mullins, 1977; Maher, 1998); whereas, acidification and gleying pedo-processes appear to eradicate 'primary' parent material minerals (Dearing *et al.,* 1995). Maher (1998) outlined that excessively wet soils are unable to form significant amounts of pedogenic ferrimagnets, whereas well-drained, or intermittently wet/dry, soils show most magnetic enhancement, similar to findings by Williams and Cooper (1990). Wang *et al.* (2008) exemplify this further, elaborating that flooded, saturated or poorly drained soils are frequently anaerobic, leading to dissolution of strongly magnetic minerals, especially magnetite and maghemite (refer to Appendix 1.2). Lu (2000) indicated reduction state is an important factor responsible for loss of superparamagnetic ferromagnetic minerals in soils (refer to Appendix 1.3 for explanation). Whilst analysing sedimentary sections, Nabel *et al.* (1999) associated minimum magnetic susceptibility (χ) values in palaeosols and hydromorphic horizons. However, a study conducted by Maier *et al.* (2006) suggests that soil moisture influences on conductivity can be overlooked.

Magiera *et al.* (2006) demonstrated that forest topsoils can show higher χ than topsoils of grassland, due to filtration of pollution effects. As well as defining environment conditions from magnetic measurements of topsoils, Hanesch and Petersen (1999) found it possible to identify vertical structures in soil profiles that would not, otherwise, have been evident in the general pedological horizons. Fine *et al.* (1992) also related magnetic properties to morphological or chemical discontinuities; therefore, suggesting that χ can be used to evaluate the suitability of pedons for chronosequence studies.

1.8 Summary

Rising sea level will effect coastal dune environments through land encroachment, raised groundwater and migration of ecological zones, the processes of which may be interrupted by 'coastal squeeze' resulting in loss of habitat. Information on sand dune system responses to coastal change is vital for nature conservation and protection of residential areas. Pedogenic information, concerning development trends and timescales, can be employed to predict these dune system responses to the effects of sea level fluctuations. Therefore, a greater understanding of past and present pedo-dynamic behaviour is essential.

The Sefton coast is currently undergoing severe coastal erosion at Formby Point, threatening the town of Formby behind the dune system barrier, as well the complex mosaic of internationally-important dune habitats and associated soil environments. As a result, ~1000 years of environmental change has been exposed in buried soils in sedimentary sequences in dune cliffs. Based on these concepts, the Sefton coast has been chosen for detailed pedological investigation. Physico-chemical soil properties have been used in numerous coastal soil studies, especially in north-west Europe, to classify and identify pedogenic trends and timescales. These techniques can be applied to the Sefton coast to establish a thorough understanding and awareness of soil environments and how they can be used to model dune habitat response to coastal change for dune management purposes.

CHAPTER 2

Materials and methods

Chapter 2 details the sampling techniques and analytical methods used to classify and assess soil properties and display their spatial distributions. The sections are described in sequential order of completion, beginning with initial desktop dune environment determinations, followed by field sampling techniques, laboratory analyses, both statistical and Geographical Information System (GIS) computation and subsequent modelling. Multi-proxy analysis offers a means of characterising soils and sediments for inter-profile comparison and environmental interpretation (Fullen and Catt, 2004; Pye and Blott, 2004b). Figure 2.1 displays the individual levels of investigation along with associated section numbers and general themes of study. Desktop processes were conducted solely at the University of Wolverhampton. Laboratory procedures were conducted at the University of Wolverhampton, U.K., Edge Hill University, U.K., and the Vivekananda Institute of Hill Agriculture, India.

2.1 Mapping dune environments

A description of numerous land utilization surveys and vegetation surveys is given in Mackay (1993). To assess the present spatial landscape of the Sefton dune macro-system, analyses of aerial photography, along with comparative analyses of both the land and vegetation surveys, were conducted using GIS tools.

Two phases of survey and map development of the sand dune vegetation resource of the Sefton coast, covering 1970 ha, were conducted by Sefton Metropolitan Borough Council (SMBC), initially in 1988/89 and between April 2003 and July 2004. These applied both Co-ordination of Information on the Environment (CORINE) (CORINE, 1991) and National Vegetation Classification (NVC) (Rodwell, 2000) definitions. The vegetation boundaries, mapped in the field in 2003/04 and verified by aerial photographs, were digitized in MapInfo GIS (version 6.5). Across the 5,369 GIS polygons, 2,513 quadrats were recorded, resulting in 563 vegetation categories, corresponding to 61 broad NVC community types.

These existing vegetation datasets and aerial photographs from MapInfo GIS (version 6.5) (courtesy of SMBC) were converted into ArcView GIS (version 3.3) software. The initial CORINE classification vegetation map of the area based on habitat categories was modified to the NVC, a classification based on vegetation type, not the physical environment, enabling the vegetation data to be more readily utilized. Classification of existing NVC types (n = 61) into 13 feasible parcels of land for this research, associated with both dune morphology and vegetation environments, was achieved by reference to Rodwell (2000). The 13 dune environments represent areas of blown sand remaining outside residential development; (i) amenity grassland (golf clubs), (ii) arable, (iii) bare sand (beach, blowouts), (iv) heath community, (v) pasture, including grazed, mowed and natural grasslands, (vi) embryo dune community, (vii) fixed dune

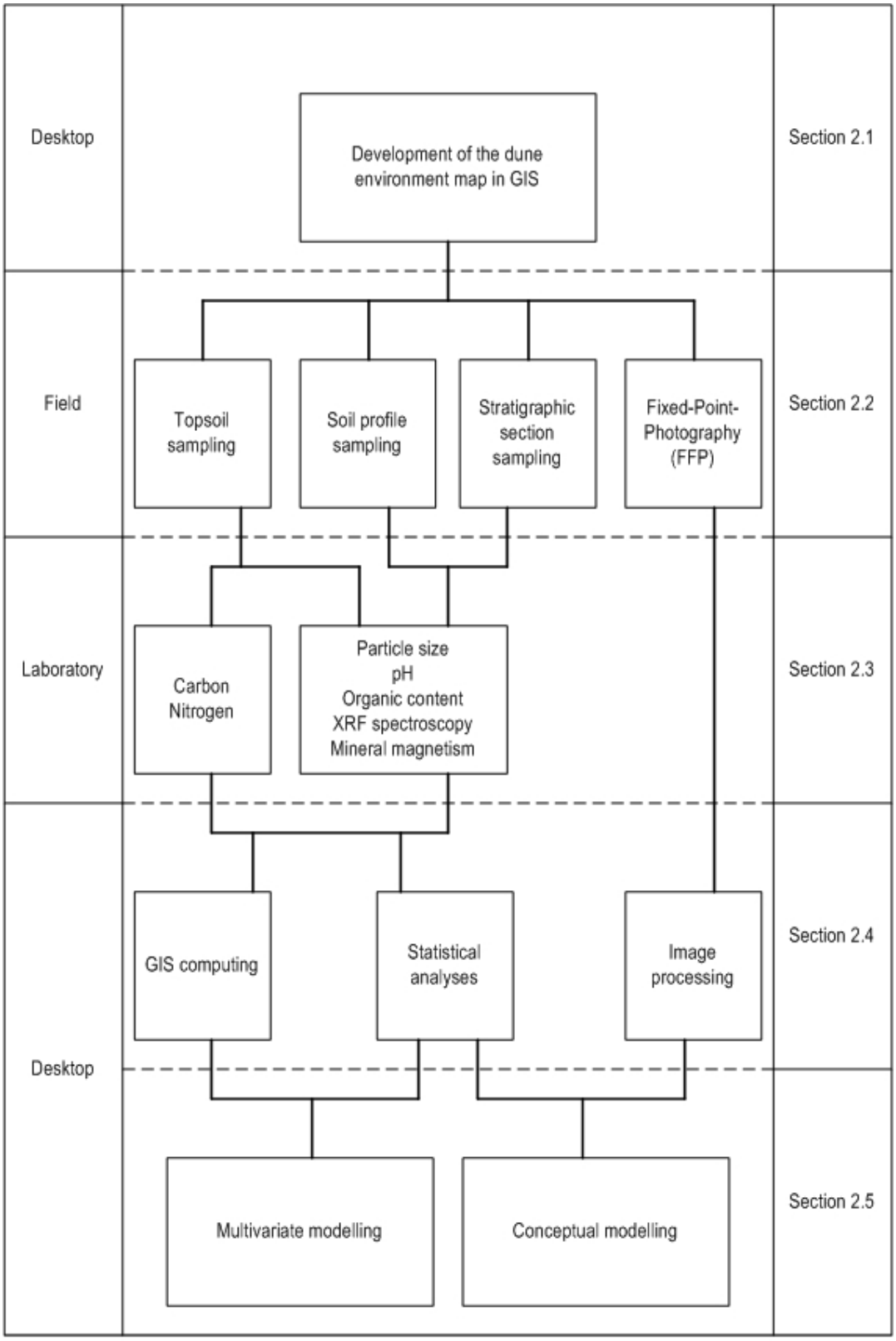

Figure 2.1 Flow diagram displaying individual levels of investigation (centre) along with associated section numbers (left) and general themes of study (right).

community, (viii) mobile dune community, (ix) coniferous plantation, (x) salt marsh community, (xi) scrub, (xii) slack community and (xiii) deciduous woodland.

The embryo dune environment was incorporated into the bare sand category, as embryo dunes represent a geomorphological feature within the landscape, rather than a classified parcel of land that can be associated with soil development. Areas not associated with natural dune succession (amenity grassland, arable and salt marsh community) were excluded from further analyses to prevent data anomalies. However, although not distinguished through vegetation analysis, the existence of an area of felled coniferous woodland became apparent during field observations. As the felled area is integrated into the fixed dune vegetation on the dune environment map it is represented on a transparent overlay in GIS. Ten classified dune environments are used to represent the overall dune landscape profile.

2.2 Sampling procedures

This section presents precise procedures for the sampling of soil with reference to the Soil Survey of England and Wales, now known as the National Soil Resources Institute (NSRI) (Hodgson, 1997). The location of each sample site was chosen following permission from landowners, then recorded using a Garmin Etrex Global-Positioning-System (GPS) instrument set to Ordnance Survey Great Britain (OSGB) and Magnetic North (stated accuracy of <15 m). Following Walden *et al*. (1999), wherever possible, care was taken to ensure that all sampling equipment used was plastic to avoid contaminating samples.

2.2.1 Topsoil sampling

A simple random sampling procedure, where all topsoil samples are given an equal probability, is best practice when surveying a landscape, as bias is minimized and analysis simplified. However, simple random sampling can be vulnerable to sampling error, as the randomness of the selection may result in a sample that does not reflect the population. For example, some dune environments on the Sefton coast may be over-represented, while some may be under-represented, or not even represented at all. Systematic sampling techniques are also not ideal, as it was possible that very small, but essential, dune environments may be overlooked.

As it has already been decided that the Sefton dune sampling area contains 10 distinct landscape categories, based on geomorphology and vegetation type (Section 2.1), it was decided that a Probability Proportional to Size (PPS) sampling technique (Rosén, 1997) was the best option to optimize results. The sampling procedure was organized by these dune landscape categories. Each category was sampled as an independent sub-population, out of which representative topsoil samples were randomly selected, assuring that those in smaller sites had the same probability of getting into the sample as those in larger sites.

The following procedure was carried out. Firstly, all of the broad NVC community vegetation type GIS polygons (Section 2.1), in the categorized dune environment being sampled (e.g.

mobile dune) were listed alongside their spatial area; of which, the running cumulative spatial area was calculated. It was decided that five vegetation polygons would be sampled within the categorized dune environment, with two samples from each polygon. This gave a total sample size of 10 samples from each of the 10 categorized dune environments; therefore, resulting in 100 samples for the total Sefton dunes area. The total area of the categorized environment in question was divided by five (the number of polygons intended to sample). The result was used as the Sampling Interval (SI). A number was chosen between 1 and the SI at random, to become the Random Start (RS). The following series was calculated: RS; RS+SI; RS+2SI; RS+3SI; RS+4SI.

The outcome of this calculation resulted in five numbers, each corresponding to a cumulative area and associated polygon on the original list which was subsequently selected for sampling. Selection of samples within the polygon was also conducted randomly. Occasionally, a very large polygon contained more than one of the series of numbers. In this case, that polygon was then counted as two sites and twice the allocated number of samples was taken. Therefore, for some larger dune environments (e.g. fixed dunes), five polygons resulted in more than 10 samples, producing a total sample population of 113 samples taken across the Sefton dunes. Consequently, the sample populations for each dune environment appear weighted according to the spatial extent of that category in the landscape, with larger environments containing more samples.

Topsoil (0-5 cm) samples (n = 113) were collected and georeferenced from across the entire dune system, incorporating each of the chosen 10 classified dune environments for soil property determinations. Similar ground-truth testing of methodological approaches are described by Rühl *et al*. (2007), where ground data were used to link virtual GIS derived data with field data for accurate assessment of the applied methodology. For each point, multiple samples (n = 5) were taken over a ~1 m^2 area and combined to become one representation, rather than a single sample taken from a specific point (Lees, 1994, 1999; Booth, 2002; Booth *et al.,* 2004). The topsoil sample, including sufficient soil for replicate analyses, was transferred into clean, pre-labelled, self-seal plastic bags. Qualitative information of soil type was recorded where relevant. Similar methodology descriptions can be found in Costantini *et al*. (2007) and Repe (2007).

2.2.2 Soil profile sampling

Prior to soil profile sampling, a log of field flora species was recorded at each site using the subjective DAFOR (Dominant**,** Abundant**,** Frequent**,** Occasional**,** Rare) abundance scale. Plant nomenclature followed Stace (1997). A single soil pit was dug for each of the classified dune environments; mobile dune (SD 29393 12160), fixed dune (SD 29437 11546), dune slack (SD 29392 12141), dune heath (SD 29443 08918), dune pasture (SD 27732 07865), scrubland (SD 28171 09841), deciduous woodland (SD 27881 09349), coniferous woodland (SD 27647 08459) and felled coniferous woodland (SD 28868 10456). A soil pit was not dug for the bare sand dune environment, as it failed to exhibit any soil development. A buried soil, recently exposed

on the beach (SD 26995 06576), was also sampled via the soil profile technique. Photographic documentation of the entire soil profile sampling procedure is shown in Figure 2.2. Following site description recordings, each soil pit was dug ~1.5 m depth (Hodgson, 1997); firstly by removing the turf and then carefully placing removed soil adjacent to the pit (Figure 2.2, Plates A and B). The profile was photographed and described following the Soil Survey Field Handbook (Hodgson, 1997). To assist discussion and comparison of soils, it was convenient to designate soil horizons by a letter notation, the same symbol being applied to analogous horizons in profiles of similar type. The notation adopted in this thesis has been modified from Hall and Folland's (1967) Memoirs of the Soil Survey of Great Britain, incorporating further horizon definitions (refer to Chapter 1, Table 1.1). All horizons were measured, bulk sampled, and colour determinations made using the Munsell Soil Colour Chart. A plastic square-shaped tube, 1 m length, was hammered into the ground to collect an entire profile sample (Figure 2.2, Plates C and D). After removal of the plastic tube containing the profile sample (Figure 2.2, Plate E), the soil pit was re-filled and re-turfed in horizon order to create minimal damage to the active soil processes and landscape aesthetics (Figure 2.2, Plate F).

2.2.3 Stratigraphic section sampling

When sampling the stratigraphic exposure (SD 27534 08981), the limits of the visible horizons were marked on the face. A photographic documentation of the entire exposed stratigraphic section sampling procedure is shown in Figure 2.3. Samples were removed sequentially, at 2 cm intervals, from a representative vertical slice that extended far enough into the face of the exposure to retrieve sufficient soil from the thinnest horizon. The top horizon was sampled first and all surplus soil removed to leave a clean step before subsequent sampling (Figure 2.3D). Samples were placed into clean, pre-labelled, self-seal, plastic bags.

2.3 Laboratory techniques

This section presents procedures for standard soil laboratory analyses, referring to the International Soil Reference and Information Centre (ISRIC) (van Reeuwijk, 2002) and the Soil Survey of England and Wales (Avery and Bascomb, 1982). Where the degree of instrumental error is relatively low; however, to have confidence in data interpretation, it was desirable to include regular replicate sub-samples and re-runs of samples to ensure both representative and accurate data are obtained. All presented results, with the exception of soil pH, are expressed to three decimal places. This is done for consistency of the work, rather than an indication of the detection limits of instruments employed or the variables used.

2.3.1 General sample preparation and storage

Due to the possible changes resulting from long-term storage, all samples were usually prepared for analysis within two weeks of collection (Oldfield *et al*., 1992). Following removal of the top face of the square-shaped plastic tube, the sediment retained within was dissected into 1 cm slices and numbered consecutively from the surface downwards, representing 1 m of stratigraphy. Each slice was placed into clean, pre-labelled, self-seal, plastic bags. Thorough

Plate A.

Plate B.

Plate C.

Plate D.

Plate E.

Plate F.

Figure 2.2 Photographic documentation of soil profile sampling procedure, using the slack profile (SD 29390 12144) as an example. Plate A) identification of suitable representative site and turf removal that will cause minimal habitat damage. Plate B) digging of the soil profile, until required depth or water table is reached. Material is placed adjacent to the pit. Visible horizons are identified, sketched and measured prior to sampling. Plate C) plastic, flat channel tubing is hammered into the ground. Plate D) hammering ceases once tubing is completely submerged, or an unpassable object is encountered. Plate E) tubing, containing sampled soil profile is removed. Plate F) turf is replaced and site is left in a condition as close to its original state as possible.

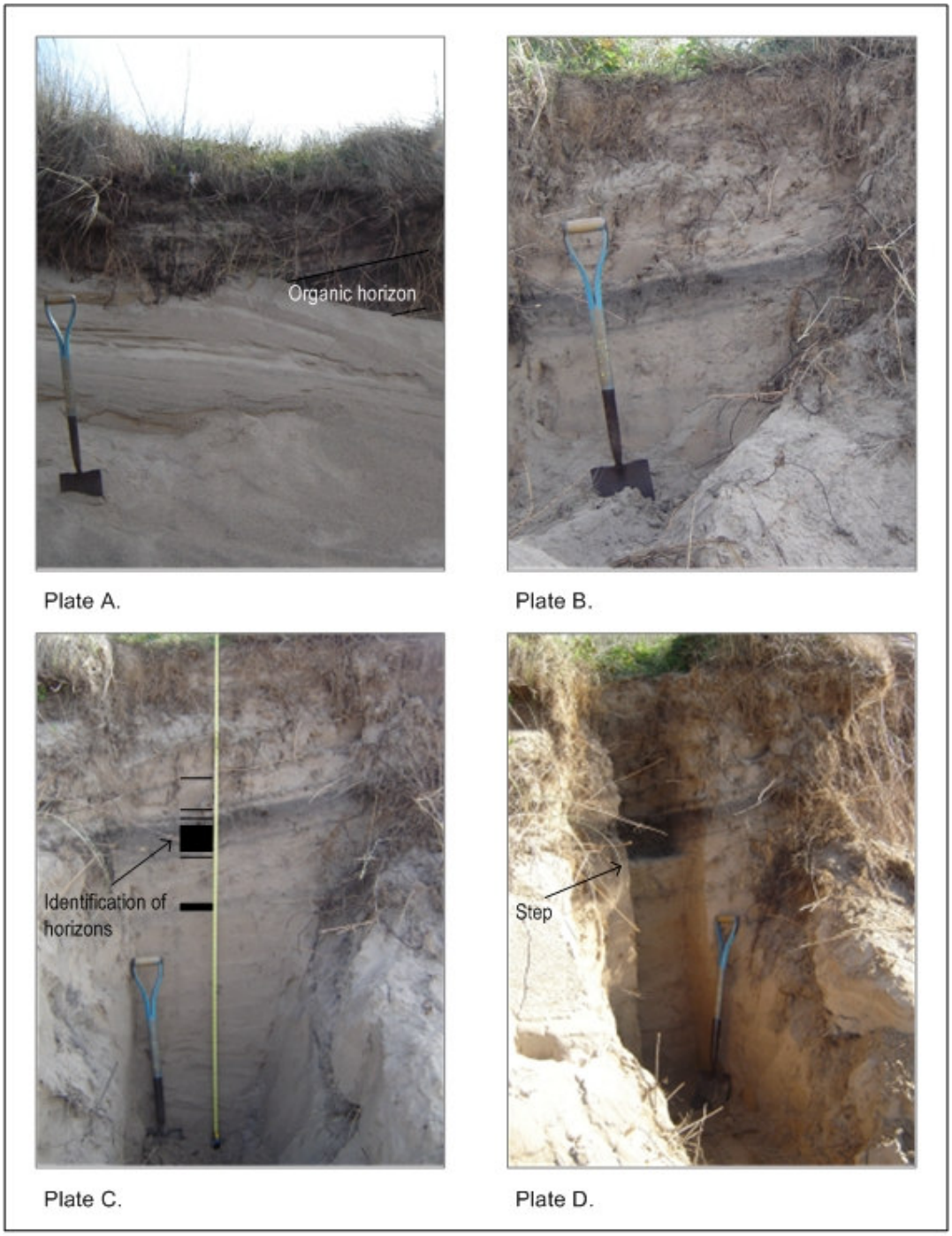

Figure 2.3 Photographic documentation of exposed stratigraphic section (SD 27534 08981) sampling procedure. Face direction is seaward. Spade for scale is 97 cm long. Plate A) identification of suitable representative full stratigraphic sequence, achieved by recognization of a thick organic horizon and several thinner ones. Plate B) exposure face scraped to reveal full representation of buried organic horizons. Plate C) visible horizons identified, sketched and measured prior to sampling. Plate D) samples were removed at 2 cm intervals, from a vertical slice in the exposure face, beginning with the surface horizon. A clean step was left between each sample.

mixing of samples prior to sub-sampling and correct use of a sample splitter was conducted to reduce possible sources of error. Samples were prepared by air-drying ~70 g for 3-days at <40ºC, then bagged in clean, pre-labelled, self-seal sample bags. Dry colour determinations were made using the Munsell Soil Colour Chart. Any remaining sediment was frozen for possible future use.

2.3.2 Particle size determinations

Prior to particle size analysis, sample dispersal was achieved by agitating ~2 g of soil with Calgon solution (40 g sodium hexametaphosphate: 1 litre distilled water) (Gerrard, 2000; Booth *et al.,* 2003), which chemically repels any electrostatic bonds between clay particles. Macroscopic traces of organic matter and shell pieces were removed manually, after Booth (2002) concluded the use of hydrogen peroxide to remove organic matter (Gale and Hoare, 1991) was unnecessary, and that the technique of removing organic matter by hand was an acceptable approach.

Particle size distributions were then determined by insertion of the Calgon/soil solution into a Malvern Mastersizer Long-bed X laser granulometer, with a MSX17 automated sample presentation unit, which allowed rapid and accurate measurement of particle sizes within 0.1-2000 μm range (Syvitski, 1991). Once an optical density of >10% was achieved, measurements were attained with a Low Angle Laser Light Scattering (LALIS) laser, through two separate lenses with overlapping ranges (45 nm: 0.1-80 μm; 1000 nm: 4-2000 μm). The technique is based on the principle that as suspended particles pass through a laser beam, the angle of diffracted light is inversely proportional to the particle sizes, the resulting pattern is focused onto a series of detectors and computed into particle size values by Malvern v1.2 software. According to Booth (2002) this approach, using the Fraunhofer theory (Bohren and Huffman, 1998; Lehner *et al*., 1998) assumes all sizes of particles scatter with equal efficiencies, and that all particles are opaque and transmit no light. Since these assumptions are not always correct, the latest Malvern instrumentation and software has been designed to compensate for these influences and, using Mie theory (Bohren and Huffman, 1998; Lehner *et al*., 1998), allows the refractive index of the materials to be taken into account when calculating particle size values. When measuring well-sorted, relatively homogeneous sediments, a single measurement may be sufficient to provide a representative result (Pye and Blott, 2004b); whereas, due to the mixed mineralogy of soils, it was deemed necessary to record a minimum of three measurements and take a mean of the obtained results.

The grain-size description outcome is based on the Wentworth scale, a negative logarithmic relation (Woodroffe, 2002). There are slight differences between categorized particle size range selections in different national systems (FitzPatrick, 1986; Brady and Weil, 1999; Ashman and Puri, 2002; Booth *et al.,* 2003). Therefore, both the Soil Survey of England and Wales (or NSRI) definitions (Syvitski, 1991; Gerrard, 2000; Fullen and Catt, 2004) and those of the United States

Department of Agriculture (USDA) (Woodroffe, 2002; Booth *et al.,* 2003) were measured (Table 2.1).

A range of statistical summary parameters to characterize particle size distribution, including median, mean, sorting, skewness and kurtosis (Folk, 1964), was obtained using Malvern Mastersizer Operator software package. Assuming the sediment has derived from similar source areas and been transported and deposited by similar processes, it has been decided that grain-size spectra would approximate better to a geometric scale, based on a log-normal distribution (Christiansen *et al.,* 1984; Fieller *et al.,* 1984).

Table 2.1 Categorized particle size ranges for the National Soil Resources Institute (NSRI) (formerly Soil Survey of England and Wales) and the U.S. Department of Agriculture (USDA)

National Soil Resources Institute		United States Department of Agriculture	
		Very coarse sand	1000-2000 µm
Coarse sand	600-2000 µm	Coarse sand	500-1000 µm
Medium sand	200-600 µm	Medium sand	250-500 µm
Fine sand	60-200 µm	Fine sand	100-250 µm
Coarse silt	20-60 µm	Very fine sand	50-100 µm
Medium silt	6-20 µm	Coarse silt	20-50 µm
Fine silt	2-6 µm	Fine silt	2-20 µm
Clay	<2 µm	Clay	<2 µm

2.3.3 Soil pH

The reaction of a soil is the degree of acidity or alkalinity, expressed as the soil pH, and is determined by the comparative activity or concentrations of H^+ and OH^- ions (Brady and Weil, 1999). A suspension of 10 g soil and 25 ml of distilled water was placed on a reciprocating flask shaker for 15 minutes (Avery and Bascomb, 1982). The pH of the soil solution was measured by a pH meter, with a glass-calomel combination electrode inserted into the supernatant suspension (van Reeuwijk, 2002), stirred and left at room temperature for 10 minutes until a stable reading was obtained. A minimum of three replicate readings were conducted to ensure accuracy.

2.3.4 Organic loss on ignition

According to Fullen and Catt (2004), it is usually impossible to determine the precise percentage of soil organic matter (SOM) in a soil sample; therefore, there is no satisfactory universal method for organic determinations (Jankauskas *et al.,* 2005). However, percentages of organic matter content were determined by calculating the percentage loss of soil weight after ignition, at 375ºC in a muffle Carbolite GSM 11/8 furnace, for 16 hours (Ball, 1964; Bengtsson and Enell, 1986; Fullen and Booth, 2006; Jankauskas *et al.,* 2006). This low temperature treatment was

used to ensure depletion of carbon and hydrogen present in organic matter, yet avoid weight loss due to loss of carbonates and structural water from clays, which can occur at higher temperatures (Ball, 1964; Fullen and Booth, 2006). Post-ignition, the samples were placed in a dessicator until cool and then re-weighed.

2.3.5 Elemental analysis by X-ray fluorescence spectroscopy

X-ray fluorescence (XRF) spectroscopy was used to rapidly identify and quantify elements within the soil samples, instead of timely Cation Exchange Capacity (CEC) methods. Although both techniques differ in the sample excitation mode, Galván *et al*. (2009) state results obtained from both procedures are compatible. XRF determines elemental composition from concentrations as low as 1 ppm to 100% by weight. Dried fine-earth was finely ground inside a tungsten carbide ball mill for 10 minutes and then 8.5 g of sample was fused with 1.5 g of Licowax C Micropowder PM (Hoechstwax) FluXana BM-0002-1 binding-wax. This preparation was then pressed with an applied pressure of 10 tonnes into the form of a rigid smooth-surface disk. The formed disk, typically 20-50 mm diameter, was analysed by XRF spectroscopy for 49 elements. In principle, these are all the elements except those below Na in the Periodic System (van Reeuwijk, 2002). The ARL 8410 XRF spectrometer is programmed to determine contents of the following elements: Major elements (expressed as oxides): Al, Fe, Si, Ca, Mg, K, Na, P, Ti and Mn; and Minor elements (expressed as elements): Cu, Cr, Ni, Rb, Sr, Ba, Co, Ga, La, Nb, Pb, V, Zn and Zr.

An element is identified by its characteristic X-ray emission wavelength or energy, whereas the concentration is quantified by measuring the intensity of its emission. The technique is based on the principle that high-energy primary X-ray photons have sufficient energy to tap electrons out of the innermost orbital to create unstable ions within the sample (Jenkins, 1988). Fluorescence is when an electron from an outer orbital will subsequently occupy the vacant space to regain stability, emitting energy in the process that is specific to known elements.

2.3.6 Total soil organic carbon and total soil nitrogen

Dried topsoil samples were passed through a 0.2 mm sieve, placed in clean, clear, self-seal plastic bags and labelled at the University of Wolverhampton, and then transported to the Vivekananda Institute of Hill Agriculture, Almora, India, for analyses. Total soil organic carbon (SOC) and total soil nitrogen (TSN) were determined, according to methods conducted by Kundu *et al.* (2007), by the dry combustion method using a FOSS Hareus CHN-O-Rapid analyser. Some ≤10 mg, but ideally 2-3 mg, of soil was placed in an autosampler and exposed to oxygen. At ~990ºC, the material becomes mineralized, and CO is formed. Complete oxidation is reached at a tungsten trioxide catalyst, resulting in CO_2, H_2O and NO_2, with some excess O_2, which subsequently flows through a silica tube packed with copper granules at ~500ºC. This binds the remaining oxygen and reduces the nitric/nitrous oxides to produce the analytically important CO_2, H_2O and N_2. Separation of these gases was achieved by zone chromatography (Rowell, 1994).

2.3.7 Mineral magnetic analyses

Each sample was tightly packed, to attain total immobilization, into a clean, pre-weighed and labelled 10 cc styrene pot. Sample pots were then re-weighed to allow mass specific values to be calculated, before placing a lid on top and sealing with sellotape. Finally, a reference line was drawn across the top of the lid and down one side of the pot to be used as an orientation mark for all future magnetic remanence measurements.

Each sample was subjected to a series of routine mineral magnetic analyses, detailed explanations of which are available in Thompson and Oldfield (1986) and Walden *et al*. (1999) and are shown in Table 2.2. Single sample mass specific magnetic susceptibility (χ) measurements were made using a Bartington MS2 magnetic susceptibility meter connected to a Bartington MS2B dual frequency susceptibility sensor. Measurements were taken at both low frequency (0.47 kHz; (χ_{LF})) and high frequency (4.70 kHz; (χ_{HF})). A steady biasing 0.04 mT anhysteretic remanent magnetisation (ARM) field was induced in the samples and the resultant remanence was measured by a Molspin magnetometer connected to a personal computer, which is controlled by Winspin software supplied by John Walden, University of St. Andrews. The samples were, subsequently, exposed to a demagnetisation field, in a Molspin alternating field demagnetiser, to remove the ARM that had been induced. All samples were then placed into a pulse magnetiser and exposed to successively increasing sizes of 'forward' magnetic fields, until a total saturation field of 1000 mT was generated, representing the Saturated Isothermal Remanent Magnetisation ($SIRM_{1000mT}$). By applying a 'reversed' magnetic field of 100 mT, the $SIRM_{1000mT}$ was destroyed, determining the s-ratio. After each 'forward' and 'reverse' field, an Isothermal Remanent Magnetisation (IRM) was measured.

2.4 Data interrogation and presentation

The varied nature of the data produced in this study means several spatial, graphical and statistical techniques have been employed to interrogate and display the results.

2.4.1 Geographical Information Systems (GIS) analysis

A geo-referenced base map (using OSGB co-ordinate system) for the study area was created in ArcView GIS (version 3.3) (see Section 2.1). Figure 2.4 visually presents the following analysis in GIS. Firstly, an outline, or mask, of the area boundary was mapped to create a single polygon representative of the entire dune area under investigation. Grid cell size, or resolution, of 1 pixel = 10 m was determined following Burrough and McDonnell (1998). Geo-referenced points were plotted on the base map with both x- and y-coordinate values, each representing topsoil samples in the field. The topsoil characteristics spatial database, gained from laboratory analyses, was merged with the coordinate values to create a table of attributes. A software routine was then performed to allow the attribute, or z-values, for the selected variable to be attached to each of the points, from which an interpolated surface of each of the specific variables was created individually. Interpolation quantitative values were automatically assigned to infinite mid-points between the data points within the masked boundary, to display spatial

Table 2.2 Mineral magnetic parameters used in this research and their basic interpretations (after Banerjee *et al.*, 1981; King *et al.*, 1982; Yu and Oldfield, 1989; Hutchinson, 1995; and Walden *et al.*, 1996). Refer to Appendices 1.1-1.3 for explanations of magnetic domains and behaviour

Magnetic variables	Interpretation
χ	Mass specific *Magnetic Susceptibility* (χ) is a measure of magnetic mineral concentrations in a sample (Sandgren and Thompson, 1990). It is measured within a small magnetic field and is reversible (no remanence is induced). Its value is roughly proportional to the concentration of ferrimagnetic minerals (Appendix 1.2) within the sample, although in materials with little or no ferrimagnetic component and a relatively large antiferromagnetic component, the latter may dominate the signal (Walden *et al.*, 1996).
$\chi_{FD\%}$	Frequency dependent χ is a measure of occurrence of very fine magnetic domains on the superparamagnetic (SP) to stable single domain (SSD) boundary (Appendix 1.3).
χ_{ARM}	Mass specific *Anhysteretic Remanent Magnetisation* (ARM) is induced in the samples by combining a peak AF field of 100mT with a DC biasing field of 0.04mT (Yu and Oldfield, 1989). Here it is represented as susceptibility (χ) of ARM. It is particularly sensitive to the concentration of magnetic grains of SSD size (Banerjee *et al.*, 1981; King *et al.*, 1982).
SIRM	Mass specific *Saturation Isothermal Remanent Magnetisation* (SIRM) is the highest amount of magnetic remanence that can be produced in a sample by applying a large magnetic field, measured on a mass specific basis. A saturating field of 1T has been used. The value of SIRM is related to concentrations of all remanence-carrying minerals in the sample but is also dependent upon the assemblage of mineral types and their magnetic domain size (Walden *et al.*, 1996).
Magnetisation variables (forward field ratios) i.e. %soft and %hard	The percentage of the final SIRM acquired at selected, increasing field strengths, is calculated. Forward field ratios are shown against a horizontal scale of percentage saturation at 20mT (100(IRM_{+20mT}/SIRM)), 40mT (100(IRM_{+40mT}/SIRM)), 300mT (100(IRM_{+300mT}/SIRM)) and 500mT (100(IRM_{+500mT}/SIRM)). These values help discriminate between ferrimagnetic and imperfect antiferromagnetic mineral types (Appendix 1.2), since the latter are likely to be the main contributors to remanence acquired above the second field (Hutchinson, 1995). At low fields, the magnetically 'hard' canted antiferromagnetic minerals such as haematite or geothite are unlikely to contribute to the IRM, even at fine domain sizes. The value is approximately proportional to the concentration of the magnetically 'softer' ferrimagnetic minerals (e.g. magnetite) within the sample, although also domain size dependent. At high fields the magnetically 'soft' ferrimagnetic minerals are likely to have been saturated and any subsequent growth of IRM will be due to magnetically 'harder' canted antiferromagnetic component within the sample. The value is approximately proportional to the concentration of canted antiferromagnetic minerals (e.g. haematite and geothite) within the sample.
Backfield Ratios i.e. S-ratio (IRM_{-100mT})	Various demagnetisation parameters can be obtained by applying one or more reversed magnetic fields to a previously saturated sample. The loss of magnetisation at each backfield can be expressed as a ratio of $IRM_{backfield}$/SIRM, and therefore gives a result between +1 and -1 normalised for concentration. Such ratios can be used to discriminate between ferrimagnetic and canted antiferromagnetic mineral types. For example, using the 100mT backfield ratio, minerals which are relatively easy to demagnetise (e.g. magnetite) have relatively low values (referred to as 'soft' magnetic behaviour). Minerals that show a stronger resistance to demagnetisation (e.g. haematite) show relatively high 100mT backfield ratios (referred to as 'hard' magnetic behaviour) (Walden *et al.*, 1996).
ARM/χ	The ratio of these variables can indicate the concentration of ferrimagnetic grain size variations (e.g. a high ratio indicates the presence of SSD grains) (Appendix 1.3).
SIRM/ARM	In samples dominated by ferrimagnetic minerals, the ratio of these variables is indicative of relative magnetic domain size variations (e.g. a low ratio indicates the presence of SSD grains) (Appendix 1.3).
SIRM/χ	The ratio of these variables can be diagnostic of either magnetic mineralogy (e.g. a low ratio might indicate paramagnetic minerals (Appendix 1.1), and a high ratio might indicate the importance of haematite or geothite) or where samples have similar mineral types and concentrations, it can be diagnostic of magnetic domain size variations (e.g. a high ratio indicates SSD ferrimagnetic grains, and a low ratio indicates the importance of SP or multidomain (MD) grains) (Appendix 1.3).

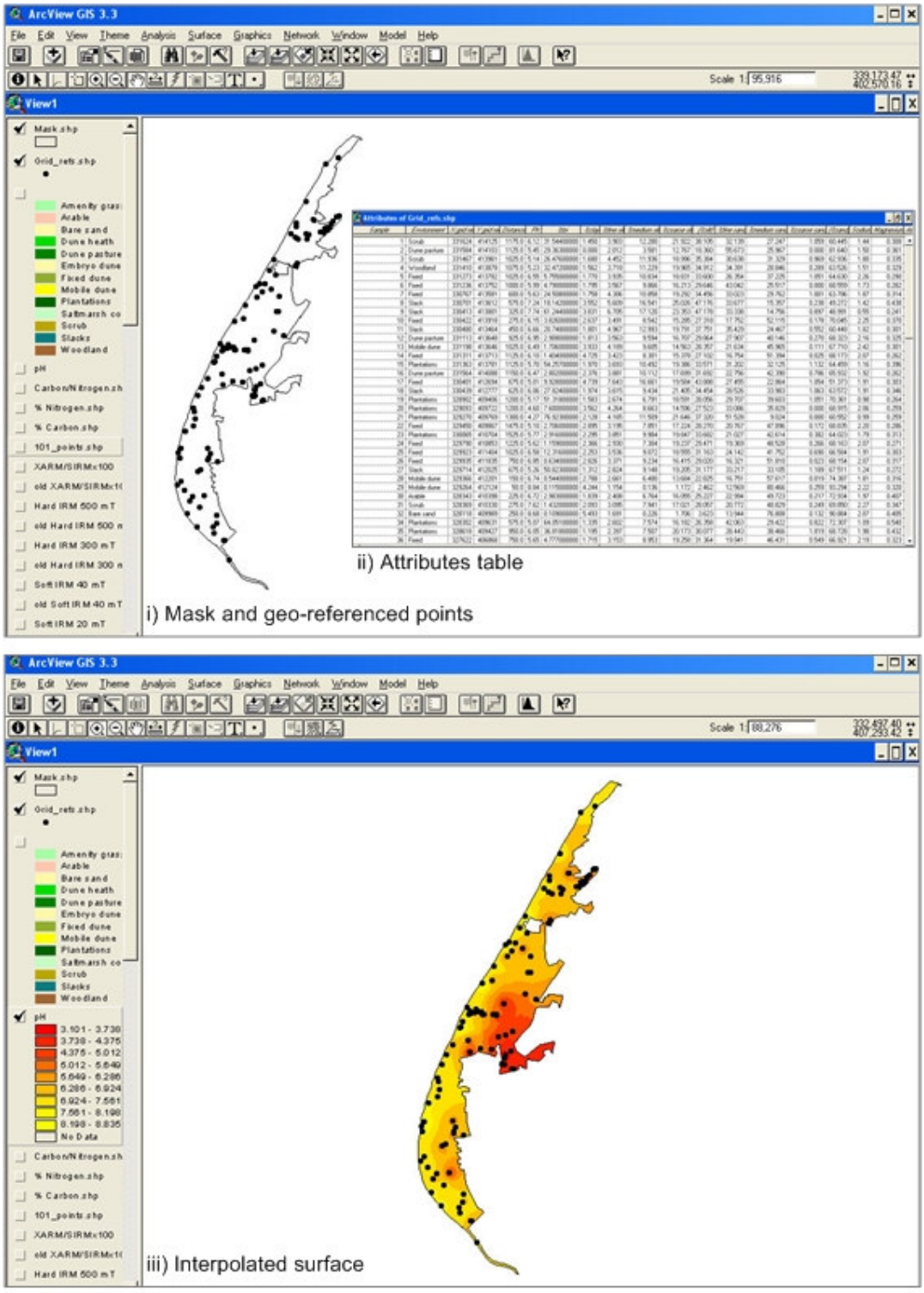

Figure 2.4 Visual representation of GIS analysis: i) creation of mask polygon and plotting of geo-referenced sample points using coordinate values; ii) a table of attributes was merged to each of the points from which, iii) an interpolated surface of the specific variables, in this case pH, was created. Interpolation quantitative values were automatically assigned to infinite mid-points between the data points within the masked boundary, to display spatial patterns of soil characteristics.

patterns of soil characteristics. As the sample points are representative, rather than transectional or from a grid, interpolation was achieved by nearest neighbour analysis (Andrews *et al.*, 2002), as it is possible to accurately calculate diagonal values.

2.4.2 Statistical analysis

Descriptive statistics were calculated using Microsoft Excel (XP) software. The Anderson-Darling normality test was performed on all data, the outcome of which was a non-normally distributed data majority. Therefore, all non-parametric data analyses were performed. Using MINITAB PC (version 15), sample comparisons were determined by Spearman's Rank. The statistical approaches, including Mann-Whitney tests and Kruskal-Wallis tests, are routine for random samples, thorough explanations of which are available in standard statistical data-analysis texts (e.g. Ebdon, 1978; Davis, 1986; Stuttard, 1994) and are also presented in Table 2.3.

2.4.3 Multivariate factor analysis

Properties of sample sets can be compared objectively on a simple, univariate basis, but this approach does not determine how sample sets respond to groups of variables simultaneously. To achieve this, multivariate analyses must be employed. Data-sets produced in this study are multivariate, i.e. each observational unit is characterized by several variables (Manly, 1994). Factor analysis is a form of multivariate statistical analysis that assumes underlying data are a small set of common factors, which are extracted by the analysis (Kovach, 1995). The remaining variance in the data is considered to be the 'uniqueness' or 'error' proportion (Davis, 1986, 2002; Kovach, 1995; Charlesworth and Lees, 1997, 2001). Factor analysis is similar to principal components analysis (PCA), in detecting interrelations, or high correlations, between variables, except the factors are chosen so as to maximize the correlation between the original variables rather than to maximize the variance (Kovach, 1995; Walden and Smith, 1995; Schneeweiss and Mathes, 1995). Factor analysis is similar to cluster analysis in that it locates groups of samples, but in numerical terms is similar to principal co-ordinates analysis (Kovach, 1995; Walden and Smith, 1995). However, no single unique solution occurs in factor analysis, as is the case in PCA.

To perform factor analysis, it is first necessary to standardize the raw data matrix to remove the effects of different parameters being measured on different scales. If a common standardization procedure is used on the raw data matrix prior to factor analysis, a common set of factors is extracted. Both the parameter factor and sample factor loadings are relative to this (Davis, 2002). The two most significant, uncorrelated, factors account for most variation within the data set and occupy axes in 'multidimensional factor space'. Therefore, any two factors can be presented as perpendicular axes in two dimensional space (Walden and Smith, 1995), from which attempts can be made to label the underlying causes. Original variables are loaded on each of the factors with those plotted in close proximity being considered highly correlated.

Table 2.3 Description of each statistical data test performed in this thesis (taken from MINITAB PC (version 15))

Statistical test used	Description of statistical test
Anderson-Darling	A one-sample hypothesis test determines whether the sample population is non-normal. The null hypothesis for a normality test states that the population is normal. The alternative hypothesis states that the population is non-normal. Anderson-Darling compares the empirical cumulative distribution function of the sample data with the distribution expected if the data were normal. If this observed difference is sufficiently large, the test will reject the null hypothesis of population normality, which means that non-parametric statistical tests are required.
Spearman's Rank correlation	Spearman's Rank correlation measures the degree of dependence between two variables. The number of raw scores are converted into ranks. Then the differences between the ranks of each observation on the two variables are calculated. The correlation coefficient assumes a value between -1 and +1. If one variable tends to increase as the other decreases, the correlation coefficient is negative. Conversely, if the two variables tend to increase together the correlation coefficient is positive.
Mann-Whitney	A 2-sample rank test of the equality of two population medians, calculating the corresponding point estimate and confidence interval . This test assumes that the data are independent random samples from two populations and whose variances are equal and a scale that is continuous or ordinal (possesses natural ordering) if discrete. The 2-sample rank test is slightly less powerful (the confidence interval is wider on the average) than the 2-sample test with pooled sample variance when the populations are normal, and considerably more powerful (confidence interval is usually narrower) for many other populations.
Kruskal-Wallis	Tests the equality of medians for two or more populations, by ranks. This test is a generalization of the procedure used by the Mann-Whitney test and offers a non-parametric alternative to the one-way Analysis of Variance. An assumption for this test is that the samples from the different populations are independent random samples from continuous distributions.
Multivariate Factor Analysis	Factor analysis, a parametric statistical analysis, like principal components analysis summarizes the data covariance structure in a few dimensions of the data. However, the emphasis in factor analysis is the identification of underlying "factors" that might explain the dimensions associated with large data variability.

Table 2.4 shows the mathematical steps of the procedure (Walden and Smith, 1995; Davis, 1986, 2002), involving a range of basic matrix algebra operations on the original raw data matrix (of *n* samples by *m* parameters). In this case, analysis is carried out using MINITAB PC (version 15). However, because this technique is mathematical and not statistical, the results are not subjected to any significance testing. Factor analysis cannot quantify the relative proportions of each variable, as it only shows changes in the balance between sources.

Figure 2.5 shows a hypothetical factor plot to illustrate how factor analysis results can be interpreted in an environmental situation. In this example, factor analysis was performed on a multivariate dataset of twelve parameters, which were measured on five sample populations (A-E) each containing different numbers of samples (perhaps representing topsoil samples from different dune environments). The parameter and sample loadings for the first two factors extracted from analysis (Factor 1 and Factor 2) have been used to generate the factor plot. Attempts are made at identifying underlying causes to, subsequently, 'label' or 'name' each factor (expressed in brackets after the factor is first mentioned in the text).

Table 2.5 shows that the first two factors extracted explain 74.29% of variation in the parameters. Factor 1 ('name' (e.g. representing distance inland)) has broadly separated the sample populations C, D and E from sample populations A and B. This indicates that Factor 1 (distance) provides a means of discriminating these groups, suggesting that those sample populations negatively loaded on Factor 1 have different characteristics to those positively loaded on Factor 1. The spread of sample loadings along Factor 2 ('name' (e.g. representing depth of sample)) separates sample population A from sample populations C and D. This indicates that Factor 2 (depth) provides an effective means of discriminating between these groups, suggesting that those sample populations negatively loaded on Factor 2 have different characteristics to the group positively loaded on Factor 2. However, Factor 2 has failed to separate sample populations B and E, which have both positive and negative Factor 2 loadings.

The distribution of parameter loadings shows that the parameters are influenced by Factors 1 and 2. Parameters 2, 3, 5, 6, 7, 8, 9, 11 and 12 are influenced by Factor 1, while parameters 1, 4 and 10 are influenced by Factor 2. This suggests that Parameters 2, 3, 6, 7 and 9 provide the strongest means of discriminating between the sample populations. As parameters 9 and 3 have plotted close together, this suggests that the sample populations are responding to these two variables in a similar manner (i.e. they are strongly positively correlated). Parameter 2 plots opposite parameter 3, suggesting parameter 2 has a negative correlation with parameter 3.

Theoretically, if sample population A represented a seaward dune environment topsoil and sample population D represented an inland dune environment topsoil, the factor plot could be applied as a semi-quantitative approach for assigning such topsoil dune environments to another sample population (F). In these circumstances, any population F samples plotted amongst population A samples are more likely dominated by soil characteristics associated with

Table 2.4 Procedure for simultaneous R- and Q-mode Factor Analysis (after Davis, 1986; 2002; Walden and Smith, 1995)

Step	Procedure
1	Compile a raw data matrix of *n* samples (rows) by *m* parameters (columns) denoted by [X], as in convential matrix algebra.
2	[X] is standardized to give [W]. Each element of [X] has its column (parameter) mean subtracted from it. It is then divided by the product of the column (parameter) standard deviation (s) and the square root of *n*.
3	[W]' is created by transposing [W]. This involves turning the rows of [W] into the columns of [W]' and the columns into rows.
4	[R] is created by matrix multiplication of [W]' · [W]. The matrix [R] represents a correlation matrix between the parameters.
5	Eigenvectors and eigenvalues (distinct properties of the matrix) are extracted from [R]. The eigenvectors are used to form a matrix [U]. The eigenvalues can be used to compute the percentage of the total variation in the original data set explained by the new 'underlying' factors.
6	The square roots of the eigenvalues are placed in the top left to bottom right diagonal elements of a matrix [^]. All other elements in this matrix are set to zero.
7	$[A^R]$ is computed by multiplication from [U] · [^]. The matrix $[A^R]$ contains the R-mode (parameter) factor loadings. Each column represents the loadings of the original parameters on an individual factor (column 1 on factor 1, etc.). These are the values used when plotting the parameters in 'factor space' in the form of scatter diagrams.
8	$[A^Q]$ is computed by multiplication from [W] · [U]. The matrix $[A^Q]$ contains the Q-mode (sample) factor loadings. Each column represents the loadings of the original parameters on an individual factor (column 1 on factor 1, etc.). These are the values used when plotting the samples in 'factor space' in the form of scatter diagrams.

Table 2.5 Hypothetical summary results from an hypothetical factor analysis using twelve hypothetical parameters

Factors	Eigenvalues	Total variance (%)	Cumulative eigenvalues	Cumulative total variance (%)
1	6.595	54.955	6.595	54.955
2	2.321	19.338	8.915	74.294
3	0.959	7.992	9.874	82.286
4	0.834	6.950	10.708	89.235
5	0.463	3.857	11.171	93.093
6	0.358	2.981	11.529	96.074
7	0.192	1.600	11.721	97.673
8	0.126	1.051	11.847	98.724
9	0.068	0.568	11.915	99.293
10	0.052	0.434	11.967	99.726
11	0.020	0.166	11.987	99.893
12	0.013	0.107	12.000	100.000

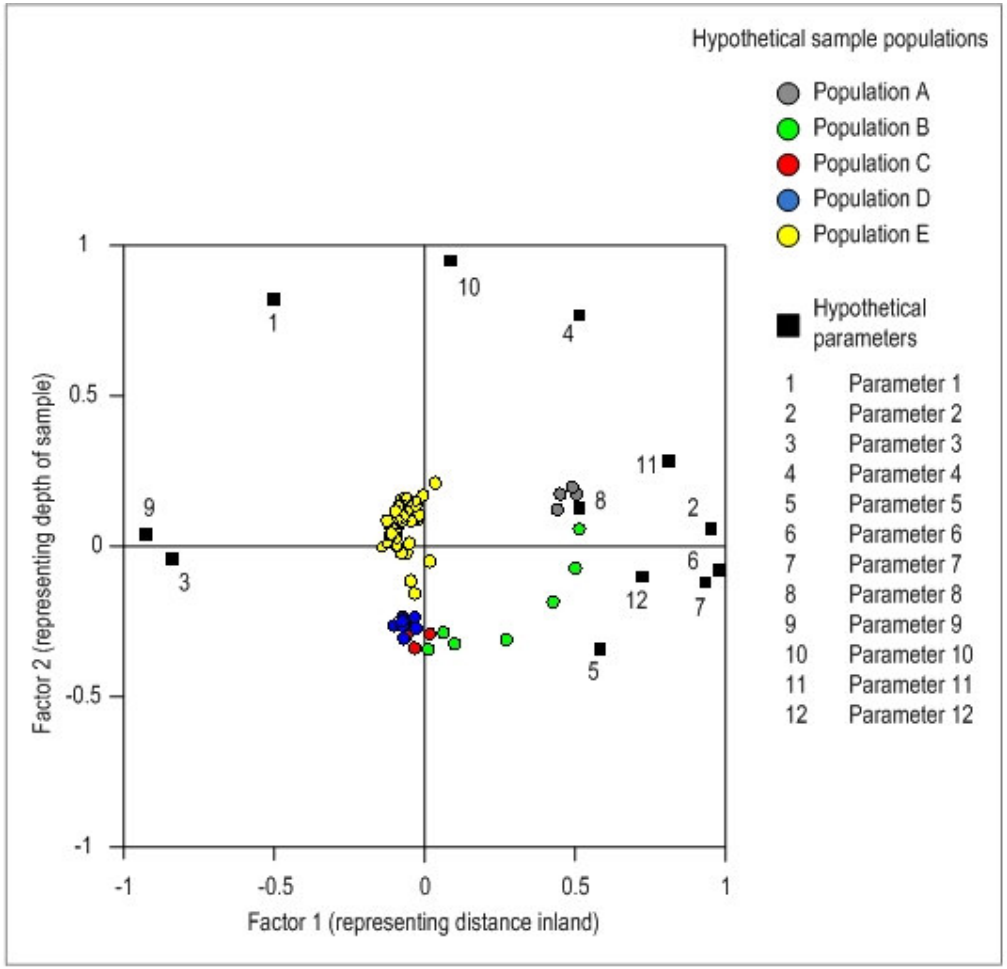

Figure 2.5 Hypothetical example of a simultaneous R- and Q-mode factor analysis plot of Factor 1 versus Factor 2, based on twelve hypothestical parameters.

seaward dune environments and, any population F samples plotting amongst population D samples are more likely dominated by inland soil characteristics. Any population F samples plotting between populations A and D represent a mixture of characteristics.

2.5 Photographic surveys and analysis

The entire coastal margin of the study area (~11.5 km) was photographed, 01/08/06-03/08/06, to gain insights into the diversity of the frontal dune environment and to investigate the transition from depositional to erosional environments. The survey initiated in the north of the study area (SD 30047 13484) and continued south, around Formby Point, until the no-access point of the Altcar Rifle Range (SD 28197 04703) was reached. The grid reference of every 20th photograph was recorded using GPS. Photographs were taken perpendicular to, at 35 paces (~25 m), from the frontal dune toe, allowing 20-25 m of dune landscape to be captured within the frame. To ensure capture of the entire length of the coast, and to aid analysis, ranging poles were placed at both the left- and right-hand edges of the photograph frame (i.e. the previous right-hand pole became the left-hand pole in the subsequent photograph).

A Fixed-Point-Photographic (FPP) survey was conducted to analyse whether dune geomorphological dynamics and vegetation change are evident on both a seasonal and annual timescale, to understand local rates of coastal change. Three monitoring stations were selected for FPP analysis, at which the highest point of each of the landscapes was geo-referenced; (i) Station 1, Birkdale sand dunes (SD 30379 13735); (ii) Station 2, Formby Point mobile dunes (SD 28016 09924) and (iii) Station 3, Raven Meols Hills Nature Reserve (SD 28092 05113). Photographs were taken from fixed angles; north, east, south and west, determined using a prismatic compass. Inclusive of the initial survey in November 2006, the survey has been conducted seasonally, in February, May and August, every year as an ongoing programme, from the same geo-referenced points. Occasionally the view from the previous year's photo point was obscured by vegetation/dune height growth. If an alternative clearer dune-view could not be obtained within ~25 m, the photo was not used (Zier and Baker, 2006).

The image-processing software Adobe Photoshop CS2 (version 9, 2005) was used to digitally match photosets by layering one photo over the other for alignment. Within a photo comparison, morphological features were analysed for increase, decrease or stability, based on already successful methodologies (Zier and Baker, 2006). An increase in extent was documented when a major dune morphological feature or vegetation type clearly occurred in new areas not occupied in the previous year's photograph. A decrease in extent was recorded when a dune morphological feature or vegetation type clearly occupied less area than in the previous year's photograph. The degree of increase or decrease was recorded as either moderate or extensive. However, the distinction between moderate and extensive changes is subjective, and estimations of area change are problematic. Vertical dune growth can sometimes block the view of areas, making them appear smaller due to sand encroachment.

CHAPTER 3

Distinguishing dune environments using topsoil (0-5 cm) pedo-characteristics

Chapter 3 characterizes the physico-chemical properties of contemporary topsoils (0-5 cm; n = 113 samples) for 10 natural and semi-natural dune environments, on the Sefton coast, to evaluate the existence of environments with distinct pedo-properties. A map of 13 classified dune environments, created using ArcView GIS (version 3.3), is introduced and described, from which 10 key dune environments are selected for analysis. Identification of spatial pedo-variations is presented as GIS images. Factor analysis attempts to group and separate dune environment topsoil pedo-characteristics, followed by interpretation and discussion of findings.

3.1 Introduction

The biological diversity of sand dunes is maintained when dune morphology and vegetation succession are encouraged. Over-stabilization of the dunes is, potentially, as great a threat as erosion, resulting in accelerated succession rates and ultimate loss of biological diversity (Doody, 1989; Kutiel *et al.,* 2000). The varying dune habitat environments of the Sefton coast support ideal conditions for successionally young slack habitats, which give rise to an ecologically significant dune system. Successful management of this landscape requires accurate baseline land cover maps (Gibson and Looney, 1992; Lucas *et al.,* 2002).

Existing vegetation descriptions and maps of the Sefton coast (e.g. Smith, 1978; Payne, 1983; Rothwell, 1985; Edmondson *et al*., 1993) suggest great variability. As soil-type may be a factor influencing species distribution (e.g. Beltman *et al.,* 1992), baseline maps of topsoil pedo-characteristics and patterns in pedogenesis, will aid the understanding of current environmental processes in operation on the dune landscape, minimizing potential future loss of natural resources.

3.2 Spatial variations in dune environments

The 61 broad NVC community boundaries, mapped in the field in by Sefton Metropolitan Borough Council (SMBC) in 2003/04, have identified 13 classified dune environments on the Sefton coast (refer to Chapter 2, Section 2.1). Figure 3.1 presents a map of the 13 dune environments, from which ten environments are chosen for topsoil analysis, excluding areas not associated with natural dune succession (amenity grassland, arable and salt marsh community). For the purpose of topsoil/sediment analysis, the geomorphological embryo dune environment is incorporated into the bare sand category. The ten dune topsoil environments are as follows; i) bare sand, ii) mobile dune community, iii) fixed dune community, iv) dune heath, v) slack community; vi) pasture, vii) scrub, viii) deciduous woodland, ix) coniferous plantation and x) felled coniferous woodland (an area not distinguished through vegetation analysis, but identified during field observations).

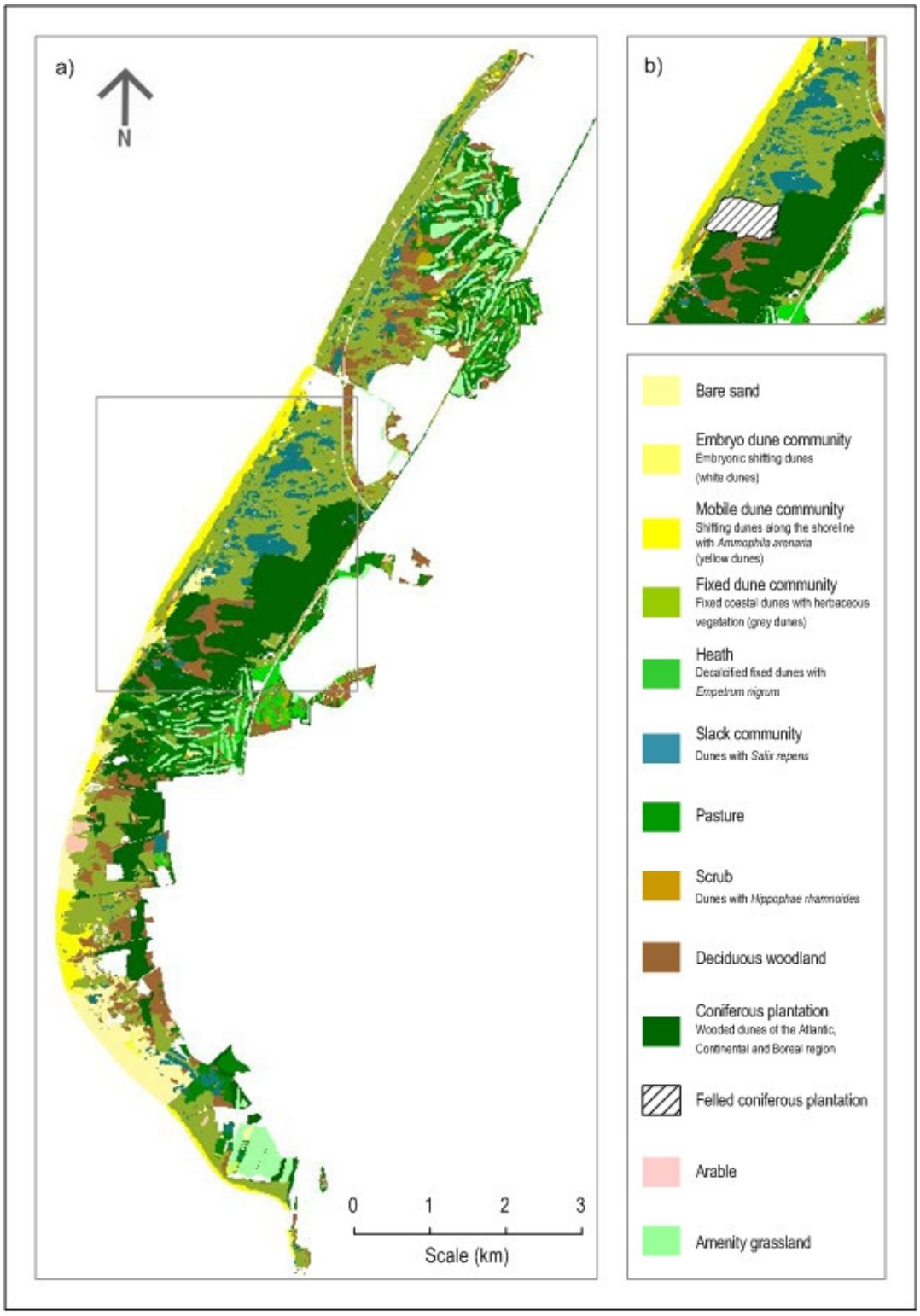

Figure 3.1 Map of dune environments on the Sefton coast, created in ArcView GIS (version 3.3): a) NVC data and EU habitat classifications (excluding saltmarsh community as areas are too small to be visible) and b) phase 2 felled area, conducted during winter 1995/96.

A complete successional series of plant communities (Smithson *et al.,* 2002), across the full width of blown sand, is not evident on the dune environments map (Figure 3.1). Therefore, the following order of dune environments described is based on a proposed path of natural dune succession, initiating on the backshore and proceeding inland. However, this is not an accurate indication of development over time; for example, erosion processes have exposed hind land environments on the backshore. Some environments have also been anthropogenically altered, such as artificially stabilized dunes and felled areas.

3.2.1 Bare sand and mobile dune community environments

Embryo dunes, or unvegetated advancing dunes, are present on the accreting coastline sections, north and south of the erosion limit. Mobile dunes occur landward of the embryo dunes, represented as ridges parallel to the coast. They are clearly visible, spanning almost the entire length of the project area, except for the stabilized 'green beach' formation in the northern extremity and where they are truncated by erosion around Formby Point. Expanses of bare sand, around Formby Point, suggest blowout formation and subsequent transgressive sand sheets, caused by recreational pressure at beach access points (Pye, 1990).

3.2.2 Fixed dune community environments

The most common and widespread environmental community is fixed dune, expanses of which are found at both Birkdale sand dunes and Ainsdale NNR. At some localities, fixed dune communities occupy the entire width of the coast. Interspersed with slack habitats, this landscape is most likely to be the result of an irregular series of hummock dunes with incipient blowouts and parabolic dunes, which Pye (1990) suggested were prograding seaward pre-1800. However, recent erosion has exposed these environments on the coast around Formby Point, with no evidence of protecting mobile dune barriers between the land and the sea.

3.2.3 Slack community environments

Slack environments have successfully been identified by distinct vegetation differences. However, evident by the polygon shapes, two geomorphological stages of slack development exist. The older, secondary slacks, at Birkdale and Ainsdale, have a mainly east-west orientation suggesting an origin from large blowouts (Pethick, 1984; Edmondson *et al*., 1993). The younger, primary dune slacks, occurring behind the mobile dunes at Ainsdale, are associated with a later phase of dune development, where successive shore-parallel dune ridges have cut off former beach surfaces. Slack environments in the southern extremity are limited. Smith (1978) pointed out that natural dune slacks south of Formby Point have been largely eliminated by extensive modification for asparagus cultivation.

3.2. 4 Heath and pasture environments

Following fixed dunes, acid heath is normally the pursuing successional stage (James and Wharfe, 1989). But this environment is fragmented on the Sefton coast, occupying only the eastern fringes where building development has occurred. According to Edmondson *et al*.

(1993), Freshfield dune heath was formerly a golf course and, therefore, cannot be classed as a natural dune environment. The polygon shape of heath communities on golf courses, often interspersed with pastures, suggest occupation of former slacks. Pastures, known to succeed from alkaline fixed dune and slack communities (Edmondson *et al.,* 1993), appear to occupy the edges of larger slacks or totally colonize older slack hollows. Large expanses of pasture environments are located in the southern extremity, having developed on relict agricultural plots.

3.2.5 Woodland environments

Natural scrub areas (i.e. colonized by native species) are generally sparse, but on Birkdale sand dunes, vegetation succession appears to have initiated in phases of slack development, progressing to scrub and even deciduous woodland, probably following the trend of stability and accretion in this vicinity. Areas of deciduous woodland further south tend to be surrounded by coniferous plantations, probably developed due to the sheltering properties of pine woodland from coastal erosion and deposition of aeolian-derived sand. Coniferous plantations occupy large areas of the central dune system. The 'phase 2' area of felled coniferous woodland, felled winter 1995-1996, is not evident on the dune environments map. Instead, the area is represented by vegetation associated with fixed dune community.

3.3 General statistical description of Sefton coastal dune topsoil pedo-characteristics

Figure 3.2 shows the location of the topsoil sample points (n = 113) for the entire study area, further details of which are given in Table 3.1. Table 3.2 reports topsoil pedo-characteristics for the entire coast (n = 113). The pH values (3.10-8.84) show a wide transverse from acid to alkaline across the dune system, which would be expected from a coastal environment. SOM (0.10-77.17%) also varies greatly. Mean particle size ranges from fine sand (95.70 µm) to medium sand (259.50 µm), with a median value of 178.80 µm (fine sand). Clay (0.00-6.92%) is generally very low across the dunes, only contributing to a median 2.14%.

Sefton dune sediments are highly siliceous (<41% Si). However, levels are relatively low compared with other coastal dune systems in north-west Europe, where some exceed 85% Si (e.g. Saye and Pye, 2006). Following Si, C and Na are the most abundant geochemical parameters. However, they only contribute a combined median 4% to the total. The extremely low levels of Al (0.00-1.37%) and Fe (<0.01-4.03%) indicate a low feldspar and heavy mineral content, respectively; whereas, the low Ca content (0.03-8.15%) indicates an overall low shell content. C (0.02-6.14%) is relatively high in comparison to N (<0.01-0.50%) across the dune system, resulting in a high C:N ratio.

Magnetic concentration-dependent parameters (χ_{LF} 0.28-17.72 $x10^{-7}m^3kg^{-1}$; χ_{ARM} 0.01-0.70 $x10^{-7}m^3kg^{-1}$; SIRM 38.07-11,786.52 $x10^{-5}m^2kg^{-1}$) show the topsoils contain low-moderate quantities of magnetic minerals, which are comparable with other European topsoils (Maher, 1986, 1998; Dearing *et al.,* 1996; Booth *et al.,* 2005, 2006). Soft parameters (IRM_{20mT} and IRM_{40mT}), indicate the content of ferrimagnetic 'magnetite-type' soft minerals (4.51-58.88%),

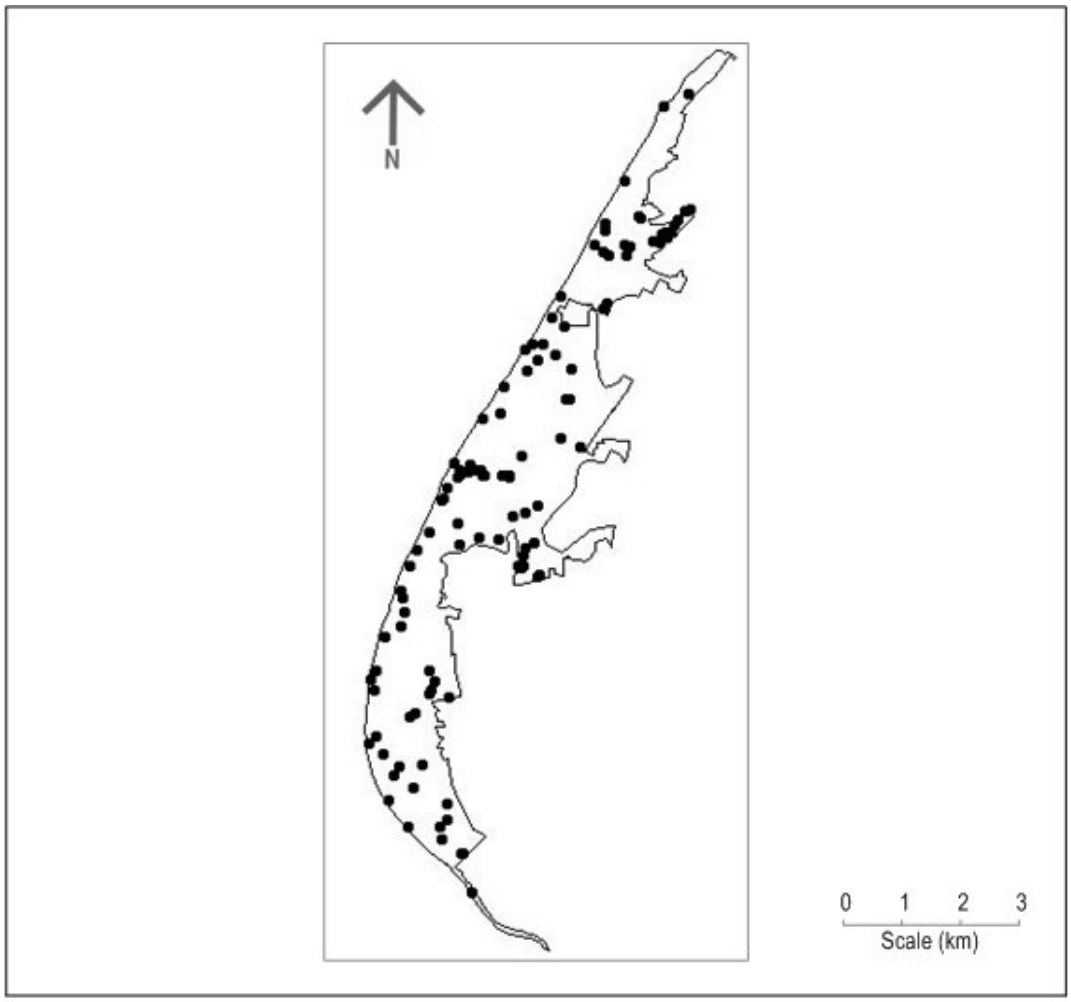

Figure 3.2 Masked study area showing georeferenced topsoil sample points, created in ArcView GIS (version 3.3).

Table 3.1 List of identified dune environments, with associated number of samples and mean distance from MHW

	Dune environment	Number of samples (n)	Mean distance from MHW (m)
Natural succession	Bare sand	9	203
	Mobile dune	12	226
	Fixed dune	18	832
	Heath	9	1724
	Slack	11	439
	Pasture	10	661
	Scrub	10	484
	Deciduous woodland	14	635
Modified	Coniferous plantation	10	1001
	Felled	10	476

Table 3.2 Summary data* for topsoil physico-chemical characteristics of the Sefton coast (n = 113)

Parameters	Units	Mean	Median	SD	CV	Min	Max
pH	mol/ltr	6.433	6.670	1.309	20.352	3.100	8.840
SOM	%	9.432	2.959	16.131	171.022	0.101	77.165
Sand	%	72.052	69.808	8.907	12.362	48.991	96.067
Silt	%	25.486	28.164	9.502	37.285	0.396	47.178
Clay	%	2.462	2.142	1.115	45.313	0.000	6.918
Mean particle size	µm	181.752	178.802	31.885	17.543	95.701	259.500
Median particle size	µm	186.057	190.865	41.096	22.088	57.419	258.096
Sorting		1.661	1.715	0.324	19.478	0.404	2.389
Skewness	γ_1	0.573	0.617	0.152	26.546	0.014	0.762
Kurtosis	g_1	1.485	0.949	1.173	78.999	0.863	6.059
Carbon	%	2.038	2.314	1.610	79.016	0.018	6.136
Nitrogen	%	0.145	0.145	0.114	78.082	0.002	0.501
Sodium	%	2.107	1.960	1.450	68.812	0.551	11.530
Magnesium	%	0.324	0.321	0.100	30.889	0.000	0.625
Aluminium	%	0.272	0.242	0.178	65.453	0.000	1.365
Silicon	%	34.352	37.050	8.166	23.770	0.210	40.910
Phosphorus	%	0.048	0.030	0.045	94.571	0.005	0.221
Sulphur	%	0.047	0.011	0.077	164.713	0.000	0.345
Chlorine	%	1.072	0.012	6.409	598.057	0.006	41.240
Potassium	%	0.543	0.569	0.116	21.371	0.000	0.759
Calcium	%	0.928	0.805	1.002	107.909	0.033	8.148
Iron	%	0.984	0.894	0.454	46.133	0.004	4.030
χ_{LF}	$10^{-7}m^3kg^{-1}$	1.809	1.347	1.955	108.048	0.275	17.718
$\chi_{FD\%}$	%	2.382	1.942	1.869	78.478	0.000	12.000
χ_{ARM}	$10^{-7}m^3kg^{-1}$	0.042	0.025	0.076	179.155	0.006	0.702
SIRM	$10^{-5}Am^2kg^{-1}$	320.645	156.655	1104.086	344.333	38.066	11786.516
$Soft_{IRM20mT}$	$10^{-5}Am^2kg^{-1}$	41.243	27.623	57.645	139.771	5.015	531.047
$Soft_{IRM40mT}$	$10^{-5}Am^2kg^{-1}$	98.256	60.194	154.697	157.443	16.249	1515.741
$Hard_{IRM300mT}$	$10^{-5}Am^2kg^{-1}$	21.080	15.291	19.722	93.558	3.549	147.036
$Hard_{IRM500mT}$	$10^{-5}Am^2kg^{-1}$	10.102	7.571	8.592	85.055	0.497	51.604
$Soft_{\%20mT}$	%	17.182	17.011	5.431	31.612	4.506	29.219
$Soft_{\%40mT}$	%	39.106	40.338	7.213	18.444	12.860	58.881
$Hard_{\%300mT}$	%	10.136	9.274	4.902	48.361	1.247	33.587
$Hard_{\%500mT}$	%	5.308	4.529	3.398	64.015	0.202	16.424
S-ratio	(none)	-0.640	-0.642	0.082	-12.761	-0.996	-0.253
ARM/χ	$10^{-2}Am^{-1}$	0.023	0.020	0.015	63.568	0.005	0.106
SIRM/ARM	(None)	223.336	206.913	97.335	43.582	34.126	527.100
χ_{ARM}/SIRM	$10^{-5}Am^2kg^{-1}$	1.777	0.015	1.269	71.454	0.596	9.203
SIRM/χ	$10^{-2}Am^{-1}$	133.442	127.764	55.168	41.342	58.339	665.238

**Mean; Median; SD = standard deviation; CV = percentage coefficient of variation; Min = minimum value; Max = maximum value. Values are shown to 3 decimal places for consistency, not accuracy.*

while Hard parameters (IRM_{300mT} and IRM_{500mT}), indicate the content of canted antiferromagnetic 'haematite-type' hard minerals (1.25-33.59%). This indicates most samples display a greater influence of magnetically-soft minerals (e.g. Magnetite (Fe_3O_4) and Maghaemite (γFe_2O_3)) than magnetically-hard minerals (e.g. Haematite (αFe_2O_3) and Goethite ($\alpha FeOOH$)). However, some samples contain contrasting magnetic mineralogies and concentration differences, supported by the S-ratio (-1.00- -0.25). ARM/χ values (0.01-0.11 $x10^{-2}$ Am^{-1}) are extremely low suggesting all topsoil dune environments contain coarse (multidomain) magnetic domain sizes, with fewer fine (stable single domain) magnetic materials.

3.4 Statistical descriptions of individual dune environment topsoil pedo-characteristics

Summary data for the physico-chemical characteristics of each of the dune environment topsoils are described and both null (H_0) and alternative (H_1) hypotheses were tested. Table 3.3 compares the medians of each of the dune environment topsoil sample populations for each parameter, while Figure 3.3 presents population distributions for selected parameters. Non-parametric Mann-Whitney U tests (Tables 3.4-10) compare the differences between these median values. The 'p' value is a measure of the level of significance at which the null (or alternative) hypothesis must be accepted. For example, if the 'p' value is equal to or less than the level of significance chosen, the null hypothesis can be rejected. Thus using a probability level of 95% (0.95) and therefore a significance level of 5% (0.05), the null hypothesis would be rejected if the 'p' value fell below 0.05 (Walden, 1990). The results of non-parametric Kruskal-Wallis tests (data not presented) show no differences between more than two of the dune environment topsoil sample populations for each parameter, independent of each other (refer to Table 2.3).

Tested Hypotheses	
Null Hypothesis (H_0)	There was no significant difference between the medians of each of the sample populations compared to each other.
Alternative Hypothesis (H_1)	There was a significant difference between the medians of each of the sample populations compared to each other.

3.4.1 Bare sand community topsoil pedo-characteristics

Table 3.11 presents the summary data for the physico-chemical characteristics of the bare sand environment topsoil samples (n = 9). The pH (7.62-8.68) clearly represented an alkaline environment. SOM (0.11-0.33%) is extremely low, corresponding to the lowest median (0.23%) for the entire dune system. Mean particle size (210.57-249.13 µm) categorizes this environment as medium sand, with sand contributing a median 88.62% to the textural total. Clay is very high (3.53-5.72%) representing the highest median (3.94%) for the entire coast. This is characteristic of muddy sediments, which suggests that there are large areas of clay-sized particles in the northern half of the Irish Sea, indicative of low energy environments. This mineralogical environment is emphasized by the relatively high values of $Soft_{IRM40mT}$ (20.10-172.57

Table 3.3 Median values for each parameter within each dune topsoil environment

Parameters	Units	Bare sand (n = 9)	Mobile dune (n = 12)	Fixed dune (n = 18)	Heath (n = 9)	Slack (n = 11)	Pasture (n = 10)	Scrub (n = 10)	Deciduous wood (n = 14)	Coniferous (n = 0)	Felled area (n = 10)
pH	mol/ltr	8.000	7.670	6.365	3.950	6.860	6.945	7.190	6.380	5.120	6.360
SOM	%	0.225	0.271	1.984	6.612	7.522	2.767	1.900	4.814	35.297	2.742
Sand	%	88.616	84.482	68.366	67.550	64.760	70.964	73.381	69.861	67.777	71.995
Silt	%	7.737	12.145	28.645	31.119	33.114	26.675	24.709	28.591	30.859	26.376
Clay	%	3.939	3.461	2.504	1.722	1.974	2.361	2.047	1.543	1.777	2.019
Mean particle size	µm	238.405	216.780	179.068	163.329	161.355	172.596	185.889	176.115	162.119	184.267
Median particle size	µm	241.144	226.581	199.660	167.949	154.247	183.235	196.704	187.339	164.887	199.865
Sorting		1.205	1.412	1.841	1.676	1.798	1.721	1.646	1.689	1.771	1.770
Skewness	γ_1	0.421	0.465	0.696	0.596	0.559	0.666	0.652	0.612	0.492	0.668
Kurtosis	g_1	3.951	2.574	0.949	0.891	0.934	0.958	0.944	0.933	0.950	0.936
Carbon	%	0.071	0.160	1.274	3.557	2.351	1.850	2.522	2.643	3.177	2.756
Nitrogen	%	0.007	0.010	0.090	0.251	0.147	0.154	0.216	0.186	0.211	0.212
Sodium	%	2.060	2.115	2.070	1.770	1.820	2.005	1.865	1.965	1.405	1.960
Magnesium	%	0.410	0.330	0.314	0.186	0.332	0.324	0.328	0.362	0.289	0.273
Aluminium	%	0.271	0.179	0.207	0.306	0.171	0.256	0.230	0.324	0.321	0.218
Silicon	%	37.810	38.315	39.370	34.940	32.100	37.365	36.660	36.100	22.060	38.000
Phosphorus	%	0.015	0.020	0.018	0.052	0.053	0.032	0.033	0.041	0.104	0.018
Sulphur	%	0.000	0.000	0.000	0.029	0.094	0.015	0.003	0.023	0.129	0.002
Chlorine	%	0.010	0.013	0.009	0.016	0.025	0.011	0.010	0.014	0.032	0.010
Potassium	%	0.552	0.548	0.598	0.540	0.527	0.586	0.564	0.575	0.423	0.566
Calcium	%	1.544	1.007	0.643	0.090	1.201	0.733	0.876	0.548	0.461	0.513
Iron	%	0.967	0.857	0.865	0.669	1.152	0.951	1.073	0.931	0.783	0.942
χ_{LF}	$10^{-7}m^3kg^{-1}$	1.012	0.902	1.062	1.102	1.198	2.111	1.513	2.115	1.671	1.582
χ_{FD}	%	1.743	1.833	2.655	1.571	2.041	1.996	2.231	1.850	2.000	1.456
χ_{ARM}	$10^{-7}m^3kg^{-1}$	0.012	0.015	0.019	0.020	0.027	0.031	0.025	0.037	0.031	0.032
SIRM	$10^{-5}Am^2kg^{-1}$	120.887	111.582	136.523	151.136	103.476	277.442	177.632	289.205	228.924	205.729
$Soft_{IRM20mT}$	$10^{-5}Am^2kg^{-1}$	22.714	15.938	18.504	33.537	23.263	48.873	32.105	36.336	29.775	38.209
$Soft_{IRM40mT}$	$10^{-5}Am^2kg^{-1}$	51.640	38.355	47.395	58.757	44.297	119.222	74.420	104.381	69.557	85.424
$Hard_{IRM300mT}$	$10^{-5}Am^2kg^{-1}$	18.761	10.098	14.302	14.589	10.527	19.640	32.782	26.706	16.236	15.140
$Hard_{IRM500mT}$	$10^{-5}Am^2kg^{-1}$	10.261	5.114	4.617	8.252	5.765	9.522	14.347	14.248	6.986	9.444
$Soft_{\%20mT}$	%	18.790	20.375	13.378	22.190	17.319	16.310	16.902	17.372	12.592	19.253
$Soft_{\%40mT}$	%	41.990	45.048	31.914	43.310	38.526	43.302	38.964	40.468	31.913	41.541
$Hard_{\%300mT}$	%	15.519	10.142	9.748	9.320	8.775	7.981	12.349	8.724	7.714	7.941
$Hard_{\%500mT}$	%	11.321	6.286	3.532	5.381	4.280	3.568	6.474	5.025	3.398	3.633
S-ratio	(none)	-0.649	-0.635	-0.623	-0.566	-0.668	-0.669	-0.628	-0.627	-0.660	-0.653
ARM/χ	$10^{-2}Am^{-1}$	0.015	0.018	0.022	0.023	0.023	0.022	0.017	0.022	0.021	0.017
SIRM/ARM	(None)	248.514	212.580	195.150	218.636	150.267	202.282	269.335	207.105	199.375	253.595
χ_{ARM}/SIRM	$10^{-5}Am^2kg^{-1}$	0.013	0.015	0.016	0.014	0.021	0.016	0.012	0.015	0.016	0.012
SIRM/χ	$10^{-2}Am^{-1}$	119.478	118.861	133.894	137.201	113.338	135.219	113.968	139.710	132.453	125.762

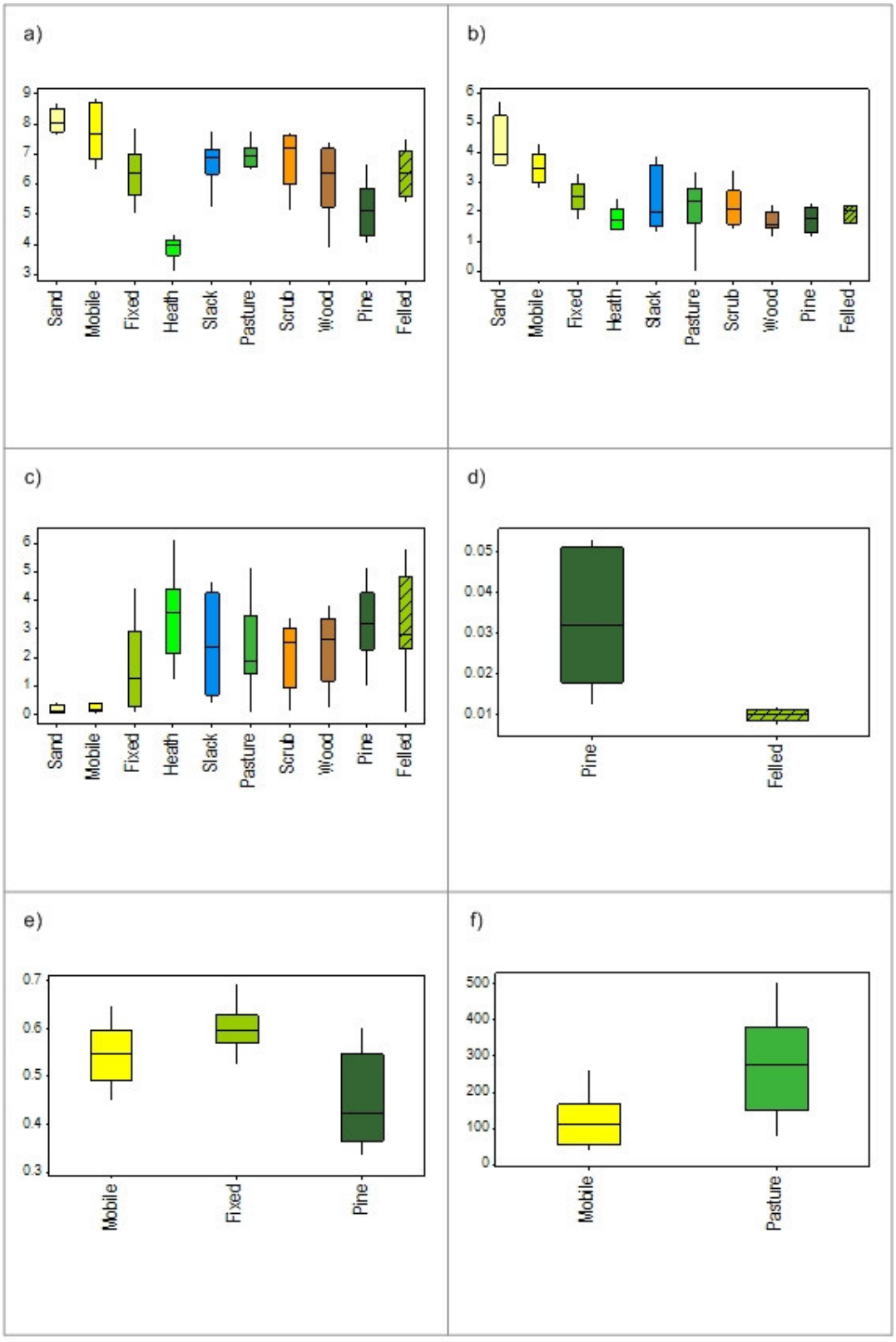

Figure 3.3 Box plots of topsoil sample population distributions for selected parameters: a) pH; b) Clay%; c) C%; d) Cl%; e) K% and f) SIRM x10^{-5}Am^{2}kg^1.

Table 3.4 Mann-Whitney U test results for topsoil parameters. Tables show MINITAB '*p*' values (**bold** text is significant (**p* <0.05; ***p* <0.01; ****p* <0.001)) for; a) pH; b) SOM%; c) Sand%; d) Silt%; e) Clay% and f) Mean particle size (µm)

a)	Bare sand	Mobile	Fixed	Heath	Slack	Pasture	Scrub	Wood	Pine
Mobile	0.337								
Fixed	**<0.001*****	**0.002****							
Heath	**<0.001*****	**<0.001*****	**<0.001*****						
Slack	**<0.001*****	**0.018***	0.234	**<0.001*****					
Pasture	**0.001****	**0.032****	0.131	**<0.001*****	0.833				
Scrub	**<0.001*****	**0.038****	0.222	**<0.001*****	0.647	0.791			
Wood	**<0.001*****	**0.001****	0.649	**<0.001*****	0.218	0.121	0.084		
Pine	**<0.001*****	**<0.001*****	**0.004****	**0.001****	**0.001****	**0.001****	**0.003****	**0.024***	
Felled	**<0.001*****	**0.003****	0.886	**<0.001*****	0.307	0.241	0.151	0.747	**0.013***

b)	Bare sand	Mobile	Fixed	Heath	Slack	Pasture	Scrub	Wood	Pine
Mobile	0.374								
Fixed	**<0.001*****	**0.001****							
Heath	**<0.001*****	**0.002****	**0.048***						
Slack	**<0.001*****	**0.001****	**0.008****	0.362					
Pasture	**<0.001*****	**0.004****	0.905	**0.016***	**0.022***				
Scrub	**0.004****	**0.011***	0.549	0.307	0.098	0.910			
Wood	**<0.001*****	**<0.001*****	**0.018***	0.729	0.396	**0.013***	0.107		
Pine	**<0.001*****	**<0.001*****	**0.001****	0.079	0.170	**0.001****	**0.007****	**0.038***	
Felled	**<0.001*****	**0.002****	0.518	0.066	**0.032***	0.427	0.910	0.057	**0.004****

c)	Bare sand	Mobile	Fixed	Heath	Slack	Pasture	Scrub	Wood	Pine
Mobile	0.303								
Fixed	**<0.001*****	**<0.001*****							
Heath	**<0.001*****	**0.001****	0.117						
Slack	**<0.001*****	**<0.001*****	**0.041***	0.403					
Pasture	**<0.001*****	**0.013***	0.172	**0.020***	**0.012***				
Scrub	**<0.001*****	**0.011***	0.204	0.066	**0.022***	1.000			
Wood	**<0.001*****	**0.003****	0.314	**0.015***	**0.013***	0.747	0.520		
Pine	**<0.001*****	**0.001****	0.457	0.653	0.245	0.089	0.089	0.065	
Felled	**<0.001*****	**0.012***	0.143	**0.004****	**0.004****	1.000	0.653	0.637	**0.037***

d)	Bare sand	Mobile	Fixed	Heath	Slack	Pasture	Scrub	Wood	Pine
Mobile	0.271								
Fixed	**<0.001*****	**<0.001*****							
Heath	**<0.001*****	**<0.001*****	**0.042***						
Slack	**<0.001*****	**<0.001*****	**0.021***	0.543					
Pasture	**<0.001*****	**0.008****	0.457	**0.016***	**0.008****				
Scrub	**<0.001*****	**0.008****	0.303	0.066	**0.018***	1.000			
Wood	**<0.001*****	**<0.001*****	0.662	**0.015***	**0.013***	0.501	0.429		
Pine	**<0.001*****	**<0.001*****	0.172	0.488	0.245	0.064	0.104	0.107	
Felled	**<0.001*****	**0.008****	0.316	**0.003****	**0.004****	0.903	0.540	0.637	**0.016***

e)	Bare sand	Mobile	Fixed	Heath	Slack	Pasture	Scrub	Wood	Pine
Mobile	0.051								
Fixed	**<0.001*****	**0.009****							
Heath	**<0.001*****	**0.002****	**0.003****						
Slack	**0.002****	**0.029***	0.178	0.288					
Pasture	**<0.001*****	**0.003****	0.222	0.111	0.805				
Scrub	**<0.001*****	**0.004****	0.089	0.153	0.972	0.678			
Wood	**<0.001*****	**0.002****	**<0.001*****	0.729	0.163	0.057	0.065		
Pine	**0.001****	**0.003****	**0.008****	0.903	0.379	0.212	0.273	0.619	
Felled	**<0.001*****	**0.003****	**0.029***	0.216	1.000	0.438	1.000	**0.022***	0.307

f)	Bare sand	Mobile	Fixed	Heath	Slack	Pasture	Scrub	Wood	Pine
Mobile	0.696								
Fixed	**<0.001*****	**0.001****							
Heath	**<0.001*****	**0.001****	**0.029***						
Slack	**<0.001*****	**<0.001*****	**0.014***	0.543					
Pasture	**<0.001*****	**0.005****	0.981	0.111	**0.038***				
Scrub	**<0.001*****	**0.011***	0.204	**0.037***	**0.018***	0.521			
Wood	**<0.001*****	**0.001****	0.985	0.055	**0.023***	0.838	0.230		
Pine	**<0.001*****	**0.005****	0.981	0.111	**0.038***	1.000	0.521	0.838	
Felled	**<0.001*****	**0.017***	0.095	**0.002****	**0.004****	0.391	0.713	0.197	0.391

Table 3.5 Mann-Whitney U test results for topsoil parameters. Tables show MINITAB '*p*' values (**bold** text is significant (**p* <0.05; ***p* <0.01; ****p* <0.001)) for; a) C%; b) N% (n = 101); c) Na% and d) Mg% (n = 112)

a)	Bare sand	Mobile	Fixed	Heath	Slack	Pasture	Scrub	Wood	Pine
Mobile	0.303								
Fixed	**0.004****	**0.012***							
Heath	**<0.001*****	**<0.001*****	**0.014***						
Slack	**0.003****	**0.004****	0.270	0.244					
Pasture	**0.002****	**0.004****	0.257	0.206	0.807				
Scrub	**0.002****	**0.006****	0.280	**0.046***	0.961	0.850			
Wood	**<0.001*****	**<0.001*****	0.154	0.062	1.000	0.733	0.515		
Pine	**0.003****	**0.003****	**0.043***	0.680	0.284	0.303	0.093	0.148	
Felled	**0.003****	**0.005****	**0.045***	0.791	0.341	0.206	0.348	0.350	0.860

b)	Bare sand	Mobile	Fixed	Heath	Slack	Pasture	Scrub	Wood	Pine
Mobile	0.394								
Fixed	**0.006****	**0.022***							
Heath	**<0.001*****	**<0.001*****	**0.012***						
Slack	**0.002****	**0.004****	0.229	0.341					
Pasture	**0.002****	**0.004****	0.163	0.206	0.961				
Scrub	**0.001****	**0.002****	0.069	0.540	0.807	0.385			
Wood	**<0.001*****	**<0.001*****	0.072	0.217	0.968	0.852	0.556		
Pine	**0.003****	**0.004****	**0.025***	1.000	0.284	0.303	0.704	0.254	
Felled	**0.003****	**0.006****	**0.039***	0.930	0.397	0.348	0.653	0.350	0.814

c)	Bare sand	Mobile	Fixed	Heath	Slack	Pasture	Scrub	Wood	Pine
Mobile	0.356								
Fixed	0.535	0.465							
Heath	**0.013***	**0.003****	**0.011***						
Slack	**0.044***	**0.005****	**0.009****	0.732					
Pasture	0.624	0.147	0.315	0.066	0.105				
Scrub	0.178	**0.019***	0.071	0.270	0.481	0.308			
Wood	0.329	**0.045***	0.147	0.108	0.239	0.619	0.578		
Pine	**0.025***	**0.008****	**0.008****	0.391	0.379	0.059	0.121	0.107	
Felled	0.488	0.070	0.160	0.289	0.275	0.762	0.850	1.000	0.112

d)	Bare sand	Mobile	Fixed	Heath	Slack	Pasture	Scrub	Wood	Pine
Mobile	0.082								
Fixed	**<0.001*****	0.106							
Heath	**<0.001*****	**0.002****	**<0.001*****						
Slack	**0.008****	0.712	0.589	**0.001****					
Pasture	**0.003****	0.489	0.514	**<0.001*****	0.916				
Scrub	**0.001****	0.644	0.183	**<0.001*****	0.805	0.545			
Wood	0.078	0.918	0.052	**0.002****	0.494	0.279	0.320		
Pine	**0.020***	0.291	0.498	**0.025***	0.379	0.345	0.427	0.242	
Felled	**0.008****	0.138	0.482	**0.004****	0.481	0.385	0.308	0.188	0.970

Table 3.6 Mann-Whitney U test results for topsoil geochemical parameters. Tables show MINITAB '*p*' values (**bold** text is significant (**p* <0.05; ***p* <0.01; ****p* <0.001)) for; a) Al%; b) Si%; c) P% and d) S% (n = 112)

a)	Bare sand	Mobile	Fixed	Heath	Slack	Pasture	Scrub	Wood	Pine
Mobile	0.145								
Fixed	0.666	0.207							
Heath	**0.042***	**0.003****	**0.046***						
Slack	0.362	0.518	0.742	**0.033***					
Pasture	0.653	0.070	0.328	0.348	0.342				
Scrub	0.967	0.291	0.564	0.391	0.647	0.791			
Wood	0.073	**0.001****	**0.007****	0.431	**0.029***	0.208	0.254		
Pine	0.079	**0.003****	**0.026***	0.775	0.062	0.273	0.345	0.725	
Felled	0.967	0.138	0.633	0.094	0.418	0.791	0.970	**0.033***	0.121

b)	Bare sand	Mobile	Fixed	Heath	Slack	Pasture	Scrub	Wood	Pine
Mobile	0.644								
Fixed	0.138	0.241							
Heath	**0.027***	0.095	**0.011***						
Slack	**0.012***	**0.025***	**0.001****	0.068					
Pasture	0.540	0.410	**0.042***	0.153	0.062				
Scrub	0.270	0.277	**0.026***	0.596	0.170	0.623			
Wood	**0.025***	0.057	**0.002****	0.592	0.286	0.121	0.501		
Pine	**0.006****	**0.013***	**0.001****	0.055	0.170	**0.014***	**0.026***	0.107	
Felled	0.967	0.621	**0.031***	0.111	**0.012***	0.762	0.385	**0.050***	**0.007****

c)	Bare sand	Mobile	Fixed	Heath	Slack	Pasture	Scrub	Wood	Pine
Mobile	0.456								
Fixed	0.360	0.740							
Heath	**0.002****	**0.043***	**0.011***						
Slack	**0.001****	**0.013***	**0.002****	0.494					
Pasture	**0.004****	0.060	0.093	0.079	0.085				
Scrub	**0.014***	0.081	0.075	0.540	0.139	0.706			
Wood	**<0.001*****	**0.006****	**0.001****	0.925	0.494	0.057	0.306		
Pine	**0.001****	**0.007****	**0.002****	0.066	0.307	0.064	0.089	0.169	
Felled	0.391	1.000	0.940	**0.031***	**0.012***	0.186	0.241	**0.021***	**0.005****

d)	Bare sand	Mobile	Fixed	Heath	Slack	Pasture	Scrub	Wood	Pine
Mobile	0.804								
Fixed	0.095	0.298							
Heath	**0.002****	**0.030***	**0.008****						
Slack	**<0.001*****	**<0.001*****	**0.001****	**0.040***					
Pasture	**0.016***	**0.081***	0.132	0.086	**0.022***				
Scrub	**0.046***	0.106	0.353	0.391	0.098	0.910			
Wood	**<0.001*****	**0.011***	**0.007****	0.777	0.059	0.188	0.429		
Pine	**<0.001*****	**<0.001*****	**<0.001*****	0.055	0.699	**0.011***	0.064	**0.038***	
Felled	0.111	0.307	0.841	**0.028***	**0.004****	0.257	0.473	**0.028***	**0.001****

Table 3.7 Mann-Whitney U test results for topsoil geochemical parameters. Tables show MINITAB '*p*' values (**bold** text is significant (**p* <0.05; ***p* <0.01; ****p* <0.001)) for; a) Cl%; b) K%; c) Ca% and d) Fe% (n = 112)

a)	Bare sand	Mobile	Fixed	Heath	Slack	Pasture	Scrub	Wood	Pine
Mobile	0.434								
Fixed	0.281	0.057							
Heath	0.133	0.303	**0.011***						
Slack	**0.040***	0.065	**<0.001*****	0.197					
Pasture	0.713	0.339	0.152	0.055	**0.038***				
Scrub	0.967	0.717	0.209	0.348	0.062	0.850			
Wood	0.244	0.644	**0.021***	0.749	0.230	0.410	0.277		
Pine	**0.005****	**0.007****	**<0.001*****	**0.034***	0.307	**0.003****	**0.008****	0.070	
Felled	0.438	**0.041***	0.861	**0.003****	**0.004****	0.273	0.385	0.056	**<0.001****

b)	Bare sand	Mobile	Fixed	Heath	Slack	Pasture	Scrub	Wood	Pine
Mobile	0.414								
Fixed	0.389	**0.028***							
Heath	0.659	0.915	**0.015***						
Slack	0.197	0.644	**0.007****	0.323					
Pasture	0.838	0.249	0.407	0.236	0.098				
Scrub	0.596	0.531	**0.022***	1.000	0.275	0.212			
Wood	0.729	0.440	0.117	0.508	0.286	0.396	0.539		
Pine	**0.025***	0.075	**0.001****	**0.037***	0.149	**0.009****	**0.045***	**0.047***	
Felled	0.488	0.621	**0.047***	0.775	0.245	0.345	1.000	0.704	**0.038***

c)	Bare sand	Mobile	Fixed	Heath	Slack	Pasture	Scrub	Wood	Pine
Mobile	**0.008****								
Fixed	**<0.001*****	**0.014***							
Heath	**<0.001*****	**0.002****	**<0.001*****						
Slack	0.704	0.230	**0.004****	**<0.001*****					
Pasture	**0.001****	0.060	0.183	**<0.001*****	**0.032***				
Scrub	**0.007****	0.621	**0.047***	**<0.001*****	0.130	0.273			
Wood	**0.001****	0.157	0.827	**0.001****	**0.015***	0.429	0.188		
Pine	**0.004****	0.156	0.900	**0.008****	**0.022***	0.308	0.162	0.838	
Felled	**0.001****	0.060	0.821	**<0.001*****	**0.008****	0.241	0.141	0.578	0.910

d)	Bare sand	Mobile	Fixed	Heath	Slack	Pasture	Scrub	Wood	Pine
Mobile	0.214								
Fixed	0.360	0.493							
Heath	**0.008****	**0.051***	**0.001****						
Slack	0.362	**0.039***	0.110	**0.001****					
Pasture	0.653	0.199	0.238	**0.006****	0.379				
Scrub	0.462	**0.044***	0.060	**0.003****	0.597	0.273			
Wood	0.777	0.190	0.258	**0.006****	0.239	0.930	0.254		
Pine	0.055	0.410	**0.029***	0.131	**0.010***	**0.031***	**0.026***	**0.028***	
Felled	1.000	0.249	0.467	**0.008****	0.379	0.623	0.734	0.661	0.064

Table 3.8 Mann-Whitney U test results for topsoil parameters. Tables show MINITAB '*p*' values (**bold** text is significant (**p* <0.05; ***p* <0.01; ****p* <0.001)) for; a) χ_{LF} x$10^{-7}m^3kg^{-1}$; b) $\chi_{FD\%}$; c) χ_{ARM} x$10^{-7}m^3kg^{-1}$; d) SIRM x$10^{-5}Am^2kg^1$; e) $Soft_{IRM20mT}$ x$10^{-5}Am^2kg^{-1}$ and f) $Soft_{IRM40mT}$ x$10^{-5}Am^2kg^{-1}$(n = 113)

a)	Bare sand	Mobile	Fixed	Heath	Slack	Pasture	Scrub	Wood	Pine
Mobile	0.644								
Fixed	0.662	0.320							
Heath	0.724	0.414	0.980						
Slack	0.447	0.282	0.770	0.704					
Pasture	0.079	**0.011***	**0.026***	0.066	0.085				
Scrub	0.066	**0.023***	0.052	0.111	0.073	0.678			
Wood	**0.035***	**0.003****	**0.004****	**0.022***	**0.017***	0.884	0.930		
Pine	0.094	**0.027***	**0.006****	0.079	**0.032***	0.623	0.910	0.169	
Felled	0.153	**0.044***	0.131	0.236	0.218	1.000	0.791	0.747	0.970

b)	Bare sand	Mobile	Fixed	Heath	Slack	Pasture	Scrub	Wood	Pine
Mobile	0.943								
Fixed	0.440	0.459							
Heath	0.860	0.749	0.898						
Slack	0.403	0.644	0.982	0.820					
Pasture	0.653	0.818	0.867	0.967	0.888				
Scrub	0.414	0.575	0.666	0.713	0.699	0.910			
Wood	0.706	0.857	0.470	0.925	0.603	0.747	0.953		
Pine	0.807	0.767	0.811	0.967	0.860	0.970	0.940	0.725	
Felled	0.903	0.921	0.943	0.775	0.597	0.734	0.791	0.930	0.734

c)	Bare sand	Mobile	Fixed	Heath	Slack	Pasture	Scrub	Wood	Pine
Mobile	0.804								
Fixed	0.117	0.103							
Heath	0.158	0.127	0.817						
Slack	0.111	0.079	0.234	0.447					
Pasture	**0.010***	**0.003****	**0.037***	0.094	0.418				
Scrub	0.111	0.106	0.518	0.744	1.000	0.385			
Wood	**0.004****	**<0.001*****	**0.004****	**0.041***	0.565	0.930	0.254		
Pine	**0.006****	**0.004****	**0.033***	0.178	0.751	0.970	0.186	0.619	
Felled	**0.020***	**0.027***	0.157	0.236	0.916	0.521	0.571	0.501	0.970

d)	Bare sand	Mobile	Fixed	Heath	Slack	Pasture	Scrub	Wood	Pine
Mobile	0.696								
Fixed	0.368	0.144							
Heath	0.480	0.214	0.817						
Slack	0.704	0.479	0.406	0.403					
Pasture	**0.031***	**0.002****	**0.014***	0.111	**0.007****				
Scrub	0.111	**0.032***	0.144	0.270	0.085	0.970			
Wood	**0.013***	**<0.001*****	**0.002****	**0.035***	**<0.001*****	0.838	0.838		
Pine	**0.046***	**0.006****	**0.012***	0.178	**0.004****	0.345	0.910	0.230	
Felled	0.094	**0.038***	0.204	0.236	0.073	0.850	0.910	0.661	0.970

e)	Bare sand	Mobile	Fixed	Heath	Slack	Pasture	Scrub	Wood	Pine
Mobile	0.749								
Fixed	0.777	0.597							
Heath	0.185	0.082	0.076						
Slack	0.939	0.926	0.875	0.149					
Pasture	0.079	**0.027***	**0.009****	0.540	0.053				
Scrub	0.079	**0.044***	**0.020***	0.488	0.062	1.000			
Wood	**0.003****	**0.013***	**<0.001*****	0.270	**0.002****	0.661	0.464		
Pine	0.153	0.307	**0.047***	0.540	0.113	0.104	0.521	**0.021***	
Felled	0.072	0.052	**0.026***	0.653	0.062	1.000	0.910	0.704	0.345

f)	Bare sand	Mobile	Fixed	Heath	Slack	Pasture	Scrub	Wood	Pine
Mobile	0.749								
Fixed	0.898	0.512							
Heath	0.377	0.214	0.341						
Slack	0.879	0.601	0.840	0.362					
Pasture	**0.037***	**0.005****	**0.006****	0.131	**0.010***				
Scrub	0.131	0.060	0.065	0.488	0.073	0.678			
Wood	**0.009****	**0.003****	**<0.001*****	0.083	**0.003****	0.877	0.556		
Pine	0.111	0.070	**0.004****	0.713	**0.027***	0.212	0.850	**0.044***	
Felled	0.079	**0.027***	**0.018***	0.206	0.062	0.970	0.910	0.687	0.678

Table 3.9 Mann-Whitney U test results for topsoil parameters. Tables show MINITAB '*p*' values (**bold** text is significant (**p* <0.05; ***p* <0.01; ****p* <0.001)) for; a) $HardIRM_{300mT}$ $x10^{-5}Am^2kg^{-1}$; b) $Hard_{IRM500mT}$ $x10^{-5}Am^2kg^{-1}$; c) $Soft_{\%20mT}$; d) $Soft_{\%40mT}$; e) $Hard_{\%300mT}$ and f) $Hard_{\%500mT}$ (n = 113)

a)	Bare sand	Mobile	Fixed	Heath	Slack	Pasture	Scrub	Wood	Pine
Mobile	0.060								
Fixed	0.396	0.112							
Heath	0.427	0.095	0.939						
Slack	0.129	0.644	0.381	0.447					
Pasture	0.653	**<0.001*****	0.065	0.111	**0.010***				
Scrub	0.236	**0.004****	**0.023***	0.055	**0.015***	0.427			
Wood	0.270	**0.001****	**0.008****	**0.018***	**0.004****	0.230	0.578		
Pine	0.967	**0.019***	0.303	0.307	0.073	0.521	0.199	0.065	
Felled	0.775	0.060	0.303	0.438	0.149	0.678	0.241	0.747	1.000

b)	Bare sand	Mobile	Fixed	Heath	Slack	Pasture	Scrub	Wood	Pine
Mobile	**0.017***								
Fixed	**0.022***	0.849							
Heath	0.331	0.051	0.054						
Slack	**0.040***	0.689	0.637	0.095					
Pasture	0.540	**0.023***	**0.014***	0.838	**0.018***				
Scrub	0.713	**0.005****	**0.007****	0.153	**0.015***	0.212			
Wood	0.637	**0.001****	**<0.001*****	0.108	**0.001****	0.074	0.930		
Pine	0.111	0.138	0.222	0.391	0.307	0.186	**0.031***	**0.009****	
Felled	0.713	0.156	0.131	0.775	0.307	1.000	0.385	0.364	0.427

c)	Bare sand	Mobile	Fixed	Heath	Slack	Pasture	Scrub	Wood	Pine
Mobile	0.644								
Fixed	**0.022***	**0.024***							
Heath	0.112	0.337	**<0.001****						
Slack	0.494	0.340	0.092	0.081					
Pasture	0.713	0.489	0.187	0.079	0.972				
Scrub	0.540	0.307	0.131	**0.016***	0.916	0.970			
Wood	0.925	0.589	0.065	0.139	0.805	0.792	0.704		
Pine	**0.013***	**0.023***	0.222	**0.002****	**0.027***	0.089	0.089	**0.033***	
Felled	0.903	0.410	**0.029***	**0.046***	0.647	0.678	0.791	1.000	**0.031***

d)	Bare sand	Mobile	Fixed	Heath	Slack	Pasture	Scrub	Wood	Pine
Mobile	0.303								
Fixed	**0.001****	**<0.001*****							
Heath	0.659	0.303	**<0.001*****						
Slack	0.494	0.230	**0.003****	0.224					
Pasture	0.540	0.818	**0.020***	0.596	0.275				
Scrub	0.270	**0.038***	0.240	0.131	0.550	0.141			
Wood	0.469	0.173	**0.003****	0.395	0.978	0.429	0.464		
Pine	**0.003****	**0.002****	0.905	**<0.001*****	**0.010***	**0.038***	0.308	**0.008****	
Felled	0.775	0.249	**<0.001*****	1.000	0.307	0.521	0.212	0.464	**0.001****

e)	Bare sand	Mobile	Fixed	Heath	Slack	Pasture	Scrub	Wood	Pine
Mobile	**0.021***								
Fixed	**0.002****	0.626							
Heath	**0.002****	0.414	0.738						
Slack	**0.003****	0.340	0.637	0.939					
Pasture	**0.006****	0.093	0.144	0.206	0.550				
Scrub	0.111	0.668	0.240	0.178	0.193	0.162			
Wood	**0.002****	0.173	0.314	0.469	0.805	0.334	0.151		
Pine	**<0.001*****	**0.027***	**0.023***	0.066	0.170	0.791	**0.045***	0.169	
Felled	**<0.001*****	0.156	0.222	0.391	0.597	0.791	0.089	0.704	0.385

f)	Bare sand	Mobile	Fixed	Heath	Slack	Pasture	Scrub	Wood	Pine
Mobile	**0.030***								
Fixed	**0.001****	0.122							
Heath	**0.042***	0.644	0.105						
Slack	**0.006****	0.372	0.574	0.197					
Pasture	**0.005****	0.277	0.905	0.131	0.504				
Scrub	**0.031***	0.921	0.187	1.000	0.307	0.385			
Wood	**0.006****	0.341	0.134	0.592	0.396	0.169	0.429		
Pine	**<0.001*****	0.052	0.518	**0.002****	**0.038***	0.623	0.064	**0.002****	
Felled	**0.002****	0.070	0.867	0.055	0.379	0.910	0.162	0.057	0.385

Table 3.10 Mann-Whitney U test results for topsoil parameters. Tables show MINITAB '*p*' values (**bold** text is significant (**p* <0.05; ***p* <0.01; ****p* <0.001)) for; a) S-ratio, b) ARM/χ x10^{-2}Am^{-1}, c) SIRM/ARM, d) χ_{ARM}/SIRM x10^{-5}Am^{-1} and e) SIRM/χ x10^{-2}Am^{-1} (n = 113)

a)	Bare sand	Mobile	Fixed	Heath	Slack	Pasture	Scrub	Wood	Pine
Mobile	0.696								
Fixed	0.396	0.485							
Heath	**0.042***	0.082	**0.048***						
Slack	0.595	0.601	0.121	**0.028***					
Pasture	0.307	0.121	0.014	**0.006****	0.460				
Scrub	0.438	0.767	0.981	0.153	0.342	**0.045***			
Wood	0.682	0.700	0.582	**0.035***	0.366	**0.050***	0.747		
Pine	0.206	0.373	0.058	**0.013***	0.972	0.473	0.121	0.151	
Felled	0.540	0.339	0.080	**0.008****	0.916	0.345	0.141	0.188	0.521

b)	Bare sand	Mobile	Fixed	Heath	Slack	Pasture	Scrub	Wood	Pine
Mobile	0.214								
Fixed	0.173	0.783							
Heath	**0.034***	0.374	0.817						
Slack	0.058	0.207	0.357	0.543					
Pasture	0.206	0.489	0.792	0.903	0.699				
Scrub	0.838	0.489	0.260	0.066	0.149	0.212			
Wood	0.176	0.738	0.864	1.000	0.338	0.704	0.364		
Pine	0.079	0.668	0.429	0.307	0.275	0.571	0.186	0.704	
Felled	0.488	0.489	0.119	**0.031***	0.098	0.186	0.850	0.279	0.104

c)	Bare sand	Mobile	Fixed	Heath	Slack	Pasture	Scrub	Wood	Pine
Mobile	0.110								
Fixed	0.341	0.882							
Heath	0.158	0.972	0.625						
Slack	0.058	0.166	0.111	0.058					
Pasture	0.270	0.921	0.684	0.775	0.245				
Scrub	0.838	0.177	0.260	0.348	**0.032***	0.241			
Wood	0.469	0.662	0.747	0.875	0.067	0.578	0.364		
Pine	0.307	0.818	0.649	0.653	0.062	0.910	0.473	0.838	
Felled	0.967	0.121	0.326	0.178	**0.038***	0.385	0.678	0.396	0.427

d)	Bare sand	Mobile	Fixed	Heath	Slack	Pasture	Scrub	Wood	Pine
Mobile	0.110								
Fixed	0.341	0.882							
Heath	0.158	0.972	0.625						
Slack	0.058	0.166	0.111	0.058					
Pasture	0.270	0.921	0.684	0.775	0.245				
Scrub	0.838	0.177	0.260	0.348	**0.032***	0.241			
Wood	0.469	0.662	0.747	0.875	0.067	0.578	0.364		
Pine	0.307	0.818	0.649	0.653	0.062	0.910	0.473	0.838	
Felled	0.967	0.121	0.326	0.178	**0.038***	0.385	0.678	0.396	0.427

e)	Bare sand	Mobile	Fixed	Heath	Slack	Pasture	Scrub	Wood	Pine
Mobile	0.859								
Fixed	**0.004****	**0.015***							
Heath	**0.002****	**0.004****	0.227						
Slack	0.197	0.132	**<0.001*****	**<0.001*****					
Pasture	0.131	0.156	0.719	0.713	**0.032***				
Scrub	0.838	0.818	0.072	0.055	0.460	0.212			
Wood	**0.002****	**0.004****	0.482	0.592	**<0.001*****	0.792	0.050		
Pine	0.066	0.138	0.905	0.348	**0.012***	0.734	0.162	0.396	
Felled	0.178	0.448	0.065	**0.031***	**0.027***	0.308	0.385	**0.024***	0.385

Table 3.11 Summary data* for topsoil physico-chemical characteristics of the bare sand environment (n = 9)

Parameters	Units	Mean	Median	SD	CV	Min	Max
pH	mol/ltr	8.088	8.000	0.382	4.722	7.620	8.680
SOM	%	0.210	0.225	0.067	31.893	0.108	0.325
Sand	%	88.401	88.616	4.056	4.588	81.687	95.335
Silt	%	7.278	7.737	4.315	59.292	0.726	14.769
Clay	%	4.321	3.939	0.859	19.872	3.525	5.716
Mean particle size	µm	236.029	238.405	13.401	5.678	210.570	249.134
Median particle size	µm	238.870	241.144	9.526	3.988	221.291	250.137
Sorting		1.139	1.205	0.366	32.101	0.488	1.531
Skewness	γ_1	0.414	0.421	0.165	39.763	0.075	0.699
Kurtosis	g_1	3.853	3.951	1.614	41.887	1.352	6.059
Carbon	%	0.297	0.071	0.529	178.278	0.018	1.665
Nitrogen	%	0.021	0.007	0.035	168.005	0.002	0.112
Sodium	%	2.034	2.060	0.175	8.588	1.790	2.410
Magnesium	%	0.432	0.410	0.078	18.151	0.359	0.625
Aluminium	%	0.241	0.271	0.096	39.783	0.110	0.431
Silicon	%	37.700	37.810	1.396	3.680	35.950	40.540
Phosphorus	%	0.017	0.015	0.006	36.708	0.011	0.032
Sulphur	%	0.000	0.000	0.000		0.000	0.001
Chlorine	%	0.015	0.010	0.011	76.283	0.007	0.043
Potassium	%	0.590	0.552	0.082	13.853	0.519	0.759
Calcium	%	1.611	1.544	0.426	26.437	1.074	2.579
Iron	%	1.024	0.967	0.291	28.386	0.702	1.646
χ_{LF}	$10^{-7}m^3kg^{-1}$	1.302	1.012	1.127	86.527	0.336	3.853
χ_{FD}	%	1.914	1.743	1.352	70.627	0.000	5.000
χ_{ARM}	$10^{-7}m^3kg^{-1}$	0.018	0.012	0.011	62.633	0.007	0.043
SIRM	$10^{-5}Am^2kg^{-1}$	149.528	120.887	119.903	80.188	41.398	410.980
$Soft_{IRM20mT}$	$10^{-5}Am^2kg^{-1}$	24.068	22.714	15.409	64.021	9.382	59.533
$Soft_{IRM40mT}$	$10^{-5}Am^2kg^{-1}$	60.196	51.640	48.071	79.858	20.099	172.572
$Hard_{IRM300mT}$	$10^{-5}Am^2kg^{-1}$	23.025	18.761	18.555	80.587	5.919	63.074
$Hard_{IRM500mT}$	$10^{-5}Am^2kg^{-1}$	14.832	10.261	12.059	81.303	2.885	40.849
$Soft_{\%20mT}$	%	18.285	18.790	3.855	21.082	12.529	24.534
$Soft_{\%40mT}$	%	41.826	41.990	4.280	10.232	36.209	48.551
$Hard_{\%300mT}$	%	15.707	15.519	3.707	23.602	9.457	23.500
$Hard_{\%500mT}$	%	10.543	11.321	4.162	39.476	4.115	16.205
S-ratio	(none)	-0.650	-0.649	0.075	-11.541	-0.820	-0.563
ARM/χ	$10^{-2}Am^{-1}$	0.017	0.015	0.007	40.484	0.010	0.032
SIRM/ARM	(None)	244.601	248.514	73.803	30.173	121.344	349.041
χ_{ARM}/SIRM	$10^{-5}Am^2kg^{-1}$	1.428	0.013	0.560	39.245	0.900	2.588
SIRM/χ	$10^{-2}Am^{-1}$	118.134	119.478	9.868	8.354	103.784	137.515

Table 3.12 Summary data* for topsoil physico-chemical characteristics of the mobile dune community environment (n = 12)

Parameters	Units	Mean	Median	SD	CV	Min	Max
pH	mol/ltr	7.717	7.670	0.868	11.247	6.490	8.840
SOM	%	2.148	0.271	6.043	281.295	0.101	21.289
Sand	%	83.158	84.482	9.528	11.458	67.710	96.067
Silt	%	13.261	12.145	10.319	77.818	0.396	30.817
Clay	%	3.582	3.461	1.296	36.182	1.279	6.918
Mean particle size	µm	220.342	216.780	32.877	14.921	168.459	259.500
Median particle size	µm	225.436	226.581	29.661	13.157	159.175	258.096
Sorting		1.287	1.412	0.506	39.330	0.404	2.049
Skewness	γ_1	0.488	0.465	0.220	44.999	0.014	0.743
Kurtosis	g_1	2.584	2.574	1.595	61.733	0.950	6.058
Carbon	%	0.506	0.160	0.916	181.221	0.021	3.170
Nitrogen	%	0.040	0.010	0.075	188.898	0.003	0.262
Sodium	%	2.895	2.115	2.726	94.157	1.810	11.530
Magnesium	%	0.338	0.330	0.126	37.311	0.001	0.485
Aluminium	%	0.164	0.179	1.000	608.989	0.000	0.321
Silicon	%	34.700	38.315	11.317	32.613	0.210	40.860
Phosphorus	%	0.038	0.020	0.054	143.059	0.005	0.188
Sulphur	%	0.019	0.000	0.050	256.503	0.000	0.164
Chlorine	%	3.449	0.013	11.901	345.099	0.008	41.240
Potassium	%	0.507	0.548	0.169	33.329	0.001	0.647
Calcium	%	1.028	1.007	0.435	42.348	0.033	1.742
Iron	%	0.811	0.857	0.306	37.757	0.004	1.214
χ_{LF}	$10^{-7}m^3kg^{-1}$	1.047	0.902	0.746	71.254	0.275	2.731
χ_{FD}	%	2.054	1.833	1.328	64.640	0.125	4.135
χ_{ARM}	$10^{-7}m^3kg^{-1}$	0.018	0.015	0.009	48.889	0.010	0.036
SIRM	$10^{-5}Am^2kg^{-1}$	119.345	111.582	75.804	63.517	38.066	261.926
$Soft_{IRM20mT}$	$10^{-5}Am^2kg^{-1}$	23.308	15.938	17.008	72.970	5.015	61.022
$Soft_{IRM40mT}$	$10^{-5}Am^2kg^{-1}$	51.646	38.355	33.821	65.486	16.249	113.487
$Hard_{IRM300mT}$	$10^{-5}Am^2kg^{-1}$	10.483	10.098	4.631	44.180	4.700	19.221
$Hard_{IRM500mT}$	$10^{-5}Am^2kg^{-1}$	5.542	5.114	3.548	64.023	1.726	14.496
$Soft_{\%20mT}$	%	19.457	20.375	5.740	29.503	10.511	26.698
$Soft_{\%40mT}$	%	43.411	45.048	6.622	15.253	31.702	51.266
$Hard_{\%300mT}$	%	10.605	10.142	4.160	39.223	3.383	17.621
$Hard_{\%500mT}$	%	6.400	6.286	4.295	67.102	0.659	16.424
S-ratio	(none)	-0.645	-0.635	0.088	-13.637	-0.845	-0.515
ARM/χ	$10^{-2}Am^{-1}$	0.021	0.018	0.008	40.222	0.012	0.036
SIRM/ARM	(None)	200.090	212.580	55.073	27.524	106.490	269.112
χ_{ARM}/SIRM	$10^{-5}Am^2kg^{-1}$	1.712	0.015	0.579	33.852	1.175	3.551
SIRM/χ	$10^{-2}Am^{-1}$	119.547	118.861	15.777	13.197	90.275	146.533

*Mean; Median; SD = standard deviation; CV = percentage coefficient of variation; Min = minimum value; Max = maximum value. Values are shown to 3 decimal places for consistency, not accuracy.

$x10^{-5}Am^{-2}kg^{-1}$), likely to be magnetically-soft minerals, such as Magnetite (Fe_3O_4) and Maghaemite (γFe_2O_3).

3.4.2 Mobile dune community topsoil pedo-characteristics

Table 3.12 presents summary data for the mobile dune topsoil samples (n = 12). The pH (6.49-8.84) represents the beginning of an alkaline-neutral transitional environment in dune succession. SOM (0.10-21.29%) represents the second lowest median (0.27%) for the entire dune system. Mean particle size (168.46-259.50 µm) categorizes this environment as medium sand, with sand contributing a median 84.48% to the textural total. These values, alongside those of the bare sand topsoils, are significantly different (p <0.05) from all other remaining dune topsoils. The very low levels of C (0.02-3.17%) and N (<0.01-0.26) calculated for bare sand and mobile dune topsoils combined, are significantly different (p <0.01) from all other topsoils (Figure 3.3c). Magnetic concentration-dependent parameters show lower quantities of magnetic minerals (χ_{LF} 0.28-2.73 $x10^{-7}m^3kg^{-1}$; χ_{ARM} 0.01-0.04 $x10^{-7}m^3kg^{-1}$; SIRM 38.07-261.93 $x10^{-5}m^2kg^{-1}$) in the mobile dune topsoils, than the bare sand environment.

3.4.3 Fixed dune community topsoil pedo-characteristics

Table 3.13 presents summary data for the fixed dune topsoil samples (n = 18). The pH (5.01-7.83) represents a neutral-acidic transitional environment in dune succession, in which SOM values (0.41-24.51%) had increased. Mean particle size (124.29-203.17 µm) represents the fixed dunes as the first successional environment to be categorized as fine sand. Sand only contributes to a median 68.37% of the textural total. C (0.06-4.44%) and N (0.01-0.39%) increased as dune succession continued, while K (0.53-0.69) is significantly higher (p <0.05) from mobile dunes (Figure 3.4e). Mg (0.26-0.40%) decreased and is significantly different (p <0.001) from bare sand. SIRM (60.24-432.76 $x10^{-5}m^2kg^{-1}$) shows almost double concentrations of magnetic minerals than in mobile dune topsoils.

3.4.4 Heath topsoil pedo-characteristics

Table 3.14 presents summary data for the dune heath topsoil samples (n = 9). The lowest pH values (3.10-4.31) occur in the heath topsoils and are significantly lower (p <0.01) from all other topsoils (Figure 3.3a). Although heath has overall lowest percentages of clay (1.33-2.46%) for the entire dune system, values are only significantly different (p <0.05) from bare sand and mobile topsoils (Figure 3.3b). Increased C (1.21-6.14%), N (0.10-0.35%) and P (33.76-38.93%) were observed, with N and P significantly higher (p <0.01) on fixed dunes. Decreases were evident in Na (1.35-2.19%), Mg (0.11-0.28%) and especially Ca (0.07-0.12%), which is significantly different (p <0.01) from all remaining dune environments, except coniferous plantations.

3.4.5 Slack community topsoil pedo-characteristics

Table 3.15 presents summary data for the slack topsoil samples (n = 11). SOM (0.94-61.24%) was significantly higher (p <0.01) than on the comparable-aged fixed dunes. Despite being

Table 3.13 Summary data* for topsoil physico-chemical characteristics of the fixed dune environment (n = 18)

Parameters	Units	Mean	Median	SD	CV	Min	Max
pH	mol/ltr	6.391	6.365	0.831	13.001	5.010	7.830
SOM	%	4.426	1.984	6.013	135.840	0.406	24.508
Sand	%	68.673	68.366	5.707	8.310	51.373	77.897
Silt	%	28.651	28.645	5.558	19.397	19.020	43.888
Clay	%	2.676	2.504	0.880	32.887	1.715	4.739
Mean particle size	µm	173.907	179.068	19.818	11.396	124.294	203.174
Median particle size	µm	184.074	199.660	38.462	20.895	65.518	218.357
Sorting		1.854	1.841	0.176	9.515	1.649	2.389
Skewness	γ_1	0.656	0.696	0.128	19.526	0.252	0.762
Kurtosis	g_1	1.179	0.949	0.647	54.877	0.863	3.036
Carbon	%	1.647	1.274	1.416	85.965	0.063	4.437
Nitrogen	%	0.114	0.090	0.106	93.001	0.005	0.390
Sodium	%	2.039	2.070	0.210	10.317	1.570	2.290
Magnesium	%	0.314	0.314	0.039	12.577	0.262	0.395
Aluminium	%	0.214	0.207	0.098	45.704	0.054	0.360
Silicon	%	38.438	39.370	2.913	7.579	30.340	40.910
Phosphorus	%	0.027	0.018	0.024	86.483	0.007	0.105
Sulphur	%	0.014	0.000	0.037	260.368	0.000	0.152
Chlorine	%	0.011	0.009	0.005	45.004	0.006	0.023
Potassium	%	0.599	0.598	0.043	7.175	0.527	0.691
Calcium	%	0.620	0.643	0.361	58.199	0.123	1.210
Iron	%	0.907	0.865	0.142	15.601	0.752	1.311
χ_{LF}	$10^{-7}m^3kg^{-1}$	1.191	1.062	0.629	52.796	0.419	3.153
χ_{FD}	%	2.496	2.655	1.648	65.997	0.000	5.462
χ_{ARM}	$10^{-7}m^3kg^{-1}$	0.024	0.019	0.013	53.479	0.012	0.059
SIRM	$10^{-5}Am^2kg^{-1}$	156.641	136.523	82.625	52.748	60.240	432.761
$Soft_{IRM20mT}$	$10^{-5}Am^2kg^{-1}$	21.862	18.504	12.771	58.417	8.384	64.562
$Soft_{IRM40mT}$	$10^{-5}Am^2kg^{-1}$	51.325	47.395	27.208	53.010	17.425	143.598
$Hard_{IRM300mT}$	$10^{-5}Am^2kg^{-1}$	14.941	14.302	8.094	54.178	3.677	37.216
$Hard_{IRM500mT}$	$10^{-5}Am^2kg^{-1}$	6.073	4.617	4.717	77.675	0.497	17.438
$Soft_{\%20mT}$	%	14.298	13.378	4.332	30.301	9.603	25.040
$Soft_{\%40mT}$	%	33.220	31.914	5.309	15.983	27.618	48.118
$Hard_{\%300mT}$	%	9.926	9.748	3.868	38.970	3.814	19.956
$Hard_{\%500mT}$	%	4.331	3.532	3.204	73.977	0.231	13.273
S-ratio	(none)	-0.621	-0.623	0.050	-8.097	-0.705	-0.537
ARM/χ	$10^{-2}Am^{-1}$	0.022	0.022	0.008	37.971	0.008	0.035
SIRM/ARM	(None)	227.476	195.150	105.043	46.178	116.115	443.407
χ_{ARM}/SIRM	$10^{-5}Am^2kg^{-1}$	1.631	0.016	0.616	37.788	0.708	2.705
SIRM/χ	$10^{-2}Am^{-1}$	133.546	133.894	11.714	8.771	102.489	151.185

Table 3.14 Summary data* for topsoil physico-chemical characteristics of the heath community environment (n = 9)

Parameters	Units	Mean	Median	SD	CV	Min	Max
pH	mol/ltr	3.863	3.950	0.367	9.495	3.100	4.310
SOM	%	6.814	6.612	3.952	58.001	1.826	13.770
Sand	%	66.798	67.550	1.901	2.847	64.075	69.035
Silt	%	31.441	31.119	1.871	5.951	29.018	33.838
Clay	%	1.761	1.722	0.398	22.595	1.331	2.462
Mean particle size	µm	166.010	163.329	7.186	4.328	159.083	177.322
Median particle size	µm	172.757	167.949	12.600	7.294	159.069	196.540
Sorting		1.727	1.676	0.112	6.506	1.582	1.887
Skewness	γ_1	0.596	0.596	0.061	10.164	0.528	0.701
Kurtosis	g_1	0.895	0.891	0.025	2.826	0.865	0.954
Carbon	%	3.421	3.557	1.560	45.593	1.212	6.136
Nitrogen	%	0.223	0.251	0.087	39.250	0.098	0.351
Sodium	%	1.752	1.770	0.236	13.459	1.350	2.190
Magnesium	%	0.189	0.186	0.047	24.892	0.111	0.277
Aluminium	%	0.304	0.306	0.064	21.052	0.207	0.434
Silicon	%	35.697	34.940	1.906	5.341	33.760	38.930
Phosphorus	%	0.047	0.052	0.016	34.945	0.017	0.067
Sulphur	%	0.036	0.029	0.022	61.041	0.000	0.058
Chlorine	%	0.018	0.016	0.008	45.855	0.008	0.037
Potassium	%	0.555	0.540	0.030	5.359	0.508	0.596
Calcium	%	0.092	0.090	0.017	18.537	0.073	0.117
Iron	%	0.705	0.669	0.125	17.786	0.601	0.978
χ_{LF}	$10^{-7}m^3kg^{-1}$	1.202	1.102	0.658	54.766	0.418	2.222
χ_{FD}	%	2.746	1.571	2.555	93.015	0.748	8.511
χ_{ARM}	$10^{-7}m^3kg^{-1}$	0.026	0.020	0.014	53.715	0.010	0.050
SIRM	$10^{-5}Am^2kg^{-1}$	176.225	151.136	105.121	59.651	52.876	360.189
$Soft_{IRM20mT}$	$10^{-5}Am^2kg^{-1}$	38.022	33.537	23.396	61.531	12.351	80.859
$Soft_{IRM40mT}$	$10^{-5}Am^2kg^{-1}$	75.144	58.757	45.474	60.516	23.244	142.312
$Hard_{IRM300mT}$	$10^{-5}Am^2kg^{-1}$	14.500	14.589	5.932	40.908	6.085	20.927
$Hard_{IRM600mT}$	$10^{-5}Am^2kg^{-1}$	9.232	8.252	4.986	54.009	2.845	18.443
$Soft_{\%20mT}$	%	21.790	22.190	4.025	18.473	15.744	27.476
$Soft_{\%40mT}$	%	42.461	43.310	3.052	7.188	38.877	48.358
$Hard_{\%300mT}$	%	9.180	9.320	1.951	21.248	5.696	11.886
$Hard_{\%600mT}$	%	5.780	5.381	2.139	37.005	2.575	10.518
S-ratio	(none)	-0.599	-0.566	0.158	-26.338	-0.996	-0.457
ARM/χ	$10^{-2}Am^{-1}$	0.022	0.023	0.003	12.325	0.018	0.026
SIRM/ARM	(None)	208.699	218.636	26.304	12.604	170.696	240.452
χ_{ARM}/SIRM	$10^{-5}Am^2kg^{-1}$	1.528	0.014	0.206	13.484	1.306	1.840
SIRM/χ	$10^{-2}Am^{-1}$	142.693	137.201	14.358	10.062	126.497	162.130

Mean; Median; SD = standard deviation; CV = percentage coefficient of variation; Min = minimum value; Max = maximum value. Values are shown to 3 decimal places for consistency, not accuracy.

assumed younger, this topsoil also had significantly higher SOM (p <0.05) than pasture and felled topsoils. The lowest percentage of sand (median 64.76%) contributing to the textural total occurred in the slacks, alongside the highest percentages of silt (median 33.11%). Clay was significantly different (p <0.05) from bare sand and mobile dune topsoils (Figure 3.3b). C (0.38-4.66%) was higher than in the fixed dunes, while Na (0.55-2.19%) and Si (13.17-39-50%) concentrations fell. Despite overall levels of Ca (0.36-8.15%) decreasing with dune succession, they were significantly higher (p <0.01) in slacks than on fixed dunes. Magnetic concentration-dependent parameters (χ_{LF} 0.69-2.74 x10^{-7}m^{3}kg^{-1}; χ_{ARM} 0.01-0.12 x10^{-7}m^{3}kg^{-1}; SIRM 81.08-272.77 x10^{-5}m^{2}kg^{-1}) were extremely low compared to fixed dunes and heath topsoils, with χ_{LF} significantly different (p <0.05) from all previous dune succession environments.

3.4.6 Pasture topsoil pedo-characteristics

Table 3.16 presents summary data for the pasture topsoil samples (n = 10). In terms of succession, C (0.09-5.10%) was significantly lower (p <0.05) than in the heath (Figure 3.3c). SIRM (78.25-504.26 x10^{-5}m^{2}kg^{-1}) was significantly different (p <0.01) from mobile dune topsoils, with almost double concentrations of magnetic minerals (Figure 3.3f). Magnetic mineralogical-dependent parameters ($Soft_{IRM20mT}$ and $Soft_{IRM40mT}$) had the highest combined value (60.49%), indicating the presence of ferrimagnetic 'magnetite-type' soft mineralogy.

3.4.7 Scrub topsoil pedo-characteristics

Table 3.17 presents summary data for the scrub topsoil samples (n = 10). Magnetic concentration-dependent parameters (χ_{LF} 0.62-17.72 x10^{-7}m^{3}kg^{-1}; χ_{ARM} 0.01-0.70 x10^{-7}m^{3}kg^{-1}; SIRM 66.12-11786.52 x10^{-5}m^{2}kg^{-1}) were extreme, representing the highest topsoil values for all environments on the Sefton coast. Increases in Hard parameters (IRM_{300mT} and IRM_{500mT}), were significantly different (p <0.01) from fixed dunes, indicating a greater influence of canted antiferromagnetic 'haematite-type' hard minerals (1.45-45.90%) in scrub topsoils. Relatively high SIRM/ARM (113.74-527.10) and SIRM/χ (93.53-665.24 x10^{-2}Am^{-1}) ratios suggest these topsoils possibly contained more coarse (multidomain) magnetic materials than previous successional environments.

3.4.8 Deciduous woodland topsoil pedo-characteristics

Table 3.18 presents summary data for the deciduous woodland topsoil samples (n = 14). Although woodland topsoils are acidic (3.89-7.37), the pH in heath topsoils was significantly lower (p <0.001) (Figure 3.3a). SOM (2.36-77.17%) represented the second highest on the entire Sefton coast, second to coniferous plantation. Na (0.66-10.33%) was extremely high, as was Cl (0.01-38.69%), reaching similar values to those found in bare sand sediments, indicating a high salt (NaCl) content.

Table 3.15 Summary data* for topsoil physico-chemical characteristics of the slack environment (n = 11)

Parameters	Units	Mean	Median	SD	CV	Min	Max
pH	mol/ltr	6.733	6.860	0.665	9.876	5.260	7.740
SOM	%	18.709	7.522	20.431	109.201	0.940	61.244
Sand	%	63.335	64.760	7.819	12.346	48.991	72.405
Silt	%	34.380	33.114	7.137	20.759	25.275	47.178
Clay	%	2.285	1.974	0.933	40.828	1.312	3.831
Mean particle size	µm	153.385	161.355	29.749	19.395	98.924	195.689
Median particle size	µm	141.557	154.247	50.543	35.705	57.419	215.412
Sorting		1.873	1.798	0.166	8.838	1.671	2.151
Skewness	γ_1	0.488	0.559	0.165	33.790	0.209	0.701
Kurtosis	g_1	0.931	0.934	0.025	2.657	0.886	0.973
Carbon	%	2.448	2.351	1.613	65.876	0.379	4.656
Nitrogen	%	0.163	0.147	0.101	61.888	0.032	0.288
Sodium	%	1.682	1.820	0.471	27.984	0.551	2.190
Magnesium	%	0.335	0.332	0.071	21.272	0.241	0.476
Aluminium	%	0.253	0.171	0.242	95.787	0.039	0.912
Silicon	%	30.960	32.100	7.474	24.140	13.170	39.500
Phosphorus	%	0.072	0.053	0.047	64.971	0.017	0.148
Sulphur	%	0.123	0.094	0.115	93.445	0.000	0.345
Chlorine	%	0.030	0.025	0.023	77.040	0.009	0.090
Potassium	%	0.530	0.527	0.086	16.278	0.367	0.706
Calcium	%	2.361	1.201	2.419	102.447	0.361	8.148
Iron	%	1.489	1.152	0.978	65.665	0.684	4.030
χ_{LF}	$10^{-7}m^3kg^{-1}$	1.264	1.198	0.599	47.375	0.692	2.735
χ_{FD}	%	2.644	2.041	1.982	74.963	0.198	5.882
χ_{ARM}	$10^{-7}m^3kg^{-1}$	0.048	0.027	0.041	86.897	0.006	0.122
SIRM	$10^{-5}Am^2kg^{-1}$	131.117	103.476	61.131	46.624	81.078	272.774
$Soft_{IRM20mT}$	$10^{-5}Am^2kg^{-1}$	23.586	23.263	15.189	64.402	8.999	61.443
$Soft_{IRM40mT}$	$10^{-5}Am^2kg^{-1}$	53.955	44.297	31.086	57.616	25.433	135.513
$Hard_{IRM300mT}$	$10^{-5}Am^2kg^{-1}$	12.011	10.527	5.954	49.566	4.226	21.558
$Hard_{IRM500mT}$	$10^{-5}Am^2kg^{-1}$	5.876	5.765	2.886	49.120	1.099	10.540
$Soft_{S20mT}$	%	17.289	17.319	5.334	30.851	9.895	25.594
$Soft_{S40mT}$	%	40.229	38.526	6.482	16.112	31.369	49.680
$Hard_{S300mT}$	%	9.304	8.775	3.161	33.981	4.865	15.931
$Hard_{S500mT}$	%	4.826	4.280	2.636	54.629	1.265	10.842
S-ratio	(none)	-0.660	-0.668	0.069	-10.516	-0.787	-0.569
ARM/χ	$10^{-2}Am^{-1}$	0.038	0.023	0.033	86.368	0.005	0.106
SIRM/ARM	(None)	161.454	150.267	124.407	77.054	34.126	454.545
χ_{ARM}/SIRM	$10^{-5}Am^2kg^{-1}$	3.649	0.021	3.189	87.380	0.691	9.203
SIRM/χ	$10^{-2}Am^{-1}$	106.743	113.338	21.949	20.562	58.339	135.330

Table 3.16 Summary data* for topsoil physico-chemical characteristics of the pasture environment (n = 10)

Parameters	Units	Mean	Median	SD	CV	Min	Max
pH	mol/ltr	6.845	6.945	0.629	9.190	5.450	7.730
SOM	%	4.775	2.767	8.698	182.148	0.335	29.363
Sand	%	72.401	70.964	6.197	8.559	64.829	82.024
Silt	%	25.484	26.675	6.125	24.034	14.638	32.471
Clay	%	2.115	2.361	0.942	44.544	0.000	3.338
Mean particle size	µm	178.181	172.596	19.149	10.747	146.636	212.017
Median particle size	µm	190.097	183.235	23.586	12.408	146.096	222.451
Sorting		1.683	1.721	0.250	14.849	1.140	1.963
Skewness	γ_1	0.647	0.666	0.080	12.384	0.449	0.716
Kurtosis	g_1	1.364	0.958	0.827	60.644	0.893	3.072
Carbon	%	2.340	1.850	1.466	62.659	0.085	5.095
Nitrogen	%	0.180	0.154	0.132	73.325	0.009	0.501
Sodium	%	1.976	2.005	0.252	12.741	1.500	2.440
Magnesium	%	0.327	0.324	0.051	15.635	0.262	0.442
Aluminium	%	0.284	0.256	0.171	60.444	0.097	0.686
Silicon	%	36.224	37.365	4.598	12.692	23.890	40.110
Phosphorus	%	0.039	0.032	0.032	80.742	0.019	0.126
Sulphur	%	0.034	0.015	0.069	203.308	0.000	0.230
Chlorine	%	0.018	0.011	0.023	127.237	0.008	0.083
Potassium	%	0.582	0.586	0.053	9.033	0.498	0.667
Calcium	%	0.800	0.733	0.288	36.032	0.411	1.262
Iron	%	0.959	0.951	0.181	18.868	0.638	1.250
χ_{LF}	$10^{-7}m^3kg^{-1}$	2.000	2.111	0.904	45.208	0.693	3.331
χ_{FD}	%	2.327	1.996	1.467	63.045	0.719	5.398
χ_{ARM}	$10^{-7}m^3kg^{-1}$	0.057	0.031	0.048	85.234	0.016	0.147
SIRM	$10^{-5}Am^2kg^{-1}$	279.804	277.442	128.211	45.822	78.251	504.258
$Soft_{IRM20mT}$	$10^{-5}Am^2kg^{-1}$	50.675	48.873	38.353	75.684	11.828	147.337
$Soft_{IRM40mT}$	$10^{-5}Am^2kg^{-1}$	125.294	119.222	79.159	63.178	39.174	296.913
$Hard_{IRM300mT}$	$10^{-5}Am^2kg^{-1}$	20.407	19.640	6.712	32.893	12.015	34.104
$Hard_{IRM500mT}$	$10^{-5}Am^2kg^{-1}$	9.660	9.522	3.418	35.388	5.594	15.031
$Soft_{S20mT}$	%	17.516	16.310	17.516	100.000	8.025	29.219
$Soft_{S40mT}$	%	42.969	43.302	9.747	22.685	26.582	58.881
$Hard_{S300mT}$	%	9.663	7.981	7.821	80.937	2.718	30.279
$Hard_{S500mT}$	%	4.511	3.568	3.305	73.255	1.524	11.899
S-ratio	(none)	-0.688	-0.669	0.060	-8.730	-0.784	-0.614
ARM/χ	$10^{-2}Am^{-1}$	0.028	0.022	0.019	65.197	0.009	0.063
SIRM/ARM	(None)	205.776	202.282	94.499	45.923	81.263	347.866
χ_{ARM}/SIRM	$10^{-5}Am^2kg^{-1}$	1.904	0.016	0.992	52.133	0.903	3.865
SIRM/χ	$10^{-2}Am^{-1}$	141.851	135.219	33.176	23.388	99.765	205.531

*Mean; Median; SD = standard deviation; CV = percentage coefficient of variation; Min = minimum value; Max = maximum value. Values are shown to 3 decimal places for consistency, not accuracy.

Table 3.17 Summary data* for topsoil physico-chemical characteristics of the scrub environment (n = 10)

Parameters	Units	Mean	Median	SD	CV	Min	Max
pH	mol/ltr	6.831	7.190	0.962	14.081	5.140	7.700
SOM	%	8.494	1.900	11.637	137.009	0.105	31.544
Sand	%	71.499	73.381	6.156	8.610	60.445	78.983
Silt	%	26.345	24.709	6.676	25.340	17.624	38.105
Clay	%	2.156	2.047	0.655	30.396	1.450	3.393
Mean particle size	µm	181.707	185.889	19.860	10.930	142.813	201.977
Median particle size	µm	185.379	196.704	39.032	21.055	108.661	220.621
Sorting		1.720	1.646	0.145	8.440	1.537	1.985
Skewness	γ_1	0.613	0.652	0.125	20.331	0.368	0.735
Kurtosis	g_1	1.450	0.944	0.931	64.247	0.872	3.443
Carbon	%	2.118	2.522	1.168	55.153	0.144	3.385
Nitrogen	%	0.186	0.216	0.102	55.063	0.011	0.305
Sodium	%	1.868	1.865	0.258	13.787	1.440	2.270
Magnesium	%	0.335	0.328	0.033	9.990	0.297	0.389
Aluminium	%	0.351	0.230	0.389	110.916	0.038	1.365
Silicon	%	35.414	36.660	4.165	11.760	28.300	39.790
Phosphorus	%	0.047	0.033	0.034	71.441	0.011	0.099
Sulphur	%	0.064	0.003	0.103	162.054	0.000	0.296
Chlorine	%	0.016	0.010	0.011	66.867	0.008	0.040
Potassium	%	0.559	0.564	0.041	7.375	0.494	0.636
Calcium	%	0.969	0.876	0.426	43.939	0.255	1.667
Iron	%	1.196	1.073	0.518	43.286	0.624	2.440
χ_{LF}	$10^{-7}m^3kg^{-1}$	3.847	1.513	5.168	134.330	0.618	17.718
χ_{FD}	%	2.149	2.231	1.137	52.884	0.000	4.144
χ_{ARM}	$10^{-7}m^3kg^{-1}$	0.126	0.025	0.232	183.840	0.009	0.702
SIRM	$10^{-5}Am^2kg^{-1}$	1478.365	177.632	3642.469	246.385	66.120	11786.516
$Soft_{IRM20mT}$	$10^{-5}Am^2kg^{-1}$	101.449	32.105	161.384	159.078	14.439	531.047
$Soft_{IRM40mT}$	$10^{-5}Am^2kg^{-1}$	262.516	74.420	462.544	176.196	28.346	1515.741
$Hard_{IRM300mT}$	$10^{-5}Am^2kg^{-1}$	47.774	32.782	44.755	93.681	9.768	147.036
$Hard_{IRM500mT}$	$10^{-5}Am^2kg^{-1}$	16.599	14.347	10.776	64.922	2.883	33.967
$Soft_{\%20mT}$	%	16.436	16.902	5.466	33.260	4.506	21.838
$Soft_{\%40mT}$	%	36.019	38.964	10.230	28.402	12.860	46.983
$Hard_{\%300mT}$	%	13.236	12.349	9.019	68.141	1.247	33.587
$Hard_{\%500mT}$	%	6.050	6.474	3.819	63.123	0.202	12.317
S-ratio	(none)	-0.602	-0.628	0.137	-22.807	-0.752	-0.253
ARM/χ	$10^{-2}Am^{-1}$	0.021	0.017	0.017	80.818	0.007	0.063
SIRM/ARM	(None)	297.839	269.335	157.253	52.798	113.738	527.100
χ_{ARM}/SIRM	$10^{-5}Am^2kg^{-1}$	1.371	0.012	0.730	53.232	0.596	2.761
SIRM/χ	$10^{-2}Am^{-1}$	177.885	113.968	175.599	98.715	93.525	665.238

Table 3.18 Summary data* for topsoil physico-chemical characteristics of the deciduous woodland environment (n = 14)

Parameters	Units	Mean	Median	SD	CV	Min	Max
pH	mol/ltr	6.138	6.380	1.078	17.556	3.890	7.370
SOM	%	12.977	4.814	20.576	158.560	2.357	77.165
Sand	%	70.581	69.861	3.727	5.280	63.526	75.545
Silt	%	27.654	28.591	4.018	14.531	21.421	34.912
Clay	%	1.765	1.543	0.695	39.376	1.152	3.955
Mean particle size	µm	174.022	176.115	18.462	10.609	135.338	199.237
Median particle size	µm	176.498	187.339	32.429	18.374	94.248	210.388
Sorting		1.676	1.689	0.128	7.618	1.490	1.831
Skewness	γ_1	0.575	0.612	0.137	23.868	0.162	0.730
Kurtosis	g_1	0.969	0.933	0.088	9.043	0.890	1.169
Carbon	%	2.324	2.643	1.241	53.408	0.230	3.816
Nitrogen	%	0.166	0.186	0.092	55.158	0.023	0.324
Sodium	%	2.446	1.965	2.303	94.155	0.660	10.330
Magnesium	%	0.341	0.362	0.122	35.961	0.001	0.475
Aluminium	%	0.336	0.324	0.123	36.672	0.110	0.578
Silicon	%	31.508	36.100	12.114	38.448	0.213	38.910
Phosphorus	%	0.057	0.041	0.041	71.511	0.021	0.181
Sulphur	%	0.051	0.023	0.077	150.079	0.000	0.291
Chlorine	%	2.786	0.014	10.334	370.985	0.009	38.690
Potassium	%	0.512	0.575	0.179	35.045	0.001	0.627
Calcium	%	0.685	0.548	0.497	72.591	0.039	1.447
Iron	%	0.921	0.931	0.323	35.114	0.005	1.381
χ_{LF}	$10^{-7}m^3kg^{-1}$	2.178	2.115	1.253	57.555	0.853	6.065
χ_{FD}	%	2.088	1.850	1.441	69.016	0.000	4.348
χ_{ARM}	$10^{-7}m^3kg^{-1}$	0.045	0.037	0.029	64.653	0.020	0.122
SIRM	$10^{-5}Am^2kg^{-1}$	300.389	289.205	164.132	54.640	116.451	782.615
$Soft_{IRM20mT}$	$10^{-5}Am^2kg^{-1}$	53.701	36.336	37.691	70.187	25.466	160.417
$Soft_{IRM40mT}$	$10^{-5}Am^2kg^{-1}$	120.421	104.381	73.141	60.737	54.965	329.713
$Hard_{IRM300mT}$	$10^{-5}Am^2kg^{-1}$	27.561	26.706	16.403	59.514	6.103	68.178
$Hard_{IRM600mT}$	$10^{-5}Am^2kg^{-1}$	15.676	14.248	11.558	73.731	5.270	51.604
$Soft_{\%20mT}$	%	18.166	17.372	6.108	33.625	9.566	28.529
$Soft_{\%40mT}$	%	39.997	40.468	6.042	15.105	31.438	50.640
$Hard_{\%300mT}$	%	9.048	8.724	3.028	33.465	5.241	18.164
$Hard_{\%600mT}$	%	5.145	5.025	1.616	31.406	2.268	8.138
S-ratio	(none)	-0.634	-0.627	0.048	-7.506	-0.728	-0.563
ARM/χ	$10^{-2}Am^{-1}$	0.022	0.022	0.009	39.783	0.010	0.037
SIRM/ARM	(None)	236.683	207.105	106.643	45.057	124.477	457.402
χ_{ARM}/SIRM	$10^{-5}Am^2kg^{-1}$	1.553	0.015	0.576	37.112	0.687	2.523
SIRM/χ	$10^{-2}Am^{-1}$	138.710	139.710	14.007	10.098	116.751	168.409

**Mean; Median; SD = standard deviation; CV = percentage coefficient of variation; Min = minimum value; Max = maximum value. Values are shown to 3 decimal places for consistency, not accuracy.*

3.4.9 Coniferous plantation topsoil pedo-characteristics

Table 3.19 presents summary data for the coniferous plantation topsoil samples (n = 10). The plantation topsoil pH (4.06-6.66) was higher (p <0.001) than heath topsoil (Figure 3.3a), but represented the second lowest for all environments on the Sefton dunes; whereas SOM (2.92-76.92%) represented the highest. This environment was not as siliceous (median Si 22.06%) as other coastal environments; however P values (0.02-0.22%) were the highest when compared to those of all other environments. K (<0.01-0.60%) was significantly lower (p <0.001) than newly developed fixed dune topsoils (Figure 3.3e).

3.4.10 Felled topsoil pedo-characteristics

Table 3.20 presents summary data for the felled topsoil samples (n = 10). The pH (5.41-7.49) represented an acidic-neutral transitional environment, similar to the fixed dune topsoils. SOM (0.64-13.42%) was significantly lower (p <0.01) than the plantation topsoil. P (0.01-0.07%) and Cl (<0.01-0.08%) drastically decreased (p <0.01) following felling (Figure 3.3d).

3.5 Spatial characterization of pedo-characteristics using ArcView GIS (version 3.3)

Statistical and graphical techniques indicate significant variations in pedo-characteristics of Sefton topsoils. However, Mann-Whitney U tests and bivariate plots fail to show the geographical relation between adjacent samples. Therefore, the topsoil data have been used to generate GIS images, determining the nature of spatial variations. Baseline maps were created in ArcView GIS (version 3.3), forming visual representations of pedo-characteristics and patterns. The masked boundary excludes unsampled areas (amenity grassland, arable and saltmarsh communities).

3.5.1 Spatial patterns in the pH parameter

Figure 3.4a shows pH to vary widely across the dune system. Alongshore, bare sand and mobile dune sediments were neutral to alkaline (6.9-8.8) along the entire length of the coast. This margin appears to increase dramatically in width directly behind the erosional point (Area i) and continues to the edge of the urban area of Formby. Fixed dunes and pastures to the north (Areas ii and iii) and south (Area iv) increase in acidity (5.0-6.3), with coniferous plantations and heath, in the central-eastern area of the dune landscape (Area v), displaying highly acidic topsoils (3.1-3.7).

3.5.2 Spatial patterns in the SOM parameter

Figure 3.4b shows SOM to be consistent (0.1-25.8%) throughout the dune system. However, slightly higher levels (<34.3%) were associated with the northern fixed dunes (Area iii) and central scrub (Area vi), while the highest values (34.3-68.6%) occurred within deciduous woodland and coniferous plantations (Area v). There were five locations (1-5) of exceptionally high values (68.6-77.1%) that belonged to individual samples, rather than interpolated mid-points. When placed as an overlay on the dune environments map, it is clear that these localities were associated with the edge of slack environments.

Table 3.19 Summary data* for topsoil physico-chemical characteristics of the coniferous plantation environment (n = 10)

Parameters	Units	Mean	Median	SD	CV	Min	Max
pH	mol/ltr	5.155	5.120	0.879	17.048	4.060	6.660
SOM	%	33.785	35.297	27.500	81.398	2.916	76.923
Sand	%	67.314	67.777	3.622	5.381	60.552	72.307
Silt	%	30.805	30.859	3.446	11.187	26.358	37.320
Clay	%	1.881	1.777	0.717	38.115	1.141	3.562
Mean particle size	µm	156.869	162.119	28.006	17.853	95.701	182.822
Median particle size	µm	154.678	164.887	34.315	22.185	85.869	201.337
Sorting		1.763	1.771	0.156	8.856	1.438	1.933
Skewness	γ_1	0.554	0.492	0.118	21.292	0.433	0.748
Kurtosis	g_1	0.969	0.950	0.067	6.965	0.898	1.083
Carbon	%	3.184	3.177	1.387	43.580	1.007	5.096
Nitrogen	%	0.229	0.211	0.096	41.798	0.095	0.370
Sodium	%	2.241	1.405	2.699	120.444	0.890	9.820
Magnesium	%	0.297	0.289	0.146	49.184	0.001	0.540
Aluminium	%	0.327	0.321	0.117	35.837	0.169	0.571
Silicon	%	24.420	22.060	11.787	48.266	0.223	39.220
Phosphorus	%	0.111	0.104	0.075	68.150	0.020	0.221
Sulphur	%	0.123	0.129	0.087	71.120	0.011	0.267
Chlorine	%	3.943	0.032	12.367	313.678	0.012	39.140
Potassium	%	0.420	0.423	0.173	41.212	0.001	0.600
Calcium	%	0.676	0.461	0.613	90.660	0.043	1.961
Iron	%	0.735	0.783	0.284	38.646	0.004	1.031
χ_{LF}	$10^{-7}m^3kg^{-1}$	1.760	1.671	0.669	38.008	1.073	3.530
χ_{FD}	%	3.069	2.000	3.480	113.387	0.000	12.000
χ_{ARM}	$10^{-7}m^3kg^{-1}$	0.036	0.031	0.015	43.372	0.019	0.076
SIRM	$10^{-5}Am^2kg^{-1}$	237.709	228.924	100.234	42.167	122.646	472.657
$Soft_{IRM20mT}$	$10^{-5}Am^2kg^{-1}$	28.032	29.775	8.055	28.734	16.527	36.964
$Soft_{IRM40mT}$	$10^{-5}Am^2kg^{-1}$	76.280	69.557	27.276	35.758	49.217	141.456
$Hard_{IRM300mT}$	$10^{-5}Am^2kg^{-1}$	17.227	16.236	7.031	40.816	3.549	28.136
$Hard_{IRM500mT}$	$10^{-5}Am^2kg^{-1}$	6.937	6.986	2.426	34.966	2.713	10.345
$Soft_{\%20mT}$	%	12.709	12.592	4.187	32.943	6.749	22.239
$Soft_{\%40mT}$	%	33.022	31.913	4.214	12.761	29.276	42.851
$Hard_{\%300mT}$	%	7.286	7.714	2.096	28.764	2.893	10.216
$Hard_{\%500mT}$	%	3.060	3.398	0.908	29.679	1.675	4.122
S-ratio	(none)	-0.659	-0.660	0.042	-6.321	-0.715	-0.564
ARM/χ	$10^{-2}Am^{-1}$	0.020	0.021	0.003	16.570	0.015	0.025
SIRM/ARM	(None)	214.517	199.375	58.547	27.292	144.327	322.401
χ_{ARM}/SIRM	$10^{-5}Am^2kg^{-1}$	1.553	0.016	0.371	23.895	0.974	2.176
SIRM/χ	$10^{-2}Am^{-1}$	133.134	132.453	17.190	12.912	109.251	165.264

Table 3.20 Summary data* for topsoil physico-chemical characteristics of the felled coniferous environment (n = 10)

Parameters	Units	Mean	Median	SD	CV	Min	Max
pH	mol/ltr	6.344	6.360	0.788	12.423	5.410	7.490
SOM	%	3.917	2.742	3.678	93.905	0.642	13.422
Sand	%	71.346	71.995	2.693	3.774	67.792	75.640
Silt	%	26.602	26.376	2.961	11.129	21.046	30.614
Clay	%	2.052	2.019	0.534	25.999	1.594	3.314
Mean particle size	µm	185.821	184.267	13.051	7.023	161.875	205.688
Median particle size	µm	198.401	199.865	16.912	8.524	163.990	219.534
Sorting		1.746	1.770	0.111	6.372	1.578	1.875
Skewness	γ_1	0.657	0.668	0.047	7.218	0.586	0.719
Kurtosis	g_1	1.086	0.936	0.456	41.984	0.885	2.299
Carbon	%	3.214	2.756	1.743	54.247	0.058	5.767
Nitrogen	%	0.207	0.212	0.096	46.565	0.004	0.312
Sodium	%	1.900	1.960	0.263	13.827	1.540	2.230
Magnesium	%	0.305	0.273	0.081	26.460	0.197	0.422
Aluminium	%	0.239	0.218	0.094	39.548	0.101	0.385
Silicon	%	37.332	38.000	2.027	5.429	32.360	39.730
Phosphorus	%	0.028	0.018	0.019	67.190	0.013	0.068
Sulphur	%	0.013	0.002	0.027	205.926	0.000	0.088
Chlorine	%	0.010	0.010	0.002	16.727	0.007	0.012
Potassium	%	0.558	0.566	0.045	8.029	0.492	0.616
Calcium	%	0.598	0.513	0.429	71.740	0.154	1.298
Iron	%	1.073	0.942	0.343	31.943	0.649	1.537
χ_{LF}	$10^{-7}m^3kg^{-1}$	2.741	1.582	2.366	86.321	0.601	6.934
χ_{FD}	%	2.383	1.456	2.126	89.214	0.223	6.122
χ_{ARM}	$10^{-7}m^3kg^{-1}$	0.041	0.032	0.028	69.942	0.014	0.096
SIRM	$10^{-5}Am^2kg^{-1}$	344.289	205.729	297.238	86.334	69.627	860.075
$Soft_{IRM20mT}$	$10^{-5}Am^2kg^{-1}$	61.557	38.209	56.720	92.142	10.807	183.292
$Soft_{IRM40mT}$	$10^{-5}Am^2kg^{-1}$	142.094	85.424	124.309	87.484	31.326	355.542
$Hard_{IRM300mT}$	$10^{-5}Am^2kg^{-1}$	27.758	15.140	23.052	83.047	6.485	69.581
$Hard_{IRM600mT}$	$10^{-5}Am^2kg^{-1}$	13.305	9.444	12.284	92.326	0.600	38.162
$Soft_{\%20mT}$	%	17.894	19.253	3.778	21.114	10.967	21.462
$Soft_{\%40mT}$	%	41.889	41.541	2.612	6.235	36.288	44.992
$Hard_{\%300mT}$	%	8.459	7.941	2.158	25.510	6.047	12.128
$Hard_{\%600mT}$	%	3.680	3.633	1.770	48.093	0.609	6.350
S-ratio	(none)	-0.655	-0.653	0.030	-4.628	-0.711	-0.600
ARM/χ	$10^{-2}Am^{-1}$	0.017	0.017	0.004	23.990	0.011	0.024
SIRM/ARM	(None)	239.074	253.595	62.715	26.232	150.760	328.733
χ_{ARM}/SIRM	$10^{-5}Am^2kg^{-1}$	1.411	0.012	0.419	29.726	1.119	2.423
SIRM/χ	$10^{-2}Am^{-1}$	124.837	125.762	12.000	9.612	102.398	140.249

*Mean; Median; SD = standard deviation; CV = percentage coefficient of variation; Min = minimum value; Max = maximum value. Values are shown to 3 decimal places for consistency, not accuracy.

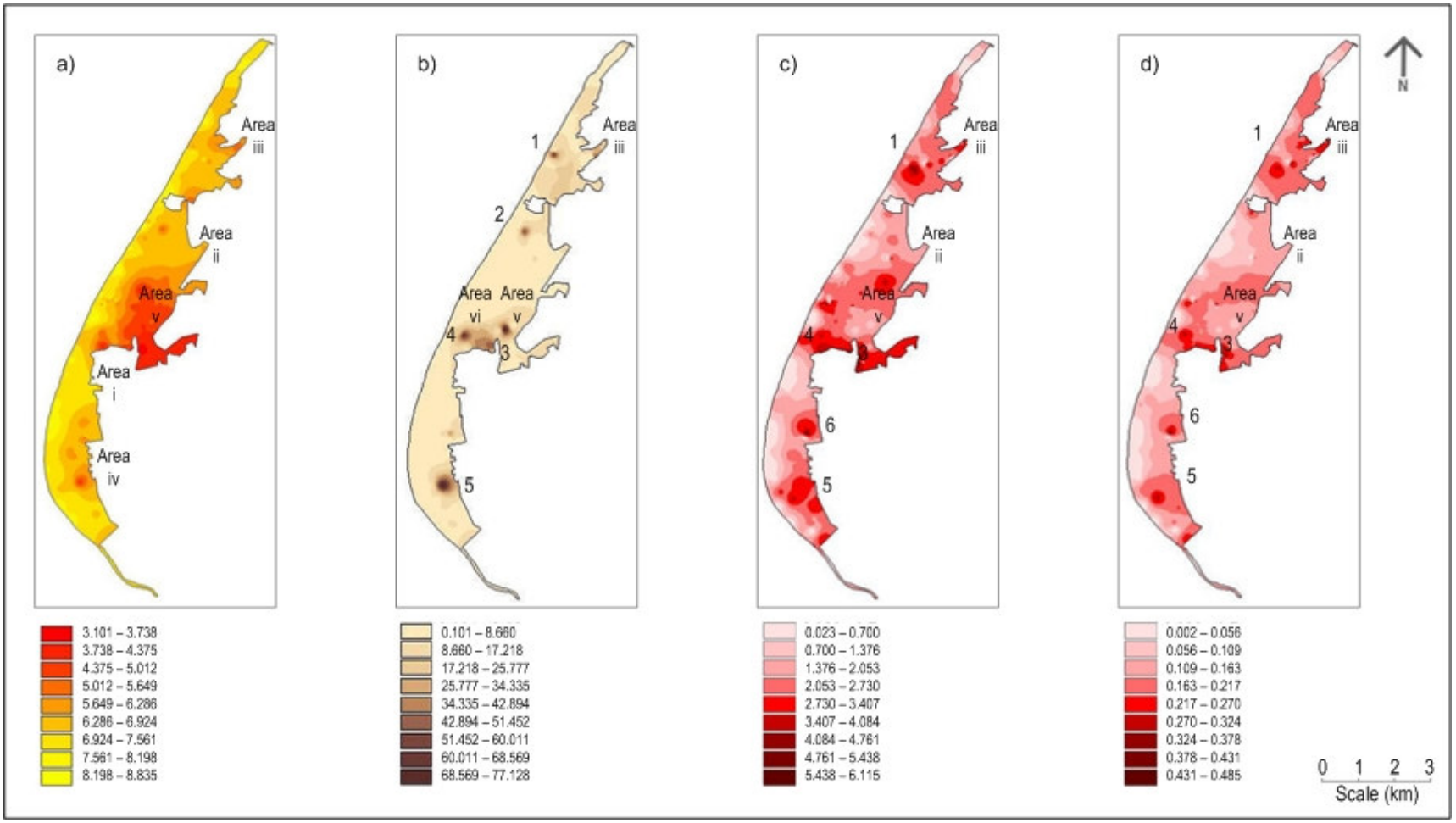

Figure 3.4 Spatial distributions of; a) pH; b) SOM%; c) C% and d) N% (Areas i-vi represent regions of interest and points 1-7 indicate sites of extreme parameter values).

3.5.3 Spatial patterns in the geochemistry parameters

Figures 3.4c,d show similar distributions of C and N, respectively, with lower values of C (0.02-0.70%) and N (<0.01-0.11%) occurring on the seaward edge. However, samples associated with slack topsoils (1-6) had relatively high C (>4.1%) and N (>0.3%) concentrations, which may have influenced interpolated values, resulting in some fixed dune areas (Areas ii and iii) appearing to have greater concentrations than in reality. Low C and N (<2.1% and <0.2%, respectively) (Area v) were associated with fixed dune topsoils that were interspersed with coniferous plantations.

Figure 3.5a shows moderate Na (>3.0%) throughout the dune system, although levels dropped (<3.0%) in heath topsoils (Area i) and locations surrounding Formby Golf Course (Area ii). Extremely high Na (>9.1%) was associated with high P (>0.17%) (Figure 3.5e) and high Cl (>32.1%) (Figure 3.6b) in samples associated with slack topsoils (1-6). This pattern was reversed in low distributions of Mg (<0.07%) (Figure 3.5b) and K (<0.09%) (Figure 3.5c). Alongshore, Mg trends show high concentrations (>4.9%) within the erosion limit, north of Formby point (Areas i and ii) and in the far northern fixed dunes (Area iii).

Figures 3.5c and 3.6a show low S (<4.2%) and Al (<0.45%), respectively, with increased levels on the northern fixed dunes (Area iii). Although, Si is abundant (>27.3%), there were samples with extremely low values (<4.7%) that were not associated with particular environment topsoils. Ca (Figure 3.6d) and Fe (Figure 3.6e) do not vary greatly (0.0-1.8%), although levels decreased slightly inland. Highest Fe values (3.1-4.0%) were on the northern fixed dunes (Area iii), with extreme values associated with slack topsoils (Points 1 and 7 on Figure 3.6).

3.5.4 Spatial patterns in the textural parameters

Figure 3.7 displays spatial variability in the sand, silt and clay parameters, showing distinct areas of low and high values. Alongshore trends were evident as alternating lobes of fine and coarse sand (Figure 3.7a, Area i), with a distinct alteration to higher percentages of silt (>31.6%) on the northern fixed dunes (Figure 3.7b, Area ii). The clay fraction had a limited contribution to textural totals (0.1-4.6%), with exception of an area on the mobile dunes by Ainsdale Holiday Village (Figure 3.7c, Area iii), where values reached 6.2-6.9%. Two further samples display actual, rather than interpolated, relatively high clay percentages (5.4-6.2%) on the mobile dunes, north of Formby Point (Area i), which were also related to high percentages of medium sand.

The general pattern of mean particle size (Figure 3.7d) shows inland dunes to have had finer particle sizes (<173.1 µm) compared to the seaward edge (230.7-259.5 µm). However, these finer particles spanned the width of the study area in three localities (Area ii, iv and v). The finest particles (<58.0 µm) were associated with a patch in the centre of the dunes (Area vi).

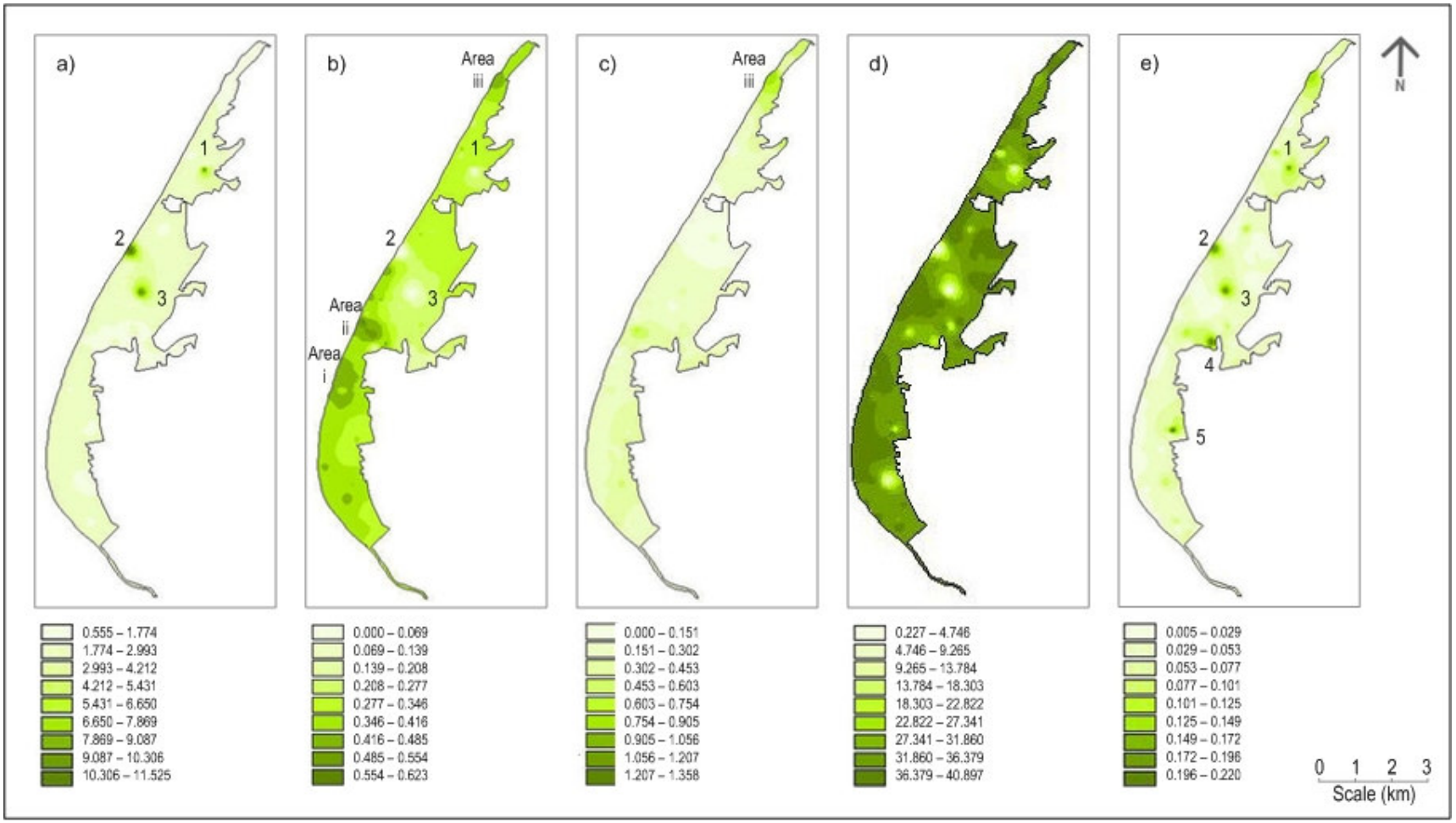

Figure 3.5 Spatial distributions of geochemical parameters: a) Na%; b) Mg%; c) Al%; d) Si% and e) P% (Areas i-iii represent regions of interest and points 1-5 indicate sites of extreme parameter values).

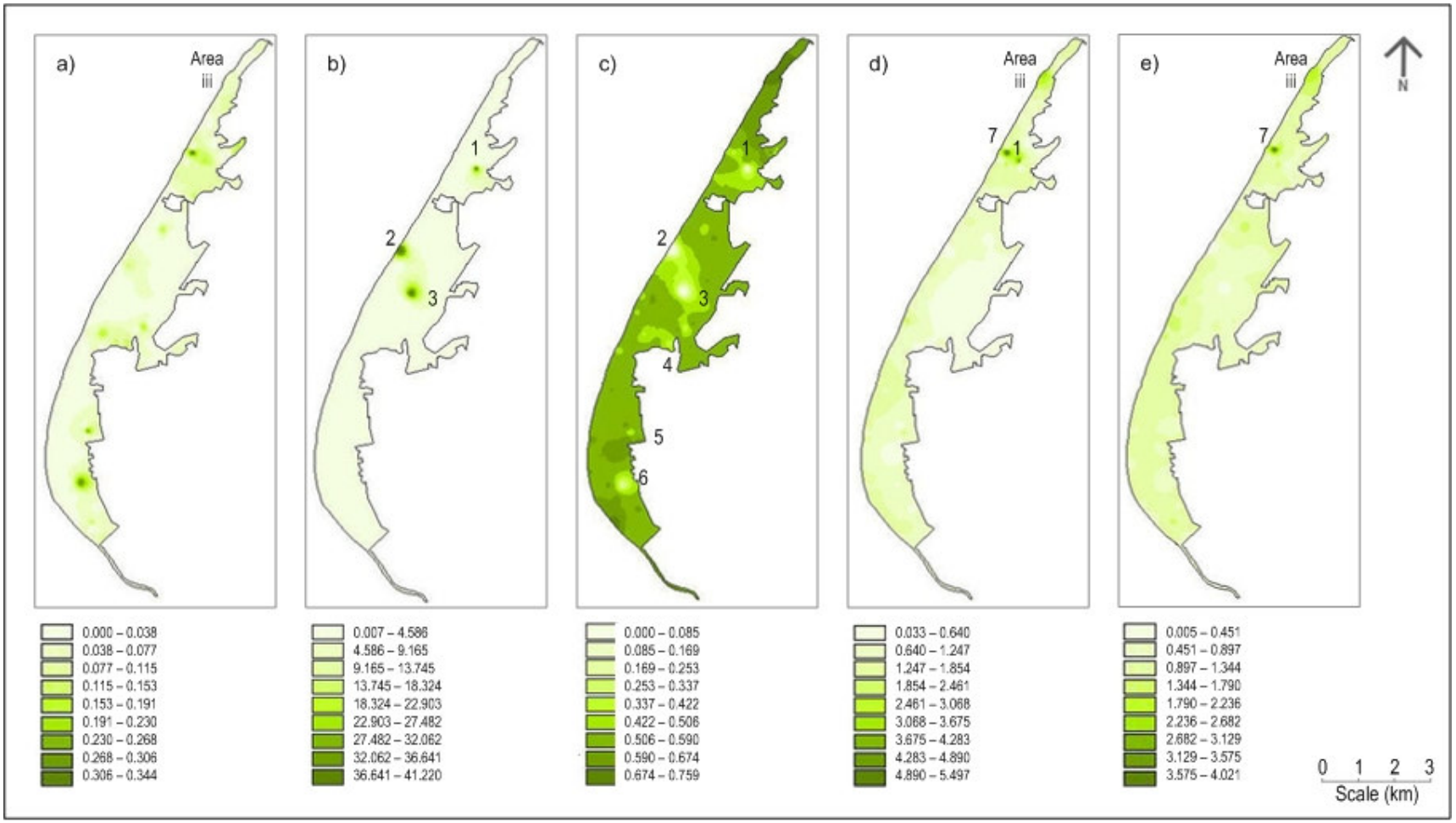

Figure 3.6 Spatial distributions of geochemical parameters: a) S%; b) Cl%; c) K%; d) Ca% and e) Fe% (Areas iii represents a region of interest and points 1-7 indicate sites of extreme parameter values).

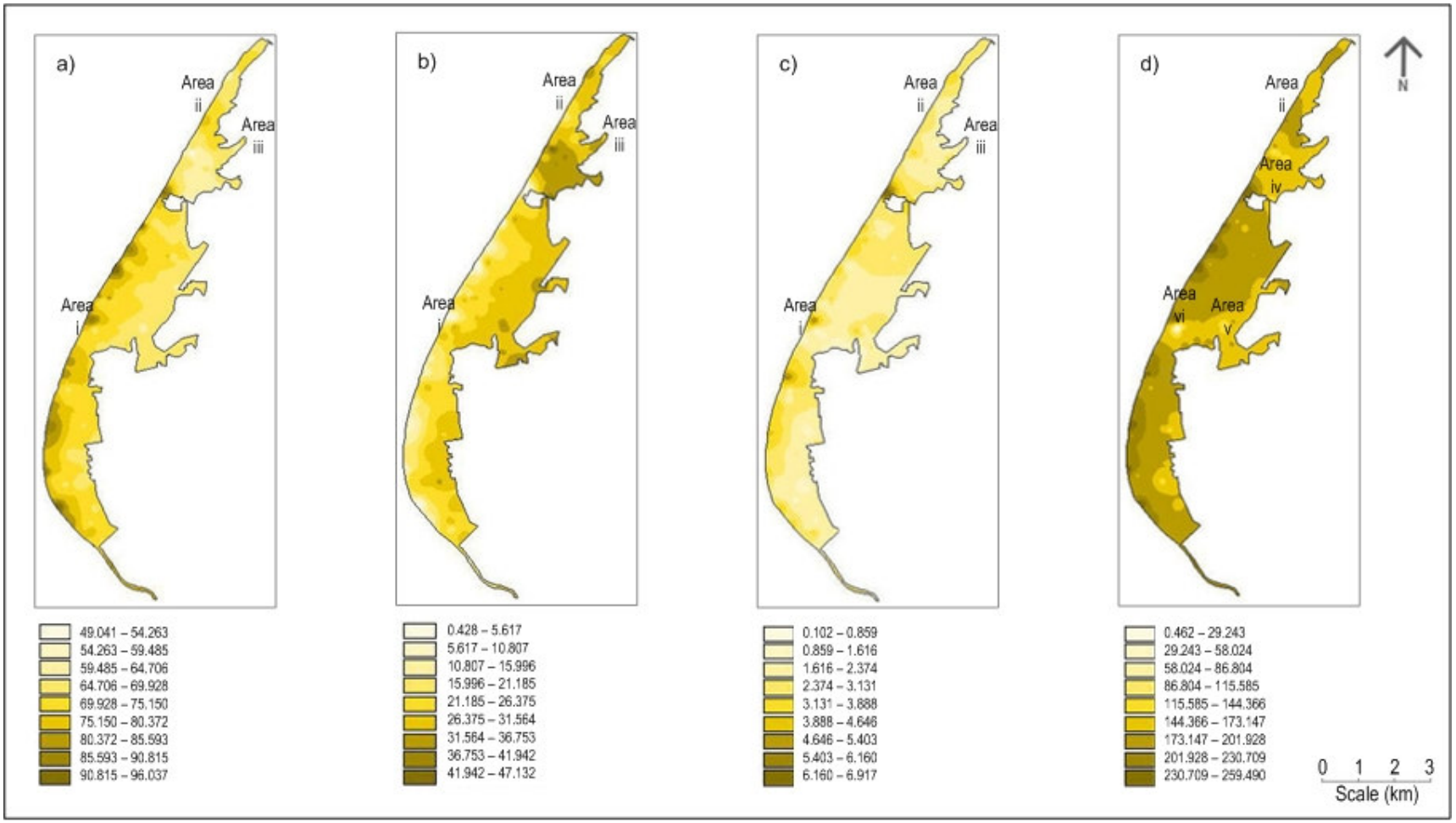

Figure 3.7 Spatial distributions of textural parameters: a) Sand%; b) Silt%; c) Clay% and d) mean particle size (μm) (Areas i-vi represent regions of interest).

3.5.5 Spatial patterns in the mineral magnetic parameters

Magnetic concentration-dependent parameters (χ_{LF}, χ_{ARM} and SIRM) (Figures 3.8a,c,d) were low-moderate across the dunes, while $\chi_{FD\%}$ values were variable, with increased values inland and in the north (Figure 3.8b). Interpolated values of χ_{LF} (Figure 3.8a) were higher (2.20-17.63 $x10^{-7}m^3kg^{-1}$) on the mobile dunes within the erosion limit (Area i) and on the northern fixed dunes (Areas ii and iii), indicating increased concentrations of ferrimagnetic minerals. Figure 3.8c identifies three areas (Areas i, ii and iii) of high χARM (>0.08 $x10^{-7}m^3kg^{-1}$), in the same locations as increased χ_{LF}. The SIRM pattern (Figure 3.8d) has a very different appearance to both of the previous parameters, with low values (<1324.0 $x10^{-5}Am^2kg^{-1}$) across the entire dune area. There was a magnetically separated area (Area iii) of high SIRM (1324.0-11,610.7 $x10^{-5}Am^2kg^{-1}$) in the northern fixed dunes.

Figures 3.9a,b illustrate spatial variability of $Soft_{IRM20mT}$ and $Soft_{IRM40mT}$. General patterns indicate increased values (>63.2 $x10^{-5}Am^2kg^{-1}$ and >182.0 $x10^{-5}Am^2kg^{-1}$, respectively) in areas i, ii and iii, suggesting higher levels of ferrimagnetic 'magnetite-type' soft minerals in these localities. However, $Hard_{IRM300mT}$ and $Hard_{IRM500mT}$ distributions (Figures 3.9c,d, respectively) not only indicate increased content of canted antiferromagnetic 'haematite-type' hard minerals in areas i, ii and iii, but also identify a greater variety in distribution values across the dunes (Areas iv, v, vi and vii). The mobile dunes in the northern erosion limit (Area i) had the highest values (51.1 - 146.3 $x10^{-5}Am^2kg^{-1}$), indicating that the western edge was characteristically enriched with magnetically hard-mineralogy, compared to eastern margins. Inconsistency of both S-ratio (Figure 3.9e) and $\chi_{FD\%}$ (Figure 3.8b) caused difficulty in interpolation, suggesting samples contained contrasting magnetic mineralogies and concentrations.

Spatial patterns of magnetic domain size dependent parameters (Figure 3.11) were very different to the previous mineral magnetic variability. Low ARM/χ (<0.1 $x10^{-2}Am^{-1}$) (Figure 3.11a) and χ_{ARM}/SIRM (<9.3 $x10^{-5}Am^2kg^{-1}$) (Figure 3.11c), alongside high SIRM/ARM (34.5-525.9) (Figure 3.11b) were particularly evident in the northern extent of the erosion limit (Area i), centre of the erosion limit (Area viii) and in the centre of Ainsdale NNR (Area ix). Patterns suggest these areas contained coarse (multidomain) magnetic domain sizes. However, patterns of increased ARM/χ and χ_{ARM}/SIRM, alongside decreased SIRM/ARM, were evident in the northern fixed dunes (Areas ii and iii), on the fringes of the urban area of Formby (Area vi) and in slack environments (Area x). This indicates the importance of fine (stable single domain) magnetic domain sizes in these localities. Increased SIRM/χ (Figure 3.11d) inland also suggests increased importance of fine (stable single domain) ferrimagnetic grains on topsoils further from the coast. The northern fixed dunes (Area iii) had the highest values (595.3-662.4 $x10^{-2}Am^{-1}$).

3.6 Further assessment using multivariate factor analysis plots

To further clarify the between-environment relationships, multivariate factor analysis was used. In each analysis, parameter and sample loadings extracted from Factors 1 and 2 were used to generate factor plots (refer to Chapter 2, Section 2.4.4).

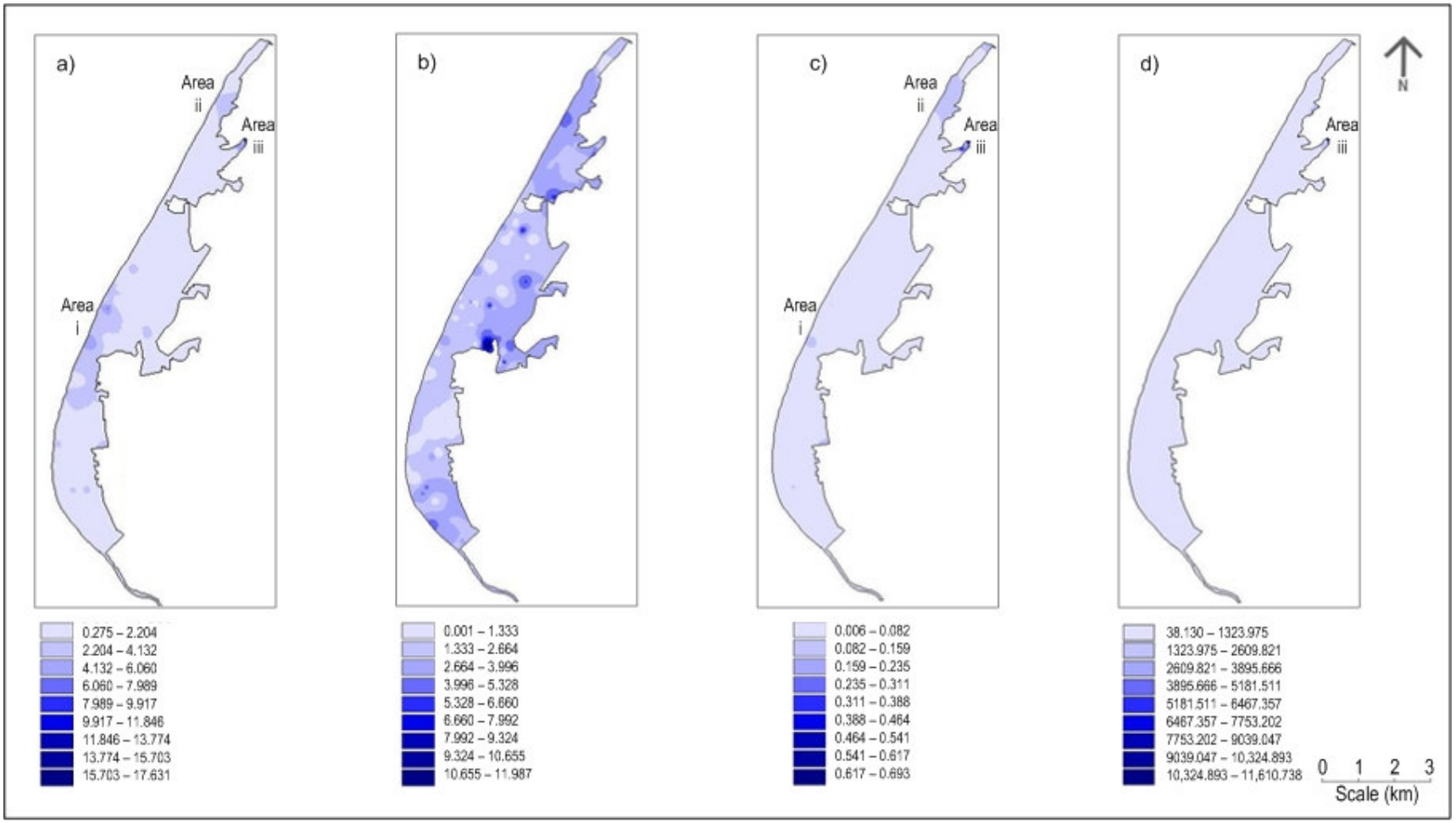

Figure 3.8 Spatial distribution of mineral magnetic concentration dependent parameters: a) χ_{LF} $x10^{-7}m^3kg^{-1}$; b) $\chi_{FD\%}$; c) χ_{ARM} $x10^{-7}m^3kg^{-1}$ and d) SIRM $x10^{-5}Am^2kg^{-1}$ (Areas i-iii represent regions of interest) .

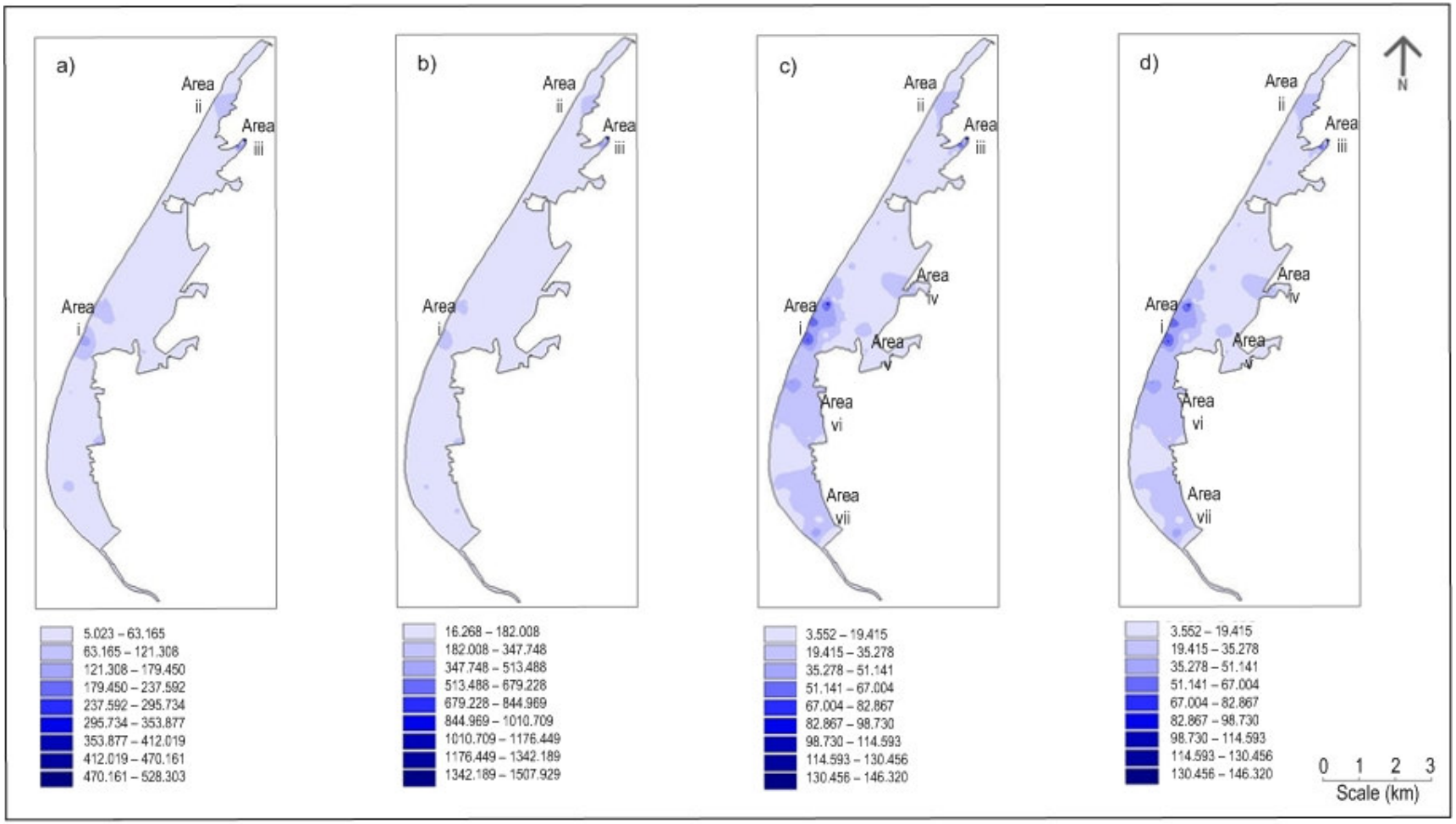

Figure 3.9 Spatial distributions of absolute magnetic mineral dependent parameters: a) $Soft_{IRM20mT}$ $x10^{-5}Am^2kg^{-1}$; b) $Soft_{IRM40mT}$ $x10^{-5}Am^2kg^{-1}$; c) $Hard_{IRM300mT}$ $x10^{-5}Am^2kg^{-1}$ and d) $Hard_{IRM500mT}$ $x10^{-5}Am^2kg^{-1}$ (Areas i-vii represent regions of interest).

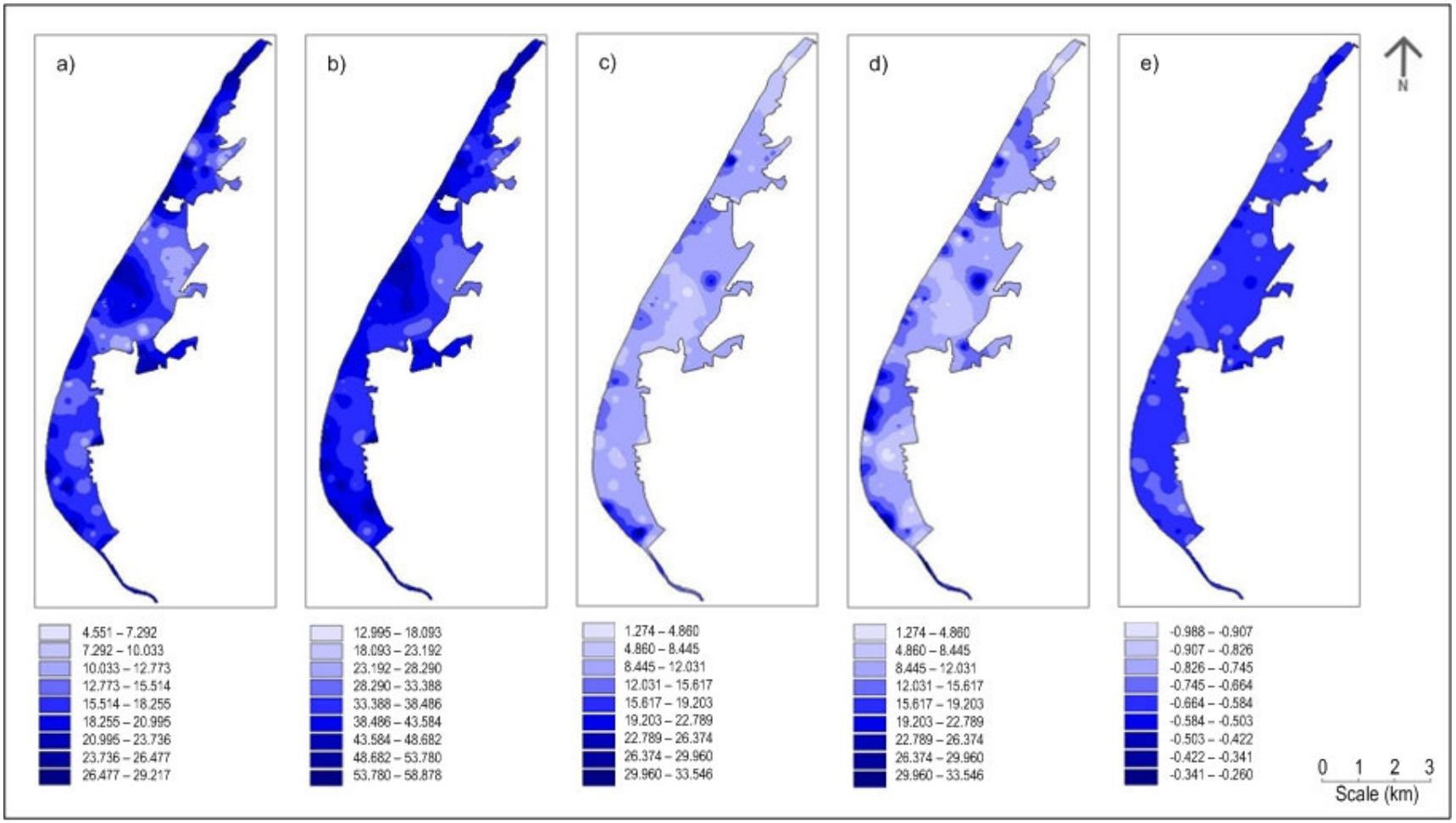

Figure 3.10 Spatial distributions of percentage magnetic mineral dependent parameters: a) $Soft_{\%20mT}$; b) $Soft_{\%40mT}$; c) $Hard_{\%300mT}$; d) $Hard_{\%500mT}$ and e) S-ratio.

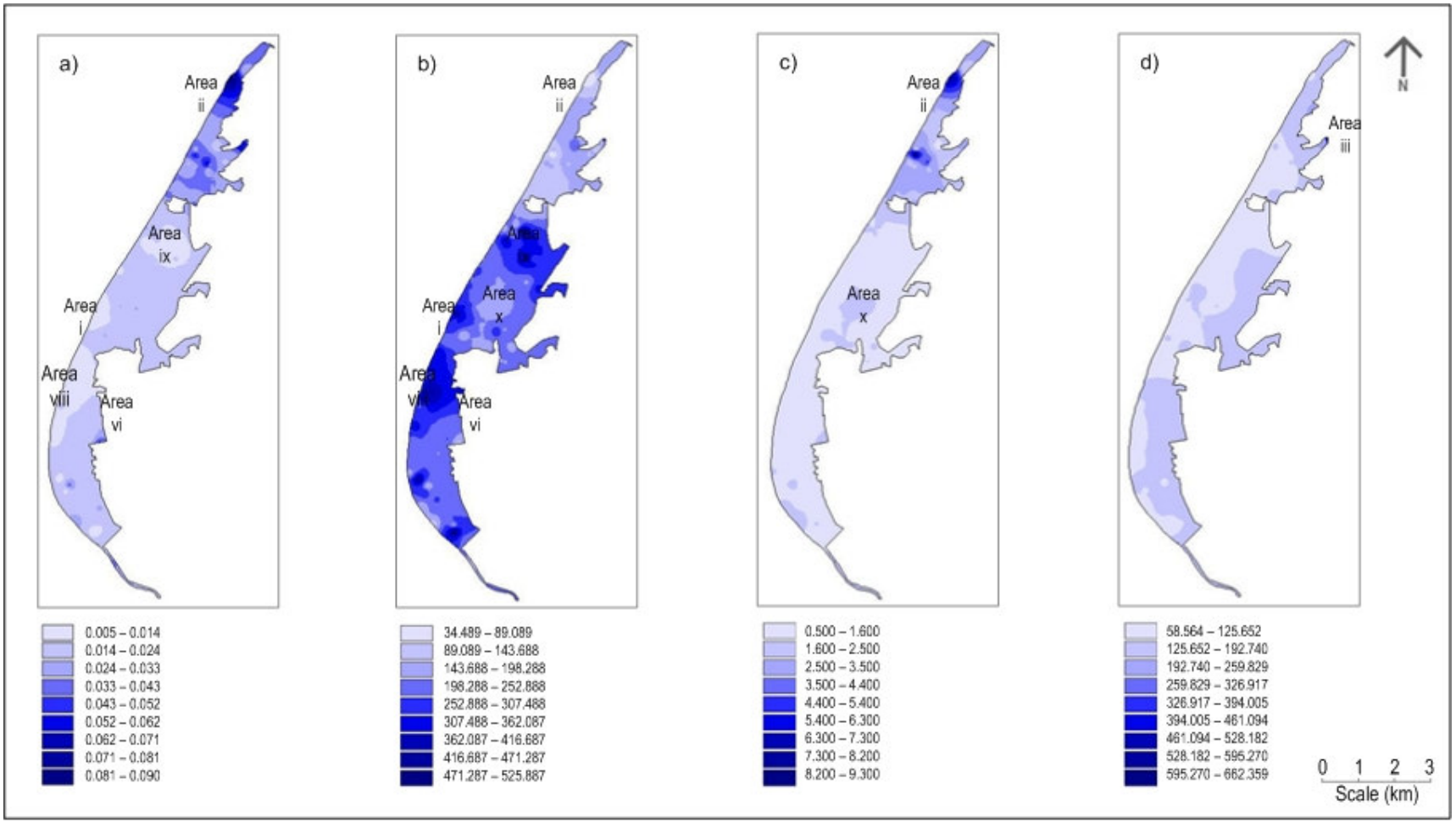

Figure 3.11 Spatial distributions of the mineral magnetic grain size dependent parameters: a) ARM/χ x10^{-2}Am^{-1}; b) SIRM/ARM; c) χ_{ARM}/SIRM x10^{-5}Am^{2}kg^{-1} and d) SIRM/χ x10^{-2}Am^{-1}(Areas i-x represent regions of interest).

3.6.1 Factor analysis using textural parameters

Factor analysis was performed using all particle size and distribution parameters. Figure 3.12a shows a factor plot created from parameter and sample loadings from Factors 1 and 2. The first two factors extracted explain 82.4% of variation in the eight parameters (Table 3.21a), indicating extremely strong positive and negative loadings on both factors. The spread of loadings indicates influences by both particle size and distribution, with some environments having notable differences between textural properties.

Factor 1 explains 65.6% of variation in the parameters, with negative loadings of silt, sorting and skewness, but positive loadings of sand, clay, mean particle size, median particle size and kurtosis. Close positioning of the particle size parameters to Factor 1, suggests an underlying energy regime occurrence. Factor 2 explains 16.8% of variation, suggesting limited influence. Only sand and kurtosis have negative loadings on Factor 2, with all remaining parameters having positive loadings. Bare sand and mobile dune community samples appear separated from the other parameters by both Factors 1 and 2, with positive loadings on Factor 1 and mostly negative loadings on Factor 2. The opposite trend is observed in most fixed dune community samples, which have a negative loading on Factor 1 and both positive and negative loadings on Factor 2. Heath and slack samples are negatively loaded on Factor 1, as are most pasture, scrub, deciduous woodland, coniferous plantation and felled community samples.

The postulated pedogenesis line indicates a texturally influenced pedo-succession. The spread of sample loadings along Factor 1 indicates most samples from inland environments are influenced by similar high percentages of silt; whereas, bare sand and mobile dune community samples appear to be influenced by both sand- and clay-sized fractions. The spread of sample loadings along Factor 2 suggest bare sand and mobile dune community samples are also characterized by coarse, unsorted particles.

3.6.2 Factor analysis using geochemical parameters

Factor analysis was initially performed using all geochemical parameters. However, the resultant plot (not presented) was chaotic and did not appear to show any obvious patterns or trends. Factor analysis was re-applied to various parameter combinations, with the resulting factor plot (Figure 3.12b) excluding some parameters from the data-set. The parameters Na, Si, P, S, Cl and K did not appear to be influenced by either Factors 1 or 2, suggesting that they provide no explanation for the pattern of sample loadings and can be considered redundant measurements.

Figure 3.12b shows a factor plot created from parameter and sample loadings from Factors 1 and 2, based on the results from a factor analysis that included only the ratio between the C and N values, Al, Fe, Mg and Ca, but excluded all remaining geochemical parameters. The first two factors extracted explain 65.4% of variation in the five parameters (Table 3.21b). The geochemical parameters have positive and negative loadings on both extracted factors, the

Table 3.21 Summary results from factor analysis of; a) selected textural; b) selected geochemical and c) selected mineral magnetic parameters

Parameter	Factors	Eigenvalues	Total variance (%)	Cumulative eigenvalues	Cumulative total variance (%)
1 Sand	1	5.250	65.619	5.250	65.619
2 Silt	2	1.344	16.803	6.594	82.422
3 Clay	3	0.959	11.985	7.553	94.407
4 Mean	4	0.262	3.275	7.815	97.682
5 Median	5	0.138	1.720	7.952	99.402
6 Sorting	6	0.041	0.515	7.993	99.917
7 Skewness	7	0.007	0.083	8.000	100.000
8 Kurtosis	8	0.000	0.000	8.000	100.000

Parameter	Factors	Eigenvalues	Total variance (%)	Cumulative eigenvalues	Cumulative total variance (%)
1 C:N ratio	1	2.158	43.155	2.158	43.155
2 Al	2	1.114	22.281	3.272	65.436
3 Fe	3	0.925	18.502	4.197	83.938
4 Mg	4	0.505	10.105	4.702	94.043
5 Ca	5	0.298	5.957	5.000	100.000

Parameter	Factors	Eigenvalues	Total variance (%)	Cumulative eigenvalues	Cumulative total variance (%)
1 χ_{frm}	1	1.797	35.935	1.797	35.935
2 $Soft_{0.400mT}$	2	1.258	25.164	3.055	61.099
3 $Hard_{0.900mT}$	3	0.979	19.584	4.034	80.684
4 $Hard_{0.500mT}$	4	0.664	13.281	4.698	93.964
5 SIRM/χ	5	0.302	6.036	5.000	100.000

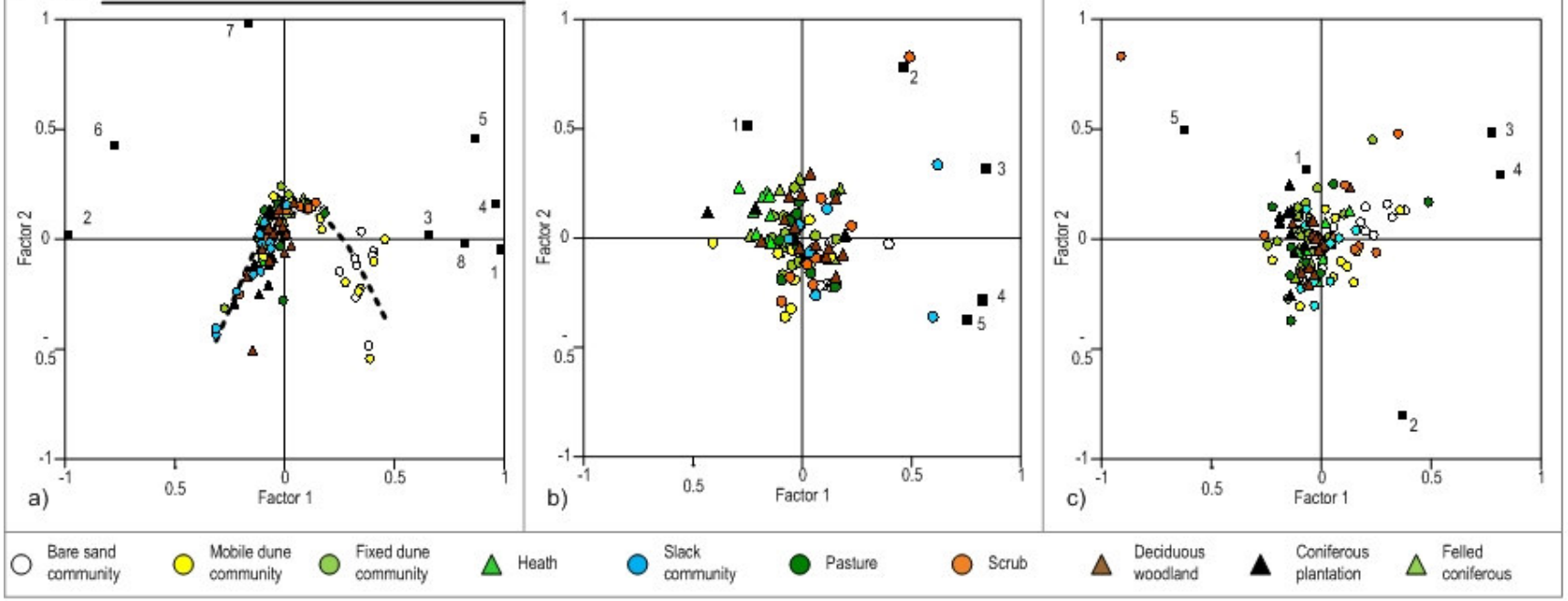

Figure 3.12 Simultaneous R- and Q-mode factor analysis plots of Factor 1 versus Factor 2, based on: a) selected topsoil textural characteristics; b) selected topsoil geochemical characteristics and c) selected topsoil mineral magnetic characteristics (dashed line represents postulated pedogenesis).

spread of which indicates they are influenced by various chemical association gradients. However, the close distribution of sample points fails to separate any grouping, therefore, indicating that any differences between geochemical properties are not notable.

Factor 1 explains 43.2% of variation in the parameters. Clustering of the sample populations in the centre makes it difficult to identify underlying causes. The C:N ratio is negatively loaded on Factor 1, whereas, the remaining parameters are positively loaded. Factor 2 explains 22.3% of variation. The C:N ratio, Al and Fe have negative loadings on Factor 2, with Mg and Ca having positive loadings. Most bare sand and mobile dune community samples have negative loadings on Factor 2. Fixed dune community samples have both positive and negative loadings on both factors, but most have a negative loading on Factor 1. Heath samples are grouped into a negative load on Factor 1 and a positive load on Factor 2. Most slack community and scrub samples appear to have positive loadings on Factor 1. Pasture and deciduous woodland samples are both positively and negatively loaded on Factors 1 and 2, whereas, most coniferous plantation and felled community samples are positively loaded on Factor 2.

The combined spread of sample loadings along both factors indicate that samples from all dune environments are influenced by combinations of all geochemistry parameters. However, it can be determined that heath samples possess a higher proportion of non-metals compared to all remaining environments, perhaps suggesting that Factor 1 represents an underlying atmospheric pollution input. Some samples from the slack community are in solitary positions on Factor 1, suggesting this environment is acting as metal sink.

3.6.3 Factor analysis using mineral magnetic parameters

Factor analysis was initially performed using all mineral magnetic parameters; however, the resultant plot (not presented) was chaotic and did not appear to show any obvious pattern. Factor analysis was re-applied to various parameter combinations until sample groupings and separations became apparent. This, ultimately, resulted in the exclusion of χ_{LF}, χ_{ARM}, SIRM, $Soft_{IRM20mT}$, $Soft_{\%20mT}$, $Soft_{\%40mT}$, $Hard_{\%300mT}$, $Hard_{\%500mT}$, S-ratio, ARM/χ, SIRM/ARM and χ_{ARM}/SIRM, from the data-set, as they did not appear to be influenced by either Factors 1 or 2, suggesting that they provide no explanation for the pattern of sample loadings and can be considered redundant measurements.

Figure 3.12c shows a factor plot created from parameter and sample loadings from Factors 1 and 2, based on the results from a factor analysis that included only $\chi_{FD\%}$, $Soft_{\%40mT}$, $Hard_{\%300mT}$, $Hard_{\%500mT}$ and SIRM/χ, but excluded all remaining mineral magnetic parameters. The first two factors extracted explain 61.1% of variation in the five parameters (Table 3.21c). The magnetic parameters have positive and negative loadings on both extracted factors, the spread of which indicates they were influenced by magnetic concentration, mineralogy and magnetic domain size gradients. However, the close distribution of sample points indicates differences between sample magnetic properties are not notable.

Factor 1 (haematite-type minerals) explains 35.9% of variation in the parameters. The $\chi_{FD\%}$ and SIRM/χ parameters are negatively loaded on Factor 1, but $Soft_{\%40mT}$, $Hard_{\%300mT}$ and $Hard_{\%500mT}$ have positive loadings. Factor 2 (domain size) explains 25.2% of variation. Only $Soft_{\%40mT}$ has a negative loading on Factor 2, with all remaining parameters having positive loadings. Bare sand and mobile dune community samples are broadly separated from the other sample populations by positive loadings on Factor 1, with most bare sand samples having a positive loading on both factors. In contrast, most fixed dune community samples have a negative loading on Factor 1 and a positive loading on Factor 2. Heath samples are negatively loaded on both factors, with slack community and scrub samples having both negative and positive loadings on both factors. Pasture and deciduous woodland samples are negatively loaded on Factor 1, as are coniferous plantation samples; whereas, felled samples are negatively loaded on both factors.

The spread of sample loadings along both factors indicates most samples from all inland dune environments have a finer ferrimagnetic domain size than the bare sand and mobile dune community samples. The spread of sample loadings along Factor 2 indicates great magnetic mineralogy variability within each dune environment. However, it can be determined that bare sand and fixed dune community samples possess higher proportions of magnetic minerals with 'hard-type' behaviour (low coercivity) compared to heath and felled environment samples.

3.6.4 Factor analysis using key physico-chemical parameters

Factor analysis was performed using only the physico-chemical parameters analysed in the previous plots (Sections 3.6.1-3.6.3). The first two factors extracted explain 48.8% of variation in the 15 parameters (Table 3.22a). Figure 3.13a shows a factor plot created from parameter and sample loadings from Factors 1 and 2, based on the results from factor analysis. Factor 1 (degree of aeolian activity) explains 30.5% of variation in the parameters, with SOM, silt, C:N ratio, Al, Fe, χ_{LF} and $\chi_{FD\%}$ having negative loadings and pH, sand, clay, Mg, Ca, $Soft_{\%40mT}$, $Hard_{\%300mT}$ and $Hard_{\%500mT}$ having positive loadings. Factor 2 (mineralogy) explains 18.3% of variation in the parameters, with pH, SOM, sand, clay, Mg, Al, Ca, Fe and χ_{LF} having negative loadings and silt, C:N ratio, $\chi_{FD\%}$, $Soft_{\%40mT}$, $Hard_{\%300mT}$ and $Hard\%_{500mT}$ having positive loadings. Bare sand and mobile dune community samples have positive loadings on Factor 1, which separates them from all remaining dune environments. In contrast, all of the coniferous plantation samples, along with most felled and deciduous woodland samples, have negative loadings on Factor 1. All heath samples and most fixed dune community samples have positive loadings on Factor 2. Slack community, pasture and scrub samples have both negative and positive loadings on both factors.

The spread of sample loadings along Factor 1 indicate textural parameters are the main influencing factor and can be used to discriminate the bare sand and mobile dune communities from the heath and coniferous plantation samples. The spread of sample loadings along Factor 2 indicates major geochemical variability within each dune environment, with some slack

Table 3.22 Summary results from factor analysis of; a) selected parameters and b) selected parameters after reclassification

Factors	Eigenvalues	Total variance (%)	Cumulative eigenvalues	Cumulative total variance (%)
1	4.579	30.529	4.579	30.529
2	2.747	18.312	7.326	48.841
3	1.445	9.633	8.771	58.474
4	1.128	7.520	9.899	65.994
5	1.076	7.170	10.975	73.164
6	0.867	5.778	11.841	78.942
7	0.760	5.065	12.601	84.008
8	0.746	4.974	13.347	88.982
9	0.513	3.417	13.860	92.399
10	0.335	2.231	14.194	94.630
11	0.269	1.793	14.463	96.423
12	0.233	1.551	14.696	97.974
13	0.178	1.186	14.874	99.160
14	0.126	0.840	15.000	100.000
15	0.000	0.000	15.000	100.000

Factors	Eigenvalues	Total variance (%)	Cumulative eigenvalues	Cumulative total variance (%)
1	5.061	38.931	5.061	38.931
2	2.521	19.390	7.582	58.321
3	1.952	15.012	9.533	73.334
4	0.903	6.944	10.436	80.278
5	0.734	5.647	11.170	85.925
6	0.686	5.277	11.856	91.202
7	0.323	2.485	12.179	93.687
8	0.264	2.029	12.443	95.716
9	0.225	1.730	12.668	97.446
10	0.146	1.120	12.814	98.566
11	0.117	0.897	12.930	99.463
12	0.041	0.314	12.971	99.777
13	0.029	0.223	13.000	100.000

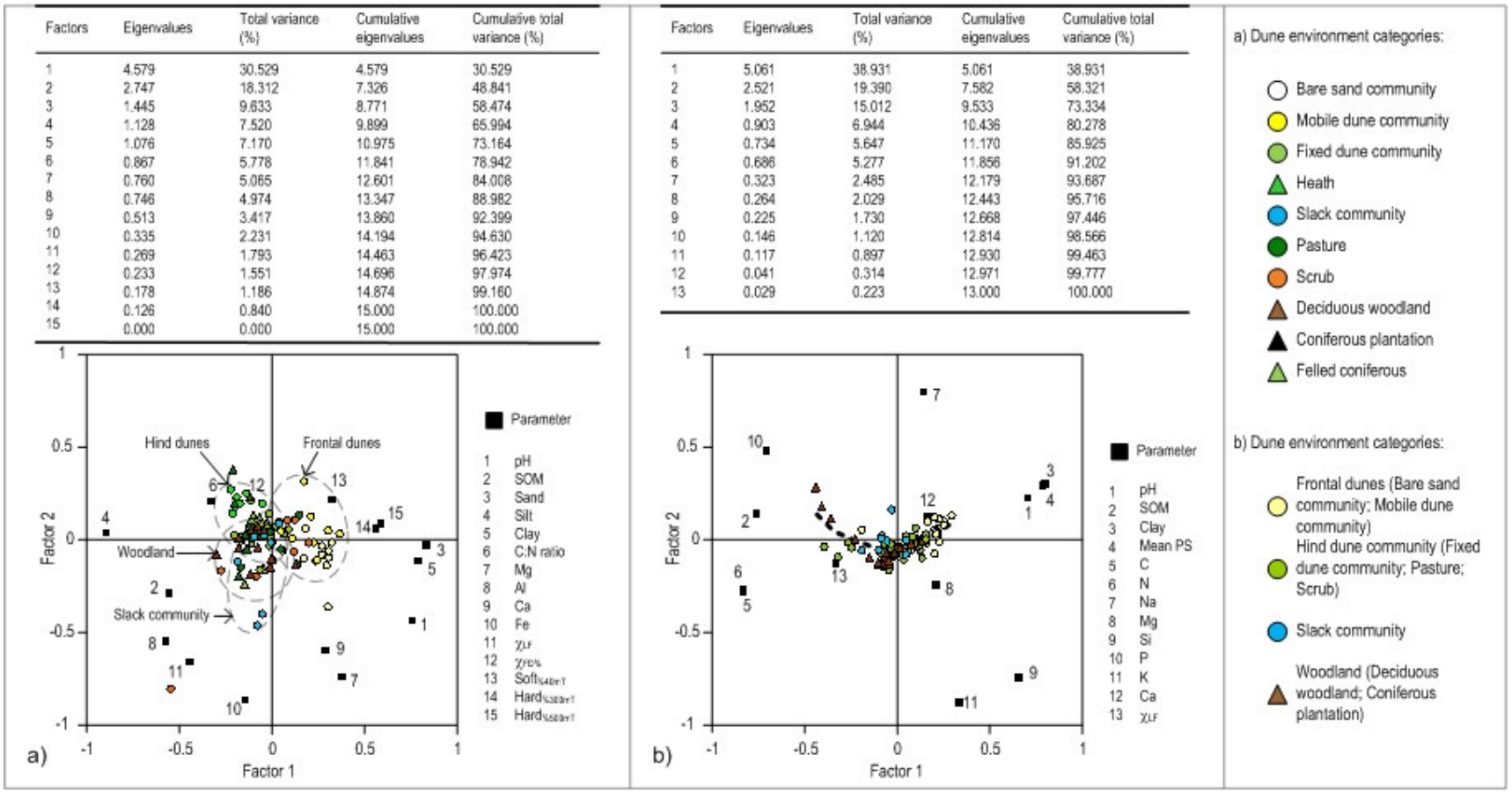

Figure 3.13 Simultaneous R- and Q-mode factor analysis plots of Factor 1 versus Factor 2, based on: a) selected topsoil characteristics and groupings and b) selected topsoil characteristics after reclassification (dashed line represents postulated pedogenesis).

community samples strongly influenced by heavy metals. Topsoils associated with advanced successional environments (i.e. fixed dune community, pasture and heath) are influenced by the C:N ratio. Despite coniferous plantation samples also being influenced by the C:N ratio, plotting of these topsoils is affected by SOM. Overall, combined spread of topsoil loadings suggests a secondary gradient, influenced by pH, evident by topsoils from seaward environments (i.e. bare sand, mobile dune community and scrub (recently exposed as a seaward environment)) plotting at opposite extremities to heath topsoils. These dune environments also appear to be influenced by Ca and magnetic mineralogies.

3.6.5 Factor analysis using key physico-chemical parameters following reclassification of dune environments

Factor analyses, so far, have identified reoccurring groupings of dune environments for most pedo-characteristics (Figure 3.13), suggesting reclassification was necessary; 'frontal dune' (bare sand; mobile dune communities), 'hind dune' (fixed dune community; pasture; scrub), 'woodland' (deciduous woodland; coniferous plantation) and slack community. The heath sample population was removed from analysis, as the topsoils appear to have independent characteristics. The felled coniferous sample population was also removed as it had similar characteristics to both the 'hind dune' and 'woodland' classifications.

Factor analysis was performed using key physico-chemical parameters (Figure 3.13b). Mineral magnetic parameters were removed, with the exception of χ_{LF}, as they displayed limited influence on topsoil characteristics. The first two factors extracted explain *5*8.3% of variation in the 13 parameters (Table 3.22b). Factor 1 (representing age of topsoil) explains 38.9% of variation in the parameters; whereas, Factor 2 (distance from the sea) explains 19.4% of variation. As acidity increases with distance inland, the alkaline frontal dune samples are positively loaded on Factor 2 with the pH parameter. As samples become more acidic they become negatively loaded on Factor 2. However, some woodland samples (presumably of an older age) are positively loaded on Factor 2, indicating alkaline characteristics. At some points along the eroding coast, both of these 'older' dune environments are in close proximity to the sea (Figure 3.1) and influenced by aeolian derived sand. Therefore, both factors have similar underlying causes, but the additional influence of erosion (possibly represented by Factor 3, explaining 15.0% of variation) has altered sample loadings.

Most of the frontal dunes samples have positive loadings on Factor 1, separating them from most of the slack and woodland topsoils. The spread of sample loadings along Factor 1 indicate that pH, SOM and particle size parameters are the major influencing parameters. The spread of sample loadings along Factor 2 indicates large geochemical variability occurs within each dune environment and, therefore, has a decreasing influence. The postulated pedogenesis line indicates a pedo-succession trend with frontal dune topsoils greatly influenced by pH, particle size and the parent material minerals Si and Ca. With distance inland, hind dune topsoils are still influenced by these parameters, but have an increasing influence of the nutrients Na, Mg

and K. Woodland topsoils are also influenced by Mg, but SOM has a greater role, alongside increased influences of C, N and P. Slack topsoils appear to be mainly influenced by Mg, Ca and χ_{LF}.

3.7 Discussion: Dynamics in topsoil pedo-characteristics on Sefton coastal dunes

The entire coastal unit, from the seaward edge to inland, can be regarded as a linear environmental system, in which topsoil characteristics vary with distance from MHW. The general marked trend is an overall decrease in mean particle size from west to east (i.e. inland), as coarser sand derived from aeolian processes is incapable of reaching far inland and increases in silt-sized particles are generally associated with pedogenesis. High values of finer clay-sized particles would have accumulated throughout the dune system, as a result of *in situ* weathering and increased levels of airborne dust. However, this is only evident on the seaward edge, with overall decreases in the percentages of clay inland. This suggests eluviation of clay-sized particles from topsoils proceeds with time.

The decreasing value of aeolian-derived sand inland is evidence of stabilization of the dune system as vegetation colonization progresses. SOM content accumulation increases inland, suggesting soil development, is dependent on decelerated aeolian processes (Ranwell, 1972). Parent material has a lesser influence on these topsoil characteristics on stable surfaces, where the processes operating within the organic horizons (e.g. biocycling of nutrients, decomposing litter and atmospheric deposition (Stutter *et al.,* 2003)) appear to control pedogenesis.

There are considerable variations between all geochemical concentrations across the dune landscape, likely to be due to varying leaching rates, translocation rates, atmospheric inputs, evapotranspiration, plant uptake and SOM content. C appears to increase with dune succession, as does N. However, the high C:N ratio suggests that denitrification processes may be active. K varies greatly, possibly due to a close association with uptake and storage by various vegetation types (James *et al.,* 1986). Leaching, and/or eluviation, appears to have resulted in losses of minerals from topsoils, confirmed by decreasing Mg, Ca and Fe, with distance inland. This, in turn, has led to increased acidification with distance from the sea. To gain an understanding of the timescale involved in this process, evidence from Newborough Warren sand dunes, Anglesey (Ranwell, 1959), show that topsoils with an initial calcium carbonate ($CaCO_3$) concentration of <5 %, similar to the Sefton coast, lose all carbonate through leaching within 300-400 years.

Due to the uniform nature of sand dune sediments, any differences in mineral magnetics cannot simply be explained by contrasting parent material, unlike previous work (e.g. Booth *et al.,* 2005, 2006). However, the overall low concentrations of magnetic minerals can be associated with the diamagnetic character of quartz (SiO_2) and calcite ($CaCO_3$) (Dearing, 1999).

3.7.1 Identifying frontal dunes using topsoil pedo-characteristics

In order to review trends in topsoil development, on a spatial pedo-succession basis, analysis of each dune pedo-environment is required with reference to potential successional order. Frontal seaward dunes have relatively high alkalinity due to the abundance of calcareous bare sand ($CaCO_3$), reflecting shell content and high quartz (SiO_2) concentrations. However, variations do exist within this depositional zone, which are likely to be caused by differential rates of aeolian erosion and deposition, as calcareous sand, transported from the frontal dunes, is often deposited inland during high energy regimes. This dune roll-back process results in large blowouts, evident as areas of high pH along the coast.

Comparisons of spatial variations in textural parameters provide an indication of sediment source and depositional conditions (Knight *et al.*, 2002; Saye and Pye, 2006). For example, the distribution pattern of mean particle size suggests frontal dunes, characterized by coarse, unsorted particles of sand- and clay-sized fractions, is responding to local variations in wave and wind energy regimes, which are strongly dependent on exposure rather than soil processes (James *et al.,* 1986; Saye and Pye, 2006). Prevailing winds on the Sefton coast are strong south-westerly (James and Wharfe, 1989) and are capable of transporting silt-sized particles inland.

According to James *et al.* (1986), the marine source for Na, K and Mg is important on the Sefton coast, with higher levels of Na on frontal dunes than elsewhere, reflecting high atmospheric inputs alongside a relatively low uptake by limited biomass. Although not significantly different (p >0.05), higher N and C in mobile dune community topsoils, compared with bare sand community sediment can be associated with increased SOM and cover of *Ammophila arenaria* in the former (Jones *et al.,* 2004). This suggests differences can be detected between topsoils of bare sand and unstable blowouts, with those of frontal dunes.

3.7.2 Identifying fixed dune environments using topsoil pedo-characteristics

Sediment accumulation north of Formby Point has resulted in stabilization of the northern fixed dune landscape. Increased SOM, likely to be the result of expanding vegetation cover, accounts for increased store of exchangeable cations, Na, K, Ca and Mg. Mg and K in fixed dune community topsoils are greater than in bare sand and mobile dune communities, indicating that even the shallowest topsoils can become more productive than bare sand alone after stabilization. High K in accreting northern and southern extremities confirms continued vegetation- and pedo-succession (Odum, 1969). Subsequently, pH fell from alkaline to neutral-slightly acidic. Payne (1983) noted acidity is slow to develop on these dunes, as the parent material is highly alkaline. In fact, Salisbury (1925) considered that it takes 200 years for the pH of soils on the Sefton coast to fall to 6.4 from original values of 8.2 at the top of the beach.

3.7.3 Identifying heath environments using topsoil pedo-characteristics

The dune heath accounts for a very small area of the Sefton dunes. However, it has potential to increase spatially, due to rapid colonization of the fixed dunes by heath vegetation, if management were not to be maintained (Edmondson *et al.,* 1993). Subsequent, extremely acidic conditions of the semi-natural dune heath environment might alter soil characteristics to such an extent, that it would be impossible for natural fixed dune vegetation to survive. This would also be applicable to C levels in the topsoil, if the heathland were allowed to expand. This accords with findings by Ordóñez *et al.* (2007). Presently, differences in C are insignificant (p >0.05) among the inland dune environments (i.e. successional environments post-fixed dune communities), apart from slight increases in the semi-natural dune heath. This concept is further confirmed by Vestin *et al.* (2006), who associated high SOM with high C and low pH. Mean particle size decreased in heath topsoils, with an overall decrease in clay suggesting eluviation, or weathering, of clays has proceeded with age in these topsoils.

3.7.4 Identifying slack environments using topsoil pedo-characteristics

Wet slacks, interspersed within the fixed dune environment, have higher SOM than comparable-aged dry fixed dune community topsoils, pasture and felled areas, similar to findings by Ranwell (1959). However, they have very similar SOM to heath, scrub, deciduous woodland and coniferous plantation topsoils. Ranwell (1972) highlighted that in most dune systems, well-developed wet slacks overlie clay deposits, accounting for high clay content in Ainsdale NNR. Although not measured in this research, it is widely known in the literature (e.g. Williams and Cooper, 1990), that increases in soil moisture characteristics are related to decreases in particle size, which corresponds to these wet slack settings.

Slack topsoils are influenced by high Fe, often associated with pollution; suggesting slack environments are acting as heavy metal sinks. Despite levels of Ca generally decreasing with dune succession, levels increase in the slacks. As losses of Mg, Ca and Fe are caused by leaching processes, increases in these minerals confirm waterlogged slacks do act as sinks. Since slacks are where the water table comes to the surface, they might be expected to be sinks for any dissolved minerals, which have been leached out of the dunes by rainwater. Previous environmental magnetism research (e.g. Mullins, 1977; Wang *et al.*, 2008) associated low χ_{LF} with dissolution of strongly magnetic minerals under reducing conditions. This appears to be true of slack topsoils on the Sefton coast, as χ_{LF} values are low in these environments compared with dry dune environments. This suggests low concentrations of magnetic minerals are evidence of waterlogged sites or topsoils developed in poorly drained areas where the water table fluctuates seasonally.

3.7.5 Identifying scrub and deciduous woodland environments using topsoil pedo-characteristics

Temporal increases in SOM has increased the capacity of the scrub and deciduous woodland topsoils to retain nutrients. The C:N ratio is generally much higher in presumably older scrub

and deciduous woodland, than in younger fixed dune community and pasture soils. Therefore, a balance between N gain and loss seems to be reached following stabilization and colonization of scrub-like species of the dune surface. However, coastal erosion processes, active on Formby point, have destroyed the mobile dune barrier environments, consequently, exposing previous inland woody habitats on the foreshore. Subsequent burial of these scrub and woodland environments, by new mobile dunes, is evident in low K concentrations across the bare sand community, scrub and woodland topsoils, where values would normally be expected to be higher in more pedogenically-advanced topsoils.

Increased storminess may have resulted in development of the large, coarse-grained sand sheets inland, burying existing scrub and deciduous woodland topsoils. This is reflected by high values of χ_{LF} in scrub topsoils and bare sand sediments, associated with well-drained, freshly deposited sand (Williams and Cooper, 1990), making it difficult to discriminate between these topsoils.

3.7.6 Identifying coniferous plantation environments using topsoil pedo-characteristics

Afforestation affected the nature and transformation of SOM and associated nutrients on topsoils under coniferous plantations on the Sefton coast, similar to findings by Chen *et al*. (2007). The major impact on topsoil characteristics has been through the deposition of a thick acidic pine needle litter layer. Guo *et al.* (2007) suggested slower turnover of litter plays a role in decreasing C, as under such rapidly developing acidic conditions, litter breakdown inhibits SOM accumulation. Berendse (1998) suggested that during succession, litter of woody species contains increased phenols and organic compounds, slowing decomposition rates. C and N stocks in coniferous plantation topsoils have limited variability compared to open fixed dune community topsoils, possibly resulting from increased biomass in the former, causing depletion of excess available C and N in the soil (Jones *et al.,* 2004). This suggests afforestation caused minor changes in C and N, similar to findings by McKinley *et al.* (2008). On the other hand, enhanced SOM mineralization and associated P appears to have, consequently, improved P availability in coniferous plantation topsoils, similar to findings by Beltman *et al.* (1992), who associated high P with high SOM on Irish dunes.

Mineralogy across the dunes is generally soft magnetite-type and this is especially notable in heath topsoils. However, magnetic mineralogical data show relative amounts of haematite-type to magnetite-type minerals to be greater in coniferous plantation topsoils, compared to all other dune environments. This may be associated with secondary magnetic minerals, developed by pedogenesis and higher levels of Fe. Low χ_{LF} may be explained by the diamagnetic characteristic of SOM (Williams and Cooper, 1990).

3.7.7 Identifying felled environments using topsoil pedo-characteristics

Due to potentially large quantities of nutrients removed, it has generally been considered, clear felling can lead to decreased soil-available reserves of limiting nutrients (e.g. Olsson *et al*.,

2000; Merino *et al.*, 2004). However, following felling on the Sefton coast, enhanced decomposition and leaching has resulted in increased movement of some minerals, encouraging plant colonization (Atkinson and Sturgess, 1991). Colonization of plants will have begun to recycle nutrients, accounting for losses in SOM and P from clear-felled topsoils compared with coniferous plantation topsoils. C and N remain the same under clear-felled topsoils as under coniferous plantation topsoils. According to Staaf and Berg (1982), this is not characteristic of such environments, as C would be expected to be lost at higher rates through respiration than N. However, Merino *et al.* (2004) proposed changes in C and N cannot be reliably detected after such short time periods (i.e. ~15 years).

The pH values of felled topsoils are higher than coniferous plantation topsoils, highlighting that during the last decade, since felling began; acidic plantation topsoils are reverting back to natural fixed dune community topsoil characteristics. This should, in turn, encourage successful growth of dune plants characteristic of young, calcareous dunes. High SOM retains water better than bare sand, and this may be an important factor in the rapid establishment of fixed dune vegetation on clear-felled sites (Sturgess, 1992, 1993).

3.7.8 Limitations when distinguishing dune environment topsoil pedo-characteristics

Individual dune environments can be successfully distinguished by comparing differences of the medians of each of the dune environment topsoil sample populations for each pedo-characteristic using Mann-Whitney U tests (Section 3.4). Therefore, the null hypothesis (H_0) can be rejected, accepting the alternative hypothesis (H_1), that there are significant differences (p <0.05) between sample populations. However, there are no statistically significant differences between more than two of the dune environment topsoil sample populations for each pedo-characteristic, independent of each other, using the Kruskal-Wallis test. Therefore, the null hypothesis (H_0) can be accepted, stating that there are no significant differences between the sample populations.

An explanation for the acceptance of the null hypothesis is that classification of dune environments, using vegetation analysis (refer to Chapter 2, Section 2.1), was insufficient, implying that pedo-surfaces could not be distinguished for the 10 classified dune environments, as some sample population values were similar both intra- and inter-dune environments. For most pedo-characteristics, a separation could be made between 'frontal dune' topsoils (i.e. bare sand and mobile dune communities) and remaining environments. Heath topsoils, and to some extent slack community topsoils, appear to have independent characteristics. 'Hind dune' topsoils (i.e. fixed dune community, pasture, scrub, deciduous woodland, coniferous plantation and felled community) appear to group together as one classified environment with similar topsoil pedo-characteristics. Woodland topsoils (i.e. deciduous woodland and coniferous plantation) could be separated further from the hind dunes, although not to the same extent. Difficulties occurred during this separation due to topsoils from the felled area having some characteristics similar to coniferous plantation topsoils and some similar to fixed dune

community topsoils. Implications of these findings are that, rather than distinguishing dune environments, linkages can be made instead, identifying close relationships between topsoils undergoing pedo-succession.

Despite these findings, inter-environment vegetation still remains variable on the dune environments map. This implies that further research is required, including a detailed vegetation survey to determine floral differences, and a detailed investigation of pedo-characteristics within the soil profiles, to identify soil-forming processes (e.g. leaching, clay translocation, podzolization, decalcification, gleying and salinization) that may further distinguish, or link, dune environments. It is also possible that there is a lot more 'cycling' in the dune system than originally observed, with stable dune surfaces de-stabilizing and re-stabilizing, resulting in fixed dune topsoil samples likely to include characteristics of both mobile and hind dune topsoils.

3.8 Summary

Distinct soil characteristics are apparent within the Sefton dune landscape and can be confidently associated with individual dune environments by digitizing reliable data into a GIS and conducting Mann-Whitney tests. In general terms:

- Topsoil pH becomes more acidic with dune pedo-succession.
- Topsoill organic matter (SOM) increases with dune pedo-succession.
- Mean particle size of topsoils decreases with dune pedo-succession.
- Percentages of clay-sized particles also decrease with dune pedo-succession.
- Percentages of Mg, Ca and Fe generally decrease with dune pedo-succession, while percentages of C and N increase. Remaining geochemical parameters vary due to fluctuating leaching rates, eluviation, translocation rates, atmospheric inputs, evapotranspiration and plant uptake.
- Magnetic concentration parameters show limited variation with dune pedo-succession, although low values are associated with slack community topsoils. Magnetic mineralogy is predominantly soft magnetite-type, with coarse (multidomain) magnetic domain sizes and few fine (stable single domain) magnetic materials. However, relative amounts of hard haematite-type to soft magnetite-type minerals increase with dune pedo-succession.

Simultaneous R- and Q-mode factor analyses has shown great potential for separating 'frontal dune' topsoils (i.e. bare sand and mobile dune communities) from heath topsoils, slack community topsoils and 'hind dune' topsoils (i.e. fixed dune community, pasture, scrub, deciduous woodland and coniferous plantation). Separations have also been made between well-drained (dry dune environments) and poorly-drained (slack environment) topsoils.

It seems that linking dune environments, rather than trying to distinguish them, can identify relationships between topsoils undergoing pedo-succession. However, for this it is necessary to reclassify the dune environments into fewer categories. This runs the risk of losing some pedo-

environments that do appear to have very distinct vegetation habitats. Further research into classifying the soil profiles may resolve this issue.

CHAPTER 4

Pedogenesis in dune environments: implications for succession

Chapter 4 identifies down-profile variations in pedo-characteristics, in an attempt to classify dune pedo-environments and determine influences on pedogenic development. Soil profiles and associated flora counts from each dune environment (n = 9) are described in proposed order of succession. The extent of relationships between parameters down-profile are identified through statistical and graphical techniques. Results of statistical analyses are summarized and presented in conceptual tables and figures, to identify influential soil-forming pedo-characteristics.

4.1 Introduction

In order to group or separate dune environments using pedo-characteristics, it was necessary to reclassify the dune topsoils into fewer categories (Chapter 3; Section 3.9). Classification of a soil profile from each topsoil pedo-environment, into NSRI categories will, ultimately, reduce sample populations. As these independent soil bodies each have distinct soil-forming processes (e.g. leaching, clay translocation, podzolization, decalcification, gleying and salinization) (Gerrard, 2000; Smithson *et al*., 2002; Fullen and Catt, 2004), pedogenic trends under varying dune ecological environments will be established.

4.2 Classification of soil profiles using general statistical descriptions of pedo-characteristics

Figure 4.1 shows the locations of the soil profiles. The numbering indicates the following order of dune environment and associated soil profile descriptions, based on a hypothetical path of natural topsoil succession (determined in Chapter 3), as suggested by Hodgson (1997). Flora counts (plant nomenclature follows Stace (1997) throughout) associated with each soil profile are presented. However, vegetation data from the embryo dunes and phase one felling (felled in 1992) are presented in Appendix 2. Graphical representations of each soil profile are presented.

As the Cu horizon is generally not affected by biological activity, technically it is not part of the soil profile (Gerrard, 2000). Therefore, a separation was made between the upper organic/mineral soil component of each profile (i.e. the combination of all layers/horizons excluding the parent material (Cu)) (following Dearing *et al.,* (1995) methodologies) and the lower parent material component of each profile. This was for classification purposes, with the separated upper soil profile component referred to as the organo-mineral soil component. Therefore, only the organo-mineral soil component of each profile is used for statistical analysis.

4.2.1 Mobile dune community pedo-characteristics

The mobile dune community soil profile location (Figure 4.1) was determined by a 'frontal dune' topsoil pedo-environment (i.e. bare sand, incorporating embryo dune and mobile dune communities) (Chapter 3, Section 3.7.1). Marram grass (*Ammophila arenaria*) was the dominant

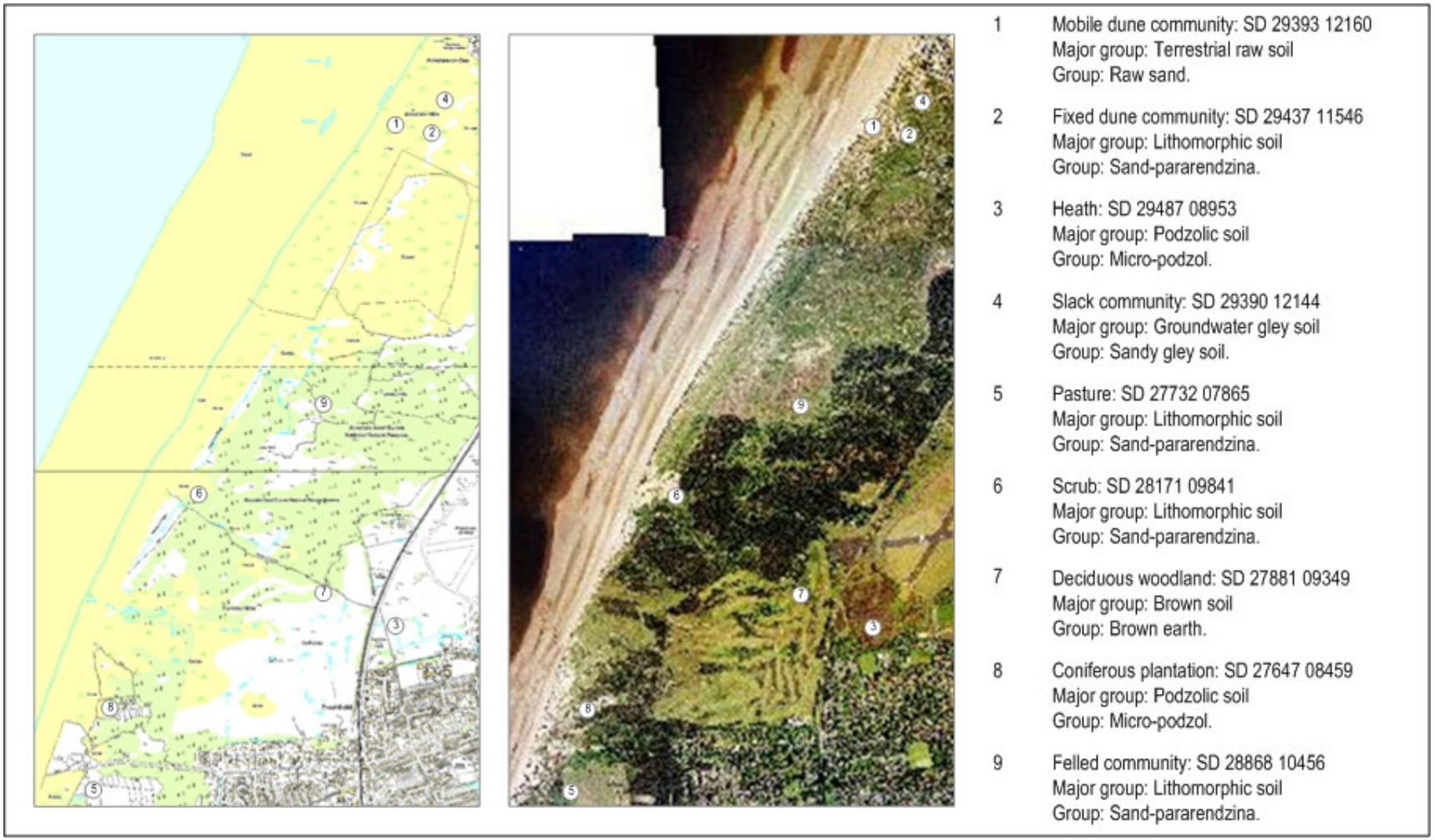

1 Mobile dune community: SD 29393 12160
Major group: Terrestrial raw soil
Group: Raw sand.

2 Fixed dune community: SD 29437 11546
Major group: Lithomorphic soil
Group: Sand-pararendzina.

3 Heath: SD 29487 08953
Major group: Podzolic soil
Group: Micro-podzol.

4 Slack community: SD 29390 12144
Major group: Groundwater gley soil
Group: Sandy gley soil.

5 Pasture: SD 27732 07865
Major group: Lithomorphic soil
Group: Sand-pararendzina.

6 Scrub: SD 28171 09841
Major group: Lithomorphic soil
Group: Sand-pararendzina.

7 Deciduous woodland: SD 27881 09349
Major group: Brown soil
Group: Brown earth.

8 Coniferous plantation: SD 27647 08459
Major group: Podzolic soil
Group: Micro-podzol.

9 Felled community: SD 28868 10456
Major group: Lithomorphic soil
Group: Sand-pararendzina.

Figure 4.1 Location and NRSI (Source Avery, 1980) of each soil profile. Ascending profile numbers are based on a hypothetical path of pedogenesis.

species type of this parallel seaward dune ridge community (Table 4.1a), occurring on freshly deposited sand and actively building dunes. Sea spurge (*Euphorbia paralias*) and red fescue (*Festuca rubra*) are typical of semi-fixed dune environments (Payne, 1983) and, therefore, only occurred in the sheltered, leeward side of dunes.

Figure 4.2 represents the terrestrial raw sand (Avery, 1980), consisting of little altered mineral material, with a thin layer of SOM (7.2%) at the surface. Slight horizonation was evidenced by a greyish brown (10YR 5/2) horizon at 1-3 cm, with neutral pH (7.1), less SOM (3.2%) and 25% silt-sized particles. The yellowish brown (10YR 5/4) sediment of the Cu horizon had pH 8.1, reflecting the abundance of Na (0.85-3.20%) and Ca (0.65-1.92%), SOM 0.5% and 89% sand-sized particles.

Figures 4.3 and 4.4 show great variation in texture, nutrient and magnetic properties down-profile, as most of the profile was comprised of mixed terrestrial raw sand due to active geomorphological processes. Identification of the very shallow soil was evident by the marked decrease in alkalinity and increased SOM above 3 cm depth, where increased percentages of silt-sized particles were also observed.

Tables 4.2a,b show the organo-mineral soil component had altered physico-chemical values (e.g. pH 7.14; SOM 4.51%; Silt 24.82%) compared to the entire profile (pH 8.02; SOM 0.69%; silt 8.17%). Nutrient enrichment in the upper horizons is evident but minimal (Al 0.04-0.12%; P 0.02-0.04%; S <0.01-0.02), whereas, Ca decreased from 1.17% to 0.82%. Increased magnetic concentrations in the surface horizons (χ_{LF} 1.15 $x10^{-7}m^3kg^{-1}$; χ_{ARM} 0.02 $x10^{-7}m^3kg^{-1}$; SIRM 124.18 $x10^{-5}m^2kg^{-1}$), compared to the entire profile (χ_{LF} 0.53 $x10^{-7}m^3kg^{-1}$; χ_{ARM} 0.01 $x10^{-7}m^3kg^{-1}$; SIRM 62.52 $x10^{-5}m^2kg^{-1}$), show magnetic enhancement of the organo-mineral soil component. The content of ferrimagnetic 'magnetite (Fe_3O_4)-type' soft minerals throughout the profile (IRM_{20mT} 10.92; IRM_{40mT} 27.15) was higher than canted antiferromagnetic 'haematite (αFe_2O_3)-type' hard minerals (IRM_{300mT} 7.22; IRM_{500mT} 4.76). However, ferrimagnetic minerals increased in the organo-mineral soil component (IRM_{20mT} 22.67; IRM_{40mT} 52.42, while canted antiferromagnetic minerals remained consistent.

4.2.2 Fixed dune community pedo-characteristics

The fixed dune community soil profile location (Figure 4.1) was determined by a fixed dune topsoil pedo-environment (Chapter 3, Section 3.7.2). Table 4.1b shows marram grass (*Ammophila arenaria*) to be less abundant but remaining frequent. Red fescue (*Festuca rubra*), a short grass, dominated this area, possibly indicating trampled ground, followed by dewberry (*Rubus caesius*). Other grasses, such as yorkshire fog (*Holcus lanatus*) occurred occasionally, with creeping willow (*Salix repens*) occurring abundantly in localized areas. The occurrence of polypody (*Polypodium vulgare*) indicates a dense vegetation type offering shade (Edmondson *et al.,* 1993). According to Payne (1983) the presence of wild parsnip (*Pastinaca sativa*) suggests this area may have been a slack hollow.

Table 4.1a Plant species on the mobile dune (SD 29353 12170)

Vernacular name	Latin name	DAFOR	Notes
Marram grass	*Ammophila arenaria*	Abundant/dominant	
Cat's ear	*Hypochaeris radicata*	Frequent	
Sea spurge	*Euphorbia paralias*	Frequent	
Ragwort	*Senecio jacobaea*	Occasional	
Hound's tongue	*Cynoglossum officinale*	Occasional	
Dune Fescue grass	*Vulpia membranacea*	Occasional	
Sticky mouse ear	*Cerastium glomeratum*	Occasional	
Wavy hair grass	*Deschampsia flexuosa*	Occasional	
Bryophytes		Occasional	
Prickly Sow-thistle	*Sonchus asper*	Rare	
Sea holly	*Eryngium maritimum*	Rare	
Evening primrose	*Oenothera sp.*	Rare	
Blue fleabane	*Erigeron acer*	Rare	
Rough hawkbit	*Leontodon hispidus*	Rare	
Smooth hawkbit	*Leontodon autumnalis*	Rare	
Eyebright	*Euphrasia officinalis*	Rare	
Carline thistle	*Carlina vulgaris*	Rare	
Canadian fleabane	*Conyza canadensis*	Rare	
Short-fruited willowherb	*Epilobium obscurum*	Rare	
Red fescue	*Festuca rubra*		Semi-fixed community.
Hedge parsley	*Torilis japonica*		Semi-fixed community.

Table 4.1b Plant species on the fixed dune (SD 29775 11634)

Vernacular name	Latin name	DAFOR	Notes
Sand sedge	*Carex arenaria*	Abundant	
Dewberry	*Rubus caesius*	Abundant	
Red fescue	*Festuca rubra*	Abundant/dominant	
Bryophytes		Abundant/dominant	
Marram grass	*Ammophila arenaria*	Frequent	Pine has never colonized.
Rose-bay willowherb	*Chamerion angustifolium*	Frequent	
Wild parsnip	*Pastinaca sativa*	Frequent	
Autumn hawkbit	*Leontodon autumnalis*	Frequent	
Field wood rush	*Luzula campestris*	Frequent	
Creeping willow	*Salix repens*	Local/abundant	
Pink centaury	*Centaurium erythraea*	Occasional	
Self-heal	*Prunella vulgaris*	Occasional	
Broad-leaved willowherb	*Epilobium montanum*	Occasional	
Intermediate polypody	*Polypodium interjectum*	Occasional	
Yorkshire fog	*Holcus lanatus*	Occasional	
Tall oat grass	*Arrhenatherum elatius*	Occasional	
Asparagus	*Asparagus officinalis*	Occasional	
Cat's ear	*Hypochaeris radicata*	Occasional	
Portland spurge	*Euphorbia portlandica*	Occasional	
Rest-harrow	*Ononis spinosa*	Occasional	
Hound's tongue	*Cynoglossum officinale*	Occasional	
Common milkwort	*Polygala vulgaris*	Occasional	
Creeping white clover	*Trifolium repens*	Occasional	
Hare bell	*Campanula rotundifolia*	Occasional	
Mouse-ear-hawk reed	*Pilosella officinarum*	Rare	
Sweet vernal grass	*Anthoxanthum odoratum*	Rare	
Yellow wort	*Blackstonia perfoliata*	Rare	
Fairy flax	*Linum catharticum*	Rare	
Eye bright	*Euphrasia officinalis*	Rare	
Spring hairgrass	*Aira praecox*	Rare	
Stork's bill	*Erodium cicutarium*	Rare	
Little Mouse-ear chickweed	*Cerastium semidecandrum*	Rare/occasional	

Table 4.1c Plant species in the heath (SD 29443 08918)

Vernacular name	Latin name	DAFOR	Notes
Common heather	*Calluna vulgaris*	Abundant/dominant	
Wavy hair grass	*Deschampsia flexuosa*	Abundant/frequent	
Sand sedge	*Carex arenaria*	Abundant/frequent	
Sheep's fescue	*Festuca ovina*	Frequent	
Cat's ear	*Hypochaeris radicata*	Frequent	
Sheep's sorrel	*Rumex acetosella*	Frequent	
Bryophytes		Local/abundant	
Common oak	*Quercus robur*	Occasional	
Silver birch	*Betula pendula*	Occasional	
Birch	*Betula spp.*	Occasional	
Heath bedstraw	*Galium saxatile*	Occasional	
Bird's foot trefoil	*Lotus corniculatus*	Occasional	
St John's wort	*Hypericum perforatum*	Rare	
Rose-bay willowherb	*Chamerion angustifolium*	Rare	
Heath grass	*Danthonia decumbens*	Rare	
Common gorse	*Ulex europaeus*		Peripheral.

Mobile dune soil profile description

Profile ID: MD
Date of survey: 17/02/2008

Site description

Location: 1000 m SSW of Ainsdale Beach car park entrance.
Grid reference: SD 29393 12160
Landform: Top of dune ridge.
Land use: Managed retreat.
Weather: Clear, bright, sub-zero temperature.

Soil description

Drainage: Well-drained.
Surface cover: Bare sand interspersed with bryophytes and marram grass.
Profile depth: 84 cm
Soil depth: 3 cm
NSRI Major group: Terrestrial raw soil


a) Photograph facing south

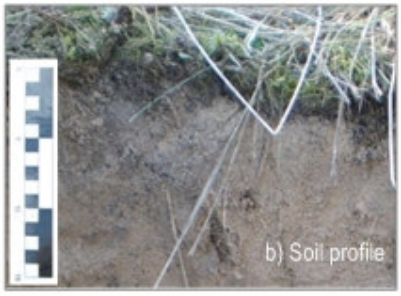
b) Soil profile

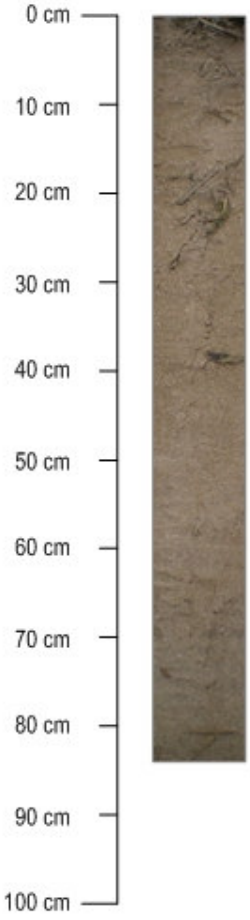

Layer/ Horizon	Depth (cm)	Field description
F	0-1	Very dark grey (10YR 3/1) moist and dark greyish brown (10YR 4/2) dry; loose sand; stoneless; clear smooth boundary to:
A	1-3	Greyish brown (10YR 5/2) moist and brown (10YR 5/3) dry; loose sand; stoneless; clear diffuse boundary to:
Cu	3-84	Yellowish brown (10 YR 5/4) moist and pale brown (10YR 6/3) dry; loose sand; stoneless; many fine (1-2 mm) fibrous roots grading into medium (2-5 mm) fibrous roots with depth.

Layer/Horizon	F	A	Cu
Sand 600-2000 µm %	73	73	89
Silt 2-60 µm %	25	25	7
Clay <2 µm %	2	2	4
SOM %	7.2	3.2	0.5
pH in water (1:2.5)	7.1	7.1	8.1

Figure 4.2 Soil profile description for mobile dune community. Scale on Plate b) is 15 cm.

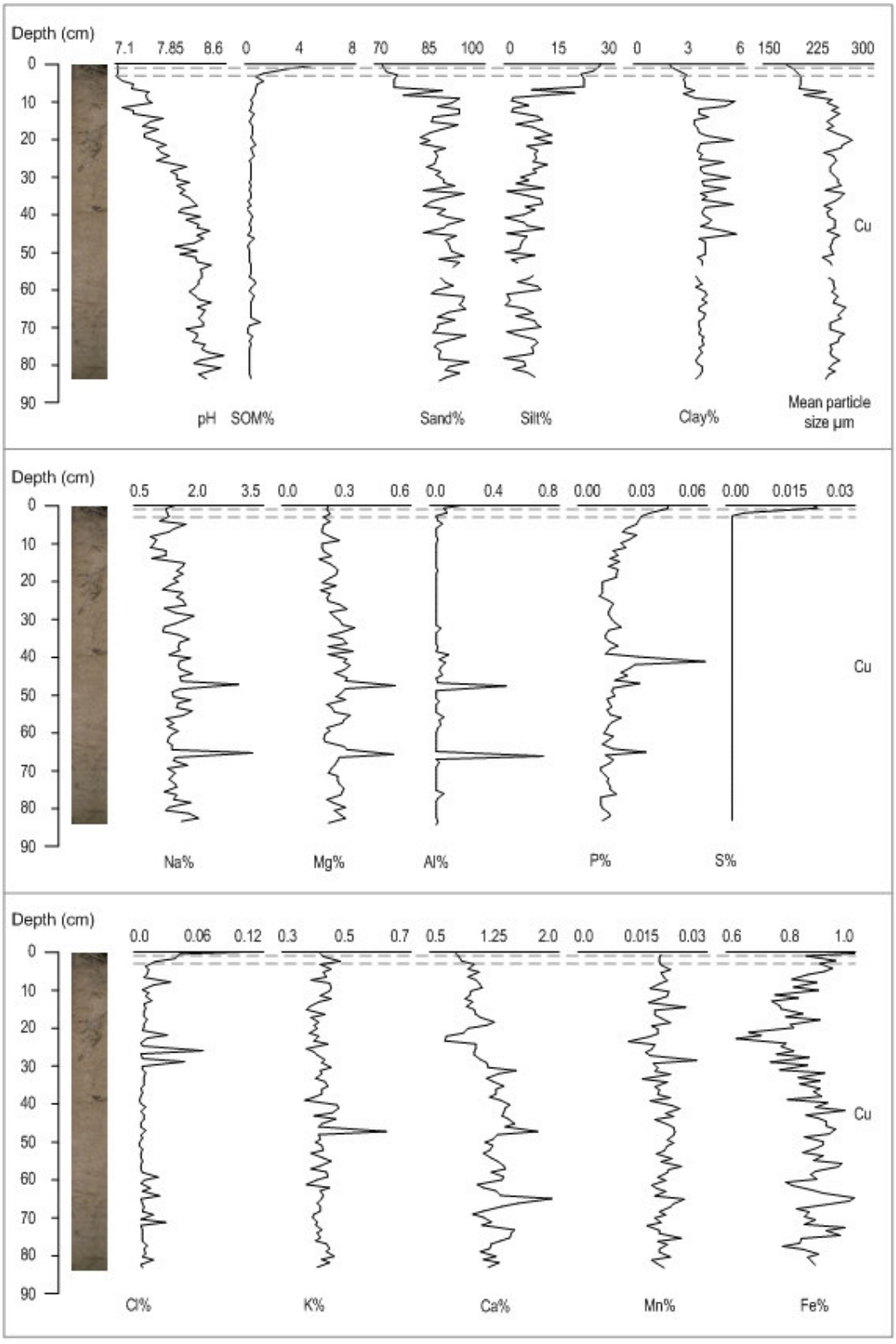

Figure 4.3 Down-profile changes in mobile dune soil characteristics; pH, SOM, texture and geochemical properties (dashed lines show horizon boundaries).

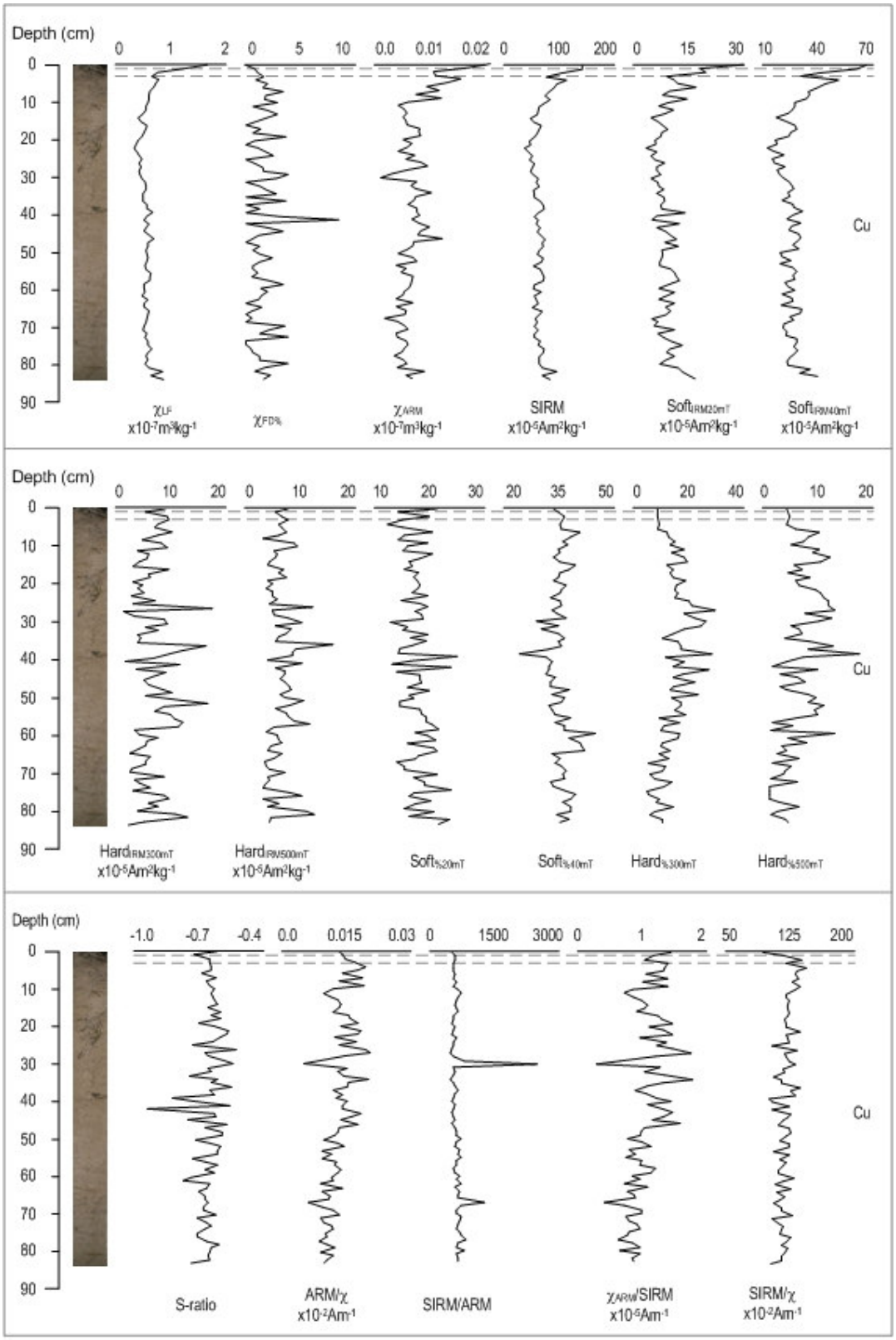

Figure 4.4 Down-profile changes in mobile dune soil mineral magnetic characteristics (dashed lines show horizon boundaries).

Table 4.2a Summary data* for mobile dune profile characteristics (n = 84)

Parameters	Units	Mean	Median	SD	CV	Min	Max
pH	mol/ltr	8.020	8.160	0.397	4.954	7.130	8.660
SOM	%	0.689	0.472	0.897	130.195	0.000	7.211
Sand	%	87.980	88.346	5.247	5.964	72.621	95.740
Silt	%	8.165	7.873	5.586	68.415	0.785	25.532
Clay	%	3.856	3.795	0.730	18.935	1.847	5.873
Mean particle size	µm	243.679	246.306	17.101	7.018	183.265	274.009
Median particle size	µm	246.161	247.143	12.641	5.135	189.125	281.020
Sorting		1.136	1.156	0.357	31.417	0.426	1.918
Skewness	γ_1	0.425	0.393	0.146	34.311	0.021	0.750
Kurtosis	g_1	3.406	3.640	1.272	37.358	0.757	5.968
Sodium	%	1.461	1.430	0.338	23.150	0.850	3.200
Magnesium	%	0.256	0.249	0.062	24.372	0.169	0.549
Aluminium	%	0.044	0.019	0.094	212.697	0.017	0.725
Phosphorus	%	0.019	0.016	0.008	41.927	0.011	0.059
Sulphur	%	0.001	0.001	0.003	196.677	0.001	0.021
Chlorine	%	0.016	0.011	0.017	107.038	0.007	0.138
Potassium	%	0.434	0.430	0.033	7.658	0.381	0.640
Calcium	%	1.172	1.170	0.217	18.482	0.647	1.920
Manganese	%	0.019	0.019	0.003	12.987	0.011	0.028
Iron	%	0.854	0.862	0.074	8.680	0.618	1.033
χ_{LF}	$10^{-7}m^3kg^{-1}$	0.528	0.505	0.165	31.216	0.291	1.585
χ_{FD}	%	1.592	1.325	1.436	90.166	0.001	9.023
χ_{ARM}	$10^{-7}m^3kg^{-1}$	0.007	0.006	0.003	46.569	0.001	0.021
SIRM	$10^{-5}Am^2kg^{-1}$	62.515	59.512	16.978	27.158	35.054	136.236
$Soft_{IRM20mT}$	$10^{-5}Am^2kg^{-1}$	10.916	10.161	3.458	31.675	5.761	29.207
$Soft_{IRM40mT}$	$10^{-5}Am^2kg^{-1}$	27.154	26.368	7.475	27.529	14.432	61.327
$Hard_{IRM300mT}$	$10^{-5}Am^2kg^{-1}$	7.219	6.226	4.081	56.535	0.771	20.006
$Hard_{IRM500mT}$	$10^{-5}Am^2kg^{-1}$	4.760	4.163	3.445	72.367	0.024	18.010
$Soft_{\%20mT}$	%	17.536	17.347	3.054	17.414	11.294	25.886
$Soft_{\%40mT}$	%	43.571	43.563	4.230	9.708	32.069	54.814
$Hard_{\%300mT}$	%	11.578	10.096	6.350	54.841	1.612	39.100
$Hard_{\%500mT}$	%	7.610	6.592	5.333	70.074	0.040	28.855
S-ratio	(none)	-0.648	-0.642	0.074	-11.426	-0.993	-0.494
ARM/χ	$10^{-2}Am^{-1}$	0.013	0.013	0.005	34.710	0.002	0.023
SIRM/ARM	(None)	346.430	300.423	289.248	83.494	157.182	2695.720
χ_{ARM}/SIRM	$10^{-5}Am^2kg^{-1}$	1.090	1.046	0.354	32.454	0.117	1.998
SIRM/χ	$10^{-2}Am^{-1}$	119.360	119.796	11.894	9.965	85.801	150.690

Table 4.2b Summary data* for mobile dune organo-mineral soil (refer to Section 5.2) characteristics (n = 3)

Parameters	Units	Mean	Median	SD	CV	Min	Max
pH	mol/ltr	7.140	7.140	0.000	0.000	7.140	7.140
SOM	%	4.506	4.517	2.711	60.163	1.789	7.211
Sand	%	73.051	72.737	0.647	0.886	72.621	73.795
Silt	%	24.816	25.287	1.035	4.172	23.629	25.532
Clay	%	2.133	1.976	0.389	18.239	1.847	2.576
Mean particle size	µm	190.311	190.522	6.942	3.648	183.265	197.145
Median particle size	µm	202.899	200.817	14.925	7.356	189.125	218.756
Sorting		1.640	1.648	0.028	1.700	1.609	1.663
Skewness	γ_1	0.643	0.625	0.064	9.873	0.591	0.714
Kurtosis	g_1	0.937	0.930	0.022	2.384	0.919	0.962
Sodium	%	1.307	1.260	0.117	8.969	1.220	1.440
Magnesium	%	0.214	0.213	0.006	2.602	0.209	0.220
Aluminium	%	0.123	0.097	0.070	57.032	0.070	0.203
Phosphorus	%	0.039	0.042	0.005	11.933	0.034	0.042
Sulphur	%	0.015	0.019	0.009	63.189	0.004	0.021
Chlorine	%	0.074	0.045	0.055	74.847	0.039	0.138
Potassium	%	0.452	0.439	0.034	7.531	0.427	0.491
Calcium	%	0.817	0.821	0.042	5.108	0.774	0.857
Manganese	%	0.019	0.019	0.000	1.336	0.019	0.019
Iron	%	0.940	0.941	0.093	9.891	0.847	1.033
χ_{LF}	$10^{-7}m^3kg^{-1}$	1.153	1.174	0.444	38.516	0.698	1.585
χ_{FD}	%	0.648	0.833	0.578	89.082	0.001	1.111
χ_{ARM}	$10^{-7}m^3kg^{-1}$	0.016	0.017	0.005	32.700	0.011	0.021
SIRM	$10^{-5}Am^2kg^{-1}$	124.178	136.034	20.710	16.677	100.265	136.236
$Soft_{IRM20mT}$	$10^{-5}Am^2kg^{-1}$	22.670	20.158	5.711	25.193	18.646	29.207
$Soft_{IRM40mT}$	$10^{-5}Am^2kg^{-1}$	52.424	56.486	11.486	21.909	39.460	61.327
$Hard_{IRM300mT}$	$10^{-5}Am^2kg^{-1}$	8.432	9.867	2.625	31.130	5.402	10.026
$Hard_{IRM500mT}$	$10^{-5}Am^2kg^{-1}$	4.710	4.666	1.544	32.780	3.188	6.275
$Soft_{\%20mT}$	%	18.420	20.104	4.156	22.564	13.686	21.470
$Soft_{\%40mT}$	%	41.967	41.462	2.897	6.903	39.355	45.083
$Hard_{\%300mT}$	%	7.073	7.253	3.021	42.716	3.965	10.000
$Hard_{\%500mT}$	%	3.869	4.613	1.324	34.223	2.340	4.654
S-ratio	(none)	-0.658	-0.648	0.066	-10.024	-0.728	-0.597
ARM/χ	$10^{-2}Am^{-1}$	0.014	0.014	0.001	6.492	0.013	0.015
SIRM/ARM	(None)	248.910	251.592	47.112	18.927	200.515	294.624
χ_{ARM}/SIRM	$10^{-5}Am^2kg^{-1}$	1.294	1.248	0.253	19.574	1.066	1.566
SIRM/χ	$10^{-2}Am^{-1}$	115.136	116.028	28.900	25.101	85.801	143.580

Mean; SD = standard deviation; CV = percentage coefficient of variation; Min = minimum value; Max = maximum value. Values are shown to 3 decimal places for consistency, not accuracy.

Figure 4.5 represents the sand-pararendzina (Avery, 1980) in an early stage of development. SOM accumulation was initially 4.8% in the H layer (0-5 cm), which became incorporated into a brown (10YR 5/3) shallow Ah horizon (5-18 cm), reaching a level of 1.1%. The pH increased from 6.3 (H) to 6.9 (Ah), but values remained similar for sand, silt and clay.

Figures 4.6 and 4.7 identify soil formation above 18 cm, most marked by an abrupt decrease in both sand and clay percentages and increases in silt-sized particles, the trends of which are replicated in changes in magnetic grain size parameters at this depth. The highest SOM (7.52%) and increasing values of all absorbed cations, with the exception of Fe, were restricted to the upper 5 cm, whereas, magnetic concentrations peaked in the upper Ah horizon (χ_{LF} 1.56 $x10^{-7}m^3kg^{-1}$; SIRM 215.22 $x10^{-5}m^2kg^{-1}$). The underlying Cu horizon retained sedimentary characteristics.

Tables 4.3a,b show the organo-mineral soil component had dissimilar physico-chemical values (e.g. pH 6.76; SOM 2.13%; Sand 72.91; Silt 24.41%) compared to the entire profile (pH 7.36; SOM 0.94%; Sand 83.24; Silt 12.89%). Nutrient enrichment in the upper horizons was evident for all geochemical parameters, excluding Fe. However, only Al (0.02-0.24%), P (0.01-0.09%) and S (<0.01-0.10) peaked at the surface. Highly ferrimagnetic minerals increased in the organo-mineral soil component (IRM_{20mT} 19.61; IRM_{40mT} 60.60), compared to the entire profile (IRM_{20mT} 14.81; IRM_{40mT} 41.01), while canted antiferromagnetic minerals remained similar.

4.2.3 Dune heath pedo-characteristics

The dune heath soil profile location (Figure 4.1) was determined by a heath topsoil pedo-environment (Chapter 3, Section 3.7.3). This area was associated with mixed acidic grassland with common heather (*Calluna vulgaris*) and wavy hair-grass (*Deschampsia flexuosa*) (Table 4.1c), a pedo-environment that has undergone leaching and loss of minerals. Edmondson *et al.* (1993), however, pointed out that rather than occurring on ridges, these areas occur in dry hollows that may once have been nutrient-rich slacks.

Figure 4.8 represents the humic podzol (Avery, 1980). A very dark greyish brown (10YR 3/2) surface L layer (0-2 cm) was evident where SOM was highest (24.8%). The H layer (2-11 cm) contained 4.0% SOM, which became incorporated into a dark brown (10YR 3/3) Ah horizon (11-24 cm) with 1.5% SOM. A slight variation in colour identified a dark brown (10YR 4/3) B horizon (24-32 cm) with 0.8% SOM. The pH decreased from 4.4 (H) to 4.2 (Ah) to 4.1 (B), but values remained similar for sand, silt and clay. The underlying Cu horizon retained characteristics similar to dune sediments, apart from decreased pH (4.3).

Figures 4.9 and 4.10 identify soil formation above 32 cm, most marked by decreases in both sand and clay alongside increases in silt. This profile-trend was replicated in decreased Al and changes in magnetic grain size parameters at this depth. However, increases in Al, P

Fixed dune soil profile description

Profile ID: FD
Date of survey: 10/10/2007

Site description

Location: 1250 m SSE of Ainsdale DC, 1100 m W of point where coastal road crosses railway line.
Grid reference: SD 29437 11546
Landform: Top of a mound.
Land use: Managed grazing.
Weather: Overcast, following heavy rain previous day, ~15ºC.

Soil description

Drainage: Well-drained.
Surface cover: Bryophytes and grasses on undulating surface.
Profile depth: 63 cm
Soil depth: 18 cm
NSRI Major group: Lithomorphic soil

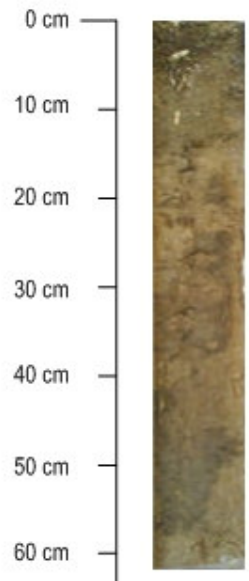

Layer/ Horizon	Depth (cm)	Field description
H	0-5	Dark greyish brown (10YR 4/2) moist and dark greyish brown (10YR 4/2) dry; loose sand; stoneless; abundant very fine (<1 mm) fibrous roots; smooth boundary to:
Ah	5-18	Brown (10YR 5/3) moist and brown (10YR 5/3) dry; loose sand; stoneless; common fine (1-2 mm) fibrous roots; smooth boundary to:
Cu1	18-38	Brown (10YR 5/3) moist and brown (10YR 5/3) dry; loose sand; stoneless; rare medium (2-5 mm) fibrous roots; gradual smooth boundary to:
Cu2	38-63	Brown (10YR 5/3) moist and pale brown (10YR 6/3) dry; loose sand; stoneless.

Layer/Horizon	H	Ah	Cu
Sand 600-2000 µm %	73	73	88
Silt 2-60 µm %	25	24	8
Clay <2 µm %	2	3	4
SOM %	4.8	1.1	0.5
pH in water (1:2.5)	6.3	6.9	7.6

Figure 4.5 Soil profile description for fixed dune community. Scale on Plate b) is 15 cm.

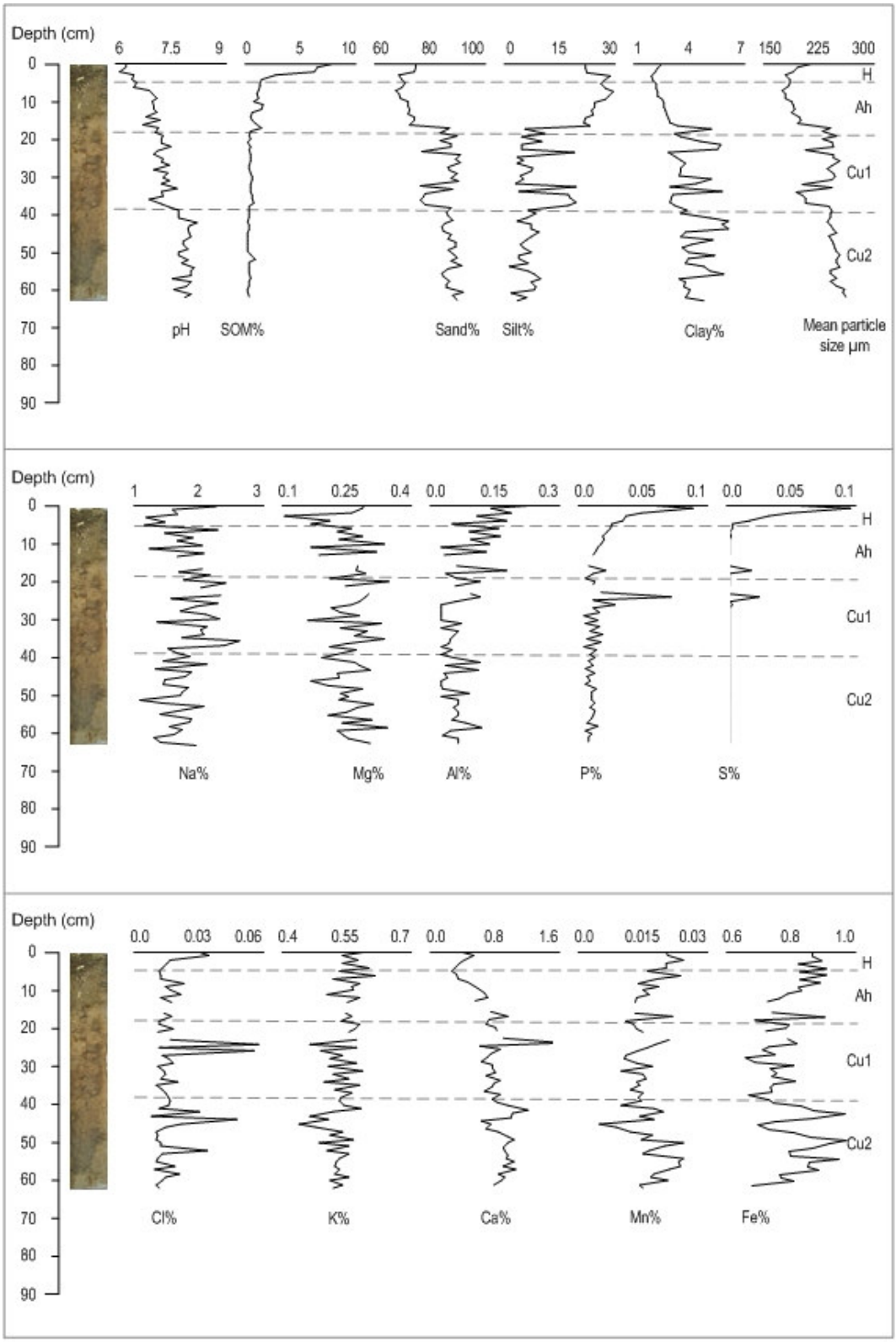

Figure 4.6 Down-profile changes in fixed dune soil characteristics; pH, SOM, texture and geochemical composition (dashed lines show horizon boundaries).

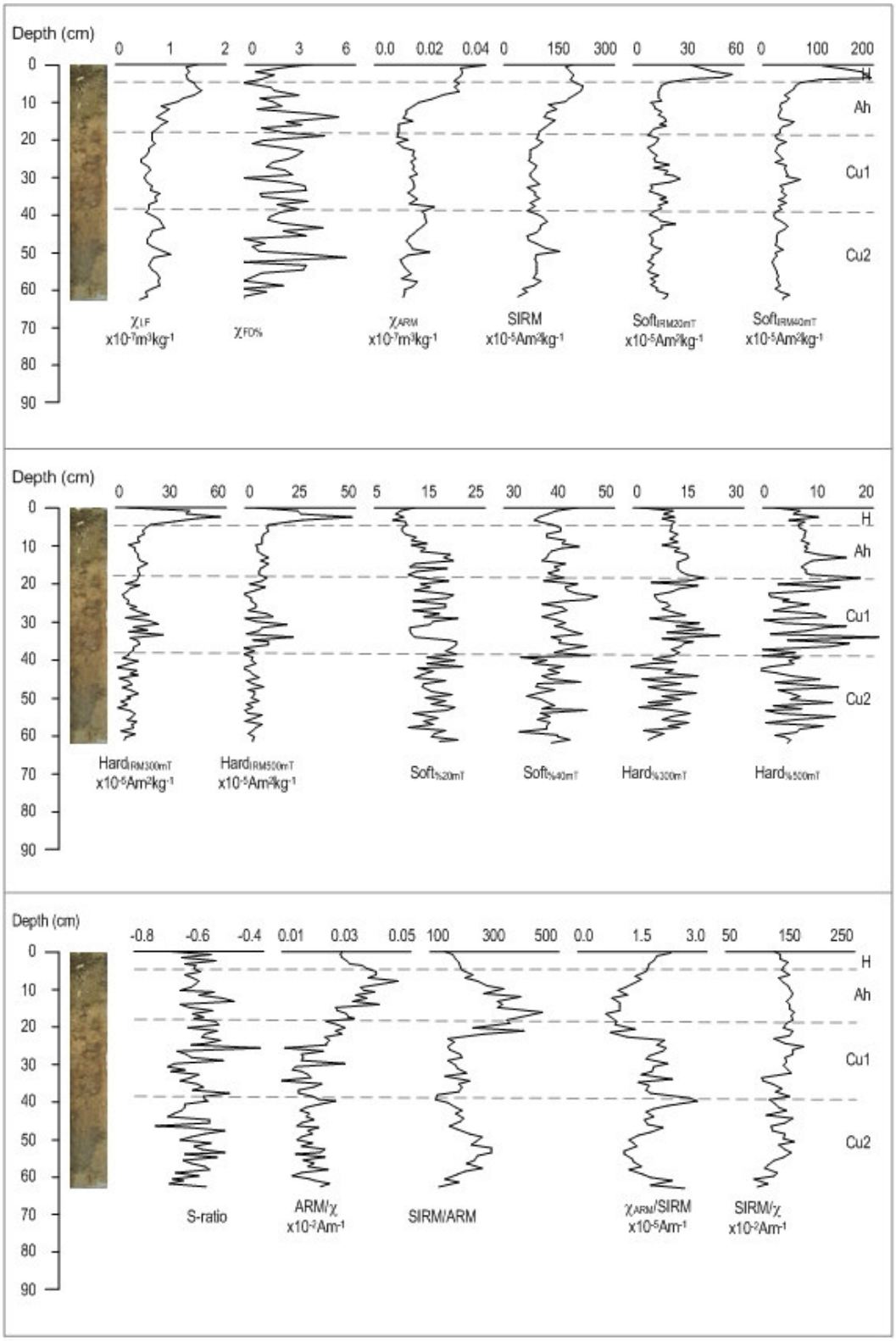

Figure 4.7 Down-profile changes in fixed dune soil mineral magnetic characteristics (dashed lines show horizon boundaries).

Table 4.3a Summary data* for fixed dune profile characteristics (n = 63)

Parameters	Units	Mean	Median	SD	CV	Min	Max
pH	mol/ltr	7.364	7.300	0.528	7.164	6.100	8.210
SOM	%	0.938	0.526	1.351	143.936	0.210	7.521
Sand	%	83.241	86.919	7.902	9.493	67.773	93.350
Silt	%	12.889	8.460	8.812	68.368	2.170	29.943
Clay	%	3.870	3.678	1.217	31.456	1.943	6.402
Mean particle size	µm	226.169	239.631	25.082	11.090	177.794	260.976
Median particle size	µm	233.080	240.950	16.827	7.219	200.364	260.386
Sorting		1.497	1.487	0.288	19.254	0.756	2.001
Skewness	γ_1	0.536	0.463	0.141	26.244	0.298	0.744
Kurtosis	g_1	3.448	4.178	1.689	48.978	0.913	5.662
Sodium	%	1.766	1.715	0.363	20.541	1.040	2.640
Magnesium	%	0.259	0.261	0.051	19.586	0.107	0.353
Aluminium	%	0.068	0.054	0.051	75.498	0.017	0.243
Phosphorus	%	0.018	0.013	0.016	88.664	0.004	0.091
Sulphur	%	0.005	0.000	0.016	314.829	0.000	0.099
Chlorine	%	0.017	0.014	0.011	63.932	0.007	0.060
Potassium	%	0.543	0.543	0.040	7.280	0.431	0.628
Calcium	%	0.771	0.779	0.270	35.034	0.195	1.753
Manganese	%	0.021	0.021	0.003	12.906	0.014	0.027
Iron	%	0.795	0.791	0.075	9.396	0.657	0.963
χ_{LF}	$10^{-7}m^3kg^{-1}$	0.801	0.704	0.294	36.697	0.430	1.585
χ_{FD}	%	1.896	1.744	1.334	70.370	0.001	5.446
χ_{ARM}	$10^{-7}m^3kg^{-1}$	0.016	0.014	0.007	43.199	0.008	0.039
SIRM	$10^{-5}Am^2kg^{-1}$	108.806	92.031	42.154	38.743	42.654	215.223
$Soft_{IRM20mT}$	$10^{-5}Am^2kg^{-1}$	14.805	14.238	5.089	34.371	7.066	29.133
$Soft_{IRM40mT}$	$10^{-5}Am^2kg^{-1}$	41.007	37.610	15.992	38.998	13.886	82.092
$Hard_{IRM300mT}$	$10^{-5}Am^2kg^{-1}$	9.850	9.380	3.814	38.725	1.480	20.559
$Hard_{IRM500mT}$	$10^{-5}Am^2kg^{-1}$	4.967	4.524	2.788	56.140	0.244	14.635
$Soft_{\%20mT}$	%	13.997	13.135	2.790	19.931	10.015	20.687
$Soft_{\%40mT}$	%	37.665	37.488	3.400	9.026	30.370	48.745
$Hard_{\%300mT}$	%	9.725	8.952	4.238	43.581	1.616	24.650
$Hard_{\%500mT}$	%	4.693	4.514	2.756	58.723	0.356	17.547
S-ratio	(none)	-0.604	-0.607	0.040	-6.585	-0.711	-0.503
ARM/χ	$10^{-2}Am^{-1}$	0.020	0.020	0.005	26.322	0.011	0.036
SIRM/ARM	(None)	228.803	204.163	73.575	32.157	118.597	456.293
χ_{ARM}/SIRM	$10^{-5}Am^2kg^{-1}$	1.499	1.538	0.428	28.542	0.688	2.648
SIRM/χ	$10^{-2}Am^{-1}$	135.395	138.719	14.661	10.828	94.905	166.207

Table 4.3b Summary data* for fixed dune organo-mineral soil (refer to Section 5.2) characteristics (n = 18)

Parameters	Units	Mean	Median	SD	CV	Min	Max
pH	mol/ltr	6.757	6.855	0.354	5.234	6.100	7.210
SOM	%	2.125	1.304	2.121	99.828	0.541	7.521
Sand	%	72.909	72.405	4.572	6.271	67.773	88.468
Silt	%	24.410	24.846	5.245	21.489	6.159	29.943
Clay	%	2.681	2.538	0.772	28.789	1.943	5.373
Mean particle size	µm	194.217	191.069	14.215	7.319	177.794	239.534
Median particle size	µm	211.628	210.023	10.055	4.751	200.364	242.708
Sorting		1.837	1.853	0.107	5.851	1.457	2.001
Skewness	γ_1	0.699	0.710	0.060	8.539	0.470	0.744
Kurtosis	g_1	1.301	0.991	1.034	79.417	0.913	5.345
Sodium	%	1.693	1.640	0.375	22.151	1.120	2.290
Magnesium	%	0.246	0.265	0.063	25.759	0.107	0.340
Aluminium	%	0.120	0.130	0.063	52.629	0.019	0.243
Phosphorus	%	0.030	0.023	0.021	69.792	0.008	0.091
Sulphur	%	0.017	0.002	0.028	164.471	0.000	0.099
Chlorine	%	0.017	0.014	0.011	63.932	0.007	0.060
Potassium	%	0.566	0.568	0.033	5.820	0.504	0.628
Calcium	%	0.480	0.461	0.220	45.806	0.195	0.990
Manganese	%	0.023	0.023	0.002	10.786	0.020	0.027
Iron	%	0.830	0.823	0.057	6.901	0.722	0.901
χ_{LF}	$10^{-7}m^3kg^{-1}$	1.165	1.255	0.286	24.571	0.755	1.585
χ_{FD}	%	1.973	1.635	1.316	66.705	0.001	5.023
χ_{ARM}	$10^{-7}m^3kg^{-1}$	0.022	0.022	0.010	45.236	0.009	0.039
SIRM	$10^{-5}Am^2kg^{-1}$	163.428	174.004	34.487	21.102	109.884	215.223
$Soft_{IRM20mT}$	$10^{-5}Am^2kg^{-1}$	19.609	19.761	4.898	24.978	11.547	29.133
$Soft_{IRM40mT}$	$10^{-5}Am^2kg^{-1}$	60.595	64.392	13.663	22.548	37.478	82.092
$Hard_{IRM300mT}$	$10^{-5}Am^2kg^{-1}$	12.759	13.034	2.934	22.993	8.734	20.173
$Hard_{IRM500mT}$	$10^{-5}Am^2kg^{-1}$	6.527	5.875	2.252	34.504	2.435	10.153
$Soft_{\%20mT}$	%	12.033	11.589	1.932	16.056	10.015	17.247
$Soft_{\%40mT}$	%	37.042	36.864	2.468	6.663	34.022	41.935
$Hard_{\%300mT}$	%	7.935	8.047	1.400	17.648	4.208	10.062
$Hard_{\%500mT}$	%	3.969	3.984	0.964	24.278	1.745	5.713
S-ratio	(none)	-0.626	-0.625	0.034	-5.361	-0.711	-0.572
ARM/χ	$10^{-2}Am^{-1}$	0.018	0.017	0.005	26.564	0.011	0.026
SIRM/ARM	(None)	272.605	260.966	87.967	32.269	151.143	456.293
χ_{ARM}/SIRM	$10^{-5}Am^2kg^{-1}$	1.268	1.206	0.397	31.319	0.688	2.078
SIRM/χ	$10^{-2}Am^{-1}$	141.628	144.696	7.779	5.493	124.461	153.350

Mean; SD = standard deviation; CV = percentage coefficient of variation; Min = minimum value; Max = maximum value. Values are shown to 3 decimal places for consistency, not accuracy.

Dune heathland soil profile description

Profile ID: DH
Date of survey: 07/07/2006

Site description

Location: Nr Woodvale Aero Club, Freshfield, Formby; ~1 km W of A565.
Grid reference: SD 29487 08953
Landform: Flat ground.
Land use: Managed heath.
Weather: Drizzle and warm; following a dry winter.

Soil description

Drainage: Well-drained.
Surface cover: Common heather with fresh plant litter
Profile depth: 79 cm
Soil depth: 32 cm
NSRI Major group: Podzolic soil


a) Photograph facing south


b) Soil profile

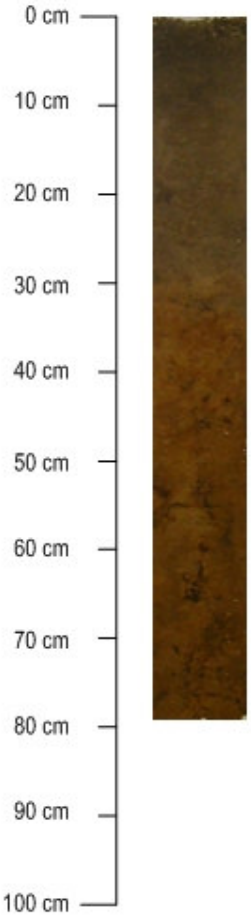

Layer/ Horizon	Depth (cm)	Field description
L	0-2	Very dark greyish brown (10 YR 3/2) moist and dark brown (10YR 3/3) dry; smooth boundary to:
H	2-11	Very dark greyish brown (10 YR 3/2) moist and dark brown (10YR 3/3) dry; loose sand; stoneless; single grain soil with no observable aggregation; common fine (0.5-2 mm) macropores; common fine (1-2 mm) fibrous roots; smooth boundary to:
Ah	11-24	Dark brown (10 YR 3/3) moist and dark brown (10YR 3/3) dry; loose sand; stoneless; 5% diffuse fine mottling; very fine (<0.5 mm) macropores; few fine (1-2 mm) fibrous roots; abrupt boundary to:
B	24-32	Dark brown (10 YR 4/3) moist and dark brown (10YR 4/3) dry; loose sand; stoneless; 25% diffuse fine mottling; very fine (<0.5 mm) macropores; few fine (1-2 mm) fibrous roots; sharp boundary to:
Cu	32-79	Yellowish brown (10 YR 5/4) moist and dark yellowish brown (10 YR 4/6) dry; loose sand; stoneless; 25% diffuse fine mottling; very fine (<0.5 mm) macropores; few fine (1-2 mm) fibrous roots.

Layer/Horizon		L	H	Ah	B	Cu
Sand	600-2000 µm %	93	88	86	88	96
Silt	2-60 µm %	7	11	13	11	3
Clay	<2 µm %	<1	1	1	1	1
SOM %		24.8	4.0	1.5	0.8	0.5
pH in water (1:2.5)		4.5	4.4	4.2	4.1	4.3

Figure 4.8 Soil profile description for heath. Scale on Plate b) is 15 cm.

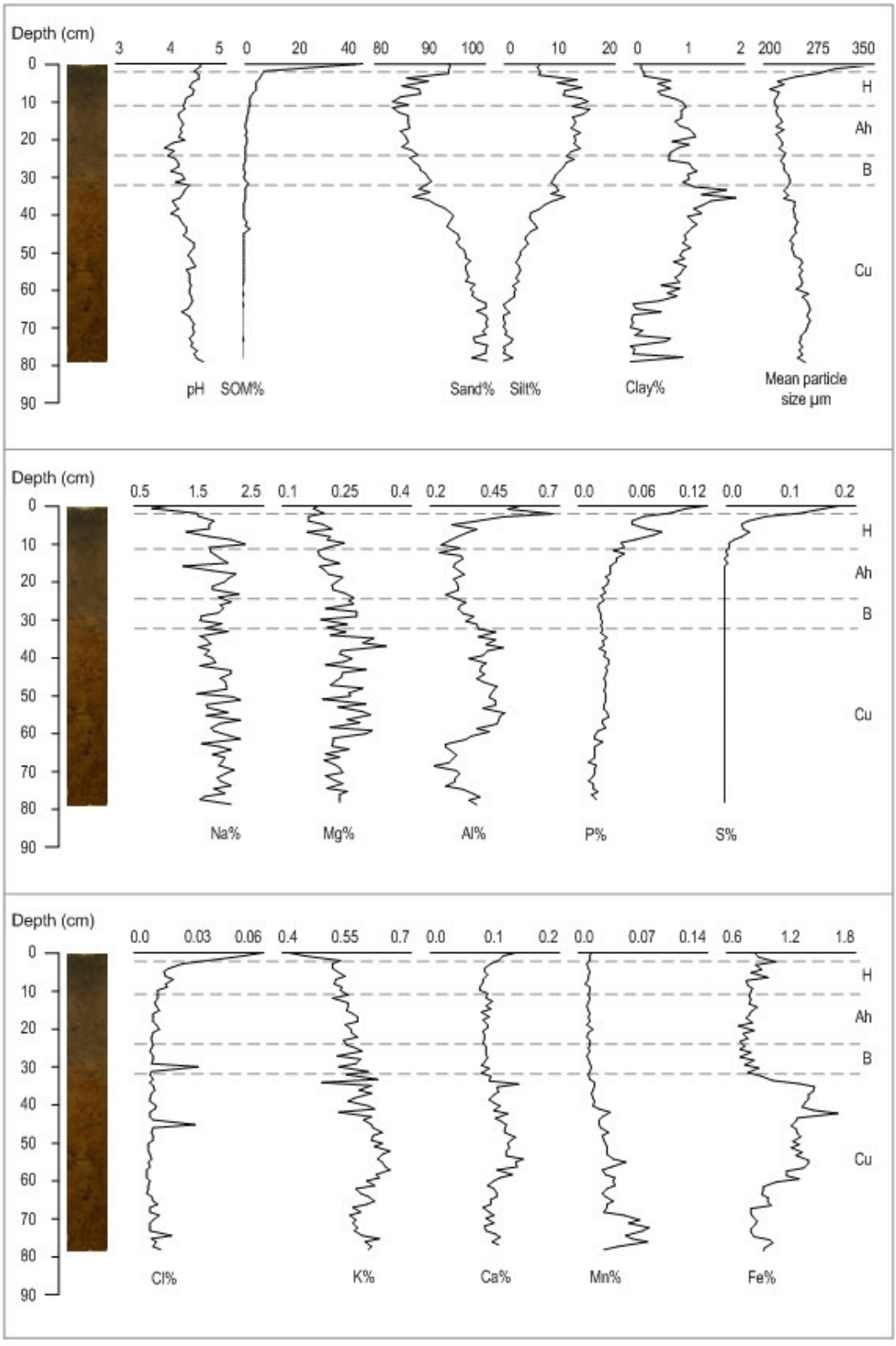

Figure 4.9 Down-profile changes in heath soil characteristics; pH, SOM, texture and geochemical properties (dashed lines show horizon boundaries).

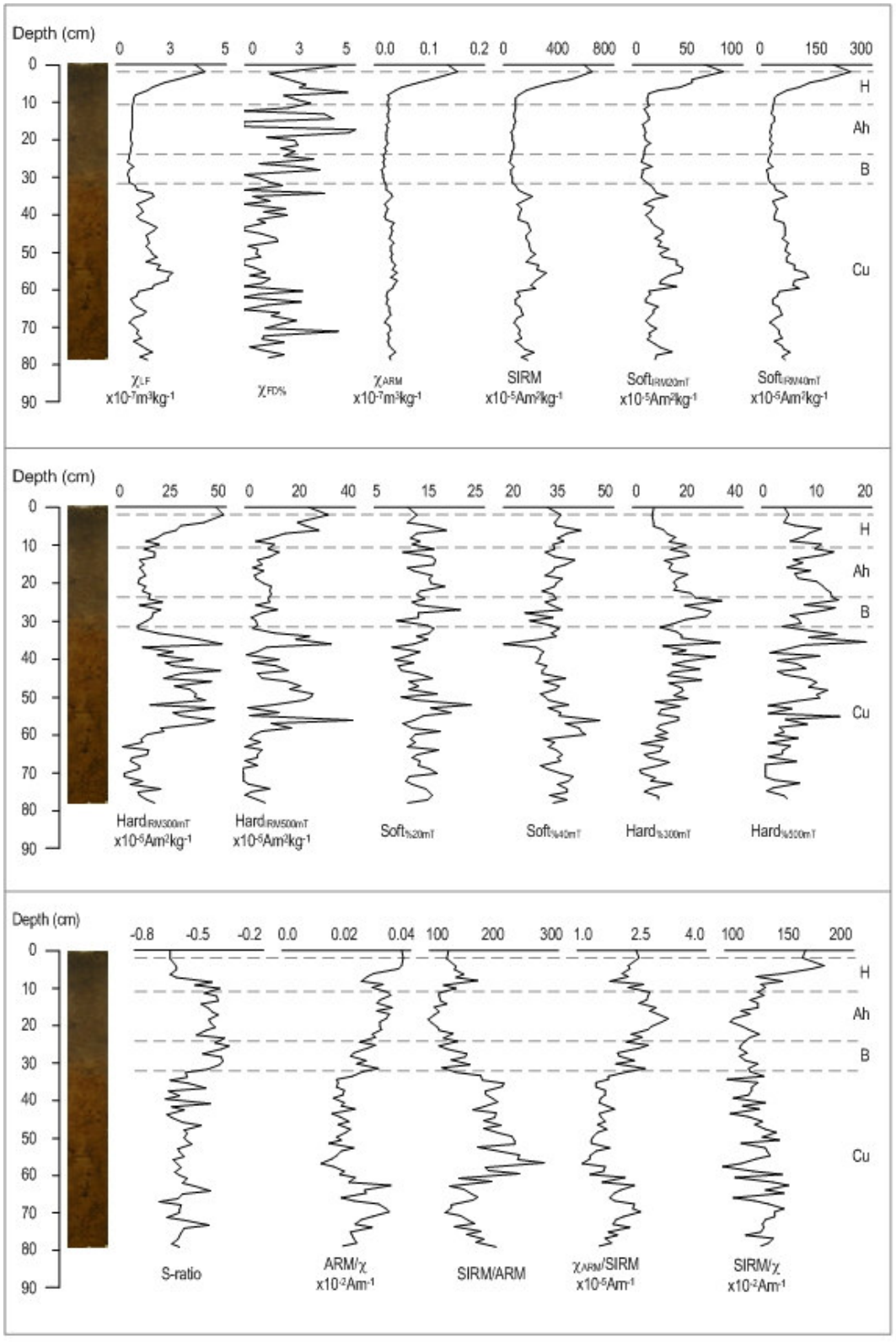

Figure 4.10 Down-profile changes in heath dune soil mineral magnetic characteristics (dashed lines show horizon boundaries).

and S, alongside magnetic mineral concentrations, occurred at 11 cm. SOM remained constant (<1.0%) throughout the Ah and B horizons, except for one peak at 32 cm (2.25%) and another at 44 cm (2.54%), positioned just below the B horizon. This may be evidence of leached soluble organic decomposition products being re-precipitated to form an organic subsoil (Bh) horizon (Fullen and Catt, 2004) that was not visible in the field. This is reflected in a second and third magnetic enhancement in the B and upper Cu (or Bh) horizons, respectively. The lowest pH value (3.91) was recorded in the Ah horizon, with values increasing gradually in the B horizon and furthermore with depth. This pattern is reflected in overall decreases in the alkaline elements Na, Mg, Ca and K. These values increased immediately below the B horizon, possibly providing further evidence of an incipient Bh horizon. Decreased magnetic mineral concentrations, alongside increased S-ratios (-0.53- -0.83) clearly identifies the combined Ah and B horizons to have experienced more influence from antiferromagnetic minerals.

Tables 4.4a,b show the organo-mineral soil component had dissimilar physico-chemical values (e.g. SOM 3.46%; Silt 11.73%) compared to the entire profile (SOM 1.68%; Silt 6.69%). S peaked at the surface (0.18%), whereas, decreases in Ca (0.09%), Mn (0.01%) and Fe (0.84%) occurred in the organo-mineral soil component. Ferrimagnetic minerals dominated in both the entire profile and organo-mineral soil component alone. Therefore, a decrease in the SIRM/ARM ratio in the soil (132.84) compared to the profile (167.03) indicates an increase in the influence of stable single domain magnetic grain sizes in the former.

4.2.4 Slack community pedo-characteristics

The slack community soil profile location (Figure 4.1) was determined by a slack topsoil pedo-environment (Chapter 3, Section 3.7.4). Vegetation types in this slack range from early successional species to the local abundance of creeping willow (Table 4.5a), which is indicative of a wet slack prone to waterlogging (Brodie, 1996). This species-rich wet slack contained many coastal rarities, such as marsh helleborine (*Epipactis palustris*) and grass-of-Parnassus (*Parnassia palustris*) occurring frequently. The presence of both Yorkshire fog and red fescue around the slack edges represented drier phases of slack vegetation development.

Figure 4.11 represents the groundwater gley (Avery, 1980) with a shallow H layer (0-2 cm) that contained 8.3% SOM. A very shallow dark brown (10YR 3/3) Ah(g) horizon (2-4 cm), low in SOM (1.6%) and displaying large black (10YR 2/1) mottles, graded into a relatively deep (4-22 cm) Cg horizon, showing evidence of fine mottling and low SOM (1.0%). A change in colour (10YR 4/2) identified the sedimentary characteristics of the Cu1 horizon (>22 cm) that was permanently waterlogged. This was interrupted at 33-35 cm by the occurrence of a red (7.5YR 4/4), iron oxide coated concretion/nodule; evidence of a BhFe horizon. The pH increased from 7.4 (H, Ag) to 7.9 (Cg) to 8.1 (Cu). Sand-sized particles increased from 63% (H) to 76% (Ag), alongside decreased silt-sized particles from 34% (H) to 20% (Ag), but remained similar to sedimentary characteristics in the Cu2 horizon.

Table 4.4a Summary data* for heath profile characteristics (n = 79)

Parameters	Units	Mean	Median	SD	CV	Min	Max
pH	mol/ltr	4.298	4.320	0.142	3.298	3.910	4.590
SOM	%	1.680	0.712	4.869	289.928	0.102	42.182
Sand	%	92.560	93.260	5.263	5.686	83.411	100.000
Silt	%	6.692	6.079	5.055	75.544	0.000	15.711
Clay	%	0.748	0.853	0.400	53.398	0.000	1.821
Mean particle size	µm	243.175	243.462	18.533	7.621	212.066	334.455
Median particle size	µm	237.755	239.517	8.751	3.681	215.326	260.081
Sorting		0.788	0.872	0.349	44.366	0.350	1.397
Skewness	γ_1	0.249	0.325	0.237	94.899	-0.077	0.634
Kurtosis	g_1	2.042	2.051	0.887	43.408	1.025	3.709
Sodium	%	1.798	1.810	0.240	13.370	0.820	2.250
Magnesium	%	0.236	0.236	0.037	15.692	0.163	0.342
Aluminium	%	0.362	0.351	0.086	23.851	0.203	0.693
Phosphorus	%	0.030	0.025	0.020	65.473	0.010	0.124
Sulphur	%	0.009	0.000	0.030	338.816	0.000	0.178
Chlorine	%	0.011	0.009	0.008	69.538	0.007	0.056
Potassium	%	0.580	0.580	0.043	7.489	0.417	0.656
Calcium	%	0.101	0.096	0.017	17.379	0.077	0.150
Manganese	%	0.023	0.017	0.016	68.956	0.007	0.074
Iron	%	1.020	0.936	0.229	22.405	0.714	1.657
χ_{LF}	$10^{-7}m^3kg^{-1}$	1.227	1.025	0.677	55.184	0.513	4.060
χ_{FD}	%	1.516	1.167	1.296	85.489	0.001	4.975
χ_{ARM}	$10^{-7}m^3kg^{-1}$	0.030	0.025	0.023	75.572	0.012	0.155
SIRM	$10^{-5}Am^2kg^{-1}$	158.942	132.060	104.924	66.014	57.431	641.821
$Soft_{IRM20mT}$	$10^{-5}Am^2kg^{-1}$	21.371	17.633	13.908	65.078	7.187	82.445
$Soft_{IRM40mT}$	$10^{-5}Am^2kg^{-1}$	55.209	43.413	37.488	67.901	16.587	229.911
$Hard_{IRM300mT}$	$10^{-5}Am^2kg^{-1}$	20.662	17.299	11.716	56.703	3.552	47.984
$Hard_{IRM500mT}$	$10^{-5}Am^2kg^{-1}$	10.128	7.754	8.240	81.360	0.248	39.077
$Soft_{\%20mT}$	%	13.540	13.052	2.461	18.173	8.650	22.163
$Soft_{\%40mT}$	%	34.432	34.390	3.626	10.530	21.074	46.150
$Hard_{\%300mT}$	%	14.270	14.060	6.213	43.540	2.928	31.291
$Hard_{\%500mT}$	%	6.858	6.446	4.323	63.037	0.239	19.944
S-ratio	(none)	-0.540	-0.569	0.078	-14.429	-0.680	-0.379
ARM/χ	$10^{-2}Am^{-1}$	0.025	0.024	0.006	24.996	0.013	0.038
SIRM/ARM	(None)	167.025	164.220	39.233	23.489	102.004	278.589
χ_{ARM}/SIRM	$10^{-5}Am^2kg^{-1}$	1.984	1.912	0.460	23.190	1.127	3.079
SIRM/χ	$10^{-2}Am^{-1}$	126.609	125.632	13.889	10.970	100.049	173.402

Table 4.4b Summary data* for heath organo-mineral soil (refer to Section 5.2) characteristics (n = 32)

Parameters	Units	Mean	Median	SD	CV	Min	Max
pH	mol/ltr	4.246	4.225	0.163	3.833	3.910	4.540
SOM	%	3.458	1.369	7.509	217.189	0.634	42.182
Sand	%	87.496	86.510	2.782	3.180	83.411	93.507
Silt	%	11.733	12.637	2.610	22.247	6.301	15.711
Clay	%	0.771	0.840	0.277	35.919	0.190	1.150
Mean particle size	µm	233.792	227.226	24.476	10.469	212.066	334.455
Median particle size	µm	230.488	229.936	8.107	3.517	215.326	260.081
Sorting		1.113	1.090	0.123	11.018	0.874	1.397
Skewness	γ_1	0.455	0.490	0.124	27.248	0.117	0.634
Kurtosis	g_1	2.434	2.593	0.531	21.807	1.245	3.315
Sodium	%	1.742	1.765	0.296	16.987	0.820	2.250
Magnesium	%	0.218	0.213	0.033	14.992	0.163	0.278
Aluminium	%	0.339	0.309	0.097	28.638	0.224	0.693
Phosphorus	%	0.043	0.033	0.026	59.913	0.018	0.124
Sulphur	%	0.022	0.000	0.045	203.103	0.000	0.178
Chlorine	%	0.015	0.011	0.011	74.334	0.008	0.056
Potassium	%	0.547	0.552	0.037	6.713	0.417	0.605
Calcium	%	0.089	0.087	0.012	13.163	0.077	0.136
Manganese	%	0.011	0.011	0.002	14.543	0.007	0.014
Iron	%	0.835	0.831	0.075	8.963	0.714	1.066
χ_{LF}	$10^{-7}m^3kg^{-1}$	1.061	0.720	0.904	85.144	0.513	4.060
χ_{FD}	%	2.237	2.305	1.445	64.593	0.001	4.975
χ_{ARM}	$10^{-7}m^3kg^{-1}$	0.035	0.022	0.036	103.130	0.012	0.155
SIRM	$10^{-5}Am^2kg^{-1}$	147.512	86.829	155.001	105.077	57.431	641.821
$Soft_{IRM20mT}$	$10^{-5}Am^2kg^{-1}$	19.808	11.732	19.232	97.093	7.187	82.445
$Soft_{IRM40mT}$	$10^{-5}Am^2kg^{-1}$	51.222	29.797	53.977	105.378	16.587	229.911
$Hard_{IRM300mT}$	$10^{-5}Am^2kg^{-1}$	18.507	15.280	9.836	53.146	10.242	47.984
$Hard_{IRM500mT}$	$10^{-5}Am^2kg^{-1}$	10.714	9.397	7.050	65.807	3.187	30.430
$Soft_{\%20mT}$	%	13.866	13.255	2.357	16.997	9.497	20.159
$Soft_{\%40mT}$	%	34.317	34.333	2.859	8.330	26.807	41.064
$Hard_{\%300mT}$	%	16.332	14.852	5.831	35.701	7.476	31.291
$Hard_{\%500mT}$	%	8.829	8.345	3.300	37.374	4.032	14.633
S-ratio	(none)	-0.481	-0.458	0.078	-16.194	-0.631	-0.379
ARM/χ	$10^{-2}Am^{-1}$	0.030	0.030	0.004	14.160	0.022	0.038
SIRM/ARM	(None)	132.842	130.355	18.410	13.858	102.004	177.384
χ_{ARM}/SIRM	$10^{-5}Am^2kg^{-1}$	2.407	2.409	0.321	13.339	1.771	3.079
SIRM/χ	$10^{-2}Am^{-1}$	127.069	122.727	17.253	13.578	105.845	173.402

**Mean; SD = standard deviation; CV = percentage coefficient of variation; Min = minimum value; Max = maximum value. Values are shown to 3 decimal places for consistency, not accuracy.*

Table 4.5a Plant species in the slack (SD 29392 12141)

Vernacular name	Latin name	DAFOR	Notes
Grass-of-Parnassus	*Parnassia palustris*	Frequent	
Marsh orchids	*Dactylorhiza incarnata*	Frequent	
Yellow sedge	*Carex viridula*	Frequent	
Lesser spearwort	*Ranunculus flammula*	Frequent	
Creeping bentgrass	*Agrostis stolonifera*	Frequent	
Marsh helleborine	*Epipactis palustris*	Frequent	
Blue sedge	*Carex flacca*	Frequent	
Creeping willow	*Salix repens*	Local/abundant	
Spike rush	*Eleocharis quinqueflora*	Local/abundant	
Bryophytes		Local/abundant	
Common spike rush	*Eleocharis palustris*	Local/frequent	
Creeping white clover	*Trifolium repens*	Local/frequent	
Pink centaury	*Centaurium erythraea*	Occasional	
Self-heal	*Prunella vulgaris*	Occasional	
Marsh pennywort	*Hydrocotyle vulgaris*	Occasional	
Watermint	*Mentha aquatica*	Occasional	
Brookweed	*Samolus valerandi*	Occasional	
Daisy	*Bellis perennis*	Occasional	
Eyebright	*Euphrasia officinalis*	Occasional	
Red fescue	*Festuca rubra*	Occasional	
Yorkshire fog	*Holcus lanatus*	Occasional	
Common milkwort	*Polygala vulgaris*	Occasional	
Grey willow	*Salix cinerea*	Rare	
Bog pimpernel	*Anagallis tenella*	Rare	
False Fox-sedge	*Carex otrubae*	Rare	
Jointed rush	*Juncus articulatus*	Rare	
Sand sedge	*Carex arenaria*	Rare	
Yellow common fleabane	*Pulicaria dysenterica*	Rare	
Forget-me-not m.laxa	*Myosotis arvensis*	Rare	
Knotted pearl wort	*Sagina nodosa*	Rare	
Purple loosestrife	*Lythrum salicaria*	Rare	
Round-leaved winter-green	*Pyrola rotundifolia*	Rare-local/frequent	
Grey club rush	*Schoenoplectus tabernaemontani*		Additional species.
Marsh bedstraw	*Galium palustre*		Additional species.
Marsh willowherb	*Epilobium palustre*		Additional species.
Colt's foot	*Tussilago farfara*		Additional species.
Smooth hawkbit	*Leontodon autumnalis*		Additional species.
Broad-leaved reed mace	*Typha latifolia*		

Table 4.5b Plant species in the pasture (SD 27518 08099)

Vernacular name	Latin name	DAFOR	Notes
Dewberry	*Rubus caesius*	Abundant	Maritime influence; scrub.
Sand sedge	*Carex arenaria*	Abundant	
Red fescue	*Festuca rubra*	Abundant	Lowland.
Tall oat grass	*Arrhenatherum elatius*	Abundant	Ungrazed, yet disturbed.
Common bent grass	*Agrostis capillaris*	Abundant	
Common ragwort	*Senecio jacobaea*	Locally abundant	Poisonous to grazers.
Rose-bay willowherb	*Chamerion angustifolium*	Locally abundant	Colonises bare ground.
Pink centaury	*Centaurium erythraea*	Occasional	Maritime influence.
Red clover	*Trifolium pratense*	Occasional	
Creeping white clover	*Trifolium repens*	Occasional	
Nettle	*Urtica dioica*	Occasional	Disturbance.
Hound's tongue	*Cynoglossum officinale*	Occasional	
Hop trefoil	*Trifolium campestre*	Occasional	
Bird's foot trefoil	*Lotus corniculatus*	Occasional	
Ladies bedstraw	*Galium verum*	Occasional	Bare ground.
Harebell	*Campanula rotundifolia*	Rare	Rabbit warrens.
Dove's foot Crane's bill	*Geranium molle*	Rare	
Spring hairgrass	*Airapraecox*	Rare	
Bramble	*Rubus fruticosus agg.*		
Stork's bill	*Erodium cicutarium*		Bare ground.
Annual meadow grass	*Poa annua L.*		Bare ground.
Mouse-ear chickweed	*Cerastium semidecandrum*		Bare ground.
Bugloss	*Anchusa officinalis*		
Soft brome	*Bromus hordeaceus*		
Yorkshire fog	*Holcus lanatus*		
Asparagus	*Asparagus officinalis*		
Dock	*Rumex crispus*		
Marram grass	*Ammophila arenaria*		
Bryophytes			
Autumn hawkbit	*Leontodon autumnalis*		

Dune slack soil profile description

Profile ID: DS
Date of survey: 15/06/2008

Site description

Location: Inland of mobile dune ridge; 780 m SSW of Ainsdale Discovery Centre.
Grid reference: SD 29390 12144
Landform: Flat, boggy; foot of dune ridge.
Land use: Managed; species conservation.
Weather: Clear and bright, ~15ºC.

Soil description

Drainage: Poorly-drained.
Surface cover: Creeping willow and flowering plants.
Profile depth: 60 cm
Soil depth: 35 cm
NSRI Major group: Groundwater gley soil

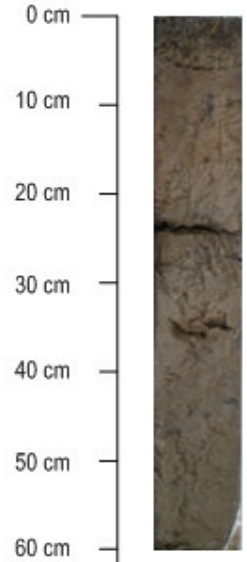

Layer/ Horizon	Depth (cm)	Field description
H	0-2	Very dark greyish brown (10 YR 3/2) moist and greyish brown (10YR 5/2) dry; stoneless; smooth clear boundary.
Ah(g)	2-4	Dark brown (10 YR 3/3) moist and light brownish gray (10YR 6/2) dry; loose sand; stoneless; many distinct large mottles; one distinct very large black (10 YR 2/1) mottle; few medium (2-5 mm) fibrous roots; smooth boundary.
Cg	4-22	Yellowish brown (10 YR 5/3 5/4) moist and pale brown (10YR 6/3) dry; loose sand; stoneless; 25% distinct fine mottling; abundant medium (2-5 mm) fibrous roots; diffuse unclear boundary.
Cu1	22-33	Dark greyish brown (10 YR 4/2) moist and pale brown (10 YR 6/3) dry; loose sand; stoneless; 25% distinct fine mottling; rare large decomposing organic material; unclear boundary.
BhFe	33-35	Dark greyish brown (10 YR 4/2) moist and pale brown (10 YR 6/3) dry; loose sand; red (7.5 YR 4/4) iron oxide coatings on concretions/nodules; unclear boundary.
Cu2	35-60	Dark yellowish brown (10 YR 4/4) moist and pale brown (10 YR 6/3) dry; loose sand; stoneless.

Layer/Horizon		H	Ah(g)	Cg	Cu1	BhFe	Cu2
Sand	600-2000 µm %	63	76	86	86	85	87
Silt	2-60 µm %	34	20	8	8	9	7
Clay	<2 µm %	3	4	6	6	6	6
SOM %		8.3	1.6	1.0	0.5	0.4	0.8
pH in water (1:2.5)		7.4	7.4	7.9	8.1	8.0	8.2

Figure 4.11 Soil profile description for slack community. Scale on Plate b) is 15 cm.

Figures 4.12 and 4.13 identify soil formation above 22 cm, evident by decreased pH and overall increased clay, although a marked decrease in clay was observed in the lower Cg horizon above the water table. This was also reflected in magnetic grain size parameters indicating the presence of stable single domain grains. The H layer contained highest values of SOM (12.26%), P (0.05%), Ca (7.39%) and Mn (0.16%), while Na increased in the Cg horizon alongside decreases in Mg, K, Ca and Mn. Two further peaks in SOM were observed at 4 cm (8.03%), marking the Ah(g)/Cg boundary and at 41 cm (10.01%) in the Cu1 horizon, associated with peaks in Al (0.48%), S (0.73%) and Cl (0.09%) alongside troughs in Na (0.69%) and K (0.29%). Decreasing ARM/χ and χ_{ARM}/SIRM ratios, alongside an increasing SIRM/ARM ratio, indicated higher importance of either superparamagnetic or multidomain magnetic grains in the permanently waterlogged part of the soil. The presence of SP grains was further confirmed by peaks in $\chi_{FD\%}$ in both the Ah(g) (8.20%, 3 cm) and Cg horizons (6.47%, 7 cm; 10.84%, 15 cm).

Magnetic mineral concentrations were measured as very low throughout the profile, apart from vastly increased values in the BhFe horizon (χ_{LF} 18.24 x10^{-7}m^{3}kg^{-1}; χ_{ARM} 0.95 x10^{-7}m^{3}kg^{-1}; SIRM 6932.43 x10^{-5}m^{2}kg^{-1}). The extremely high content of minerals comprising soft magnetic behaviour at this depth was demonstrated by the very low S-ratio (-0.93). These peaks coincided with peaks in Ca (3.43%) and Fe (1.82%).

Tables 4.6a,b show the organo-mineral soil component had dissimilar physico-chemical values (e.g. pH 7.80; Silt 11.21%) compared to the entire profile (pH 8.01; Silt 8.80%). Decreased Al (0.04%) and S (0.01%) occurred in the organo-mineral soil component, alongside slightly increased Mn (0.03%). A decreased SIRM/ARM ratio in the aerated soil (129.93) indicated the importance of stable single domain magnetic grains sizes, as opposed to superparamagnetic or multidomain magnetic grains in the permanently/seasonally waterlogged soil profile.

4.2.5 Pasture pedo-characteristics

The pasture soil profile location (Figure 4.1) was determined by a pasture dune topsoil pedo-environment (Chapter 3, Section 3.7.2). This particular area of dune pasture had colonized a relict asparagus field that had been abandoned for some decades (Lewis and Cowell, 2002). Dominated by red fescue (Table 4.5b), the area was also being invaded by rose-bay willowherb (*Chamerion angustifolium*) and bramble (*Rubus fruticosus*). Base-rich conditions were evident by the presence of red fescue (*Festuca rubra*) and common bent grass (*Agrostis capillaries*).

Figure 4.14 represents another sand-pararendzina (Avery, 1980), although in a later stage of development with the first appearance of an F layer (0-3 cm), overlying the H layer (3-8 cm) that contained 6.2% SOM. Evidence of a regular ridged and furrowed cultivation surface was indicative of a dark greyish brown (10YR 4/2) Ap horizon (8-22 cm), with 1.2% SOM. The pH decreased slightly from the organic layers (6.7-6.8) to the A horizon (6.5). Silt-sized particles increased to 24% in the H horizon, but decreased back to 19% in the A horizon. The underlying

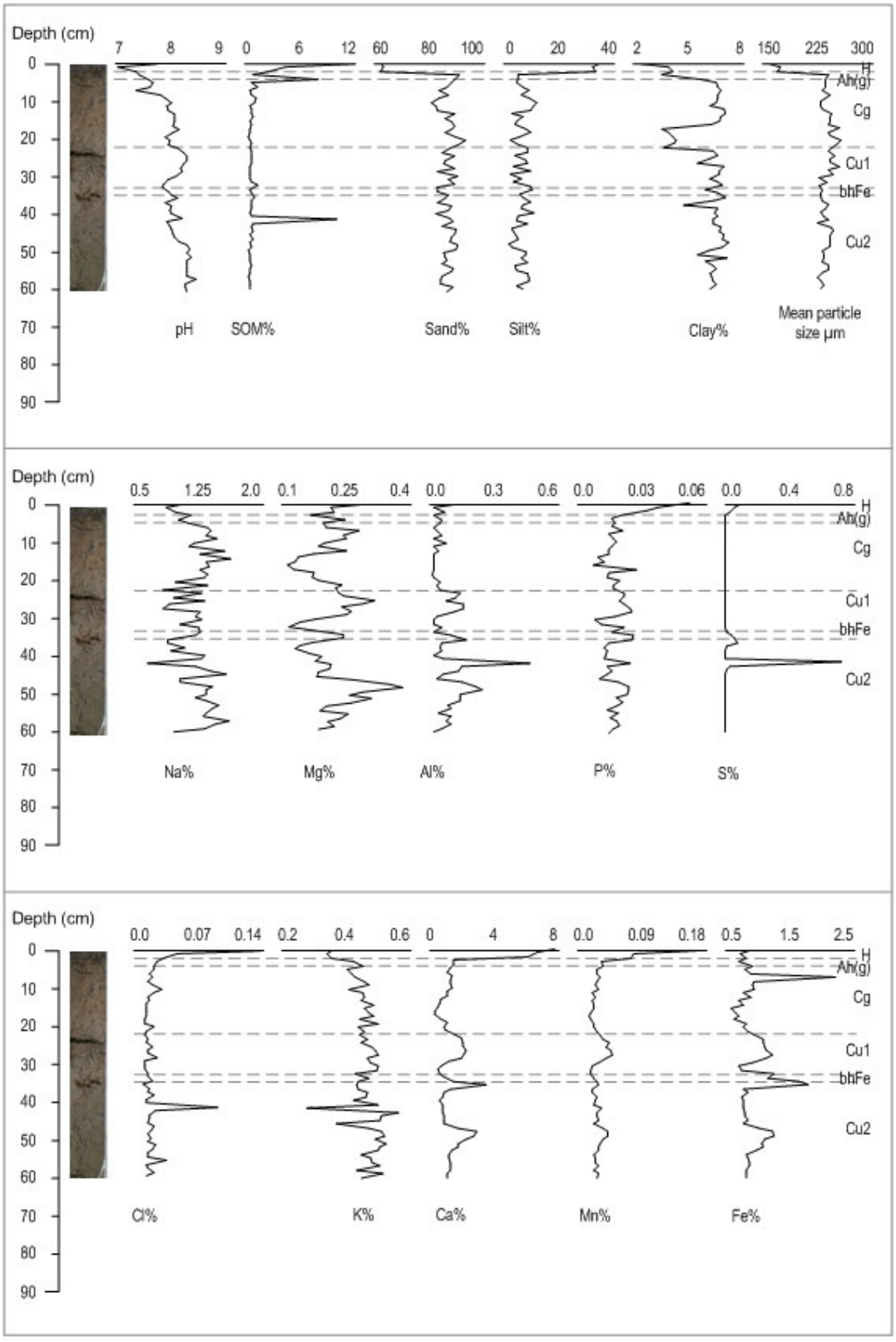

Figure 4.12 Down-profile changes in slack soil characteristics; pH, SOM, texture and geochemical properties (dashed lines show horizon boundaries).

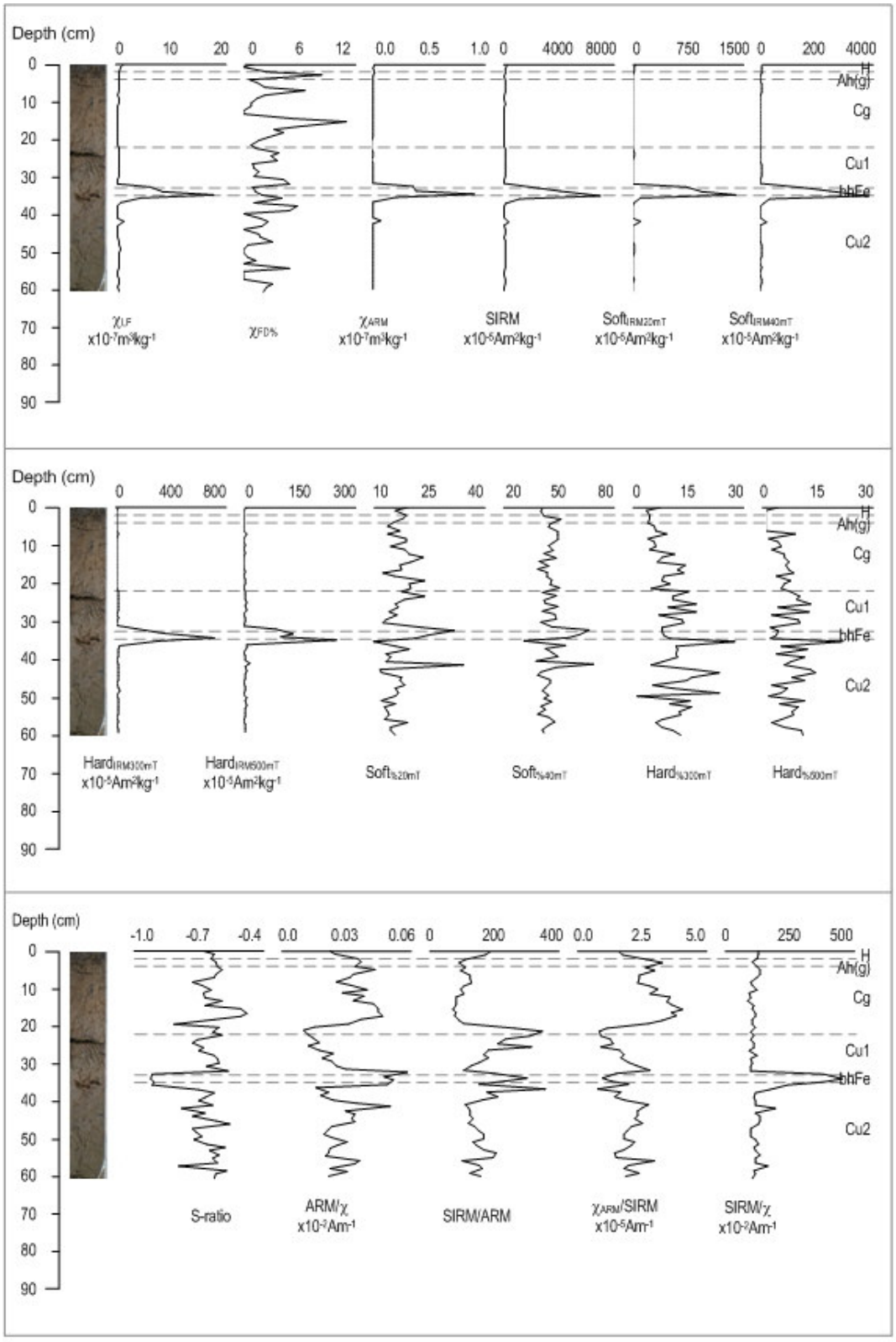

Figure 4.13 Down-profile changes in slack soil mineral magnetic characteristics (dashed lines show horizon boundaries).

Table 4.6a Summary data* for slack profile characteristics (n = 60)

Parameters	Units	Mean	Median	SD	CV	Min	Max
pH	mol/ltr	8.010	8.030	0.264	3.291	7.060	8.420
SOM	%	1.070	0.450	2.206	206.164	0.213	12.259
Sand	%	85.333	86.497	5.781	6.775	62.236	92.670
Silt	%	8.804	7.587	6.303	71.599	2.746	35.093
Clay	%	5.863	6.269	1.127	19.231	2.159	7.079
Mean particle size	µm	238.161	240.768	18.045	7.577	158.102	260.874
Median particle size	µm	244.103	246.713	17.848	7.312	150.730	264.750
Sorting		1.613	1.547	0.243	15.079	1.164	2.076
Skewness	γ_1	0.532	0.484	0.118	22.282	0.391	0.755
Kurtosis	g_1	4.947	5.239	1.203	24.312	0.577	6.038
Sodium	%	1.229	1.280	0.205	16.698	0.690	1.620
Magnesium	%	0.219	0.215	0.057	26.149	0.116	0.384
Aluminium	%	0.082	0.056	0.077	93.615	0.018	0.475
Phosphorus	%	0.019	0.017	0.007	35.836	0.008	0.051
Sulphur	%	0.020	0.001	0.095	472.594	0.001	0.728
Chlorine	%	0.019	0.013	0.021	112.059	0.008	0.153
Potassium	%	0.460	0.465	0.047	10.312	0.286	0.560
Calcium	%	1.687	1.387	1.271	75.308	0.533	7.391
Manganese	%	0.028	0.023	0.021	74.402	0.013	0.160
Iron	%	0.979	0.896	0.279	28.460	0.616	2.271
χ_{LF}	$10^{-7}m^3kg^{-1}$	1.113	0.470	2.656	238.538	0.204	18.242
χ_{FD}	%	2.244	1.649	2.193	97.710	0.001	10.843
χ_{ARM}	$10^{-7}m^3kg^{-1}$	0.046	0.012	0.140	305.496	0.004	0.945
SIRM	$10^{-5}Am^2kg^{-1}$	302.767	58.694	1058.692	349.672	25.450	6932.430
$Soft_{IRM20mT}$	$10^{-5}Am^2kg^{-1}$	67.124	9.511	244.347	364.023	3.264	1478.642
$Soft_{IRM40mT}$	$10^{-5}Am^2kg^{-1}$	164.223	25.338	603.130	367.262	10.140	3773.900
$Hard_{IRM300mT}$	$10^{-5}Am^2kg^{-1}$	32.773	6.039	111.237	339.414	1.208	727.763
$Hard_{IRM500mT}$	$10^{-5}Am^2kg^{-1}$	13.338	4.157	38.623	289.576	0.369	248.466
$Soft_{\%20mT}$	%	17.476	16.882	4.304	24.628	10.566	34.223
$Soft_{\%40mT}$	%	44.567	43.590	6.564	14.728	29.352	68.458
$Hard_{\%300mT}$	%	10.812	10.414	5.081	46.995	1.538	27.800
$Hard_{\%500mT}$	%	6.691	5.808	3.995	59.705	0.808	22.063
S-ratio	(none)	-0.661	-0.634	0.096	-14.592	-0.926	-0.464
ARM/χ	$10^{-2}Am^{-1}$	0.029	0.029	0.011	37.805	0.010	0.059
SIRM/ARM	(None)	161.905	146.497	65.720	40.591	77.925	357.534
χ_{ARM}/SIRM	$10^{-5}Am^2kg^{-1}$	2.218	2.144	0.771	34.765	0.878	4.030
SIRM/χ	$10^{-2}Am^{-1}$	139.054	122.586	66.419	47.765	94.373	454.061

Table 4.6b Summary data* for slack organo-mineral soil (refer to Section 5.2) characteristics (n = 22)

Parameters	Units	Mean	Median	SD	CV	Min	Max
pH	mol/ltr	7.800	7.915	0.284	3.642	7.060	8.130
SOM	%	1.676	0.468	2.964	176.846	0.214	12.259
Sand	%	83.534	86.223	8.909	10.665	62.236	92.670
Silt	%	11.205	7.603	9.554	85.269	3.177	35.093
Clay	%	5.261	6.096	1.482	28.164	2.159	6.920
Mean particle size	µm	234.024	242.271	27.999	11.964	158.102	260.874
Median particle size	µm	239.899	247.562	28.045	11.690	150.730	264.580
Sorting		1.623	1.553	0.320	19.712	1.164	2.076
Skewness	γ_1	0.541	0.477	0.134	24.779	0.391	0.755
Kurtosis	g_1	4.509	5.008	1.552	34.418	0.871	5.830
Sodium	%	1.264	1.300	0.186	14.697	0.900	1.620
Magnesium	%	0.203	0.201	0.051	24.895	0.116	0.303
Aluminium	%	0.039	0.022	0.028	72.948	0.018	0.131
Phosphorus	%	0.020	0.017	0.009	48.507	0.008	0.051
Sulphur	%	0.009	0.001	0.024	259.075	0.001	0.100
Chlorine	%	0.023	0.016	0.030	128.966	0.009	0.153
Potassium	%	0.439	0.453	0.042	9.500	0.345	0.500
Calcium	%	1.894	1.252	1.937	102.286	0.533	7.391
Manganese	%	0.032	0.022	0.033	102.853	0.013	0.160
Iron	%	0.897	0.843	0.324	36.158	0.616	2.271
χ_{LF}	$10^{-7}m^3kg^{-1}$	0.470	0.427	0.258	55.049	0.204	1.427
χ_{FD}	%	2.814	1.890	2.882	102.395	0.001	10.843
χ_{ARM}	$10^{-7}m^3kg^{-1}$	0.014	0.013	0.006	41.701	0.004	0.031
SIRM	$10^{-5}Am^2kg^{-1}$	57.265	47.795	36.345	63.467	25.450	189.005
$Soft_{IRM20mT}$	$10^{-5}Am^2kg^{-1}$	10.249	9.063	6.822	66.564	3.264	36.619
$Soft_{IRM40mT}$	$10^{-5}Am^2kg^{-1}$	25.010	22.878	14.380	57.497	10.140	75.642
$Hard_{IRM300mT}$	$10^{-5}Am^2kg^{-1}$	4.145	3.566	2.753	66.412	2.022	15.172
$Hard_{IRM500mT}$	$10^{-5}Am^2kg^{-1}$	2.821	2.435	1.608	56.998	0.369	6.450
$Soft_{\%20mT}$	%	18.015	18.363	2.856	15.854	12.826	23.935
$Soft_{\%40mT}$	%	44.178	44.105	3.826	8.662	37.726	50.748
$Hard_{\%300mT}$	%	7.829	6.888	3.114	39.772	4.101	14.477
$Hard_{\%500mT}$	%	5.189	5.312	1.907	36.763	0.808	8.600
S-ratio	(none)	-0.625	-0.621	0.077	-12.290	-0.818	-0.464
ARM/χ	$10^{-2}Am^{-1}$	0.033	0.033	0.010	29.096	0.010	0.047
SIRM/ARM	(None)	129.927	111.731	65.166	50.156	77.925	350.935
χ_{ARM}/SIRM	$10^{-5}Am^2kg^{-1}$	2.779	2.811	0.832	29.929	0.895	4.030
SIRM/χ	$10^{-2}Am^{-1}$	119.126	118.931	12.994	10.908	94.373	142.348

Mean; SD = standard deviation; CV = percentage coefficient of variation; Min = minimum value; Max = maximum value. Values are shown to 3 decimal places for consistency, not accuracy.

Dune pasture soil profile description

Profile ID: DP
Date of survey: 10/10/2007


a) Photograph facing east

Site description

Location: 100 m SSW of Victoria Road Car Park, SW of Freshfield Caravan Park.
Grid reference: SD 27732 07865
Landform: Relic-furrowed field.
Land use: Abandoned agricultural land.
Weather: Overcast morning; heavy rain previous day, ~15ºC.


b) Soil profile

Soil description

Drainage: Well-drained.
Surface cover: Very dense meadow vegetation (sand sedge).
Profile depth: 87 cm
Soil depth: 22 cm
NSRI Major group: Lithomorphic soil

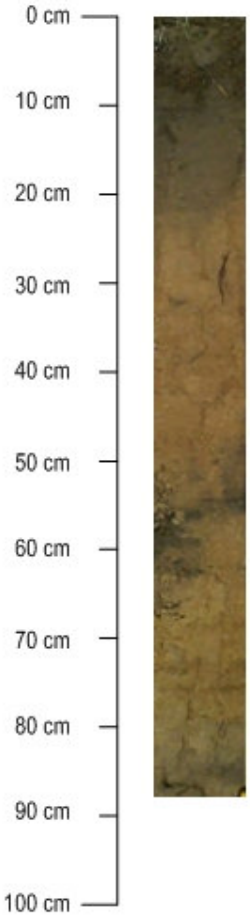

Layer/ Horizon	Depth (cm)	Field description
F	0-3	Dark greyish brown (10YR 4/2) moist and brown (10YR 5/3) dry; smooth boundary to:
H	3-8	Dark greyish brown (10YR 4/2) moist and dark greyish brown (10YR 4/2) dry; loose sand; stoneless; abundant medium (2-5 mm) fibrous roots; clear boundary to:
Ah/Ap	8-22	Dark greyish brown (10YR 4/2) moist and greyish brown (10YR 5/2) dry; loose sand; stoneless; few medium (2-5 mm) fibrous roots; diffuse boundary to:
Cu	22-54	Yellowish brown (10YR 5/4) moist and brown (10YR 5/3) dry; loose sand; stoneless; rare medium (2-5 mm) fibrous roots with dark staining; abrupt boundary to:
bAh1	54-59	Very dark greyish brown (10YR 3/2) moist and greyish brown (10YR 5/2) dry; smooth boundary to:
bAh2	59-79	Yellowish brown (10YR 5/4) moist and brown (10YR 5/3) dry; loose sand; stoneless; common diffuse fine mottling; unclear boundary to:
bCu	79-87	Dark greyish brown (10YR 4/2) moist and pale brown (10YR 6/3) dry; loose sand; stoneless.

Layer/Horizon		F	H	Ah/ Ap	Cu	bAh1	bAh2	bCu
Sand	600-2000 µm %	78	73	77	82	77	83	67
Silt	2-60 µm %	17	24	19	12	19	10	28
Clay	<2 µm %	5	3	4	6	4	7	5
SOM %		1.6	6.2	1.2	0.4	1.0	0.4	0.8
pH in water (1:2.5)		6.7	6.8	6.5	7.3	7.0	7.9	7.6

Figure 4.14 Soil profile description for pasture. Scale on Plate b) is 15 cm.

Cu horizon retained sedimentary characteristics. Pedogenic processes were disturbed by renewed sand deposition burying an existing soil profile, evident by a very dark greyish brown (10YR 3/2) bAh1 horizon at 54-59 cm, where SOM increased slightly to 1%. The yellowish brown (10YR 5/4) bAh2 horizon (59-79 cm) was associated with increased sand (83%) and clay (7%) and decreased silt (10%) relative to the bCu horizon.

Figures 4.15 and 4.16 identify soil formation above 22 cm, evident by overall decreased clay, although a marked increase in clay was observed in the lower Ah/Ap horizon, alongside increased χ_{LF} (1.80 x$10^{-7}$$m^3$$kg^{-1}$). P increased in the upper 22 cm and peaked at 5 cm (0.08%), whereas Ca values decreased, which was reflected in increased concentrations of magnetic minerals. The H layer contained highest values of SOM (8.67%) and Mn (0.03%), alongside lowest values of K (0.41%). Ca decreased from 0.74% at the surface to 0.16% in the Ah/Ap horizon and only increased gradually down-profile to beyond the root zone (54 cm). The bAh1 horizon was further identified by a decrease in pH (6.30) and clay (2.33%), alongside peaks in P (0.03%), S (<0.01%), Cl (0.03%), magnetic concentration parameters (χ_{LF} 1.19 x$10^{-7}$$m^3$$kg^{-1}$; SIRM 157.25 x$10^{-5}$$m^2$$kg^{-1}$) and magnetic minerals ($Soft_{IRM20mT}$ 26.46 x$10^{-5}$$Am^2$$kg^{-1}$; $Soft_{IRM40mT}$ 55.57 x$10^{-5}$$Am^2$$kg^{-1}$). There was also a clear increase in the presence of hard, haematite-type, magnetic minerals in the bAh1 horizon ($Hard_{IRM300mT}$ 43.95 x$10^{-5}$$Am^2$$kg^{-1}$).

Tables 4.7a,b show the organo-mineral soil component had dissimilar physico-chemical values (e.g. pH 6.59; SOM 2.40%) compared to the entire profile (pH 7.26; SOM 0.98%). Increased P (0.04%) and S (0.02%) occurred in the organo-mineral soil component, alongside decreased Ca (0.46%). Magnetic concentration parameter increases (χ_{LF} 1.20 x$10^{-7}$$m^3$$kg^{-1}$; χ_{ARM} 0.04 x$10^{-7}$$m^3$$kg^{-1}$; SIRM 152.40 x$10^{-5}$$Am^2$$kg^{-1}$) were associated with increased ferrimagnetic magnetic minerals ($Soft_{IRM20mT}$ 23.31 x$10^{-5}$$Am^2$$kg^{-1}$; $Soft_{IRM40mT}$ 57.88 x$10^{-5}$$Am^2$$kg^{-1}$). A decline in the SIRM/ARM ratio (127.36) indicated further importance of stable single domain magnetic grains sizes in the organo-mineral soil component.

4.2.6 Scrub pedo-characteristics

The scrub soil profile location (Figure 4.1) was determined by a scrub topsoil pedo-environment (Chapter 3, Section 3.7.5). This environment, sheltered by coniferous plantations, was colonized by deciduous scrub. The first appearance of sea buckthorn (*Hippophae rhamnoides*) (Table 4.8), although initially introduced as a stabilizing technique (Edmondson *et al.,* 1993), indicates an increasingly acidic substrate. Native species, such as creeping willow (*Salix repens*), silver birch (*Betula pendula*) and hawthorn (*Crataegus monogyna*) were also colonizing the dune scrub, alongside the invasion of pine (*Pinus*) seedlings. This mixed birch-hawthorn scrub is indicative of a previous dry slack environment, supported by the presence of ground-layer grass species, such as tall oat grass (*Arrhenatherum elatius*), meadowsweet (*Filipendula ulmaria*) and rose-bay willowherb (*Chamerion angustifolium*). The occasional presence of Little mouse-ear chickweed, on the seaward margins, indicated the dry conditions of aeolian-derived bare sand;

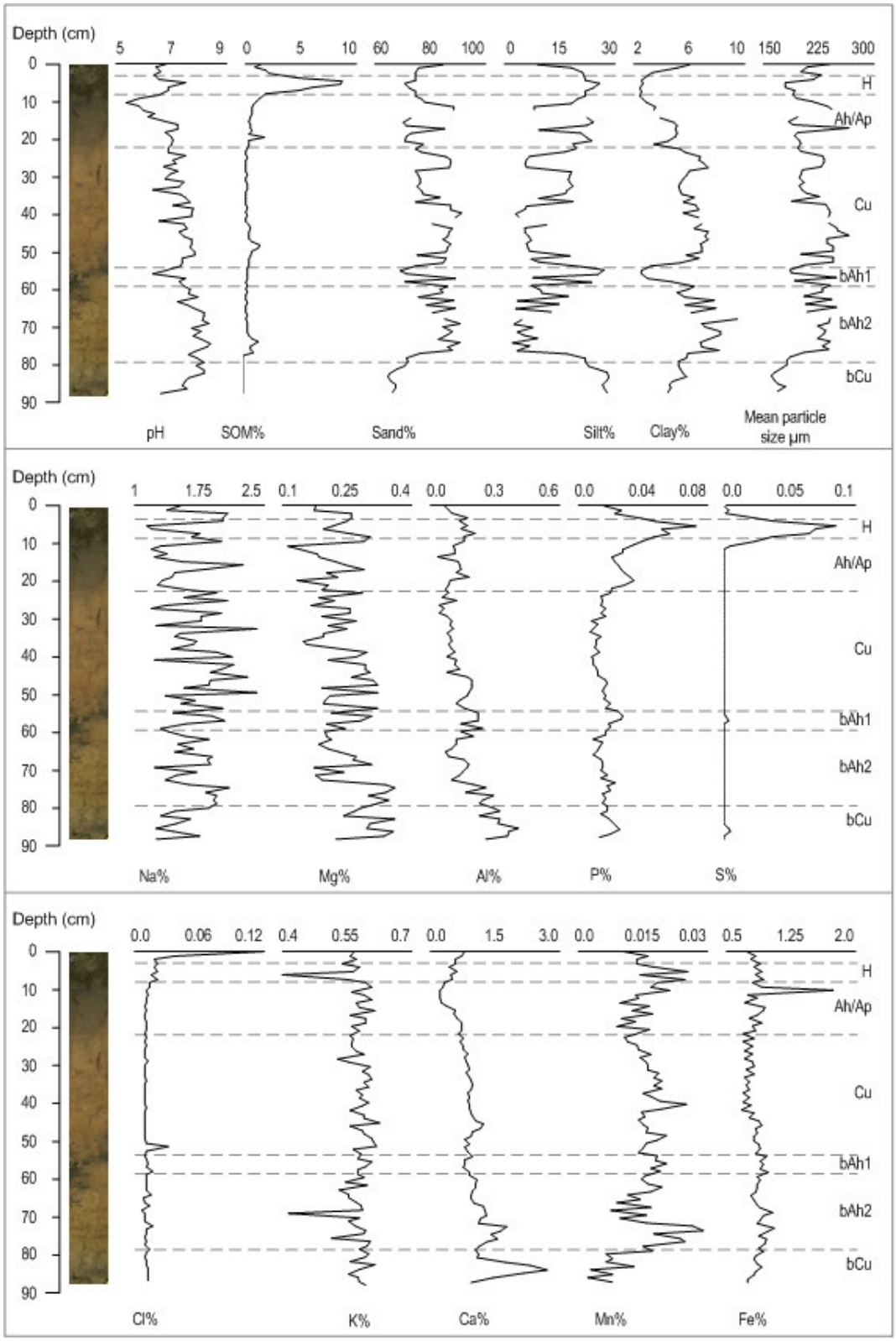

Figure 4.15 Down-profile changes in pasture soil characteristics; pH, SOM, texture and geochemical properties (dashed lines show horizon boundaries).

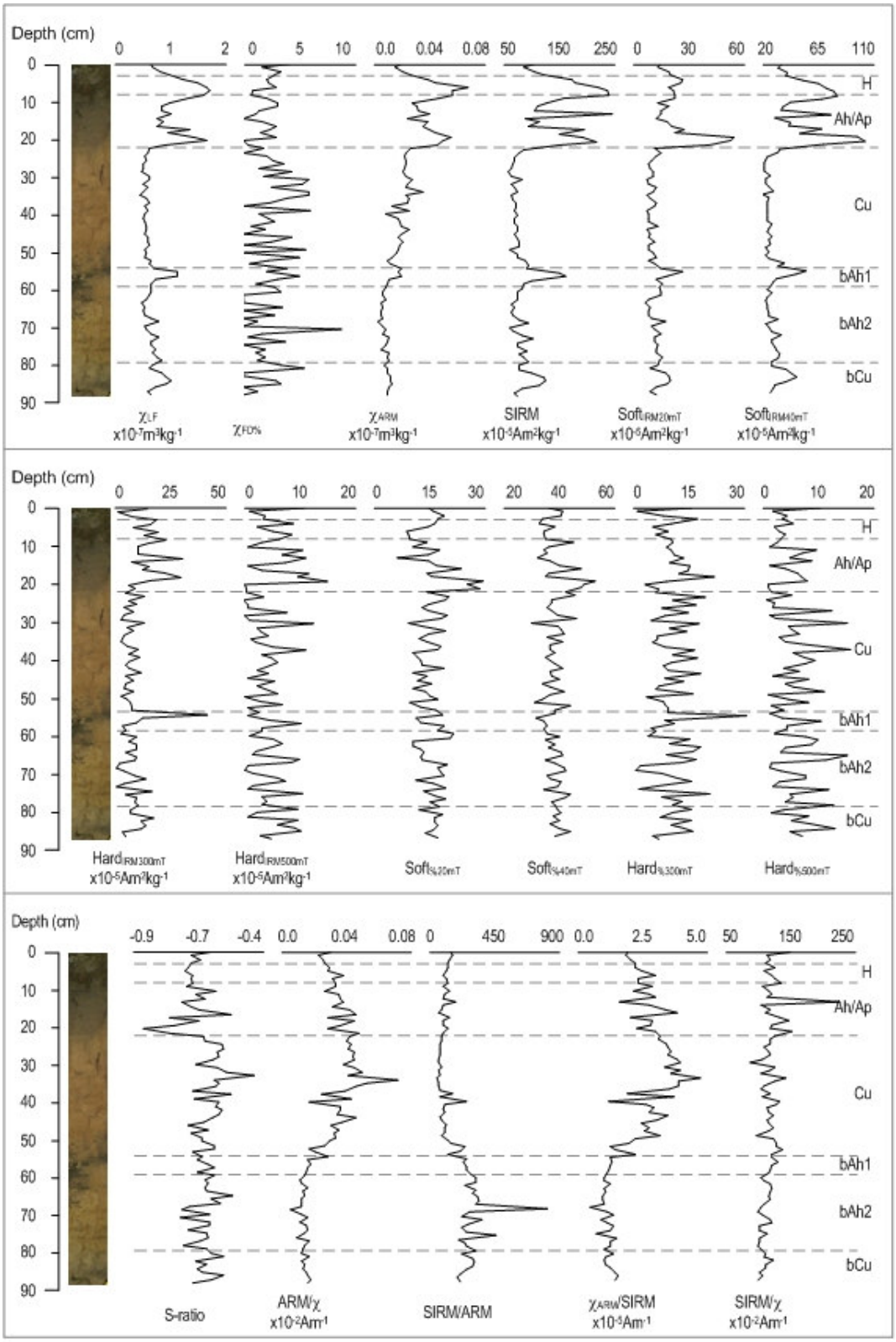

Figure 4.16 Down-profile changes in pasture soil mineral magnetic characteristics (dashed lines show horizon boundaries).

Table 4.7a Summary data* for pasture profile characteristics (n = 85)

Parameters	Units	Mean	Median	SD	CV	Min	Max
pH	mol/ltr	7.256	7.380	0.618	8.512	5.410	8.320
SOM	%	0.980	0.486	1.541	157.337	0.210	8.770
Sand	%	79.103	77.195	7.316	9.249	64.662	91.056
Silt	%	15.401	17.568	8.403	54.563	2.713	29.540
Clay	%	5.496	5.631	1.723	31.346	2.228	9.740
Mean particle size	µm	212.933	207.968	26.537	12.462	158.472	266.687
Median particle size	µm	222.475	221.867	19.908	8.948	175.667	252.441
Sorting		1.870	1.960	0.272	14.566	1.225	2.313
Skewness	γ_1	0.642	0.702	0.121	18.926	0.431	0.795
Kurtosis	g_1	3.470	3.579	1.971	56.792	0.927	6.446
Sodium	%	1.680	1.650	0.338	20.119	1.110	2.490
Magnesium	%	0.246	0.245	0.057	23.298	0.119	0.362
Aluminium	%	0.159	0.141	0.080	50.665	0.038	0.414
Phosphorus	%	0.022	0.019	0.012	51.956	0.009	0.076
Sulphur	%	0.004	0.000	0.015	347.168	0.000	0.088
Chlorine	%	0.013	0.010	0.013	102.015	0.007	0.123
Potassium	%	0.579	0.584	0.033	5.633	0.410	0.627
Calcium	%	0.889	0.856	0.421	47.353	0.162	2.628
Manganese	%	0.021	0.021	0.003	15.814	0.012	0.030
Iron	%	0.837	0.828	0.135	16.166	0.663	1.784
χ_{LF}	$10^{-7}m^3kg^{-1}$	0.792	0.669	0.336	42.425	0.453	1.870
χ_{FD}	%	2.221	2.113	1.842	82.934	0.000	8.805
χ_{ARM}	$10^{-7}m^3kg^{-1}$	0.021	0.019	0.014	66.126	0.003	0.067
SIRM	$10^{-5}Am^2kg^{-1}$	95.207	74.130	46.241	48.569	53.597	244.193
$Soft_{IRM20mT}$	$10^{-5}Am^2kg^{-1}$	14.347	11.820	8.499	59.239	6.224	54.596
$Soft_{IRM40mT}$	$10^{-5}Am^2kg^{-1}$	35.842	28.228	17.935	50.041	20.057	105.137
$Hard_{IRM300mT}$	$10^{-5}Am^2kg^{-1}$	10.132	8.848	7.128	70.349	0.517	43.954
$Hard_{IRM500mT}$	$10^{-5}Am^2kg^{-1}$	4.457	3.419	3.406	76.403	0.000	14.148
$Soft_{\%20mT}$	%	15.141	14.639	3.981	26.295	6.077	28.839
$Soft_{\%40mT}$	%	37.767	37.350	4.185	11.082	28.969	52.299
$Hard_{\%300mT}$	%	10.594	9.776	5.033	47.509	0.924	29.915
$Hard_{\%500mT}$	%	5.021	4.143	3.820	76.078	0.000	15.649
S-ratio	(none)	-0.637	-0.633	0.061	-9.591	-0.864	-0.448
ARM/χ	$10^{-2}Am^{-1}$	0.026	0.028	0.013	50.876	0.004	0.071
SIRM/ARM	(None)	188.806	143.415	115.428	61.136	63.391	814.879
χ_{ARM}/SIRM	$10^{-5}Am^2kg^{-1}$	2.219	2.190	1.096	49.392	0.385	4.954
SIRM/χ	$10^{-2}Am^{-1}$	119.031	118.319	16.107	13.532	90.416	224.743

Table 4.7b Summary data* for pasture organo-mineral soil (refer to Section 5.2) characteristics (n = 22)

Parameters	Units	Mean	Median	SD	CV	Min	Max
pH	mol/ltr	6.593	6.680	0.505	7.659	5.410	7.450
SOM	%	2.404	1.127	2.566	106.711	0.569	8.770
Sand	%	76.159	74.614	5.542	7.277	70.124	88.060
Silt	%	20.150	22.770	5.798	28.777	8.532	26.965
Clay	%	3.692	3.331	1.219	33.032	2.228	6.029
Mean particle size	µm	205.992	196.328	23.738	11.524	178.153	266.687
Median particle size	µm	212.270	212.921	18.961	8.932	175.667	240.862
Sorting		1.947	1.979	0.277	14.236	1.323	2.247
Skewness	γ_1	0.674	0.705	0.095	14.062	0.483	0.779
Kurtosis	g_1	1.906	1.161	1.232	64.614	1.052	4.687
Sodium	%	1.578	1.495	0.355	22.518	1.110	2.310
Magnesium	%	0.218	0.214	0.051	23.251	0.119	0.304
Aluminium	%	0.126	0.128	0.042	33.715	0.038	0.209
Phosphorus	%	0.036	0.030	0.014	39.305	0.017	0.076
Sulphur	%	0.017	0.000	0.027	164.992	0.000	0.088
Chlorine	%	0.019	0.011	0.024	127.096	0.009	0.123
Potassium	%	0.572	0.577	0.041	7.187	0.410	0.617
Calcium	%	0.461	0.508	0.190	41.218	0.162	0.742
Manganese	%	0.021	0.020	0.003	14.195	0.017	0.028
Iron	%	0.867	0.826	0.219	25.281	0.682	1.784
χ_{LF}	$10^{-7}m^3kg^{-1}$	1.195	1.058	0.396	33.110	0.674	1.870
χ_{FD}	%	1.960	2.105	1.145	58.396	0.000	4.145
χ_{ARM}	$10^{-7}m^3kg^{-1}$	0.039	0.039	0.013	34.837	0.015	0.067
SIRM	$10^{-5}Am^2kg^{-1}$	152.403	146.648	54.577	35.811	81.818	244.193
$Soft_{IRM20mT}$	$10^{-5}Am^2kg^{-1}$	23.309	20.289	11.757	50.440	11.820	54.596
$Soft_{IRM40mT}$	$10^{-5}Am^2kg^{-1}$	57.880	52.291	22.027	38.056	29.870	105.137
$Hard_{IRM300mT}$	$10^{-5}Am^2kg^{-1}$	15.408	14.920	7.796	50.599	1.122	32.479
$Hard_{IRM500mT}$	$10^{-5}Am^2kg^{-1}$	5.695	5.503	4.075	71.547	0.376	14.148
$Soft_{\%20mT}$	%	15.874	14.873	5.919	37.289	6.077	28.839
$Soft_{\%40mT}$	%	38.186	35.449	6.073	15.904	31.415	52.299
$Hard_{\%300mT}$	%	10.377	10.159	4.602	44.350	1.372	21.394
$Hard_{\%500mT}$	%	3.975	3.435	2.980	74.978	0.174	10.009
S-ratio	(none)	-0.685	-0.684	0.067	-9.810	-0.864	-0.533
ARM/χ	$10^{-2}Am^{-1}$	0.033	0.031	0.007	21.218	0.021	0.047
SIRM/ARM	(None)	127.362	129.242	28.037	22.014	79.208	192.823
χ_{ARM}/SIRM	$10^{-5}Am^2kg^{-1}$	2.582	2.431	0.570	22.068	1.629	3.965
SIRM/χ	$10^{-2}Am^{-1}$	128.070	120.978	25.309	19.762	106.013	224.743

**Mean; SD = standard deviation; CV = percentage coefficient of variation; Min = minimum value; Max = maximum value. Values are shown to 3 decimal places for consistency, not accuracy.*

Table 4.8 Plant species in the scrub (SD 28155 09854)

Vernacular name	Latin name	DAFOR	Notes
Dewberry	*Rubus caesius*	Abundant	
Rest-harrow	*Ononis repens*	Frequent	
Marram grass	*Ammophila arenaria*	Frequent	
Sand sedge	*Carex arenaria*	Frequent	
Red fescue	*Festuca rubra*	Frequent	
Eyebright	*Euphrasia officinalis*	Frequent	
Birch	*Betula spp.*	Frequent	
Creeping willow	*Salix repens*	Locally abundant	Typical of damp conditions.
Bryophytes		Locally abundant	
Ragwort	*Senecio jacobaea*	Occasional	
Hawthorn	*Crataegus monogyna*	Occasional	
Silver birch	*Betula pendula*	Occasional	
Wood angelica	*Angelica venenosa*	Occasional	
Little Mouse-ear chickweed	*Cerastium semidecandrum*	Occasional	
Portland spurge	*Euphorbia portlandica*	Occasional	
Self-heal	*Prunella vulgaris*	Occasional	
Sand wort	*Arenaria serpyllifolia*	Occasional	
Field wood rush	*Luzula campestris*	Occasional	
Common milkwort	*Polygala vulgaris*	Occasional	
Pink centaury	*Centaurium erythraea*	Occasional	
Yellowwort	*Blackstonia perfoliata*	Occasional	Lime indicator.
Asparagus	*Asparagus officinalis*	Occasional	
Bird's-foot-trefoil	*Lotus corniculatus*	Occasional/frequent	
Wall pepper	*Sedum acre*	Occasional/frequent	
Yorkshire fog	*Holcus lanatus*	Occasional/frequent	
Rose-bay willowherb	*Chamerion angustifolium*	Occasional/frequent	
Carline thistle	*Carlina vulgaris*	Occasional/frequent	
Autumn hawkbit	*Leontodon autumnalis*	Occasional/frequent	
Ploughman's spikenard	*Inula conyza*	Occasional/frequent	
Cat's ear	*Hypochaeris radicata*	Occasional/frequent	
Sea buckthorne	*Hippophae rhamnoides*	Occasional/rare	
Hound's tongue	*Cynoglossum officinale*	Rare	
Spear thistle	*Cirsium vulgare*	Rare	
Common sedge	*Carex nigra*	Rare	
Mouse-ear-hawkweed	*Pilosella officinarum*	Rare	
Wild Strawberry	*Fragaria vesca*	Rare	
Yellow rattle	*Rhinanthus minor*	Rare	
Dog rose	*Rosa canina*	Rare	
Agrimony	*Agrimonia eupatoria*	Rare	
Pine seedlings	*Pinus sylvestris*	Rare	
Fairy flax	*Linum catharticum*	Rare	
Blue fleabane	*Erigeron acer*	Rare	
Intermediate polypody	*Polypodium interjectium*	Rare	
Common knapweed	*Centaurea nigra*	Rare	
Sowthistle	*Sonchus asper*	Rare	
Creeping white clover	*Trifolium repens*		Colonised pathways.
Tall oat grass	*Arrhenatherum elatius*		Typical of slacks.
Stork's bill	*Erodium cicutarium*		
Meadowsweet	*Filipendula ulmaria*		Typical of slacks.

whereas, the occurrence of polypody and wild strawberry (*Fragaria vesca*) is typical of a north-facing dune ridge community (Edmondson *et al.,* 1993).

Figure 4.17 represents the sand-pararendzina (Avery, 1980), in an advanced stage of development. A thick humus (1-7 cm, SOM 3.8%) has influenced pedogenic trends and movement of complexes into the Ah horizon (7-13 cm) by acidification, where pH reached 6.7 and incorporation of SOM (4.4%) was evident in the distinct dark brown (10YR 3/3) layer. A brown (10YR 5/3), leached, eluvial A horizon (13-35 cm), with decreased SOM (0.8%), occurred immediately below. The pH altered down-profile, acidic-neutral, although values were similar (6.6-7.0). Both sand- and silt-sized particles increased in the Ah horizon (70% and 28%, respectively), while clay (2%) decreased. The underlying Cu horizon retained sedimentary characteristics.

Figures 4.18 and 4.19 identify soil formation above 13 cm, evident by decreased pH and mean particle size alongside increased SOM and silt. These changes in pedo-characteristics are associated with higher levels of absorbed cations, except for K where a decrease was observed. Peak values of SOM (15.16%), Mg (0.46%), P (0.06%), S (0.03%) and Ca (2.11%) occurred in the H layer. However, peaks in Al (0.36%) Mn (0.05%) and Fe (1.70%), alongside the lowest recorded value for Ca (0.45%) were observed in the upper Ah horizon, associated with peaks in magnetic concentration parameters (χ_{LF} 6.29 $x10^{-7}m^3kg^{-1}$; χ_{ARM} 0.09 $x10^{-7}m^3kg^{-1}$; SIRM 788.86 $x10^{-5}Am^2kg^{-1}$) and increased magnetic minerals ($Soft_{IRM20mT}$ 109.11 $x10^{-5}$ Am^2kg^{-1}; $Soft_{IRM40mT}$ 292.94 $x10^{-5}Am^2kg^{-1}$; $Hard_{IRM300mT}$ 81.02 $x10^{-5}Am^2kg^{-1}$).

Tables 4.9a,b show the organo-mineral soil component had dissimilar physico-chemical values (e.g. pH 6.63; SOM 4.09%; Silt 24.67%) compared to the entire profile (pH 7.01; SOM 1.42%; Silt 14.66%). Increased Mg (0.37%), Al (0.23%), P (0.04%), S (0.01%) and Fe (1.36%) occurred in the organo-mineral soil component. Magnetic concentration parameter increases (χ_{LF} 4.05 $x10^{-7}m^3kg^{-1}$; χ_{ARM} 0.05 $x10^{-7}m^3kg^{-1}$; SIRM 486.64 $x10^{-5}Am^2kg^{-1}$) were associated with increased ferrimagnetic magnetic minerals ($Soft_{IRM20mT}$ 61.81 $x10^{-5}Am^2kg^{-1}$; $Soft_{IRM40mT}$ 182.01 $x10^{-5}Am^2kg^{-1}$). An increase in the SIRM/ARM ratio (323.54) indicates an additional presence of superparamagnetic or multidomain grains in the organo-mineral soil component.

4.2.7 Deciduous woodland pedo-characteristics

The deciduous woodland soil profile location (Figure 4.1) was determined by a deciduous woodland topsoil pedo-environment (Chapter 3, Section 3.7.5). The presence of meadowsweet (*Filipendula ulmaria*), broad bruckler fern (*Dryopteris dilatata*), woody night shade (*Solanum dulcamara*) and purple loosestrife (*Lythrum salicaria*) (Table 4.10a) suggests this stand of white birch woodland colonized a previous slack environment, as they are all species associated with damp conditions. Dewberry (*Rubus caesius*) was abundant in the shrub layer, while rose-bay willowherb (*Chamerion angustifolium*) was frequent in the ground flora.

Scrubland soil profile description

Profile ID: SL
Date of survey: 02/08/2007

Site description

Location: Off Fisherman's Path, Ainsdale NNR; ~2.5 km W of A565
Grid reference: SD 28171 09841
Landform: Top of dune mound.
Land use: Managed retreat.
Weather: Still, overcast; rain previous night.

Soil description

Drainage: Well-drained.
Surface cover: Dewberry scrub with aeolian derived sand.
Profile depth: 60 cm
Soil depth: 35 cm
NSRI Major group: Lithomorphic soil

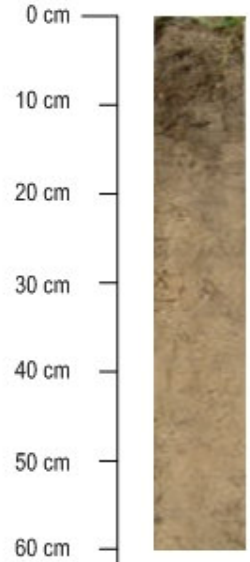

Layer/ Horizon	Depth (cm)	Field description
L	0-2	Brown (10 YR 5/3) moist and brown (10YR 5/3) dry; smooth boundary to:
H	2-7	Brown (10 YR 5/3) moist and brown (10YR 5/3) dry; loose sand; stoneless; single grain soil with no observable aggregation; few coarse (5-10 mm) woody roots; common medium (2-5 mm) woody roots; many fine (1-2 mm) fibrous roots; clear, smooth boundary to:
Ah	7-13	Dark brown (10 YR 3/3) moist and dark greyish brown (10YR 4/2) dry; loose sand; stoneless; single grain soil with no observable aggregation; few coarse (5-10 mm) woody roots; common medium (2-5 mm) woody roots; many fine (1-2 mm) fibrous roots; clear, smooth boundary to:
A	13-35	Brown (10 YR 5/3) moist and brown (10YR 5/3) dry; loose sand; stoneless; few coarse (5-10 mm) and medium (2-5 mm) woody roots; common fine (1-2 mm) fibrous roots; diffuse boundary to:
Cu	35-60	Brown (10 YR 5/3) moist and pale brown (10YR 6/3) dry; loose sand; stoneless; few coarse (5-10 mm) and medium (2-5 mm) woody roots; common fine (1-2 mm) fibrous roots.

Layer/Horizon		L	H	Ah	A	Cu
Sand	600-2000 µm %	76	75	70	80	86
Silt	2-60 µm %	21	23	28	15	9
Clay	<2 µm %	3	2	2	5	5
SOM %		2.3	4.4	4.4	0.8	0.6
pH in water (1:2.5)		6.6	6.6	6.7	7.0	7.2

Figure 4.17 Soil profile description for scrub. Scale on Plate b) is 15 cm.

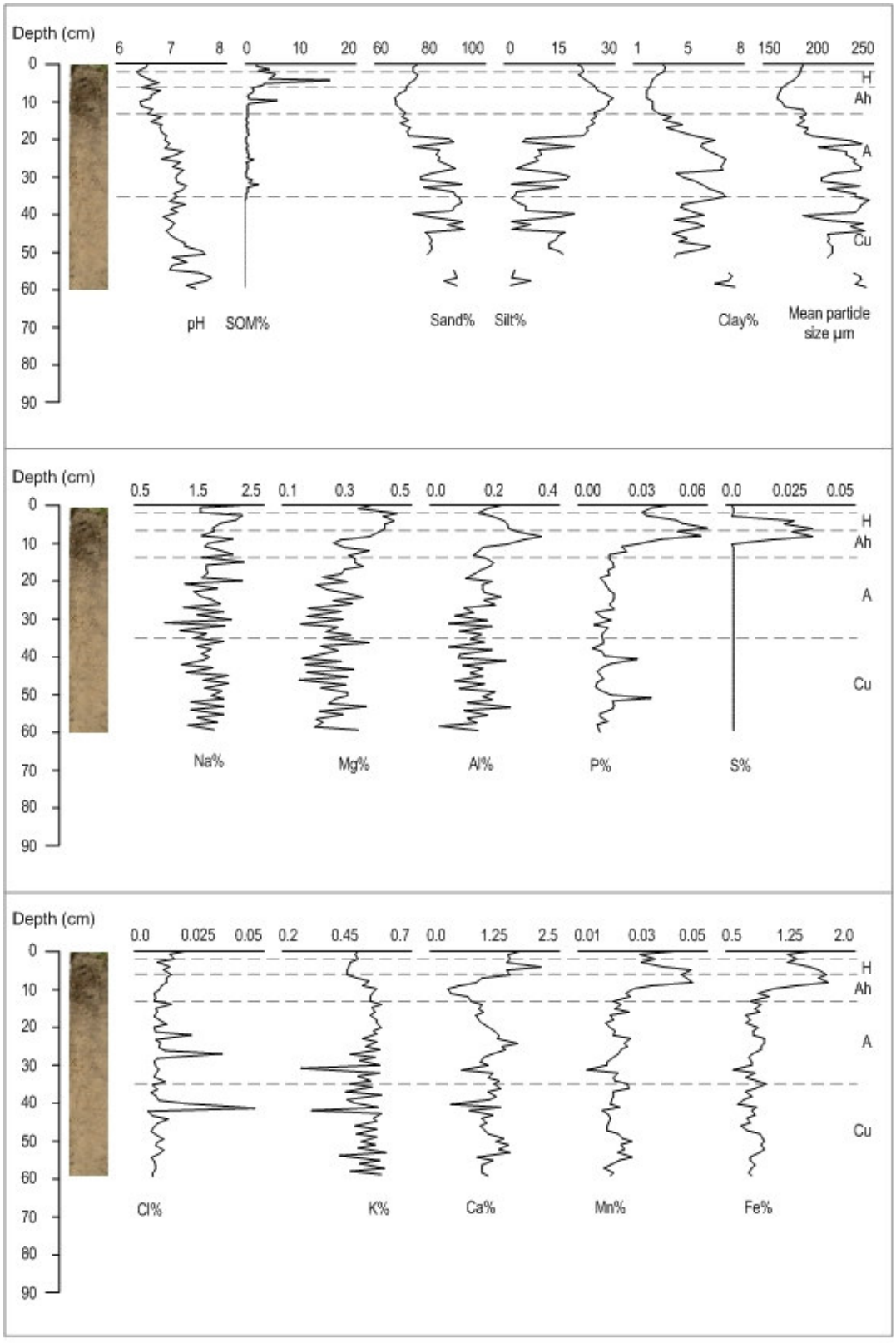

Figure 4.18 Down-profile changes in scrub soil characteristics; pH, SOM, texture and geochemical properties (dashed lines show horizon boundaries).

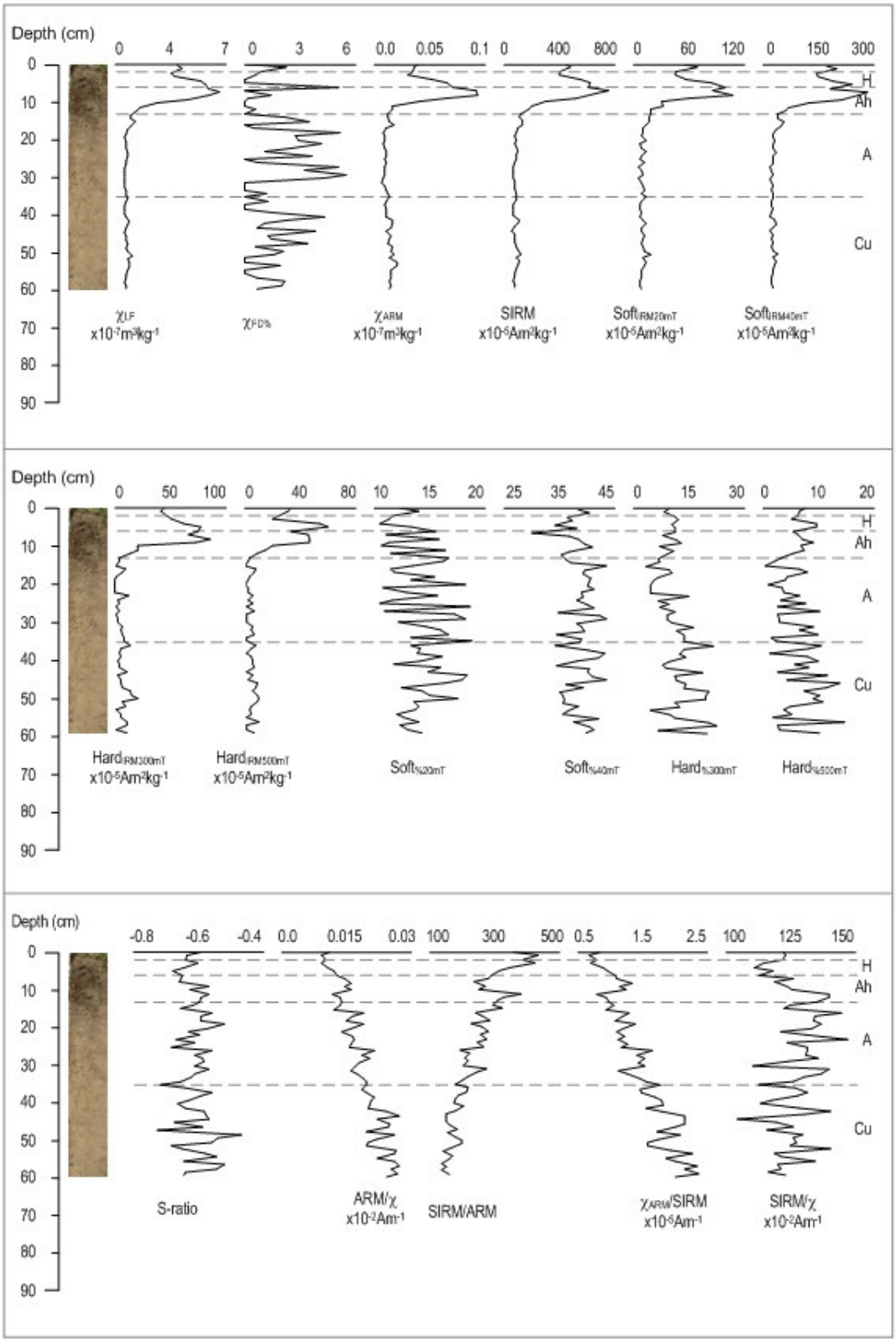

Figure 4.19 Down-profile changes in scrub soil mineral magnetic characteristics (dashed lines show horizon boundaries).

Table 4.9a Summary data* for scrub profile characteristics (n = 60)

Parameters	Units	Mean	Median	SD	CV	Min	Max
pH	mol/ltr	7.010	7.020	0.294	4.200	6.460	7.720
SOM	%	1.423	0.548	2.294	161.135	0.217	15.155
Sand	%	80.841	80.868	7.248	8.965	68.708	92.783
Silt	%	14.664	15.235	8.598	58.631	2.480	29.495
Clay	%	4.495	4.219	1.709	38.015	1.797	7.467
Mean particle size	µm	210.842	210.984	26.160	12.407	163.517	248.402
Median particle size	µm	220.291	224.647	22.936	10.412	166.558	247.534
Sorting		1.691	1.671	0.205	12.124	1.273	2.090
Skewness	γ_1	0.614	0.677	0.129	20.979	0.402	0.776
Kurtosis	g_1	3.448	3.677	1.885	54.657	0.943	6.191
Sodium	%	1.676	1.660	0.285	17.014	0.940	2.340
Magnesium	%	0.291	0.293	0.072	24.883	0.163	0.456
Aluminium	%	0.166	0.167	0.065	39.290	0.020	0.365
Phosphorus	%	0.018	0.014	0.012	68.052	0.007	0.058
Sulphur	%	0.004	0.001	0.008	224.609	0.001	0.034
Chlorine	%	0.011	0.009	0.006	56.424	0.006	0.047
Potassium	%	0.530	0.550	0.061	11.448	0.292	0.607
Calcium	%	1.156	1.148	0.313	27.090	0.395	2.106
Manganese	%	0.024	0.022	0.007	29.809	0.012	0.046
Iron	%	0.944	0.847	0.262	27.708	0.598	1.704
χ_{LF}	$10^{-7}m^3kg^{-1}$	1.369	0.633	1.602	117.029	0.443	6.294
χ_{FD}	%	1.495	1.053	1.598	106.959	0.001	5.369
χ_{ARM}	$10^{-7}m^3kg^{-1}$	0.021	0.014	0.020	93.595	0.008	0.094
SIRM	$10^{-5}Am^2kg^{-1}$	167.895	79.302	189.242	112.714	52.562	788.856
$Soft_{IRM20mT}$	$10^{-5}Am^2kg^{-1}$	22.430	11.851	24.375	108.673	6.885	109.107
$Soft_{IRM40mT}$	$10^{-5}Am^2kg^{-1}$	64.039	31.734	70.089	109.448	21.956	292.935
$Hard_{IRM300mT}$	$10^{-5}Am^2kg^{-1}$	18.196	9.856	20.145	110.710	3.631	81.022
$Hard_{IRM500mT}$	$10^{-5}Am^2kg^{-1}$	10.899	5.693	14.543	133.426	0.177	60.872
$Soft_{\%20mT}$	%	14.126	13.908	2.505	17.731	10.280	19.120
$Soft_{\%40mT}$	%	39.106	39.554	2.987	7.637	29.722	44.493
$Hard_{\%300mT}$	%	11.438	11.247	4.465	39.037	3.455	22.113
$Hard_{\%500mT}$	%	5.997	6.090	3.421	57.039	0.131	14.574
S-ratio	(none)	-0.609	-0.610	0.046	-7.506	-0.718	-0.479
ARM/χ	$10^{-2}Am^{-1}$	0.019	0.019	0.005	27.913	0.009	0.028
SIRM/ARM	(None)	229.538	212.310	71.850	31.302	132.857	426.764
χ_{ARM}/SIRM	$10^{-5}Am^2kg^{-1}$	1.494	1.479	0.432	28.887	0.736	2.364
SIRM/χ	$10^{-2}Am^{-1}$	125.846	125.310	8.625	6.854	104.942	145.540

Table 4.9b Summary data* for scrub organo-mineral soil (refer to Section 5.2) characteristics (n = 13)

Parameters	Units	Mean	Median	SD	CV	Min	Max
pH	mol/ltr	6.628	6.640	0.122	1.843	6.460	6.850
SOM	%	4.088	3.428	3.624	88.655	1.342	15.155
Sand	%	73.053	73.200	2.971	4.067	68.708	76.958
Silt	%	24.671	24.761	3.245	13.152	20.270	29.495
Clay	%	2.276	2.211	0.402	17.642	1.797	3.015
Mean particle size	µm	176.238	174.044	9.330	5.294	163.517	188.346
Median particle size	µm	185.809	185.430	13.957	7.512	166.558	205.716
Sorting		1.706	1.712	0.062	3.624	1.614	1.790
Skewness	γ_1	0.648	0.673	0.044	6.821	0.580	0.698
Kurtosis	g_1	1.245	1.078	0.360	28.930	0.943	2.040
Sodium	%	1.816	1.740	0.273	15.038	1.520	2.340
Magnesium	%	0.374	0.379	0.061	16.396	0.264	0.456
Aluminium	%	0.232	0.240	0.063	27.114	0.152	0.365
Phosphorus	%	0.038	0.038	0.012	32.195	0.020	0.058
Sulphur	%	0.013	0.001	0.014	109.988	0.001	0.034
Chlorine	%	0.013	0.013	0.003	25.969	0.008	0.020
Potassium	%	0.510	0.503	0.037	7.307	0.464	0.574
Calcium	%	1.191	1.469	0.534	44.866	0.395	2.106
Manganese	%	0.035	0.034	0.008	21.935	0.024	0.046
Iron	%	1.360	1.342	0.265	19.500	0.888	1.704
χ_{LF}	$10^{-7}m^3kg^{-1}$	4.046	4.051	1.622	40.095	1.282	6.294
χ_{FD}	%	0.822	0.195	1.407	171.057	0.001	4.936
χ_{ARM}	$10^{-7}m^3kg^{-1}$	0.050	0.041	0.025	50.089	0.017	0.094
SIRM	$10^{-5}Am^2kg^{-1}$	486.638	497.483	185.080	38.032	177.517	788.856
$Soft_{IRM20mT}$	$10^{-5}Am^2kg^{-1}$	61.805	59.020	27.187	43.988	20.113	109.107
$Soft_{IRM40mT}$	$10^{-5}Am^2kg^{-1}$	182.012	189.726	68.560	37.668	63.375	292.935
$Hard_{IRM300mT}$	$10^{-5}Am^2kg^{-1}$	50.906	49.880	21.236	41.715	16.214	81.022
$Hard_{IRM500mT}$	$10^{-5}Am^2kg^{-1}$	34.134	33.305	16.165	47.359	9.318	60.872
$Soft_{\%20mT}$	%	12.658	11.491	2.226	17.588	10.294	16.626
$Soft_{\%40mT}$	%	37.551	37.667	3.141	8.365	29.722	41.691
$Hard_{\%300mT}$	%	10.380	11.100	1.709	16.469	7.383	12.853
$Hard_{\%500mT}$	%	6.881	6.489	1.572	22.843	4.890	9.541
S-ratio	(none)	-0.623	-0.635	0.032	-5.216	-0.672	-0.571
ARM/χ	$10^{-2}Am^{-1}$	0.012	0.012	0.003	20.392	0.009	0.016
SIRM/ARM	(None)	323.544	321.773	63.464	19.615	229.562	426.764
χ_{ARM}/SIRM	$10^{-5}Am^2kg^{-1}$	1.007	0.976	0.201	19.944	0.736	1.368
SIRM/χ	$10^{-2}Am^{-1}$	122.536	122.237	8.367	6.828	111.198	138.442

Mean; SD = standard deviation; CV = percentage coefficient of variation; Min = minimum value; Max = maximum value. Values are shown to 3 decimal places for consistency, not accuracy.

Table 4.10a Plant species in the deciduous woodland (SD 27880 09354)

Vernacular name	Latin name	DAFOR	Notes
White birch	*Betula pubescens*	Abundant	
Dewberry	*Rubus caesius*	Abundant	
Silver birch	*Betula pendula*	Frequent	
Yorkshire fog	*Holcus lanatus*	Frequent	
Rose-bay willowherb	*Chamerion angustifolium*	Frequent	
Common male fern	*Dryopteris filix-mas*	Frequent	
Broad bruckler fern	*Dryopteris dilatata*	Frequent	Typical of damp conditions.
Cleavers	*Galium aparine*	Frequent	
Tall oat grass	*Arrhenatherum elatius*	Frequent/locally-ab	
Bryophytes		Locally abundant	
Hawthorn	*Crataegus monogyna Jacq.*	Occasional	Scrub layer.
Creeping willow	*Salix repens*	Occasional	
Marsh thistle	*Cirsium palustre*	Occasional	
Broad-leaved helleborine	*Epipactis helleborine*	Occasional	
Intermediate polypody	*Polypodium interjectum*	Occasional	
Dog rose	*Rosa canina*	Occasional	
Broad-leaved willowherb	*Epilobium montanum*	Occasional	
Spear thistle	*Cirsium vulgare*	Rare	
Meadowsweet	*Filipendula ulmaria*	Rare	Typical of damp conditions.
Common horsetail	*Equisetum arvense*	Rare	
Creeping bent grass	*Agrostis stolonifera*	Rare	
Watermint	*Mentha aquatica*	Rare	
Woody night shade	*Solanum dulcamara*	Rare	Typical of damp conditions.
Honeysuckle	*Lonicera periclymenum*	Rare	
Purple loosestrife	*Lythrum salicaria*	Rare	Typical of marsh conditions.
Wood avens	*Geum urbanum*	Rare	
Sea buckthorne	*Hippophae rhamnoides*	Rare	
Common broom	*Cytisus scoparius*		Appears on edge of habitat.
Sand sedge	*Carex arenaria*		Appears on edge of habitat.
Creeping white clover	*Trifolium repens*		Colonised pathways.
Common gorse	*Ulex europaeus*		
Sow thistle	*Sonchus asper*		

Table 4.10b Plant species in the coniferous plantation (SD 27646 08462)

Vernacular name	Latin name	DAFOR	Notes
Scots pine	*Pinus sylvestris*	Dominant	
Mouse-ear chickweed	*Cerastium fontanum*	Rare	Exists in areas of sunlight.
Common ragwort	*Senecio jacobaea*	Rare	Exists in areas of sunlight.
Spear thistle	*Cirsium vulgare*	Rare	Exists in areas of sunlight.
Elder	*Sambucus nigra*	Rare	
Sycamore seedlings	*Acer pseudoplatanus*	Rare	
Nettle	*Urtica dioica*	Rare	
Intermediate polypody	*Polypodium interjectum*	Rare	
Bryophytes		Rare	
Yorkshire fog	*Holcus lanatus*	Rare	
Sand sedge	*Carex arenaria*	Rare	Appears on edge of habitat.

Table 4.10c Plant species in the felled phase 2 area (SD 29090 10384)

Vernacular name	Latin name	DAFOR	Notes
Common ragwort	*Senecio jacobaea*	Frequent	
Heath speedwell	*Veronica officinalis*	Frequent	
Dewberry	*Rubus caesius*	Frequent	
Yorkshire fog	*Holcus lanatus*	Frequent	
Field wood rush	*Luzula campestris*	Frequent	
Creeping willow	*Salix repens*	Local/abundant	
Mouse-ear chickweed	*Cerastium fontanum*	Occasional	
Common bent grass	*Agrostis capillaris*	Occasional	
Red fescue	*Festuca rubra*	Occasional	
Stork's bill	*Erodium cicutarium*	Rare	
Sow thistle	*Sonchus asper*	Rare	
Mouse-ear-hawk reed	*Pilosella officinarum*	Rare	
Pink centaury	*Centaurium erythraea*	Rare	

Figure 4.20 represents the brown earth (Avery, 1980) with the no separation between the L and H layers (0-11 cm) identifiable in the field. However, the L layer (0-4 cm) characteristics (SOM 70.2%; pH 4.8) are different to those of the H layer (4-11 cm; SOM 37.3%; pH 4.1). SOM became incorporated into a very dark greyish brown (10YR 3/2) Ah horizon (11-15 cm), reaching 3.5%, while pH decreased to 3.9. Values for silt-sized particles decreased to 19%, while sand and clay remained similar. A dark greyish brown (10YR 4/2); mottled B horizon (15-25 cm) occurred immediately below, with decreased SOM (1.1%). The underlying Cu horizon retained sedimentary characteristics.

Figures 4.21 and 4.22 identify soil formation above 25 cm, evident by decreased pH and clay with increased silt. Peak values of SOM (78.76%), mean particle size (401.07 µm), Mg (0.42%), Cl (1.13%) and Mn (0.09%) occurred in the L layer, with Na and K showing lowest values (0.28%; 0.22%, respectively). Peaks in silt (27.13%), Al (0.60%), P (0.12%), S (0.32%), and Fe (1.24%), were observed in the H layer, associated with peaks in magnetic concentration parameters (χ_{LF} 7.74 $x10^{-7}m^3kg^{-1}$; χ_{ARM} 0.17 $x10^{-7}m^3kg^{-1}$; SIRM 909.10 $x10^{-5}Am^2kg^{-1}$) and increased magnetic minerals ($Soft_{IRM20mT}$ 147.86 $x10^{-5}Am^2kg^{-1}$; $Soft_{IRM40mT}$ 336.93 $x10^{-5}Am^2kg^{-1}$; $Hard_{IRM300mT}$ 97.94 $x10^{-5}Am^2kg^{-1}$; $Hard_{IRM500mT}$ 54.60 $x10^{-5}Am^2kg^{-1}$). Levels of K rose again (0.58%) in the Ah horizon as Ca dropped, alongside a peak in SIRM/ARM indicative of increased superparamagnetic or multidomain grains. The lowest values of Ca (0.09%) are recorded in the B horizon. Peaks in $\chi_{FD\%}$ in the B horizon, followed by steady increases down profile, are indicative of the presence of superparamagnetic grains.

Tables 4.11a,b show the organo-mineral soil component had dissimilar physico-chemical values (e.g. pH 4.12; SOM 22.17%; Sand 75.73%; Silt 21.98%; Clay 2.30%) compared to the entire profile (pH 6.68; SOM 7.09%; Sand 83.39%; Silt 11.47%; Clay 5.14%). Increased Al (0.32%), P (0.05%), S (0.09%) and Cl (0.08%) occurred in the organo-mineral soil component, alongside decreased Ca (0.39%). Magnetic concentration parameter increases (χ_{LF} 2.10 $x10^{-7}m^3kg^{-1}$; χ_{ARM} 0.05 $x10^{-7}m^3kg^{-1}$; SIRM 250.12 $x10^{-5}Am^2kg^{-1}$) were associated with increased ferrimagnetic magnetic minerals ($Soft_{IRM20mT}$ 41.46 $x10^{-5}Am^2kg^{-1}$; $Soft_{IRM40mT}$ 90.20 $x10^{-5}Am^2kg^{-1}$). An increase in the SIRM/ARM ratio (167.96) indicates the additional presence of superparamagnetic or multidomain grains in the organo-mineral soil component.

4.2.8 Coniferous plantation pedo-characteristics

The coniferous plantation soil profile location (Figure 4.1) was determined by a deciduous woodland topsoil pedo-environment (Chapter 3, Section 3.7.6). Scots pine woodland (*Pinus sylvestris*) had relatively low species diversity (Table 4.10b). Despite this, the plantation does have some ground flora bryophyte species. Where light has penetrated through the canopy at woodland edges, ground cover is occupied by sand sedge (*Carex arenaria*), together with Little mouse-ear chickweed (*Cerastium fontanum*) and spear thistle (*Cirsium vulgare*). Common ragwort (*Senecio jacobaea*) and stinging nettle (*Urtica dioica*) were signs of disturbance. Natural

Deciduous woodland soil profile description

Profile ID: DW
Date of survey: 17/02/2008

Site description

Location: ~500 m along Fisherman's Path from the railway.
Grid reference: SD 27881 09349
Landform: Relic slack.
Land use: Natural woodland.
Weather: Clear, bright; subzero temperatures.

Soil description

Drainage: Well-drained.
Surface cover: Frozen; dense scrub vegetation (birch).
Profile depth: 80 cm
Soil depth: 25 cm
NSRI Major group: Brown soil


a) Photograph facing east


b) Soil profile

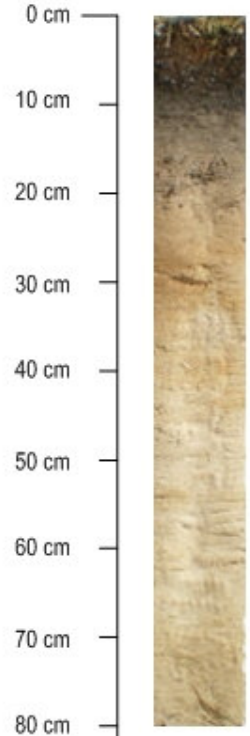

Layer/ Horizon	Depth (cm)	Field description
L	0-4	Black (10 YR 2/1) moist and very dark greyish brown (10YR 3/2) dry; abrupt boundary to:
H	4-11	Black (10 YR 2/1) moist and very dark greyish brown (10YR 3/2) dry; loose sand; stoneless; sharp boundary to:
Ah	11-15	Very dark greyish brown (10 YR 3/2) moist and greyish brown (10YR 5/2) dry; loose sand; stoneless; common coarse (5-10 mm) and medium (2-5 mm) woody roots; diffuse boundary to:
B	15-25	Dark greyish brown (10 YR 4/2) moist and brown (10YR 5/3) dry; loose sand; stoneless; 15% diffuse mottles; diffuse boundary to:
Cu1	25-43	Yellowish brown (10 YR 5/4) moist and yellowish brown (10 YR 5/4) dry; loose sand; stoneless; abundant fine (1-2 mm) fibrous roots; diffuse boundary to:
Cu2	43-68	Brown (10 YR 5/3) moist and pale brown (10YR 6/3) dry; loose sand; stoneless; 5% small diffuse mottles; diffuse boundary to:
Cu3	68-80	Yellowish brown (10 YR 5/4) moist and light yellowish brown (10YR 6/4) dry; loose sand; stoneless.

Layer/Horizon		L	H	Ah	B	Cu
Sand	600-2000 µm %	76	73	79	76	87
Silt	2-60 µm %	22	25	19	21	6
Clay	<2 µm %	2	2	2	3	7
SOM %		70.2	37.3	3.5	1.1	0.6
pH in water (1:2.5)		4.8	4.1	3.9	4.0	7.8

Figure 4.20 Soil profile description for deciduous woodland. Scale on Plate b) is 15 cm.

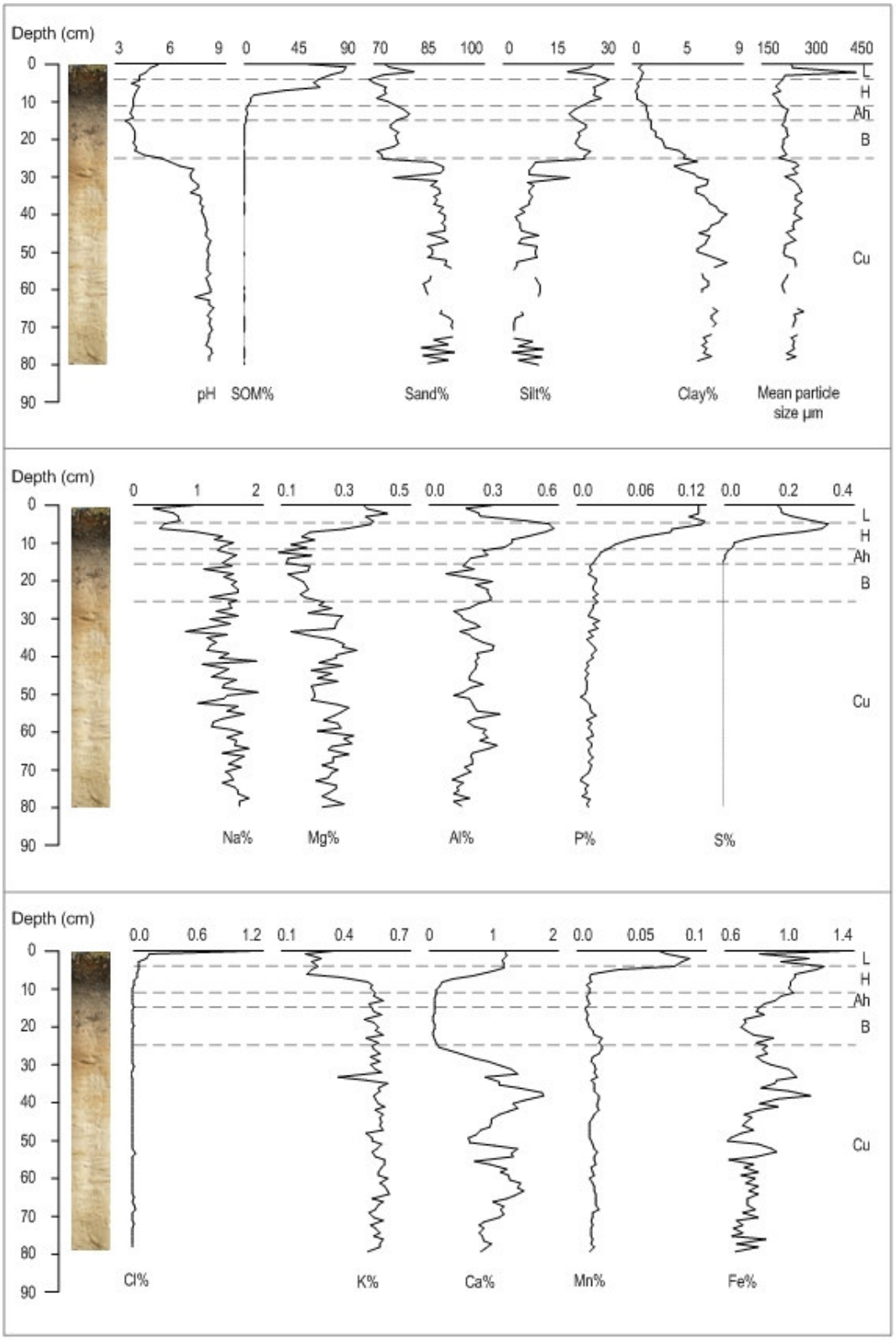

Figure 4.21 Down-profile changes in deciduous woodland soil characteristics; pH, SOM, texture and geochemical properties (dashed lines show horizon boundaries).

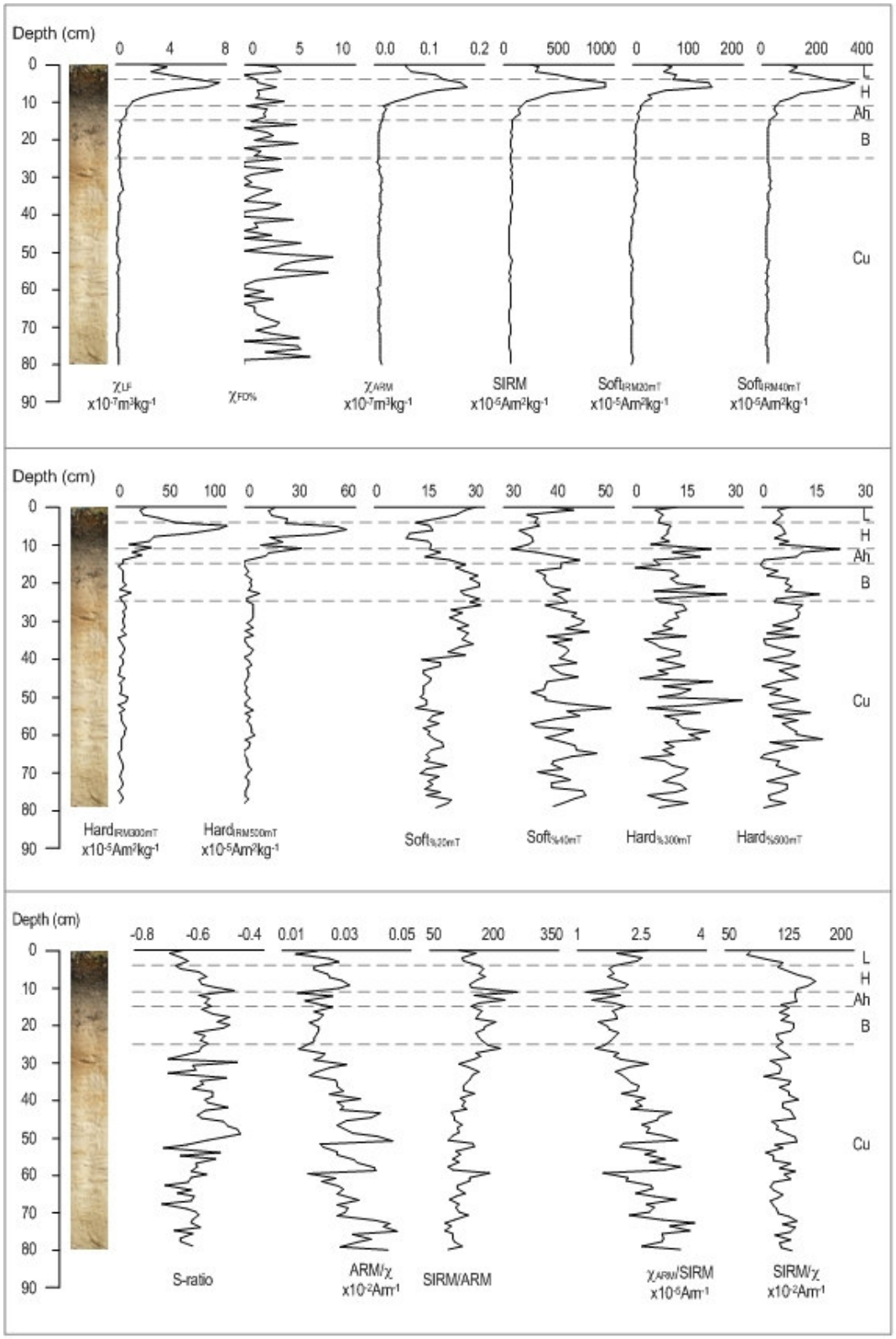

Figure 4.22 Down-profile changes in deciduous woodland soil mineral magnetic characteristics (dashed lines show horizon boundaries).

Table 4.11a Summary data* for deciduous woodland profile characteristics (n = 80)

Parameters	Units	Mean	Median	SD	CV	Min	Max
pH	mol/ltr	6.678	7.770	1.807	27.065	3.550	8.370
SOM	%	7.087	0.750	18.786	265.062	0.108	81.548
Sand	%	83.386	85.203	6.236	7.479	70.346	91.600
Silt	%	11.472	8.390	8.184	71.342	1.813	28.107
Clay	%	5.142	6.203	2.172	42.250	1.279	8.117
Mean particle size	µm	229.010	228.059	26.976	11.779	183.793	401.071
Median particle size	µm	225.473	229.072	22.759	10.094	151.978	250.593
Sorting		1.683	1.602	0.200	11.889	1.349	2.353
Skewness	γ_1	0.544	0.493	0.129	23.709	0.174	0.799
Kurtosis	g_1	4.059	5.008	1.819	44.812	0.922	6.122
Sodium	%	1.391	1.475	0.337	24.253	0.280	1.970
Magnesium	%	0.245	0.253	0.061	24.768	0.109	0.417
Aluminium	%	0.249	0.226	0.098	39.349	0.091	0.597
Phosphorus	%	0.025	0.016	0.029	113.513	0.005	0.118
Sulphur	%	0.027	0.000	0.073	270.735	0.000	0.315
Chlorine	%	0.036	0.012	0.126	356.014	0.006	1.126
Potassium	%	0.525	0.547	0.091	17.303	0.218	0.615
Calcium	%	0.862	0.971	0.485	56.288	0.077	1.816
Manganese	%	0.018	0.014	0.015	84.378	0.009	0.087
Iron	%	0.844	0.811	0.151	17.864	0.613	1.363
χ_{LF}	$10^{-7}m^3kg^{-1}$	0.899	0.371	1.472	163.801	0.207	7.740
χ_{FD}	%	1.975	1.494	1.895	95.952	0.000	8.163
χ_{ARM}	$10^{-7}m^3kg^{-1}$	0.022	0.011	0.034	150.411	0.007	0.172
SIRM	$10^{-5}Am^2kg^{-1}$	105.985	43.653	179.185	169.067	27.085	917.951
$Soft_{IRM20mT}$	$10^{-5}Am^2kg^{-1}$	18.217	9.442	27.052	148.495	3.461	147.857
$Soft_{IRM40mT}$	$10^{-5}Am^2kg^{-1}$	39.570	18.146	62.608	158.220	10.037	336.926
$Hard_{IRM300mT}$	$10^{-5}Am^2kg^{-1}$	10.935	5.400	17.436	159.457	0.815	97.936
$Hard_{IRM500mT}$	$10^{-5}Am^2kg^{-1}$	6.278	2.592	10.334	164.618	0.020	54.603
$Soft_{\%20mT}$	%	19.028	18.222	5.308	27.897	9.153	29.427
$Soft_{\%40mT}$	%	39.753	40.031	3.275	8.238	31.735	49.292
$Hard_{\%300mT}$	%	11.356	11.190	4.776	42.056	1.992	28.319
$Hard_{\%500mT}$	%	6.130	5.803	3.970	64.771	0.069	20.830
S-ratio	(none)	-0.596	-0.600	0.059	-9.866	-0.719	-0.467
ARM/χ	$10^{-2}Am^{-1}$	0.028	0.028	0.007	25.569	0.015	0.046
SIRM/ARM	(None)	138.815	134.735	34.790	25.062	83.009	260.912
χ_{ARM}/SIRM	$10^{-5}Am^2kg^{-1}$	2.398	2.332	0.571	23.796	1.204	3.784
SIRM/χ	$10^{-2}Am^{-1}$	117.010	115.941	12.503	10.686	77.043	151.188

Table 4.11b Summary data* for deciduous woodland organo-mineral soil (refer to Section 5.2) characteristics (n = 25)

Parameters	Units	Mean	Median	SD	CV	Min	Max
pH	mol/ltr	4.124	4.010	0.381	9.232	3.550	5.330
SOM	%	22.167	3.349	29.546	133.287	0.538	81.548
Sand	%	75.728	75.581	2.744	3.624	70.346	81.364
Silt	%	21.976	21.995	2.991	13.608	16.774	28.107
Clay	%	2.295	2.079	0.967	42.115	1.279	4.936
Mean particle size	µm	218.390	211.564	39.917	18.278	183.793	401.071
Median particle size	µm	202.859	216.335	25.508	12.574	151.978	250.593
Sorting		1.822	1.827	0.183	10.062	1.524	2.248
Skewness	γ_1	0.607	0.666	0.167	27.559	0.174	0.773
Kurtosis	g_1	1.695	1.446	0.700	41.311	0.922	2.978
Sodium	%	1.191	1.370	0.440	36.970	0.280	1.660
Magnesium	%	0.224	0.192	0.092	40.939	0.109	0.417
Aluminium	%	0.316	0.291	0.135	42.743	0.091	0.597
Phosphorus	%	0.051	0.024	0.041	80.899	0.012	0.118
Sulphur	%	0.086	0.017	0.110	128.063	0.000	0.315
Chlorine	%	0.084	0.021	0.221	264.214	0.010	1.126
Potassium	%	0.457	0.525	0.130	28.550	0.218	0.581
Calcium	%	0.394	0.119	0.460	116.710	0.077	1.239
Manganese	%	0.025	0.012	0.026	102.056	0.009	0.087
Iron	%	0.937	0.916	0.174	18.599	0.697	1.363
χ_{LF}	$10^{-7}m^3kg^{-1}$	2.101	0.929	2.219	105.604	0.345	7.740
χ_{FD}	%	1.764	1.449	1.409	79.849	0.001	4.950
χ_{ARM}	$10^{-7}m^3kg^{-1}$	0.049	0.018	0.051	105.222	0.008	0.172
SIRM	$10^{-5}Am^2kg^{-1}$	250.117	121.515	272.073	108.778	39.137	917.951
$Soft_{IRM20mT}$	$10^{-5}Am^2kg^{-1}$	41.455	21.919	39.544	95.390	10.549	147.857
$Soft_{IRM40mT}$	$10^{-5}Am^2kg^{-1}$	90.201	46.929	94.752	105.046	14.763	336.926
$Hard_{IRM300mT}$	$10^{-5}Am^2kg^{-1}$	24.637	13.314	26.588	107.917	1.219	97.936
$Hard_{IRM500mT}$	$10^{-5}Am^2kg^{-1}$	14.604	11.492	15.499	106.126	0.085	54.603
$Soft_{\%20mT}$	%	20.825	22.572	6.393	30.699	9.153	29.058
$Soft_{\%40mT}$	%	37.598	37.470	3.071	8.168	31.735	43.611
$Hard_{\%300mT}$	%	10.793	10.058	5.136	47.586	1.992	24.732
$Hard_{\%500mT}$	%	6.310	5.589	4.535	71.874	0.136	20.830
S-ratio	(none)	-0.586	-0.588	0.055	-9.384	-0.695	-0.485
ARM/χ	$10^{-2}Am^{-1}$	0.023	0.022	0.004	17.521	0.015	0.031
SIRM/ARM	(None)	167.963	166.137	30.690	18.272	116.297	260.912
χ_{ARM}/SIRM	$10^{-5}Am^2kg^{-1}$	1.925	1.890	0.327	16.972	1.204	2.701
SIRM/χ	$10^{-2}Am^{-1}$	119.782	121.894	17.409	14.534	77.043	151.188

Mean; SD = standard deviation; CV = percentage coefficient of variation; Min = minimum value; Max = maximum value. Values are shown to 3 decimal places for consistency, not accuracy.

regeneration of sycamore (*Acer pseudoplatanus*) seedlings, suggests the woodland may have been thinned in the past.

Figure 4.23 represents another podzol (Avery, 1980), further defined as a micropodzol by James (1993), which was very different to that under the heath. A thick (0-10 cm) accumulation of pine-needle litter (pH 5.5; SOM 50.9%) overlaid a well developed black (10YR 2/1) H layer (10-12 cm) with pH 4.2. Both horizons had similar percentages of sand, silt and clay. SOM dropped to 4.4% in the thick (12-24 cm) bleached greyish brown (10YR 5/2 dry) E horizon, where levels of sand-sized particles decreased (68%) alongside increased silt (29%) and clay (3%). A weakly developed B horizon (24-42 cm) was evident by rusty-mottles and very low SOM (1.7%). The underlying Cu horizon retained sedimentary characteristics.

Figures 4.24 and 4.25 identify soil formation above 42 cm, evident by decreased pH and increased silt. Peaked values of SOM (80.70%), Mg (0.52%), P (0.09%), S (0.19%) Ca (1.46%), Mn (0.04%) and Fe (1.32%) occurred in the L layer, with Na and K showing lowest values (0.82%; 0.27%, respectively), associated with high numbers of superparamagnetic or multidomain magnetic grain sizes (ARM/χ 0.01 $x10^{-2}Am^{-1}$; SIRM/ARM 264.13). Peaks in Al (0.83%) and Cl (0.12%), with lowest values of mean particle size (156.24 µm), were observed in the H layer. These were associated with peaks in magnetic concentration parameters (χ_{LF} 9.93 $x10^{-7}m^3kg^{-1}$; χ_{ARM} 0.27 $x10^{-7}m^3kg^{-1}$; SIRM 1395.60 $x10^{-5}Am^2kg^{-1}$), magnetic minerals ($Soft_{IRM20mT}$ 158.69 $x10^{-5}Am^2kg^{-1}$; $Soft_{IRM40mT}$ 439.81 $x10^{-5}Am^2kg^{-1}$; $Hard_{IRM300mT}$ 77.31 $x10^{-5}Am^2kg^{-1}$; $Hard_{IRM500mT}$ 55.43 $x10^{-5}Am^2kg^{-1}$) and stable single domain magnetic grains (SIRM/χ 145.56 $x10^{-2}Am^{-1}$). Lowest levels of Mg (0.16%), Al (0.17%), P (<0.0%), Ca (0.13%) and Mn (0.01%) were recorded in the E horizon, where magnetic domain sizes were similar to the B horizon, being slightly coarser than the horizons above. Ca remained low throughout the B horizon.

Tables 4.12a,b show the physico-chemical characteristics of the organo-mineral soil component did not vary greatly with those from the entire soil profile. However, the organo-mineral soil component had lower pH (4.80) alongside increased Al (0.33%) and Fe (0.92%).

4.2.9 Felled coniferous woodland pedo-characteristics

The felled coniferous woodland soil profile location (Figure 4.1) was determined by a felled coniferous woodland topsoil pedo-environment (Chapter 3, Section 3.7.7). Initial responses to clear-felling are the establishment of weed communities (Sturgess, 1992), allowing colonization of light-demanding ground flora species, including Yorkshire fog (*Holcus lanatus*) and common ragwort (*Senecio jacobaea*) (Table 4.10c). These species were also present on the edges of the pine plantations, as well as on fixed dunes, confirming this area underwent pine removal and that these species were benefiting from post-felling nutrient release and absence of competition (Sturgess, 1993).

Coniferous plantation soil profile description

Profile ID: CP
Date of survey: 02/08/2007

Site description

Location: 200 m NNW of Victoria Road Car Park, SW of Freshfield Caravan Park; National Trust.
Grid reference: SD 27647 08459
Landform: Top of dune ridge.
Land use: Recreational.
Weather: Very bright, >18°C.

Soil description

Drainage: Well-drained.
Surface cover: Scott's pine; bare sand, fresh needle litter.
Profile depth: 52 cm
Soil depth: 42 cm
NSRI Major group: Podzolic soil


a) Photograph facing west


b) Soil profile

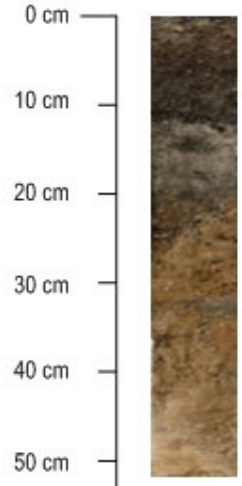

Layer/ Horizon	Depth (cm)	Field description
L	0-10	Very dark brown (10 YR 2/2) moist and very dark greyish brown (10YR 3/2) dry; abrupt boundary to:
H	10-12	Black (10 YR 2/1) moist and very dark grey (10YR 3/1) dry; sharp boundary to:
E	12-24	Dark greyish brown (10 YR 4/2) moist and greyish brown (10YR 5/2) dry; loose sand; stoneless; common coarse (5-10 mm) woody roots; clear boundary to:
B	24-42	Dark greyish brown (10 YR 4/2) moist and brown (10 YR 5/3) dry; loose sand; stoneless; 25% diffuse mottles; few coarse (5-10 mm) woody roots; common medium (2-5 mm) woody roots; diffuse boundary to:
Cu	42-52	Yellowish brown (10 YR 5/4) moist and brown (10YR 5/3) dry; loose sand; stoneless; few very coarse (>10 mm) woody roots; many coarse (5-10 mm) woody roots.

Layer/Horizon		L	H	E	B	Cu
Sand	600-2000 µm %	74	75	68	72	76
Silt	2-60 µm %	25	24	29	24	18
Clay	<2 µm %	1	1	3	4	6
SOM %		50.9	47.5	4.4	1.7	0.5
pH in water (1:2.5)		5.5	4.2	4.5	4.7	7.1

Figure 4.23 Soil profile description for coniferous plantation. Scale on Plate b) is 15 cm.

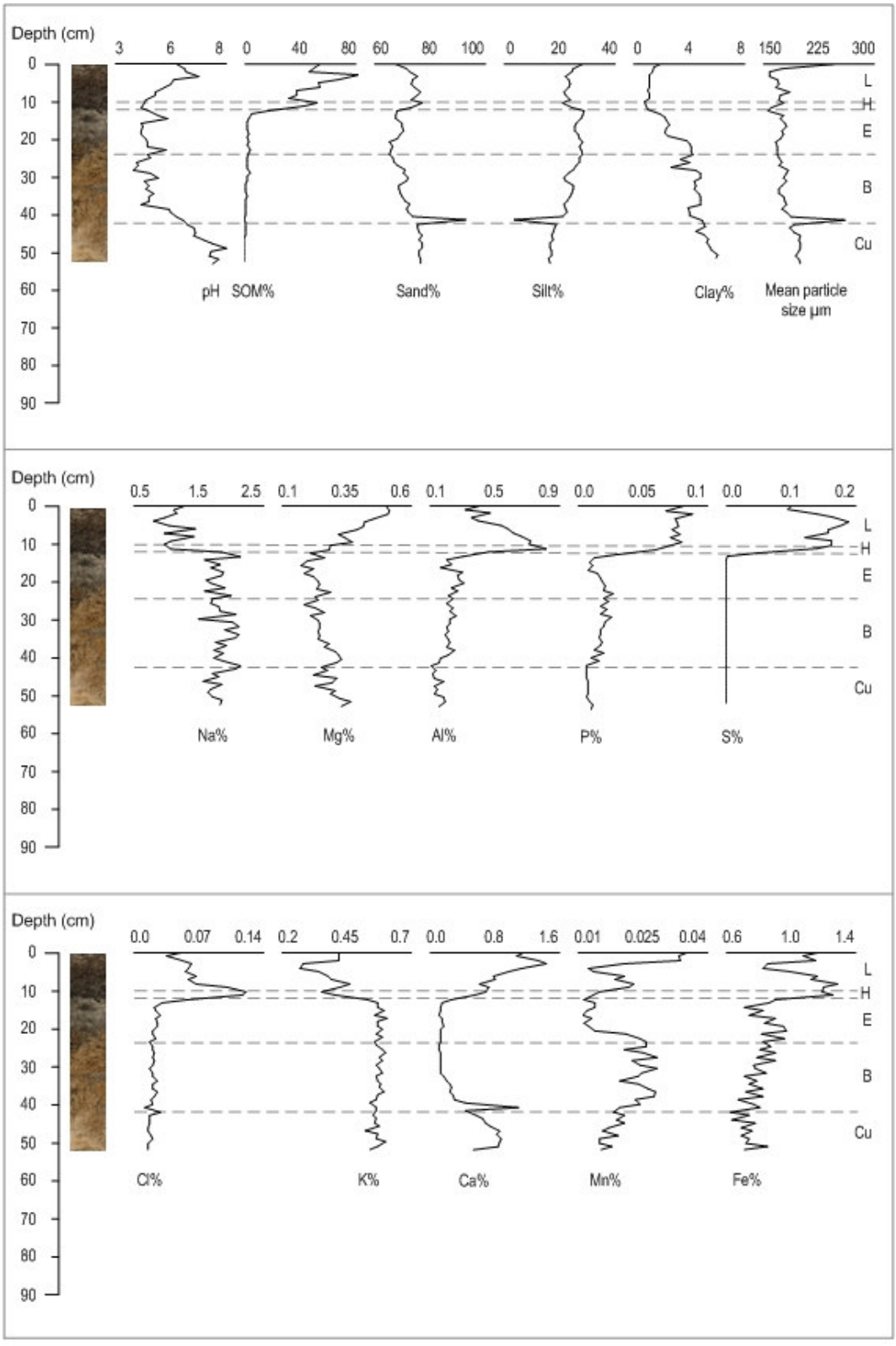

Figure 4.24 Down-profile changes in coniferous plantation soil characteristics; pH, SOM, texture and geochemical properties (dashed lines show horizon boundaries).

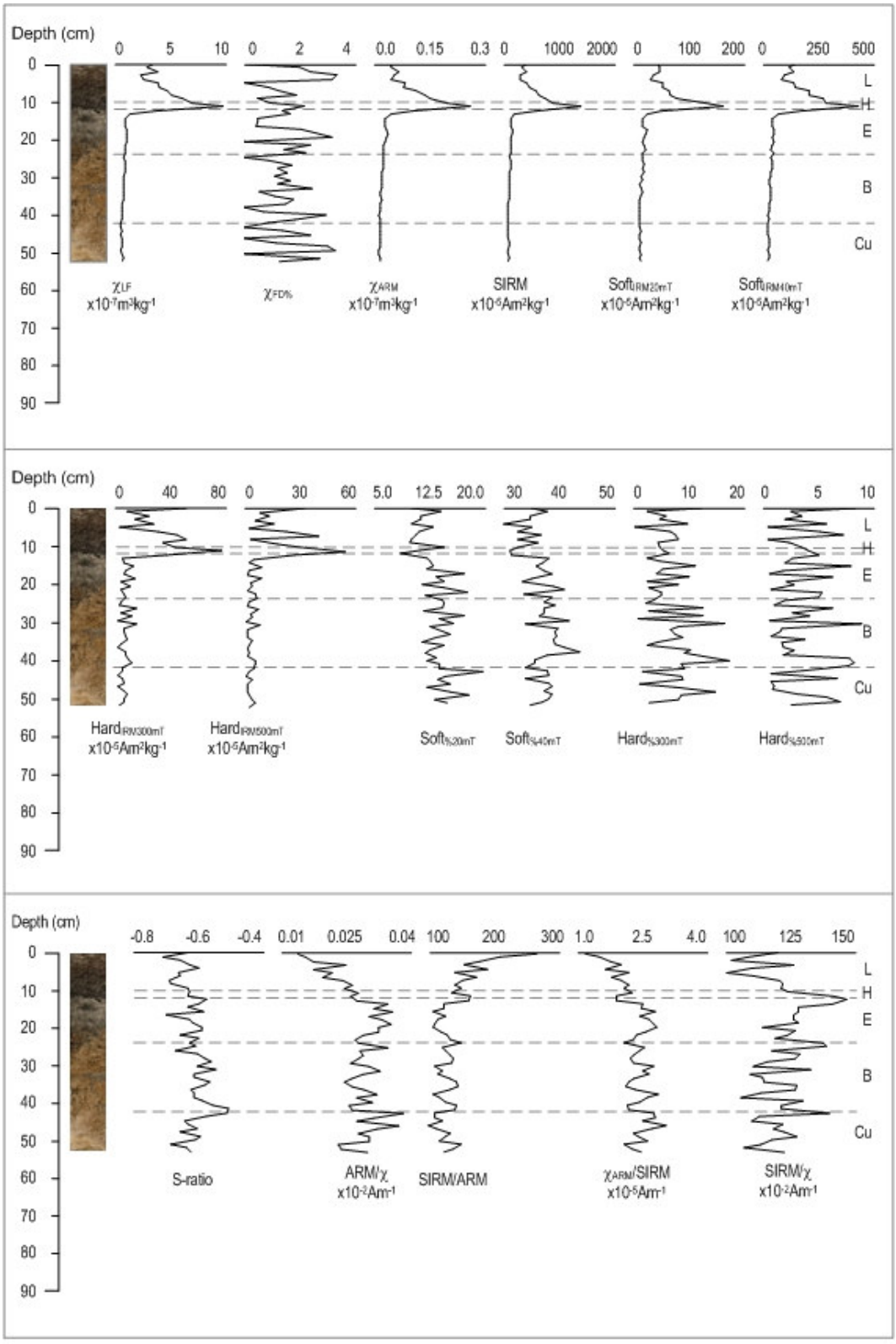

Figure 4.25 Down-profile changes in coniferous plantation soil mineral magnetic characteristics (dashed lines show horizon boundaries).

Table 4.12a Summary data* for coniferous plantation profile characteristics (n = 52)

Parameters	Units	Mean	Median	SD	CV	Min	Max
pH	mol/ltr	5.242	4.825	1.139	21.732	3.730	7.910
SOM	%	13.297	2.114	21.541	162.005	0.229	80.696
Sand	%	72.373	72.054	4.420	6.107	65.973	91.893
Silt	%	24.003	24.871	4.924	20.513	3.822	30.397
Clay	%	3.623	4.259	1.667	46.010	0.929	6.331
Mean particle size	µm	180.511	176.015	18.062	10.006	156.237	258.027
Median particle size	µm	188.377	195.028	25.940	13.770	129.187	242.949
Sorting		1.936	2.022	0.239	12.363	1.299	2.225
Skewness	γ_1	0.657	0.737	0.153	23.275	0.319	0.788
Kurtosis	g_1	1.610	1.138	1.003	62.279	0.944	5.179
Sodium	%	1.698	1.770	0.360	21.226	0.820	2.190
Magnesium	%	0.287	0.265	0.087	30.314	0.164	0.527
Aluminium	%	0.296	0.231	0.175	59.238	0.112	0.834
Phosphorus	%	0.030	0.019	0.026	86.192	0.008	0.088
Sulphur	%	0.036	0.000	0.066	182.889	0.000	0.193
Chlorine	%	0.030	0.018	0.026	86.002	0.008	0.121
Potassium	%	0.531	0.570	0.089	16.808	0.265	0.612
Calcium	%	0.496	0.301	0.387	78.005	0.124	1.458
Manganese	%	0.020	0.020	0.006	32.537	0.010	0.035
Iron	%	0.885	0.845	0.171	19.274	0.637	1.317
χ_{LF}	$10^{-7}m^3kg^{-1}$	1.700	0.856	1.989	117.015	0.407	9.931
χ_{FD}	%	1.444	1.368	0.993	68.760	0.001	3.306
χ_{ARM}	$10^{-7}m^3kg^{-1}$	0.044	0.025	0.050	113.859	0.014	0.265
SIRM	$10^{-5}Am^2kg^{-1}$	208.163	104.312	256.783	123.357	53.328	1395.602
$Soft_{IRM20mT}$	$10^{-5}Am^2kg^{-1}$	25.330	14.336	29.168	115.150	7.453	158.687
$Soft_{IRM40mT}$	$10^{-5}Am^2kg^{-1}$	72.987	37.998	83.500	114.403	18.914	439.810
$Hard_{IRM300mT}$	$10^{-5}Am^2kg^{-1}$	13.310	6.346	16.003	120.234	0.923	77.311
$Hard_{IRM500mT}$	$10^{-5}Am^2kg^{-1}$	7.461	3.162	11.270	151.042	0.385	55.427
$Soft_{\%20mT}$	%	13.408	13.491	2.283	17.024	8.523	20.014
$Soft_{\%40mT}$	%	36.927	37.383	2.802	7.588	30.316	43.875
$Hard_{\%300mT}$	%	7.078	6.811	3.967	56.054	0.662	17.188
$Hard_{\%500mT}$	%	3.432	2.635	2.455	71.529	0.444	8.653
S-ratio	(none)	-0.610	-0.608	0.043	-7.036	-0.702	-0.501
ARM/χ	$10^{-2}Am^{-1}$	0.029	0.029	0.005	18.281	0.014	0.039
SIRM/ARM	(None)	137.827	134.145	28.115	20.399	101.656	264.127
χ_{ARM}/SIRM	$10^{-5}Am^2kg^{-1}$	2.351	2.341	0.379	16.138	1.189	3.090
SIRM/χ	$10^{-2}Am^{-1}$	121.489	121.547	9.919	8.165	101.117	145.561

Table 4.12b Summary data* for coniferous plantation organo-mineral soil (refer to Section 5.2) characteristics (n = 42)

Parameters	Units	Mean	Median	SD	CV	Min	Max
pH	mol/ltr	4.803	4.515	0.731	15.229	3.730	6.660
SOM	%	16.345	2.653	22.971	140.538	0.335	80.696
Sand	%	71.394	70.880	4.372	6.123	65.973	91.893
Silt	%	25.444	25.756	4.355	17.117	3.822	30.397
Clay	%	3.162	3.226	1.507	47.661	0.929	5.159
Mean particle size	µm	176.955	174.015	18.249	10.313	156.237	258.027
Median particle size	µm	182.530	192.152	25.519	13.980	129.187	242.949
Sorting		1.918	1.992	0.263	13.695	1.299	2.225
Skewness	γ_1	0.634	0.722	0.162	25.534	0.319	0.788
Kurtosis	g_1	1.228	1.118	0.670	54.560	0.944	5.179
Sodium	%	1.671	1.770	0.391	23.425	0.820	2.190
Magnesium	%	0.286	0.253	0.094	33.075	0.164	0.527
Aluminium	%	0.330	0.253	0.178	54.002	0.112	0.834
Phosphorus	%	0.035	0.021	0.026	76.474	0.008	0.088
Sulphur	%	0.044	0.000	0.070	158.659	0.000	0.193
Chlorine	%	0.034	0.021	0.028	80.427	0.008	0.121
Potassium	%	0.523	0.571	0.097	18.557	0.265	0.612
Calcium	%	0.433	0.230	0.401	92.779	0.124	1.458
Manganese	%	0.021	0.021	0.007	33.748	0.010	0.035
Iron	%	0.918	0.861	0.173	18.810	0.637	1.317
χ_{LF}	$10^{-7}m^3kg^{-1}$	1.974	0.904	2.127	107.730	0.407	9.931
χ_{FD}	%	1.427	1.404	0.934	65.416	0.001	3.306
χ_{ARM}	$10^{-7}m^3kg^{-1}$	0.051	0.028	0.054	106.191	0.014	0.265
SIRM	$10^{-5}Am^2kg^{-1}$	242.360	116.600	275.271	113.579	56.669	1395.602
$Soft_{IRM20mT}$	$10^{-5}Am^2kg^{-1}$	29.040	15.365	31.375	108.041	7.599	158.687
$Soft_{IRM40mT}$	$10^{-5}Am^2kg^{-1}$	84.605	43.625	89.169	105.395	19.410	439.810
$Hard_{IRM300mT}$	$10^{-5}Am^2kg^{-1}$	15.394	7.175	17.152	111.419	0.923	77.311
$Hard_{IRM500mT}$	$10^{-5}Am^2kg^{-1}$	8.777	3.991	12.175	138.708	0.422	55.427
$Soft_{\%20mT}$	%	12.984	12.782	2.083	16.040	8.523	17.794
$Soft_{\%40mT}$	%	36.798	37.061	3.019	8.204	30.316	43.875
$Hard_{\%300mT}$	%	7.026	6.247	3.983	56.693	0.662	17.188
$Hard_{\%500mT}$	%	3.517	2.635	2.481	70.550	0.444	8.653
S-ratio	(none)	-0.607	-0.607	0.045	-7.433	-0.702	-0.501
ARM/χ	$10^{-2}Am^{-1}$	0.028	0.028	0.005	19.308	0.014	0.039
SIRM/ARM	(None)	140.967	135.629	29.763	21.114	108.507	264.127
χ_{ARM}/SIRM	$10^{-5}Am^2kg^{-1}$	2.304	2.316	0.385	16.705	1.189	2.894
SIRM/χ	$10^{-2}Am^{-1}$	122.451	122.746	10.445	8.530	101.117	145.561

*Mean; SD = standard deviation; CV = percentage coefficient of variation; Min = minimum value; Max = maximum value. Values are shown to 3 decimal places for consistency, not accuracy.

Figure 4.26 represents the sand-pararendzina (Avery, 1980), overlying the micropodzol of James (1993). The dark greyish brown (10YR 3/2) H layer (0-3 cm) contained 19.2% SOM, which overlaid a thin (3-5 cm) buried pine-needle litter layer (bL) where SOM increased to 26.6 and pH decreased to 4.3. A dark greyish brown (10YR 4/2) B horizon (5-12 cm) was evident, with very low SOM (1.3%). The underlying Cu horizon retained sedimentary characteristics.

Figures 4.27 and 4.28 identify soil formation above 12 cm, evident by decreased pH and increased silt. Peak values of P (0.09%) and Cl (0.20%) occurred in the H layer, with clay showing lowest values (0.11%). Peaks in SOM (34.19%) and S (0.14%), with lowest values of pH (4.20) and K (0.43%), were observed in the bL layer, associated with peaks in magnetic concentration parameters (χ_{LF} 3.77 $x10^{-7}m^3kg^{-1}$; χ_{ARM} 0.11 $x10^{-7}m^3kg^{-1}$; SIRM 550.25 $x10^{-5}Am^2kg^{-1}$) and magnetic minerals ($Soft_{IRM20mT}$ 52.72 $x10^{-5}Am^2kg^{-1}$; $Soft_{IRM40mT}$ 198.14 $x10^{-5}Am^2kg^{-1}$; $Hard_{IRM300mT}$ 57.03 $x10^{-5}Am^2kg^{-1}$; $Hard_{IRM500mT}$ 48.25 $x10^{-5}Am^2kg^{-1}$). The highest value of Mn (0.03%) occurred in the bB horizon alongside the lowest Ca (0.13%), associated with high numbers of superparamagnetic or multidomain magnetic grain sizes (ARM/χ 0.05 $x10^{-2}Am^{-1}$).

Tables 4.13a,b show the organo-mineral soil component had dissimilar physico-chemical values (e.g. pH 5.14; SOM 10.16%; Sand 70.74%; Silt 26.51%; Clay 2.75%) compared to the entire profile (pH 7.35; SOM 1.89%; Sand 82.45%; Silt 13.49%; Clay 4.06%). Increased Al (0.26%), P (0.04%), S (0.04%) and Cl (0.04%) occurred in the organo-mineral soil component, alongside decreased Ca (0.41%). Magnetic concentration parameter increases (χ_{LF} 1.86 $x10^{-7}m^3kg^{-1}$; SIRM 272.70 $x10^{-5}Am^2kg^{-1}$) were associated with increased ferrimagnetic magnetic minerals ($Soft_{IRM20mT}$ 27.56 $x10^{-5}Am^2kg^{-1}$; $Soft_{IRM40mT}$ 104.85 $x10^{-5}Am^2kg^{-1}$; $Hard_{IRM300mT}$ 25.65$x10^{-5}Am^2kg^{-1}$; $Hard_{IRM500mT}$ 17.20 $x10^{-5}Am^2kg^{-1}$). A decrease in the SIRM/ARM ratio (135.15) indicates increased stable single domain grains in the organo-mineral soil component.

4.3 Distinguishing soil profiles using pedo-characteristics

Table 4.14 compares the medians of each of the organo-mineral soil component of the soil profile populations for each parameter; while, Figure 4.29 presents population distributions for selected parameters. To distinguish the soil profiles, both null (H_0) and alternative (H_1) hypotheses were tested. Non-parametric Mann-Whitney U tests were used to compare the differences of these medians.

Tested Hypotheses	
Null Hypothesis (H_0)	There was no significant difference between the medians of each of the sample populations compared to each other.
Alternative Hypothesis (H_1)	There was a significant difference between the medians of each of the sample populations compared to each other.

Clear-felled soil profile description

Profile ID: CF
Date of survey: 10/10/2007

Site description

Location: 1125 m NWW of seaward end of Fisherman's Path, Northern end of Long Slack.
Grid reference: SD 28868 10456
Landform: Top of dune mound.
Land use: Managed grazing.
Weather: Overcast; heavy rain previous day; ~15°C.

Soil description

Drainage: Well-drained.
Surface cover: Bryophytes, sand sedge; tree stumps.
Profile depth: 81 cm
Soil depth: 1 2 cm
NSRI Major group: Lithomorphic soil


a) Photograph facing east


b) Soil profile

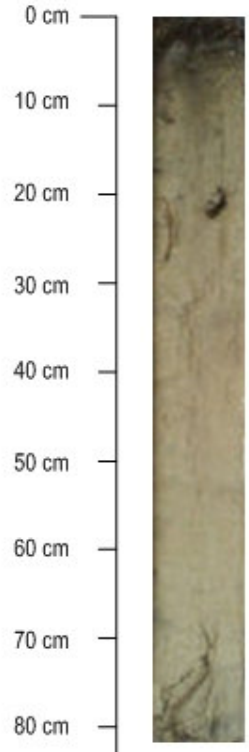

Layer/ Horizon	Depth (cm)	Field description
H	0-3	Dark greyish brown (10YR 3/2) moist and dark greyish brown (10YR 4/2) dry; abrupt boundary to:
bL	3-5	Very dark greyish brown (10YR 3/2) moist and dark greyish brown (10YR 4/2) dry; abrupt boundary to:
bB	5-12	Dark greyish brown (10YR 4/2) moist and greyish brown (10YR 5/2) dry; loose sand; stoneless; abundant fine (1-2 mm) fibrous roots; few medium (2-5 mm) woody roots; unclear boundary to:
bCu1	12-72	Brown (10YR 5/3) moist and brown (10 YR 5/3) dry; loose sand; stoneless; one large root (20 mm); few medium (2-5 mm) roots; unclear boundary to:
bCu2	72-81	Brown (10YR 5/3) moist and brown (10 YR 5/3) dry; loose sand; stoneless; few medium (2-5 mm) roots.

Layer/Horizon		H	bL	bB	Cu
Sand	600-2000 µm %	70	67	72	85
Silt	2-60 µm %	29	31	24	11
Clay	<2 µm %	1	2	4	4
SOM %		19.2	26.6	1.3	0.4
pH in water (1:2.5)		5.2	4.3	5.4	7.7

Figure 4.26 Soil profile description for clear-felled community. Scale on Plate b) is 15 cm.

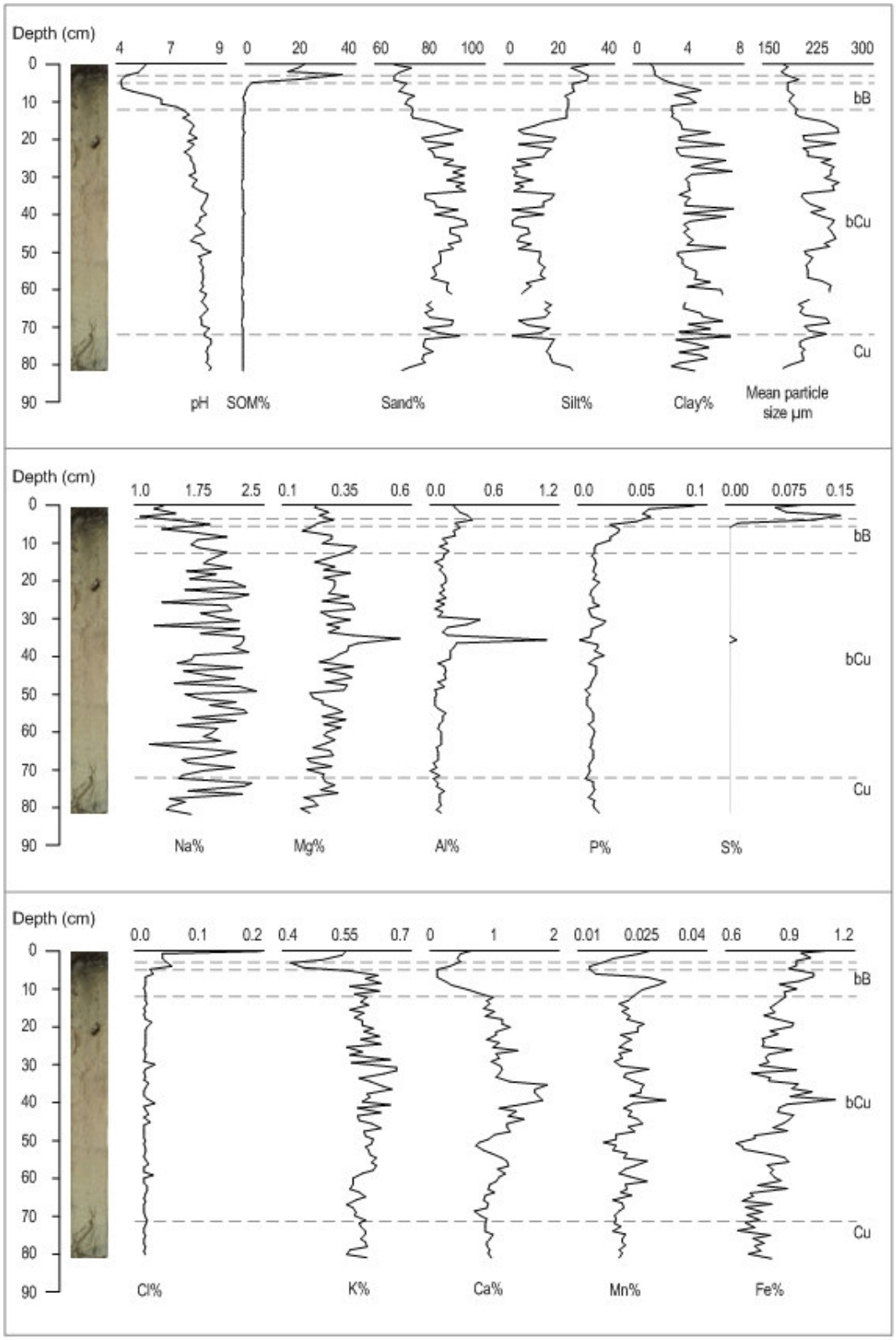

Figure 4.27 Down-profile changes in felled coniferous soil characteristics; pH, SOM, texture and geochemical properties (dashed lines show horizon boundaries).

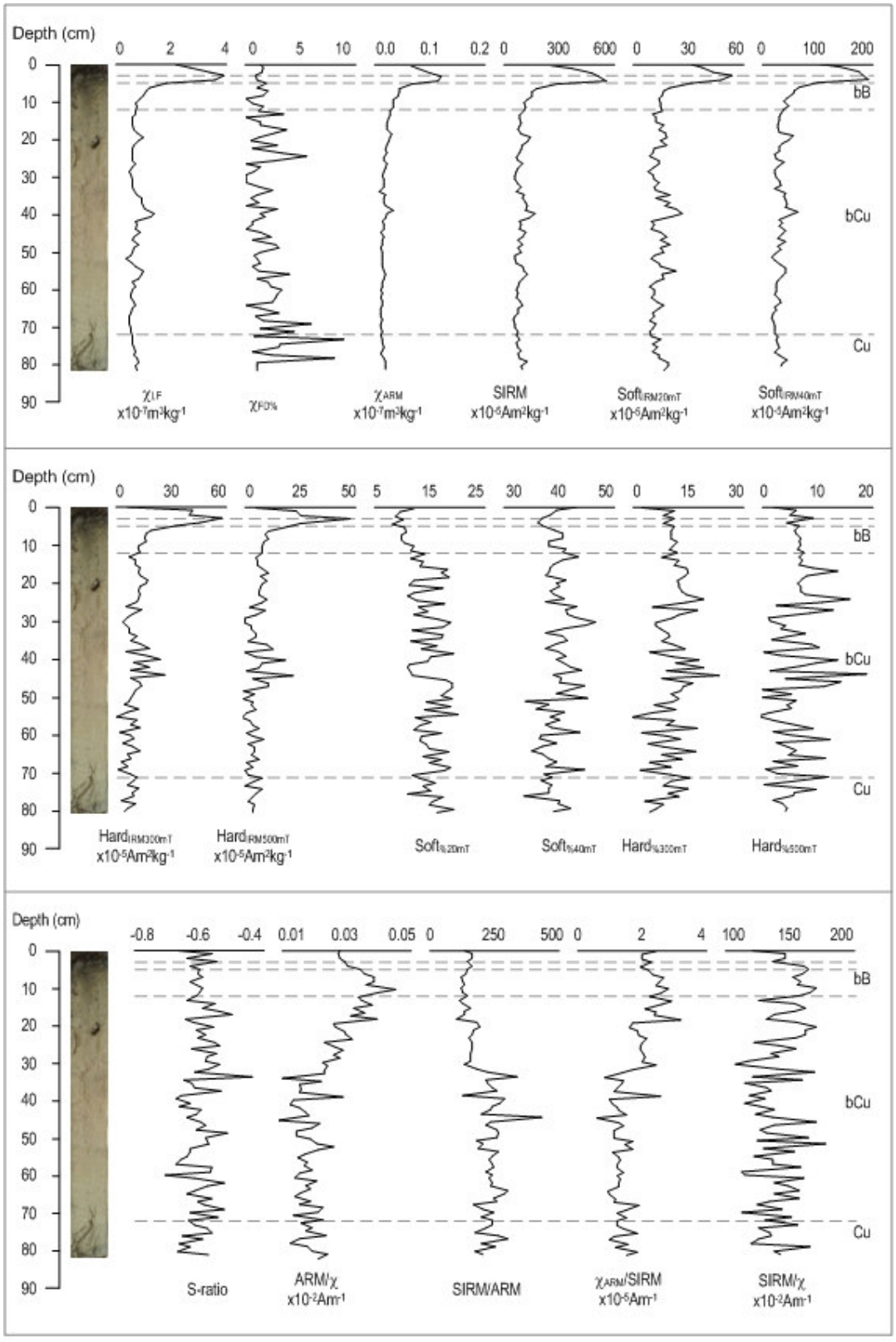

Figure 4.28 Down-profile changes in felled coniferous soil mineral magnetic characteristics (dashed lines show horizon boundaries).

Table 4.13a Summary data* for felled coniferous plantation profile characteristics (n = 81)

Parameters	Units	Mean	Median	SD	CV	Min	Max
pH	mol/ltr	7.352	7.750	1.025	13.942	4.180	8.270
SOM	%	1.885	0.451	5.485	290.933	0.205	34.185
Sand	%	82.451	82.521	7.496	9.092	67.262	100.000
Silt	%	13.488	13.740	8.178	60.631	0.000	31.342
Clay	%	4.062	3.844	1.440	35.443	0.000	7.354
Mean particle size	µm	217.876	212.698	22.140	10.162	176.666	254.927
Median particle size	µm	225.124	223.580	18.650	8.284	155.273	250.759
Sorting		1.582	1.585	0.264	16.703	1.049	2.269
Skewness	γ_1	0.594	0.687	0.140	23.619	0.386	0.766
Kurtosis	g_1	3.521	3.726	1.592	45.203	0.638	6.226
Sodium	%	1.872	1.840	0.340	18.162	1.090	2.450
Magnesium	%	0.286	0.278	0.066	23.140	0.166	0.570
Aluminium	%	0.170	0.138	0.135	79.381	0.030	1.114
Phosphorus	%	0.015	0.012	0.014	89.507	0.000	0.095
Sulphur	%	0.006	0.000	0.023	375.478	0.000	0.136
Chlorine	%	0.016	0.011	0.024	155.394	0.009	0.223
Potassium	%	0.593	0.594	0.039	6.596	0.426	0.671
Calcium	%	0.997	0.984	0.342	34.329	0.135	1.860
Manganese	%	0.021	0.021	0.003	16.001	0.012	0.031
Iron	%	0.826	0.814	0.101	12.291	0.636	1.116
χ_{LF}	$10^{-7}m^3kg^{-1}$	0.820	0.644	0.631	76.958	0.356	3.773
χ_{FD}	%	1.804	1.290	1.677	92.940	0.001	9.091
χ_{ARM}	$10^{-7}m^3kg^{-1}$	0.021	0.014	0.021	99.805	0.006	0.115
SIRM	$10^{-5}Am^2kg^{-1}$	114.878	89.874	92.005	80.089	52.866	550.253
$Soft_{IRM20mT}$	$10^{-5}Am^2kg^{-1}$	15.451	13.722	8.160	52.809	7.798	52.719
$Soft_{IRM40mT}$	$10^{-5}Am^2kg^{-1}$	45.134	35.058	34.320	76.042	20.832	198.139
$Hard_{IRM300mT}$	$10^{-5}Am^2kg^{-1}$	11.749	9.931	9.478	80.672	0.001	57.029
$Hard_{IRM500mT}$	$10^{-5}Am^2kg^{-1}$	7.393	5.760	7.220	97.664	0.001	48.248
$Soft_{\%20mT}$	%	14.673	14.423	3.089	21.054	8.477	20.519
$Soft_{\%40mT}$	%	39.655	39.513	2.716	6.849	33.342	47.074
$Hard_{\%300mT}$	%	10.486	10.654	4.203	40.086	0.001	22.835
$Hard_{\%500mT}$	%	6.463	6.347	3.997	61.837	0.001	19.408
S-ratio	(none)	-0.605	-0.611	0.048	-7.977	-0.717	-0.434
ARM/χ	$10^{-2}Am^{-1}$	0.024	0.023	0.008	34.061	0.010	0.047
SIRM/ARM	(None)	198.712	198.157	60.209	30.300	99.577	435.024
χ_{ARM}/SIRM	$10^{-5}Am^2kg^{-1}$	1.727	1.585	0.522	30.228	0.722	3.154
SIRM/χ	$10^{-2}Am^{-1}$	139.616	135.822	16.942	12.135	105.440	175.395

Table 4.13b Summary data* for felled coniferous plantation organo-mineral soil (refer to Section 5.2) characteristics (n = 12)

Parameters	Units	Mean	Median	SD	CV	Min	Max
pH	mol/ltr	5.135	5.075	0.826	16.086	4.180	6.730
SOM	%	10.162	3.018	11.440	112.583	0.685	34.185
Sand	%	70.741	71.044	2.608	3.687	67.262	74.710
Silt	%	26.509	25.476	3.252	12.269	22.315	31.342
Clay	%	2.749	2.632	1.304	47.418	1.108	4.862
Mean particle size	µm	187.070	185.602	6.490	3.469	176.666	200.956
Median particle size	µm	195.066	207.809	21.017	10.774	155.273	216.225
Sorting		1.881	1.811	0.193	10.261	1.563	2.269
Skewness	γ_1	0.648	0.716	0.125	19.334	0.430	0.766
Kurtosis	g_1	1.010	1.011	0.086	8.540	0.907	1.131
Sodium	%	1.590	1.650	0.290	18.214	1.090	2.100
Magnesium	%	0.259	0.247	0.058	22.252	0.172	0.393
Aluminium	%	0.260	0.260	0.086	33.254	0.119	0.418
Phosphorus	%	0.040	0.032	0.023	58.054	0.013	0.095
Sulphur	%	0.040	0.006	0.050	126.882	0.000	0.136
Chlorine	%	0.040	0.021	0.059	146.540	0.010	0.223
Potassium	%	0.555	0.560	0.068	12.159	0.426	0.635
Calcium	%	0.412	0.417	0.216	52.313	0.135	0.769
Manganese	%	0.021	0.024	0.007	31.173	0.012	0.031
Iron	%	0.953	0.940	0.074	7.737	0.845	1.115
χ_{LF}	$10^{-7}m^3kg^{-1}$	1.858	1.454	1.157	62.272	0.657	3.773
χ_{FD}	%	1.229	1.370	0.570	46.347	0.001	2.000
χ_{ARM}	$10^{-7}m^3kg^{-1}$	0.061	0.051	0.031	51.349	0.031	0.115
SIRM	$10^{-5}Am^2kg^{-1}$	272.702	213.494	162.919	59.742	110.611	550.253
$Soft_{IRM20mT}$	$10^{-5}Am^2kg^{-1}$	27.563	24.867	14.354	52.079	13.748	52.719
$Soft_{IRM40mT}$	$10^{-5}Am^2kg^{-1}$	104.848	87.723	58.873	56.151	42.032	198.139
$Hard_{IRM300mT}$	$10^{-5}Am^2kg^{-1}$	25.646	17.264	16.283	63.491	6.179	57.029
$Hard_{IRM500mT}$	$10^{-5}Am^2kg^{-1}$	17.202	10.978	12.264	71.292	5.661	48.248
$Soft_{\%20mT}$	%	10.547	10.544	1.184	11.228	8.477	12.454
$Soft_{\%40mT}$	%	39.085	38.759	2.206	5.645	36.009	43.519
$Hard_{\%300mT}$	%	9.642	10.428	2.528	26.217	2.487	12.027
$Hard_{\%500mT}$	%	6.386	6.611	1.745	27.332	2.279	9.523
S-ratio	(none)	-0.613	-0.610	0.034	-5.523	-0.678	-0.553
ARM/χ	$10^{-2}Am^{-1}$	0.036	0.036	0.006	16.346	0.029	0.047
SIRM/ARM	(None)	135.152	131.877	15.317	11.333	113.506	157.783
χ_{ARM}/SIRM	$10^{-5}Am^2kg^{-1}$	2.351	2.382	0.261	11.096	1.991	2.767
SIRM/χ	$10^{-2}Am^{-1}$	150.735	154.472	13.650	9.056	119.637	168.386

**Mean; SD = standard deviation; CV = percentage coefficient of variation; Min = minimum value; Max = maximum value. Values are shown to 3 decimal places for consistency, not accuracy.*

Table 4.14 Median values for each parameter within each dune organo-mineral soil (refer to Section 5.2)

Parameters	Units	Mobile dune	Fixed dune	Heath	Slack	Pasture	Scrub	Deciduous wood	Coniferous	Felled area
pH	mol/ltr	7.140	6.855	4.225	7.915	6.680	6.640	4.010	4.515	5.075
SOM	%	4.517	1.304	1.369	0.468	1.127	3.428	3.349	2.653	3.018
Sand	%	72.737	72.405	86.510	86.223	74.614	73.200	75.581	70.880	71.044
Silt	%	25.287	24.846	12.637	7.603	22.770	24.761	21.995	25.756	25.476
Clay	%	1.976	2.538	0.840	6.096	3.331	2.211	2.079	3.226	2.632
Mean particle size	µm	190.522	191.069	227.226	242.271	196.328	174.044	211.564	174.015	185.602
Median particle size	µm	200.817	210.023	229.936	247.562	212.921	185.430	216.335	192.152	207.809
Sorting		1.648	1.853	1.090	1.553	1.979	1.712	1.827	1.992	1.811
Skewness	γ_1	0.625	0.710	0.490	0.477	0.705	0.673	0.666	0.722	0.716
Kurtosis	g_1	0.930	0.991	2.593	5.008	1.161	1.078	1.446	1.118	1.011
Sodium	%	1.260	1.640	1.765	1.300	1.495	1.740	1.370	1.770	1.650
Magnesium	%	0.213	0.265	0.213	0.201	0.214	0.379	0.192	0.253	0.247
Aluminium	%	0.097	0.130	0.309	0.022	0.128	0.240	0.291	0.253	0.260
Phosphorus	%	0.042	0.023	0.033	0.017	0.030	0.038	0.024	0.021	0.032
Sulphur	%	0.019	0.002	0.000	0.001	0.000	0.001	0.017	0.000	0.006
Chlorine	%	0.045	0.014	0.011	0.016	0.011	0.013	0.021	0.021	0.021
Potassium	%	0.439	0.568	0.552	0.453	0.577	0.503	0.525	0.571	0.560
Calcium	%	0.821	0.461	0.087	1.252	0.508	1.469	0.119	0.230	0.417
Manganese	%	0.019	0.023	0.011	0.022	0.020	0.034	0.012	0.021	0.024
Iron	%	0.941	0.823	0.831	0.843	0.826	1.342	0.916	0.861	0.940
χ_{LF}	$10^{-7}m^3kg^{-1}$	1.174	1.255	0.720	0.427	1.058	4.051	0.929	0.904	1.454
χ_{FD}	%	0.833	1.635	2.305	1.890	2.105	0.195	1.449	1.404	1.370
χ_{ARM}	$10^{-7}m^3kg^{-1}$	0.017	0.022	0.022	0.013	0.039	0.041	0.018	0.028	0.051
SIRM	$10^{-5}Am^2kg^{-1}$	136.034	174.004	86.829	47.795	146.648	497.483	121.515	116.600	213.494
$Soft_{IRM20mT}$	$10^{-5}Am^2kg^{-1}$	20.158	19.761	11.732	9.063	20.289	59.020	21.919	15.365	24.867
$Soft_{IRM40mT}$	$10^{-5}Am^2kg^{-1}$	56.486	64.392	29.797	22.878	52.291	189.726	46.929	43.625	87.723
$Hard_{IRM300mT}$	$10^{-5}Am^2kg^{-1}$	9.867	13.034	15.280	3.566	14.920	49.880	13.314	7.175	17.264
$Hard_{IRM500mT}$	$10^{-5}Am^2kg^{-1}$	4.666	5.875	9.397	2.435	5.503	33.305	11.492	3.991	10.978
$Soft_{\%20mT}$	%	20.104	11.589	13.255	18.363	14.873	11.491	22.572	12.782	10.544
$Soft_{\%40mT}$	%	41.462	36.864	34.333	44.105	35.449	37.667	37.470	37.061	38.759
$Hard_{\%300mT}$	%	7.253	8.047	14.852	6.888	10.159	11.100	10.058	6.247	10.428
$Hard_{\%500mT}$	%	4.613	3.984	8.345	5.312	3.435	6.489	5.589	2.635	6.611
S-ratio	(none)	-0.648	-0.625	-0.458	-0.621	-0.684	-0.635	-0.588	-0.607	-0.610
ARM/χ	$10^{-2}Am^{-1}$	0.014	0.017	0.030	0.033	0.031	0.012	0.022	0.028	0.036
SIRM/ARM	(None)	251.592	260.966	130.355	111.731	129.242	321.773	166.137	135.629	131.877
χ_{ARM}/SIRM	$10^{-5}Am^2kg^{-1}$	1.248	1.206	2.409	2.811	2.431	0.976	1.890	2.316	2.382
$SIRM/\chi$	$10^{-2}Am^{-1}$	116.028	144.696	122.727	118.931	120.978	122.237	121.894	122.746	154.472

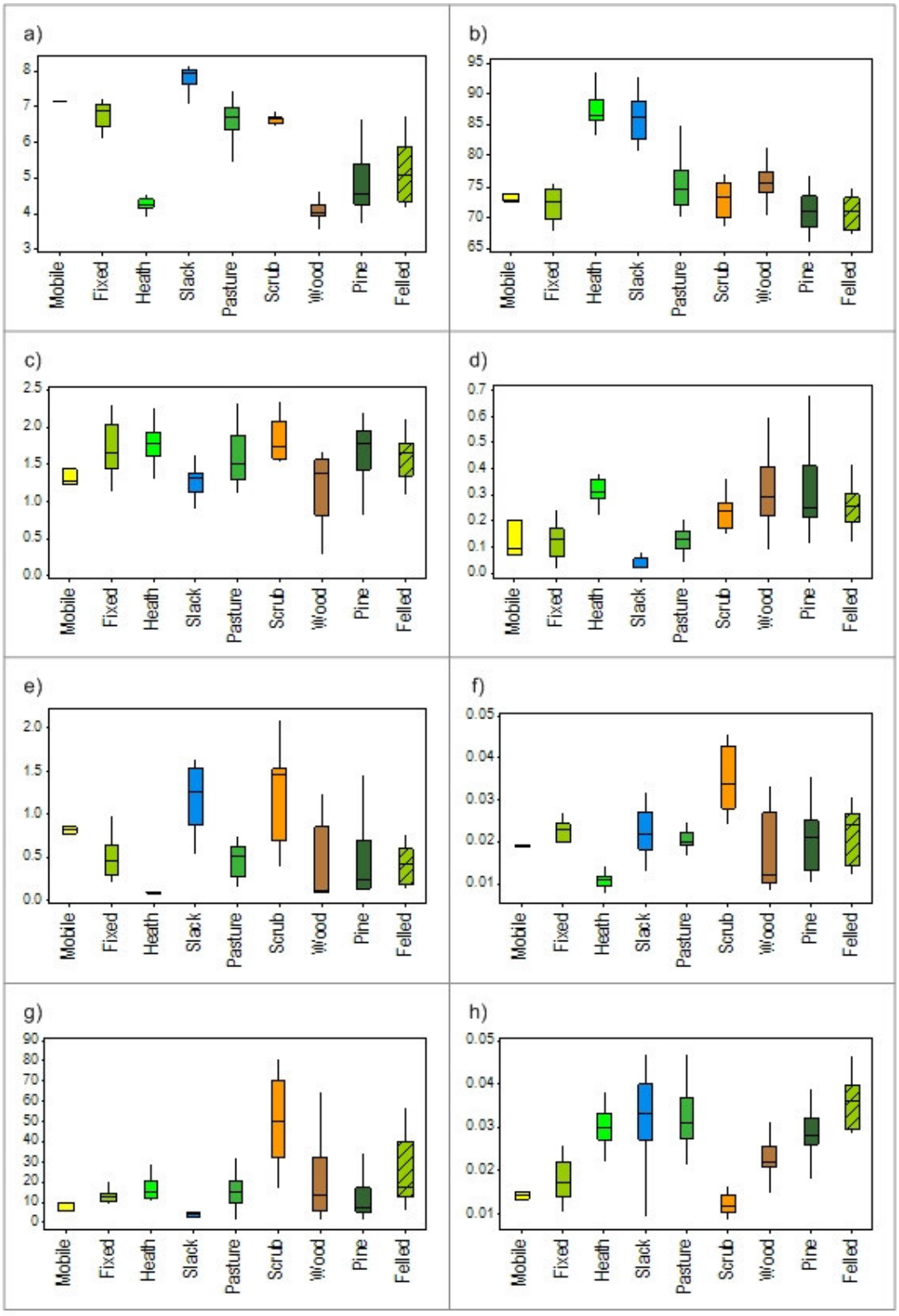

Figure 4.29 Box plots of soil profile sample population distributions for selected parameters: a) pH; b) Sand%; c) Na%; d) Al%; e) Ca%; f) Mn; g) $Hard_{IRM300mT}$ $x10^{-5}Am^2kg^{-1}$ and h) ARM/χ $x10^{-2}Am^{-1}$.

Results of non-parametric Kruskal-Wallis tests (data not presented) show no differences between more than two of the dune environment organo-mineral soil component sample populations for each parameter, independent of each other.

4.3.1 Distinguishing soil profiles using pH

Organo-mineral soils from all of the dune environments are significantly different from each other (p <0.05) (Figure 4.29a). The pH values for the organo-mineral soil component of the mobile dune terrestrial raw sand (pH 7.14) were significantly different (p <0.05) than all other dune environments, with the highest significant differences (p <0.01) occurring with the micro-podzols of both the heath (pH 4.23) and coniferous plantation (pH 4.52), along with the deciduous woodland brown earth (pH 4.01) (Table 4.15a). The fixed dune (pH 6.86), pasture (pH 6.68) and scrub (pH 6.64) organo-mineral soils were significantly different (p <0.05) from all dune environments, suggesting pH can be used to classify these soils as sand-pararednzinas. The pH of the slack groundwater gley (pH 7.92) was significantly different (p <0.05) from all environments; as was the deciduous woodland brown earth (p <0.01), highlighting both of these profiles as having isolated pH characteristics. The heath micro-podzol pH was also highly significantly different (p <0.01) from all dune environments; whereas, the coniferous plantation micro-podzol displayed similar values to the felled dune environment (pH 5.08), suggesting this profile can not be classified as either a micro-podzol or a sand-pararendzina using pH characteristics.

4.3.2 Distinguishing soil profiles using SOM

The SOM values for the organo-mineral soil component of the mobile dune terrestrial raw sand (4.52%) were similar to most dune environments, with the exception of the slack groundwater gley (0.47%; p <0.05) (Table 4.15b). The fixed dune (1.30%) and pasture (1.13%) sand-pararendzinas cannot be isolated from the remaining dune environments using SOM characteristics; whereas, the slack groundwater gley was significantly different (p <0.05) from all environments, highlighting this profile as having separate SOM characteristics. Organo-mineral soils associated with scrub (3.43%), deciduous woodland (3.35%) and coniferous plantation (2.65%) environments, all displayed similar SOM values to each other and were significantly different (p <0.05) from all other dune environments, suggesting SOM is a function of vegetation cover in these environments, rather than soil-mineralogy.

4.3.3 Distinguishing soil profiles using textural characteristics

Sand (Table 4.15c), silt (Table 4.15d) and clay (Table 4.15e) showed highly significant differences (p <0.01) between the heath organo-mineral soil (86.51%, 12.64%, 0.84%, respectively) and most dune environments, with the exception of similar values of sand with the slack groundwater gley (86.22%) (Figure 4.29b). The groundwater gley displayed its own significant differences in sand (p <0.05), silt (7.60%) and clay (6.10%; p <0.01) from all other environments. This, alongside significant differences (p <0.05) in sand between the coniferous plantation organo-mineral soil (70.88%) and most remaining dune environments, suggests

Table 4.15 Mann-Whitney U test results for soil parameters. Tables show '*p*' values (**bold** text is significant (**p* <0.05; ***p* <0.01; ****p* <0.001)) for; a) pH; b) SOM%; c) Sand%; d) Silt%; e) Clay% and f) Mean particle size (µm)

a)	Mobile	Fixed	Heath	Slack	Pasture	Scrub	Wood	Pine
Fixed	**0.039***							
Heath	**0.005****	**<0.001*****						
Slack	**0.014***	**<0.001*****	**<0.001*****					
Pasture	**0.049***	0.283	**<0.001*****	**<0.001*****				
Scrub	**0.011***	0.262	**<0.001*****	**<0.001*****	0.851			
Wood	**0.006****	**<0.001*****	**0.004****	**<0.001*****	**<0.001*****	**<0.001*****		
Pine	**0.005****	**<0.001*****	**<0.001*****	**<0.001*****	**<0.001*****	**<0.001*****	**<0.001*****	
Felled	**0.012***	**<0.001*****	**<0.001*****	**<0.001*****	**<0.001*****	**<0.001*****	**<0.001*****	0.228

b)	Mobile	Fixed	Heath	Slack	Pasture	Scrub	Wood	Pine
Fixed	0.063							
Heath	0.125	0.725						
Slack	**0.041***	**0.003****	**<0.001*****					
Pasture	0.143	0.828	0.379	**0.003****				
Scrub	0.501	**0.009****	**0.021***	**<0.001*****	**0.018***			
Wood	1.000	**0.020***	**0.015***	**<0.001*****	**0.006****	0.691		
Pine	0.802	**0.001****	**0.002****	**<0.001*****	**0.001****	0.929	0.785	
Felled	0.943	0.103	0.186	**0.001****	0.054	0.978	0.471	0.388

c)	Mobile	Fixed	Heath	Slack	Pasture	Scrub	Wood	Pine
Fixed	0.651							
Heath	**0.005****	**<0.001*****						
Slack	**0.049***	**<0.001*****	0.208					
Pasture	0.337	**0.038***	**<0.001*****	**0.001****				
Scrub	0.788	0.412	**<0.001*****	**<0.001*****	0.146			
Wood	0.088	**0.002****	**<0.001*****	**<0.001*****	0.453	**0.019***		
Pine	0.211	0.144	**<0.001*****	**<0.001*****	**<0.001*****	**0.049***	**<0.001*****	
Felled	0.130	0.133	**<0.001*****	**0.001****	**0.002****	0.068	**<0.001*****	0.827

d)	Mobile	Fixed	Heath	Slack	Pasture	Scrub	Wood	Pine
Fixed	0.880							
Heath	**0.005****	**<0.001*****						
Slack	**0.049***	**<0.001*****	**0.003****					
Pasture	**0.029***	**0.007****	**<0.001*****	**0.001****				
Scrub	0.893	0.535	**<0.001*****	**<0.001*****	**0.026***			
Wood	0.088	**0.004****	**<0.001*****	**<0.001*****	0.643	**0.015***		
Pine	0.539	0.379	**<0.001*****	**<0.001*****	**<0.001*****	0.223	**<0.001*****	
Felled	0.718	0.849	**<0.001*****	**0.001****	**0.008****	0.532	**0.009****	0.417

e)	Mobile	Fixed	Heath	Slack	Pasture	Scrub	Wood	Pine
Fixed	0.097							
Heath	**0.005****	**<0.001*****						
Slack	**0.008****	**<0.001*****	**<0.001*****					
Pasture	**0.029***	**0.007****	**<0.001*****	**0.001****				
Scrub	0.687	0.057	**<0.001*****	**<0.001*****	**<0.001*****			
Wood	0.941	**0.040***	**<0.001*****	**<0.001*****	**<0.001*****	0.415		
Pine	0.351	0.406	**<0.001*****	**<0.001*****	0.151	0.127	0.069	
Felled	0.613	0.916	**<0.001*****	**<0.001*****	0.059	0.644	0.390	0.411

f)	Mobile	Fixed	Heath	Slack	Pasture	Scrub	Wood	Pine
Fixed	0.802							
Heath	**0.005****	**<0.001*****						
Slack	**0.049***	**<0.001*****	**0.002****					
Pasture	0.337	0.099	**<0.001*****	**0.002****				
Scrub	0.060	**<0.001*****	**<0.001*****	**<0.001*****	**<0.001*****			
Wood	**0.018***	**<0.001*****	**<0.001*****	**<0.001*****	0.074	**<0.001*****		
Pine	**0.017***	**<0.001*****	**<0.001*****	**<0.001*****	**<0.001*****	0.714	**<0.001*****	
Felled	0.516	0.112	**<0.001*****	**0.001****	**0.007****	**0.011***	**<0.001*****	**<0.001*****

micro-podzols can be identified using the sand textural parameter. Clay was significantly different (p <0.05) in the pasture organo-mineral soil (3.33%) compared to most dune environments, except for the coniferous plantation (3.23%) and felled organo-mineral (2.63%) soils. Deciduous woodland also showed significant differences (p <0.05) in sand (75.58%) and silt (22.00%) from most dune environments, except for pasture (74.61%) and coniferous plantation organo-mineral soils for sand and, except for mobile dune (25.29%) and pasture organo-mineral soil (22.77%), for silt.

Significant differences in mean particle size exist between the heath (227.23 µm; p <0.01), slack (242.27 µm; p <0.05), scrub (174.04 µm; p <0.01), deciduous woodland (211.56 µm; p <0.05), coniferous plantation (174.02 µm; p <0.05) and felled (185.60 µm; p <0.05) organo-mineral soils (Table 4.15f). This indicates the mean particle size textural variable can be used as a tool in the classification of groundwater gleys, brown earths and micro-podzols on sand dunes.

4.3.4 Distinguishing soil profiles using geochemical properties

Na in the slack groundwater gley (1.30%) was highly significantly different (p <0.01) from most dune environments, with the exception of the mobile dune (1.26%) and deciduous woodland (1.37%) organo-mineral soils (Figure 4.29c; Table 4.16a). Otherwise, Na remained relatively constant throughout the organo-mineral soil component of each of the pedo-environment profiles. Mg in the scrub organo-mineral soil (0.38%) was highly significantly different (p <0.05) with all other environments, indicating Mg can be used to indentify this environment (Table 4.16b). Al (Figure 4.29d; Table 4.16c) and P (Table 4.16d) can be used to identify the groundwater gley (0.02%) from all other profiles (p <0.05). The use of Al was also true for identification of fixed dune and pasture sand-pararendzinas. However, the scrub organo-mineral soil (0.24%) displayed highly significant differences (p <0.001) to both these environments, suggesting this profile was acting differently from the other sand-pararendzinas. S showed limited variability between profiles and, therefore, cannot be used to successfully classify dune environments (Table 4.16e).

Cl in the heath organo-mineral soil was significantly different (p <0.05) from most dune environments, with the exception of the pasture and scrub organo-mineral soils (Table 4.16f). K_2 in the slack groundwater gley was significantly different (p <0.05) from most dune environments, with the exception of the mobile dune organo-mineral soil (Table 4.17a). The scrub organo-mineral soil K was also significantly different (p <0.05) from most dune environments, although values were similar to those of the deciduous woodland organo-mineral soil. Significant differences (p <0.05) in both Ca (Figure 4.29e; Table 4.17b) and Mn (Figure 4.29f; Table 4.17c) were evident for heath, scrub and deciduous woodland organo-mineral soils. Given the well-developed nature of vegetation in these environments, it is suggested the nutrient content was a function of vegetation succession over time, rather than soil-type. The scrub organo-mineral soil was the only soil to display significantly different (p <0.05) values of Fe from any other dune environment (Table 4.17d).

Table 4.16 Mann-Whitney U test results for soil parameters. Tables show '*p*' values (**bold** text is significant (**p* <0.05; ***p* <0.01; ****p* <0.001)) for; a) Na%; b) Mg%; c) Al%; d) P%; e) S% and f) Cl%

a)	Mobile	Fixed	Heath	Slack	Pasture	Scrub	Wood	Pine
Fixed	0.118							
Heath	**0.020***	0.519						
Slack	0.770	**<0.001*****	**<0.001*****					
Pasture	0.242	0.352	0.055	**0.003****				
Scrub	**0.011***	0.324	0.871	**<0.001*****	**0.036***			
Wood	0.941	**0.001****	**<0.001*****	0.647	**0.023***	**<0.001*****		
Pine	0.117	0.993	0.777	**<0.001*****	0.283	0.546	**<0.001*****	
Felled	0.112	0.626	0.078	**0.003****	0.746	0.103	**0.010***	0.275

b)	Mobile	Fixed	Heath	Slack	Pasture	Scrub	Wood	Pine
Fixed	0.240							
Heath	0.977	**0.040***						
Slack	0.587	**0.039***	0.228					
Pasture	1.000	0.114	1.000	0.260				
Scrub	**0.011***	**<0.001*****	**<0.001*****	**<0.001*****	**<0.001*****			
Wood	0.235	0.279	0.115	0.966	0.437	**<0.001*****		
Pine	0.065	0.460	**<0.001*****	**<0.001*****	**0.005****	**0.001****	**0.001***	
Felled	0.130	0.799	**0.018***	**0.017***	0.072	**0.001****	0.054	0.662

c)	Mobile	Fixed	Heath	Slack	Pasture	Scrub	Wood	Pine
Fixed	0.955							
Heath	**0.005****	**<0.001*****						
Slack	**0.014***	**<0.001*****	**<0.001*****					
Pasture	0.770	0.848	**<0.001*****	**<0.001*****				
Scrub	0.060	**<0.001*****	**<0.001*****	**<0.001*****	**<0.001*****			
Wood	**0.021***	**<0.001*****	0.162	**<0.001*****	**<0.001*****	**0.039***		
Pine	**0.009****	**<0.001*****	**0.017***	**<0.001*****	**<0.001*****	0.106	0.746	
Felled	**0.036***	**<0.001*****	**0.010***	**<0.001*****	**<0.001*****	0.328	0.307	0.581

d)	Mobile	Fixed	Heath	Slack	Pasture	Scrub	Wood	Pine
Fixed	0.162							
Heath	0.659	**0.018***						
Slack	**0.017***	**0.049***	**<0.001*****					
Pasture	0.296	**0.040***	0.666	**<0.001*****				
Scrub	0.946	**0.037***	0.851	**<0.001*****	0.528			
Wood	0.656	0.291	0.390	**0.001****	0.647	0.623		
Pine	0.228	0.993	**0.006****	**0.012***	**0.028***	0.064	0.158	
Felled	0.718	0.131	0.948	**0.006****	0.843	0.892	1.000	0.180

e)	Mobile	Fixed	Heath	Slack	Pasture	Scrub	Wood	Pine
Fixed	0.288							
Heath	0.331	0.146						
Slack	**0.049***	0.965	0.355					
Pasture	0.380	0.121	0.840	0.296				
Scrub	0.687	0.443	0.157	0.720	0.189			
Wood	0.941	0.548	0.051	0.212	0.056	0.559		
Pine	0.285	**0.035***	0.707	**0.024***	0.983	0.056	**0.035***	
Felled	0.829	0.516	0.063	0.815	**0.032***	0.849	0.884	**0.038***

f)	Mobile	Fixed	Heath	Slack	Pasture	Scrub	Wood	Pine
Fixed	**0.009****							
Heath	**0.010***	**0.009****						
Slack	**0.022***	0.848	**0.016***					
Pasture	**0.011***	0.069	0.333	0.142				
Scrub	**0.011***	**0.037***	0.573	0.082	0.798			
Wood	0.181	**0.034***	**<0.001*****	**0.027***	**0.001****	**0.001****		
Pine	0.080	**0.001****	**<0.001*****	**0.005****	**<0.001*****	**<0.001*****	0.800	
Felled	0.097	0.318	**0.006****	0.272	**0.035***	0.054	0.390	0.388

Table 4.17 Mann-Whitney U test results for soil parameters. Tables show '*p*' values (**bold** text is significant (**p* <0.05; ***p* <0.01; ****p* <0.001)) for; a) K%; b) Ca%; c) Mn% and d) Fe%

a)	Mobile	Fixed	Heath	Slack	Pasture	Scrub	Wood	Pine
Fixed	**0.009****							
Heath	**0.010***	0.090						
Slack	0.770	**<0.001*****	**<0.001*****					
Pasture	**0.014***	0.281	**0.001****	**<0.001*****				
Scrub	**0.044***	**0.001****	**0.005****	**<0.001*****	**<0.001*****			
Wood	0.334	**0.001****	**0.002****	**0.031***	**<0.001*****	0.976		
Pine	0.195	0.670	0.190	**<0.001*****	0.158	**0.049***	**0.001***	
Felled	0.051	1.000	0.377	**<0.001*****	0.418	**0.047***	0.625	0.625

b)	Mobile	Fixed	Heath	Slack	Pasture	Scrub	Wood	Pine
Fixed	**0.022***							
Heath	**0.005****	**<0.001*****						
Slack	0.072	**<0.001*****	**<0.001*****					
Pasture	**0.007****	0.918	**<0.001*****	**<0.001*****				
Scrub	0.346	**0.001****	**<0.001*****	0.798	**<0.001*****			
Wood	0.158	**0.028***	**<0.001*****	**<0.001*****	**0.019***	**<0.001*****		
Pine	0.072	0.059	**<0.001*****	**<0.001*****	0.065	**<0.001*****	**0.012***	
Felled	**0.012***	0.472	**<0.001*****	**<0.001*****	0.418	**0.001****	0.077	0.423

c)	Mobile	Fixed	Heath	Slack	Pasture	Scrub	Wood	Pine
Fixed	**0.009****							
Heath	**0.005****	**<0.001*****						
Slack	0.358	0.399	**<0.001*****					
Pasture	0.087	**0.039***	**<0.001*****	0.557				
Scrub	**0.011***	**<0.001*****	**<0.001*****	**0.001****	**<0.001*****			
Wood	0.265	**0.009****	**0.007****	**0.004****	**0.007****	**0.005****		
Pine	0.400	0.293	**<0.001*****	0.358	0.794	**<0.001*****	**0.027***	
Felled	0.718	0.982	**<0.001*****	0.815	0.627	**0.001****	0.062	0.460

d)	Mobile	Fixed	Heath	Slack	Pasture	Scrub	Wood	Pine
Fixed	0.065							
Heath	**0.048***	0.939						
Slack	0.195	0.545	0.628					
Pasture	0.087	0.848	0.979	0.681				
Scrub	**0.031***	**<0.001*****	**<0.001*****	**<0.001*****	**<0.001*****			
Wood	0.882	0.080	**0.040***	0.127	0.059	**<0.001*****		
Pine	0.413	0.124	**0.048***	0.255	0.125	**<0.001*****	0.627	
Felled	1.000	**<0.001*****	**<0.001*****	**0.007****	**0.001****	**0.001****	0.685	0.072

4.3.5 Distinguishing soil profiles using mineral magnetics

Levels of both χ_{LF} (0.72 $x10^{-7}m^3kg^{-1}$) (Table 4.18a) and SIRM (86.23 $x10^{-5}Am^2kg^{-1}$) (Table 4.18d) in the heath organo-mineral soil were significantly different (p <0.01; p <0.05; respectively) from most dune environments, except for mobile dune (1.17 $x10^{-7}m^3kg^{-1}$, 136.03 $x10^{-5}Am^2kg^{-1}$ respectively) and deciduous woodland (0.93 $x10^{-7}m^3kg^{-1}$, 121.52 $x10^{-5}Am^2kg^{-1}$ respectively) organo-mineral soils. Whereas, the slack χ_{LF} (0.43 $x10^{-7}m^3kg^{-1}$) and SIRM (47.80 $x10^{-5}Am^2kg^{-1}$) and scrub χ_{LF} (4.05 $x10^{-7}m^3kg^{-1}$) and SIRM (497.48 $x10^{-5}Am^2kg^{-1}$) organo-mineral soils were significantly different (p <0.05) from all dune environments. The scrub organo-mineral soil was the only pedo-environment to display significant differences (p <0.05) in $\chi_{FD\%}$ (0.2%) from the other dune environments (Table 4.18b). The organo-mineral soil associated with the felled environment showed significant differences (p <0.05) in χ_{ARM} (0.05 $x10^{-7}m^3kg^{-1}$) from most dune environments, excluding the scrub (0.04 $x10^{-7}m^3kg^{-1}$) and deciduous woodland (0.02 $x10^{-7}m^3kg^{-1}$) organo-mineral soils (Table 4.18c).

Levels of magnetic minerals represented by $Soft_{IRM20mT}$ (Table 4.18e) in the heath organo-mineral soil (11.73 $x10^{-5}Am^2kg^{-1}$) were significantly different (p <0.01) from most dune environments, except for mobile dune (20.16 $x10^{-5}Am^2kg^{-1}$) and coniferous plantation (15.37 $x10^{-5}Am^2kg^{-1}$) organo-mineral soils. The slack and scrub organo-mineral soils had significantly different (p <0.05) $Soft_{IRM20mT}$, $Soft_{IRM40mT}$ (Table 4.18f) and $Hard_{IRM300mT}$ (Figure 4.29g; Table 4.19a) with all dune environments. $Hard_{IRM500mT}$ in the slack organo-mineral soil (2.44 $x10^{-5}Am^2kg^{-1}$) was significantly different (p <0.05) from most dune environments, except for the mobile dune (4.67 $x10^{-5}Am^2kg^{-1}$) and coniferous (3.99 $x10^{-5}Am^2kg^{-1}$) plantation organo-mineral soils (Table 4.19b). $Hard_{IRM500mT}$ in the felled organo-mineral soil (10.98 $x10^{-5}Am^2kg^{-1}$) was also significantly different (p <0.05) from most dune environments, except for the heath (9.40 $x10^{-5}Am^2kg^{-1}$) and deciduous woodland (5.59 $x10^{-5}Am^2kg^{-1}$) organo-mineral soils. However, the scrub organo-mineral soil showed significant differences (p <0.05) in $Hard_{IRM500mT}$ (6.49 $x10^{-5}Am^2kg^{-1}$) with all dune environments.

$Soft_{\%20mT}$ in the fixed dune organo-mineral soil (11.59%) was significantly different (p <0.05) from most dune environments, except for scrub (11.49%) and coniferous plantation (12.78%) organo-mineral soils (Table 4.19c). The slack groundwater gley (18.36%) was also significantly different (p <0.05) from most dune environments, apart from the mobile dune (20.10%) and deciduous woodland (22.57%) organo-mineral soils; whereas, the deciduous woodland organo-mineral soil showed significant differences (p <0.05) from most dune environments, apart from both the mobile dune and slack organo-mineral soils. However, the felled organo-mineral soil (10.54%) was significantly different (p <0.05) from all other dune environments. $Soft_{\%40mT}$, $Hard_{\%300mT}$ and $Hard_{\%500mT}$ in the heath organo-mineral soil were significantly different (p <0.05) from all other dune environments (Table 4.19d-f, respectively). $Soft_{\%40mT}$ in the slack groundwater gley (44.11%) was also significantly different (p <0.01) from most dune environments, apart from the mobile dune organo-mineral soil (41.46%). The S-ratio in the heath organo-mineral soil (-0.46) was significantly different (p <0.05) from all other dune

Table 4.18 Mann-Whitney U test results for soil parameters. Tables show '*p*' values (**bold** text is significant (**p* <0.05; ***p* <0.01; ****p* <0.001)) for; a) χ_{LF} x$10^{-7}m^3kg^{-1}$; b) $\chi_{FD\%}$; c) χ_{ARM} x$10^{7}m^3kg^{-1}$; d) SIRM x$10^{-5}Am^2kg^{-1}$; e) $Soft_{IRM20mT}$ x$10^{-5}Am^2kg^{-1}$ and f) $Soft_{IRM40mT}$ x$10^{-5}Am^2kg^{-1}$

a)	Mobile	Fixed	Heath	Slack	Pasture	Scrub	Wood	Pine
Fixed	0.960							
Heath	0.332	**0.001****						
Slack	**0.014***	**<0.001*****	**<0.001*****					
Pasture	0.900	0.838	**0.001****	**<0.001*****				
Scrub	**0.022***	**<0.001*****	**0.001****	**<0.001*****	**<0.001*****			
Wood	0.941	0.740	0.618	**0.001****	0.823	**0.005****		
Pine	0.874	0.345	**0.010***	**<0.001*****	0.416	**<0.001*****	0.488	
Felled	0.516	0.320	**0.003****	**<0.001*****	0.227	**0.002****	0.446	0.344

b)	Mobile	Fixed	Heath	Slack	Pasture	Scrub	Wood	Pine
Fixed	0.088							
Heath	0.065	0.400						
Slack	0.181	0.786	0.934					
Pasture	0.094	0.828	0.523	0.814				
Scrub	0.687	**0.003****	**0.003****	**0.006****	**0.007****			
Wood	0.137	0.546	0.196	0.376	0.376	**0.019***		
Pine	0.145	0.203	**0.012***	0.149	0.085	**0.013***	0.521	
Felled	0.149	0.138	**0.017***	0.207	**0.048***	**0.032***	0.372	0.603

c)	Mobile	Fixed	Heath	Slack	Pasture	Scrub	Wood	Pine
Fixed	0.514							
Heath	0.097	0.463						
Slack	0.531	0.052	**<0.001*****					
Pasture	**0.017***	**<0.001*****	**0.002****	**<0.001*****				
Scrub	**0.031***	**<0.001*****	**0.012***	**<0.001*****	0.267			
Wood	0.766	0.649	0.526	0.122	0.400	0.207		
Pine	**0.031***	**0.009****	**0.019***	**<0.001*****	0.309	0.151	0.148	
Felled	**0.012***	**<0.001*****	**<0.001*****	**<0.001*****	**0.050***	0.497	0.095	**0.018***

d)	Mobile	Fixed	Heath	Slack	Pasture	Scrub	Wood	Pine
Fixed	0.097							
Heath	0.141	**<0.001*****						
Slack	**0.017***	**<0.001*****	**<0.001*****					
Pasture	0.427	0.321	**0.002****	**<0.001*****				
Scrub	**0.011***	**<0.001*****	**<0.001*****	**<0.001*****	**<0.001*****			
Wood	1.000	0.614	0.793	**0.001****	0.790	**0.003****		
Pine	0.802	0.092	**0.015***	**<0.001*****	0.567	**<0.001*****	0.472	
Felled	0.097	0.169	**0.001****	**<0.001*****	**0.020***	**0.008****	0.168	0.472

e)	Mobile	Fixed	Heath	Slack	Pasture	Scrub	Wood	Pine
Fixed	0.514							
Heath	0.085	**0.003****						
Slack	**0.014***	**<0.001*****	**0.001****					
Pasture	0.646	0.596	**0.001****	**<0.001*****				
Scrub	**0.022***	**<0.001*****	**<0.001*****	**<0.001*****	**<0.001*****			
Wood	0.941	0.438	**0.001****	**<0.001*****	0.601	**0.021***		
Pine	0.400	0.406	0.051	**<0.001*****	0.211	**<0.001*****	0.148	
Felled	0.943	0.320	**0.009****	**<0.001*****	0.652	**0.001****	0.961	0.293

f)	Mobile	Fixed	Heath	Slack	Pasture	Scrub	Wood	Pine
Fixed	**0.291**							
Heath	0.110	**<0.001*****						
Slack	**0.017***	**<0.001*****	**0.005****					
Pasture	0.834	0.439	**0.001***	**<0.001*****				
Scrub	**0.011***	**<0.001*****	**<0.001*****	**<0.001*****	**<0.001*****			
Wood	0.941	0.580	0.432	**0.004****	0.757	**0.002****		
Pine	0.666	0.116	**0.001****	**<0.001*****	0.558	**<0.001*****	0.521	
Felled	0.130	0.095	**<0.001*****	**<0.001*****	**0.017***	**0.007****	0.108	**0.018***

Table 4.19 Mann-Whitney U test results for soil parameters. Tables show '*p*' values (**bold** text is significant (**p* <0.05; ***p* <0.01; ****p* <0.001)) for; a) $Hard_{IRM300mT}$ $x10^{-5}Am^2kg^{-1}$; b) $Hard_{IRM500mT}$ $x10^{-5}Am^2kg^{-1}$; c) $Soft_{\%20mT}$; d) $Soft_{\%40mT}$; e) $Hard_{\%300mT}$ and f) $Hard_{\%500mT}$

a)	Mobile	Fixed	Heath	Slack	Pasture	Scrub	Wood	Pine
Fixed	**0.039***							
Heath	**0.005****	**0.013***						
Slack	**0.022***	**<0.001*****	**<0.001*****					
Pasture	0.087	0.283	0.304	**<0.001*****				
Scrub	**0.011***	**<0.001*****	**<0.001*****	**<0.001*****	**<0.001*****			
Wood	0.373	0.721	0.642	**<0.001*****	0.840	**0.002****		
Pine	0.874	0.058	**0.002****	**<0.001*****	**0.041***	**<0.001*****	0.216	
Felled	**0.025***	**0.012***	0.284	**<0.001*****	0.101	**0.003****	0.236	**0.007****

b)	Mobile	Fixed	Heath	Slack	Pasture	Scrub	Wood	Pine
Fixed	0.248							
Heath	0.056	**0.034***						
Slack	0.072	**<0.001*****	**<0.001*****					
Pasture	0.834	0.439	**0.006****	**0.021***				
Scrub	**0.011***	**<0.001*****	**<0.001*****	**<0.001*****	**<0.001*****			
Wood	0.504	0.307	0.993	**0.004****	0.065	**0.001****		
Pine	0.767	0.077	**0.002****	0.086	0.838	**<0.001*****	0.115	
Felled	**0.017***	**0.001****	0.057	**<0.001*****	**0.001****	**0.013***	0.292	**0.001****

c)	Mobile	Fixed	Heath	Slack	Pasture	Scrub	Wood	Pine
Fixed	**0.018***							
Heath	0.056	**0.005****						
Slack	0.646	**<0.001*****	**<0.001*****					
Pasture	0.531	**0.012***	0.146	**0.032***				
Scrub	**0.044***	0.412	0.116	**<0.001*****	0.085			
Wood	0.414	**<0.001*****	**<0.001*****	0.112	**0.012***	**0.001****		
Pine	**0.031***	0.065	0.127	**<0.001*****	**0.016***	0.389	**<0.001*****	
Felled	**0.012***	**0.026***	**<0.001*****	**<0.001*****	**0.004****	**0.010***	**<0.001*****	**<0.001*****

d)	Mobile	Fixed	Heath	Slack	Pasture	Scrub	Wood	Pine
Fixed	**0.031***							
Heath	**0.008****	**0.001****						
Slack	0.380	**<0.001*****	**<0.001*****					
Pasture	0.168	0.634	**0.041***	**0.001****				
Scrub	**0.044***	0.459	**0.001****	**<0.001*****	0.484			
Wood	**0.045***	0.453	**<0.001*****	**<0.001*****	0.488	0.782		
Pine	**0.019***	0.803	**0.001****	**<0.001*****	0.972	0.389	0.368	
Felled	0.097	**0.029***	**<0.001*****	**0.001****	0.109	0.314	0.095	**0.017***

e)	Mobile	Fixed	Heath	Slack	Pasture	Scrub	Wood	Pine
Fixed	0.651							
Heath	**0.011***	**<0.001*****						
Slack	0.770	0.407	**<0.001*****					
Pasture	0.195	**0.014***	**0.001****	**0.025***				
Scrub	0.060	**0.001****	**<0.001*****	**0.011***	0.746			
Wood	0.181	**0.038***	**<0.001*****	**0.019***	0.992	0.479		
Pine	0.874	0.127	**<0.001*****	0.312	**0.003****	**0.002****	**0.002****	
Felled	0.097	**0.002****	**<0.001*****	**0.050***	1.000	0.370	0.910	**0.016***

f)	Mobile	Fixed	Heath	Slack	Pasture	Scrub	Wood	Pine
Fixed	0.880							
Heath	**0.016***	**<0.001*****						
Slack	0.195	**0.014***	**<0.001*****					
Pasture	0.834	0.559	**<0.001*****	0.080				
Scrub	**0.011***	**<0.001*****	0.104	**0.013***	**0.005****			
Wood	0.235	**0.014***	**0.005****	0.543	0.056	0.176		
Pine	0.666	0.127	**<0.001*****	**0.006****	0.616	**<0.001*****	**0.006****	
Felled	**0.036***	**<0.001*****	**0.044***	0.054	**0.018***	0.828	0.355	**0.002****

environments (Table 4.20a). The pasture organo-mineral soil (-0.68) was significantly different (p <0.01) from most dune environments, apart from the mobile dune organo-mineral soil (-0.65).

The ratios of ARM/χ, SIRM/ARM and χ_{ARM}/SIRM in the mobile organo-mineral soil (0.01 x10^{-2}Am^{-1}, 251.59, 1.25 x10^{-5}Am^{2}kg^{-1}, respectively) were significantly different (p <0.05) from most dune environments, with the exception of both the fixed dune (0.02 x10^{-2}Am^{-1}, 260.97, 1.21 x10^{-5}Am^{2}kg^{-1}, respectively) and scrub (0.01 x10^{-2}Am^{-1}, 321.77, 0.98 x10^{-5}Am^{2}kg^{-1}, respectively) organo-mineral soils Tables 4.20b-d). Reflecting this, both the fixed dune and scrub organo-mineral soil ARM/χ ratios were highly significantly different (p <0.01) from most dune environments, apart from the mobile dune organo-mineral soil (Figure 4.29h), while SIRM/ARM and χ_{ARM}/SIRM ratios were very highly significantly different (p <0.001). The felled organo-mineral soil ARM/χ (0.04 x10^{-2}Am^{-1}) was significantly different (p <0.05) from most dune environments, except for the slack (0.03 x10^{-2}Am^{-1}) and pasture (0.03 x10^{-2}Am^{-1}) organo-mineral soils; whereas, the slack SIRM/ARM (111.73) and χ_{ARM}/SIRM (2.81 x10^{-5}Am^{2}kg^{-1}) ratios were significantly different to most dune environments, except for the organo-mineral soil pasture (129.24, 2.43 x10^{-5}Am^{2}kg^{-1}, respectively). The deciduous woodland organo-mineral soil had significantly different ARM/χ (0.02 x10^{-2}Am^{-1}; p <0.01), SIRM/ARM (166.14; p <0.05) and χ_{ARM}/SIRM (1.89 x10^{-5}Am^{2}kg^{-1}; p <0.05) ratios from all dune environments, suggesting magnetic domain size parameters can be used to identify and classify brown earth profiles. The ARM/χ of the coniferous plantation organo-mineral soil (0.03 x10^{-2}Am^{-1}) was significantly different (p <0.05) from most dune environments, with the exception of the heath organo-mineral soil (0.03 x10^{-2}Am^{-1}), also suggesting this magnetic domain size parameter can be used to identify and classify micro-podzols. The SIRM/χ ratio in the fixed dune organo-mineral soil (144.70 x10^{-2}Am^{-1}) was significantly different (p <0.05) from most dune environments, apart from the mobile dune soil (116.03 x10^{-2}Am^{-1}); whereas, the felled organo-mineral soil (154.47 x10^{-2}Am^{-1}) was significantly different (p <0.05) from all dune environments (Table 4.20e).

4.3.6 Classification of soil profiles using Mann-Whitney U tests

Kruskal-Wallis tests showed no differences between the dune environment organo-mineral soil component sample populations for each parameter. It was decided that if a sample population (e.g. Heath) showed significant pedo-differences (Mann-Whitney U test p-values) to at least six other dune environments, then it can be considered as having different pedo-characteristics, although not statistically significant.

Table 4.21 shows pedo-characteristic parameters that could be used to identify organo-mineral soils associated with each dune environment. Value of pH is the most appropriate pedo-characteristic in identifying a soil belonging to a specific dune environment on the Sefton coast, as values were significantly different in every dune environment. SOM was only useful in identifying dune slack soils. Textural variables were of no significance in identifying either the mobile or fixed dune soils; whereas mean particle size could be used to identify most remaining soils, except for pasture, which requires silt and clay data. Geochemical parameters have no

Table 4.20 Mann-Whitney U test results for soil parameters. Tables show '*p*' values (**bold** text is significant (**p* <0.05; ***p* <0.01; ****p* <0.001)) for; a) S-ratio; b) ARM/χ x10^{-2}Am^{-1}; c) SIRM/ARM; d) χ_{ARM}/SIRM x10^{-5}Am^{-1} and e) SIRM/χ x10^{-2}Am^{-1}

a)	Mobile	Fixed	Heath	Slack	Pasture	Scrub	Wood	Pine
Fixed	0.393							
Heath	**0.016***	**<0.001*****						
Slack	0.587	0.817	**<0.001*****					
Pasture	0.477	**0.001****	**<0.001*****	**0.003***				
Scrub	0.346	0.920	**<0.001*****	0.959	**0.001****			
Wood	0.102	**0.010***	**<0.001*****	**0.023***	**<0.001*****	**0.046***		
Pine	0.180	0.116	**<0.001*****	0.140	**<0.001*****	0.247	0.096	
Felled	0.279	0.459	**<0.001*****	0.377	**0.001****	0.497	0.089	0.655

b)	Mobile	Fixed	Heath	Slack	Pasture	Scrub	Wood	Pine
Fixed	0.291							
Heath	**0.005****	**<0.001*****						
Slack	**0.017***	**<0.001*****	0.083					
Pasture	**0.007****	**<0.001*****	0.399	0.581				
Scrub	0.226	**0.002****	**<0.001*****	**<0.001*****	**<0.001*****			
Wood	**0.008****	**0.002****	**<0.001*****	**<0.001*****	**<0.001*****	**<0.001*****		
Pine	**0.006****	**<0.001*****	0.090	**0.012***	**0.040***	**<0.001*****	**<0.001*****	
Felled	**0.012***	**<0.001*****	**0.016***	0.552	0.144	**<0.001*****	**<0.001*****	**0.001****

c)	Mobile	Fixed	Heath	Slack	Pasture	Scrub	Wood	Pine
Fixed	**0.880**							
Heath	**0.005****	**<0.001*****						
Slack	**0.022***	**<0.001*****	**0.010***					
Pasture	**0.007****	**<0.001*****	0.304	0.201				
Scrub	0.106	0.069	**<0.001*****	**<0.001*****	**<0.001*****			
Wood	**0.014***	**<0.001*****	**<0.001*****	**<0.001*****	**<0.001*****	**<0.001*****		
Pine	**0.007****	**<0.001*****	0.352	**0.002****	0.069	**<0.001*****	**<0.001*****	
Felled	**0.012***	**<0.001*****	0.666	**0.024***	0.288	**<0.001*****	**<0.001*****	0.909

d)	Mobile	Fixed	Heath	Slack	Pasture	Scrub	Wood	Pine
Fixed	0.880							
Heath	**0.005****	**<0.001*****						
Slack	**0.022***	**<0.001*****	**0.010***					
Pasture	**0.007****	**<0.001*****	0.304	0.201				
Scrub	0.106	0.069	**<0.001*****	**<0.001*****	**<0.001*****			
Wood	**0.014***	**<0.001*****	**<0.001*****	**<0.001*****	**<0.001*****	**<0.001*****		
Pine	**0.007****	**<0.001*****	0.352	**0.002****	0.069	**<0.001*****	**<0.001*****	
Felled	**0.012***	**<0.001*****	0.666	**0.024***	0.288	**<0.001*****	**<0.001*****	0.909

e)	Mobile	Fixed	Heath	Slack	Pasture	Scrub	Wood	Pine
Fixed	0.063							
Heath	0.434	**<0.001*****						
Slack	1.000	**<0.001*****	0.151					
Pasture	0.531	**0.001****	0.788	0.307				
Scrub	0.687	**<0.001*****	0.625	0.442	0.905			
Wood	0.941	**<0.001*****	0.412	0.558	0.662	0.806		
Pine	0.699	**<0.001*****	0.780	0.400	0.983	0.804	0.790	
Felled	**0.036***	**0.026***	**0.001****	**<0.001*****	**0.001****	**<0.001*****	**<0.001*****	**<0.001*****

Table 4.21 Summary of parameters (minimum and maximum values) suitable for identification of organo-mineral soils on sand dunes (results derived from significant Mann-Whitney U Test *p*-values)

Parameters	Units	Mobile dune (Terrestrial raw sand)	Fixed dune (Sand-pararendzina)	Pasture (Sand-pararendzina)	Slack (Groundwater gley)	Deciduous wood (Brown earth)	Heath (Micro-podzol)	Coniferous (Micro-podzol)	Scrub	Felled area
pH	mol/ltr	7.1	6.1 – 7.2	5.4 – 7.5	7.1 – 8.1	3.6 – 5.3	3.9 – 4.5	3.7 – 6.7	6.5 – 6.9	4.2 – 6.7
SOM	%				0.2 – 12.3					
Sand	%				62.2 – 92.7	70.3 – 81.4	83.4 – 93.5	66.0 – 92.0		
Silt	%			8.5 – 27.0	3.2 – 35.1	16.8 – 28.1	6.3 – 15.7			
Clay	%			2.2 – 6.0	2.2 – 6.9		0.2 – 1.2			
Mean particle size	µm				158.1 – 260.9	183.8 – 401.1	212.1 – 334.5	156.2 – 258.0	163.5 – 188.3	176.7 – 201.0
Sodium	%				0.9 – 1.6					
Magnesium	%								0.3 – 0.5	
Aluminium	%		0.02	0.04 – 0.20	0.02 – 0.13		0.22 – 0.69			
Phosphorus	%				0.01 – 0.05					
Chlorine	%						0.01 – 0.06			
Potassium	%				0.3 – 0.5				0.5 – 0.6	
Calcium	%				0.5 – 7.4	0.1 – 1.2	0.1		0.4 – 2.1	
Manganese	%					0.01 – 0.09	0.01		0.02 – 0.05	
Iron	%								0.9 – 1.7	
χ_{LF}	$10^{-7}m^3kg^{-1}$				0.2 – 1.4		0.5 – 4.1		1.3 – 6.3	
χ_{FD}	%								0.0 – 4.9	
χ_{ARM}	$10^{-7}m^3kg^{-1}$									0.03 – 0.12
SIRM	$10^{-5}Am^2kg^{-1}$				25.4 – 189.0		57.4 – 641.8		177.5 – 788.9	
$Soft_{IRM20mT}$	$10^{-5}Am^2kg^{-1}$				3.3 – 36.6		7.2 – 82.4		20.1 – 109.1	
$Soft_{IRM40mT}$	$10^{-5}Am^2kg^{-1}$				10.1 – 75.6				63.4 – 292.9	
$Hard_{IRM300mT}$	$10^{-5}Am^2kg^{-1}$				2.0 – 15.2				16.2 – 81.0	
$Hard_{IRM500mT}$	$10^{-5}Am^2kg^{-1}$				0.4 – 6.5				9.3 – 60.9	5.7 – 48.2
$Soft_{\%20mT}$	%		10.0 – 17.2		12.8 – 23.9	9.2 – 29.1				8.5 – 12.5
$Soft_{\%40mT}$	%				37.7 – 50.7		26.8 – 41.1			
$Hard_{\%300mT}$	%						7.5 – 31.3			
$Hard_{\%500mT}$	%						4.0 – 14.6			
S-ratio	(none)			-0.9 - -0.5			-0.6 - -0.4			
ARM/χ	$10^{-2}Am^{-1}$	0.01 – 0.02	0.01 – 0.03			0.02 – 0.03			0.01 – 0.02	0.03 – 0.05
SIRM/ARM	(None)	200.5 – 294.6	151.1 – 456.3		77.9 – 350.9	116.3 – 260.9			229.6 – 426.8	
χ_{ARM}/SIRM	$10^{-5}Am^2kg^{-1}$	1.1 – 1.6	0.7 – 2.1		0.9 – 4.0	1.2 – 2.7			0.7 – 1.4	
SIRM/χ	$10^{-2}Am^{-1}$	85.8 – 143.6	124.5 – 153.4							119.6 – 168.4

influence in identifying mobile dune, deciduous woodland, coniferous plantation or felled soils. However, values of Cl can solely be used to identify heath soils; Na and P to identify slack soils and Mg to identify scrub soils. Mineral magnetics vary considerably between each organo-mineral soil, but both $Hard_{\%300mT}$ and $Hard_{\%500mT}$ can be used to identify heath soils, while $\chi_{FD\%}$ can solely be used to identify slack soils and χ_{ARM} to identify soils associated with felled environments.

When identifying classified soil profiles on the Sefton coast, pH is the most appropriate pedo-characteristic to use. SOM can solely be used to classify the groundwater gley. Textural variables were of no significance in classifying either the terrestrial raw sand or the sand-pararendzinas; whereas, sand could be used to identify the remaining soil classifications and clay could solely be used to classify the groundwater gley. Geochemical parameters have no influence in classifying either the terrestrial raw sand or micro-podzols. However, the groundwater gley displayed influences in Na, P and K, while Mn could solely be used to classify the brown earth. Al could be used in some instances to classify sand-pararendzinas, but this would exclude the profile from under the scrub environment. Magnetic concentration and mineralogy parameters would not be useful in identifying the terrestrial raw sand, sand-pararendzinas or micro-podzols, but could be used to identify the groundwater gley and $Soft_{\%20mT}$ could solely be used to identify the brown earth. Magnetic domain size parameters have no significant influence on terrestrial raw soils; whereas, all remaining soil classifications can be identified by these characteristics, with ARM/χ being solely used to identify micro-podzols.

4.4 Further assessment using multivariate factor analysis plots

Results of Mann-Whitney U tests have identified two-dimensional key pedo-characteristic associations with each organo-mineral soil component in terms of observed parameters. However, these data cannot identify the role of each pedo-characteristic in soil profile horizons. To achieve this, multivariate factor analysis is used to provide multi-dimensional details on both down-profile changes in physico-chemical unobserved parameters and to identify profiles belonging to the same NSRI classification.

The main advantage of using multivariate factor analysis, over univariate Mann Whitney U tests, is the reduction of parameters, by combining two or more variables into one single factor to identify any hidden dimensions that would not have been apparent from direct analysis. The resultant plot identifies groups of inter-related parameters, to observe how they relate to each other. The information gained about the interdependencies is used to reduce the number of parameters in each dataset. Factor analysis is used to estimate how much variability between parameters is due to common factors. In each case, parameter and sample loadings extracted from Factors 1 and 2 were used to generate factor plots.

4.4.1 Factor analysis of the mobile dune soil profile

Figure 4.30 shows the factor plot for the mobile dune soil profile using all physico-chemical parameters. The first two factors extracted explain 42.09% of variation (Table 4.22). Factor 1 (depth) explains 28.60% of variation in parameters, while Factor 2 (mineral properties) explains 13.49%. The spread of parameter loadings along Factor 1 indicate textural and geochemical parameter influences, with Factor 1 appearing to separate surface layers/horizons from parent material samples. Factor 2 appears to be influenced by mineral magnetic parameters, especially magnetic domain size and, does appear to separate the Cu samples into two distinct groups. The position of $\chi_{FD\%}$ in the centre of the plot indicates this parameter has no influence.

Figure 4.31a shows the textural factor plot, where the first two factors extracted explain 84.72% of variation in parameters. F layer and A horizon samples are separated from Cu samples by both factors, with negative loadings on Factor 1 and positive loadings on Factor 2. However, a small cluster of Cu samples are strongly associated with F and A samples, suggesting strong silt influences in this population. The majority of Cu samples are positively loaded on Factor 1, suggesting strong sand and clay influences that differ to the rest of the sample population.

Figure 4.31b shows the geochemical factor plot, where the first two factors extracted explain 61.98% of variation in parameters. A horizon samples are negatively loaded on Factor 1 and positively loaded on Factor 2, suggesting strong SOM, S and Cl influences, with some P influences. The clustering of Cu sample points in the centre of the plot, away from A horizon samples, suggests geochemical parameters have limited influence on parent material. Figure 4.31c shows the mineral magnetic factor plot, where the first two factors extracted explain 54.77% of variation in parameters. F layer and A horizon samples are positively loaded on both factors. The F layer sample is highly influenced by magnetic concentration influences (χ_{LF}, χ_{ARM}, SIRM), of soft 'magnetite-type' minerals. A horizon samples are shown to be influenced by concentrations of ferrimagnetic domain size variations, represented by ARM/χ. Hard 'haematite-type' minerals become more influential down-profile.

4.4.2 Factor analysis of the fixed dune soil profile

Figure 4.32 shows the factor plot for the fixed dune soil profile using all physico-chemical parameters. The first two factors extracted explain 48.12% of variation in parameters (Table 4.23). Factor 1 explains 37.20% of variation in parameters, while Factor 2 explains 10.92%. The spread of parameter loadings along Factor 1 indicates textural and geochemical parameters as the major influencing factors, while magnetic mineralogy and domain size is represented by Factor 2. H layer samples are separated from the Ah horizon samples by Factor 1; whereas, Factor 2 separates Cu samples from both the H layer and Ah horizon.

Figure 4.33a shows the textural factor plot, where the first factor extracted (depth) explains 86.51% of variation in parameters. The second factor extracted only explains 9.58% of variation and, therefore, has little relevance. H layer and Ah horizon samples are separated from the Cu

Table 4.22 Summary results from factor analysis of the mobile dune soil profile using all parameters

Factors	Eigenvalues	Total variance (%)	Cumulative eigenvalues	Cumulative total variance (%)
1	10.583	28.602	10.583	28.602
2	4.990	13.486	15.573	42.089
3	4.791	12.948	20.364	55.037
4	2.976	8.044	23.340	63.081
5	2.159	5.835	25.499	68.916
6	1.659	4.484	27.158	73.400
7	1.504	4.064	28.662	77.464
8	1.441	3.894	30.102	81.358
9	1.003	2.710	31.105	84.068
10	0.852	2.302	31.957	86.370
11	0.698	1.886	32.655	88.256
12	0.673	1.820	33.328	90.076
13	0.562	1.518	33.890	91.594
14	0.439	1.187	34.329	92.781
15	0.407	1.099	34.736	93.880
16	0.374	1.011	35.110	94.891
17	0.316	0.855	35.426	95.746
18	0.288	0.779	35.714	96.525
19	0.233	0.630	35.947	97.154
20	0.216	0.584	36.163	97.739
21	0.172	0.464	36.335	98.203
22	0.144	0.390	36.479	98.593
23	0.123	0.333	36.603	98.926
24	0.104	0.280	36.706	99.206
25	0.087	0.234	36.793	99.440
26	0.077	0.209	36.870	99.649
27	0.049	0.132	36.919	99.781
28	0.032	0.086	36.951	99.866
29	0.019	0.050	36.969	99.917
30	0.012	0.033	36.982	99.950
31	0.009	0.023	36.990	99.974
32	0.004	0.010	36.994	99.983
33	0.003	0.008	36.997	99.991
34	0.002	0.006	36.999	99.997
35	0.001	0.002	37.000	99.999
36	0.000	0.001	37.000	100.000
37	0.000	0.000	37.000	100.000

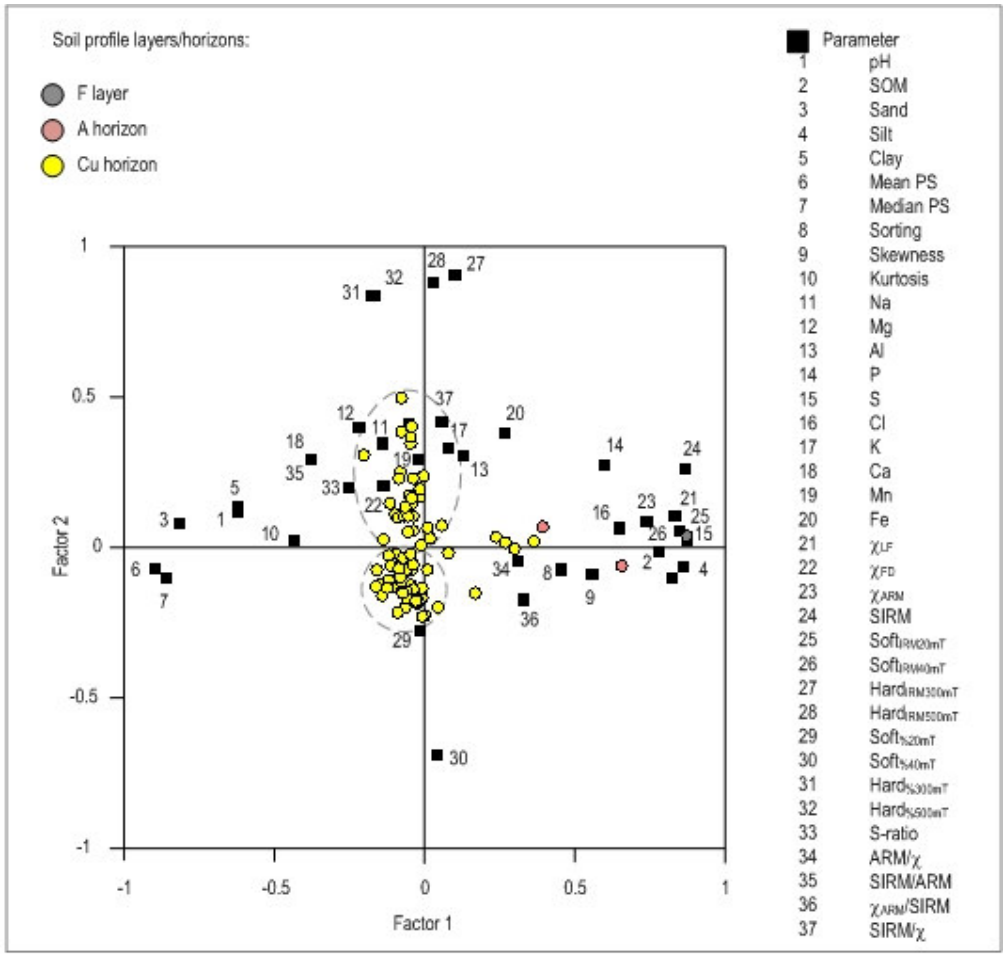

Figure 4.30 Simultaneous R- and Q-mode factor analysis plots of Factor 1 versus Factor 2, based on the mobile dune soil profile characteristics (grey dashed line represents possible grouping with a sample population).

Parameters	Factors	Eigenvalues	Total variance (%)	Cumulative eigenvalues	Cumulative total variance (%)
1 Sand	1	4.662	58.277	4.662	58.277
2 Silt	2	2.115	26.440	6.777	84.717
3 Clay	3	0.683	8.542	7.461	93.259
4 Mean	4	0.317	3.959	7.777	97.219
5 Median	5	0.127	1.590	7.905	98.809
6 Sorting	6	0.067	0.843	7.972	99.652
7 Skewness	7	0.028	0.348	8.000	100.000
8 Kurtosis	8	0.000	0.000	8.000	100.000

Parameters	Factors	Eigenvalues	Total variance (%)	Cumulative eigenvalues	Cumulative total variance (%)
1 pH	1	4.032	33.601	4.032	33.601
2 SOM	2	3.406	28.383	7.438	61.984
3 Na	3	1.251	10.427	8.689	72.411
4 Mg	4	0.962	8.013	9.651	80.424
5 Al	5	0.664	5.533	10.315	85.956
6 P	6	0.424	3.536	10.739	89.492
7 S	7	0.347	2.888	11.086	92.379
8 C	8	0.278	2.316	11.363	94.696
9 K	9	0.261	2.174	11.624	96.869
10 Ca	10	0.172	1.435	11.797	98.304
11 Mn	11	0.140	1.166	11.936	99.470
12 Fe	12	0.064	0.530	12.000	100.000

Parameters	Factors	Eigenvalues	Total variance (%)	Cumulative eigenvalues	Cumulative total variance (%)
1 χ_{LF}	1	4.828	28.397	4.828	28.397
2 χ_{FD}	2	4.484	26.374	9.311	54.771
3 χ_{ARM}	3	2.765	16.265	12.076	71.036
4 SIRM	4	1.572	9.250	13.649	80.285
5 $Soft_{IRM20mT}$	5	0.880	5.177	14.529	85.463
6 $Soft_{IRM40mT}$	6	0.788	4.638	15.317	90.101
7 $Hard_{IRM300mT}$	7	0.575	3.382	15.892	93.483
8 $Hard_{IRM500mT}$	8	0.530	3.116	16.422	96.598
9 $Soft_{S-20mT}$	9	0.322	1.892	16.743	98.490
10 $Soft_{S-40mT}$	10	0.195	1.150	16.939	99.640
11 $Hard_{S-300mT}$	11	0.027	0.161	16.966	99.801
12 $Hard_{S-500mT}$	12	0.014	0.085	16.981	99.885
13 S-ratio	13	0.010	0.056	16.990	99.942
14 ARM/χ	14	0.004	0.025	16.994	99.967
15 SIRM/ARM	15	0.003	0.019	16.998	99.986
16 χ_{ARM}/SIRM	16	0.001	0.007	16.999	99.994
17 SIRM/χ	17	0.001	0.006	17.000	100.000

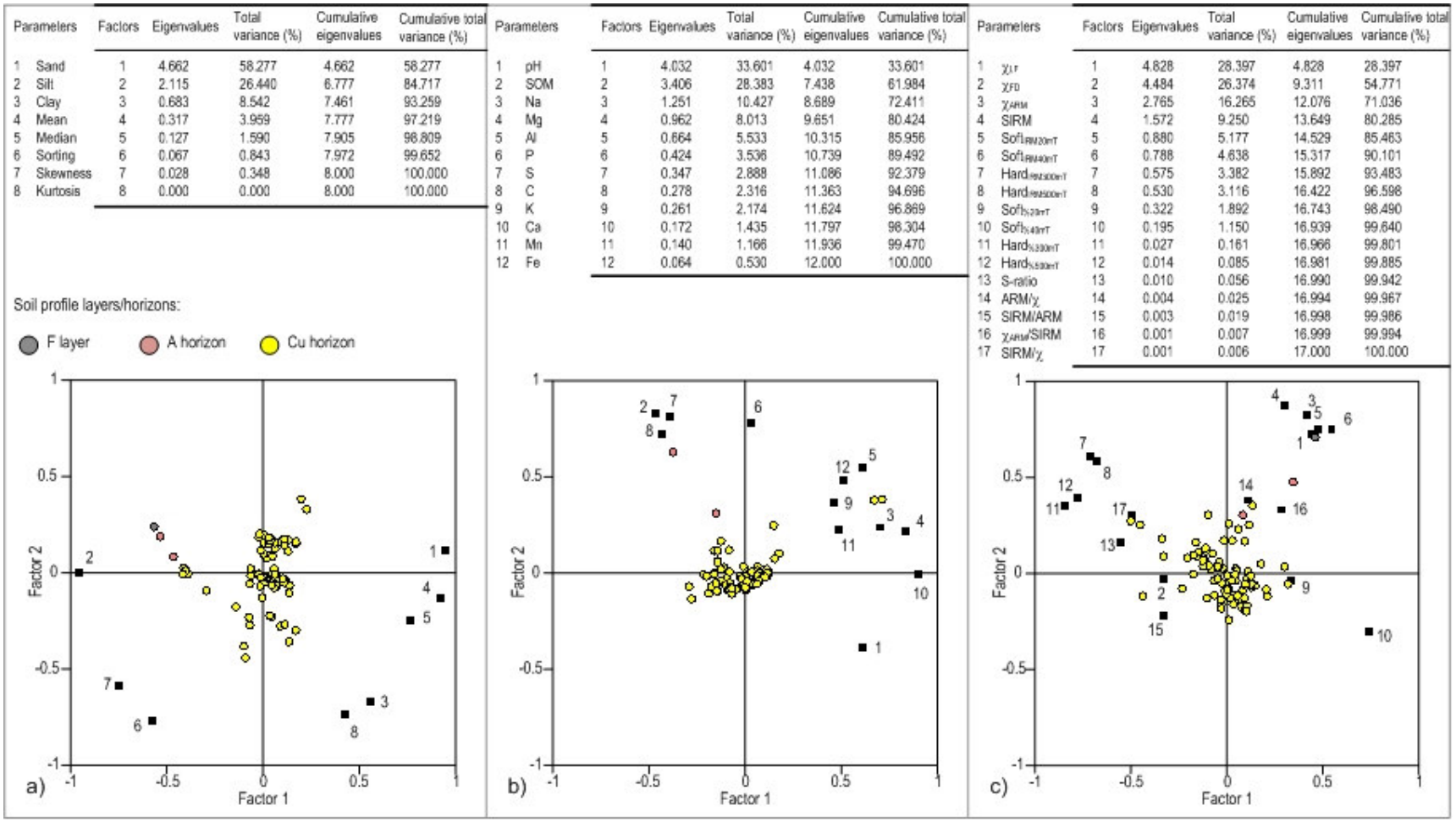

Figure 4.31 Summary results and simultaneous R- and Q-mode factor analysis plots of Factor 1 versus Factor 2, based on the mobile dune soil profile: a) textural characteristics; b) geochemical characteristics and c) mineral magnetic characteristics.

Table 4.23 Summary results from factor analysis of the fixed dune soil profile using all parameters

Factors	Eigenvalues	Total variance (%)	Cumulative eigenvalues	Cumulative total variance (%)
1	13.765	37.203	13.765	37.203
2	4.040	10.919	17.805	48.122
3	3.349	9.050	21.154	57.172
4	2.813	7.604	23.967	64.776
5	2.203	5.955	26.171	70.731
6	2.061	5.571	28.232	76.302
7	1.461	3.949	29.693	80.251
8	1.203	3.251	30.896	83.502
9	1.042	2.815	31.937	86.317
10	0.963	2.603	32.901	88.920
11	0.673	1.818	33.573	90.739
12	0.592	1.601	34.166	92.339
13	0.557	1.504	34.722	93.843
14	0.459	1.241	35.181	95.084
15	0.318	0.859	35.499	95.943
16	0.295	0.798	35.794	96.741
17	0.258	0.697	36.052	97.438
18	0.196	0.530	36.248	97.968
19	0.179	0.484	36.427	98.452
20	0.143	0.386	36.570	98.838
21	0.102	0.275	36.672	99.113
22	0.088	0.238	36.760	99.351
23	0.059	0.158	36.818	99.509
24	0.052	0.140	36.870	99.650
25	0.042	0.113	36.912	99.763
26	0.024	0.064	36.936	99.827
27	0.020	0.055	36.956	99.882
28	0.013	0.036	36.970	99.918
29	0.009	0.025	36.979	99.943
30	0.006	0.017	36.985	99.960
31	0.006	0.015	36.991	99.975
32	0.005	0.012	36.995	99.988
33	0.002	0.006	36.998	99.994
34	0.001	0.003	36.999	99.997
35	0.001	0.002	37.000	99.999
36	0.000	0.001	37.000	100.000
37	0.000	0.000	37.000	100.000

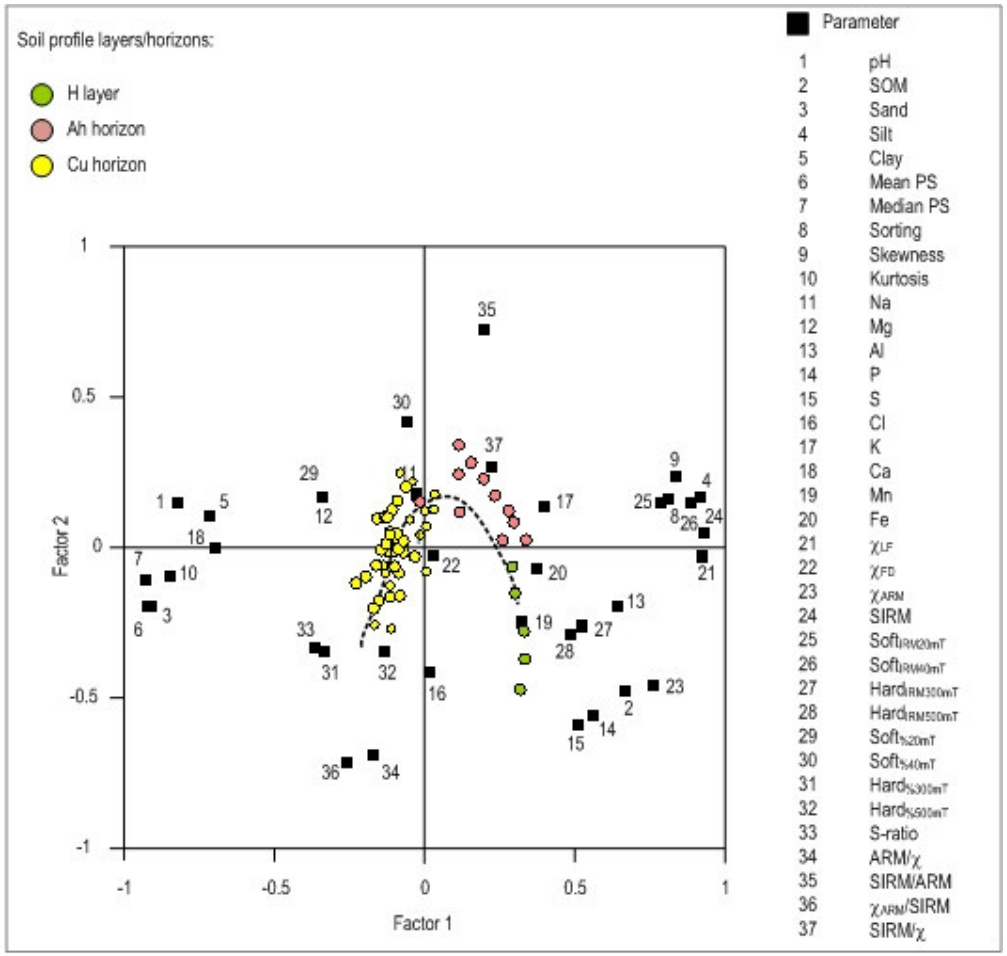

Figure 4.32 Simultaneous R- and Q-mode factor analysis plots of Factor 1 versus Factor 2, based on the fixed dune soil profile characteristics (dashed line represents postulated soil horizon development).

Parameters		Factors	Eigenvalues	Total variance (%)	Cumulative eigenvalues	Cumulative total variance (%)
1	Sand	1	6.921	86.509	6.921	86.509
2	Silt	2	0.766	9.579	7.687	96.088
3	Clay	3	0.134	1.672	7.821	97.760
4	Mean	4	0.091	1.134	7.912	98.894
5	Median	5	0.055	0.692	7.967	99.586
6	Sorting	6	0.028	0.352	7.995	99.938
7	Skewness	7	0.005	0.062	8.000	100.000
8	Kurtosis	8	0.000	0.000	8.000	100.000

Parameters		Factors	Eigenvalues	Total variance (%)	Cumulative eigenvalues	Cumulative total variance (%)
1	pH	1	4.393	36.607	4.393	36.607
2	SOM	2	2.180	18.165	6.573	54.772
3	Na	3	1.817	15.138	8.389	69.910
4	Mg	4	1.581	13.176	9.970	83.086
5	Al	5	0.490	4.086	10.461	87.172
6	P	6	0.451	3.761	10.912	90.933
7	S	7	0.329	2.744	11.241	93.678
8	C	8	0.270	2.246	11.511	95.924
9	K	9	0.204	1.696	11.714	97.620
10	Ca	10	0.141	1.174	11.855	98.794
11	Mn	11	0.113	0.938	11.968	99.733
12	Fe	12	0.032	0.267	12.000	100.000

Parameters		Factors	Eigenvalues	Total variance (%)	Cumulative eigenvalues	Cumulative total variance (%)
1	χ_{LF}	1	5.637	33.160	5.637	33.160
2	χ_{FD}	2	3.153	18.544	8.790	51.705
3	χ_{ARM}	3	2.969	17.463	11.758	69.167
4	SIRM	4	1.556	9.150	13.314	78.318
5	$Soft_{BV20mT}$	5	1.153	6.780	14.467	85.097
6	$Soft_{BV40mT}$	6	0.875	5.150	15.342	90.247
7	$Hard_{BV300mT}$	7	0.606	3.565	15.948	93.812
8	$Hard_{BV500mT}$	8	0.523	3.079	16.471	96.891
9	$Soft_{N20mT}$	9	0.373	2.192	16.844	99.083
10	$Soft_{N40mT}$	10	0.064	0.377	16.908	99.460
11	$Hard_{N300mT}$	11	0.029	0.170	16.937	99.630
12	$Hard_{N500mT}$	12	0.024	0.142	16.961	99.773
13	S-ratio	13	0.018	0.104	16.979	99.876
14	ARM/χ	14	0.015	0.089	16.994	99.965
15	SIRM/ARM	15	0.004	0.025	16.998	99.990
16	χ_{ARM}/SIRM	16	0.001	0.007	16.999	99.997
17	SIRM/χ	17	0.001	0.003	17.000	100.000

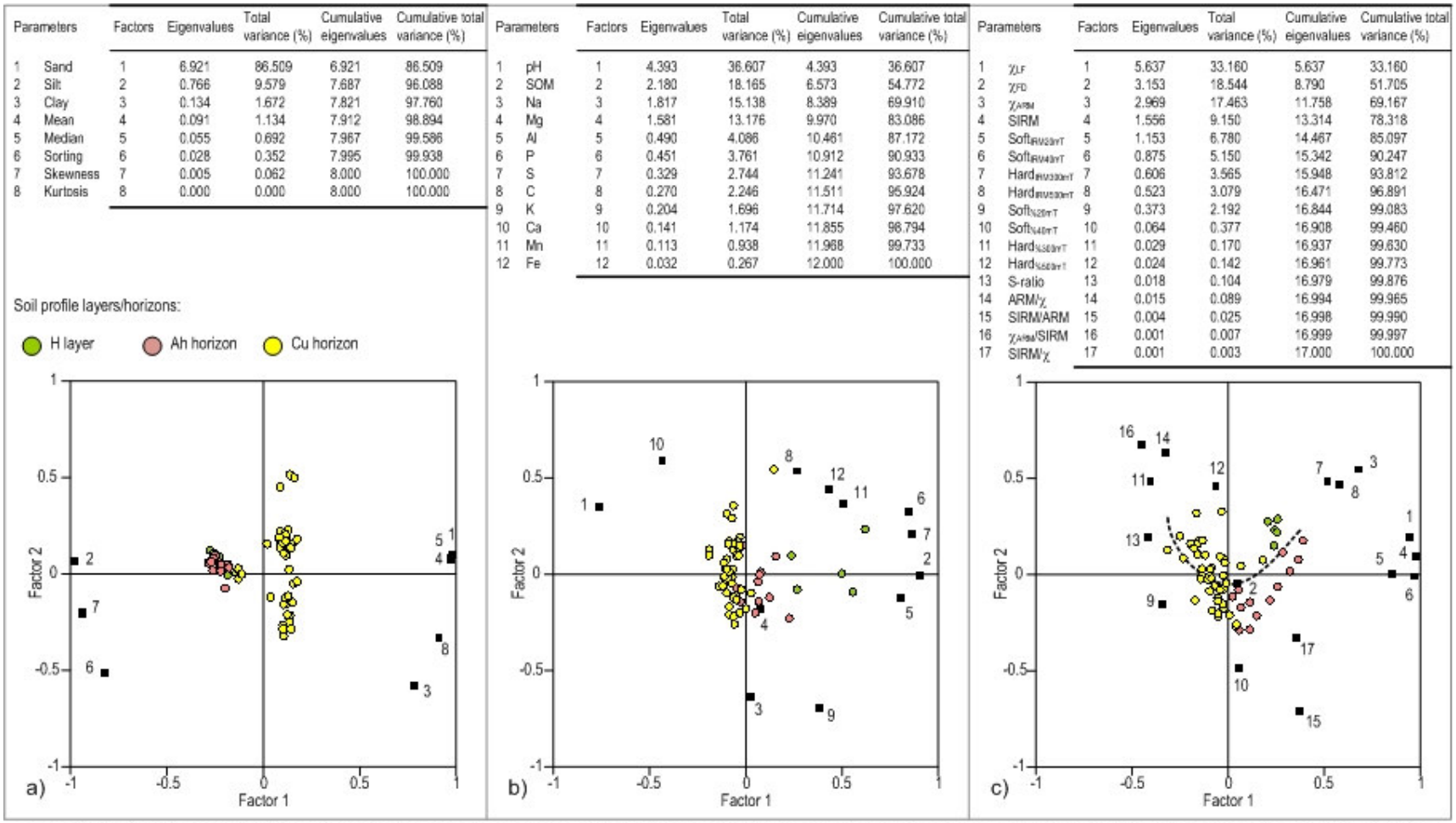

Figure 4.33 Summary results and simultaneous R- and Q-mode factor analysis plots of Factor 1 versus Factor 2, based on the fixed dune soil profile: a) textural characteristics; b) geochemical characteristics and c) mineral magnetic characteristics (dashed line represents postulated soil horizon development).

samples by Factor 2, suggesting strong silt influences; whereas, the Cu samples are positively loaded on Factor 1, suggesting strong sand and clay influences. Figure 4.33b shows the geochemical factor plot, where the first two factors extracted explain 54.77% of variation in parameters. H layer samples are positively loaded on Factor 1 (representing depth), suggesting strong SOM, P, S and Al influences. Most Ah horizon samples are positively loaded on Factor 1, but display higher influences of Cl, Fe, MnO, Na, Mg and K. Cu samples are negatively loaded on Factor 1 and are most strongly influenced by pH and Ca.

Figure 4.33c shows the mineral magnetic factor plot, where the first two factors extracted explain 51.71% of variation in parameters. H layer samples are positively loaded on both factors, suggesting strong magnetic concentration influences. Ah horizon samples are also positively loaded on Factor 1, but are positively and negatively loaded on Factor 2, suggesting strong magnetic concentration influences of variable magnetic mineralogy. Cu sample loadings indicate increasing influence of hard 'haematite-type' minerals down-profile. The position of $\chi_{FD\%}$ in the centre of the plot indicates this parameter has no influence on any of the sample populations.

4.4.3 Factor analysis of the dune pasture soil profile

Figure 4.34 shows the Factor plot for the dune pasture soil profile using all physico-chemical parameters. The first two factors extracted explain 42.62% of variation in parameters (Table 4.24). Factor 1 (possibly age) explains 30.11% of variation, while Factor 2 explains 12.51%. F layer samples are positively loaded on Factor 1 and negatively loaded on Factor 2. The H layer samples are positively loaded on both factors. The Ah horizon samples are separated from the Cu horizon by Factor 2, while Factor 1 separates the buried horizons from the Cu samples.

Figure 4.35a is a factor plot of the textural parameters, where the first two factors extracted explain 91.29% of variation. F and H layer and Ah horizon samples are positively loaded on both factors, suggesting strong sand and silt influences; whereas, the Cu and buried horizon samples are negatively loaded on Factor 1, suggesting strong clay influences. Figure 4.35b shows the geochemical factor plot, where the first two factors extracted explain 45.64% of variation in parameters. F layer samples are negatively loaded on Factor 1 and positively loaded on Factor 2, suggesting a strong Cl influence. Factor 1 separates these data from the H layer samples, which are negatively loaded on both factors, suggesting strong P and S influences. The Ah/Ap horizon samples are negatively loaded on Factor 1, influenced by the same parameters as the organic horizons. Most Cu samples are positively loaded on both factors, influenced by K and Na; whereas, the buried horizons are positively loaded on Factor 1, appearing to be influenced by Al, Mg and Ca.

Figure 4.35c shows the mineral magnetic factor plot, where the first two factors extracted explain 51.56% of variation in parameters. H layer and Ah/Ap horizon samples are positively loaded on Factor 1, suggesting strong magnetic concentration influences with soft 'magnetite-

Table 4.24 Summary results from factor analysis of the pasture soil profile using all parameters

Factors	Eigenvalues	Total variance (%)	Cumulative eigenvalues	Cumulative total variance (%)
1	11.140	30.109	11.140	30.109
2	4.628	12.509	15.768	42.618
3	3.629	9.807	19.397	52.425
4	3.200	8.648	22.597	61.073
5	2.129	5.754	24.726	66.827
6	1.852	5.006	26.578	71.833
7	1.510	4.080	28.088	75.913
8	1.208	3.264	29.296	79.178
9	1.097	2.966	30.393	82.143
10	1.009	2.727	31.402	84.870
11	0.855	2.310	32.257	87.181
12	0.733	1.982	32.990	89.163
13	0.699	1.888	33.689	91.051
14	0.582	1.574	34.271	92.625
15	0.486	1.313	34.757	93.937
16	0.387	1.045	35.144	94.983
17	0.351	0.947	35.494	95.930
18	0.290	0.783	35.784	96.713
19	0.276	0.747	36.060	97.460
20	0.196	0.530	36.257	97.991
21	0.175	0.473	36.431	98.463
22	0.126	0.340	36.557	98.803
23	0.118	0.320	36.675	99.123
24	0.098	0.264	36.773	99.386
25	0.068	0.184	36.841	99.571
26	0.048	0.131	36.890	99.702
27	0.035	0.094	36.924	99.795
28	0.024	0.065	36.948	99.860
29	0.015	0.041	36.963	99.901
30	0.013	0.035	36.976	99.936
31	0.010	0.026	36.986	99.962
32	0.008	0.021	36.994	99.983
33	0.003	0.007	36.996	99.990
34	0.002	0.005	36.998	99.995
35	0.001	0.003	36.999	99.998
36	0.001	0.002	37.000	99.999
37	0.000	0.001	37.000	100.000

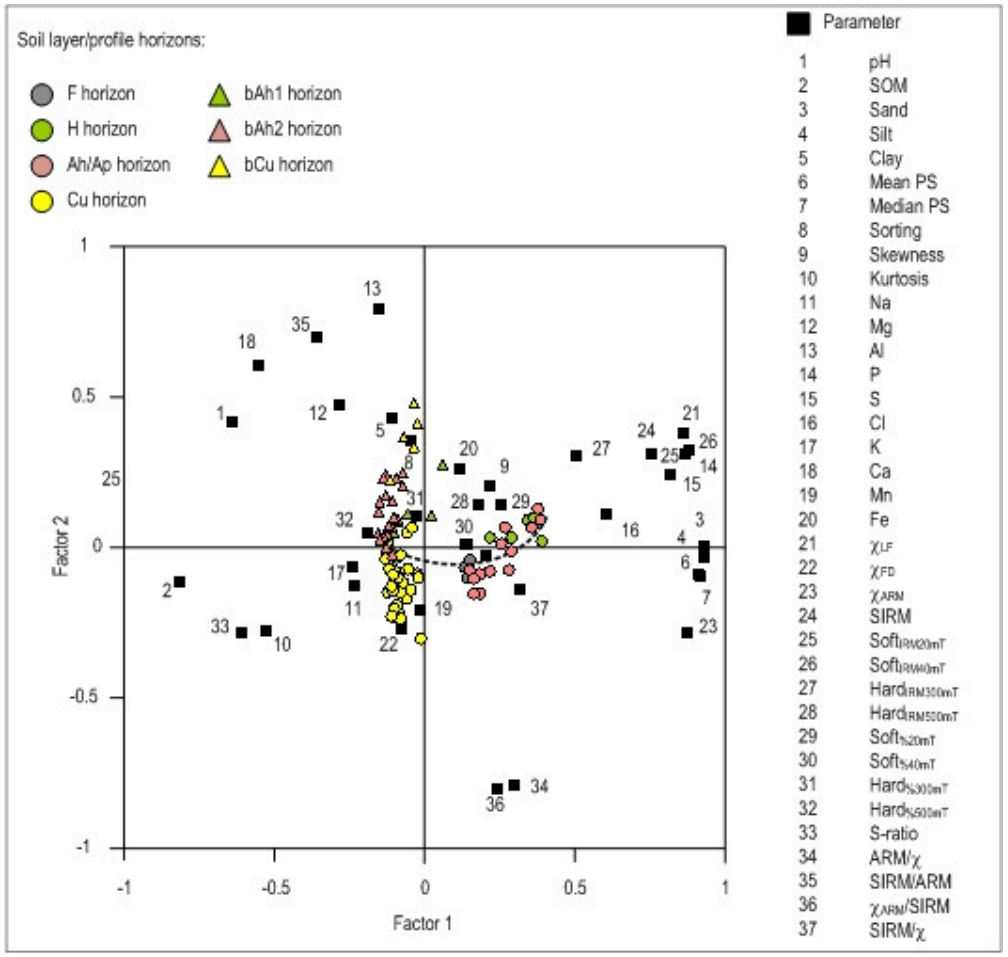

Figure 4.34 Simultaneous R- and Q-mode Factor analysis plots of Factor 1 versus factor 2, based on the pasture soil profile characteristics (dashed line represents postulated soil horizon development).

Parameters		Factors	Eigenvalues	Total variance (%)	Cumulative eigenvalues	Cumulative total variance (%)
1	Sand	1	4.259	53.233	4.259	53.233
2	Silt	2	3.044	38.056	7.303	91.289
3	Clay	3	0.320	3.994	7.623	95.284
4	Mean	4	0.238	2.981	7.861	98.264
5	Median	5	0.113	1.410	7.974	99.674
6	Sorting	6	0.020	0.253	7.994	99.927
7	Skewness	7	0.003	0.040	7.997	99.967
8	Kurtosis	8	0.003	0.033	8.000	100.000

Parameters		Factors	Eigenvalues	Total variance (%)	Cumulative eigenvalues	Cumulative total variance (%)
1	pH	1	3.313	27.606	3.313	27.606
2	SOM	2	2.164	18.037	5.477	45.643
3	Na	3	1.661	13.841	7.138	59.484
4	Mg	4	1.174	9.787	8.313	69.272
5	Al	5	1.004	8.368	9.317	77.640
6	P	6	0.896	7.470	10.213	85.110
7	S	7	0.702	5.854	10.916	90.964
8	C	8	0.410	3.416	11.326	94.381
9	K	9	0.300	2.502	11.626	96.883
10	Ca	10	0.168	1.396	11.793	98.279
11	Mn	11	0.140	1.170	11.934	99.449
12	Fe	12	0.066	0.551	12.000	100.000

Parameters		Factors	Eigenvalues	Total variance (%)	Cumulative eigenvalues	Cumulative total variance (%)
1	χ_{LF}	1	5.393	31.726	5.393	31.726
2	χ_{FD}	2	3.371	19.829	8.764	51.555
3	χ_{ARM}	3	3.000	17.645	11.764	69.200
4	SIRM	4	1.511	8.888	13.275	78.087
5	$Soft_{BV20mT}$	5	0.969	5.701	14.244	83.788
6	$Soft_{BV40mT}$	6	0.849	4.993	15.093	88.781
7	$Hard_{BV300mT}$	7	0.707	4.162	15.800	92.943
8	$Hard_{BV500mT}$	8	0.456	2.684	16.257	95.627
9	$Soft_{N20mT}$	9	0.366	2.152	16.622	97.778
10	$Soft_{N40mT}$	10	0.204	1.197	16.826	98.976
11	$Hard_{N300mT}$	11	0.081	0.474	16.907	99.450
12	$Hard_{N500mT}$	12	0.039	0.229	16.945	99.679
13	S-ratio	13	0.026	0.156	16.972	99.835
14	ARM/χ	14	0.018	0.104	16.990	99.939
15	SIRM/ARM	15	0.006	0.036	16.996	99.975
16	χ_{ARM}/SIRM	16	0.002	0.015	16.998	99.990
17	SIRM/χ	17	0.002	0.010	17.000	100.000

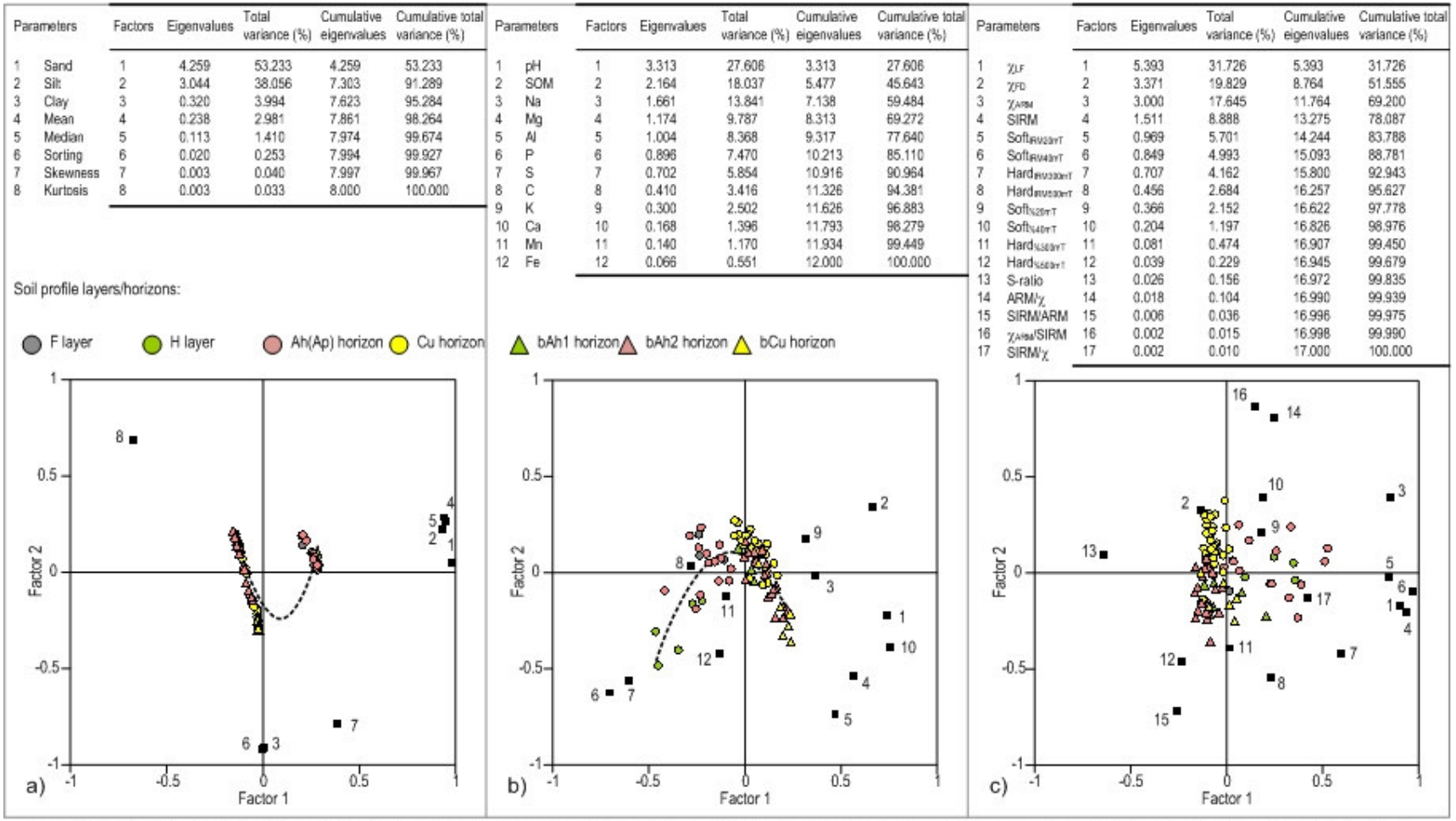

Figure 4.35 Summary results and simultaneous R- and Q-mode factor analysis plots of Factor 1 versus Factor 2, based on the pasture soil profile: a) textural characteristics; b) geochemical characteristics and c) mineral magnetic characteristics (dashed line represents postulated soil horizon development).

type' mineralogy. Cu samples are negatively loaded on Factor 1 and positively loaded on Factor 2, indicating increasing influence of a varied magnetic mineralogy and domain size down-profile. Most buried horizons are negatively loaded on both factors, suggesting a hard 'haematite-type' mineral influence.

4.4.4 Factor analysis of the scrub soil profile

Figure 4.36 shows the Factor plot for the scrub soil profile using all physico-chemical parameters. The first two factors extracted explain 59.89% of variation (Table 4.25). Factor 1 (organic content) explains 46.93% of variation in parameters, while Factor 2 explains 12.96%. The spread of parameter loadings along Factor 1 indicate textural and magnetic mineralogy parameters as the major influencing factors. L and H layers and Ah organic horizon samples have positive loadings on Factor 1, separating them from the mineral A and Cu horizon samples. Factor 2 appears to separate A horizon samples from Cu samples.

Figure 4.37a shows the textural factor plot, where the first two factors extracted explain 95.46% of variation in parameters. L and H layer and Ah horizon samples are negatively loaded on Factor 1 and positively loaded on Factor 2, separating them from the A and Cu samples by both factors. This suggests strong silt influences in the upper organic section of the profile with increasing sand and clay influences with depth. Figure 4.37b shows the geochemical factor plot, where the first two factors extracted explain 65.19% of variation in parameters. L and H layer and Ah horizon samples are positively loaded on Factor 1 and most are negatively loaded on Factor 2, suggesting strong SOM, S, P, Mn and Fe influences. Most A and Cu horizon sample points are negatively loaded on Factor 1, suggesting an influence of K and pH. The position of Cl in the centre of the plot indicates this parameter has no influence on any of the sample populations.

Figure 4.37c shows the mineral magnetic factor plot, where the first two factors extracted explain 63.36% of variation in parameters. L layer samples are positively loaded on Factor 1 and negatively loaded on Factor 2, indicating a very strong influence by magnetic domain size. H layer and Ah horizon samples are positively loaded on Factor 1, but evenly distributed on Factor 2. This also suggests a magnetic domain size influence, but highlights the increasing influence of magnetic concentration and mineralogy in these horizons. A horizon samples are exclusively negatively loaded on both factors, indicating the importance of soft 'magnetite-type' minerals and domain sizes. Most Cu samples are negatively loaded on Factor 1 and positively loaded on Factor 2, indicating an increasing influence of magnetic domain size, alongside hard 'haematite-type' minerals, down-profile.

4.4.5 Factor analysis of the slack soil profile

Figure 4.38 shows the factor plot for the slack soil profile using all physico-chemical parameters. The first two factors extracted explain 48.51% of variation (Table 4.26). Factor 1 explains 25.83% of variation in parameters, while Factor 2 explains 22.68%. The spread of parameter

Table 4.25 Summary results from factor analysis of the scrub soil profile using all parameters

Factors	Eigenvalues	Total variance (%)	Cumulative eigenvalues	Cumulative total variance (%)
1	17.366	46.934	17.366	46.934
2	4.794	12.956	22.159	59.890
3	2.630	7.108	24.789	66.998
4	1.827	4.939	26.616	71.936
5	1.761	4.761	28.378	76.697
6	1.704	4.604	30.082	81.301
7	1.090	2.947	31.172	84.248
8	1.030	2.785	32.202	87.033
9	0.811	2.193	33.014	89.226
10	0.712	1.926	33.726	91.152
11	0.541	1.463	34.268	92.615
12	0.486	1.314	34.754	93.929
13	0.421	1.138	35.175	95.067
14	0.363	0.981	35.538	96.048
15	0.299	0.807	35.836	96.855
16	0.270	0.729	36.106	97.584
17	0.196	0.530	36.302	98.114
18	0.156	0.421	36.458	98.535
19	0.149	0.402	36.607	98.938
20	0.103	0.279	36.710	99.217
21	0.087	0.235	36.797	99.453
22	0.050	0.134	36.847	99.587
23	0.035	0.095	36.882	99.681
24	0.028	0.076	36.910	99.757
25	0.023	0.062	36.933	99.819
26	0.019	0.052	36.952	99.871
27	0.013	0.034	36.965	99.905
28	0.011	0.030	36.976	99.936
29	0.010	0.027	36.986	99.963
30	0.006	0.017	36.993	99.980
31	0.004	0.010	36.996	99.990
32	0.002	0.004	36.998	99.995
33	0.001	0.002	36.999	99.997
34	0.001	0.002	36.999	99.999
35	0.000	0.001	37.000	100.000
36	0.000	0.000	37.000	100.000
37	0.000	0.000	37.000	100.000

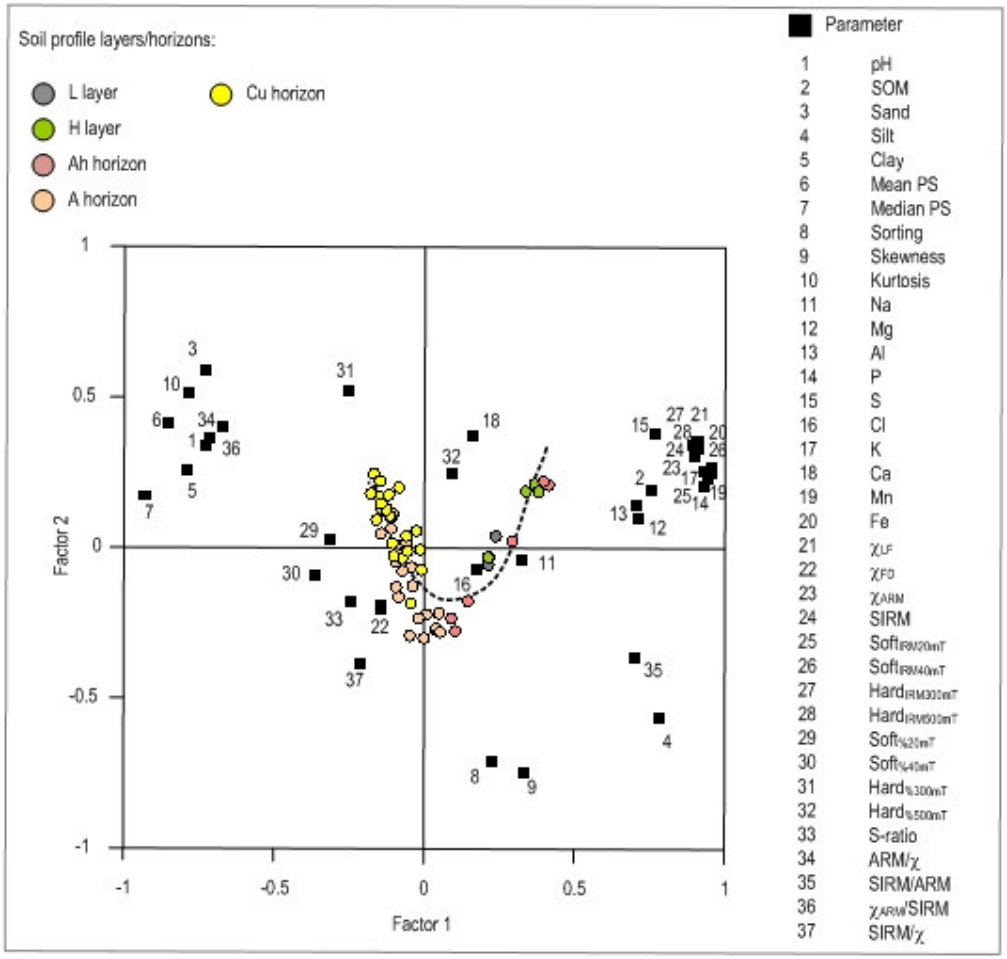

Figure 4.36 Simultaneous R- and Q-mode factor analysis plots of Factor 1 versus Factor 2, based on the scrub soil profile characteristics (dashed line represents postulated soil horizon development).

	Parameters	Factors	Eigenvalues	Total variance (%)	Cumulative eigenvalues	Cumulative total variance (%)
1	Sand	1	6.354	79.426	6.354	79.426
2	Silt	2	1.283	16.035	7.637	95.462
3	Clay	3	0.222	2.774	7.859	98.236
4	Mean	4	0.091	1.136	7.950	99.371
5	Median	5	0.030	0.374	7.980	99.746
6	Sorting	6	0.017	0.218	7.997	99.963
7	Skewness	7	0.003	0.037	8.000	100.000
8	Kurtosis	8	0.000	0.000	8.000	100.000

	Parameters	Factors	Eigenvalues	Total variance (%)	Cumulative eigenvalues	Cumulative total variance (%)
1	pH	1	5.904	49.198	5.904	49.198
2	SOM	2	1.919	15.990	7.823	65.188
3	Na	3	1.110	9.247	8.932	74.435
4	Mg	4	0.980	8.170	9.913	82.605
5	Al	5	0.683	5.688	10.595	88.293
6	P	6	0.415	3.462	11.011	91.755
7	S	7	0.385	3.206	11.395	94.962
8	C	8	0.197	1.643	11.593	96.605
9	K	9	0.168	1.400	11.761	98.005
10	Ca	10	0.151	1.262	11.912	99.266
11	Mn	11	0.059	0.491	11.971	99.757
12	Fe	12	0.029	0.243	12.000	100.000

	Parameters	Factors	Eigenvalues	Total variance (%)	Cumulative eigenvalues	Cumulative total variance (%)
1	χ_{LF}	1	8.220	48.355	8.220	48.355
2	χ_{FD}	2	2.551	15.007	10.772	63.362
3	χ_{ARM}	3	1.615	9.498	12.386	72.860
4	SIRM	4	1.184	6.965	13.570	79.825
5	$Soft_{BV20mT}$	5	0.971	5.711	14.541	85.537
6	$Soft_{BV40mT}$	6	0.844	4.962	15.385	90.499
7	$Hard_{BV300mT}$	7	0.590	3.471	15.975	93.970
8	$Hard_{BV500mT}$	8	0.485	2.853	16.460	96.823
9	$Soft_{N20mT}$	9	0.390	2.294	16.850	99.117
10	$Soft_{N40mT}$	10	0.062	0.366	16.912	99.484
11	$Hard_{N300mT}$	11	0.045	0.263	16.957	99.746
12	$Hard_{N500mT}$	12	0.021	0.123	16.978	99.869
13	S-ratio	13	0.010	0.061	16.988	99.930
14	ARM/χ	14	0.007	0.039	16.995	99.969
15	SIRM/ARM	15	0.004	0.022	16.999	99.991
16	χ_{ARM}/SIRM	16	0.001	0.008	17.000	99.999
17	SIRM/χ	17	0.000	0.001	17.000	100.000

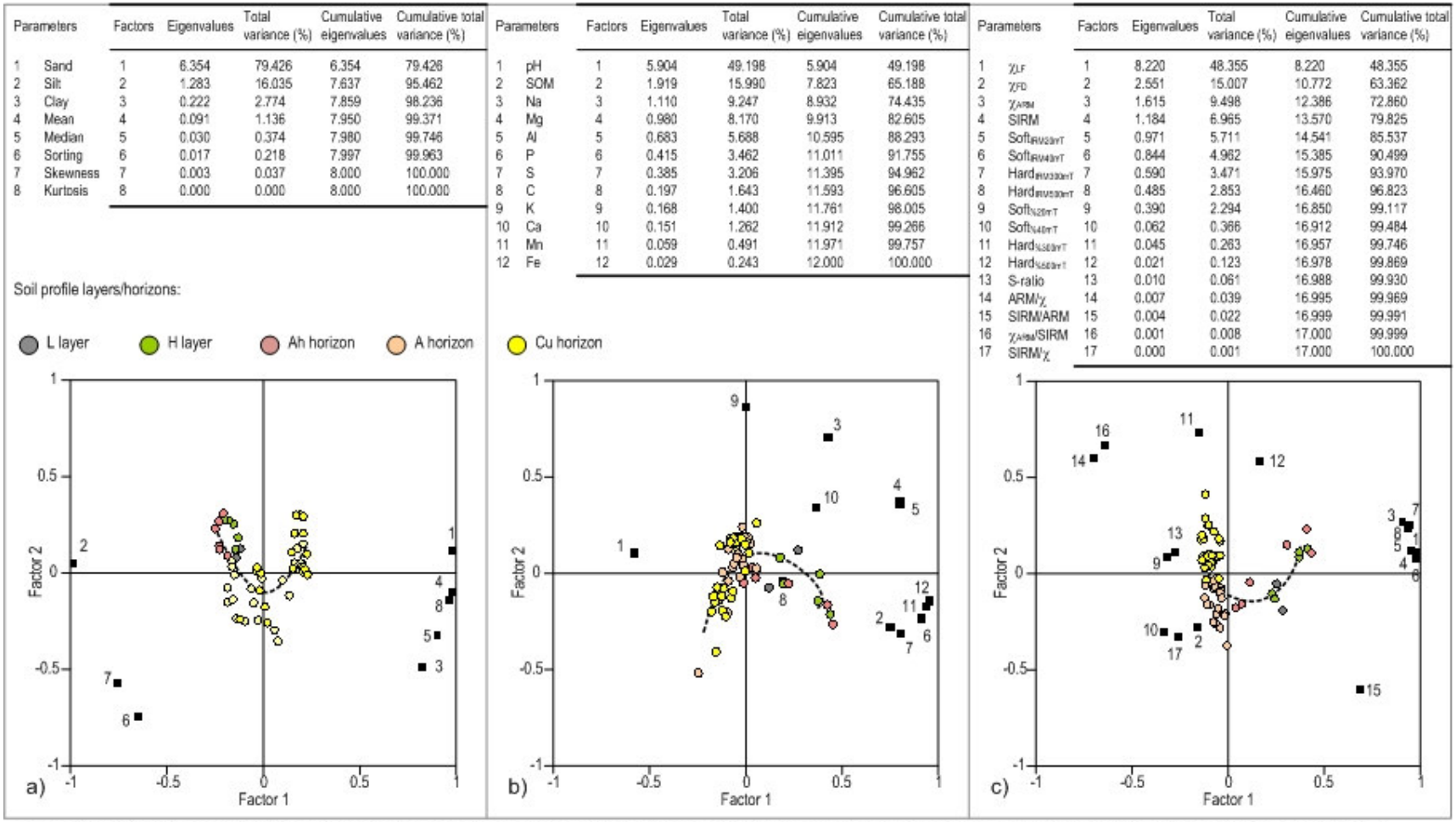

Figure 4.37 Summary results and simultaneous R- and Q-mode factor analysis plots of Factor 1 versus Factor 2, based on the scrub soil profile: a) textural characteristics; b) geochemical characteristics and c) mineral magnetic characteristics (dashed line represents postulated soil horizon development).

Table 4.26 Summary results from factor analysis of the slack soil profile using all parameters

Factors	Eigenvalues	Total variance (%)	Cumulative eigenvalues	Cumulative total variance (%)
1	9.556	25.826	9.556	25.826
2	8.391	22.680	17.947	48.506
3	3.776	10.206	21.723	58.712
4	3.101	8.380	24.824	67.092
5	2.449	6.620	27.274	73.712
6	2.173	5.872	29.446	79.584
7	1.591	4.300	31.037	83.884
8	1.032	2.788	32.069	86.673
9	0.718	1.940	32.787	88.613
10	0.686	1.853	33.472	90.466
11	0.512	1.384	33.984	91.850
12	0.498	1.346	34.483	93.196
13	0.384	1.038	34.867	94.234
14	0.349	0.942	35.215	95.177
15	0.340	0.920	35.556	96.096
16	0.234	0.634	35.790	96.730
17	0.221	0.597	36.011	97.327
18	0.191	0.516	36.202	97.843
19	0.168	0.455	36.370	98.297
20	0.133	0.360	36.503	98.657
21	0.107	0.290	36.611	98.947
22	0.102	0.274	36.712	99.222
23	0.084	0.228	36.797	99.450
24	0.061	0.166	36.858	99.616
25	0.047	0.128	36.905	99.744
26	0.037	0.101	36.943	99.845
27	0.023	0.063	36.966	99.908
28	0.013	0.036	36.979	99.944
29	0.011	0.029	36.990	99.973
30	0.005	0.014	36.995	99.986
31	0.003	0.009	36.998	99.995
32	0.001	0.003	36.999	99.998
33	0.001	0.001	37.000	100.000
34	0.000	0.000	37.000	100.000
35	0.000	0.000	37.000	100.000
36	0.000	0.000	37.000	100.000
37	0.000	0.000	37.000	100.000

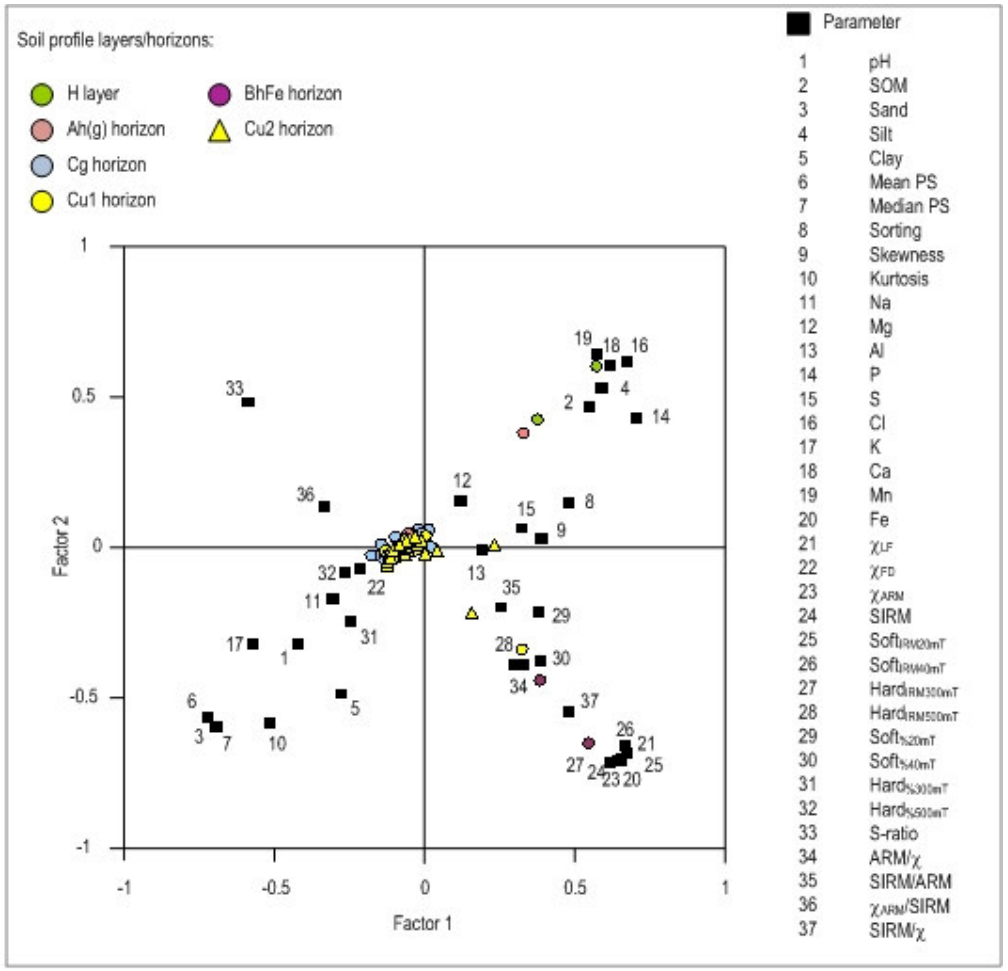

Figure 4.38 Simultaneous R- and Q-mode factor analysis plots of Factor 1 versus Factor 2, based on the slack soil profile characteristics.

loadings along Factor 1 indicate mineralogy as the major influencing factor. H layer samples are positively loaded on both factors. Factor 2 appears to separate the Cg and Cu samples from the upper organic layers.

Figure 4.39a shows the textural factor plot, where the first two factors extracted explain 88.51% of variation in parameters. H layer and some Ah(g) horizon samples are negatively loaded on Factor 1 and positively loaded on Factor 2, separating them from the Cg and Cu samples by both factors. This suggests strong silt influences in the upper organic section of the profile, with increasing sand and clay influences with depth.

Figure 4.39b shows the geochemical factor plot, where the first two factors extracted explain 61.80% of variation in parameters. The H layer samples are positively loaded on Factor 1 and negatively loaded on Factor 2, suggesting strong SOM, Cl, Mn, Ca and P influences, while Ah samples are positively loaded on both factors, representing influences of SOM, Cl and S. Cg horizon samples are positively loaded on Factor 2, displaying similar influences to the overlying Ah horizon samples. The BhFe samples are interspersed with the Cu samples, which all appear to be influenced by Fe, Na, K and pH.

Figure 4.39c shows the mineral magnetic factor plot, where the first two factors extracted explain 65.59% of variation in parameters. Most samples are negatively loaded on Factor 1 (Fe influences), the distribution of which suggests a soft 'magnetite-type' to hard 'haematite-type' mineral transition down-profile, represented by Factor 2 (depth). However, the BhFe samples are positively loaded on Factor 1, indicating very high magnetic concentrations in this horizon.

4.4.6 Factor analysis of the deciduous woodland soil profile

Figure 4.40 shows the factor plot for the deciduous woodland soil profile using all physico-chemical parameters. The first two factors extracted explain 61.03% of variation (Table 4.27). Factor 1 (organic content) explains 43.94% of variation in parameters, while Factor 2 explains 17.09%. The spread of parameter loadings along Factor 1 indicate texture and mineralogy as the major influencing factors. L layer samples are positively loaded on both factors, separated from the Ah and B horizon samples by Factor 1 and separated from Cu samples by Factor 2.

Figure 4.41a shows the textural factor plot, where the first two factors extracted explain 82.92% of variation in parameters. Most of L and H layer and Ah horizon samples are negatively loaded on Factor 1 and positively loaded on Factor 2, separating them from the B and Cu samples, suggesting a strong silt influence in these upper organic horizons. B horizon samples are negatively loaded on both factors, indicating particle sorting and skewness influences. Most Cu samples are positively loaded on Factor 1, influenced by sand and clay.

Figure 4.41b shows the geochemical factor plot, where the first two factors extracted explain 74.29% of variation in parameters. L layer samples are positively loaded on both factors,

Parameters		Factors	Eigenvalues	Total variance (%)	Cumulative eigenvalues	Cumulative total variance (%)
1	Sand	1	5.184	64.799	5.184	64.799
2	Silt	2	1.897	23.712	7.081	88.511
3	Clay	3	0.532	6.655	7.613	95.166
4	Mean	4	0.256	3.199	7.869	98.365
5	Median	5	0.095	1.191	7.965	99.556
6	Sorting	6	0.033	0.410	7.997	99.966
7	Skewness	7	0.003	0.034	8.000	100.000
8	Kurtosis	8	0.000	0.000	8.000	100.000

Parameters		Factors	Eigenvalues	Total variance (%)	Cumulative eigenvalues	Cumulative total variance (%)
1	pH	1	5.169	43.075	5.169	43.075
2	SOM	2	2.247	18.724	7.416	61.799
3	Na	3	1.697	14.146	9.113	75.945
4	Mg	4	1.030	8.583	10.143	84.528
5	Al	5	0.681	5.676	10.824	90.204
6	P	6	0.342	2.847	11.166	93.051
7	S	7	0.309	2.572	11.475	95.623
8	C	8	0.227	1.896	11.702	97.519
9	K	9	0.104	0.868	11.806	98.387
10	Ca	10	0.103	0.858	11.909	99.244
11	Mn	11	0.065	0.546	11.975	99.790
12	Fe	12	0.025	0.210	12.000	100.000

Parameters		Factors	Eigenvalues	Total variance (%)	Cumulative eigenvalues	Cumulative total variance (%)
1	χ_{LF}	1	8.490	49.942	8.490	49.942
2	χ_{FD}	2	2.660	15.645	11.150	65.587
3	χ_{ARM}	3	2.423	14.255	13.573	79.842
4	SIRM	4	0.985	5.792	14.558	85.634
5	$Soft_{BW30mT}$	5	0.932	5.482	15.490	91.116
6	$Soft_{BW40mT}$	6	0.474	2.787	15.964	93.903
7	$Hard_{BW300mT}$	7	0.332	1.951	16.295	95.854
8	$Hard_{BW500mT}$	8	0.254	1.494	16.549	97.349
9	$Soft_{N25mT}$	9	0.207	1.219	16.756	98.568
10	$Soft_{N40mT}$	10	0.125	0.735	16.881	99.302
11	$Hard_{N300mT}$	11	0.073	0.429	16.954	99.731
12	$Hard_{N500mT}$	12	0.038	0.221	16.992	99.952
13	S-ratio	13	0.006	0.033	16.997	99.985
14	ARM/χ	14	0.002	0.009	16.999	99.994
15	SIRM/ARM	15	0.001	0.005	17.000	100.000
16	χ_{ARM}/SIRM	16	0.000	0.000	17.000	100.000
17	SIRM/χ	17	0.000	0.000	17.000	100.000

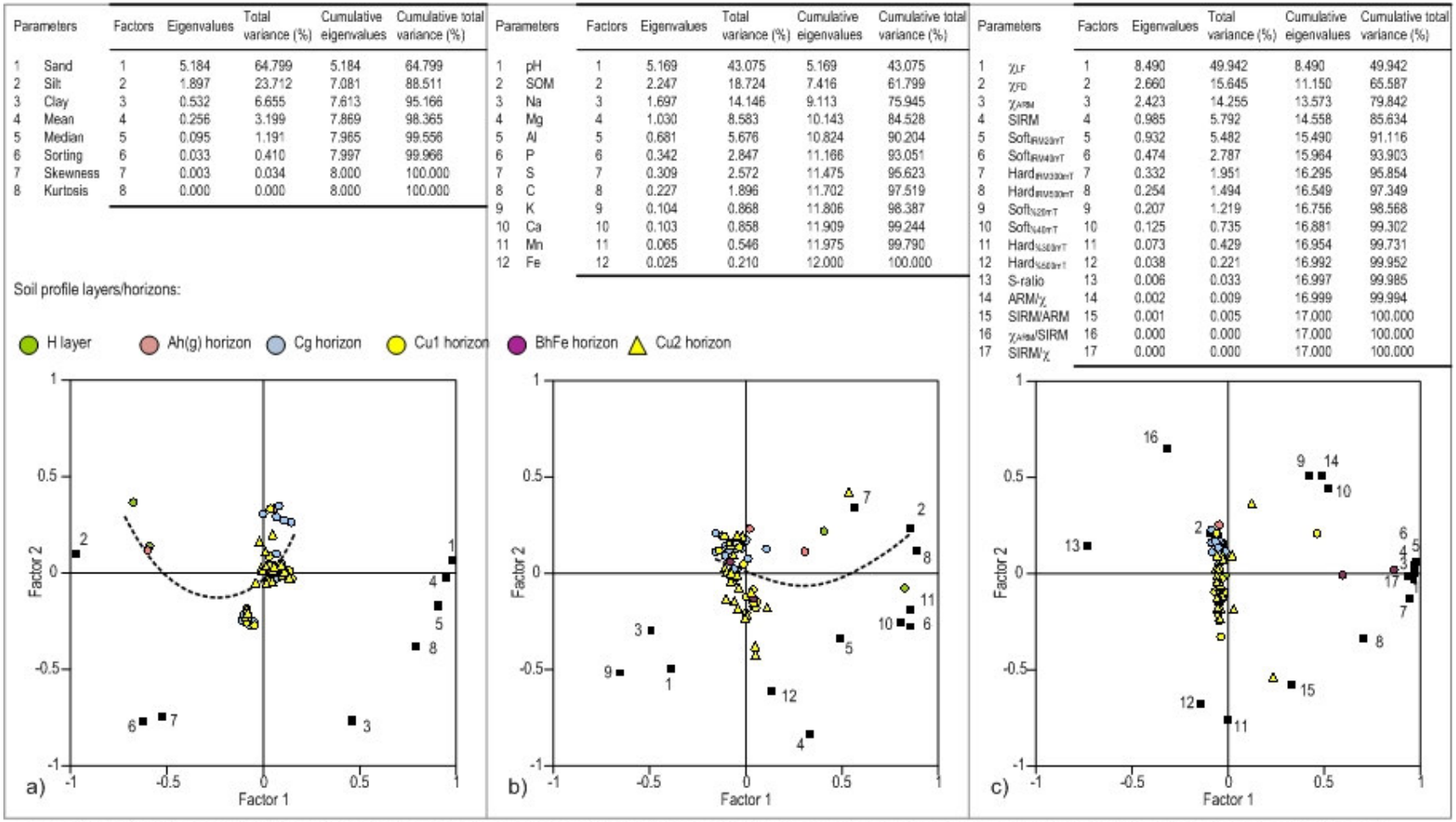

Figure 4.39 Summary results and simultaneous R- and Q-mode factor analysis plots of Factor 1 versus Factor 2, based on the slack soil profile: a) textural characteristics; b) geochemical characteristics and c) mineral magnetic characteristics (dashed line represents postulated soil horizon development).

Table 4.27 Summary results from factor analysis of the deciduous woodland soil profile using all parameters

Factors	Eigenvalues	Total variance (%)	Cumulative eigenvalues	Cumulative total variance (%)
1	16.259	43.942	16.259	43.942
2	6.323	17.090	22.582	61.032
3	3.315	8.961	25.897	69.993
4	2.440	6.594	28.337	76.586
5	1.503	4.063	29.840	80.649
6	1.231	3.327	31.071	83.976
7	1.130	3.054	32.201	87.030
8	0.849	2.295	33.050	89.324
9	0.727	1.966	33.777	91.290
10	0.622	1.682	34.400	92.972
11	0.483	1.306	34.883	94.278
12	0.387	1.045	35.270	95.323
13	0.320	0.864	35.589	96.187
14	0.301	0.814	35.891	97.002
15	0.257	0.694	36.148	97.696
16	0.184	0.497	36.332	98.193
17	0.149	0.402	36.480	98.596
18	0.129	0.349	36.610	98.945
19	0.085	0.229	36.695	99.174
20	0.056	0.151	36.750	99.325
21	0.050	0.135	36.800	99.460
22	0.047	0.126	36.847	99.586
23	0.038	0.104	36.885	99.690
24	0.029	0.078	36.914	99.769
25	0.023	0.062	36.937	99.831
26	0.019	0.052	36.956	99.882
27	0.016	0.044	36.973	99.926
28	0.008	0.020	36.980	99.946
29	0.007	0.018	36.987	99.965
30	0.005	0.014	36.992	99.979
31	0.004	0.012	36.997	99.991
32	0.002	0.005	36.998	99.996
33	0.001	0.003	36.999	99.998
34	0.000	0.001	37.000	99.999
35	0.000	0.001	37.000	100.000
36	0.000	0.000	37.000	100.000
37	0.000	0.000	37.000	100.000

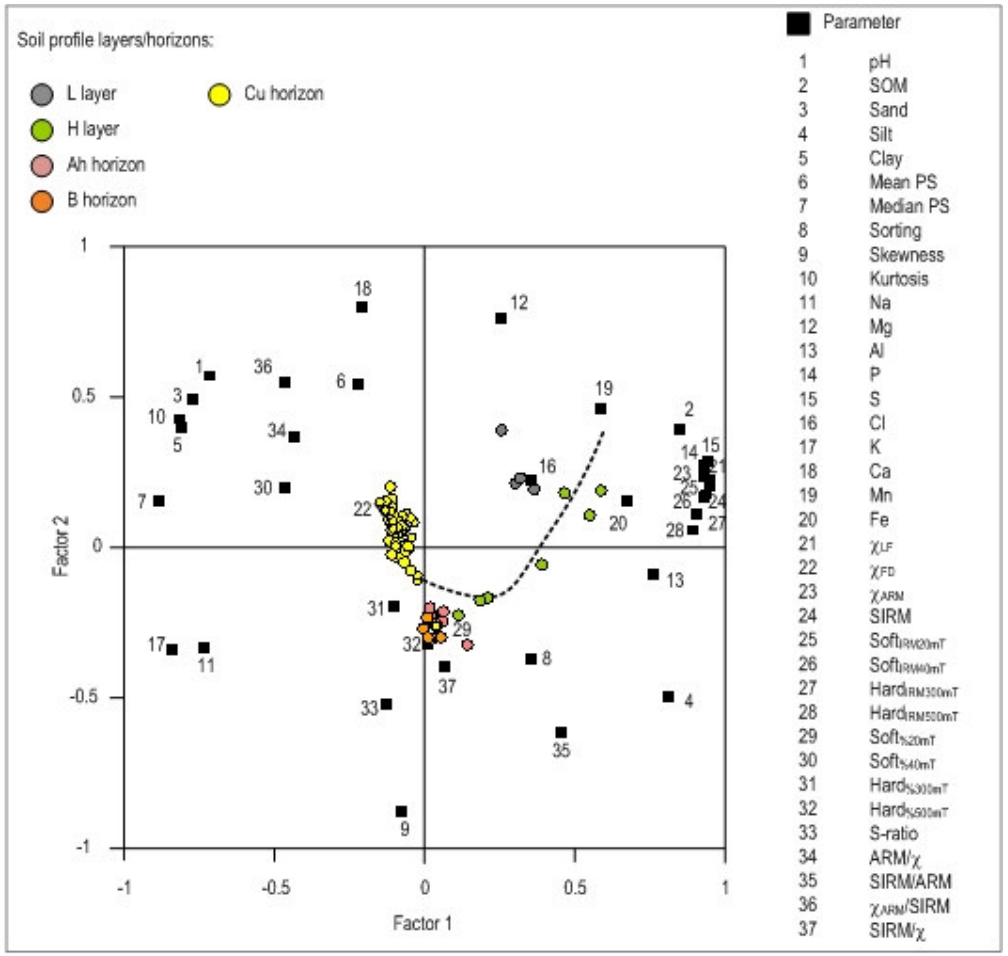

Figure 4.40 Simultaneous R- and Q-mode factor analysis plots of Factor 1 versus Factor 2, based on the deciduous woodland soil profile characteristics (dashed line represents postulated soil horizon development).

Parameters		Factors	Eigenvalues	Total variance (%)	Cumulative eigenvalues	Cumulative total variance (%)
1	Sand	1	5.378	67.229	5.378	67.229
2	Silt	2	1.255	15.694	6.634	82.923
3	Clay	3	0.916	11.454	7.550	94.377
4	Mean	4	0.357	4.459	7.907	98.836
5	Median	5	0.047	0.589	7.954	99.425
6	Sorting	6	0.032	0.402	7.986	99.827
7	Skewness	7	0.014	0.173	8.000	100.000
8	Kurtosis	8	0.000	0.000	8.000	100.000

Parameters		Factors	Eigenvalues	Total variance (%)	Cumulative eigenvalues	Cumulative total variance (%)
1	pH	1	6.595	54.955	6.595	54.955
2	SOM	2	2.321	19.338	8.915	74.294
3	Na	3	0.959	7.992	9.874	82.286
4	Mg	4	0.834	6.950	10.708	89.235
5	Al	5	0.463	3.857	11.171	93.093
6	P	6	0.358	2.981	11.529	96.074
7	S	7	0.192	1.600	11.721	97.673
8	C	8	0.126	1.051	11.847	98.724
9	K	9	0.068	0.568	11.915	99.293
10	Ca	10	0.052	0.434	11.967	99.726
11	Mn	11	0.020	0.166	11.987	99.893
12	Fe	12	0.013	0.107	12.000	100.000

Parameters		Factors	Eigenvalues	Total variance (%)	Cumulative eigenvalues	Cumulative total variance (%)
1	χ_{LF}	1	7.458	43.873	7.458	43.873
2	χ_{FD}	2	3.157	18.569	10.615	62.442
3	χ_{ARM}	3	2.270	13.353	12.885	75.795
4	SIRM	4	1.225	7.203	14.110	82.998
5	$Soft_{BV20mT}$	5	0.966	5.682	15.076	88.680
6	$Soft_{BV40mT}$	6	0.689	4.053	15.765	92.733
7	$Hard_{BV300mT}$	7	0.408	2.397	16.172	95.130
8	$Hard_{BV500mT}$	8	0.347	2.041	16.519	97.171
9	$Soft_{N20mT}$	9	0.323	1.900	16.842	99.071
10	$Soft_{N40mT}$	10	0.073	0.430	16.915	99.501
11	$Hard_{N300mT}$	11	0.040	0.234	16.955	99.735
12	$Hard_{N500mT}$	12	0.026	0.150	16.981	99.885
13	S-ratio	13	0.010	0.059	16.990	99.944
14	ARM/χ	14	0.006	0.033	16.996	99.977
15	SIRM/ARM	15	0.002	0.013	16.998	99.990
16	χ_{ARM}/SIRM	16	0.001	0.006	16.999	99.996
17	SIRM/χ	17	0.001	0.004	17.000	100.000

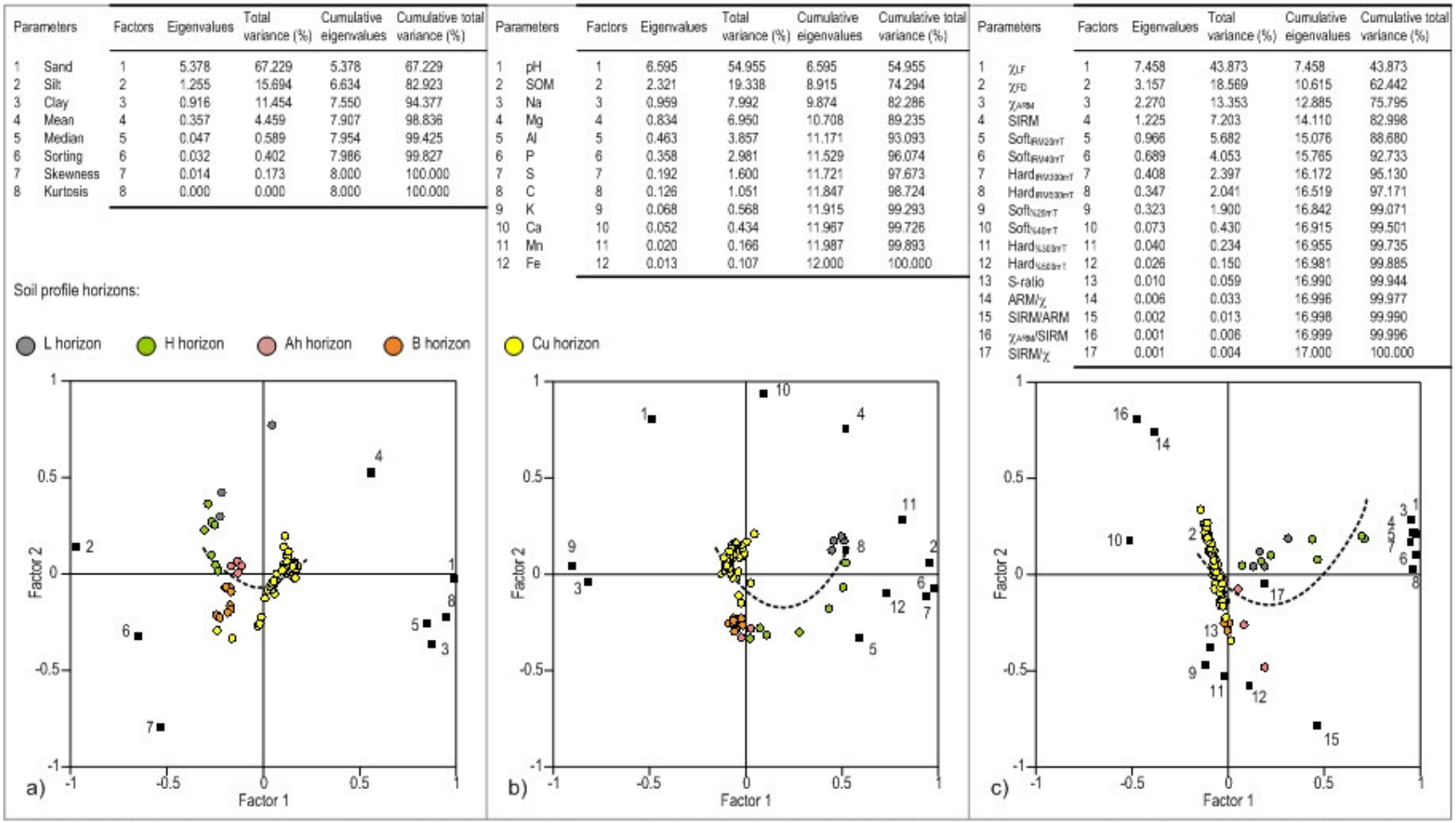

Figure 4.41 Summary results and simultaneous R- and Q-mode factor analysis plots of Factor 1 versus Factor 2, based on the deciduous woodland soil profile: a) textural characteristics; b) geochemical characteristics and c) mineral magnetic characteristics (dashed line represents postulated soil horizon development).

influenced by SOM, Cl and Mn. Most H layer samples are positively loaded on Factor 1 and negatively loaded on Factor 2. The postulated pedogenesis line indicates a decreasing influence of SOM, P and S, alongside increasing influences of Al, with H layer depth. This pattern continues through the Ah horizon and into the B horizon, which is negatively loaded on both factors. Most Cu samples are negatively loaded on Factor 1 and positively loaded on Factor 2, influenced by Na, K and pH.

Figure 4.41c shows the mineral magnetic factor plot, where the first two factors extracted explain 62.44% of variation in parameters. All L and H layer samples are positively loaded on both factors, indicating high magnetic concentrations of varying magnetic mineralogy. Most Ah horizon samples are positively loaded on Factor 1 and negatively loaded on Factor 2, suggesting this horizon is dominated by hard 'haematite-type' mineralogy. B horizon samples are negatively loaded on both factors, suggesting a varied mineralogy that becomes increasingly soft 'magnetite-type' with depth into the Cu horizon.

4.4.7 Factor analysis of the heath soil profile

Figure 4.42 shows the factor plot for the heath soil profile using all physico-chemical parameters. The first two factors extracted explain 56.36% of variation (Table 4.28). Factor 1 (depth) explains 31.28% of variation in parameters, while Factor 2 (organic content) explains 25.08%. The spread of parameter loadings along Factor 1 indicates mineralogy and grain size as the major influencing factors, however, the position of $Soft_{\%20mT}$ and $Soft_{\%40mT}$ in the centre of the plot indicate these parameters have no influence on the samples. The H layer and Ah and B horizon samples are separated from Cu horizon samples by Factor 2; whereas, Factor 1 separates the B and Cu horizons from the Ah, H and L samples.

Figure 4.43a shows the textural factor plot, where the first two factors extracted explain 87.38% of variation in parameters. L layers are negatively loaded on both factors, displaying some influence with mean particle size. However, H layer and Ah and B horizon samples are positively loaded on Factor 1, with the majority negatively loaded on Factor 2, influenced by clay and silt. Cu samples are mainly influenced by sand.

Figure 4.43b shows the geochemical factor plot, where the first two factors extracted explain 65.11% of variation in parameters. H layer samples are positively loaded on both factors, along with most Ah horizon samples, displaying a strong influence by pH, but only slight influences by SOM, Cl, P and S. B horizon samples are positively loaded on Factor 2, showing similar influences to the overlying Ah horizon population, but also displaying an increasing Na influence. Most Cu samples are negatively loaded on Factor 1, influenced by Na, K, Mn, Mg, Fe and Ca.

Figure 4.43c shows the mineral magnetic factor plot, where the first two factors extracted explain 60.21% of variation in parameters. L layer samples, along with most H layer samples,

Table 4.28 Summary results from factor analysis of the heath soil profile using all parameters

Factors	Eigenvalues	Total variance (%)	Cumulative eigenvalues	Cumulative total variance (%)
1	11.574	31.281	11.574	31.281
2	9.280	25.081	20.854	56.362
3	5.079	13.726	25.933	70.088
4	2.130	5.757	28.063	75.845
5	1.354	3.658	29.416	79.504
6	1.201	3.246	30.617	82.750
7	0.982	2.655	31.600	85.405
8	0.806	2.180	32.406	87.584
9	0.715	1.932	33.121	89.516
10	0.575	1.553	33.696	91.069
11	0.515	1.392	34.211	92.462
12	0.464	1.255	34.675	93.716
13	0.413	1.116	35.088	94.832
14	0.339	0.917	35.427	95.749
15	0.266	0.718	35.693	96.467
16	0.254	0.687	35.947	97.154
17	0.244	0.660	36.191	97.813
18	0.174	0.470	36.365	98.283
19	0.148	0.401	36.513	98.684
20	0.125	0.338	36.638	99.022
21	0.085	0.230	36.723	99.252
22	0.070	0.190	36.793	99.442
23	0.056	0.151	36.849	99.593
24	0.043	0.116	36.892	99.709
25	0.028	0.075	36.920	99.784
26	0.020	0.054	36.940	99.838
27	0.019	0.052	36.959	99.890
28	0.013	0.036	36.973	99.927
29	0.009	0.025	36.982	99.952
30	0.006	0.016	36.988	99.967
31	0.005	0.014	36.993	99.981
32	0.002	0.007	36.996	99.988
33	0.002	0.006	36.998	99.994
34	0.001	0.003	36.999	99.997
35	0.001	0.002	37.000	99.999
36	0.000	0.001	37.000	100.000
37	0.000	0.000	37.000	100.000

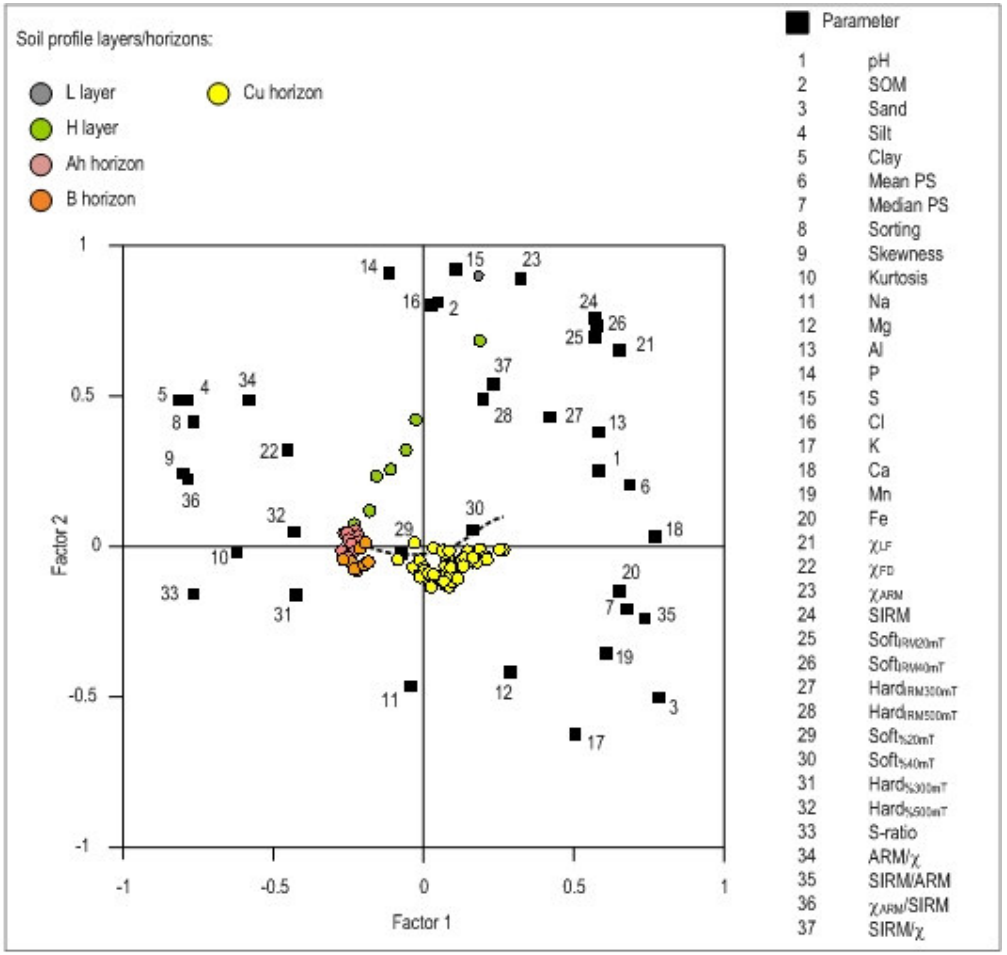

Figure 4.42 Simultaneous R- and Q-mode factor analysis plots of Factor 1 versus Factor 2, based on the heath soil profile characteristics (dashed line represents postulated soil horizon development).

Parameters		Factors	Eigenvalues	Total variance (%)	Cumulative eigenvalues	Cumulative total variance (%)
1	Sand	1	5.913	73.911	5.913	73.911
2	Silt	2	1.077	13.464	6.990	87.375
3	Clay	3	0.728	9.096	7.718	96.471
4	Mean	4	0.191	2.387	7.909	98.858
5	Median	5	0.046	0.578	7.955	99.436
6	Sorting	6	0.023	0.288	7.978	99.724
7	Skewness	7	0.012	0.150	7.990	99.874
8	Kurtosis	8	0.010	0.126	8.000	100.000

Parameters		Factors	Eigenvalues	Total variance (%)	Cumulative eigenvalues	Cumulative total variance (%)
1	pH	1	4.694	39.120	4.694	39.120
2	SOM	2	3.119	25.990	7.813	65.111
3	Na	3	1.504	12.535	9.317	77.646
4	Mg	4	0.778	6.485	10.096	84.131
5	Al	5	0.568	4.736	10.664	88.867
6	P	6	0.350	2.914	11.014	91.781
7	S	7	0.277	2.311	11.291	94.091
8	C	8	0.236	1.970	11.527	96.061
9	K	9	0.199	1.660	11.727	97.721
10	Ca	10	0.137	1.142	11.864	98.863
11	Mn	11	0.097	0.804	11.960	99.667
12	Fe	12	0.040	0.333	12.000	100.000

Parameters		Factors	Eigenvalues	Total variance (%)	Cumulative eigenvalues	Cumulative total variance (%)
1	χ_{LF}	1	6.704	39.437	6.704	39.437
2	χ_{FD}	2	3.532	20.776	10.236	60.212
3	χ_{ARM}	3	2.635	15.498	12.871	75.710
4	SIRM	4	1.293	7.606	14.164	83.316
5	$Soft_{BV20mT}$	5	0.846	4.979	15.010	88.296
6	$Soft_{BV40mT}$	6	0.630	3.707	15.640	92.003
7	$Hard_{BV300mT}$	7	0.617	3.630	16.258	95.632
8	$Hard_{BV500mT}$	8	0.404	2.375	16.661	98.007
9	$Soft_{N20mT}$	9	0.192	1.130	16.853	99.137
10	$Soft_{N40mT}$	10	0.069	0.405	16.922	99.543
11	$Hard_{N300mT}$	11	0.033	0.192	16.955	99.734
12	$Hard_{N500mT}$	12	0.025	0.145	16.979	99.879
13	S-ratio	13	0.010	0.060	16.990	99.939
14	ARM/χ	14	0.005	0.031	16.995	99.970
15	SIRM/ARM	15	0.003	0.015	16.997	99.985
16	χ_{ARM}/SIRM	16	0.002	0.011	16.999	99.996
17	SIRM/χ	17	0.001	0.004	17.000	100.000

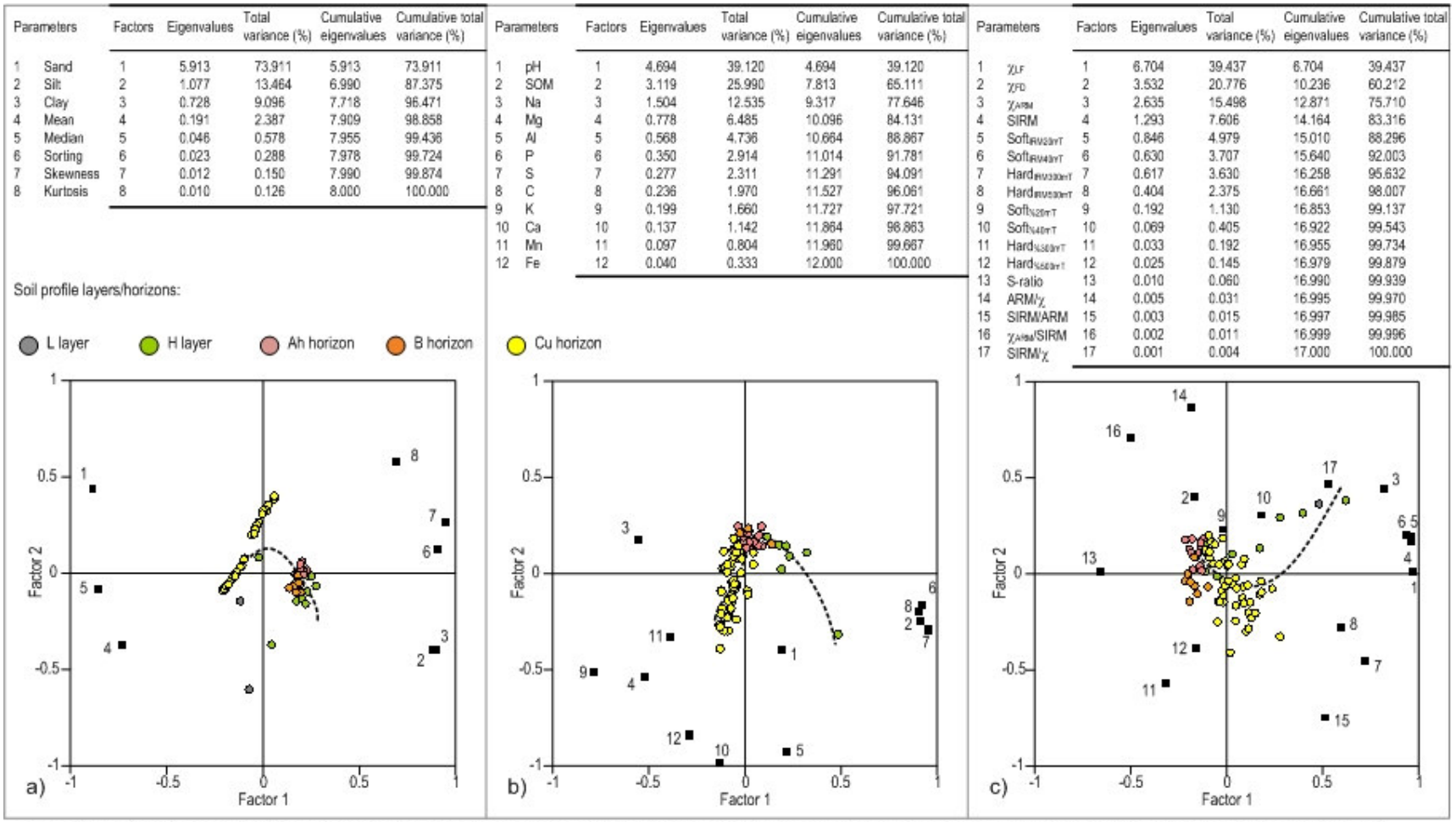

Figure 4.43 Summary results and simultaneous R- and Q-mode factor analysis plots of Factor 1 versus Factor 2, based on the heath soil profile: a) textural characteristics; b) geochemical characteristics and c) mineral magnetic characteristics (dashed line represents postulated soil horizon development).

are positively loaded on both factors, indicating high magnetic mineral concentrations. Ah horizon samples are negatively loaded on Factor 1 and positively loaded on Factor 2, suggesting this horizon is influenced by magnetic domain size. Most B horizon samples are negatively loaded on both factors, suggesting this horizon is dominated by hard 'haematite-type' mineralogy. Cu samples have both positive and negative loadings on both factors, but appear to be driven by hard 'haematite-type' minerals.

4.4.8 Factor analysis of the coniferous plantation soil profile

Figure 4.44 shows the factor plot for the coniferous plantation soil profile using all physico-chemical parameters. The first two factors extracted explain 62.84% of variation (Table 4.29). Factor 1 (organic content) explains 48.07% of variation in parameters, while Factor 2 explains 14.78%. The spread of parameter loadings along Factor 1 indicates mineralogy as the major influencing factor. Factor 2 divides the profile into organic and mineral sections.

Figure 4.45a shows the textural factor plot, where the first two factors extracted explain 89.80% of variation in parameters. L and H layers are negatively loaded on Factor 1 and positively loaded on Factor 2, displaying limited influence by textural variables. E horizon samples are negatively loaded on both factors, suggesting strong silt influences; whereas B horizon samples are just negatively loaded on Factor 2, displaying influences by silt and clay. Cu samples are positively loaded on both factors, mainly influenced by sand.

Figure 4.45b shows the geochemical factor plot, where the first two factors extracted explain 81.45% of variation in parameters. L layer samples are positively loaded on Factor 1, influenced by pH, SM, Mg, Ca, P and S. H layer samples are similar, but are increasingly influenced by Fe, Cl and Al. E horizon samples are negatively loaded on Factor 1 and positively loaded on Factor 2, displaying an increased influence of Na and K, which continues down-profile into the B and Cu horizons, where Mn becomes an important influencing factor.

Figure 4.45c shows the mineral magnetic factor plot, where the first two factors extracted explain 62.74% of variation in parameters. L and H layer samples are positively loaded on Factor 1, indicating high magnetic mineral concentrations and, as samples are dominated by ferrimagnetic minerals, SIRM/ARM influences indicate relative domain size variations. Most E horizon samples, along with all the B and Cu horizon samples, are negatively loaded on Factor 1, suggesting this horizon is influenced by magnetic domain size.

4.4.9 Factor analysis of the felled coniferous soil profile

Figure 4.46 shows the factor plot for the felled coniferous soil profile using all physico-chemical parameters. The first two factors extracted explain 51.17% of variation (Table 4.30). Factor 1 explains 39.29% of variation in parameters, while Factor 2 explains 11.88%. The spread of

Table 4.29 Summary results from factor analysis of the coniferous plantation soil profile using all parameters

Factors	Eigenvalues	Total variance (%)	Cumulative eigenvalues	Cumulative total variance (%)
1	17.784	48.065	17.784	48.065
2	5.467	14.775	23.251	62.840
3	3.435	9.284	26.686	72.124
4	2.543	6.873	29.229	78.997
5	1.559	4.214	30.788	83.211
6	0.979	2.645	31.767	85.856
7	0.939	2.537	32.705	88.393
8	0.808	2.185	33.514	90.578
9	0.642	1.735	34.156	92.313
10	0.536	1.450	34.692	93.763
11	0.486	1.312	35.178	95.075
12	0.357	0.964	35.534	96.039
13	0.308	0.834	35.843	96.873
14	0.283	0.766	36.126	97.638
15	0.189	0.512	36.316	98.150
16	0.163	0.441	36.479	98.591
17	0.132	0.358	36.611	98.949
18	0.109	0.293	36.720	99.242
19	0.056	0.151	36.776	99.393
20	0.048	0.129	36.823	99.523
21	0.043	0.115	36.866	99.638
22	0.034	0.091	36.900	99.729
23	0.030	0.081	36.930	99.810
24	0.024	0.065	36.954	99.875
25	0.015	0.040	36.969	99.915
26	0.009	0.025	36.978	99.940
27	0.007	0.018	36.984	99.958
28	0.005	0.014	36.990	99.972
29	0.004	0.010	36.993	99.982
30	0.003	0.008	36.996	99.990
31	0.002	0.005	36.998	99.995
32	0.001	0.002	36.999	99.997
33	0.001	0.002	37.000	99.999
34	0.000	0.001	37.000	99.999
35	0.000	0.000	37.000	100.000
36	0.000	0.000	37.000	100.000
37	0.000	0.000	37.000	100.000

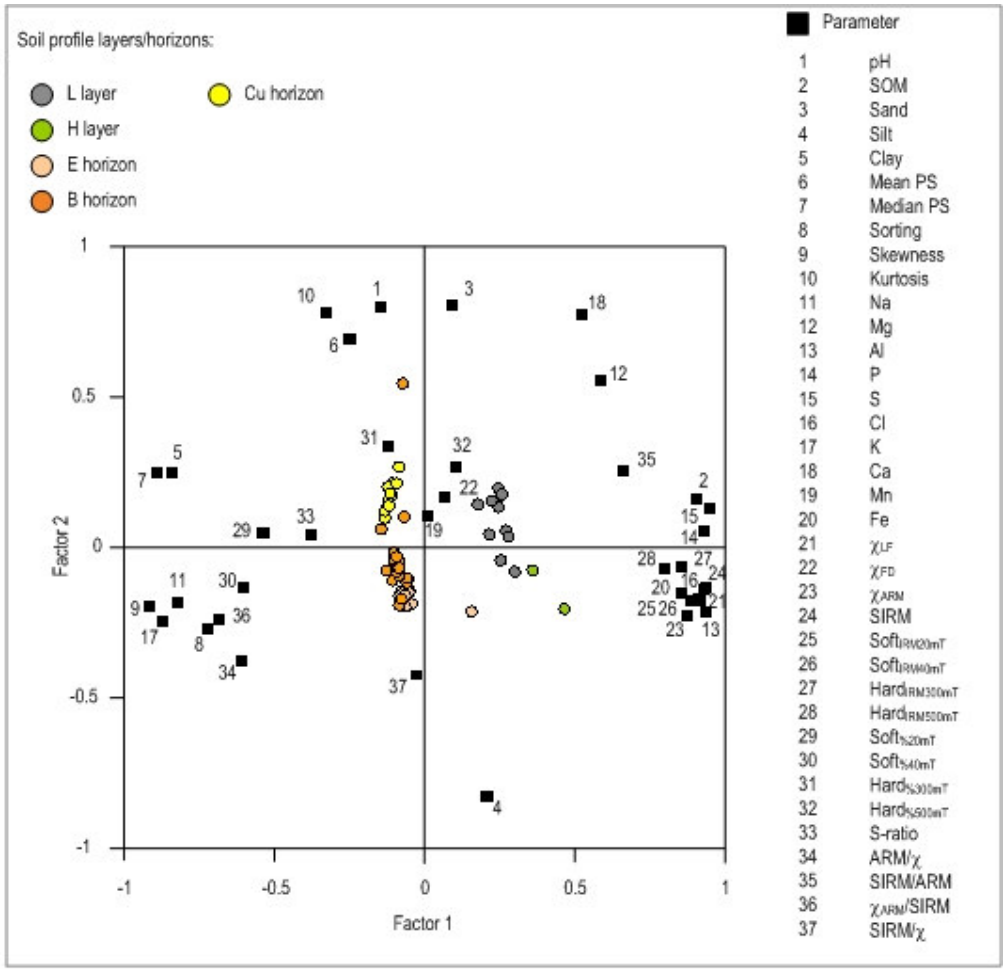

Figure 4.44 Simultaneous R- and Q-mode factor analysis plots of Factor 1 versus Factor 2, based on the coniferous plantation soil profile characteristics.

Parameters		Factors	Eigenvalues	Total variance (%)	Cumulative eigenvalues	Cumulative total variance (%)
1	Sand	1	4.148	51.845	4.148	51.845
2	Silt	2	3.037	37.959	7.184	89.804
3	Clay	3	0.474	5.923	7.658	95.727
4	Mean	4	0.212	2.645	7.870	98.372
5	Median	5	0.113	1.410	7.983	99.782
6	Sorting	6	0.015	0.193	7.998	99.975
7	Skewness	7	0.002	0.025	8.000	100.000
8	Kurtosis	8	0.000	0.000	8.000	100.000

Parameters		Factors	Eigenvalues	Total variance (%)	Cumulative eigenvalues	Cumulative total variance (%)
1	pH	1	7.626	63.546	7.626	63.546
2	SOM	2	2.149	17.907	9.774	81.453
3	Na	3	1.211	10.088	10.985	91.541
4	Mg	4	0.393	3.271	11.377	94.812
5	Al	5	0.198	1.654	11.576	96.466
6	P	6	0.174	1.453	11.750	97.918
7	S	7	0.086	0.713	11.836	98.632
8	C	8	0.069	0.577	11.905	99.209
9	K	9	0.052	0.430	11.957	99.639
10	Ca	10	0.023	0.195	11.980	99.834
11	Mn	11	0.015	0.121	11.995	99.955
12	Fe	12	0.005	0.045	12.000	100.000

Parameters		Factors	Eigenvalues	Total variance (%)	Cumulative eigenvalues	Cumulative total variance (%)
1	χ_{LF}	1	8.179	48.111	8.179	48.111
2	χ_{FD}	2	2.488	14.634	10.667	62.744
3	χ_{ARM}	3	2.301	13.537	12.968	76.281
4	SIRM	4	1.059	6.231	14.027	82.513
5	$Soft_{BV20mT}$	5	0.910	5.352	14.937	87.865
6	$Soft_{BV40mT}$	6	0.628	3.693	15.565	91.558
7	$Hard_{BV300mT}$	7	0.499	2.933	16.063	94.491
8	$Hard_{BV500mT}$	8	0.454	2.669	16.517	97.160
9	$Soft_{N20mT}$	9	0.270	1.586	16.787	98.746
10	$Soft_{N40mT}$	10	0.114	0.670	16.901	99.416
11	$Hard_{N300mT}$	11	0.048	0.280	16.948	99.696
12	$Hard_{N500mT}$	12	0.034	0.202	16.983	99.898
13	S-ratio	13	0.011	0.067	16.994	99.965
14	ARM/χ	14	0.003	0.018	16.997	99.983
15	SIRM/ARM	15	0.002	0.011	16.999	99.994
16	χ_{ARM}/SIRM	16	0.001	0.003	17.000	99.998
17	SIRM/χ	17	0.000	0.002	17.000	100.000

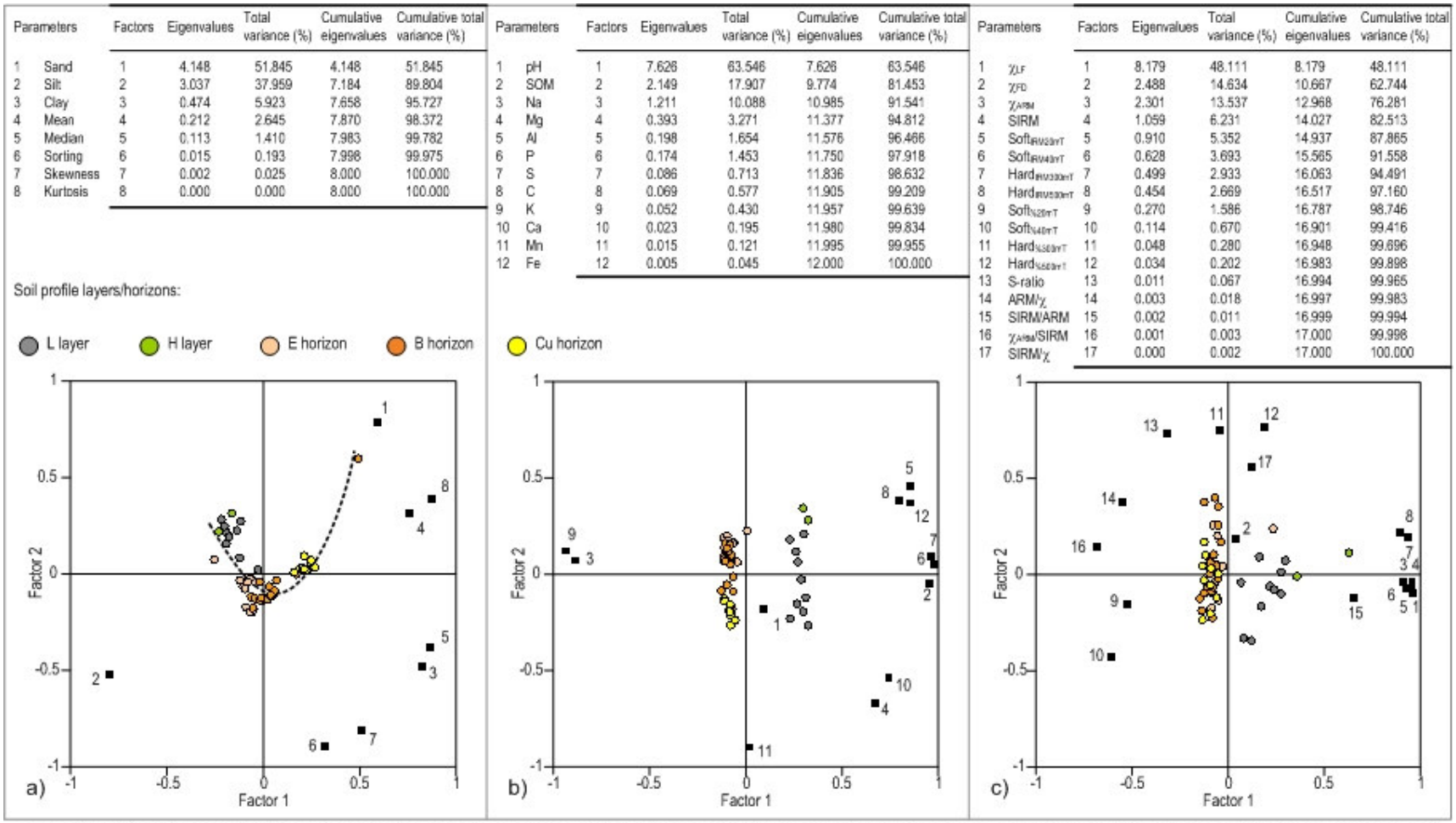

Figure 4.45 Summary results and simultaneous R- and Q-mode factor analysis plots of Factor 1 versus Factor 2, based on the coniferous plantation soil profile: a) textural characteristics; b) geochemical characteristics and c) mineral magnetic characteristics (dashed line represents postulated soil horizon development).

Table 4.30 Summary results from factor analysis of the felled coniferous plantation soil profile using all parameters

Factors	Eigenvalues	Total variance (%)	Cumulative eigenvalues	Cumulative total variance (%)
1	14.536	39.286	14.536	39.286
2	4.396	11.882	18.932	51.168
3	2.975	8.042	21.907	59.209
4	2.896	7.827	24.804	67.037
5	2.398	6.481	27.201	73.517
6	1.483	4.008	28.685	77.526
7	1.234	3.335	29.918	80.860
8	1.092	2.951	31.010	83.811
9	1.041	2.814	32.051	86.625
10	0.821	2.219	32.873	88.845
11	0.689	1.862	33.561	90.706
12	0.663	1.792	34.224	92.498
13	0.508	1.374	34.733	93.872
14	0.436	1.180	35.169	95.051
15	0.334	0.903	35.503	95.955
16	0.320	0.864	35.823	96.819
17	0.290	0.785	36.113	97.604
18	0.188	0.509	36.302	98.112
19	0.155	0.420	36.457	98.532
20	0.130	0.350	36.586	98.882
21	0.091	0.246	36.678	99.128
22	0.078	0.212	36.756	99.340
23	0.054	0.145	36.809	99.485
24	0.047	0.126	36.856	99.611
25	0.041	0.110	36.897	99.721
26	0.033	0.090	36.930	99.811
27	0.023	0.063	36.953	99.874
28	0.019	0.052	36.973	99.926
29	0.009	0.026	36.982	99.952
30	0.006	0.016	36.988	99.968
31	0.005	0.014	36.993	99.982
32	0.003	0.008	36.996	99.990
33	0.002	0.005	36.998	99.995
34	0.001	0.004	36.999	99.999
35	0.000	0.001	37.000	100.000
36	0.000	0.000	37.000	100.000
37	0.000	0.000	37.000	100.000

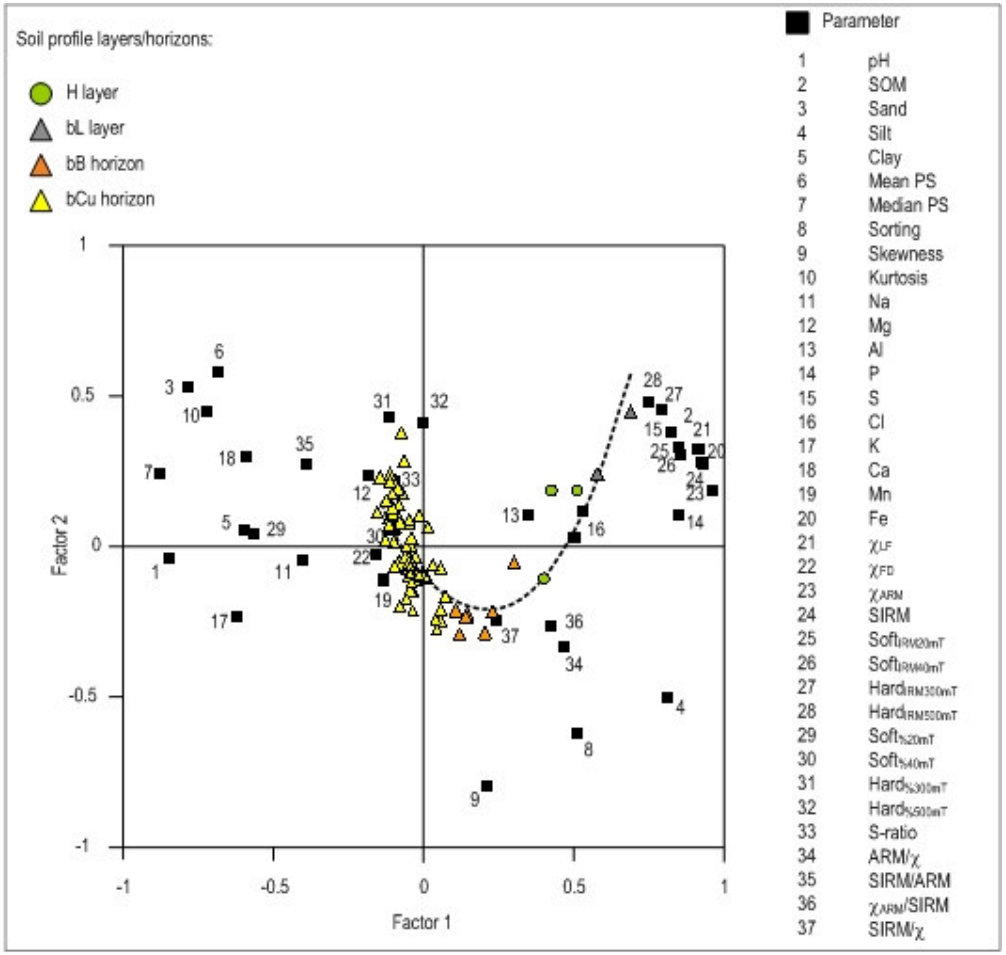

Figure 4.46 Simultaneous R- and Q-mode factor analysis plots of Factor 1 versus Factor 2, based on the felled coniferous plantation soil profile characteristics (dashed line represents postulated soil horizon development).

parameter loadings along Factor 1 indicates particle size and mineralogy as the major influencing factors.

Figure 4.47a shows the textural factor plot, where the first two factors extracted explain 89.64% of variation in parameters. H and bL layers are negatively loaded on Factor 1 and positively loaded on Factor 2, displaying slight silt influences. The bB horizon samples are negatively loaded on Factor 1, also displaying silt influences. Cu samples are positively and negatively loaded on both factors, suggesting stronger influences of sand and clay.

Figure 4.47b shows the geochemical factor plot, where the first two factors extracted explain 62.95% of variation in parameters. H layer samples are positively loaded on both factors, influenced by SOM, Cl, P and S; whereas, bL horizon samples are positively loaded on Factor 1 and negatively loaded on Factor 2, influenced solely by SOM. The bB horizon samples are positively loaded on Factor 1, influenced by SOM, Al and Fe. Most Cu samples are negatively loaded on Factor 1, influenced by Mn, Mg, Ca, Na, K and pH.

Figure 4.47c shows the mineral magnetic factor plot, where the first two factors extracted explain 58.01% of variation in parameters. Most H layer samples, along with all bL layer samples, are positively loaded on both factors, indicating high magnetic mineral concentrations. The bB horizon samples are positively loaded on Factor 1 and negatively loaded on Factor 2, slightly influenced by magnetic concentrations, but more importantly by magnetic domain size. Most Cu samples are negatively loaded on Factor 1, suggesting a magnetically soft 'magnetite-type' influence, becoming increasingly hard 'haematite-type' with depth.

4.5 Classification of soil profiles using multivariate factor analysis

Similarity in patterns between some soil profile factor plots allowed groupings to be made into classified NSRI profiles. Figure 4.48 summarizes these suggested results on individual soil profiles. Each profile is presented in postulated order of pedogenesis, following identification of pedogenic processes operating within each horizon. The strong influence of silt, SOM and Cl in the organic layer of the mobile dune soil profile suggests this represents terrestrial raw sand. Influences of both P and S in the H layers of the fixed dune and pasture soil profiles, alongside Cl in the Ah horizons, suggest these profiles are immature sand-pararendzinas. These soils have developed from terrestrial raw sand, having undergone leaching processes, which led to eluviation of Cl and resulted in desalinization. Mn and Ca storage in the upper layer of the slack soil profile suggests saturation through water-logging and provides evidence of gleying. Subsequent drying of slack environments involved the removal of Ca from the Ah and B horizons, evident in the deciduous woodland profile, resulting in decalcification, representative of brown earths. Increased SOM and acidity influences in both the heath and coniferous plantation soil profiles have led to podzolization. The following sections use multivariate factor analysis to group dune soil profiles into classified NSRI units and identify associations with dune environments.

Parameters		Factors	Eigenvalues	Total variance (%)	Cumulative eigenvalues	Cumulative total variance (%)
1	Sand	1	5.958	74.479	5.958	74.479
2	Silt	2	1.213	15.163	7.171	89.642
3	Clay	3	0.435	5.443	7.607	95.085
4	Mean	4	0.220	2.747	7.827	97.832
5	Median	5	0.109	1.363	7.936	99.195
6	Sorting	6	0.049	0.613	7.985	99.808
7	Skewness	7	0.015	0.192	8.000	100.000
8	Kurtosis	8	0.000	0.000	8.000	100.000

Parameters		Factors	Eigenvalues	Total variance (%)	Cumulative eigenvalues	Cumulative total variance (%)
1	pH	1	5.047	42.054	5.047	42.054
2	SOM	2	2.507	20.895	7.554	62.949
3	Na	3	1.327	11.057	8.881	74.006
4	Mg	4	0.864	7.196	9.744	81.202
5	Al	5	0.808	6.729	10.552	87.932
6	P	6	0.613	5.107	11.165	93.039
7	S	7	0.319	2.660	11.484	95.698
8	C	8	0.264	2.200	11.748	97.898
9	K	9	0.155	1.292	11.903	99.190
10	Ca	10	0.045	0.376	11.948	99.566
11	Mn	11	0.041	0.343	11.989	99.909
12	Fe	12	0.011	0.091	12.000	100.000

Parameters		Factors	Eigenvalues	Total variance (%)	Cumulative eigenvalues	Cumulative total variance (%)
1	χ_{LF}	1	7.066	41.566	7.066	41.566
2	χ_{FD}	2	2.795	16.442	9.861	58.008
3	χ_{ARM}	3	2.407	14.159	12.268	72.167
4	SIRM	4	1.310	7.707	13.579	79.874
5	$Soft_{BV20mT}$	5	1.127	6.628	14.705	86.502
6	$Soft_{BV40mT}$	6	0.823	4.842	15.528	91.344
7	$Hard_{BV300mT}$	7	0.637	3.745	16.165	95.089
8	$Hard_{BV500mT}$	8	0.416	2.447	16.581	97.537
9	$Soft_{N20mT}$	9	0.239	1.405	16.820	98.942
10	$Soft_{N40mT}$	10	0.076	0.444	16.896	99.386
11	$Hard_{N300mT}$	11	0.064	0.376	16.960	99.763
12	$Hard_{N500mT}$	12	0.020	0.117	16.979	99.879
13	S-ratio	13	0.011	0.067	16.991	99.946
14	ARM/χ	14	0.005	0.029	16.996	99.975
15	SIRM/ARM	15	0.003	0.017	16.999	99.991
16	χ_{ARM}/SIRM	16	0.001	0.006	17.000	99.997
17	SIRM/χ	17	0.000	0.003	17.000	100.000

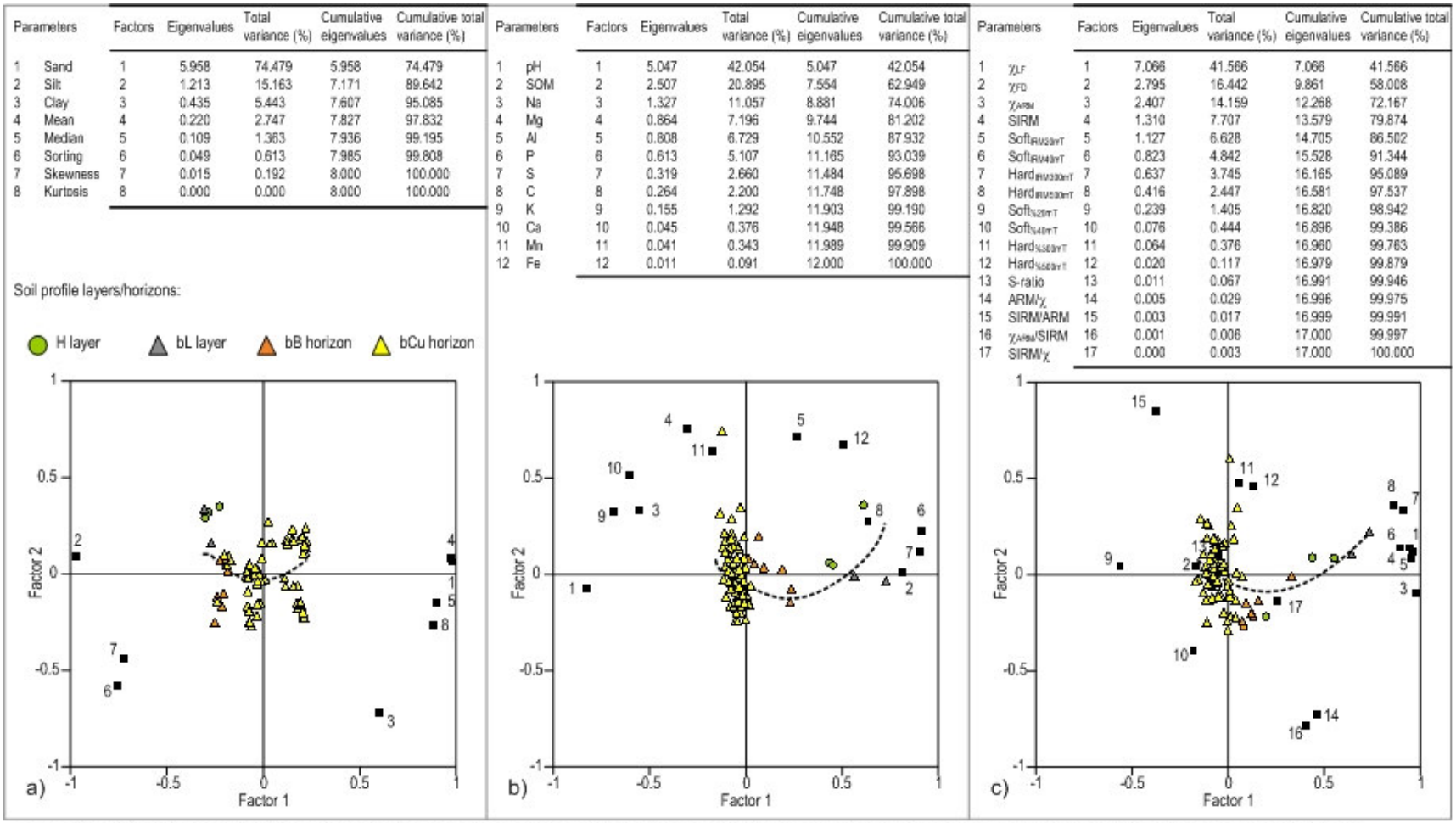

Figure 4.47 Summary results and simultaneous R- and Q-mode factor analysis plots of Factor 1 versus Factor 2, based on the felled coniferous plantation soil profile: a) textural characteristics; b) geochemical characteristics and c) mineral magnetic characteristics (dashed line represents postulated soil horizon development).

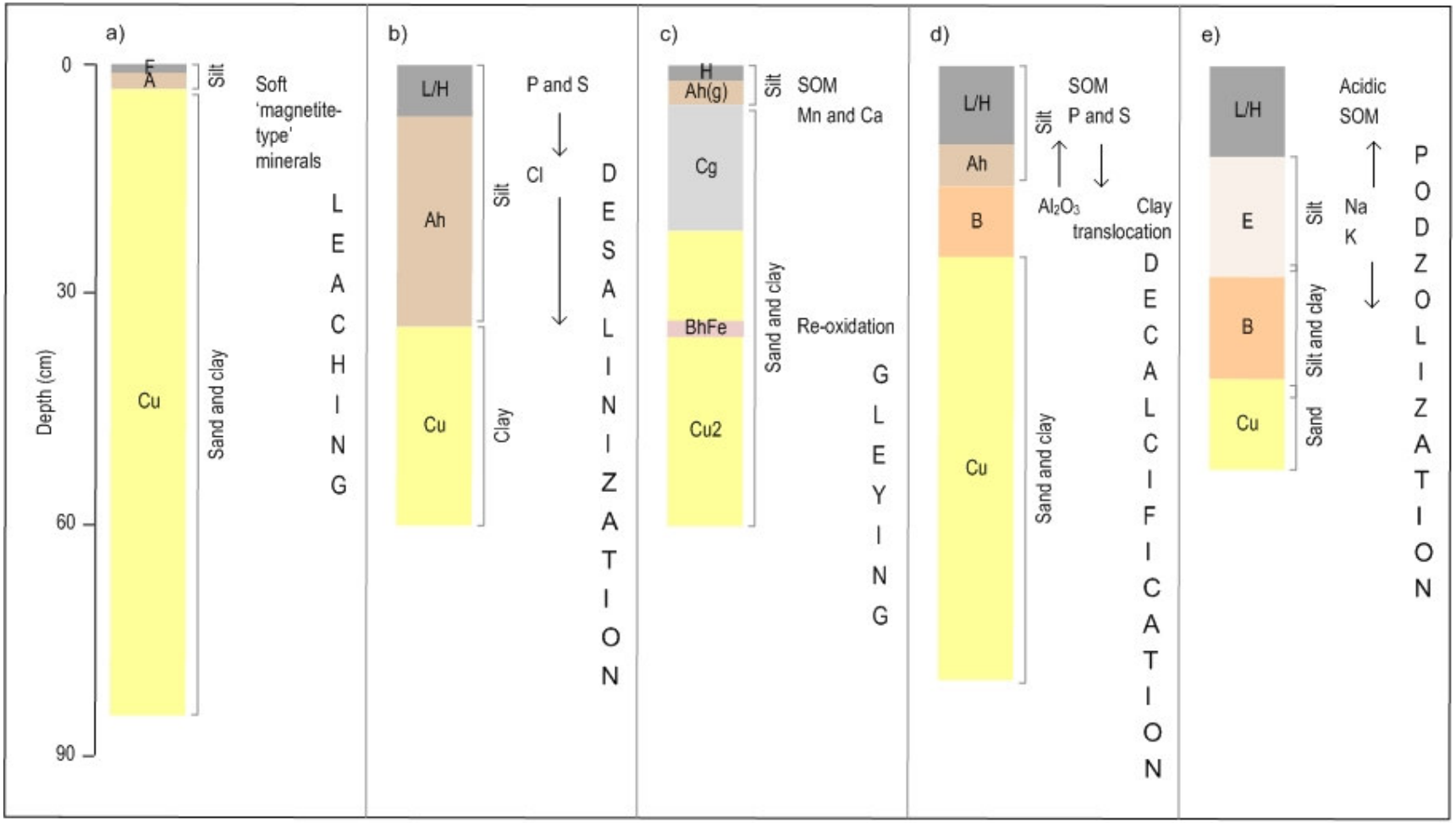

Figure 4.48 Summary of pedogenesis following the results of multivariate factor analyses with, subsequent, proposed soil profile NRSI classifications; a) raw sand; b) sand-pararendzina; c) groundwater gley; d) brown earth and e) micro-podzol.

4.5.1 Factor analysis of the organo-mineral soil components

Figure 4.49 shows the factor plot for comparing the organo-mineral components of the soil profiles (refer to Section 4.2). The first two factors extracted explain 47.97% of variation in parameters (Table 4.31). Factor 1 explains 31.03% of variation, while Factor 2 explains 16.94%. Bare sand and mobile dune communities are positively loaded on Factor 2, influenced by pH, sand and Ca, but not to the same extent as slack community samples. Fixed dune community samples do not appear to be particularly influenced by any parameters. Both deciduous and coniferous woodland samples are influenced by P and S, along with magnetic concentration and mineralogical parameters. Heath samples are plotted separately to the other sample populations, away from the postulated pedogenesis line, being strongly influenced by silt, clay and mean particle size parameters, of which the mineralogy appears to be hard 'haematite-type'. This suggests this soil profile has not developed directly as a result of natural succession, but instead may be the result of anthropogenic activity.

Figure 4.50a is a factor plot of the textural parameters, where the first two factors extracted explain 78.32% of variation. Most heath samples are positively loaded on both factors, indicating strong silt and clay influences, characteristics that appear unique to this soil profile. Most slack samples are positively loaded on Factor 1 and negatively loaded on Factor 2, suggesting a weaker silt influence alongside equal sand and clay influences. The remaining organo-mineral soil samples are grouped together and negatively loaded on Factor 1, suggesting sand influences, but cannot be differentiated further.

Figure 4.50b shows the geochemical factor plot, where the first two factors extracted explain 63.21% of variation in parameters. All mobile dune, slack and scrub organo-mineral samples are positively loaded on Factor 2, indicating strong influences by pH, Ca and Mn. Fixed dune and pasture organo-mineral samples are negatively loaded on Factor 1, suggesting influences by Na and K. Heath samples are negatively loaded on Factor 2, also influenced by Na and K, but also influenced by Al. Most deciduous woodland, coniferous plantation and felled coniferous organo-mineral soil samples are negatively loaded on Factor 2, influenced by SOM, P, S and Al.

Figure 4.50c shows the mineral magnetic factor plot, where the first two factors extracted explain 56.92% of variation in the parameters. Mobile dune organo-mineral soil samples, along with most slack samples, are negatively loaded on Factor 1 and positively loaded on Factor 2, suggesting a soft 'magnetite-type' mineralogy influence; whereas, the heath samples are negatively loaded on both factors, suggesting a stronger hard 'haematite-type' mineralogy influence. Scrub organo-mineral soil samples are positively loaded on Factor 1, suggesting high magnetic concentration. The remaining fixed dune, pasture, deciduous woodland, coniferous plantation and felled organo-mineral soil samples have both positive and negative loadings on both factors, with the 'woody' samples being slightly more influenced by magnetic concentrations.

Table 4.31 Summary results from factor analysis of the organo-mineral soil components using all parameters

Factors	Eigenvalues	Total variance (%)	Cumulative eigenvalues	Cumulative total variance (%)
1	11.481	31.029	11.481	31.029
2	6.268	16.941	17.749	47.970
3	3.986	10.774	21.735	58.744
4	2.887	7.803	24.623	66.547
5	1.960	5.299	26.583	71.846
6	1.418	3.832	28.001	75.678
7	1.345	3.635	29.346	79.313
8	1.061	2.868	30.407	82.181
9	1.034	2.794	31.441	84.975
10	0.816	2.205	32.256	87.179
11	0.779	2.106	33.036	89.286
12	0.604	1.633	33.640	90.919
13	0.507	1.371	34.147	92.290
14	0.470	1.271	34.618	93.561
15	0.422	1.141	35.040	94.702
16	0.304	0.823	35.344	95.525
17	0.292	0.790	35.637	96.315
18	0.231	0.625	35.868	96.940
19	0.185	0.500	36.053	97.440
20	0.158	0.428	36.211	97.868
21	0.135	0.366	36.347	98.234
22	0.131	0.354	36.478	98.588
23	0.118	0.319	36.596	98.907
24	0.092	0.250	36.688	99.157
25	0.067	0.182	36.755	99.339
26	0.050	0.135	36.805	99.473
27	0.043	0.116	36.848	99.589
28	0.039	0.106	36.887	99.695
29	0.031	0.085	36.918	99.780
30	0.025	0.068	36.944	99.848
31	0.021	0.056	36.964	99.904
32	0.014	0.038	36.978	99.942
33	0.012	0.031	36.990	99.973
34	0.004	0.012	36.994	99.985
35	0.003	0.008	36.998	99.993
36	0.002	0.005	36.999	99.998
37	0.001	0.002	37.000	100.000

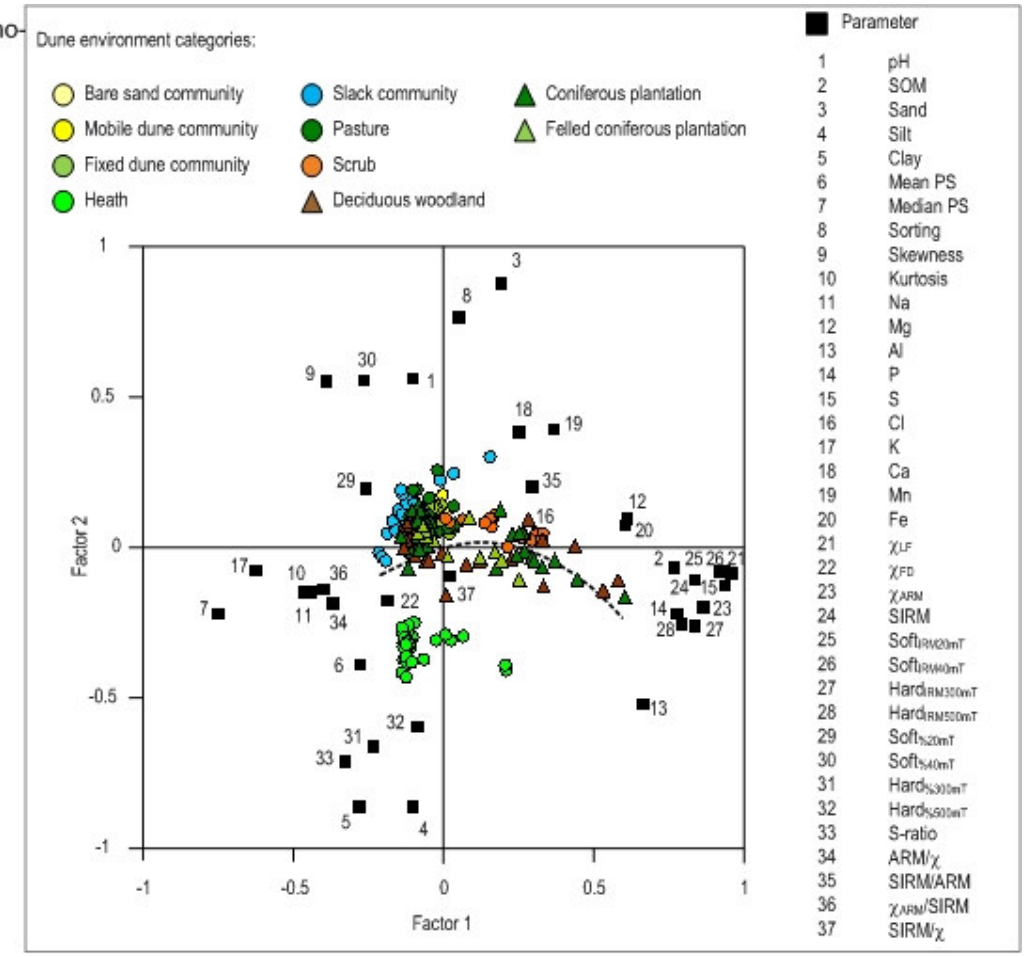

Figure 4.49 Simultaneous R- and Q-mode factor analysis plots of Factor 1 versus Factor 2, based on organo-mineral soil component characteristics (dashed line represents postulated pedogenesis).

	Parameters	Factors	Eigenvalues	Total variance (%)	Cumulative eigenvalues	Cumulative total variance (%)
1	Sand	1	4.317	53.961	4.317	53.961
2	Silt	2	1.949	24.360	6.266	78.321
3	Clay	3	1.063	13.282	7.328	91.603
4	Mean	4	0.401	5.009	7.729	96.612
5	Median	5	0.184	2.298	7.913	98.910
6	Sorting	6	0.047	0.586	7.960	99.495
7	Skewness	7	0.030	0.379	7.990	99.874
8	Kurtosis	8	0.010	0.126	8.000	100.000

	Parameters	Factors	Eigenvalues	Total variance (%)	Cumulative eigenvalues	Cumulative total variance (%)
1	pH	1	5.144	42.864	5.144	42.864
2	SOM	2	2.441	20.342	7.585	63.206
3	Na	3	1.298	10.814	8.882	74.020
4	Mg	4	0.848	7.070	9.731	81.090
5	Al	5	0.677	5.639	10.408	86.730
6	P	6	0.585	4.879	10.993	91.608
7	S	7	0.329	2.744	11.322	94.352
8	C	8	0.274	2.282	11.596	96.634
9	K	9	0.174	1.452	11.770	98.086
10	Ca	10	0.111	0.924	11.881	99.011
11	Mn	11	0.060	0.500	11.941	99.510
12	Fe	12	0.059	0.490	12.000	100.000

	Parameters	Factors	Eigenvalues	Total variance (%)	Cumulative eigenvalues	Cumulative total variance (%)
1	χ_{LF}	1	7.003	41.197	7.003	41.197
2	χ_{FD}	2	2.673	15.726	9.677	56.923
3	χ_{ARM}	3	2.553	15.018	12.230	71.941
4	SIRM	4	1.541	9.064	13.771	81.005
5	$Soft_{BV20mT}$	5	0.919	5.403	14.689	86.408
6	$Soft_{BV40mT}$	6	0.840	4.942	15.530	91.350
7	$Hard_{BV300mT}$	7	0.482	2.836	16.012	94.186
8	$Hard_{BV500mT}$	8	0.376	2.209	16.387	96.395
9	$Soft_{IL20mT}$	9	0.270	1.588	16.657	97.982
10	$Soft_{IL40mT}$	10	0.145	0.852	16.802	98.835
11	$Hard_{IL300mT}$	11	0.095	0.560	16.897	99.395
12	$Hard_{IL500mT}$	12	0.039	0.229	16.936	99.624
13	S-ratio	13	0.026	0.152	16.962	99.776
14	ARM/χ	14	0.024	0.140	16.986	99.916
15	SIRM/ARM	15	0.006	0.037	16.992	99.953
16	χ_{ARM}/SIRM	16	0.005	0.030	16.997	99.982
17	SIRM/χ	17	0.003	0.018	17.000	100.000

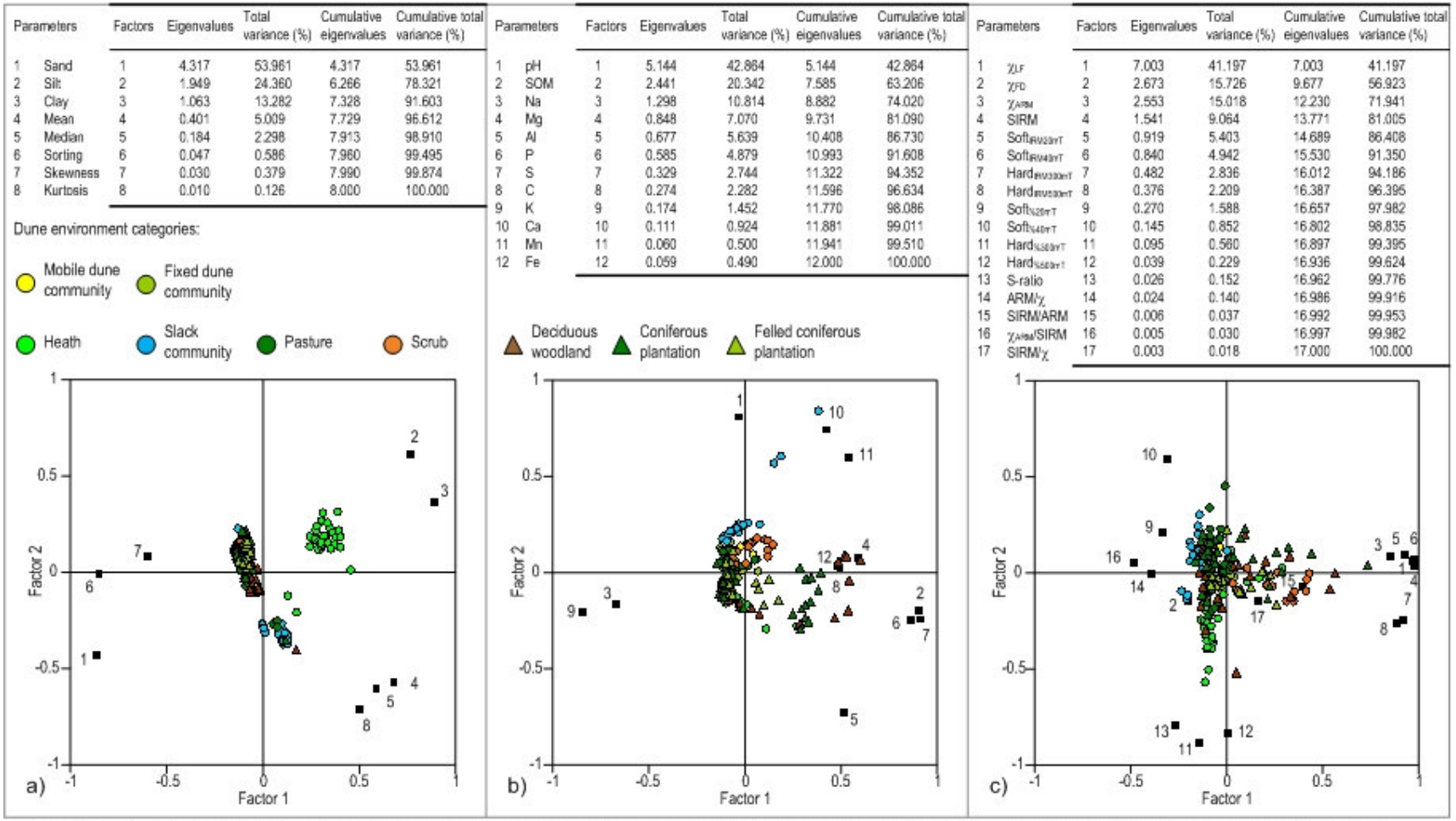

Figure 4.50 Summary results and simultaneous R- and Q-mode factor analysis plots of Factor 1 versus Factor 2, based on the organo-mineral soil components: a) textural characteristics; b) geochemical characteristics and c) mineral magnetic characteristics (dashed line represents postulated pedogenesis).

4.5.2 Factor analysis of classified soil profiles

Figure 4.51 shows the factor plot comparing the pedo-characteristics of the soil profiles once they have been classified into NRSI classifications. The first two factors extracted explain 48.29% of variation in parameters (Table 4.32). Factor 1 explains 31.12% of the variation, while Factor 2 explains 17.17%. Factor 1 appears to represent mineralogy, generally separating the acidic heath micro-podzol profile from the alkaline terrestrial raw sand and sand-pararendzina profiles and some of the deciduous and coniferous woodland samples. The distinguished heath micro-podzol sample population suggests that either; i) this soil has not developed directly as a result of natural succession, but instead may be the result of anthropogenic activity; or, ii) there is a missing soil profile that has not been identified and sampled in the field, which would link the dune environments in a non-linear fashion. Factor 2 appears to represent textural differences, separating frontal dune profiles from hind dune profiles.

Figure 4.52a is a factor plot of the textural parameters, where the first two factors extracted explain 78.61% of variation. Most micro-podzol samples associated with the heath environment are positively loaded on both factors, indicating strong silt and clay influences; whereas, most groundwater gley samples are positively loaded on Factor 1 and negatively loaded on Factor 2, suggesting a weaker silt influence alongside equal sand and clay influences. The remaining sand-pararendzina, brown earth and micro-podzol associated with the coniferous plantation samples are grouped together and negatively loaded on Factor 1, suggesting sand influences, but cannot be differentiated further.

Figure 4.52b shows the geochemical factor plot, where the first two factors extracted explain 63.60% of variation in parameters. All of the terrestrial raw sand, sand-pararendzina and groundwater gley samples are positively loaded on Factor 2, indicating strong influences by pH, Ca and Mn, with increasing influences of Na and K. Both the micro-podzol sample populations are behaving similarly to the brown earth samples, which are negatively loaded on Factor 2, also being influenced by Na, K, Al, P, S and SOM.

Figure 4.52c shows the mineral magnetic factor plot, where the first two factors extracted explain 57.17% of variation in parameters. Most terrestrial raw sand and groundwater gley samples are negatively loaded on Factor 1 and positively loaded on Factor 2, suggesting a soft ‘magnetite-type’ mineralogy influence. Sand-pararendzina, brown earth and micro-podzol sample populations have both positive and negative loadings on both factors. However, the scrub sand-pararendzina population, along with some of the brown earth and coniferous micro-podzol samples, are being slightly more influenced by magnetic concentrations. On the other hand, most micro-podzol samples are negatively loaded on Factor 1, suggesting strong magnetic mineralogy influences.

Table 4.32 Summary results from factor analysis of NRSI classified soil profiles using all parameters

Factors	Eigenvalues	Total variance (%)	Cumulative eigenvalues	Cumulative total variance (%)
1	11.514	31.119	11.514	31.119
2	6.352	17.169	17.867	48.288
3	4.050	10.945	21.916	59.233
4	2.839	7.674	24.755	66.907
5	1.986	5.366	26.741	72.273
6	1.457	3.939	28.198	76.212
7	1.321	3.569	29.519	79.781
8	1.094	2.956	30.613	82.737
9	1.014	2.740	31.626	85.477
10	0.781	2.111	32.407	87.588
11	0.771	2.085	33.179	89.672
12	0.602	1.626	33.780	91.298
13	0.500	1.352	34.281	92.650
14	0.460	1.243	34.741	93.894
15	0.378	1.021	35.118	94.914
16	0.305	0.823	35.423	95.737
17	0.280	0.758	35.703	96.495
18	0.220	0.594	35.923	97.089
19	0.168	0.454	36.091	97.543
20	0.154	0.417	36.245	97.961
21	0.134	0.361	36.379	98.322
22	0.133	0.359	36.512	98.681
23	0.115	0.311	36.627	98.993
24	0.087	0.236	36.715	99.229
25	0.061	0.164	36.775	99.393
26	0.045	0.122	36.820	99.515
27	0.039	0.104	36.859	99.619
28	0.036	0.098	36.895	99.717
29	0.030	0.081	36.925	99.798
30	0.023	0.064	36.949	99.862
31	0.019	0.051	36.968	99.912
32	0.013	0.034	36.980	99.947
33	0.011	0.029	36.991	99.976
34	0.004	0.010	36.995	99.986
35	0.003	0.008	36.998	99.994
36	0.002	0.005	36.999	99.998
37	0.001	0.002	37.000	100.000

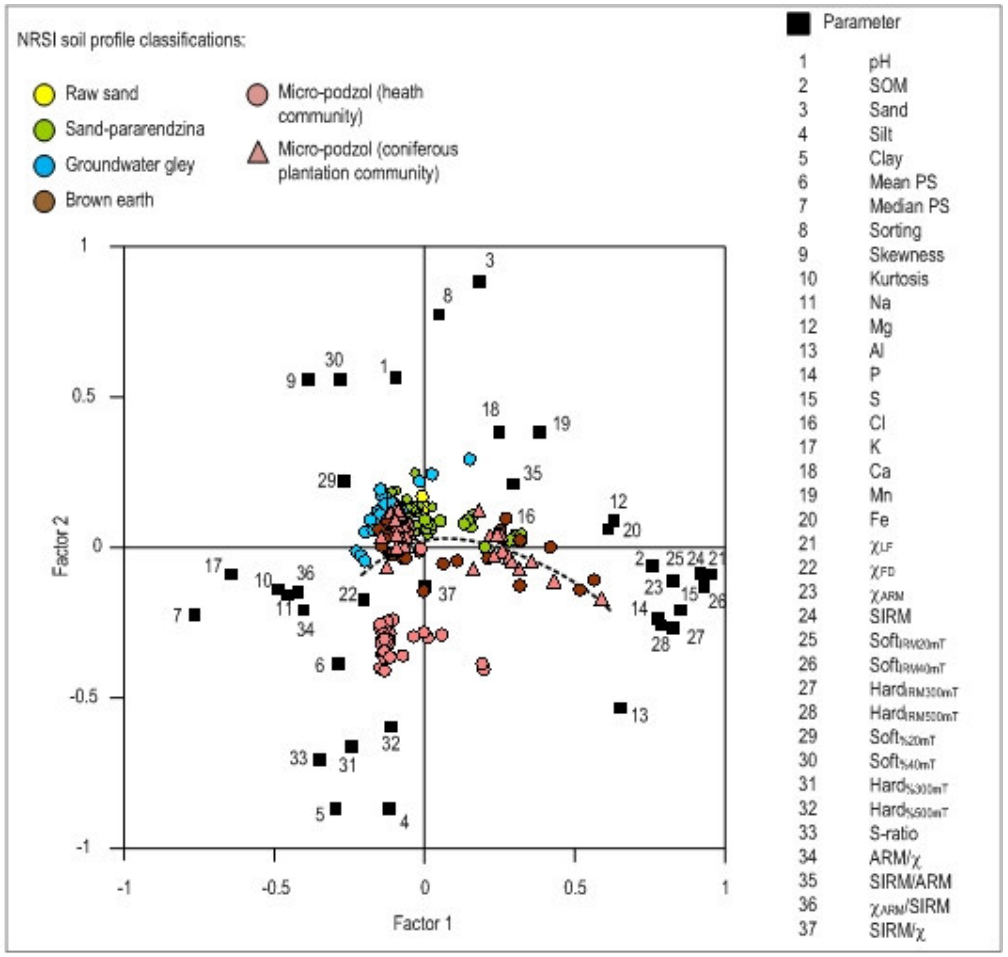

Figure 4.51 Simultaneous R- and Q-mode factor analysis plots of Factor 1 versus Factor 2, based on NRSI classified soil profile characteristics (dashed line represents postulated pedogenesis).

Parameters		Factors	Eigenvalues	Total variance (%)	Cumulative eigenvalues	Cumulative total variance (%)
1	Sand	1	4.313	53.916	4.313	53.916
2	Silt	2	1.975	24.693	6.289	78.609
3	Clay	3	1.038	12.971	7.326	91.580
4	Mean	4	0.407	5.089	7.734	96.669
5	Median	5	0.179	2.238	7.913	98.907
6	Sorting	6	0.047	0.587	7.959	99.493
7	Skewness	7	0.030	0.381	7.990	99.874
8	Kurtosis	8	0.010	0.126	8.000	100.000

Parameters		Factors	Eigenvalues	Total variance (%)	Cumulative eigenvalues	Cumulative total variance (%)
1	pH	1	5.200	43.336	5.200	43.336
2	SOM	2	2.432	20.264	7.632	63.600
3	Na	3	1.292	10.767	8.924	74.367
4	Mg	4	0.846	7.048	9.770	81.416
5	Al	5	0.677	5.640	10.447	87.056
6	P	6	0.575	4.790	11.022	91.846
7	S	7	0.319	2.655	11.340	94.501
8	C	8	0.273	2.279	11.614	96.780
9	K	9	0.168	1.399	11.781	98.178
10	Ca	10	0.105	0.874	11.886	99.052
11	Mn	11	0.058	0.483	11.944	99.535
12	Fe	12	0.056	0.465	12.000	100.000

Parameters		Factors	Eigenvalues	Total variance (%)	Cumulative eigenvalues	Cumulative total variance (%)
1	χ_{LF}	1	7.036	41.386	7.036	41.386
2	χ_{FD}	2	2.682	15.779	9.718	57.165
3	χ_{ARM}	3	2.574	15.143	12.292	72.308
4	SIRM	4	1.521	8.945	13.813	81.253
5	$Soft_{BV20mT}$	5	0.941	5.537	14.754	86.790
6	$Soft_{BV40mT}$	6	0.774	4.555	15.529	91.345
7	$Hard_{BV300mT}$	7	0.483	2.843	16.012	94.188
8	$Hard_{BV500mT}$	8	0.376	2.214	16.388	96.402
9	$Soft_{N20mT}$	9	0.274	1.612	16.662	98.014
10	$Soft_{N40mT}$	10	0.148	0.869	16.810	98.882
11	$Hard_{N300mT}$	11	0.093	0.548	16.903	99.430
12	$Hard_{N500mT}$	12	0.035	0.207	16.938	99.637
13	S-ratio	13	0.026	0.156	16.965	99.793
14	ARM/χ	14	0.022	0.129	16.987	99.922
15	SIRM/ARM	15	0.006	0.033	16.992	99.955
16	χ_{ARM}/SIRM	16	0.005	0.028	16.997	99.983
17	SIRM/χ	17	0.003	0.017	17.000	100.000

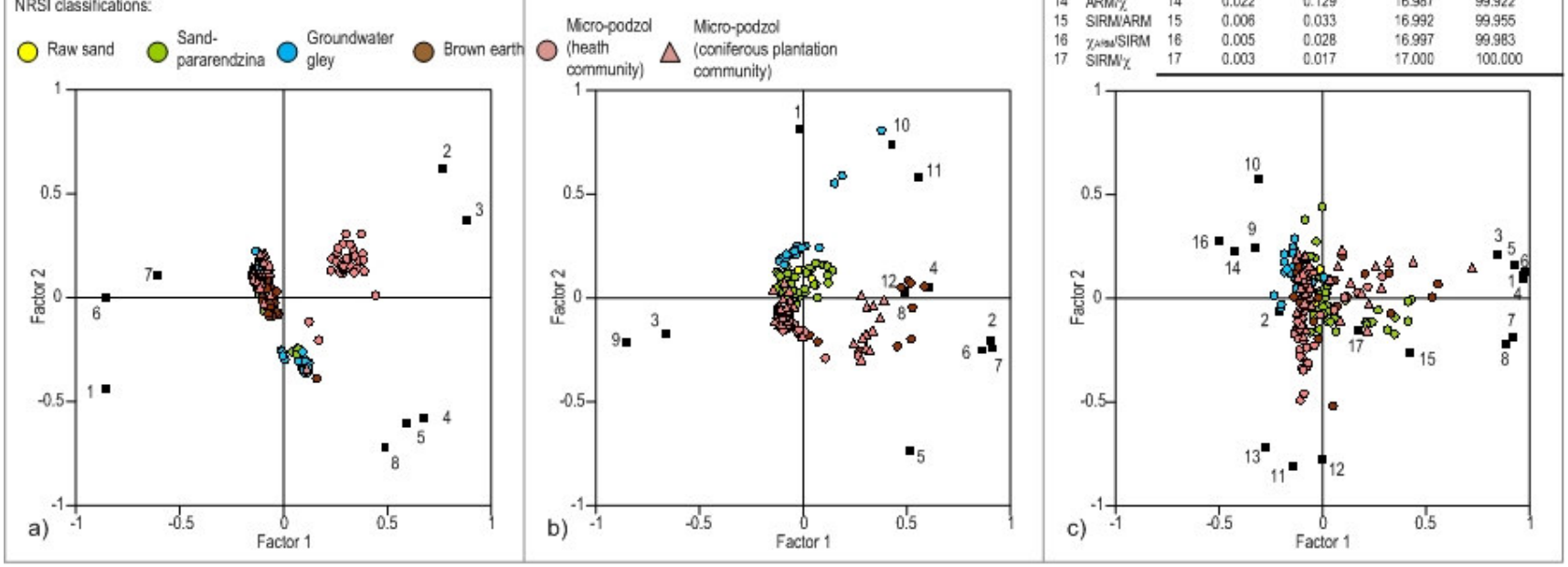

Figure 4.52 Summary results and simultaneous R- and Q-mode factor analysis plots of Factor 1 versus Factor 2, based on the soil profile NRSI classifications: a) textural characteristics; b) geochemical characteristics and c) mineral magnetic characteristics.

4.6 Discussion: Implications for pedogenic succession

4.6.1 Terrestrial raw sands

Recently deposited sand provides a sediment source for early mobile dune development. Soil development in this dune environment only consists of little-altered mineral material, with a thin layer of SOM at the surface. This has resulted in stressful conditions for the growth of most plant species and, therefore, classifies this profile as terrestrial raw sand. Pedological horizons are absent, evident by great down-profile variation in mixed terrestrial raw sand physico-chemical characteristics, resulting from active geomorphological processes. Continued growth of the dune system depends on stabilization by marram grass (*Ammophila arenaria*), a salt- and drought-tolerant species with extensive root systems.

These sandy sediments drain easily, but have a poor ability to retain moisture and are prone to leaching processes (Gerrard, 2000), evident on the Sefton dunes by low nutrient content. The mobile dune soil profile is alkaline, being significantly different from all other dune environments, and heavily influenced by Ca. Soil development only consists of decomposed organic remains incorporated with mineral material (F layer), producing a soil only capable of supporting species such as cat's ear (*Hypochaeris radicata*) and sea spurge (*Euphorbia paralias*), both of which have deep roots, along with occasional bryophytes. The peak in χ_{LF} at the surface and soft 'magnetite-type' mineralogy influence is most likely reflecting the input of ferrimagnetic minerals from atmospheric fall-out particulates, which has been identified in other magnetic properties of soil profiles (e.g. Maher, 1986; Dearing *et al.,* 1995). Values for the rest of the profile are low (<1 $x10^{-7}m^3kg^{-1}$) due to dynamic erosion/deposition processes (Crockford and Willet, 2001).

4.6.2 Sand-pararendzinas

Foredune stabilization allows terrestrial raw sand to progress to sand-pararendzinas, which are more favourable for less hardy plants. On the Sefton coast, these profiles are found under the fixed dune community, pasture and, to some extent, the scrubland and felled coniferous dune environments, identified in Chapter 3. When sand input ceases, marram grass (*Ammophila arenaria*) can no longer cope and breaks down. Subsequently, increased decaying SOM releases nutrients for plant growth, resulting in increased species diversity overlying sand-pararendzinas, across the width of the dune landscape. Plant succession is comparable to Payne's (1983) model, with fixed dunes, pasture and scrub environments supporting abundant coverage of red fescue (*Festuca rubra*) and dewberry (*Rubus caesius*).

The SOM appears to have been transformed into slower decomposing humus (F), when compared to terrestrial raw sand, altering physical conditions such as capacity to supply nutrients and soil aeration (Fullen and Catt, 2004). Carbon dioxide (CO_2) is produced during the formation of organic matter (Gerrard, 2000), which, on the Sefton dunes, has increased soil acidity and enhanced chemical breakdown of parent material. The fixed dune profile is the only sand-pararendzina to display the atmospheric-particulate derived peak in χ_{LF} at the surface

described by Maher (1986). The peak can be observed in all other profiles, but at 3-4 cm below the surface, similar to findings by Magiera *et al.* (2006).

Sand-pararendzinas on the Sefton coast are mainly influenced by alkaline Ca and Mn, although the fixed dune pedo-dynamics are affected by inputs of Na and K. The Ah horizon of the fixed dune displays a higher influence of Cl, Fe, Mn, Na, Mg and K, compared to sand-pararendzinas associated with pasture and scrub environments. This suggests the latter profiles are experiencing desalinization processes, eluviating the dissolved minerals Ca, Mg, Na and K, downwards through the soil beyond the root zone (Cu2).

Effects of ploughing on the pasture soil profile are confirmed by low χ_{LF} in the upper Ap horizon, overlying maximum χ_{LF} in the lower Ap horizon, similar to ploughed horizons identified by Lukshin *et al.* (1968). The bAh1 horizon represents the surface of a buried soil, similar to Crockford and Willett (2001), evidence of a previous stable surface with vegetation that has been, subsequently, buried by windblown material, as discussed by Jungerius (1985).

Mineral magnetic analyses of soil profiles can, in some instances, date relative soil formation (Pope, 2000), which can be used as a tool to group profiles into classifications. The χ_{LF} data for the sand-pararendzinas associated with fixed dune and pasture environments are similar (<2 $x10^{-7}m^3kg^{-1}$), suggesting they are similar age. However, the scrub soil has higher magnetic mineral concentrations, similar to the deciduous woodland, suggesting this soil may be transitional between a sand-pararendzina and brown earth.

4.6.3 Groundwater gley soil

A groundwater gley soil profile has formed under the dune slack community identified in Chapter 3. This can be distinguished by the pH being significantly different from all other environments. The upper organic H layer and Ah(g) horizon, both strongly influenced by silt content, are separated from the Cg and Cu horizons, which have increasing sand and clay influences with depth. These high percentages of clay in the lower groundwater gley profile provide a good supply of nutrients, but inhibit drainage, and therefore, the soil is waterlogged. Seasonal waterlogging has severely inhibited decomposition in the groundwater gley soil, resulting in limited SOM accumulation at the surface of the profile (H), which is significantly lower from other profiles. The H horizon is strongly influenced by Cl, Mn, Ca and P. Intermittent aeration, with consequent re-oxidation (Ragg *et al.,* 1984), has resulted in mottled Ah(g) and Cg horizons. Furthermore, these conditions have resulted in the presence of oxidized Mn aiding SOM oxidization (van Breemen and Buurman, 2002). James (1993) suggested the presence of an oxidized Ah horizon, indicating a deep summer water table.

Mineral magnetic measurements are low and unstable throughout the saturated profile, without the noticeable topsoil enhancement previously observed in dry-profiles, despite having developed from the same parent material and associated mineral magnetic characteristics as

every other profile under investigation. This result is similar to other soil studies (e.g. de Jong *et al.,* 2000; Lu, 2000; Magiera *et al.,* 2006). The presence of a Cg horizon depicts these soils as having experienced seasonal water table fluctuations, resulting in a zone of intense orange and rust-brown mottling and iron concentrations (Hall and Folland, 1967). The $\chi_{FD\%}$ values peak at >5% in the Ah(g) and Cg horizons is evidence that magnetic properties at these depths are probably controlled by the presence of SP grains (Hanesch and Petersen, 1999). This may be an indication of the presence of magnetotactic bacteria (Fassbinder *et al.,* 1990), which Oldfield (2007) described as the growth of magnetite within bacteria cells. Furthermore, at 15 cm depth, $\chi_{FD\%}$ values peak at >10%, indicating SP domains (Lu, 2000). However, $\chi_{FD\%}$ and ARM/χ are greatly decreased in the Cu1 horizon, indicating active dissolution of ferrimagnetic fine (SD) and ultrafine (SP) minerals by gleying processes (Mullins, 1977; Maher, 1986). These can be described as Fe compounds, which are redeposited in the BhFe horizon. Combined high ratios of both ARM/χ and SIRM/ARM, alongside high Fe, suggest these magnetic minerals may possibly be SP-sized coatings, on what Ragg *et al.* (1984) referred to as a ferri-manganiferous nodule.

4.6.4 Brown earth soil

Pedogenesis transforms sand-pararendzinas to brown earths advanced enough to support shrubs and trees, which, on the Sefton dunes, can be found under the deciduous woodland and, to some extent, the scrubland dune environments identified in Chapter 3. These soils may also have developed from groundwater gleys. Lowering of the water table by coniferous woodland caused subsequent drying of slacks in close proximity, allowing peat development at the soil surface. Increased aeolian derived sand to the profile has resulted in the development of well-drained brown earths.

Magnetic enhancement in this profile is in the form of a wide peak (>10 cm), similar to the Cambisol described by Magiera *et al.* (2006), also developed under deciduous woodland. The peak is located in the H layer, immediately below the L layer, which is comparable to profiles described by Strzyszcz (1989). Although previously classified as a sand-pararendzina, the topsoil χ_{LF} enhancement of the scrub profile is similar to the deciduous woodland brown earth. This, alongside the scrub organo-mineral soil displaying significantly different Fe values from any other dune profile, suggests the scrub profile is undergoing pedological change.

The L layer, in the brown earth under the deciduous woodland, is influenced by SOM, Cl and Mn. SOM, P and S influences decrease with depth, alongside increased influences of Al in the H layer and, subsequently, both the Ah and B horizons. Desalinization processes are in operation in this profile, evident by an overall low concentration of Cl down-profile. Decalcification processes have begun in the H layer, resulting in total loss of Ca from the entire Ah and B horizons. Loss of this diamagnetic mineral (Dearing, 1999) through dissolution has, subsequently, produced the effect of greater magnetic concentrations (Maher, 1986), evident by increased $Soft_{\%20mT}$, in the B horizon.

Both L and H layers and the Ah horizon are strongly influenced by silt, whereas, the B and Cu horizons are influenced by sand and clay. Clay formation and translocation is evident by increased clay concentrations in the lower B horizon and increased influences of clay in the Cu horizon, characteristic of a para-brown earth (Hanesch and Petersen, 1999). The extent of leaching is related to soil texture (Ragg *et al.,* 1984), therefore, increased percentages of silt-sized particles in the B horizon maintained ready supplies of nutrients by buffering (Gerrard, 2000).

4.6.5 Micro-podzol soils

On the Sefton coast, micro-podzol soil profiles are found under both the dune heath community and the coniferous plantation environments identified in Chapter 3. Edmondson *et al*., (1993) state that these micro-podzols have not naturally succeeded directly from fixed dunes. The authors suggest that the micro-podzol under the dune heath environment developed following deforestation to create golf courses. This modified nutrient recycling processes favourable to brown earth formation by removing basic cations in woodland, leading to podzolization and invasion of acid tolerant heath species, such as common heather (*Calluna vulgaris*). Whereas, afforestation of coniferous woodland associated with accumulation of a needle litter (L) layer, has also led to podzolization. Continuous shade under these plantations has resulted in less species diversity and exposed topsoils. The thick L layer at the surface, with high SOM, has been incorporated to a lower depth, possibly by faunal activity (Fullen and Catt, 2004), to form an H layer indicative of a well-developed soil. Both of these micro-podzols have experienced intense leaching and translocation, leading to organic acids forming complexes with Fe and Al compounds, resulting in acidic surface horizons.

Topsoil χ_{LF} data for the coniferous plantation micro-podzol are much higher than any other profile on the Sefton dunes, similar to findings by Magiera *et al.* (2006). This suggests the forest canopy is unlikely to be accumulating atmospheric particulates, as in other forest soil studies (e.g. Vadyunina and Babanin, 1972; Strzyszcz, 1989). The enhancement peak, however, occurs much lower down the profile, due to low rates of organic turnover (Dearing *et al.,* 1995), possibly explained by excess production of non-ferrimagnetic pine needles effectively diluting the magnetic signal (Maher, 1986; Williams and Cooper, 1990). Generally, MD particles of anthropogenic origin have smaller surface/volume ratios, favouring dissolution of SP domain sizes under reducing conditions (Cornell and Schwertmann, 1996). Therefore, this would be evidence of active pedogenic processes (Maher, 1986) rather than an indication of age (Pope, 2000). However, eluviation of Fe is considered too destructive a process (Duchaufour, 1982), that magnetic enhancement occurring through pedogenic reactions is unlikely. It is also unlikely that magnetotactic bacteria (Fassbinder *et al.,* 1990) caused the magnetic enhancement, as conditions are too acidic. Whereas, high magnetic mineral concentrations, in the heath micro-podzol, can be attributed to the older age of the soil; especially, when considering the flat topography of the environment and natural species invasion.

The pH values suitable for cation exchange buffering are 4.2-5.0 (Schrijver *et al.,* 2006), similar to the pH values in the heath soil profile, which are significantly more acidic from all dune environments. Overall decrease in soil acidity down-profile may be the result of sufficient leaching of cations (Na, Mg, K and Ca) and subsequent redeposition of alkaline elements towards the profile base. A result of this is the upper profile being dominated by acidic Al ions, an indication of podzolisation (Brady and Weil, 1999; Ampe and Langohr, 2003). Small peaks in SOM, along with magnetic enhancements, are identified in both the B and, more importantly, the upper Cu horizon, suggesting the possible occurrence of an organic subsoil (Bh) horizon (Fullen and Catt, 2004) that is not visible in the field.

Different to the heath micro-podzol, a bleached subsurface horizon (E) is evident above the Fe, Al and humus enriched B horizon of the coniferous plantation profile. A similar micro-podzol was described by James and Wharfe (1989) beneath a 46 year old forest of Corsican pine (*Pinus nigra*) on the Sefton coast, where a narrow bleached E horizon was described, alongside a mottled B horizon, caused by leaching of iron.

In the clay-deficient heath profile, silt plays an important role in influencing pedogenic processes and organic matter storage (Fullen and Booth, 2006; Fullen *et al.,* 2006), but this micro-podzol can not be differentiated from the sand-pararendzinas using textural variables alone. However, pedogenic processes are quite different. Increased concentrations of clay-sized particles in lower horizons of the coniferous plantation profile are likely to have resulted from eluviation of organic acids from the humus layer (H), to form complexes with Fe and Al compounds (Ragg *et al.,* 1984), rather than clay minerals. The presence of stable single domain magnetic grain sizes also supports this. However, iron redistribution, identified by James and Wharfe (1989), is not evident in the heath profile, where the combined Ah and B horizons has a greater influence of antiferromagnetic minerals, indicated by an increased S-ratio (Sandgren and Thompson, 1999). Lack of precipitation of these oxides in the B horizon, classifies this profile as a humic podzol, where darkening and reddening is a function of increasing age (Turk *et al.,* 2008). Many authors (e.g. Sandgren and Thompson, 1990; Dearing *et al.,* 1995; Hanesch and Petersen, 1999; Magiera *et al.,* 2006) have observed magnetic enhancement in B horizons of podzols, which were absent in the Sefton micro-podzols. Kapička *et al.* (2003) suggest advanced acidification and destruction of primary minerals in some soils could be enough to eliminate the magnetic signal.

Species invasion to other communities is evident by the presence of pine seedlings (*Pinus sylvestris*) in the scrub environment. This may, in the long-term, alter characteristics of lithomorphic soils in close proximity, creating an increased expanse of unnatural dune flora, the process of which may have enhanced heath establishment.

4.6.6 Reversion of a micro-podzol soil to a sand-pararendzina

Some authors believe restoration of a diverse dune flora is not possible simply by clear-felling (e.g. Sturgess, 1992, 1993; Edmondson *et al.,* 1993). The lack of tree cover has encouraged erosion of the exposed litter and surface organic horizons, which are, subsequently, buried by sheet-deposition of aeolian derived sand. Therefore, a lithomorphic soil developed under the felled community environment, overlying the micro-podzol would have previously been the contemporary soil profile of the area. The pH of the lithomorphic H layer has reverted back to values similar to fixed dune environments; however, the low pH of the bL organic layer may be sufficient to prevent successful growth of many dune plants characteristic of young, calcareous dunes. The pH of the felled dune soil profile is similar to the coniferous plantation micro-podzol, suggesting classification as either micro-podzol or sand-pararendzina, using pH characteristics, is not feasible.

In very acidic soils, such as the underlying micro-podzol, SOM breakdown can be inhibited (Gherardi *et al*., 2007), explaining the acidic, partly-decomposed plant litter (bL) above the mineral horizon (bB). High organic content retains water much better than bare sand (Sturgess, 1993) and this may be an important factor in the observed establishment of some scrub species, including Common ragwort (*Senecio jacobaea*), Creeping willow (*Salix repens*), Mouse-ear chickweed (*Cerastium fontanum*) and Sow thistle (*Sonchus asper*), on the clear-felled site. Over time it has been possible to note a gradual loss of SOM in the bL layer from 50.9% to 26.6% after 13 years of clear-cutting.

The sharp distinction between the organic litter (bL) and the mineral soil (bB), shows the E horizon, characteristic of the micro-podzol, has disappeared as the soil becomes replenished with Mg and Mn. There is little incorporation of organic matter in this mineral horizon, similar to findings by Sturgess (1991, 1993). According to Atkinson and Sturgess (1991), post-felling there would be increased movement of some minerals in the B horizon, as higher effective rainfall promotes decomposition and leaching. This may also account for the disappearance of the mineral magnetic enhancement, evident in the L layer of the coniferous plantation micro-podzol. As plants colonize, nutrients are recycled, accounting for the levelling of the felled phosphate profile with time, compared to the abrupt decrease associated with the E horizon of the micro-podzol.

4.7 Summary

Distinct variations in soil profiles were apparent between the dune environments identified in Chapter 3, which can be categorized into National Soil Resources Institute (NSRI) classifications. Simultaneous R- and Q-mode factor analyses have shown great potential for identifying pedogenic trends within soil profile horizons, which can be associated with independent dune environments.

Pedogenesis initiates as terrestrial raw sand, progressing to sand-pararendzinas and, through thickening of the humus layer and acidification by natural leaching with time, results in brown earth development. Anthropogenic afforestation and deforestation has increased acidification, resulting in micro-podzol development. Groundwater gley soils are associated with dune slacks. In general terms:

- Terrestrial raw sands are associated with mobile dune environments. Low Soil Organic Matter (SOM) and high pH, occur alongside Ca and Mn influences.
- Sand-pararendzinas are associated with fixed dune, pasture and scrub communities, although some pedo-characteristics would categorize the scrub profile as a transition between sand-pararendzina and brown earth. Deeper, more acidic humus layers overlie an A horizon with lower Ca, Mg, Na and K percentages, due to desalinization processes.
- Groundwater gley soils are associated with slack environments, with high percentages of clay and a good nutrient supply, but inhibited drainage.
- Brown earth soils are associated with deciduous woodland environments and may have developed from groundwater gleys. Desalinization processes have lowered Cl percentages; whereas, decalcification processes have resulted in loss of Ca from Ag and B horizons. Clay formation and translocation has increased clay concentrations in B and Cu horizons.
- Micro-podzols are associated with unnatural heath and coniferous plantation environments that have not succeeded directly from any other dune environment. Deep needle litter has increased soil acidity, but leaching of Na Mg K and Ca has decreased acidity down-profile. A bleached subsurface horizon (E) was evident in the coniferous plantation profile. Silt played an important role in influencing pedogenic processes in the heath profile.

CHAPTER 5

Buried soils and dune sediments: archives for past morpho-dynamics

Chapter 5 analyses an exposed stratigraphic and historic soil sequence in a frontal dune cliff, providing evidence of a dynamic, cyclic sand dune system. The temporal physico-chemical properties are presented graphically. In addition, a buried soil profile on the upper foreshore is analysed in an attempt to classify the historic pedo-environment. Factor analysis is employed to trace the beach soil profile into those exposed in the dune cliff, to provide a basis for modelling past dune morpho-dynamics.

5.1 Introduction

The frontal dunes at Formby Point are eroding at a mean rate of 3 m/yr, and during single storm events 6-14 m (Pye, 1991) (refer to Chapter 1, Section 1.4.3). Excessive sand removal has re-exposed buried soils in dune cliffs and on the upper foreshore, observed at numerous locations along the eroded section of the coast around Formby Point. This has provided a unique opportunity to investigate historic pedo-environments and to compare them to the contemporary soils. These buried environments provide evidence that the dune system operates in a cyclic nature, with seaward advancements during episodic sea regressions and associated shoreline accretion (Jungerius, 1985), interspersed with phases of dune stability resulting in species colonization and soil development.

The northern limit of the erosive section is ~1 km north of Fisherman's Path (SD 280 099) and extends southwards to between Alexandra Road (SD 273 057) and Lifeboat Road (SD 271 063). Figure 5.1 shows the location of the exposed stratigraphic section and buried soil profile at a distance of ~2.5 km apart. Identification of similar pedo-characteristics between the buried soil and buried organic layers allowed tracing of that particular organic horizon across such a macro-distance. Cyclic modelling of past dune morpho-dynamics may provide insights into the possible future behaviour of the Sefton dune complex.

5.2 Identification of stratigraphic layers using physcio-chemical characteristics (Site 1)

Figure 5.2 shows the shallow contemporary soil profile, at the surface of the stratigraphic section, to be typical of a sand-pararendzina, after Avery (1980) (refer to Chapter 4, Section 4.2). A thick organic horizon, combining both F and H layers (0-15 cm) and containing 1.0-1.4% SOM, is positioned above a greyish brown (10YR 5/2) A horizon (15-20 cm) that is comparatively low in SOM (0.5%). A relatively deep (20-84 cm) Cu horizon represents the latest phase of dune-building activity. At least three phases of environmental stabilization and subsequent soil development were represented by buried dark grey (10YR 4/1) layers. The first buried organic layer (bH1), at 82-84 cm depth, contained 4.4% SOM and 30% silt-sized particles. A very shallow sedimentary layer, representing a relatively short period of dune mobilization, separated the bH1 from the bH2. The second buried organic layer (bH2) was much

Figure 5.1 Location of stratigraphic section and exhumed soil profile. Plates: A) Exposed stratigraphic section: SD 27534 08981; B) Exhumed soil on beach: SD 27001 06592; C) and D) Examples of buried soils on the Sefton coast: grid square 294 090.

Stratigraphic section description

Profile ID: ES
Date of survey: 25/09/2006

Site description

Location: 2 km N of pedestrian beach access point to Freshfield caravan park.
Grid reference: SD 27534 08981
Landform: Cliffed hind dunes exposed on beach.

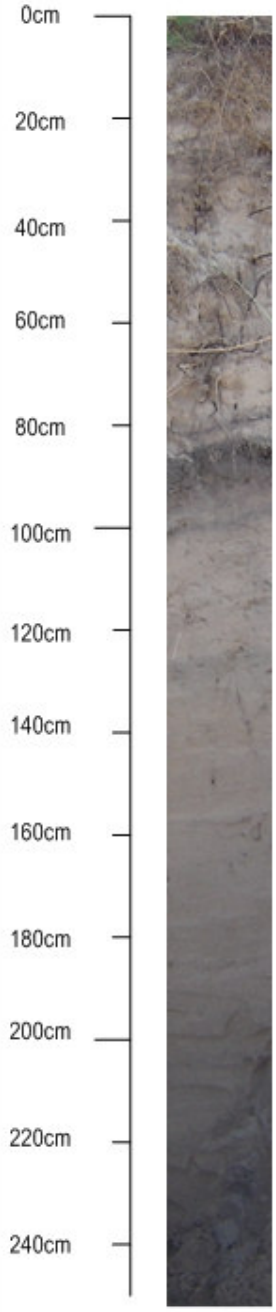

Unit	Depth	Field description
F	0-4	Greyish brown (10 YR 5/2) moist and greyish brown (10YR 5/2) dry; loose sand; stoneless; many medium (2-5 mm) fibrous roots; diffuse boundary to:
H	4-15	Greyish brown (10 YR 5/2) moist and brown (10YR 5/3) dry; loose sand; stoneless; many medium (2-5 mm) fibrous roots; clear boundary to:
A	15-20	Greyish brown (10 YR 5/2) moist and greyish brown (10YR 5/2) dry; loose sand; stoneless; many fine (1-2 mm) fibrous roots; clear boundary to:
Cu	20-84	Greyish brown (10 YR 5/2) moist and brown (10YR 5/3) dry; loose sand; stoneless; many fine (1-2 mm) fibrous roots grading into medium (2-5 mm) fibrous roots with depth; clear boundary to:
bH1	82-84	Dark grey (10 YR 4/1) moist and very dark grey (10 YR 3/1) dry; loose sand; stoneless; diffuse boundary to:
bCu1	84-86	Dark grey (10 YR 4/1) moist and greyish brown (10YR 5/2) dry; loose sand; stoneless; clear boundary to:
bH2	86-96	Dark grey (10 YR 4/1) moist and dark greyish brown (10YR 4/2) dry; loose sand; stoneless; diffuse boundary to:
bCu2	96-98	Greyish brown (10 YR 5/2) moist and greyish brown (10YR 5/2) dry; loose sand; stoneless; clear boundary to:
bH3	98-100	Dark grey (10 YR 4/1) moist and greyish brown (10YR 5/2) dry; loose sand; stoneless; diffuse boundary to:
bCu3	100-250	Brown (10 YR 5/3) moist and brown (10YR 5/3) dry; loose sand; stoneless; 5% distinct mottling.

Layer/horizon		F	H	A	Cu	bH1	bH2	bH3
Sand	60-2000 µm %	74	83	80	73	68	66	71
Silt	2-60 µm %	22	14	17	24	30	32	26
Clay	<2 µm %	4	3	3	3	2	2	3
SOM %		1.4	1.0	0.5	0.9	4.4	1.2	0.3
pH in water (1:2.5)		7.3	7.1	7.2	7.7	7.8	7.4	7.8

Figure 5.2 Stratigraphic description for exposed section at Formby Point (Site 1 on Figure 5.1).

thicker at 86-96 cm, yet contained less SOM (1.2%) than bH1. The third buried organic layer (bH3), at 98-100 cm, contained only 0.3% SOM.

Figures 5.3 and 5.4 identify historic soil formations at 82-84, 86-96 and 98-100 cm, evident by increased SOM and percentages of silt-sized particles, alongside decreased percentages of sand- and clay-sized particles. The surface of the H layer was evident by increased acidity and mean particle size, alongside the second highest values of SOM (2.81%), P (0.03%) and Fe (1.76%). The organic bands are identifiable by increased acidity (pH 7.38), P (0.04%) and S (0.03%), in conjunction with decreased Mg values (0.20%), Ca (0.28%) and Mn (0.02%). The surface of the organic bands also marks a rapid decrease in magnetic mineral concentrations down-profile.

5.3 Classification of the buried soil profile using pedo-characteristic descriptions (Site 2)

Figure 5.5 shows the buried soil profile has very distinct horizon definition, evident of a well developed mature soil. Buried under 12 cm of contemporary sediments, a thick bH layer (12-24 cm) lay at the surface of the profile and contained 14.3% SOM. A shallow dark greyish brown (10YR 4/2) bAg horizon (24-29 cm), low in SOM (1.8%) and displaying fine mottles, graded into a relatively deep (29-48 cm) light brownish grey (10YR 6/2) E horizon with very low SOM (0.7%) and becoming darker (10YR 4/2) with depth and increased moisture. The underlying dark greyish brown (10YR 4/2) B horizon gradually diffuses into the parent material. A change in colour (10YR 3/2) identified the sedimentary characteristics of the permanently waterlogged bCu horizon. The pH remained similar throughout the profile (7.1-7.6) under the alkaline (8.1) beach sediments.

Figures 5.6 and 5.7 identify soil formation above 48 cm, evident by a transition to increasing pH and higher clay values. These changes are also reflected in increased soft, magnetite-type, magnetic minerals and decreased hard, haematite-type, magnetic minerals. The surface of the bH layer was evident by further increased alkalinity and mean particle size of the overlying beach sediments. The bH horizon contained highest values of SOM (27.08%), P (0.06%) and S (0.27%), Ca (7.39%) and Mn (0.16%), while peaks in Mg (0.90%), Al (1.66%) and Cl (0.12%) occur at 53 cm in the bCu1 horizon.

Magnetic mineral concentrations are highest in the contemporary beach sediments (χ_{LF} 5.25 $x10^{-7}m^3kg^{-1}$; χ_{ARM} 0.07 $x10^{-7}m^3kg^{-1}$; SIRM 598.45 $x10^{-5}m^2kg^{-1}$). Otherwise, values were very low, or undectable, throughout the profile apart from small peaks at 22 cm at the bH/bAg boundary (χ_{LF} 1.14 $x10^{-7}m^3kg^{-1}$; χ_{ARM} 0.02 $x10^{-7}m^3kg^{-1}$; SIRM 114.36 $x10^{-5}m^2kg^{-1}$) and 62 cm in the bCu1 horizon (χ_{LF} 0.16 $x10^{-7}m^3kg^{-1}$; χ_{ARM} 0.02 $x10^{-7}m^3kg^{-1}$; SIRM 70.89 $x10^{-5}m^2kg^{-1}$). Low values of ARM/χ and χ_{ARM}/SIRM ratios, alongside high SIRM/ARM ratios, indicate the importance of either SP or MD magnetic grains in the upper and lower soil profile. However, very low values of $\chi_{FD\%}$ in the upper 30 cm suggests MD grains to be an influencing factor. The opposite trend was

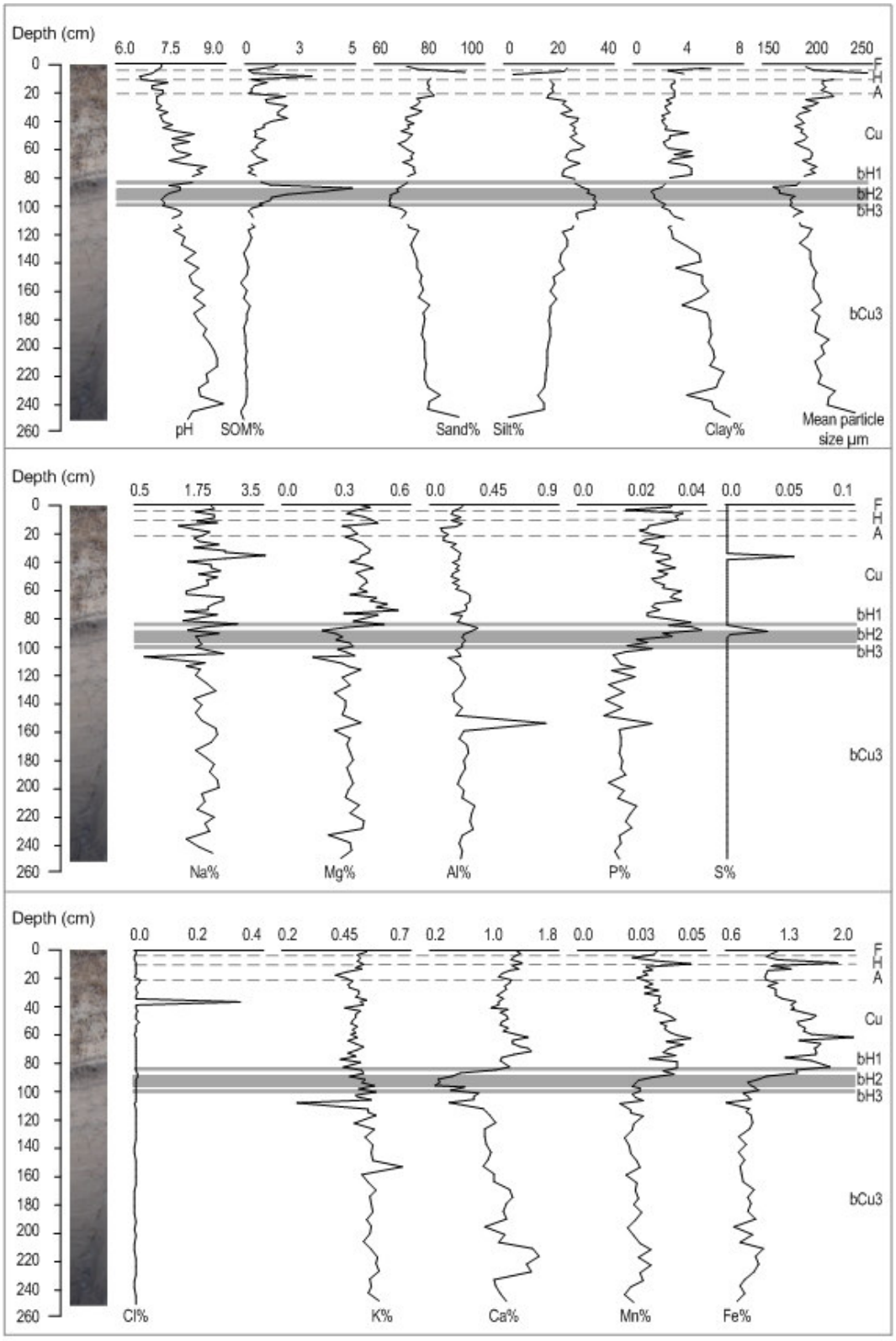

Figure 5.3 Stratigraphic section characteristics; pH, SOM, texture and geochemical composition (dashed lines show horizon boundaries and shaded areas represent organic layers).

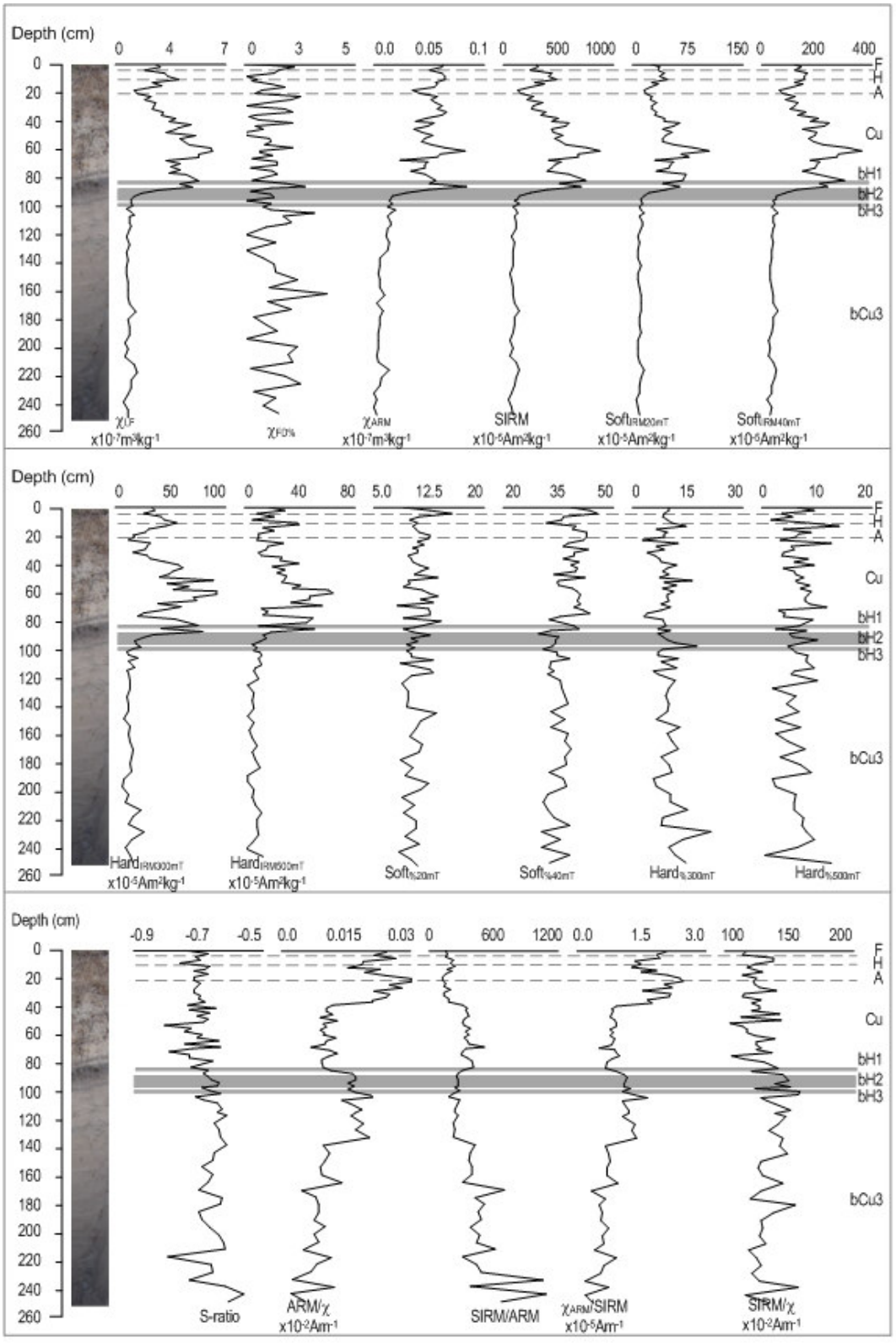

Figure 5.4 Stratigraphic section characteristics mineral magnetic characteristics (dashed lines show horizon boundaries and shaded areas represent organic layers).

Buried soil profile description

Profile ID: BS
Date of survey: 03/08/2008

Site description

Location: 500 m NNW of seaward edge of Lifeboat Road.
Grid reference: SD 27001 06592
Landform: Upper beach.
Land use: Recreation.
Weather: Clear and bright, ~20°C.

Soil description

Drainage: Tidal.
Surface cover: Bare sand; exposed soil organic surface.
Profile depth: 76 cm
Soil depth: 12-48 cm
NSRI class: Buried groundwater gley


a) Photograph facing north


b) Soil profile

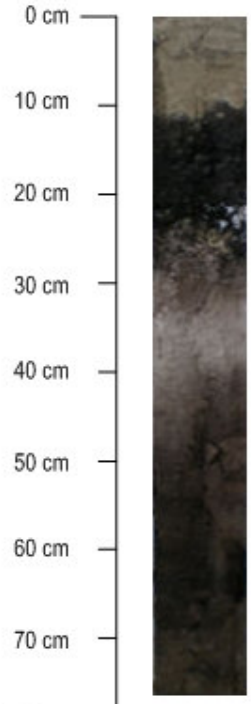

Horizon	Depth	Field description
Cu	0-12	Brown (10 YR 5/3) moist and brown (10YR 5/3) dry; loose sand stoneless; abrupt boundary to:
bH	12-24	Black (10 YR 2/1) moist and very dark brown (10YR 2/2) dry; clear smooth boundary to:
bAg	24-29	Dark greyish brown (10 YR 4/2) moist and greyish brown (10YR 5/2) dry; loose sand; stoneless; 25% distinct fine mottling; diffuse clear boundary to:
bE	29-38	Light brownish grey (10 YR 6/2) moist and very pale brown (10 YR 7/1) dry; loose sand; stoneless; diffuse boundary to:
bB	38-48	Dark greyish brown (10 YR 4/2) moist and light greyish brown (10 YR 6/2) dry; loose sand; diffuse boundary to:
bCu1	48-70	Very dark greyish brown (10 YR 3/2) moist and dark brown (10 YR 3/3) dry; loose sand; stoneless; unclear boundary to:
bCu2	70-76	Dark brown (10 YR 3/3) moist and brown (10 YR 5/3) dry; loose sand; stoneless; *tidal influence*.

Layer/horizon		Cu	bH	bAg	bE	bB	bCu
Sand	60-2000 µm %	91	61	66	71	70	70
Silt	2-60 µm %	5	37	30	23	23	25
Clay	<2 µm %	4	2	4	6	7	5
SOM %		2.3	14.3	1.8	0.7	0.6	1.2
pH in water (1:2.5)		8.1	7.5	7.6	7.3	7.1	7.3

Figure 5.5 Buried soil profile description. Scale on Plate b) is 15 cm (Site 2 on Figure 6.1).

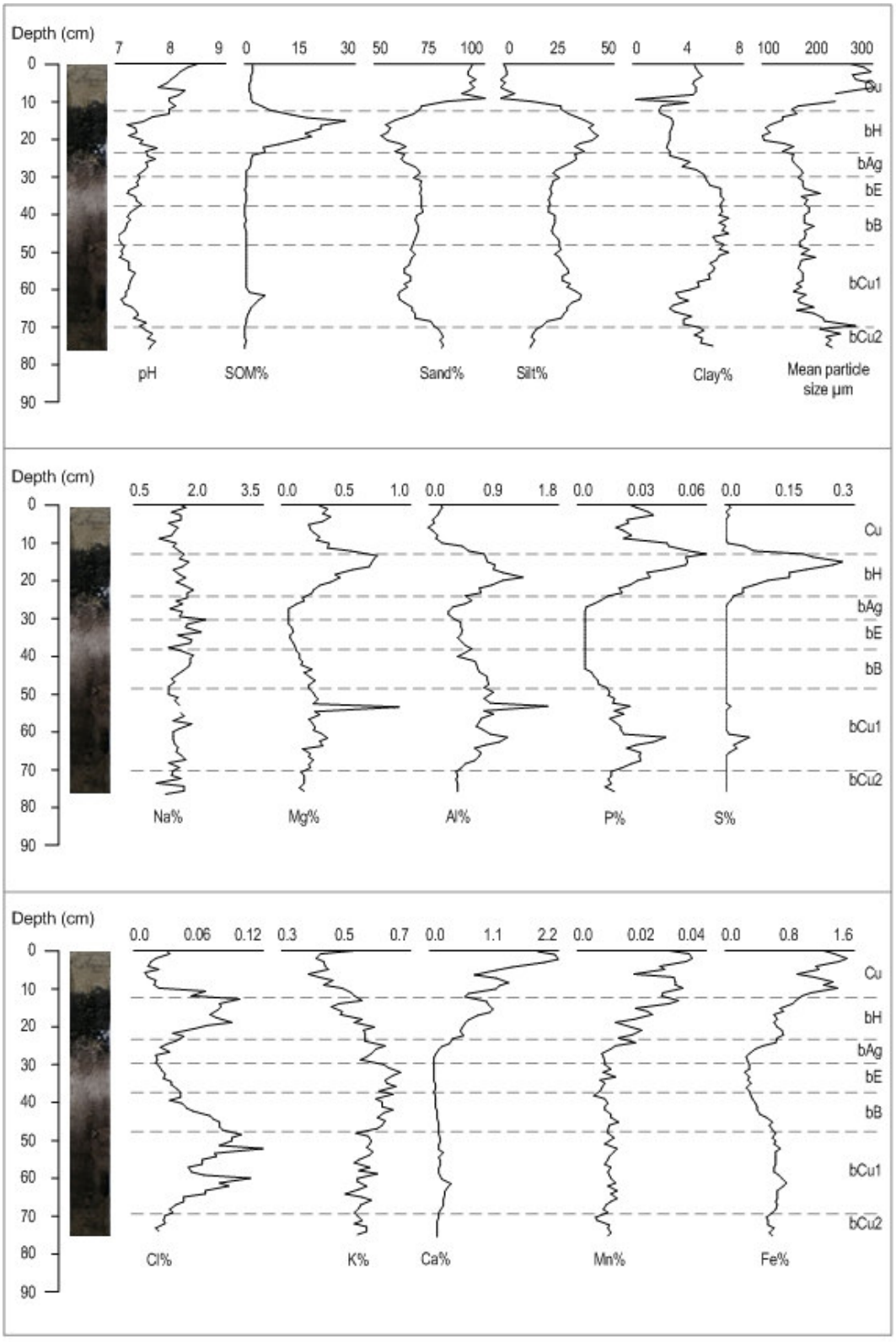

Figure 5.6 Down-profile changes in the buried soil characteristics; pH, SOM, texture and geochemical properties (dashed lines show horizon boundaries).

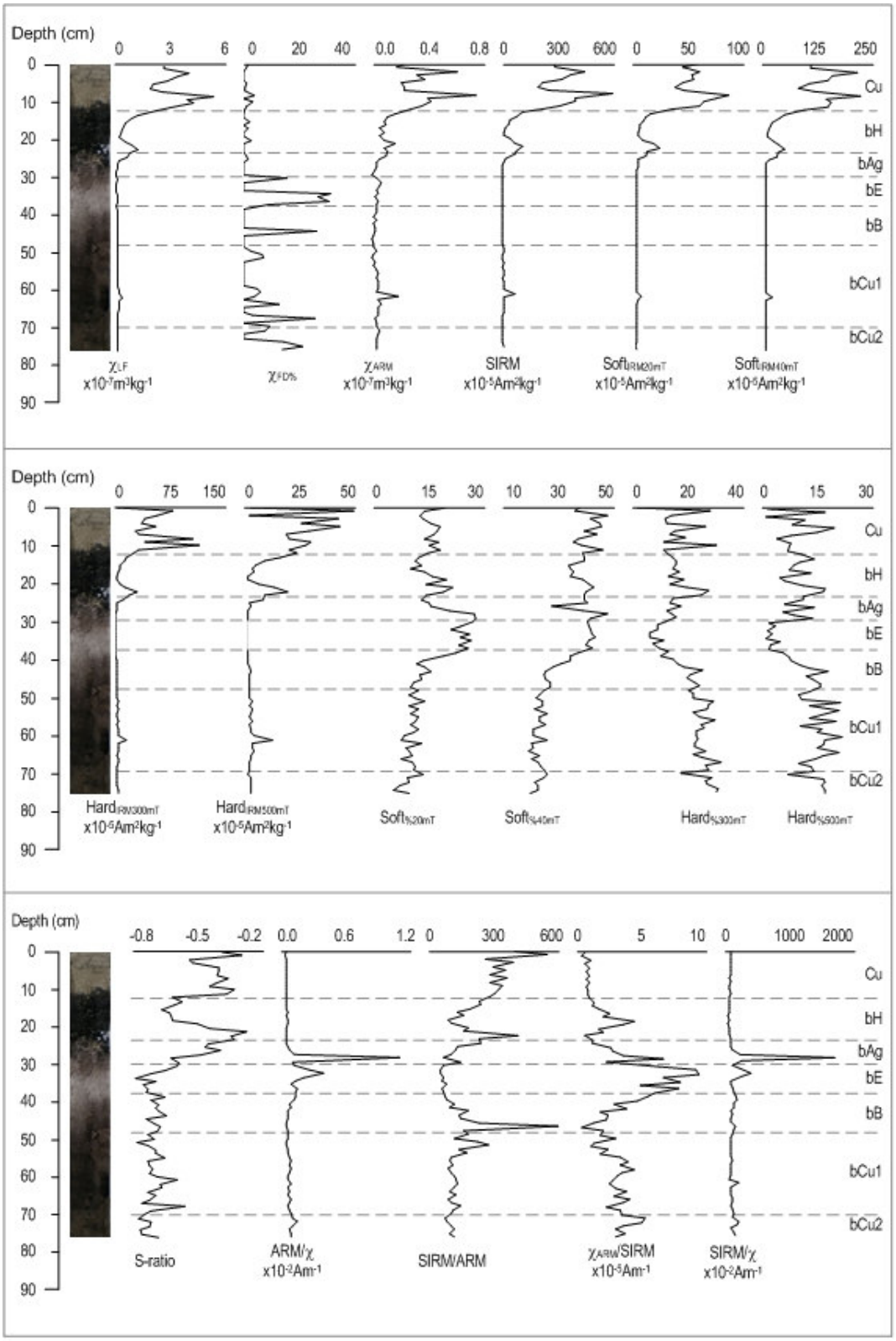

Figure 5.7 Down-profile changes in the buried soil mineral magnetic characteristics (dashed lines show horizon boundaries).

observed in the bE and bB horizons, indicating the presence of SSD grains. The predominant peak in ARM/χ (1.14 x10^{-2}Am^{-1}) and SIRM/χ (1687.62 x10^{-2}Am^{-1}) at 28 cm suggests a very strong influence of SSD magnetic grains and hard, haematite-type, mineralogy in the bAg horizon.

Tables 5.1a,b show the organo-mineral soil component had slightly different physico-chemical values (e.g. pH 7.39; SOM 5.38%; silt 28.92%) compared to the entire profile (pH 7.47; SOM 3.38%; silt 23.92%). Nutrient enrichment in the organo-mineral horizons is evident by increases in S (0.05%), but values of Ca decreased from 0.44 to 0.32%, alongside decreases in Fe from 0.68 to 0.51%. Decreased magnetic concentrations in the surface horizons (χ_{LF} 0.32 x10^{-7}m^{3}kg^{-1}; χ_{ARM} 0.01 x10^{-7}m^{3}kg^{-1}; SIRM 33.82 x10^{-5}m^{2}kg^{-1}), compared to the entire profile, including contemporary beach sediments (χ_{LF} 0.68 x10^{-7}m^{3}kg^{-1}; χ_{ARM} 0.01 x10^{-7}m^{3}kg^{-1}; SIRM 75.56 x10^{-5}m^{2}kg^{-1}), shows dissolution of magnetic minerals in the organo-mineral soil component. Although values are generally low throughout the profile, the content of ferrimagnetic 'magnetite (Fe_3O_4)-type' soft minerals (IRM_{20mT} 11.45; IRM_{40mT} 29.84) was higher than canted antiferromagnetic 'haematite (αFe_2O_3)-type' hard minerals (IRM_{300mT} 12.74 x10^{-5}m^{2}kg^{-1}; IRM_{500mT} 6.64 x10^{-5}m^{2}kg^{-1}).

5.4 Classification of buried soils using multivariate factor analysis

Results of descriptive statistics have identified key pedo-characteristics associated with both the buried organic layers in the dune cliff and the soil buried under beach sediments. Each buried soil appears to have very different properties, suggesting they developed under different dune environmental regimes. Therefore, multivariate factor analyses have been used as an attempt to identify any similarities these soils may have with the contemporary soils confidently classified in previous chapters. Of the exposed organic layers, the bH2 layer was chosen for analysis due to it being much thicker than the other organic layers. However, at just 10 cm in depth, this layer lacks further soil profile horizon definition and, therefore, will be considered as buried topsoil alone. Factor analysis on this sample population will be carried out alongside the topsoil sample populations identified in Chapter 3, Section 3.6.4. Factor analysis on the buried soil sample population will be carried out alongside the NRSI soil profile sample populations identified in Chapter 4, Section 4.5.2. However, this approach may not be ideal as buried soil characteristics may have been modified diagenetically post-burial, resulting in false palaeoenvironmental interpretations (Martini and Chesworth, 1992; Kemp *et al.*, 1994; Olson and Nettleton, 1998; Choi, 2005). In each case, parameter and sample loadings extracted from factors one and two were used to generate factor plots.

5.4.1 Factor analysis of the exposed organic layer (Site 1)

Factor analysis of key pedo-characteristics associated with topsoils (0-5 cm), allowed classification of soil properties into four distinct dune environments; 'frontal dune' (bare sand; mobile dune communities), 'hind dune' (fixed dune community; pasture; scrub), 'woodland' (deciduous woodland; coniferous plantation) and slack community (Chapter 3, Section 3.6.4). In

Table 5.1a Summary data* for the buried soil profile characteristics (n = 76) (Site 2 on Figure 6.1)

Parameters	Units	Mean	Median	SD	CV	Min	Max
pH	mol/ltr	7.473	7.375	0.357	4.773	7.010	8.510
SOM	%	3.380	0.949	5.523	163.364	0.325	27.086
Sand	%	71.541	68.940	10.648	14.883	53.430	100.000
Silt	%	23.919	25.988	10.909	45.607	0.000	43.989
Clay	%	4.540	4.599	1.592	35.079	0.000	6.950
Mean particle size	µm	183.668	172.257	42.273	23.016	102.161	294.048
Median particle size	µm	190.626	196.590	40.290	21.136	69.524	250.047
Sorting		2.085	2.174	0.493	23.644	0.501	2.579
Skewness	γ_1	0.661	0.758	0.193	29.135	0.029	0.806
Kurtosis	g_1	1.450	0.871	1.199	82.691	0.726	4.934
Sodium	%	1.539	1.530	0.210	13.675	0.970	2.180
Magnesium	%	0.263	0.233	0.167	63.465	0.060	0.900
Aluminium	%	0.607	0.636	0.301	49.551	0.016	1.660
Phosphorus	%	0.018	0.016	0.014	75.374	0.002	0.058
Sulphur	%	0.026	0.001	0.058	226.282	0.001	0.266
Chlorine	%	0.050	0.045	0.025	49.779	0.012	0.115
Potassium	%	0.546	0.554	0.064	11.747	0.375	0.664
Calcium	%	0.439	0.174	0.508	115.653	0.068	2.160
Manganese	%	0.014	0.010	0.008	115.653	0.004	0.035
Iron	%	0.676	0.641	0.305	45.157	0.262	1.542
χ_{LF}	$10^{-7}m^3kg^{-1}$	0.683	0.106	1.183	173.163	0.003	5.249
χ_{FD}	%	3.983	0.001	7.731	194.076	0.001	31.250
χ_{ARM}	$10^{-7}m^3kg^{-1}$	0.011	0.005	0.013	123.437	0.001	0.072
SIRM	$10^{-5}Am^2kg^{-1}$	75.564	13.166	128.306	169.798	5.063	598.448
$Soft_{IRM20mT}$	$10^{-5}Am^2kg^{-1}$	11.449	1.749	19.783	172.794	0.586	82.094
$Soft_{IRM40mT}$	$10^{-5}Am^2kg^{-1}$	29.636	3.119	52.991	178.808	2.412	222.314
$Hard_{IRM300mT}$	$10^{-5}Am^2kg^{-1}$	12.740	3.303	23.584	185.121	0.390	121.893
$Hard_{IRM500mT}$	$10^{-5}Am^2kg^{-1}$	6.637	1.924	10.839	163.309	0.029	49.470
$Soft_{\%20mT}$	%	14.760	13.314	5.712	38.697	5.041	28.655
$Soft_{\%40mT}$	%	32.633	34.567	8.555	26.214	19.722	47.637
$Hard_{\%300mT}$	%	18.891	19.064	7.265	38.457	1.183	31.767
$Hard_{\%500mT}$	%	10.946	11.469	5.685	51.936	0.353	21.262
S-ratio	(none)	-0.616	-0.672	0.135	-21.909	-0.786	-0.290
ARM/χ	$10^{-2}Am^{-1}$	0.064	0.035	0.137	215.346	0.007	1.137
SIRM/ARM	(None)	155.356	109.921	113.487	73.050	33.228	579.650
χ_{ARM}/SIRM	$10^{-5}Am^2kg^{-1}$	3.118	2.859	2.010	64.471	0.542	9.452
SIRM/χ	$10^{-2}Am^{-1}$	160.539	124.053	185.897	115.795	79.772	1687.618

Table 5.1b Summary data* for the buried soil, soil component characteristics (n = 36) (Site 2 on Figure 6.1)

Parameters	Units	Mean	Median	SD	CV	Min	Max
pH	mol/ltr	7.387	7.365	0.238	3.216	7.010	7.990
SOM	%	5.375	0.798	7.476	139.084	0.412	27.086
Sand	%	66.503	68.806	5.572	8.378	53.430	72.165
Silt	%	28.916	26.030	7.026	24.298	21.345	43.989
Clay	%	4.580	5.166	1.839	40.147	1.683	6.950
Mean particle size	µm	158.997	168.884	24.838	15.622	102.161	200.267
Median particle size	µm	168.624	191.120	43.573	25.840	69.524	203.043
Sorting		2.228	2.225	0.228	10.225	1.825	2.579
Skewness	γ_1	0.678	0.767	0.164	24.165	0.290	0.806
Kurtosis	g_1	0.890	0.869	0.088	9.874	0.783	1.135
Sodium	%	1.634	1.620	0.206	12.589	1.270	2.180
Magnesium	%	0.252	0.172	0.209	82.889	0.060	0.739
Aluminium	%	0.658	0.636	0.231	35.102	0.286	1.309
Phosphorus	%	0.015	0.006	0.018	119.626	0.002	0.058
Sulphur	%	0.047	0.001	0.078	165.083	0.001	0.266
Chlorine	%	0.050	0.044	0.021	42.910	0.021	0.094
Potassium	%	0.580	0.591	0.053	9.157	0.449	0.664
Calcium	%	0.320	0.138	0.320	100.248	0.068	1.069
Manganese	%	0.012	0.009	0.007	53.910	0.004	0.031
Iron	%	0.511	0.465	0.202	39.506	0.262	0.979
χ_{LF}	$10^{-7}m^3kg^{-1}$	0.315	0.084	0.462	146.754	0.003	2.185
χ_{FD}	%	4.271	0.001	9.407	220.251	0.001	31.250
χ_{ARM}	$10^{-7}m^3kg^{-1}$	0.007	0.006	0.005	76.838	0.001	0.027
SIRM	$10^{-5}Am^2kg^{-1}$	33.821	11.560	46.240	136.719	5.063	225.729
$Soft_{IRM20mT}$	$10^{-5}Am^2kg^{-1}$	5.214	1.840	6.896	132.265	1.153	33.034
$Soft_{IRM40mT}$	$10^{-5}Am^2kg^{-1}$	13.041	3.101	18.468	141.618	2.412	88.539
$Hard_{IRM300mT}$	$10^{-5}Am^2kg^{-1}$	5.511	2.368	7.720	140.087	0.390	31.372
$Hard_{IRM500mT}$	$10^{-5}Am^2kg^{-1}$	3.696	1.195	5.752	155.625	0.029	23.482
$Soft_{\%20mT}$	%	18.186	15.629	5.938	32.652	9.932	28.655
$Soft_{\%40mT}$	%	37.200	39.518	5.705	15.337	25.509	47.633
$Hard_{\%300mT}$	%	14.688	14.425	5.303	36.107	5.442	27.433
$Hard_{\%500mT}$	%	8.440	8.285	5.029	59.592	0.401	17.380
S-ratio	(none)	-0.607	-0.635	0.125	-20.598	-0.786	-0.290
ARM/χ	$10^{-2}Am^{-1}$	0.074	0.039	0.147	200.497	0.008	1.137
SIRM/ARM	(None)	136.182	112.613	110.743	81.320	33.228	579.650
χ_{ARM}/SIRM	$10^{-5}Am^2kg^{-1}$	3.731	2.789	2.484	66.575	0.542	9.452
SIRM/χ	$10^{-2}Am^{-1}$	195.343	127.351	269.491	137.958	79.772	1687.618

Mean; SD = standard deviation; CV = percentage coefficient of variation; Min = minimum value; Max = maximum value. Values are shown to 3 decimal places for consistency, not accuracy.

this section, pedo-characteristics of the buried topsoil (bH2), exposed in the stratigraphic section, are applied to the same factor plot, previously presented in Figure 4.13b, to identify the pedo-environment in which the buried soil would have developed.

The first two factors extracted explain 55.66% of variation in the 11 key parameters (Table 5.2). Figure 5.8 shows a factor plot created from parameter and sample loadings from Factors 1 and 2, based on the results from factor analysis. Factor 1 (distance) explains 34.65% of variation in the parameters, with SOM, Na, Si and χ_{LF} having negative loadings; while pH, clay, mean particle size, Mg, P, K and Ca have positive loadings. Factor 2, however, explains 21.01% of variation, with SOM, Mg, P and K having negative loadings, while pH, clay, mean particle size, Na, Si and Ca have positive loadings. Buried organic samples are plotted in the centre of the factor plot, suggesting that physico-chemical parameter influences have been lost over time. However, most buried organic samples have negative loadings on Factor 1, separating them from the frontal dune topsoils, which have positive loadings. These samples are also separated from the woodland topsoils, which are negatively loaded on Factor 2. Hind dune topsoils have both positive and negative loadings on Factor 1, as well as some positive loadings on Factor 2. The spread of this sample population suggests Ca influences, with an increasing χ_{LF} influence, likely to be associated with soil maturity. The buried organic sample population appears to be negatively loaded on Factor 2, with strong Ca influences, suggesting these samples represent a former slack environment that has since become buried under a hind dune environment.

5.4.2 Factor analysis of the buried soil profile (Site 2)

Factor analysis was used to provide details on down-profile changes in physico-chemical parameters of the soil buried under contemporary beach sediments and to identify the NSRI classification. Figure 5.9 shows the factor plot for the buried soil profile using all physico-chemical parameters. The first two factors extracted explain 57.32% of variation (Table 5.3). Factor 1 (depth) explains 40.95% of variation, while Factor 2 (organic content) explains 16.37%. The spread of parameter loadings along Factor one indicates profile depth as the major influencing factor. Factor two divides the profile into organic and mineral sections.

The bH layer is positively loaded on both factors, strongly influenced by pH and SOM. Large percentages of silt in this horizon are reflected in the magnetic mineral concentrations and magnetic mineralogy influences. Na becomes more of an influence down-profile, represented by most bAg samples being negatively loaded on Factor 1 and positively loaded on Factor 2. The bE horizon samples are negatively loaded on Factor 1 and positively loaded on Factor 2, becoming less affected by Na and more influenced by K and magnetic domain size. The bB horizon samples are all negatively loaded on Factor 1, while most are also loaded on Factor 2, suggesting this horizon is dominated by both sand- and clay-sized particles. The samples are becoming more influenced by hard, haematite-type, mineralogy at this depth, the effects of

Table 5.2 Summary results from factor analysis of the organic layer using selected parameters.

Factors	Eigenvalues	Total variance (%)	Cumulative eigenvalues	Cumulative total variance (%)
1	3.812	34.653	3.812	34.653
2	2.311	21.007	6.123	55.660
3	1.942	17.652	8.064	73.312
4	0.896	8.146	8.960	81.458
5	0.716	6.506	9.676	87.964
6	0.450	4.087	10.126	92.050
7	0.308	2.802	10.434	94.852
8	0.256	2.324	10.689	97.177
9	0.146	1.330	10.836	98.507
10	0.121	1.097	10.956	99.603
11	0.044	0.397	11.000	100.000

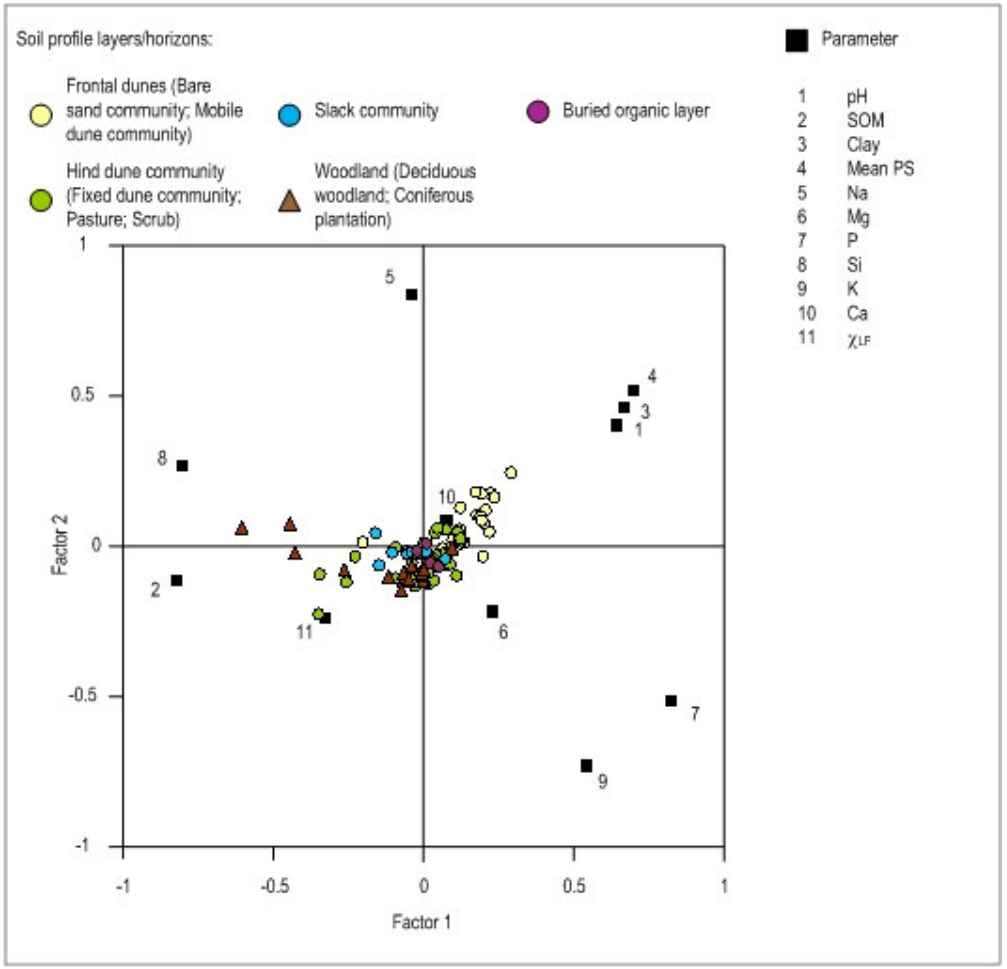

Figure 5.8 Simultaneous R- and Q-mode factor analysis plots of Factor 1 versus Factor 2, based on organic layer selected characteristics.

Table 5.3 Summary results from factor analysis of the buried soil profile using all parameters.

Factors	Eigenvalues	Total variance (%)	Cumulative eigenvalues	Cumulative total variance (%)
1	14.743	40.954	14.743	40.954
2	5.892	16.366	20.635	57.320
3	4.531	12.586	25.166	69.906
4	2.569	7.135	27.735	77.041
5	1.826	5.073	29.561	82.114
6	1.557	4.326	31.118	86.440
7	0.945	2.626	32.064	89.066
8	0.883	2.454	32.947	91.520
9	0.621	1.725	33.568	93.245
10	0.423	1.174	33.991	94.419
11	0.294	0.818	34.285	95.237
12	0.266	0.739	34.552	95.976
13	0.227	0.631	34.779	96.607
14	0.200	0.555	34.978	97.162
15	0.170	0.472	35.148	97.634
16	0.156	0.434	35.305	98.068
17	0.144	0.400	35.449	98.468
18	0.123	0.341	35.571	98.809
19	0.087	0.243	35.659	99.052
20	0.084	0.234	35.743	99.286
21	0.050	0.140	35.793	99.426
22	0.048	0.132	35.841	99.558
23	0.038	0.106	35.879	99.664
24	0.028	0.078	35.907	99.742
25	0.024	0.068	35.932	99.810
26	0.023	0.065	35.955	99.875
27	0.014	0.040	35.969	99.914
28	0.011	0.030	35.980	99.944
29	0.007	0.019	35.987	99.964
30	0.005	0.015	35.992	99.979
31	0.004	0.010	35.996	99.989
32	0.002	0.005	35.998	99.994
33	0.001	0.003	35.999	99.997
34	0.001	0.002	36.000	100.000
35	0.000	0.000	36.000	100.000
36	0.000	0.000	36.000	100.000

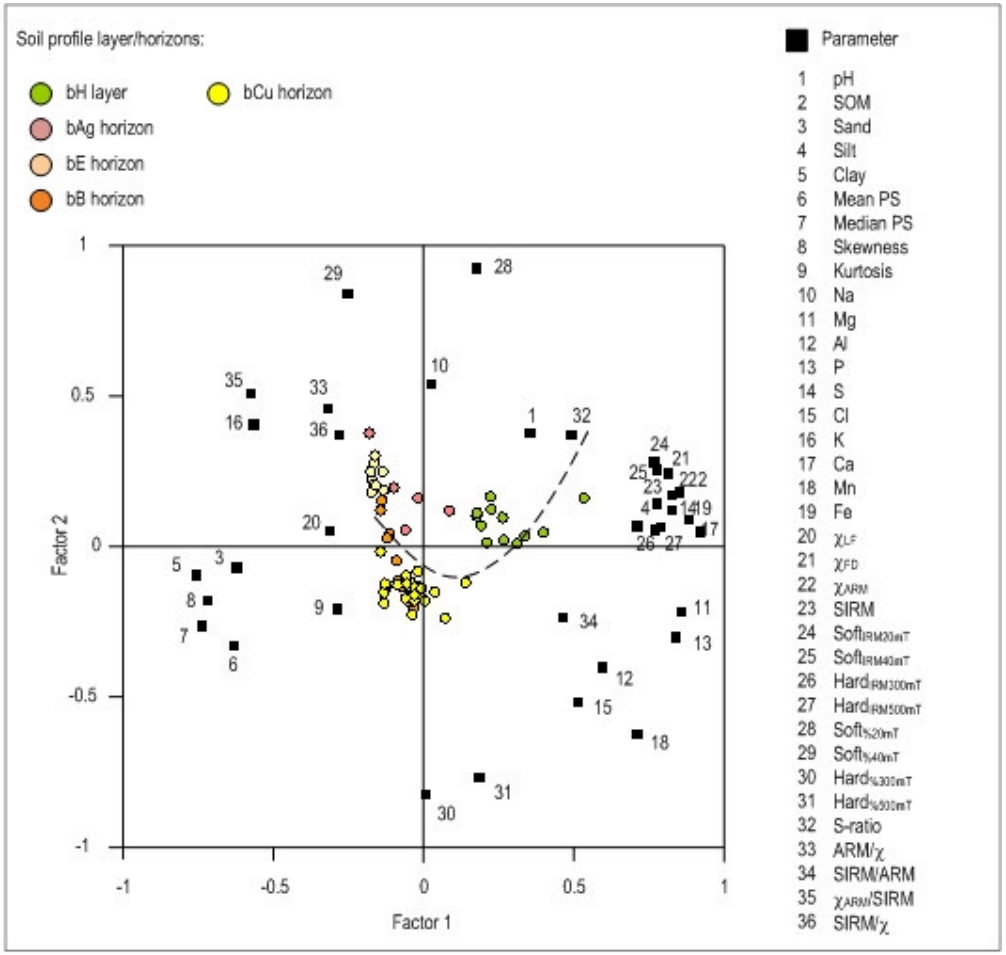

Figure 5.9 Simultaneous R- and Q-mode factor analysis plots of Factor 1 versus Factor 2, based on buried soil profile characteristics (dashed line represents postulated soil horizon development).

which are enhanced further by most bCu samples being negatively loaded on Factor 1 and all of the samples being negatively loaded on Factor 2.

5.4.3 Factor analysis of the buried soil profile and other NSRI classifications using geochemical parameters

Separation between the organo-mineral soil component and the parent material of the buried soil profile was made (Chapter 4, Section 4.2). Factor analysis of pedo-characteristics has classified soil profiles on the Sefton coast into five distinct NSRI environments; 'terrestrial raw sand' (mobile dune community), 'sand-pararendzina' (fixed dune community; pasture; scrub), 'groundwater gley' (slack community), 'brown earth' (deciduous woodland) and 'micro-podzol' (heath; coniferous plantation) (Chapter 4, Section 4.5.2). Of these analyses, the geochemical parameters proved most successful in establishing NRSI classifications. Therefore, in this section the geochemical parameters of the soil buried under contemporary beach sediments are applied to the same factor plot, previously presented in Figure 5.51b, to identify the pedo-environment that the buried soil would have developed under.

Figure 5.10 shows the factor plot for the buried soil profile using geochemical parameters. The first two factors extracted explain 60.12% of variation in the parameters (Table 5.4). Factor 1 explains 42.45% of variation, while Factor 2 (possibly age) explains 17.68%. Most of the buried soil sample population is negatively loaded on Factor 2 and both positively and negatively loaded on Factor 1. The limited influence of both Ca and Mn separates these samples from those associated with both the sand-pararendzina and groundwater gley profiles. Strong influences of K and Al suggest the buried soil profile is a well-developed and mature soil. However, the samples are separated from both the brown earth profile and the micro-podzol profile by limited influences of Fe, Ca, Cl, Mg, P and S. This suggests the buried soil represents a historic pedo-environment that is unlike any other on the Sefton dunes today. The position of sample points on the factor plot suggests this soil was more advanced than the micro-podzol. Acidic characteristics, due to leaching of Mg, Ca and Fe, may indicate a mature organic soil that developed under older vegetation, than the current plantations. However, it is likely this soil may possibly have been modified diagenetically post-burial.

5.5 Conceptual modelling of the pedo-history of the Sefton coast

Buried soils in dune cliffs along the Sefton coast provide evidence of a complex dynamic history of phases of dune activity, erosion and morphological change, interspersed with environmentally stable conditions. This provides baseline information useful for the development of a conceptual model outlining the pedo-history of the Sefton coast. The proposed cyclic model (Chapter 1, Section 1.5.5) represents five-stages in the evolution of the Sefton coast around the eroding Formby Point section, between Fisherman's Path (SD 280 099) and Lifeboat Road (SD 271 063) (Figure 5.11). The model begins by highlighting the initial phase of dune erosion, thought to have been brought about by the Little Ice Age (LIA), ~13th Century (Pye and Neal, 1993), which resulted in the shape of the dune ramp and exposed soils in existence today. The

Table 5.4 Summary results from factor analysis of the organic layer using selected parameters.

Factors	Eigenvalues	Total variance (%)	Cumulative eigenvalues	Cumulative total variance (%)
1	4.244	42.445	4.244	42.445
2	1.768	17.678	6.012	60.123
3	1.161	11.612	7.173	71.734
4	0.921	9.210	8.094	80.945
5	0.801	8.010	8.896	88.955
6	0.355	3.554	9.251	92.509
7	0.326	3.263	9.577	95.772
8	0.227	2.274	9.805	98.046
9	0.128	1.278	9.932	99.324
10	0.068	0.676	10.000	100.000

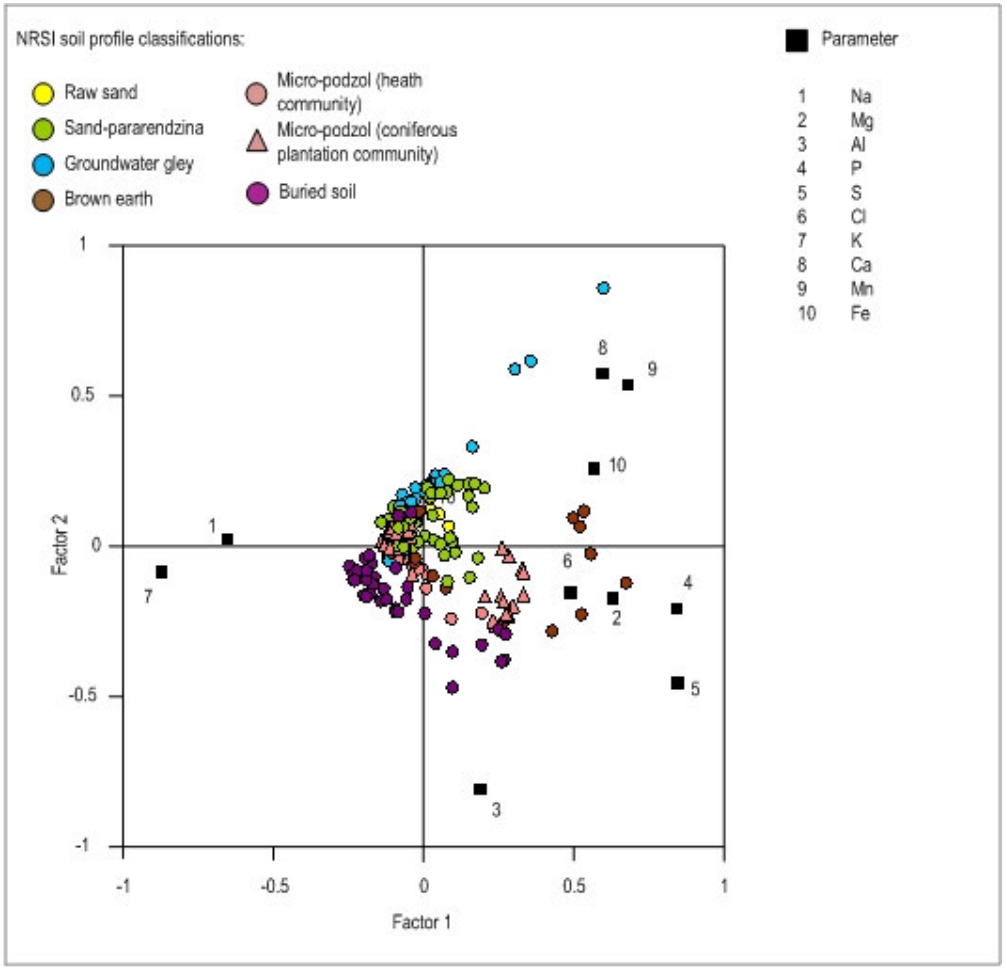

Figure 5.10 Simultaneous R- and Q-mode factor analysis plots of Factor 1 versus Factor 2, based on the organic layer selected characteristics.

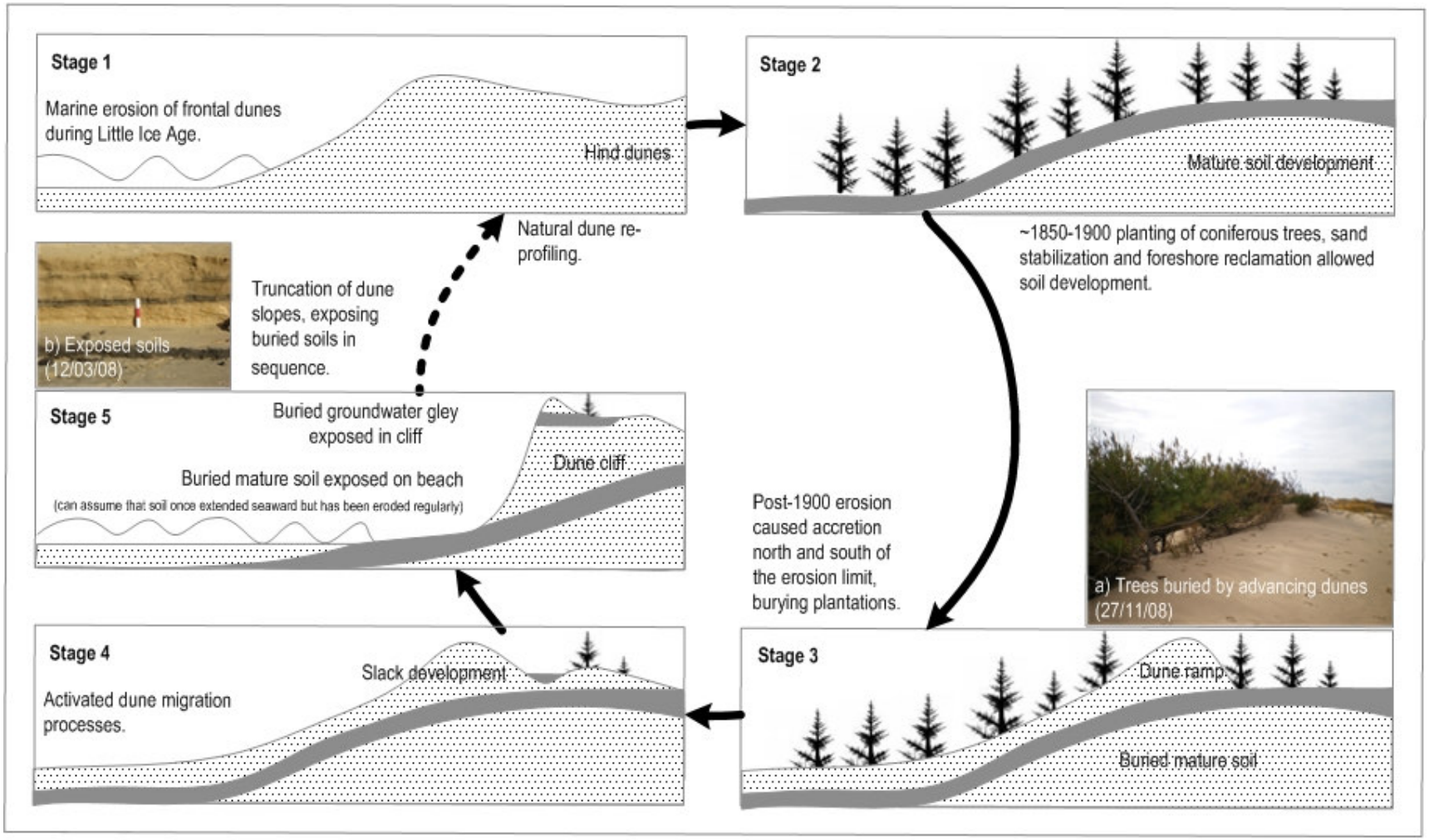

Figure 5.11 Conceptual model of the proposed five-stages in the geomorphic evolution of Formby Point (exaggerated scale).

following sections describe each stage of the conceptual model in detail, finishing with the present-day scenario. However, the cyclic nature of the model aims to suggest that this process does not necessarily have a beginning and an end circumstance, but each stage is constantly re-activated in response to environmental change.

5.5.1 Stage 1: Frontal dune transgression

Erosion of the frontal dunes occurred during a phase of increased storminess, possibly initiated during the Little Ice Age (LIA), in the 13th Century (Innes and Tooley, 1993), which eroded the coastline as far landward as the hind dunes (Pye and Neal, 1993).

5.5.2 Stage 2: Soil development and colonization

A period of marine regression and increased deposition of aeolian sediments on the foreshore, possibly due to sand stabilization and foreshore reclamation measures carried-out 1850-1900 (Pye and Neal, 1993), meant the environment became stable enough for soil development. The resulting soil profile was mature, evident by high SOM in a thick H layer, similar to that of the contemporary deciduous woodland soil profile or that of the coniferous plantation (Chapter 4, Figures 4.20 and 4.23, respectively), which have developed over the last 100 years since conifer planting began in 1887. This overlies a mottled Ag horizon. Nutrient enrichment in the organo-mineral horizons was associated with high values of S, K and Al, alongside low values of Ca and Fe. Na becomes more of an influence down-profile, suggesting that leaching processes were in operation. Limited influences of Fe, Ca, Cl, Mg and P, make this soil different from either a brown earth or micro-podzol profile, suggesting that the buried soil represents a historic pedo-environment that is unlike any other on the Sefton dunes today.

The lower elevation of the profile buried on the foreshore, along with its defined horizons, suggests this soil predates the buried organic layer in the exposed section. It may even represent a spatial continuation of the 18th Century peat deposit, identified by Innes and Tooley (1993) on Formby Moss (Chapter 1, Section 1.5.6), that was overblown by sand during the Little Ice Age. However, the presence of distinct horizon definitions suggests that this deposit represents soil development, following a phase of rapid colonization of the seaward advancing shoreline by vegetation from the hind dunes, already planted with conifers in ~1900 (e.g. Gresswell, 1953; MacDonald, 1954; Pethick, 2001; Simpson and Gee, 2001). It is important to note that using soil development as an indication of age is subjective, as the properties of A horizons do not always serve as a good indicator of soil age or maturity (Turk *et al.,* 2008). Soil development also relies on Jenny's (1941) other four factors.

5.5.3 Stage 3: Frontal dune regression and soil preservation

Post-1900 erosion at Formby Point (Plater *et al.,* 1993) resulted in available sand for renewed dune formation and mobility. Aeolian processes transported sand up dune slopes, burying the soil profile on the foreshore, diagnostic of depositional processes (Sutherland and Lee, 1994). Subsequently, this soil became preserved under 12 cm of contemporary beach and dune

sediment deposits. Burial of this dune environment is still is operation today, where coniferous plantations are being suffocated by migrating frontal dunes (Figure 5.11, Plate a).

5.5.4 Stage 4: Migration of mobile dunes and slack formations

The phase of environmental stability and dune formation was sufficient for mobilization of the frontal dunes. Deflation created slacks and, subsequent, soil development with strong Ca influences. Strong χ_{LF} influences suggest that this groundwater gley slack soil dried out, before eventually being re-buried during cyclic episodes, to finally become overlaid by a hind dune environment. This organic horizon lies at >150 cm above the buried mature soil profile, providing an indication of the time frame involved during this phase of dune migration. Thin organic horizons, separated from the buried slack soil by sand layers, indicate brief interruptions of soil development by minor influxes of dune sand.

5.5.5 Stage 5: Foredune truncation and soil exposure

Although, Stages 3 and 4 of the cyclic model are still in operation north of the erosion limit, more recent, intense, ongoing phases of dune-toe erosion have truncated gentle slopes of the migrating dune system around Formby Point. This has exposed buried soils associated with at least three phases of environmental stabilization and historic pedo-environments (Figure 5.11, Plate b). These are evident by increased acidity, SOM, silt-sized particles, P and S, alongside decreased sand- and clay-sized particles, Mg, Ca and Mn. Shallow sedimentary layers, in between the buried organic layers, represent relatively short periods of dune mobilization. A shallow, contemporary sand-pararendzina soil profile, at the surface of the stratigraphic section, represents the latest phase of dune-building activity.

Ongoing marine erosion has also exposed the lower elevated mature soil profile at the surface of the beach sediments. The permanently waterlogged nature of the bCu horizon (observed in the field), suggests this soil is likely to have undergone post-burial diagenetically modification.

5.6 Summary

The soil profile buried on the foreshore appears to represent a mature organic soil, suggesting pedogenesis occurred on a once well-drained, stable surface. Whereas, the buried organic horizon, within the exposed stratigraphic section, represents a former slack environment that has since become buried under a hind dune environment.

Both buried soils suggest the following cyclic model: i) transgression of frontal dunes and flattening of dune cliffs; ii) simultaneous soil development and colonization of the seaward advancing shoreline by woodland vegetation; iii) renewed dune formation activity and, subsequent, habitat burial and soil preservation; iv) dynamic, migrating mobile dune environment with cyclical slack formations and burials; and v) truncation of mobile dunes and soil exposure by erosion.

CHAPTER 6

A protocol to monitor Sefton dune morpho-dynamics and local rates of coastal change

Previous chapters have established pedo-succession operating on both contemporary and historic stable dune landscapes. The cyclic nature of erosion and accretion within this coastal system has exposed historic soils that were inhibited from further succession by sand burial. Chapter 6 provides a protocol for studying the Sefton coast as a dynamic system, to gain an insight into how contemporary soils may be affected by present-day coastal processes. Interactions between general elements of coastal geomorphology are considered on long-term (centuries/decades), mid-term (annual) and short-term (annual/seasonal) timescales, using photography. Analysis of vertical aerial photographs and Ordnance Survey (O.S.) Maps, identify macro-scale rates and typicalities of localized geomorphic and anthropogenic coastal change over the past century. Comparison between a dune-toe photographic survey, August 2006, with oblique aerial photographs (taken by the North West and North Wales Coastal Group, early 2008), distinguish annual meso-scale coastal change and, subsequent, soil erosion. A Fixed Point Photographic (FPP) survey identifies annual and seasonal change in dune morphological structure and topsoil burial, on a micro-scale. The Chapter finishes with a brief discussion on the Sefton dune morpho-dynamics and local rates of coastal change, which may affect pedogenesis.

6.1 Introduction

Assessment of dune pedo-system responses to coastal change requires an understanding of the causes that have influenced present day dune morphology and the timescales on which they operate. Therefore, the aim of this Chapter is to develop a protocol for studying and modelling dune processes, based on the Sefton coast. According to Pye (1990), the morphology of coastal dunes is governed by beach morphology, aeolian characteristics, vegetation cover and anthropogenic activities, effects of which can be traced back and monitored through maps and photography as long as they are available.

6.2 Monitoring long-term coastal change

Given the current trend of sea level rise since ~1850 (Houghton *et al.,* 1996), especially during the last 50 years (Shackley *et al.,* 1998; Evans *et al*., 2004), examination of long-term erosion and accretion trends aid understanding of coastline and pedo-environment future responses. Beach level dynamics and dune-toe position on the Sefton coast have been studied since the 1950s (e.g. Gresswell, 1953; Turner, 1984; Pye and Neal, 1994; Saye *et al.,* 2005; Pye and Blott, 2008). Changes in the position of the dune-toe around Formby Point have been monitored since 1958, first by Southport Corporation and since 1974 by Sefton Council Engineer and Surveyor's Department (now the Technical Services Department). However, gaps in the data have occurred. Through O.S. map and vertical aerial photography analyses, these gaps have been filled to create a fuller, more accurate database.

6.2.1 Ordnance Survey (O.S.) Map evidence of coastal dynamics

Relatively accurate information about shoreline changes along the Sefton coast has been available since 1845, when the first O.S. maps were published. Although now relatively stable, the dunes were considerably more active in the past. A period of sea regression occurred 1850-1909, when the entire shoreline accreted by ~200 m (Gresswell, 1953), evident in Figures 6.1 and 6.2. This resulted in seaward migration of hind dune environments, suggesting sand-pararendzina development. It is apparent that dune extent was greatest in 1909, with mean annual accretion rates recorded as 4.7 m/y during 1892-1906 (Smith, 1987). However, since 1906, Formby Point has been subject to erosion (Pye and Smith, 1988), initially at Victoria Road (SD 275 083), reaching a rate of 7-8 m/y during 1945-1965 (Smith, 1987) and a total landward retreat of ~400 m (Pye and Neal, 1994). Erosion limits have progressed southwards during 1929-1976 and north towards Lifeboat Road (SD 271 063) since the 1970s, which has continued to the present day (Turner, 1984) (Figures 6.3-5), constantly increasing the length of coastline and hind dune pedo-environment subject to erosion (a diagrammatic representation of Sefton's dynamic coastline, based on O.S. map evidence, after Turner (1984), is represented in Chapter 1, Figure 1.5). Continued accretion, north of the erosion limit, is currently creating a straighter coastline, with renewed frontal dune and, subsequent terrestrial raw sand development, compared to the angular profile in existence during the early 20th Century.

During the 19th and early 20th Centuries, active management was carried out by local landowners to encourage dune stability and promote shoreline accretion around Formby Point (Pye and Neal, 1994). Hind dune areas were stabilized by the establishment of ~120 ha conifer plantations (Jones *et al.,* 1993), resulting in rapid micro-podzol development. These considerable pine plantations were evident between Victoria Road (SD 275 083) and Wicks Lane (SD 270 070) on the 1909 O.S. map (Figure 6.2). However, by 1929, this plantation unit had become separated into two distinct areas (Figure 6.3), as a result of aeolian derived sand in the central section, suggesting a sand-pararendzina development overlying the buried micro-podzol environment. By 1976, the seaward edge, along with contemporary sand-pararendzina developments, appears to be disappearing as a result of localized coastal erosion (Figure 6.4).

The early 20th Century saw the beginnings of anthropogenic dune levelling of areas not occupied by trees for asparagus planting (Lewis and Cowell, 2002). This would have resulted in rapid stabilization and sand-pararendzina development. Felling was a gradual process since 1925, the methods of which included leaving small patches of planted trees to act as wind-beaks, to protect felled areas (Gresswell, 1953). This subsequently, protected the pedo-environment behind from erosion and sand burial.

Reliance on O.S. maps for accurate environmental reconstructions has its flaws. For example, a phase of deforestation was conducted on Ainsdale sand dunes during winter 1995-1996 (a map of which is presented in Chapter 1, Figure 1.14) but is not evident on the 2000 O.S. map (Figure 6.5). Therefore, supplementary aerial photography analysis is strongly required.

Figure 6.1 Ordnance Survey Map of the Sefton coast, 1850, 1:50,000 (© Crown Copyright. All rights reserved Sefton Council Licence no 100018192).

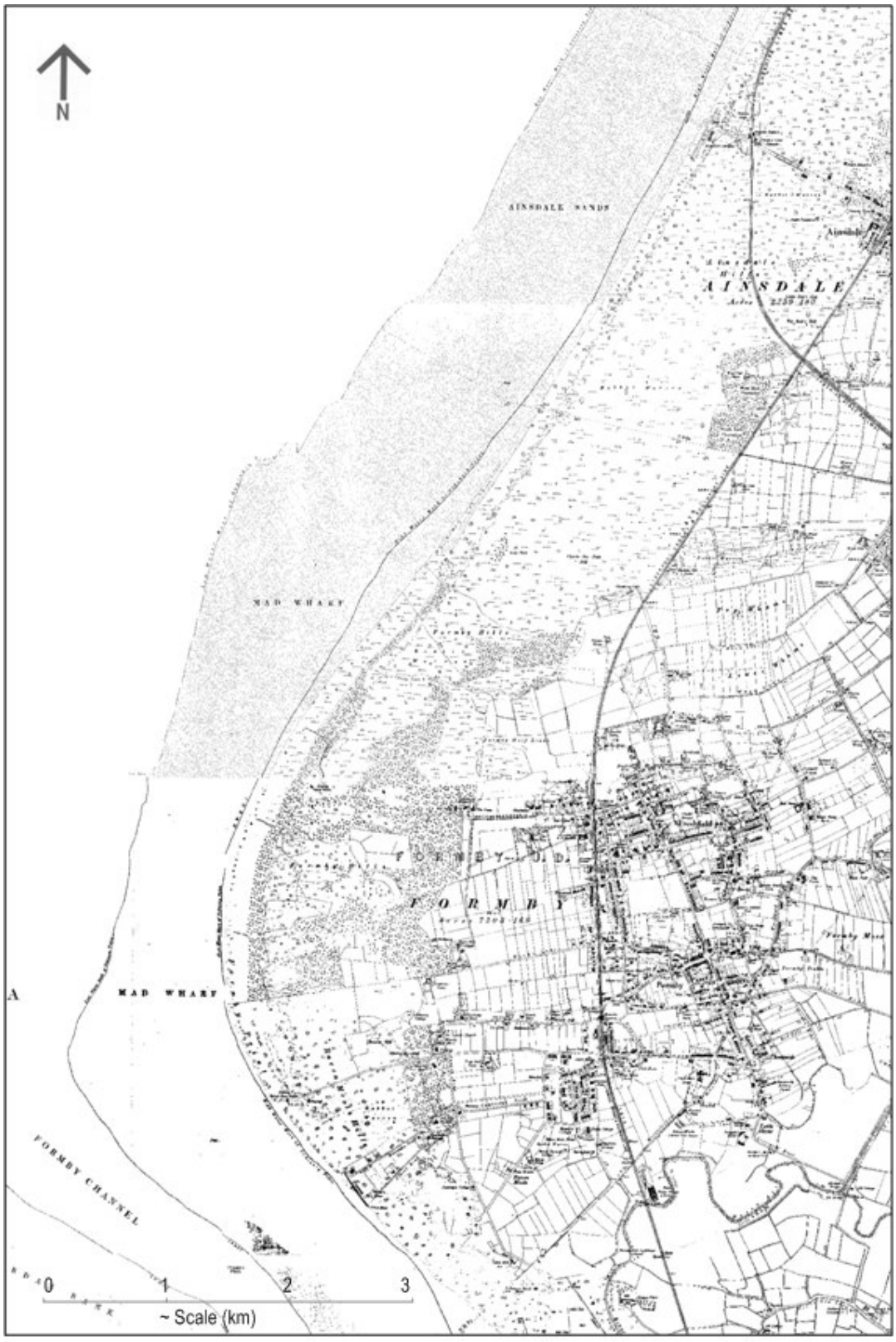

Figure 6.2 Ordnance Survey Map of the Sefton coast, 1909, 1:50,000 (© Crown Copyright. All rights reserved Sefton Council Licence no 100018192).

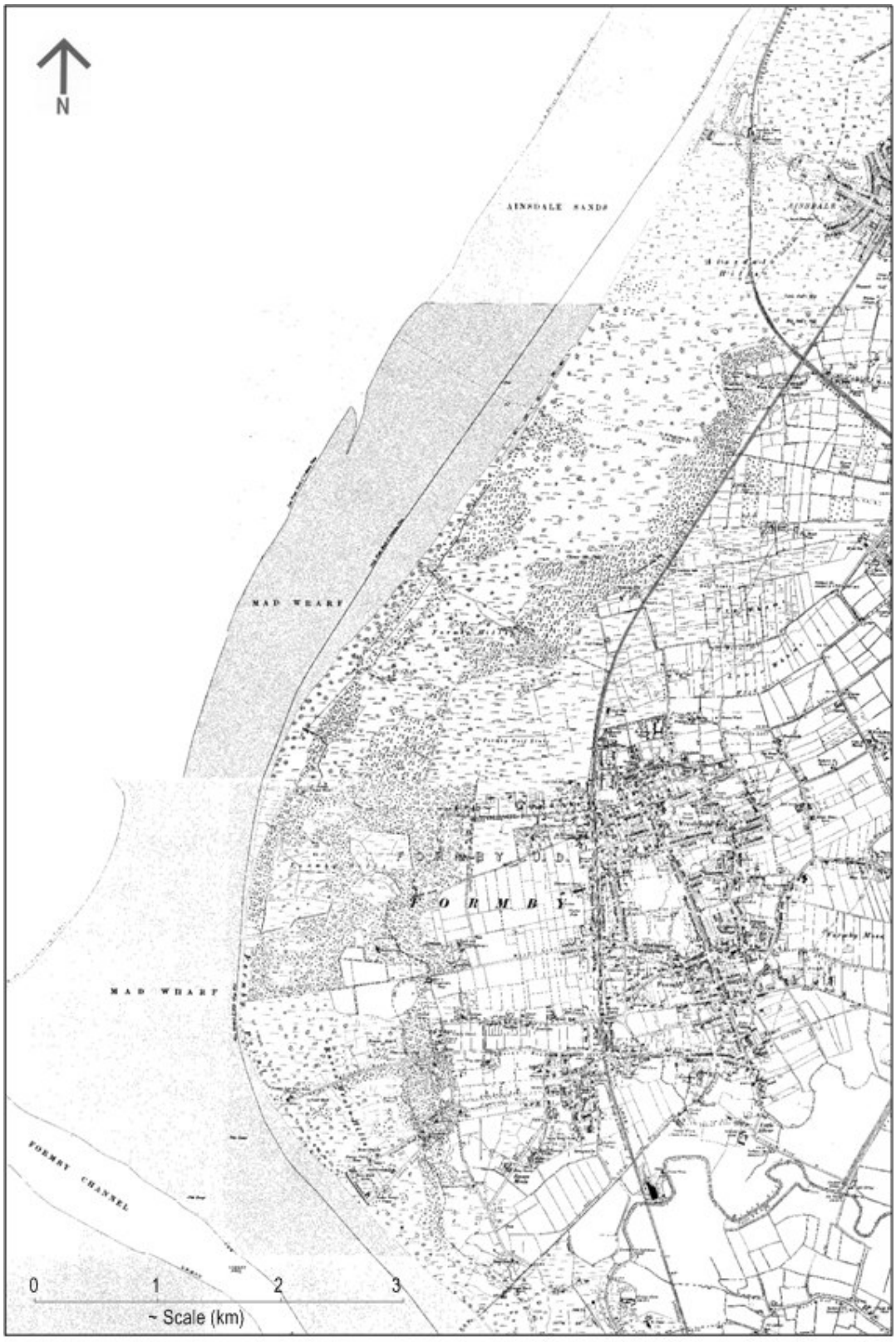

Figure 6.3 Ordnance Survey Map of the Sefton coast, 1929, 1:50,000 (© Crown Copyright. All rights reserved Sefton Council Licence no 100018192).

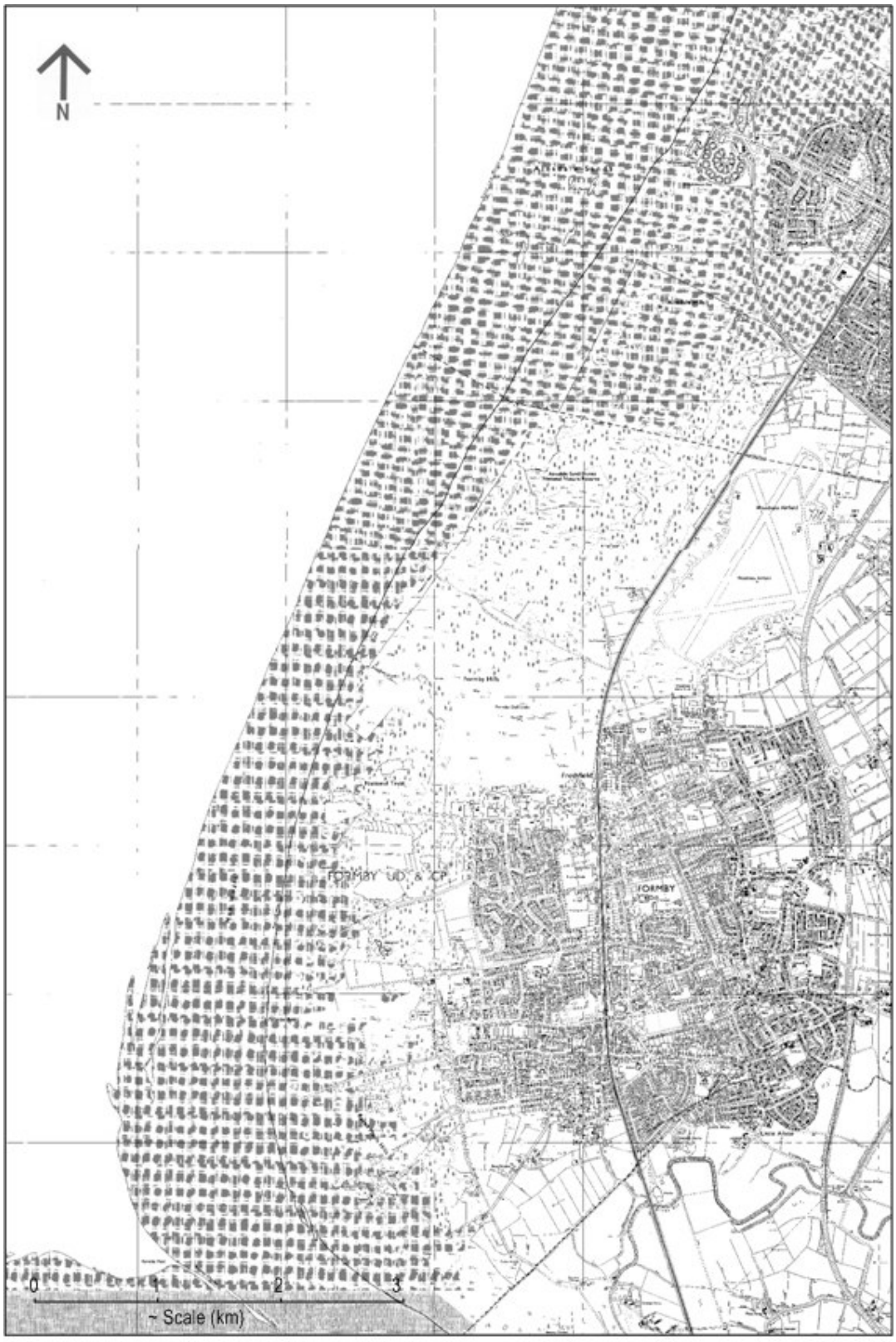

Figure 6.4 Ordnance Survey Map of the Sefton coast, 1976, 1:50,000 (© Crown Copyright. All rights reserved Sefton Council Licence no 100018192).

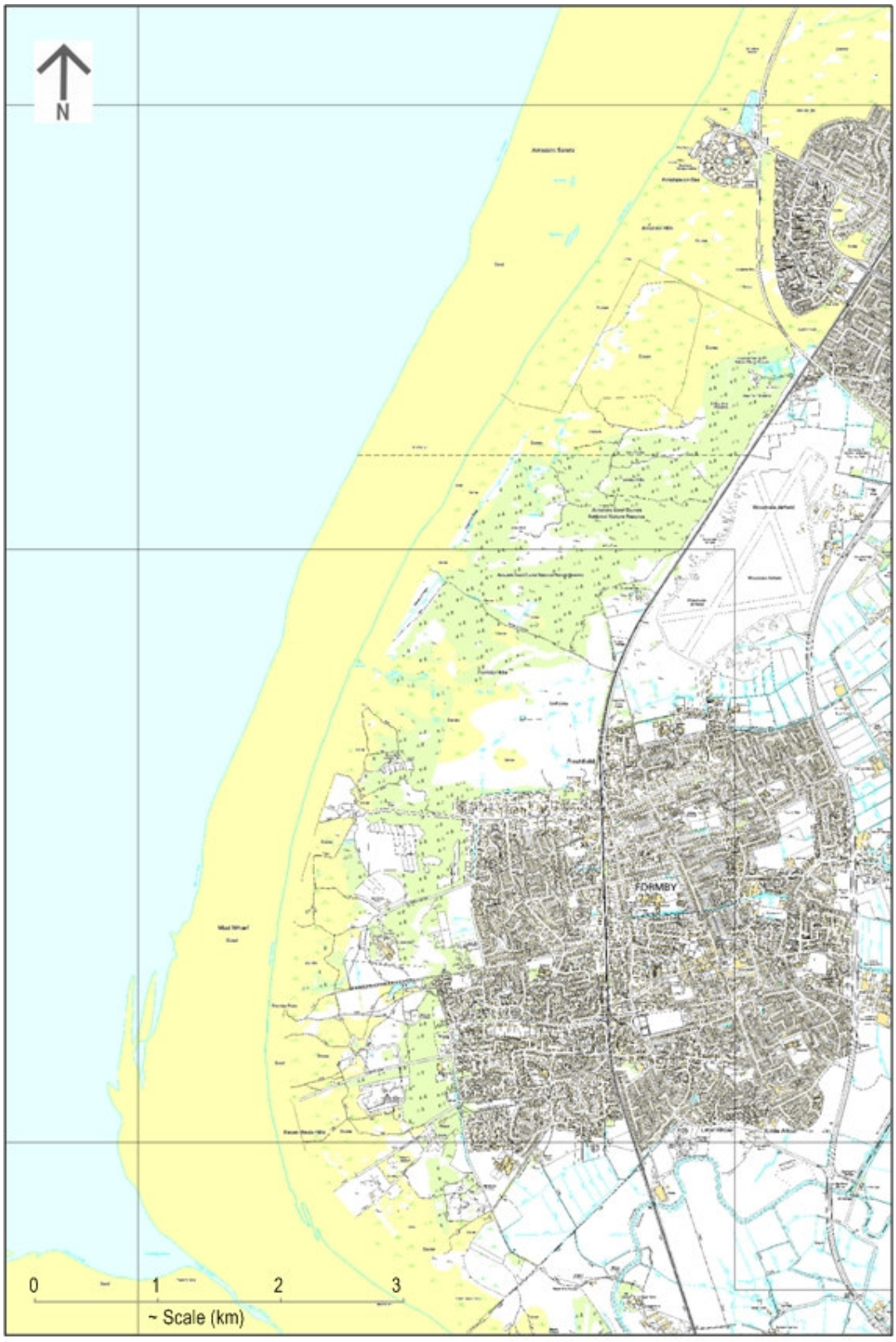

Figure 6.5 Ordnance Survey Map of the Sefton coast, 2000, 1:50,000 (© Crown Copyright. All rights reserved Sefton Council Licence no 100018192).

6.2.2 Vertical aerial photography and evidence of 20th Century erosion

The first full set of vertical aerial photography on the Sefton coast was taken in 1945 (Figure 6.6), which post-dates the 1906 onset of erosion. However, the effects of erosion on Formby Point are immediately apparent in the form of truncated parallel dunes, stretching southwards from the north at the point where the coastline changes angle. Large areas of blown sand clearly identify the extent to which this process operated, burying sand-parendzina pedo-environments. However, new foredune formation on the accreting frontal dunes at Woodvale, north of Formby Point, were evident on the 1945 aerial photograph (Figure 6.6), suggesting raw terrestrial sand profile development. Figure 6.7 demonstrates the overall movement of the dune front 1945-1997, with the erosional effect of storms on Formby Point, along with evidence of subsequent accretion and soil development in the north and south. The northern limit of dune erosion progressively moved northwards to reach Fisherman's Path (SD 280 099) by 1961 and a further kilometre north by 1997. During 1982-1997, there had been ~35 m of erosion at Fisherman's Path (SD 280 099) and Massam's Slack (SD 282 102), eroding both sand-pararendzina and groundwater gley profiles, creating a narrow, steep beach. This coincided with ~20 m of lateral accretion and terrestrial raw sand development between Albert Road (SD 275 055) and Range Lane (SD 283 054) (Pye and Neal, 1994).

Since the early 20th Century cessation of stabilization techniques, along with increased recreational pressures, the frontal dunes, and associated soils, underwent significant degradation and development of blowouts from 1900-1970s. Sand dune morphology also underwent vast changes during this period; mainly influenced by anthropogenic activities, such as agriculture (Lewis and Cowell, 2002), sand-mining and dumping of waste (Pye and Neal, 1994), as well as caravan parks, car parks, roads and golf courses evident in the aerial photographs. At public access sites, recreational pressure had caused severe dune and soil degradation. For example, Figure 6.8 shows the area adjacent to Shore Road, Ainsdale, both prior- and post-development of a holiday camp. Vehicles had access to the foreshore at this point and embryo dune terrestrial raw sands were subject to high trampling pressure. Degraded dunes were highly visible around the holiday camp in 1972; whereas, dunes in the east were partially covered by urban development, neither of which are evident on the 1961 aerial photograph. Dunes in the north had been developed into a golf course, possibly resulting in heath-type micro-podzol development along the periphery (refer to Chapter 4, Section 4.5).

Prior to restoration measures in the late 1970s, sand sheets were evident between Lifeboat Road (SD 271 063) and Victoria Road (SD 275 083) (Figure 6.9). Trampling of embryo dune vegetation and, subsequent erosion of deep gullies in foredune ridges, were contributing factors to erosion at Formby Point. Pre-1906, the 200 m wide belt of parallel dune ridges continued around Formby Point, but since 1906 these dunes have been eroded and removed between Lifeboat Road (SD 271 063) and Fisherman's Path (SD 280 099), subjecting truncated slacks and associated groundwater gley soils to marine incursion during storm events (Pye, 1990), evident in 1972 (Figure 6.10).

Figure 6.6 Aerial photography of Sefton coast, 1945 (Cities Revealed aerial photography copyright The GeoInformation Group. Imagery reproduced from M.O.D. archives).

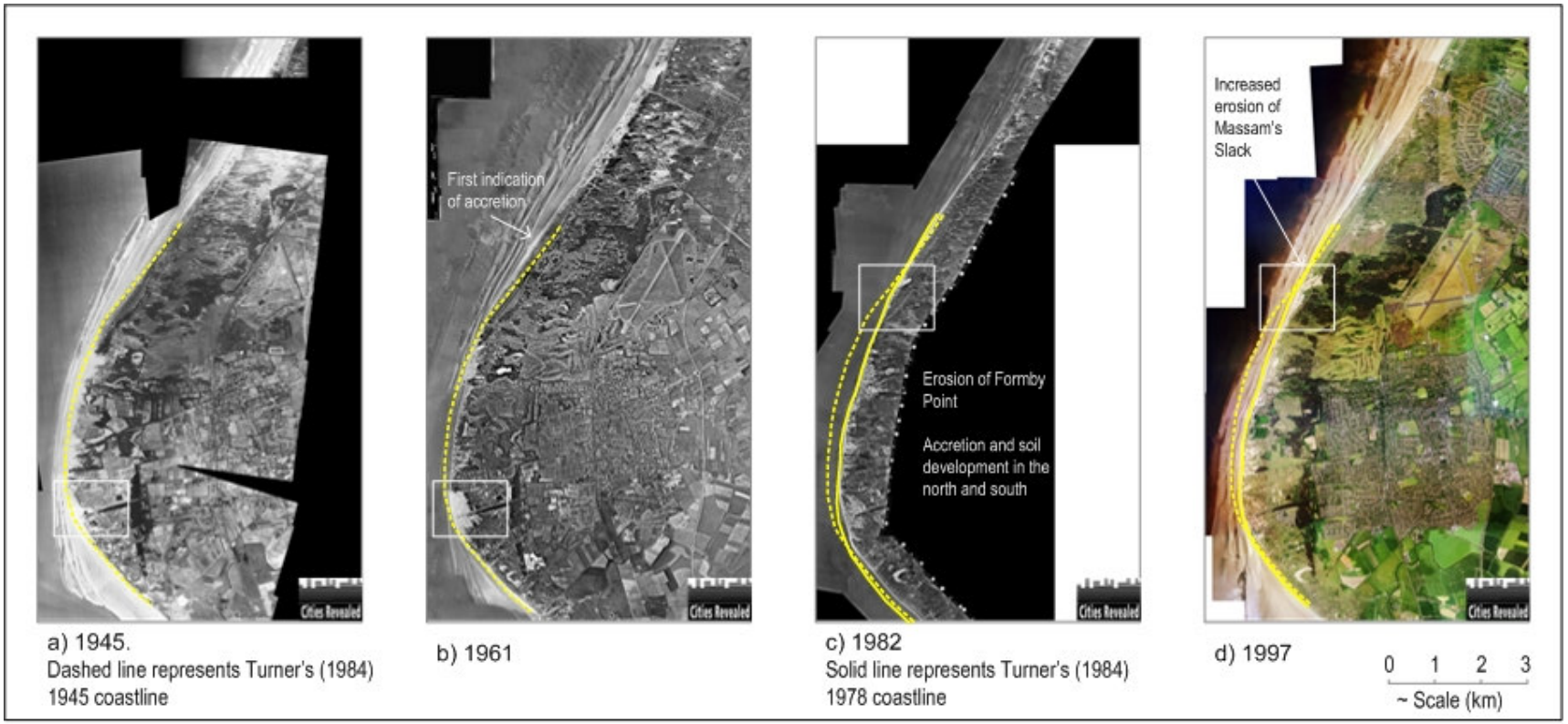

Figure 6.7 Aerial photography of the entire Sefton coast: a) 1945 (Cities Revealed aerial photography copyright The GeoInformation Group. Imagery reproduced from M.O.D. archives); b) 1961 (Cities Revealed® copyright by The GeoInformation® Group, 2007 and Crown Copyright © All rights reserved); c) 1982 and d) 1997 (Cities Revealed® copyright by The GeoInformation® Group, 2008 and Crown Copyright © All rights reserved).

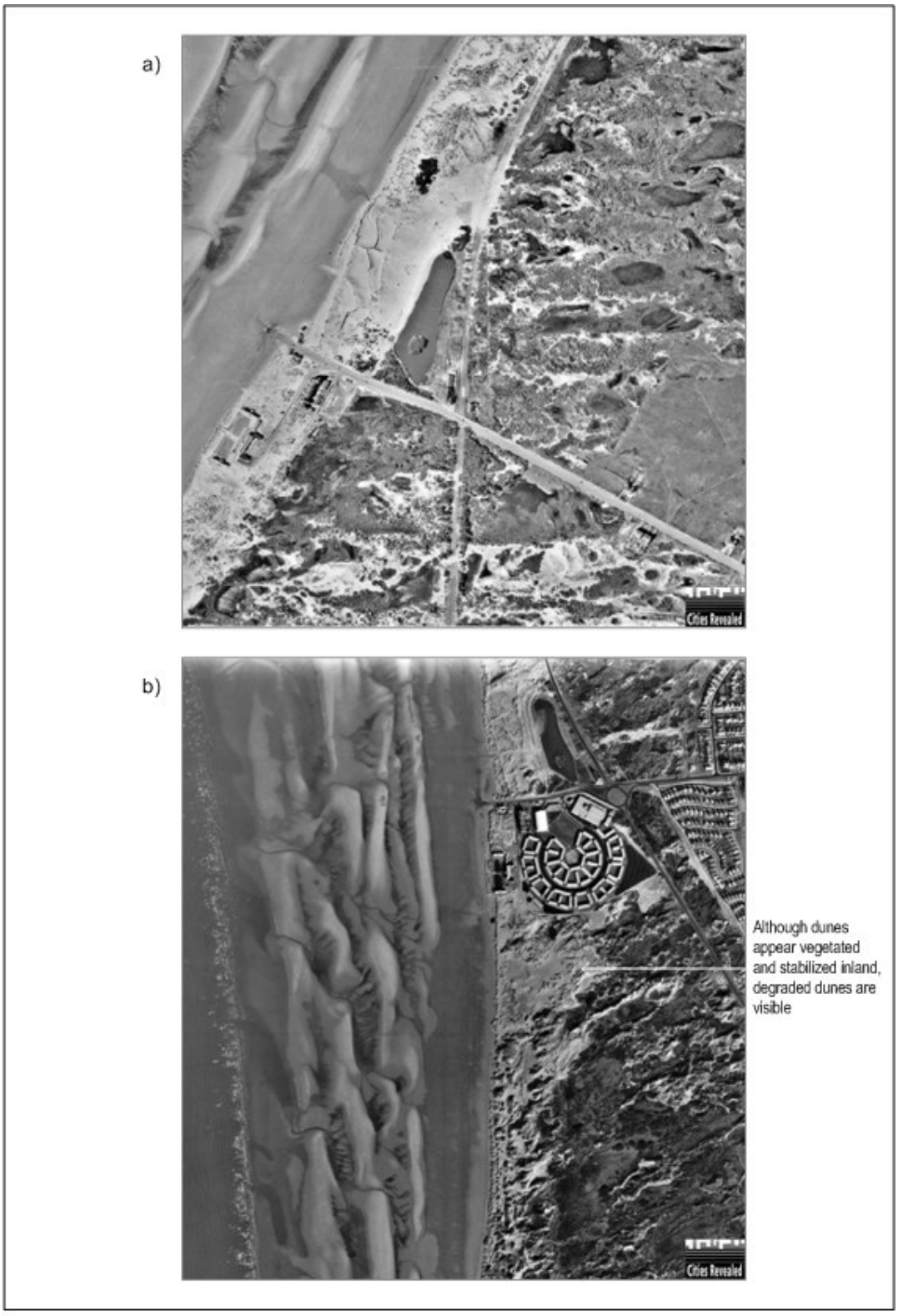

Figure 6.8 Aerial photography of Shore Road, Ainsdale (SD 299 129): a) 1961 and b) 1972 (Cities Revealed® copyright by The GeoInformation® Group, 2007 and Crown Copyright © All rights reserved).

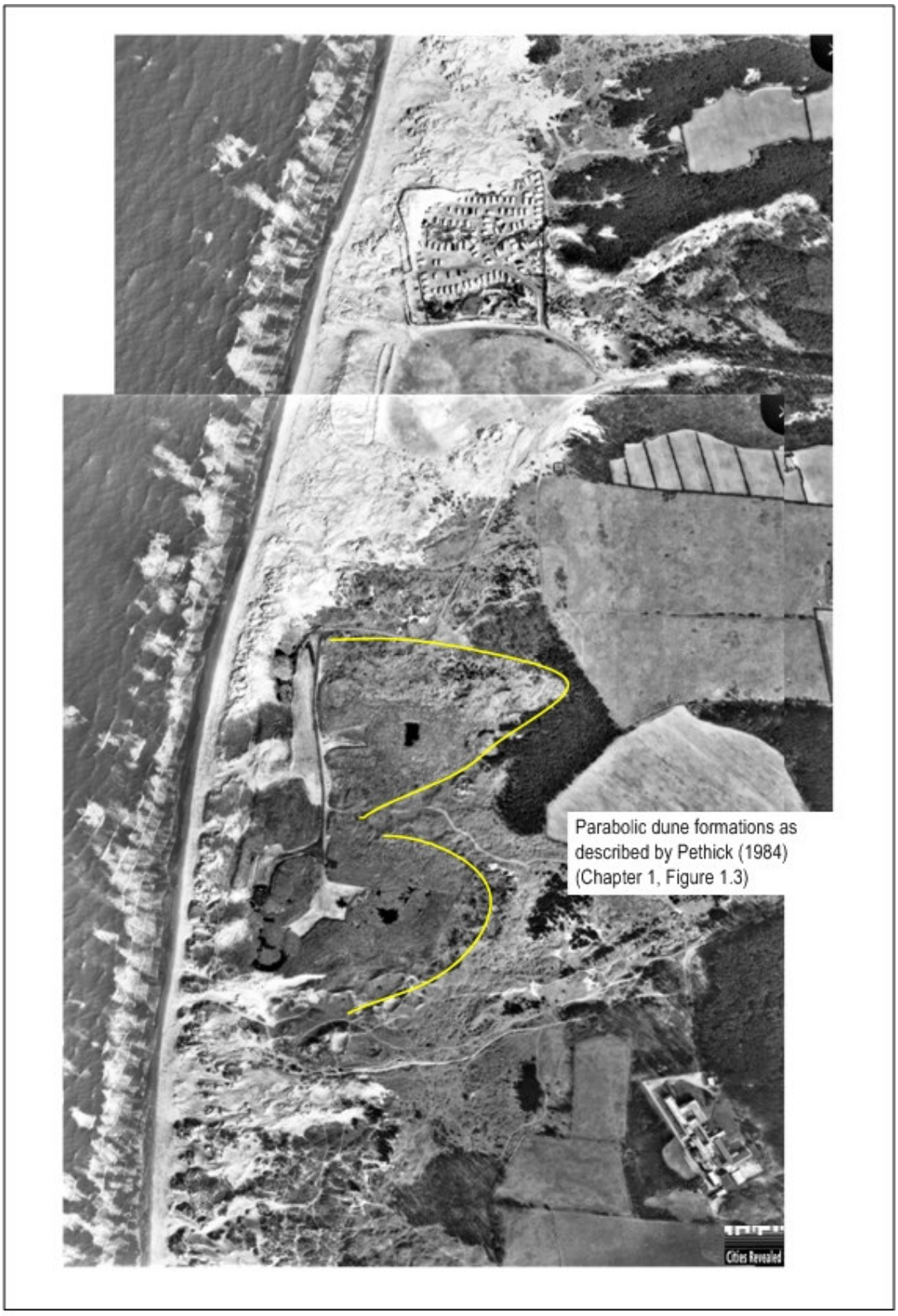

Figure 6.9 Aerial photography of sand sheets between Lifeboat Road (SD 271 063) and Victoria Road (SD 275 083), 1972 (Cities Revealed® copyright by The GeoInformation® Group, 2007 and Crown Copyright © All rights reserved).

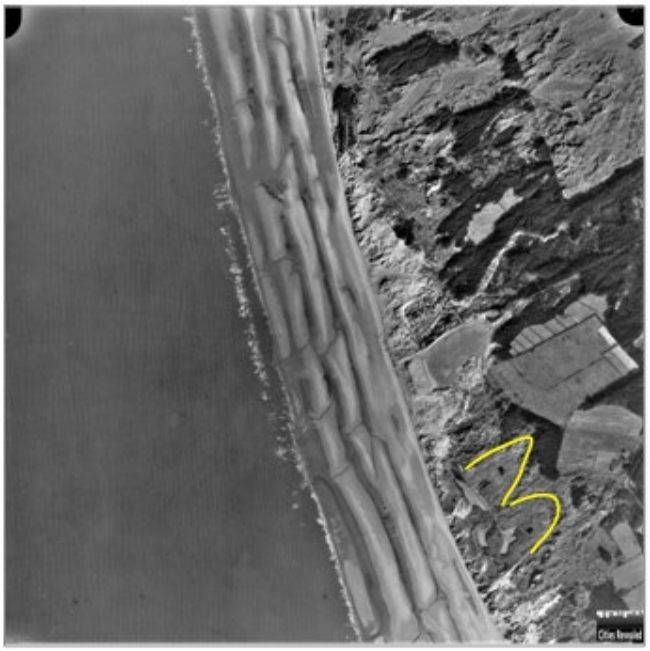

Note the same parabolic dunes that were identified in Figure 6.9. Parallel dune ridges are visible at low tide (Photographs are taken at different orientations)

Figure 6.10 Aerial photography of parallel dune ridges at Fisherman's Path (SD 279 099), 1972 (Cities Revealed® copyright by The GeoInformation® Group, 2007 and Crown Copyright © All rights reserved).

Figure 6.11 Aerial photography of conifer stands protecting Formby Golf Club (SD 285 184), 1989 (Cities Revealed® copyright by The GeoInformation® Group, 2008 and Crown Copyright © All rights reserved).

Dune restoration and protection practises, such as brushwood fencing and marram planting, began in the mid-1980s (Wheeler *et al.*, 1993) and coincided with an overall lower rate of dune activity. Extensive areas of Formby and Ainsdale continued to be planted with conifers throughout the 20th Century, creating micro-podzol pedo-environments. These plantations stabilized the landscape and acted as a wind break, protecting the town of Formby, as well as Formby Golf Club (SD 283 085), from dune burial. Such extensive conifer stands were evident in the 1989 aerial photograph (Figure 6.11), stabilizing the inland dunes and slacks and encouraging further sand-pararendzina and groundwater gley profile development. However, the effects of soil erosion were evident in the truncated foredunes and the large blowout at Massam's Slack (SD 282 102), seaward of the plantations, indicative of the perceived need for protection and stabilization techniques.

6.2.3 21st Century continued erosion

Since the onset of erosion at Formby Point the northern limit of erosion advanced northwards, to presently sit ~1 km north of Fisherman's Path (SD 280 099). The southern limit presently sits between Alexandra Road (SD 273 057) and Lifeboat Road (SD 271 063) (Pye, 1990). The present day shoreline at Formby Point lies almost in exactly the same position as during the late 18th Century, having advanced and retreated again by >300 m (Saye *et al.,* 2005). Therefore, former 19th Century hind dune topsoils are now exposed on the eroded backshore, representing a cyclical dynamism of ~200 years. A short, significant episode of erosion occurred in 2002 and the frontal dunes have only recently recovered to their former position (Pye and Blott, 2008). Figure 6.12 displays the coast's entire aerial photography, taken in 2002/2003. The eroded hind dunes at Formby Point were clearly visible, along with associated sand-pararendzinas inland buried by active sand sheets. The 21st Century coastline is much straighter than the 20th Century angular profile, due to continued accretion north and south of the erosion limit.

6.3 Mid-term coastal change

Dune-toe photographic surveys provide valuable qualitative information regarding the condition of beaches, dunes and other coastal features including pedogenesis, on mid-term, or annual, timescales. However, a limitation exists, in that only the immediate foreshore can be monitored. For that reason, in this section comparisons are made with oblique aerial photographs to highlight links with foreshore processes and inland dune dynamics. The 2006 dune toe photographic survey of the entire coastal margin of the study area (SD 30047 13484 to SD 28197 04703) is presented in Appendix 3.1.

It is apparent from the dune-toe photographic survey that dune shape differs notably along the entire length of the Sefton coast. Dunes undergoing erosion at Formby Point (Figure 6.13) display a short foreshore and steep dune-cliff appearance compared to other dunes along the coast. For example, embryo dune formations on Birkdale foreshore gently increase in gradient inland as bare sand becomes colonized and terrestrial raw sand begins to form (Figure 6.14).

Figure 6.12 Aerial photography of Sefton coast, 2002/2003 (Cities Revealed® copyright by The GeoInformation® Group, 2008 and Crown Copyright © All rights reserved).

When the dune-toe survey photographs for Formby Point are compared to the 2008 oblique aerial photographs, it is evident that sites exposed to aeolian and wave action during annual storm events are subject to morphological changes on an annual basis. Figure 6.15a and 6.15b show removal of the characteristic gentle gradient of the foredunes both north and south of the erosion limit, respectively, to be replaced by scarped dune cliffs containing exposed buried historic soils, characteristic of eroded environments.

Evident on the oblique photograph, just north of Fisherman's path (Figure 6.16), is a large expanse of dune scrub behind the main foredune landscape, suggesting presence of a sand-pararendzina/brown earth transitional soil (refer to Chapter 4, Section 4.6.2), which has undergone burial following a period of sand encroachment (evident by brown-coloured patches of vegetation visible within extensive sand sheets). This would be impossible to identify in the dune-toe survey photographs and, therefore, demonstrates the importance of using the two photographic techniques alongside each other for mid-term monitoring.

Eroded dune-cliff material from Formby Point is readily available for removal in both northern and southern directions by the process of longshore drift, creating a ready supply of material for dune formation with characteristic gentle profiles. Figures 6.17a and 6.17b show a wider foreshore, to the north and south of Formby Point, respectively, compared to the short foreshore previously described at Formby Point (note the beginning of the development of the 'green beach' geomorphological feature in Figure 6.17a). Stabilization of deflated sand supplies has supported embryo dune soil development seaward of the main foredune landscape in both localities.

6.3 Short-term coastal change

The extent of coastal aeolian processes, coupled with limited vegetation coverage and the high erodibility of dune sand and soil, make the Sefton coastal dunes susceptible to rapid morphological adjustments on a seasonal-scale. Therefore, more regular and consistent monitoring, compared to annual aerial photography analysis, is necessary to identify and record changes and trends. A Fixed Point Photographic (FPP) survey has shown the impacts of recent coastal changes on these sensitive dune pedo-environments. Both long- and mid-term photographic monitoring techniques were used to identify key areas of coastal dynamism, including erosion at Formby Point and, subsequent accretion in the northern and southern extremities. The FPP Stations refer to the highest points at each locality (Figure 6.18). Seasonal photographic surveys of dune morphology, since November 2006 to the present day are presented in Appendix 3.2, and will continue as an ongoing programme of morphological monitoring.

6.3.1 Station 1: Birkdale sand dunes (SD 30379 13735)

Station 1 represents the highest point on an accreting section of the Sefton coastline. Figure 6.19b,f shows increased winter flooding in the dune slacks from November to February,

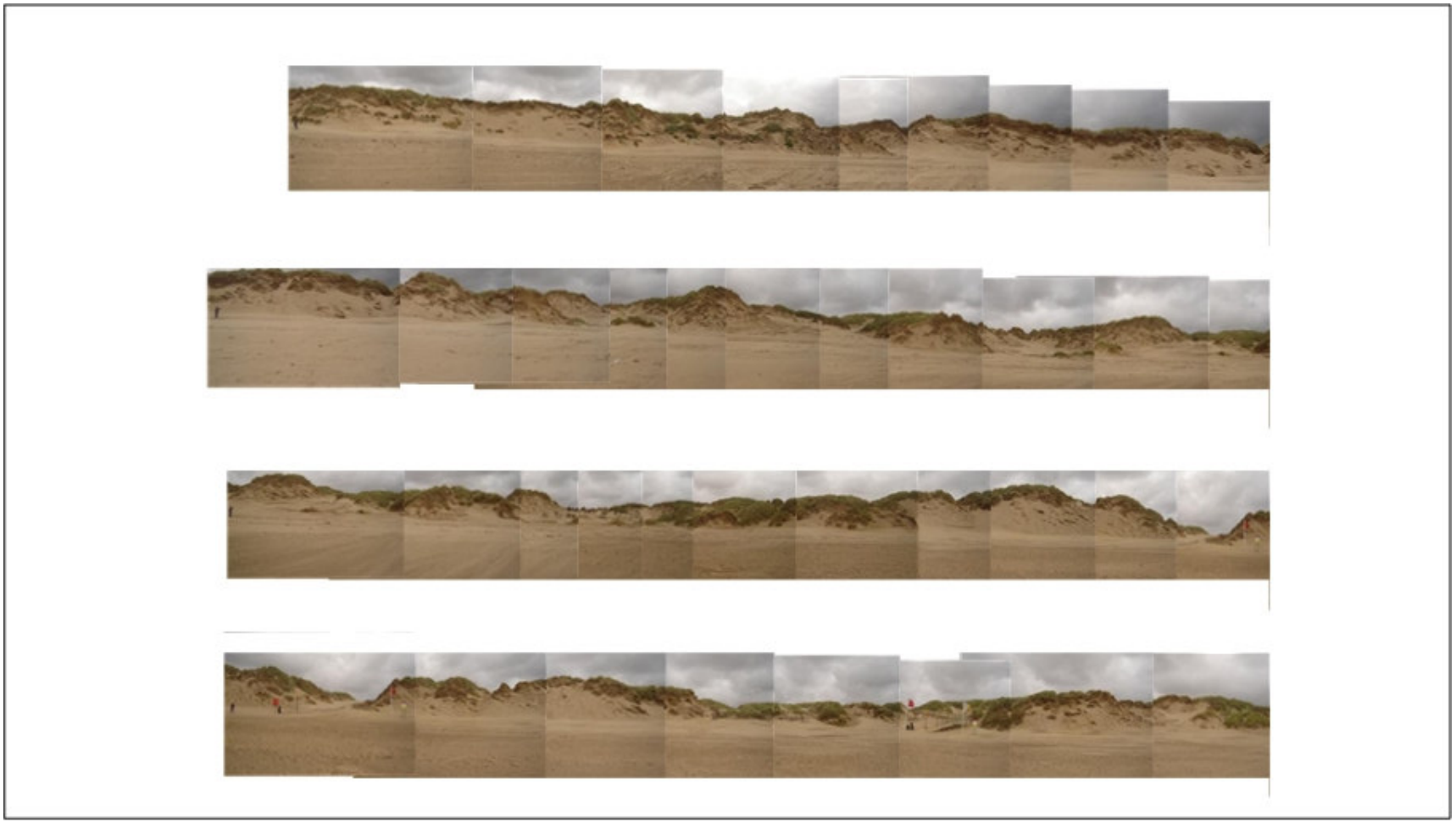

Figure 6.13 Dune-toe photographic survey of eroding dunes at Formby Point (top left photograph georeferenced: SD 27074 07654; total distance of shown photographed coast ~750 m (02/08/2006)).

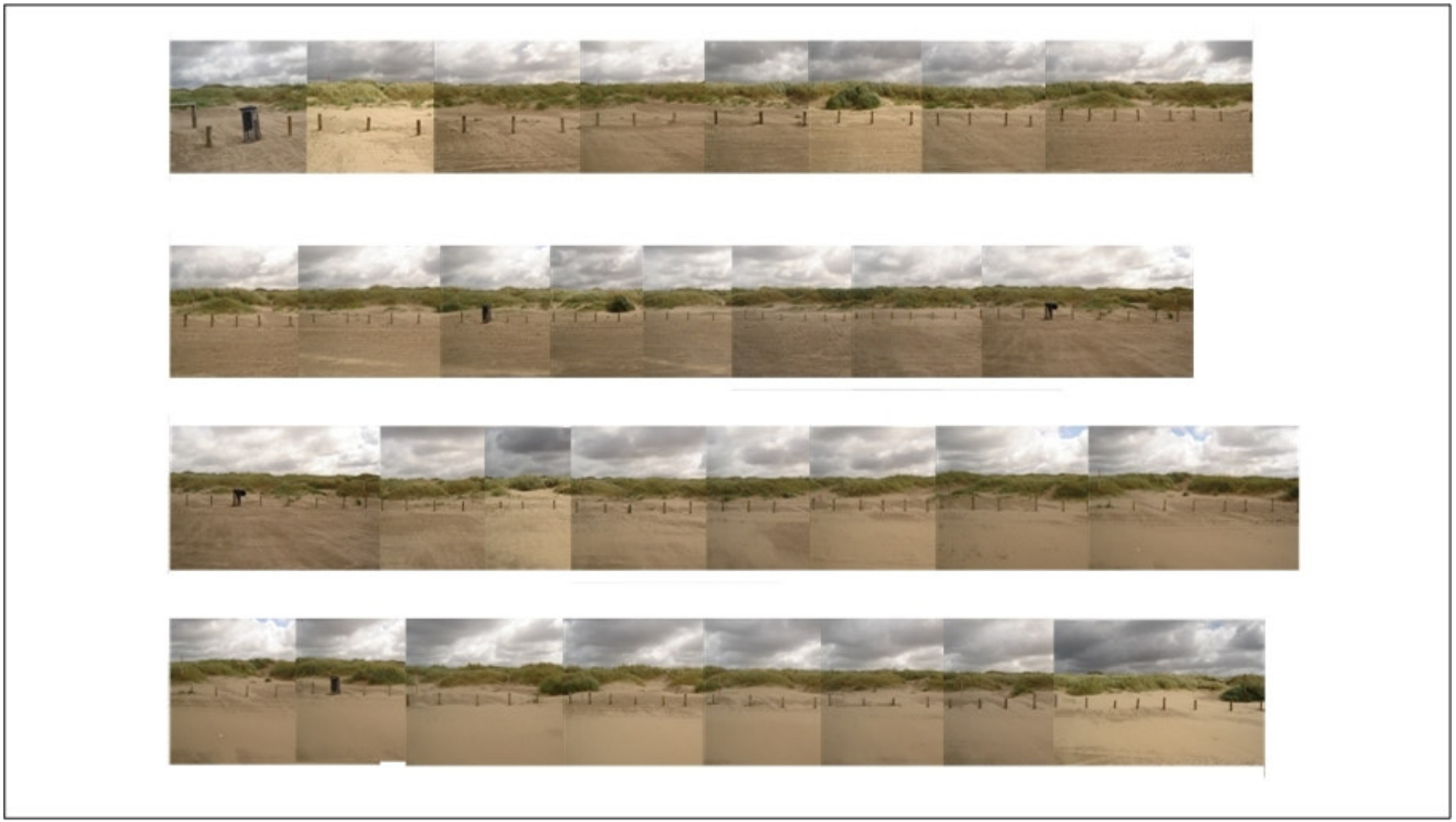

Figure 6.14 Dune-toe photographic survey of accreting dunes and embryo dune formation on Birkdale foreshore (top left photograph georeferenced: SD 30047; bottom right photograph georeference SD 29919 13245; total distance of shown photographed coast ~500 m (01/08/2006)).

a)

b)

Figure 6.15 Oblique aerial photographs, 2008; showing truncation of the characteristic gentle gradient of accreting foredunes to create cliffed dunes in an eroded environment: a) north of Formby Point (Felled area of Ainsdale sand dunes, SD 286 108) and b) south of Formby Point (Lifeboat Road, SD 271 063) (copyright of North West and North Wales Coastal Group ©).

Figure 6.16 Area where Fisherman's Path arrives at the shore (SD 278 099): a) dune toe photographic survey and b) oblique aerial photograph, 2008 (copyright of North West and North Wales Coastal Group ©).

a)

b)

Figure 6.17 Oblique aerial photographs, 2008: a) north of Formby Point (Birkdale sand dunes, SD 304 137) and b) south of Formby Point (Albert Road, SD 275 056) (copyright of North West and North Wales Coastal Group ©).

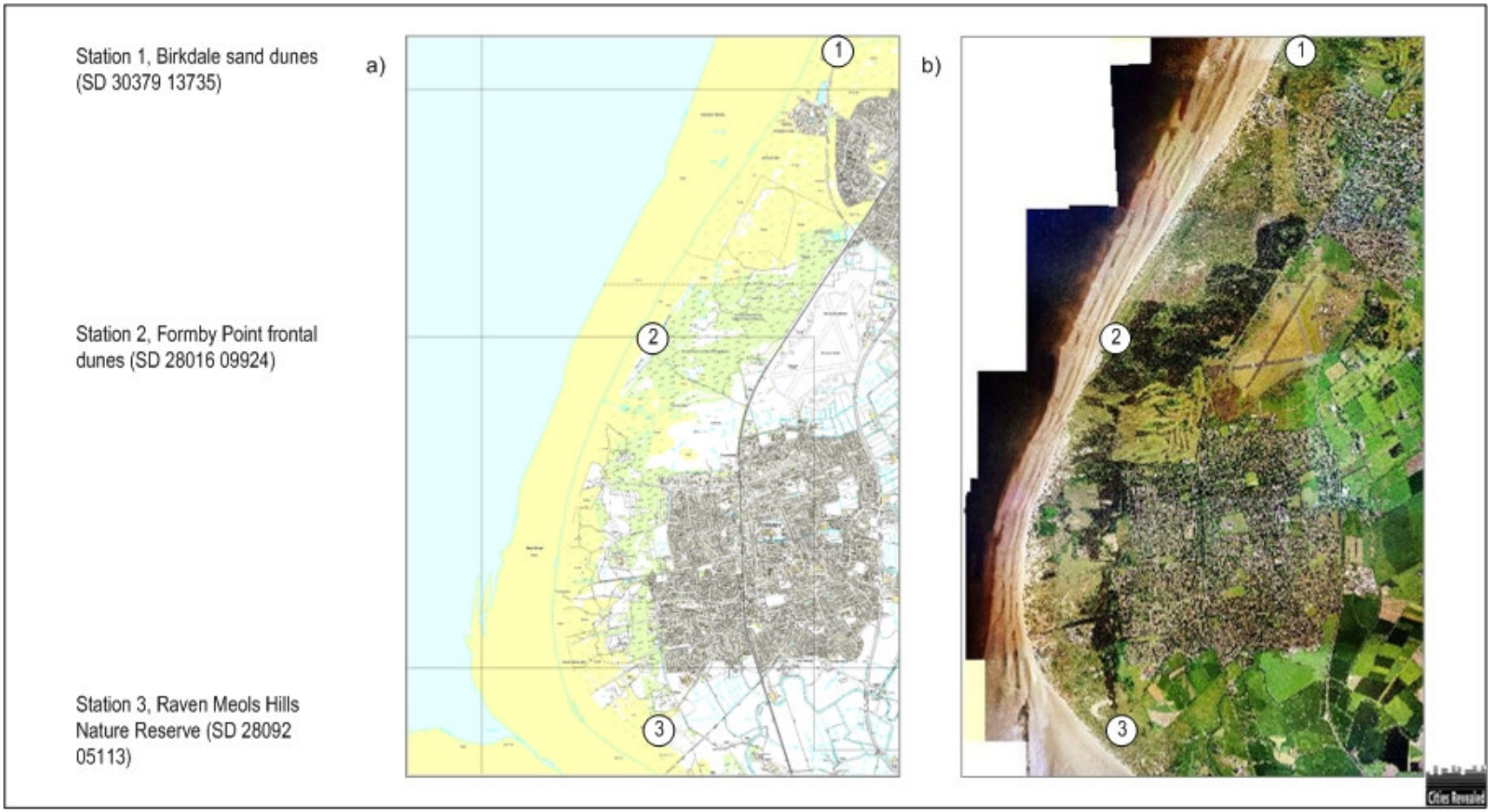

Figure 6.18 Locations of FPP Stations superimposed onto: a) Ordnance Survey Map of the Sefton coast, 2000, 1:50,000 (© Crown Copyright. All rights reserved Sefton Council Licence no 100018192) and b) aerial photography of Sefton coast, 2002/2003 (Cities Revealed® copyright by The GeoInformation® Group, 2008 and Crown Copyright © All rights reserved).

Figure 6.19 Station 1, Birkdale sand dunes (SD 30379 13735) FPP sequences for Season 1 (November 2006): a) facing north; b) facing east; c) facing south and d) facing west. Season 2 (February 2007): e) facing north; f) facing east; g) facing south and h) facing east.

saturating associated groundwater gleys. Rapid fall of the water table in summer coincides with leafing of deciduous species, indicating areas of scrub and deciduous woodland associated with brown earth soil profiles, evident in the far distance of the photographs taken in an easterly direction (Figure 6.20). Westerly photographs show natural embryo terrestrial raw sands interspersed with sand-pararendzina communities dominated by sand sedge (*Carex arenaria*), marram grass (*Ammophilia arenaria*) and red fescue (*Festuca rubra*), all of which are dune-building species characteristic of semi-fixed dune environments. During winter months the vegetation is not as vivid.

6.3.2 Station 2: Formby Point frontal dunes (SD 28016 09924)

Station 2 represents the highest point on a highly eroded section of the Sefton coastline where, after several phases of advance and retreat, the coastline lies in almost the same position as it did in the 18th Century (Turner, 1984; Saye *et al.,* 2005). Therefore, the once stabilized sand-pararendzina hind dune environments, which formed during coastline advancement, are now exposed on the eroding foreshore. FPP analysis demonstrated no change occurred between November 2006 and February 2007 (Figure 6.21). Exposed bare sand on adjacent sand dunes reveals predominant laminae, dipping in the prevailing wind direction (Figure 6.21a), providing evidence of deposition in the lee side of the peak, creating the impression that the dune is migrating landwards (Tsoar *et al.,* 2004).

The frontal dunes became extensively deflated by May 2007, possibly the result of a large storm event, resulting in collapse of the dominant landscape feature and hind dune topsoil, designated as Station 2. The collapsed dune alters the elevation of Station 2 to well below the highest point, making it no longer possible to identify the same morphological feature between several photographs (Figure 6.22). However, despite the vegetated dune obscuring the view in November 2007 (Figure 6.22i), the stable foredune-toe in the background is still visible. The photographic sequences following on from this event appear to have identified a landward migration of the dunes during the subsequent 6-9 months of monitoring.

6.3.3 Station 3: Raven Meols Hills Nature Reserve (SD 28092 05113)

Station 3 represents the highest point of the Sefton coastline that resembles a textbook successive pedo-environment, with newly developed terrestrial raw sand embryo dunes on an accreting coast, sand-pararendzina fixed hummock dunes (Figure 6.23) and successive dune pasture environments, and deciduous woodland associated with brown earth soil development inland. The overall dune status during the last three years is considered stable, with the hind dunes remaining morphologically established and only minor subtle changes in the visible amount of bare sand exposed in the hummock-fixed dunes.

6.5 Discussion

Using photography as a monitoring technique on the Sefton coast has identified an overall trend of soil erosion at Formby Point, increased accretion and soil development in the north and south

Figure 6.20 Station 1, Birkdale sand dunes (SD 30379 13735) FPP sequences for Season 4 (August 2007): a) facing north; b) facing east; c) facing south and d) facing west. Season 6 (February 2008): e) facing north; f) facing east; g) facing south and h) facing west.

Figure 6.21 Station 2, Formby Point frontal dunes (SD 28016 09924) FPP sequences for Season 1 (November 2006): a) facing north; b) facing east; c) facing south and d) facing west. Season 2 (February 2007): e) facing north; f) facing east; g) facing south and h) facing east.

Figure 6.22 Station 2, Formby Point frontal dunes (SD 28016 09924) FPP sequences for Season 2 (February 2007): a) facing north; b) facing east; c) facing south and d) facing west. Season 3 (May 2007): e) facing north; f) facing east; g) facing south and h) facing west. Season 5 (November 2007): i) facing north; j) facing east; k) facing south and l) facing east.

Figure 6.23 Station 3, Raven Meols Hills Nature Reserve (SD 28092 05113) FPP sequences for Season 1 (November 2006): a) facing north; b) facing east; c) facing south and d) facing west. Season 6 (February 2008): e) facing north; f) facing east; g) facing south and h) facing west. Season 9 (November 2008): i) facing north; j) facing east; k) facing south and l) facing east.

extremities due to longshore drift towards Birkdale and the River Alt, respectively, and stabilization in the pedologically advanced hind dunes, over century-decadal-annual-seasonal timescales. This is due to overall coastal geomorphological realignment and improved management strategies. Evidence suggests the onset of soil erosion at Formby Point, post-1900, was initially a response to increased occurrence of storm events, but was also encouraged by anthropogenic activity (Pye and Neal, 1994).

Long-term O.S. map analysis and aerial photography monitoring has recorded a slowing-down of erosion rates since dune restoration and protection practises began in the 1980s. Mid- and short-term photographic monitoring has identified renewed phases of dune activity, soil erosion and geomorphological change in predominantly environmentally stable conditions. Significant dune and soil erosion occurs only when major storm surges coincide with high tides, about once per 5-6 years (Pye, 1991) to 10 years (Pye and Smith, 1988), resulting in renewed periods of dune activity and blowout formation. Rates of erosion appear to be faster than natural dune roll-back processes, creating scarped dune cliffs with exposed eroded soils, rather than reverting to gently sloping dunes and terrestrial raw sand. Storms of lesser magnitude generally cause erosion of just part of the dune-toe (Pye and Blott, 2008) and if initial dune height is sufficient, a greater volume of sand is released per metre of retreat, retaining beach levels (Edelman, 1968).

The common assumption that sea level rise on soft coasts will cause shoreline retreat (Innes and Frank, 1988) (Chapter 1, Section 1.3) has been disproven, as O.S. maps and aerial photographs indicate erosion at Formby Point, but shoreline advance in the extreme north and south of the coastal area. It is apparent these observed trends are occurring, despite sea level rise, as a result of rapid deposition (Leatherman, 1990; French *et al.,* 1995), or the rate of frontal dune pedogenesis being sufficient to prevent long-term net erosion and maintain net progradation (Pye, 1991).

Each photographic technique can be used individually as a monitoring programme to inform the process of shoreline management. However, it is necessary to group all timescales and spatial-scales together, when monitoring dune dynamics and sedimentary processes, to gain an accurate understanding of morpho-dynamics and local rates of coastal change that can be applied to future scenarios. Furthermore, in the context of pedogenesis, this evidence suggests soils and their surrounding dune environments are influenced by a dynamic, cyclic system. For example, during episodic sea regressions, the dune landscape would have advanced seaward (Jungerius, 1985); whereas, phases of dune stability resulted in species colonization and soil development, which were, subsequently, buried by dune sand during following periods of dune activity and morpho-dynamism (Fullen *et al.,* 1999).

6.6 Summary

Ordnance Survey (O.S.) Map and aerial photographic evidence documented three centuries of coastal dune change. The evidence displayed substantial growth and subsequent deflation of

foredunes at Formby Point, sand encroachments on mobile dunes burying existing pedo-environments, accretion and soil development in northern and southern extremities and overall stability in the hind dunes. Anthropogenic activity, including the onset and demotion of management and dune stabilization practices, has been identified.

In comparison to the vertical aerial photography, which has been used to identify spatial dynamics, oblique aerial photographs have provided information about dune morphological changes on a meso-scale. Along with the dune toe photographic survey, this monitoring technique has identified dune shape to differ significantly along the entire length of the Sefton coast, depending on the erosion or accretion dynamics and topsoil coverage of that particular area.

Fixed Point Photography (FPP) analysis revealed overall dune stability in northern and southern extremities with seasonal fluctuations in the water table of dune slacks. The photographic sequences from Formby Point identified erosion and, subsequent, landward migration of the dunes on a seasonal timescale.

CHAPTER 7

Modelling pedogenesis on the Sefton dunes

Chapter 7 links the five NSRI soil profile classifications (terrestrial raw sand, sand-pararendzina, groundwater gley, brown earth and micro-podzol), identified in Chapter 4, to the five dune topsoil environments identified in Chapter 3 (frontal dune, hind dune, slack, woodland and heath/coniferous plantation), to create a geomorphopedological (GMP) map of the Sefton dunes. Statistical correlations between topsoil physico-chemical characteristics are related to soil profile organic layers to indicate pedogenic trends over distance and time. Localized geomorphic and anthropogenic coastal change, identified in Chapter 6, is used to divide the landscape into zones of erosion and accretion. Differences in topsoil characteristics between these zones are identified. Conceptual pedogenic models represent two-dimensional pedogenic pathways of NSRI classified soil profile succession on the Sefton coast, under varying erosion/accretion regimes. Theoretically, both the GMP map and conceptual models can be used to predict soil types and characteristics in similar sand dune systems.

7.1 Pedogenesis on the Sefton coastal dunes

Key topsoil characteristics were successfully assigned to grouped dune environments (frontal dune, hind dune, woodland, heath and slack) in Chapter 3, Section 3.6.4, which were associated with the existing vegetation boundaries mapped by Sefton Metropolitan Borough Council (SMBC) (refer to Chapter 2, Section 2.1). Subsequently, dune pedo-environments were assigned to NSRI soil profile classifications (terrestrial raw sand, sand-pararendzina, brown earth, micro-podzol and groundwater gley) (refer to Chapter 4, Sections 4.5-4.5.2). Figure 7.1 shows a GMP map, indirectly created by assigning NSRI soil profile classifications to topsoil characteristics across the dune landscape. The GMP map provides an indication of possible pedogenic pathways from the active coastline to the stable inland dune landscape.

The GMP map shows expanses of aeolian derived bare sand extending inland around Formby Point, indicating the actively eroding shoreline in that area. Whereas, terrestrial raw sands, represented by embryo and mobile dune community topsoil formation, are present on the accreting coastline sections, north and south of the erosion limit along almost the entire length of the project area, except for the stabilized northern extremity. At each locality, terrestrial raw sands border sand-pararendzinas, represented by fixed dune community and hind dune pasture topsoils. These appear to be the most abundant of soil classifications, the largest expansions of which are located at Birkdale sand dunes and Ainsdale NNR. In general, sand-pararendzinas are interspersed with groundwater gleys, formed in slack environments, throughout the dune landscape, although there are fewer occurrences in the south compared to the north. Brown earth development, represented by scrub and deciduous woodland topsoils, on Birkdale sand dunes appears to have initiated in relic groundwater gley localities, following stability and accretion in the area. Further areas of brown earth are interspersed amongst micro-podzols. Micro-podzol formations, represented by heath and coniferous plantation topsoils, occupy large

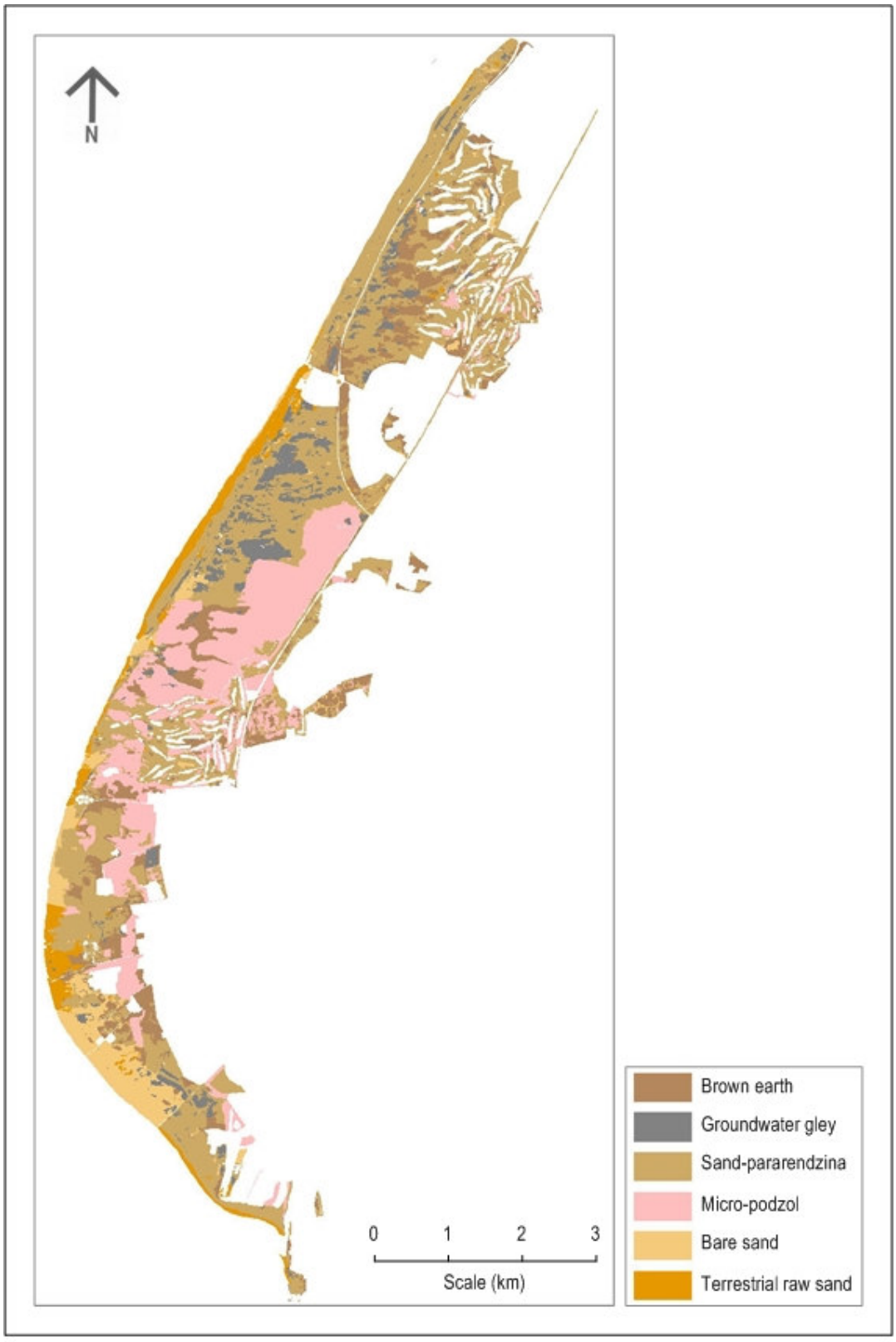

Figure 7.1 Theoretical geomorphopedological map of the Sefton coast, created in ArcView GIS (version 3.3) based on both topsoil and soil profile characteristics.

areas of the central dune system. However, smaller patches are evident in the east and surrounding golf courses.

7.2 Statistical correlation of topsoil pedo-properties on the Sefton coastal dunes

Previous chapters have identified physico-chemical soil parameters to be more influential in certain topsoil environments (Chapter 3) and soil profiles (Chapter 4). This section aims to identify which parameters influence each other during the processes involved with pedogenesis and soil succession. As these correlations are likely to be effected spatially, with time and in varying erosion/accretion regimes, statistical analyses are performed on the topsoil data sets only (Chapter 3) to gain an understanding of pedogenesis over the entire dune landscape. Data sets are interrogated using Spearman's Rank correlation (refer to Table 2.4 for description). Both null (H_0) and alternative (H_1) hypotheses were tested to compare the relationship between two parameters. Tables 7.1-6 display correlation values for every possible pairing of parameters.

Tested Hypotheses	
Null Hypothesis (H_0)	There was no significant relationship between the parameters.
Alternative Hypothesis (H_1)	There was a significant relationship between the parameters.

7.2.1 Statistical correlation between topsoil textural parameters

Table 7.1 shows, with the exception of skewness, all topsoil textural parameters displayed strong correlations (p <0.05), suggesting particle size and distribution parameters were highly dependent upon each other, whereas, the degree of symmetry of grain-size distribution had no relevance. The strongest correlation coefficients were associated with sand (r = 0.72-0.10; p <0.001; n = 112) and silt (r = 0.58-0.10; p <0.001; n = 112).

Figure 7.2a shows an extremely strong negative correlation between sand versus silt (r = 1.00; p <0.001; n = 112). However, this was to be expected as these parameters were measured as percentages and, were therefore, highly dependent upon each other. A negative correlation also exists between silt versus clay (r = 0.58; p <0.001; n = 112) (Figure 7.2b). Despite highly significant (p <0.001), the distribution of points around best-fit line shows parameters were less interdependent. There was a positive correlation between sand versus clay (r = 0.49; p <0.001; n = 112) (Figure 7.2c). The negative correlation between mean particle size versus sorting (r = -0.70; p <0.001; n = 112) (Figure 7.2d), indicates that with decreased mean particle size sediment becomes better sorted.

Figure 7.2e shows three topsoil population samples; bare sand (terrestrial raw sand), fixed dune (sand-pararendzina) and slack (groundwater gley) communities, from the 10 original dune environments for silt versus mean particle size correlation. There is evidence of separation using textural characteristics, with bare sand values falling into the medium sand-sized fraction (200-600 µm). When the data were separated into environment-specific correlations, the

Table 7.1 Statistical relationships between the particle size distribution parameters for the Sefton coast (**bold** text is significant (*p <0.05; **p <0.01; ***p <0.001)) (n = 112)

	Sand	Silt	Clay	Mean particle size	Median particle size	Sorting	Skewness
Silt	r = 0.995 ***p* <0.001***** R^2 = 0.990						
Clay	r = 0.489 ***p* <0.001***** R^2 = 0.239	r = 0.576 ***p* <0.001***** R^2 = 0.331					
Mean particle size	r = 0.904 ***p* <0.001***** R^2 = 0.817	r = 0.913 ***p* <0.001***** R^2 = 0.834	r = 0.562 ***p* <0.001***** R^2 = 0.316				
Median particle size	r = 0.823 ***p* <0.001***** R^2 = 0.677	r = 0.826 ***p* <0.001***** R^2 = 0.683	r = 0.466 ***p* <0.001***** R^2 = 0.218	r = 0.930 ***p* <0.001***** R^2 = 0.866			
Sorting	r = 0.844 ***p* <0.001***** R^2 = 0.713	r = 0.818 ***p* <0.001***** R^2 = 0.669	r = 0.227 ***p* = 0.016*** R^2 = 0.051	r = 0.699 ***p* <0.001***** R^2 = 0.448	r = 0.542 ***p* <0.001***** R^2 = 0.293		
Skewness	r = 0.165 p = 0.082 R^2 = 0.027	r = 0.174 p = 0.066 R^2 = 0.030	r = 0.163 p = 0.085 R^2 = 0.027	r = 0.023 p = 0.691 R^2 = 0.001	r = 0.288 ***p* = 0.002**** R^2 = 0.083	r = 0.469 ***p* <0.001***** R^2 = 0.220	
Kurtosis	r = 0.724 ***p* <0.001***** R^2 = 0.524	r = 0.764 ***p* <0.001***** R^2 = 0.584	r = 0.731 ***p* <0.034*** R^2 = 0.535	r = 0.692 ***p* <0.001***** R^2 = 0.479	r = 0.560 ***p* <0.001***** R^2 = 0.314	r = 0.436 ***p* <0.001***** R^2 = 0.190	r = 0.167 p = 0.078 R^2 = 0.028

r = correlation coefficient; p-value = significance of the correlation; R^2 = coefficient of determination, indicating the success of the equation in explaining the relationship between two parameters.

Table 7.2 Statistical relationships between pH and SOM (n = 113), C and N (n = 101) and geochemical parameters (n = 112) for the Sefton coast (**bold** text is significant (**p* <0.05; ***p* <0.01; ****p* <0.001))

	pH	SOM	C	N	Na	Mg	Al	Si	P	S	Cl	K	Ca
SOM	r = 0.335 **p <0.001***** R^2 = 0.112												
C	r = 0.562 **p <0.001***** R^2 = 0.361	r = 0.524 **p <0.001***** R^2 = 0.275											
N	r = 0.442 **p <0.001***** R^2 = 0.195	r = 0.491 **p <0.001***** R^2 = 0.241	r = 0.946 **p <0.001***** R^2 = 0.894										
Na	r = 0.047 p = 0.626 R^2 = 0.002	r = 0.189 **p = 0.046*** R^2 = 0.036	r = 0.152 p = 0.130 R^2 = 0.023	r = 0.163 p = 0.104 R^2 = 0.027									
Mg	r = 0.545 **p <0.001***** R^2 = 0.298	r = 0.015 p = 0.875 R^2 = 0.000	r = 0.292 **p = 0.003**** R^2 = 0.085	r = 0.229 **p = 0.021*** R^2 = 0.053	r = 0.500 **p <0.001***** R^2 = 0.250								
Al	r = 0.255 **p = 0.007**** R^2 = 0.065	r = 0.327 **p <0.001***** R^2 = 0.107	r = 0.363 **p <0.001***** R^2 = 0.132	r = 0.437 **p <0.001***** R^2 = 0.191	r = 0.018 p = 0.848 R^2 = 0.000	r = 0.069 p = 0.470 R^2 = 0.005							
Si	r = 0.236 **p = 0.012*** R^2 = 0.056	r = 0.665 **p <0.001***** R^2 = 0.442	r = 0.256 **p = 0.010*** R^2 = 0.066	r = 0.281 **p = 0.004**** R^2 = 0.079	r = 0.522 **p <0.001***** R^2 = 0.273	r = 0.339 **p <0.001***** R^2 = 0.115	r = 0.317 **p = 0.001**** R^2 = 0.100						
P	r = 0.268 **p = 0.004**** R^2 = 0.072	r = 0.652 **p <0.001***** R^2 = 0.425	r = 0.391 **p <0.001***** R^2 = 0.153	r = 0.455 **p <0.001***** R^2 = 0.207	r = 0.338 **p <0.001***** R^2 = 0.114	r = 0.238 **p = 0.012*** R^2 = 0.057	r = 0.445 **p <0.001***** R^2 = 0.198	r = 0.865 **p <0.001***** R^2 = 0.747					
S	r = 0.242 **p = 0.010*** R^2 = 0.059	r = 0.838 **p <0.001***** R^2 = 0.702	r = 0.417 **p <0.001***** R^2 = 0.174	r = 0.489 **p <0.001***** R^2 = 0.239	r = 0.119 p = 0.211 R^2 = 0.014	r = 0.002 p = 0.985 R^2 = 0.000	r = 0.477 **p <0.001***** R^2 = 0.227	r = 0.688 **p <0.001***** R^2 = 0.474	r = 0.747 **p <0.001***** R^2 = 0.558				
Cl	r = 0.047 p = 0.624 R^2 = 0.002	r = 0.001 p = 0.995 R^2 = 0.000	r = 0.059 p = 0.559 R^2 = 0.003	r = 0.066 p = 0.511 R^2 = 0.004	r = 0.969 **p <0.001***** R^2 = 0.938	r = 0.540 **p <0.001***** R^2 = 0.292	r = 0.057 p = 0.548 R^2 = 0.003	r = 0.695 **p <0.001***** R^2 = 0.483	r = 0.508 **p <0.001***** R^2 = 0.258	r = 0.065 p = 0.496 R^2 = 0.004			
K	r = 0.154 p = 0.105 R^2 = 0.024	r = 0.446 **p <0.001***** R^2 = 0.199	r = 0.086 p = 0.393 R^2 = 0.007	r = 0.069 p = 0.490 R^2 = 0.005	r = 0.649 **p <0.001***** R^2 = 0.422	r = 0.387 **p <0.001***** R^2 = 0.150	r = 0.029 p = 0.758 R^2 = 0.001	r = 0.879 **p <0.001***** R^2 = 0.773	r = 0.670 **p <0.001***** R^2 = 0.449	r = 0.422 **p <0.001***** R^2 = 0.178	r = 0.776 **p <0.001***** R^2 = 0.603		
Ca	r = 0.460 **p <0.001***** R^2 = 0.212	r = 0.143 p = 0.134 R^2 = 0.020	r = 0.291 **p = 0.003**** R^2 = 0.085	r = 0.260 **p = 0.009**** R^2 = 0.068	r = 0.198 **p = 0.036*** R^2 = 0.039	r = 0.459 **p <0.001***** R^2 = 0.211	r = 0.036 p = 0.708 R^2 = 0.001	r = 0.113 p = 0.234 R^2 = 0.013	r = 0.165 p = 0.083 R^2 = 0.027	r = 0.390 **p <0.001***** R^2 = 0.152	r = 0.147 p = 0.121 R^2 = 0.002	r = 0.001 p = 0.989 R^2 <0.001	
Fe	r = 0.231 **p = 0.014*** R^2 = 0.053	r = 0.216 **p = 0.022*** R^2 = 0.047	r = 0.045 p = 0.655 R^2 = 0.002	r = 0.093 p = 0.353 R^2 = 0.009	r = 0.413 **p <0.001***** R^2 = 0.171	r = 0.374 **p <0.001***** R^2 = 0.140	r = 0.237 **p = 0.012*** R^2 = 0.056	r = 0.041 p = 0.670 R^2 = 0.002	r = 0.062 p = 0.515 R^2 = 0.004	r = 0.342 **p <0.001***** R^2 = 0.117	r = 0.358 **p <0.001***** R^2 = 0.128	r = 0.199 **p = 0.035**** R^2 = 0.040	r = 0.543 **p <0.001***** R^2 = 0.295

r = correlation coefficient; p-value = significance of the correlation; R^2 = coefficient of determination, indicating the success of the equation in explaining the relationship between two parameters.

Table 7.3 Statistical relationships between the mineral magnetic parameters for the Sefton coast (**bold** text is significant (*p <0.05; **p <0.01; ***p <0.001)) (n = 113)

	χ_{LF}	χ_{FD}	χ_{ARM}	SIRM	$Soft_{IRM20}$	$Soft_{IRM40}$	$Hard_{IRM300}$	$Hard_{IRM500}$	$Soft_{\%20}$	$Soft_{\%40}$	$Hard_{\%300}$	$Hard_{\%500}$	S-ratio	ARM/χ	SIRM/ ARM	χ_{ARM}/ SIRM
χ_{FD}	r = 0.006 p = 0.948 R² = 0.000															
χ_{ARM}	r = 0.927 **p <0.001***** R² = 0.860	r = 0.040 p = 0.676 R² = 0.002														
SIRM	r = 0.865 **p <0.001***** R² = 0.748	r = 0.024 p = 0.799 R² = 0.001	r = 0.943 **p <0.001***** R² = 0.890													
$Soft_{IRM20}$	r = 0.738 **p <0.001***** R² = 0.545	r = 0.057 p = 0.545 R² = 0.003	r = 0.869 **p <0.001***** R² = 0.756	r = 0.898 **p <0.001***** R² = 0.807												
$Soft_{IRM40}$	r = 0.915 **p <0.001***** R² = 0.837	r = 0.010 p = 0.917 R² = 0.000	r = 0.971 **p <0.001***** R² = 0.942	r = 0.970 **p <0.001***** R² = 0.940	r = 0.938 **p <0.001***** R² = 0.880											
$Hard_{IRM300}$	r = 0.802 **p <0.001***** R² = 0.643	r = 0.073 p = 0.440 R² = 0.005	r = 0.821 **p <0.001***** R² = 0.674	r = 0.827 **p <0.001***** R² = 0.683	r = 0.853 **p <0.001***** R² = 0.728	r = 0.879 **p <0.001***** R² = 0.773										
$Hard_{IRM500}$	r = 0.171 p = 0.069 R² = 0.029	r = 0.150 p = 0.111 R² = 0.023	r = 0.198 **p = 0.034*** R² = 0.039	r = 0.179 p = 0.056 R² = 0.032	r = 0.445 **p <0.001***** R² = 0.198	r = 0.296 **p = 0.001**** R² = 0.088	r = 0.566 **p <0.001***** R² = 0.320									
$Soft_{\%20}$	r = 0.292 **p = 0.002**** R² = 0.085	r = 0.116 p = 0.220 R² = 0.013	r = 0.304 **p = 0.001**** R² = 0.092	r = 0.326 **p <0.001***** R² = 0.106	r = 0.157 p = 0.095 R² = 0.025	r = 0.281 **p = 0.002**** R² = 0.079	r = 0.367 **p <0.001***** R² = 0.135	r = 0.048 p = 0.615 R² = 0.002								
$Soft_{\%40}$	r = 0.350 **p <0.001***** R² = 0.122	r = 0.091 p = 0.335 R² = 0.008	r = 0.377 **p <0.001***** R² = 0.142	r = 0.434 **p <0.001***** R² = 0.188	r = 0.266 **p = 0.004**** R² = 0.071	r = 0.353 **p = 0.001**** R² = 0.124	r = 0.444 **p <0.001***** R² = 0.197	r = 0.052 p = 0.585 R² = 0.003	r = 0.804 **p <0.001***** R² = 0.646							
$Hard_{\%300}$	r = 0.238 **p = 0.011*** R² = 0.057	r = 0.002 p = 0.988 R² = 0.000	r = 0.312 **p = 0.001**** R² = 0.097	r = 0.264 **p = 0.005**** R² = 0.069	r = 0.346 **p <0.001***** R² = 0.120	r = 0.313 **p = 0.001**** R² = 0.098	r = 0.020 p = 0.834 R² = 0.000	r = 0.095 p = 0.316 R² = 0.009	r = 0.007 p = 0.938 R² = 0.000	r = 0.003 p = 0.727 R² = 0.001						
$Hard_{\%500}$	r = 0.221 **p = 0.018*** R² = 0.049	r = 0.005 p = 0.957 R² = 0.000	r = 0.287 **p = 0.004**** R² = 0.071	r = 0.231 **p = 0.013*** R² = 0.054	r = 0.282 **p = 0.002**** R² = 0.080	r = 0.270 **p = 0.004**** R² = 0.073	r = 0.154 p = 0.102 R² = 0.024	r = 0.274 **p = 0.003**** R² = 0.075	r = 0.227 **p = 0.015*** R² = 0.051	r = 0.197 **p = 0.036*** R² = 0.039	r = 0.622 **p <0.001***** R² = 0.387					
S-ratio	r = 0.316 **p = 0.001**** R² = 0.100	r = 0.161 p = 0.086 R² = 0.026	r = 0.202 **p = 0.031*** R² = 0.041	r = 0.015 p = 0.875 R² = 0.000	r = 0.024 p = 0.798 R² = 0.001	r = 0.143 p = 0.129 R² = 0.020	r = 0.128 p = 0.173 R² = 0.017	r = 0.070 **p <0.001***** R² = 0.005	r = 0.020 p = 0.829 R² = 0.000	r = 0.156 p = 0.097 R² = 0.024	r = 0.172 p = 0.067 R² = 0.030	r = 0.187 **p = 0.047*** R² = 0.035				
ARM/χ	r = 0.021 p = 0.821 R² = 0.000	r = 0.189 p = 0.073 R² = 0.028	r = 0.213 **p = 0.023*** R² = 0.045	r = 0.059 p = 0.535 R² = 0.003	r = 0.094 p = 0.321 R² = 0.009	r = 0.059 p = 0.534 R² = 0.003	r = 0.074 p = 0.435 R² = 0.005	r = 0.098 p = 0.301 R² = 0.010	r = 0.070 p = 0.460 R² = 0.005	r = 0.074 p = 0.431 R² = 0.006	r = 0.203 **p = 0.030*** R² = 0.041	r = 0.064 p = 0.500 R² = 0.004	r = 0.078 p = 0.407 R² = 0.006			
SIRM/ARM	r = 0.220 **p = 0.019*** R² = 0.048	r = 0.204 **p = 0.029** R² = 0.042	r = 0.134 p = 0.154 R² = 0.018	r = 0.297 **p = 0.001**** R² = 0.088	r = 0.311 **p = 0.001**** R² = 0.097	r = 0.287 **p = 0.002**** R² = 0.082	r = 0.434 **p <0.001***** R² = 0.189	r = 0.343 **p <0.001***** R² = 0.118	r = 0.264 **p = 0.005**** R² = 0.070	r = 0.307 **p = 0.001**** R² = 0.094	r = 0.100 p = 0.291 R² = 0.010	r = 0.039 p = 0.680 R² = 0.002	r = 0.127 p = 0.179 R² = 0.016	r = 0.851 **p <0.001***** R² = 0.423		
χ_{ARM}/SIRM	r = 0.107 p = 0.258 R² = 0.011	r = 0.151 p = 0.108 R² = 0.023	r = 0.034 p = 0.721 R² = 0.001	r = 0.118 p = 0.212 R² = 0.014	r = 0.136 p = 0.150 R² = 0.018	r = 0.125 p = 0.185 R² = 0.016	r = 0.230 **p = 0.014*** R² = 0.053	r = 0.198 **p = 0.034*** R² = 0.039	r = 0.094 p = 0.321 R² = 0.009	r = 0.181 p = 0.054 R² = 0.033	r = 0.117 p = 0.214 R² = 0.014	r = 0.019 p = 0.837 R² = 0.000	r = 0.168 p = 0.074 R² = 0.028	r = 0.866 **p <0.001***** R² = 0.749	r = 0.677 **p <0.001***** R² = 0.458	
SIRM/χ	r = 0.351 **p = 0.001**** R² = 0.099	r = 0.031 p = 0.748 R² = 0.001	r = 0.572 **p <0.001***** R² = 0.328	r = 0.714 **p <0.001***** R² = 0.509	r = 0.752 **p <0.001***** R² = 0.566	r = 0.634 **p <0.001***** R² = 0.402	r = 0.528 **p <0.001***** R² = 0.278	r = 0.193 **p = 0.039*** R² = 0.037	r = 0.231 **p = 0.013*** R² = 0.053	r = 0.380 **p <0.001***** R² = 0.145	r = 0.256 **p = 0.006**** R² = 0.066	r = 0.196 **p = 0.036*** R² = 0.039	r = 0.356 **p <0.001***** R² = 0.127	r = 0.209 **p = 0.026*** R² = 0.044	r = 0.238 **p = 0.011*** R² = 0.057	r = 0.128 p = 0.173 R² = 0.016

r = correlation coefficient; p-value = significance of the correlation; R^2 = coefficient of determination, indicating the success of the equation in explaining the relationship between two parameters.

Table 7.4 Statistical relationships between pH and SOM (n = 112), C and N (n = 101) and geochemical (n = 112) parameters versus particle size distribution parameters (n = 112) for the Sefton coast (**bold** text is significant (**p* <0.05; ***p* <0.01; ****p* <0.001))

	pH	SOM	C	N	Na	Mg	Al	Si	P	S	Cl	K	Ca	Fe
Sand	r = 0.580 **p <0.001***** R^2 = 0.336	r = 0.412 **p <0.001***** R^2 = 0.170	r = 0.552 **p <0.001***** R^2 = 0.304	r = 0.530 **p <0.001***** R^2 = 0.281	r = 0.142 *p* = 0.137 R^2 = 0.020	r = 0.333 **p <0.001***** R^2 = 0.111	r = 0.281 **p = 0.003**** R^2 = 0.079	r = 0.254 **p = 0.007**** R^2 = 0.065	r = 0.354 **p <0.001***** R^2 = 0.125	r = 0.480 **p <0.001***** R^2 = 0.231	r = 0.036 *p* = 0.708 R^2 = 0.001	r = 0.074 *p* = 0.440 R^2 = 0.005	r = 0.062 *p* = 0.520 R^2 = 0.004	r = 0.220 **p = 0.020*** R^2 = 0.049
Silt	r = 0.608 **p <0.001***** R^2 = 0.369	r = 0.427 **p <0.001***** R^2 = 0.182	r = 0.596 **p <0.001***** R^2 = 0.355	r = 0.577 **p <0.001***** R^2 = 0.333	r = 0.143 *p* = 0.135 R^2 = 0.020	r = 0.339 **p <0.001***** R^2 = 0.115	r = 0.303 **p = 0.001**** R^2 = 0.092	r = 0.264 **p = 0.005**** R^2 = 0.070	r = 0.370 **p <0.001***** R^2 = 0.137	r = 0.486 **p <0.001***** R^2 = 0.237	r = 0.035 *p* = 0.719 R^2 = 0.001	r = 0.079 *p* = 0.413 R^2 = 0.006	r = 0.016 *p* = 0.868 R^2 = 0.000	r = 0.195 **p = 0.040*** R^2 = 0.038
Clay	r = 0.547 **p <0.001***** R^2 = 0.299	r = 0.342 **p <0.001***** R^2 = 0.117	r = 0.726 **p <0.001***** R^2 = 0.527	r = 0.739 **p <0.001***** R^2 = 0.546	r = 0.090 *p* = 0.348 R^2 = 0.008	r = 0.254 **p = 0.007**** R^2 = 0.065	r = 0.353 **p <0.001***** R^2 = 0.124	r = 0.235 **p = 0.013*** R^2 = 0.055	r = 0.349 **p <0.001***** R^2 = 0.122	r = 0.340 **p <0.001***** R^2 = 0.115	r = 0.009 *p* = 0.925 R^2 = 0.000	r = 0.083 *p* = 0.386 R^2 = 0.007	r = 0.354 **p <0.001***** R^2 = 0.125	r = 0.087 *p* = 0.362 R^2 = 0.008
Mean particle size	r = 0.555 **p <0.001***** R^2 = 0.308	r = 0.574 **p <0.001***** R^2 = 0.330	r = 0.610 **p <0.001***** R^2 = 0.372	r = 0.623 **p <0.001***** R^2 = 0.388	r = 0.230 **p = 0.015*** R^2 = 0.053	r = 0.217 **p = 0.022*** R^2 = 0.047	r = 0.379 **p <0.001***** R^2 = 0.144	r = 0.355 **p <0.001***** R^2 = 0.126	r = 0.449 **p <0.001***** R^2 = 0.202	r = 0.630 **p <0.001***** R^2 = 0.397	r = 0.094 *p* = 0.328 R^2 = 0.009	r = 0.121 *p* = 0.208 R^2 = 0.015	r = 0.117 *p* = 0.220 R^2 = 0.014	r = 0.244 **p = 0.010*** R^2 = 0.059
Median particle size	r = 0.472 **p <0.001***** R^2 = 0.222	r = 0.716 **p <0.001***** R^2 = 0.513	r = 0.611 **p <0.001***** R^2 = 0.373	r = 0.638 **p <0.001***** R^2 = 0.407	r = 0.241 **p = 0.011*** R^2 = 0.058	r = 0.120 *p* = 0.211 R^2 = 0.014	r = 0.448 **p <0.001***** R^2 = 0.201	r = 0.485 **p <0.001***** R^2 = 0.235	r = 0.571 **p <0.001***** R^2 = 0.327	r = 0.815 **p <0.001***** R^2 = 0.665	r = 0.080 *p* = 0.405 R^2 = 0.006	r = 0.211 **p = 0.026*** R^2 = 0.045	r = 0.247 **p = 0.009**** R^2 = 0.061	r = 0.333 **p <0.001***** R^2 = 0.111
Sorting	r = 0.425 **p <0.001***** R^2 = 0.181	r = 0.182 *p* = 0.054 R^2 = 0.033	r = 0.341 **p = 0.001**** R^2 = 0.116	r = 0.323 **p = 0.001**** R^2 = 0.105	r = 0.146 *p* = 0.126 R^2 = 0.021	r = 0.240 **p = 0.011*** R^2 = 0.058	r = 0.096 *p* = 0.316 R^2 = 0.009	r = 0.001 *p* = 0.991 R^2 = 0.000	r = 0.122 *p* = 0.202 R^2 = 0.015	r = 0.194 **p = 0.041*** R^2 = 0.038	r = 0.103 *p* = 0.284 R^2 = 0.011	r = 0.078 *p* = 0.415 R^2 = 0.006	r = 0.022 *p* = 0.822 R^2 = 0.000	r = 0.185 *p* = 0.052 R^2 = 0.034
Skewness	r = 0.142 *p* = 0.136 R^2 = 0.020	r = 0.447 **p <0.001***** R^2 = 0.200	R = 0.015 *p* = 0.879 R^2 = 0.000	r = 0.009 *p* = 0.933 R^2 = 0.000	r = 0.015 *p* = 0.873 R^2 = 0.000	r = 0.199 **p = 0.037*** R^2 = 0.039	r = 0.216 **p = 0.023*** R^2 = 0.047	r = 0.425 **p <0.001***** R^2 = 0.181	r = 0.362 **p <0.001***** R^2 = 0.131	r = 0.538 **p <0.001***** R^2 = 0.290	r = 0.072 *p* = 0.455 R^2 = 0.005	r = 0.303 **p = 0.001**** R^2 = 0.092	r = 0.388 **p <0.001***** R^2 = 0.151	r = 0.204 **p = 0.032*** R^2 = 0.041
Kurtosis	r = 0.557 **p <0.001***** R^2 = 0.310	r = 0.253 **p = 0.007**** R^2 = 0.064	r = 0.542 **p <0.001***** R^2 = 0.294	r = 0.538 **p <0.001***** R^2 = 0.289	r = 0.061 *p* = 0.525 R^2 = 0.004	r = 0.315 **p = 0.001**** R^2 = 0.099	r = 0.270 **p = 0.004**** R^2 = 0.073	r = 0.173 *p* = 0.069 R^2 = 0.030	r = 0.279 **p = 0.003**** R^2 = 0.078	r = 0.264 **p = 0.005**** R^2 = 0.070	r = 0.005 *p* = 0.962 R^2 = 0.000	r = 0.008 *p* = 0.931 R^2 = 0.000	r = 0.176 *p* = 0.065 R^2 = 0.031	r = 0.013 *p* = 0.894 R^2 = 0.000

r = correlation coefficient; p-value = significance of the correlation; R^2 = coefficient of determination, indicating the success of the equation in explaining the relationship between two parameters.

Table 7.5 Statistical relationships between the mineral magnetic parameters versus particle size distribution parameters for the Sefton coast (**bold** text is significant (*p <0.05; **p <0.01; ***p <0.001)) (n = 112)

	χ_{LF}	χ_{FD}	χ_{ARM}	SIRM	$Soft_{IRM20}$	$Soft_{IRM40}$	$Hard_{IRM300}$	$Hard_{IRM500}$	$Soft_{\%20}$	$Soft_{\%40}$	$Hard_{\%300}$	$Hard_{\%500}$	S-ratio	ARM/χ	SIRM/ ARM	χ_{ARM}/ SIRM	SIRM/χ
Sand	r = 0.172 p = 0.070 R^2 = 0.030	r = 0.123 p = 0.198 R^2 = 0.015	r = 0.282 **p = 0.003** R^2 = 0.080	r = 0.152 p = 0.110 R^2 = 0.023	r = 0.179 p = 0.059 R^2 = 0.032	r = 0.171 p = 0.071 R^2 = 0.029	r = 0.074 p = 0.438 R^2 = 0.005	r = 0.067 p = 0.486 R^2 = 0.004	r = 0.214 **p = 0.023*** R^2 = 0.046	r = 0.320 **p = 0.001**** R^2 = 0.102	r = 0.362 **p <0.001***** R^2 = 0.131	r = 0.421 **p <0.001***** R^2 = 0.177	r = 0.001 p = 0.993 R^2 = 0.000	r = 0.398 **p <0.001***** R^2 = 0.158	r = 0.217 **p = 0.022*** R^2 = 0.047	r = 0.364 **p <0.001***** R^2 = 0.133	r = 0.200 **p = 0.034*** R^2 = 0.040
Silt	r = 0.187 **p = 0.048*** R^2 = 0.035	r = 0.124 p = 0.194 R^2 = 0.015	r = 0.287 **p = 0.002**** R^2 = 0.083	r = 0.158 p = 0.097 R^2 = 0.025	r = 0.194 **p = 0.040*** R^2 = 0.038	r = 0.185 p = 0.051 R^2 = 0.034	r = 0.085 p = 0.375 R^2 = 0.007	r = 0.055 p = 0.566 R^2 = 0.003	r = 0.212 **p = 0.025*** R^2 = 0.045	r = 0.315 **p = 0.001**** R^2 = 0.099	r = 0.376 **p <0.001***** R^2 = 0.142	r = 0.435 **p <0.001***** R^2 = 0.189	r = 0.006 p = 0.947 R^2 = 0.000	r = 0.371 **p <0.001***** R^2 = 0.137	r = 0.207 **p = 0.029*** R^2 = 0.043	r = 0.327 **p <0.001***** R^2 = 0.107	r = 0.207 **p = 0.028*** R^2 = 0.043
Clay	r = 0.225 **p = 0.017*** R^2 = 0.051	r = 0.076 p = 0.425 R^2 = 0.006	r = 0.192 **p = 0.043*** R^2 = 0.037	r = 0.132 p = 0.164 R^2 = 0.018	r = 0.224 **p = 0.017*** R^2 = 0.050	r = 0.207 **p = 0.029*** R^2 = 0.043	r = 0.130 p = 0.172 R^2 = 0.017	r = 0.065 p = 0.499 R^2 = 0.004	r = 0.096 p = 0.313 R^2 = 0.009	r = 0.135 p = 0.157 R^2 = 0.018	r = 0.315 **p = 0.001**** R^2 = 0.099	r = 0.345 **p <0.001***** R^2 = 0.119	r = 0.047 p = 0.620 R^2 = 0.002	r = 0.019 p = 0.840 R^2 = 0.000	r = 0.028 p = 0.770 R^2 = 0.001	r = 0.125 p = 0.190 R^2 = 0.016	r = 0.169 p = 0.075 R^2 = 0.028
Mean particle size	r = 0.232 **p = 0.014*** R^2 = 0.054	r = 0.151 p = 0.113 R^2 = 0.023	r = 0.312 **p = 0.001**** R^2 = 0.097	r = 0.158 p = 0.097 R^2 = 0.025	r = 0.195 **p = 0.039*** R^2 = 0.038	r = 0.198 **p = 0.036*** R^2 = 0.039	r = 0.127 p = 0.181 R^2 = 0.016	r = 0.003 p = 0.971 R^2 = 0.000	r = 0.288 **p = 0.002**** R^2 = 0.083	r = 0.357 **p <0.001***** R^2 = 0.127	r = 0.365 **p <0.001***** R^2 = 0.133	r = 0.432 **p <0.001***** R^2 = 0.187	r = 0.038 p = 0.692 R^2 = 0.001	r = 0.389 **p <0.001***** R^2 = 0.151	r = 0.190 **p = 0.045*** R^2 = 0.036	r = 0.357 **p <0.001***** R^2 = 0.128	r = 0.187 **p = 0.048*** R^2 = 0.035
Median particle size	r = 0.460 **p <0.001***** R^2 = 0.211	r = 0.210 **p = 0.026*** R^2 = 0.044	r = 0.396 **p <0.001***** R^2 = 0.156	r = 0.219 **p = 0.021*** R^2 = 0.048	r = 0.239 **p = 0.011*** R^2 = 0.057	r = 0.249 **p = 0.008**** R^2 = 0.062	r = 0.141 p = 0.139 R^2 = 0.020	r = 0.010 p = 0.914 R^2 = 0.000	r = 0.292 **p = 0.002**** R^2 = 0.085	r = 0.333 **p <0.001***** R^2 = 0.111	r = 0.385 **p <0.001***** R^2 = 0.148	r = 0.415 **p <0.001***** R^2 = 0.172	r = 0.088 p = 0.357 R^2 = 0.008	r = 0.475 **p <0.001***** R^2 = 0.226	r = 0.256 **p = 0.006**** R^2 = 0.065	r = 0.460 **p <0.001***** R^2 = 0.211	r = 0.210 **p = 0.026*** R^2 = 0.044
Sorting	r = 0.106 p = 0.267 R^2 = 0.011	r = 0.072 p = 0.450 R^2 = 0.005	r = 0.178 p = 0.060 R^2 = 0.032	r = 0.090 p = 0.347 R^2 = 0.008	r = 0.107 p = 0.261 R^2 = 0.011	r = 0.101 p = 0.291 R^2 = 0.010	r = 0.078 p = 0.414 R^2 = 0.006	r = 0.052 p = 0.588 R^2 = 0.003	r = 0.246 **p = 0.009**** R^2 = 0.061	r = 0.350 **p <0.001***** R^2 = 0.122	r = 0.252 **p = 0.007**** R^2 = 0.063	r = 0.372 **p <0.001***** R^2 = 0.139	r = 0.014 p = 0.887 R^2 = 0.000	r = 0.275 **p = 0.003**** R^2 = 0.075	r = 0.102 p = 0.284 R^2 = 0.010	r = 0.226 **p = 0.017*** R^2 = 0.051	r = 0.151 p = 0.111 R^2 = 0.023
Skewness	r = 0.096 p = 0.313 R^2 = 0.009	r = 0.158 p = 0.097 R^2 = 0.025	r = 0.209 **p = 0.027*** R^2 = 0.044	r = 0.125 p = 0.188 R^2 = 0.016	r = 0.089 p = 0.351 R^2 = 0.008	r = 0.107 p = 0.260 R^2 = 0.012	r = 0.011 p = 0.908 R^2 = 0.000	r = 0.005 p = 0.956 R^2 = 0.000	r = 0.008 p = 0.935 R^2 = 0.000	r = 0.078 p = 0.412 R^2 = 0.006	r = 0.064 p = 0.503 R^2 = 0.004	r = 0.011 p = 0.906 R^2 = 0.000	r = 0.166 p = 0.081 R^2 = 0.027	r = 0.284 **p = 0.002**** R^2 = 0.081	r = 0.243 **p = 0.010*** R^2 = 0.059	r = 0.344 **p <0.001***** R^2 = 0.119	r = 0.038 p = 0.687 R^2 = 0.001
Kurtosis	r = 0.100 p = 0.293 R^2 = 0.010	r = 0.101 p = 0.291 R^2 = 0.010	r = 0.153 p = 0.108 R^2 = 0.023	r = 0.075 p = 0.433 R^2 = 0.006	r = 0.121 p = 0.203 R^2 = 0.015	r = 0.106 p = 0.267 R^2 = 0.011	r = 0.003 p = 0.973 R^2 = 0.000	r = 0.109 p = 0.252 R^2 = 0.012	r = 0.114 p = 0.232 R^2 = 0.013	r = 0.201 **p = 0.034*** R^2 = 0.040	r = 0.320 **p = 0.001**** R^2 = 0.102	r = 0.376 **p <0.001***** R^2 = 0.141	r = 0.060 p = 0.532 R^2 = 0.004	r = 0.161 p = 0.089 R^2 = 0.026	r = 0.153 p = 0.107 R^2 = 0.023	r = 0.105 p = 0.269 R^2 = 0.011	r = 0.132 p = 0.166 R^2 = 0.017

r = correlation coefficient; p-value = significance of the correlation; R^2 = coefficient of determination, indicating the success of the equation in explaining the relationship between two parameters.

Table 7.6 Statistical relationships between the mineral magnetic parameters (n = 113) versus pH and SOM (n = 113), C and N (n = 101) and geochemical parameters (n = 112) for the Sefton coast (**bold** text is significant (*p <0.05; **p <0.01; ***p <0.001))

	χ_{LF}	χ_{FD}	χ_{ARM}	SIRM	$Soft_{IRM20}$	$Soft_{IRM40}$	$Hard_{IRM300}$	$Hard_{IRM500}$	$Soft_{\%20}$	$Soft_{\%40}$	$Hard_{\%300}$	$Hard_{\%500}$	S-ratio	ARM/χ	SIRM/ ARM	χ_{ARM} SIRM	SIRM/χ
pH	r = 0.033 p = 0.729 R² = 0.001	r = 0.184 p = 0.051 R² = 0.034	r = 0.095 p = 0.319 R² = 0.009	r = 0.041 p = 0.669 R² = 0.002	r = 0.064 p = 0.502 R² = 0.004	r = 0.053 p = 0.574 R² = 0.003	r = 0.072 p = 0.448 R² = 0.005	r = 0.083 p = 0.384 R² = 0.007	r = 0.006 p = 0.486 R² = 0.004	r = 0.196 **p = 0.038*** R² = 0.038	r = 0.371 **p <0.001***** R² = 0.138	r = 0.295 **p = 0.002**** R² = 0.087	r = 0.146 p = 0.122 R² = 0.021	r = 0.060 p = 0.529 R² = 0.004	rR = 0.131 p = 0.166 R² = 0.017	r = 0.053 p = 0.574 R² = 0.003	r = 0.151 p = 0.111 R² = 0.023
SOM	r = 0.186 **p = 0.048*** R² = 0.035	r = 0.301 **p = 0.001**** R² = 0.091	r = 0.250 **p = 0.008**** R² = 0.063	r = 0.150 p = 0.112 R² = 0.023	r = 0.105 p = 0.267 R² = 0.011	r = 0.144 p = 0.128 R² = 0.021	r = 0.096 p = 0.489 R² = 0.004	r = 0.036 p = 0.708 R² = 0.001	r = 0.382 **p <0.001***** R² = 0.131	r = 0.303 **p <0.001***** R² = 0.092	r = 0.271 **p = 0.004**** R² = 0.074	r = 0.278 **p = 0.003**** R² = 0.077	r = 0.122 p = 0.198 R² = 0.015	r = 0.205 **p = 0.029*** R² = 0.042	r = 0.160 p = 0.090 R² = 0.026	r = 0.263 **p = 0.005**** R² = 0.069	r = 0.084 p = 0.375 R² = 0.007
C	r = 0.240 **p = 0.016*** R² = 0.057	r = 0.003 p = 0.976 R² = 0.000	r = 0.220 **p = 0.027*** R² = 0.049	r = 0.119 p = 0.236 R² = 0.014	r = 0.245 **p = 0.013*** R² = 0.060	r = 0.212 **p = 0.033*** R² = 0.045	r = 0.180 p = 0.071 R² = 0.033	r = 0.180 p = 0.109 R² = 0.026	r = 0.095 p = 0.343 R² = 0.009	r = 0.098 p = 0.331 R² = 0.010	r = 0.325 **p = 0.001**** R² = 0.106	r = 0.312 **p = 0.001**** R² = 0.097	r = 0.025 p = 0.801 R² = 0.001	r = 0.100 p = 0.318 R² = 0.010	r = 0.196 **p = 0.049*** R² = 0.039	r = 0.037 p = 0.714 R² = 0.001	r = 0.155 p = 0.121 R² = 0.024
N	r = 0.288 **p = 0.003**** R² = 0.083	r = 0.069 p = 0.494 R² = 0.005	r = 0.309 **p = 0.002**** R² = 0.095	r = 0.191 p = 0.056 R² = 0.036	r = 0.283 **p = 0.004**** R² = 0.080	r = 0.269 **p = 0.007**** R² = 0.072	r = 0.219 **p = 0.028*** R² = 0.048	r = 0.150 p = 0.134 R² = 0.023	r = 0.144 p = 0.151 R² = 0.021	r = 0.127 p = 0.207 R² = 0.016	r = 0.320 **p = 0.001**** R² = 0.102	r = 0.312 **p = 0.002**** R² = 0.097	r = 0.003 p = 0.973 R² = 0.000	r = 0.177 p = 0.077 R² = 0.031	r = 0.261 **p = 0.030*** R² = 0.047	r = 0.100 p = 0.317 R² = 0.010	r = 0.219 **p = 0.028*** R² = 0.048
Na	r = 0.113 p = 0.235 R² = 0.013	r = 0.140 p = 0.140 R² = 0.020	r = 0.099 p = 0.298 R² = 0.010	r = 0.063 p = 0.510 R² = 0.004	r = 0.073 p = 0.443 R² = 0.005	r = 0.084 p = 0.381 R² = 0.007	r = 0.126 p = 0.185 R² = 0.016	r = 0.096 p = 0.316 R² = 0.009	r = 0.165 p = 0.083 R² = 0.027	r = 0.159 p = 0.094 R² = 0.025	r = 0.020 p = 0.834 R² = 0.000	r = 0.059 p = 0.538 R² = 0.003	r = 0.133 p = 0.163 R² = 0.018	r = 0.068 p = 0.357 R² = 0.005	r = 0.031 p = 0.749 R² = 0.001	r = 0.085 p = 0.371 R² = 0.007	r = 0.067 p = 0.480 R² = 0.005
Mg	r = 0.155 p = 0.103 R² = 0.024	r = 0.075 p = 0.434 R² = 0.006	r = 0.046 p = 0.628 R² = 0.002	r = 0.018 p = 0.848 R² = 0.000	r = 0.066 p = 0.492 R² = 0.004	r = 0.078 p = 0.413 R² = 0.006	r = 0.241 **p = 0.011*** R² = 0.058	r = 0.327 **p <0.001***** R² = 0.107	r = 0.153 p = 0.107 R² = 0.023	r = 0.025 p = 0.793 R² = 0.001	r = 0.165 p = 0.082 R² = 0.027	r = 0.162 p = 0.088 R² = 0.026	r = 0.298 **p = 0.001**** R² = 0.089	r = 0.010 p = 0.919 R² = 0.000	r = 0.178 p = 0.064 R² = 0.031	r = 0.004 p <0.968 R² = 0.000	r = 0.068 p = 0.479 R² = 0.005
Al	r = 0.607 **p <0.001***** R² = 0.368	r = 0.095 p = 0.320 R² = 0.009	r = 0.723 **p <0.001***** R² = 0.523	r = 0.641 **p <0.001***** R² = 0.411	r = 0.644 **p <0.001***** R² = 0.415	r = 0.661 **p <0.001***** R² = 0.437	r = 0.472 **p <0.001***** R² = 0.223	r = 0.274 **p = 0.003**** R² = 0.075	r = 0.097 p = 0.309 R² = 0.009	r = 0.175 p = 0.065 R² = 0.031	r = 0.317 **p = 0.001**** R² = 0.100	r = 0.172 p = 0.070 R² = 0.030	r = 0.212 **p = 0.025*** R² = 0.045	r = 0.410 **p <0.001***** R² = 0.168	rR = 0.031 p = 0.744 R² = 0.001	r = 0.176 p = 0.064 R² = 0.031	r = 0.853 **p <0.001***** R² = 0.427
Si	r = 0.087 p = 0.364 R² = 0.007	r = 0.129 p = 0.174 R² = 0.017	r = 0.151 p = 0.112 R² = 0.023	r = 0.075 p = 0.432 R² = 0.006	r = 0.054 p = 0.573 R² = 0.003	r = 0.069 p = 0.473 R² = 0.005	r = 0.041 p = 0.667 R² = 0.002	r = 0.077 p = 0.420 R² = 0.006	r = 0.082 p = 0.514 R² = 0.004	r = 0.020 p = 0.836 R² = 0.000	r = 0.265 **p = 0.005**** R² = 0.070	r = 0.188 **p = 0.047*** R² = 0.035	r = 0.049 p <0.608 R² = 0.002	r = 0.177 p = 0.062 R² = 0.031	r = 0.183 p = 0.053 R² = 0.033	r = 0.263 **p = 0.005**** R² = 0.069	r = 0.007 p = 0.942 R² = 0.000
P	r = 0.160 p = 0.091 R² = 0.026	r = 0.207 **p = 0.029*** R² = 0.043	r = 0.251 **p = 0.008**** R² = 0.063	r = 0.128 p = 0.180 R² = 0.016	r = 0.136 p = 0.151 R² = 0.019	r = 0.144 p = 0.131 R² = 0.021	r = 0.034 p <0.718 R² = 0.001	r = 0.030 p = 0.756 R² = 0.001	r = 0.122 p = 0.201 R² = 0.015	r = 0.107 p = 0.261 R² = 0.011	r = 0.331 **p <0.001***** R² = 0.110	r = 0.280 **p = 0.003**** R² = 0.078	r = 0.082 p = 0.391 R² = 0.007	r = 0.309 **p = 0.001**** R² = 0.095	r = 0.207 **p = 0.029*** R² = 0.043	r = 0.324 **p <0.001***** R² = 0.105	r = 0.078 p = 0.411 R² = 0.006
S	r = 0.327 **p <0.001***** R² = 0.107	r = 0.187 **p = 0.049*** R² = 0.035	r = 0.468 **p <0.001***** R² = 0.219	r = 0.329 **p <0.001***** R² = 0.108	r = 0.289 **p = 0.002**** R² = 0.084	r = 0.319 **p = 0.001**** R² = 0.102	r = 0.168 p = 0.078 R² = 0.028	r = 0.008 p = 0.930 R² = 0.000	r = 0.264 **p = 0.005**** R² = 0.070	r = 0.250 **p = 0.008**** R² = 0.062	r = 0.320 **p = 0.001**** R² = 0.103	r = 0.309 **p = 0.001**** R² = 0.095	r = 0.072 p = 0.448 R² = 0.005	r = 0.441 **p <0.001***** R² = 0.195	r = 0.208 **p = 0.028*** R² = 0.043	r = 0.465 **p <0.001***** R² = 0.216	r = 0.250 **p = 0.008**** R² = 0.063
Cl	r = 0.074 p = 0.436 R² = 0.006	r = 0.086 p = 0.367 R² = 0.007	r = 0.051 p = 0.597 R² = 0.003	r = 0.032 p = 0.738 R² = 0.001	r = 0.050 p = 0.603 R² = 0.002	r = 0.054 p = 0.570 R² = 0.003	r = 0.117 p = 0.217 R² = 0.014	r = 0.102 p = 0.288 R² = 0.010	r = 0.135 p = 0.157 R² = 0.018	r = 0.129 p = 0.175 R² = 0.017	r = 0.084 p = 0.377 R² = 0.007	r = 0.004 p = 0.963 R² = 0.000	r = 0.115 p = 0.225 R² = 0.013	r = 0.033 p = 0.729 R² = 0.001	r = 0.066 p = 0.488 R² = 0.004	r = 0.006 p = 0.953 R² = 0.000	r = 0.055 p = 0.563 R² = 0.003
K	r = 0.010 p = 0.921 R² = 0.000	r = 0.006 p = 0.954 R² = 0.000	r = 0.041 p = 0.665 R² = 0.002	r = 0.044 p = 0.642 R² = 0.002	r = 0.043 p = 0.651 R² = 0.002	r = 0.039 p = 0.685 R² = 0.001	r = 0.061 p = 0.524 R² = 0.004	r = 0.046 p = 0.628 R² = 0.002	r = 0.012 p = 0.898 R² = 0.000	r = 0.042 p = 0.659 R² = 0.002	r = 0.161 p = 0.090 R² = 0.026	r = 0.146 p = 0.124 R² = 0.021	r = 0.072 p = 0.448 R² = 0.005	r = 0.097 p = 0.308 R² = 0.009	r = 0.020 p = 0.832 R² = 0.000	r = 0.023 p = 0.810 R² = 0.001	r = 0.148 p = 0.120 R² = 0.022
Ca	r = 0.009 p = 0.928 R² = 0.000	r = 0.044 p = 0.642 R² = 0.002	r = 0.097 p = 0.311 R² = 0.009	r = 0.017 p = 0.858 R² = 0.000	r = 0.031 p = 0.747 R² = 0.001	r = 0.022 p = 0.819 R² = 0.000	r = 0.003 p = 0.974 R² = 0.000	r = 0.067 p = 0.483 R² = 0.004	r = 0.002 p = 0.987 R² = 0.000	r = 0.113 p = 0.234 R² = 0.013	r = 0.060 p = 0.532 R² = 0.004	r = 0.113 p = 0.234 R² = 0.013	r = 0.226 **p = 0.016*** R² = 0.051	r = 0.489 **p <0.001***** R² = 0.240	r = 0.138 p = 0.146 R² = 0.019	r = 0.668 **p <0.001***** R² = 0.446	r = 0.141 p = 0.139 R² = 0.020
Fe	r = 0.457 **p <0.001***** R² = 0.209	r = 0.008 p = 0.936 R² = 0.000	r = 0.412 **p <0.001***** R² = 0.170	r = 0.344 **p <0.001***** R² = 0.118	r = 0.372 **p <0.001***** R² = 0.139	r = 0.386 **p <0.001***** R² = 0.149	r = 0.385 **p <0.001***** R² = 0.148	r = 0.276 p = 0.003 R² = 0.076	r = 0.218 **p = 0.021*** R² = 0.047	r = 0.107 p = 0.259 R² = 0.012	r = 0.152 p = 0.111 R² = 0.023	r = 0.178 p = 0.060 R² = 0.032	r = 0.149 p = 0.117 R² = 0.022	r = 0.243 **p = 0.010*** R² = 0.059	r = 0.127 p = 0.183 R² = 0.016	r = 0.424 **p <0.001***** R² = 0.180	r = 0.162 p = 0.087 R² = 0.026

r = correlation coefficient; p-value = significance of the correlation; R² = coefficient of determination, indicating the success of the equation in explaining the relationship between two parameters.

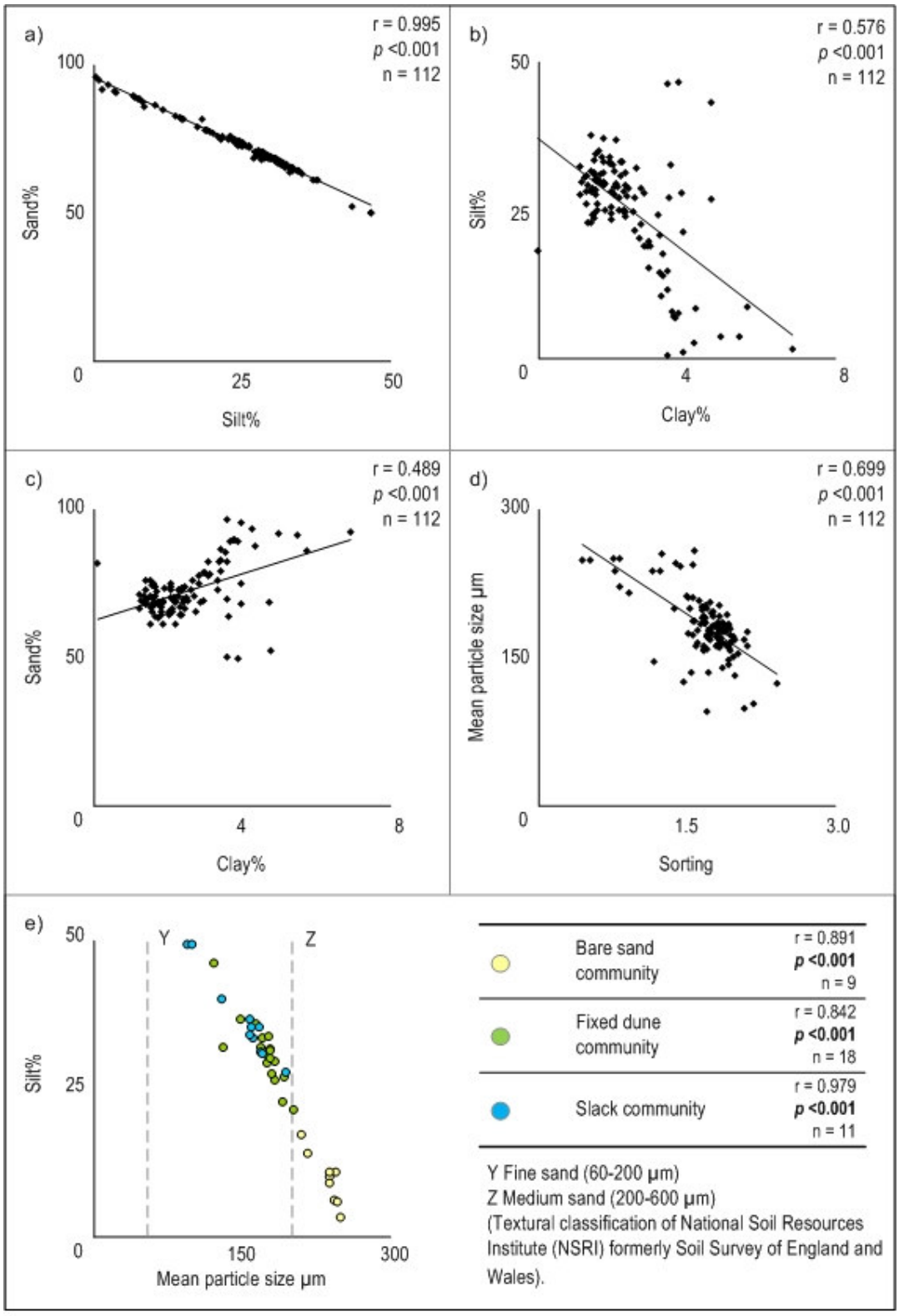

Figure 7.2 Bivariate plots for particle size parameters: a) sand versus silt; b) silt versus clay; c) sand versus clay; d) mean particle size versus sorting and e) silt versus mean particle size for selected dune environments (**bold** text is significant (p <0.05).

significance of the particle size association continued to be evident for each population, bare sand ($r = 0.89$; $p < 0.001$; $n = 9$), fixed dune ($r = 0.84$; $p < 0.001$; $n = 18$) and slack communities ($r = 0.98$; $p < 0.001$; $n = 11$).

7.2.2 Statistical correlation between pH, SOM and geochemical topsoil parameters

Table 7.2 shows geochemical topsoil parameters displayed strong correlations ($p < 0.05$) with at least eight other geochemical parameters, suggesting major oxides were highly dependent upon each other. Strongest correlation coefficients were evident for C versus N ($r = 0.95$; $p < 0.001$; $n = 101$) and Na versus Cl ($r = 0.97$; $p < 0.001$; $n = 112$). Whereas, weakest correlation coefficients were associated with Mg versus S ($r < 0.01$; $p = 0.985$ (NS); $n = 112$) and K versus Ca ($r < 0.01$; $p = 0.989$ (NS); $n = 112$).

Figure 7.3a shows a negative correlation between pH versus SOM ($r = 0.34$; $p < 0.001$; $n = 113$), indicating decreased pH was associated with increased SOM. This pattern was similar to pH versus C ($r = 0.56$; $p < 0.001$; $n = 101$) (Figure 7.3b), which corresponded with strong positive correlations between SOM versus C ($r = 0.52$; $p < 0.001$; $n = 101$) (Figure 7.3d) and SOM versus N ($r = 0.49$; $p < 0.001$; $n = 101$) (Figure 7.3e). This suggests SOM contributed to high C concentrations and low pH. Figure 7.3c shows alkaline samples correlated positively with high levels of Mg ($r = 0.55$; $p < 0.001$; $n = 112$). A strong positive correlation between P versus SOM ($r = 0.65$; $p < 0.001$; $n = 112$) (Figure 7.3f) indicates increased P was related to increased SOM.

Figure 7.3g shows three topsoil population samples, fixed dune community (sand-pararendzina), heath and coniferous plantation (micro-podzols), from the 10 original dune environments for pH versus SOM correlation. Although these populations all fell into the acid division, they still showed evidence of separation. When the data were separated into environment-specific correlations, the significance of pH and SOM association continued to be evident for heath topsoils ($r = 0.68$; $p < 0.05$; $n = 9$). However, the association became insignificant for both fixed dune community and coniferous plantation topsoils.

Figure 7.4 shows a selection of significantly correlated ($p < 0.05$) geochemical parameters. Figures 7.4a and 7.4b show very different relationships with Si versus P and Si versus K, respectively. High Si values had a strong negative correlation with P ($r = 0.87$; $p < 0.001$; $n = 112$), indicating that as Si values increased, P values decreased. Whereas, the opposite trend was observed in the strong positive correlation between SiO_2 versus K_2O ($r = 0.88$; $p < 0.001$; $n = 112$). Figure 7.4c shows P was positively correlated with S ($R = 0.75$; $p < 0.001$; $n = 112$), while Figure 7.4d shows a positive correlation between Ca versus Fe ($r = 0.54$; $p < 0.001$; $n = 112$), indicating that increases in the alkaline earth metal Ca were associated with increased transition metal Fe. Figure 7.4e shows the mobile dune community, heath and deciduous woodland populations for Si versus P. The significance of the association continued to be evident for both the mobile dune community ($r = 0.96$; $p < 0.001$; $n = 12$) and

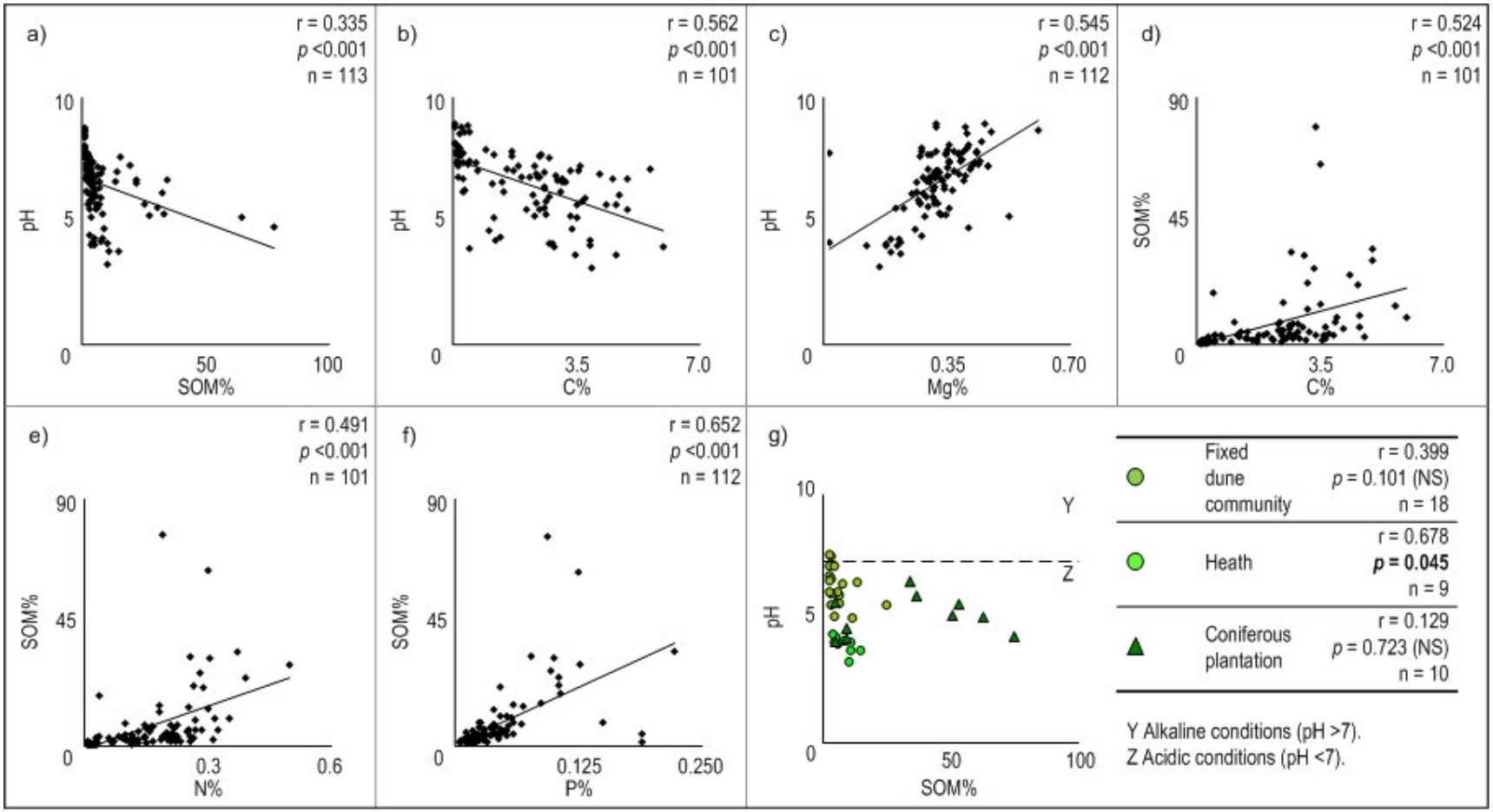

Figure 7.3 Bivariate plots for pH, SOM and selected geochemical parameters: a) pH versus SOM; b) pH versus C; c) pH versus Mg; d) SOM versus C; e) SOM versus N; f) SOM versus P and g) selected dune environments (**bold** text is significant (p <0.05)) for pH versus SOM.

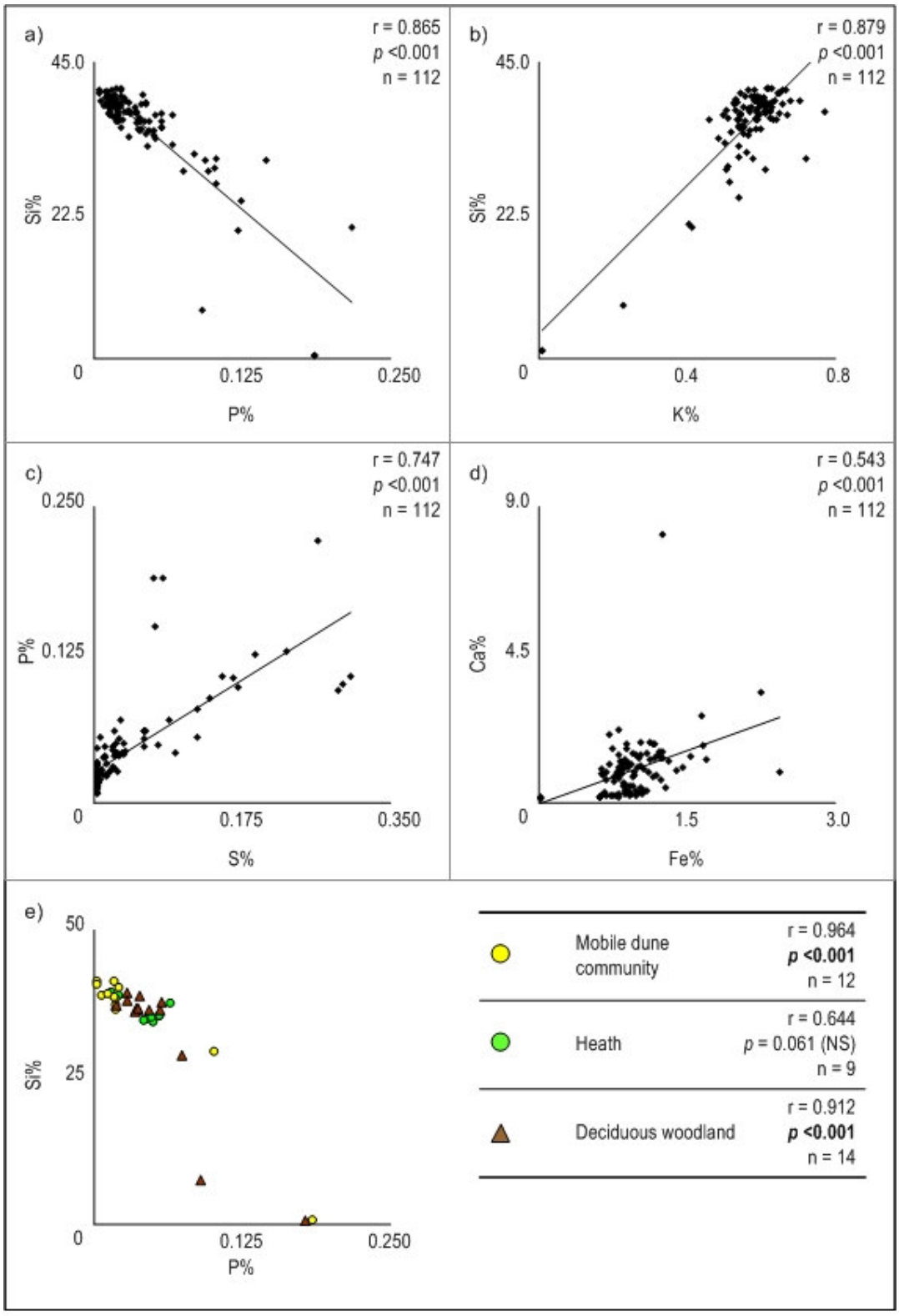

Figure 7.4 Bivariate plots for selected geochemical parameters: a) Si versus P; b) Si versus K; c) P versus S; d) Ca versus Fe and e) selected dune environments (**bold** text is significant (p <0.05)) for Si versus P.

deciduous woodland (r = 0.91; p <0.001; n = 14) topsoils. However, the association was insignificant in heath topsoils.

7.2.3 Statistical correlation between mineral magnetic topsoil parameters

Table 7.3 shows, with the exception of χ_{FD}, S-ratio and χ_{ARM}/SIRM, most mineral magnetic topsoil parameters displayed strong correlations (p <0.05), suggesting they were highly dependent upon each other. Strongest correlation coefficients were evident between magnetic concentration dependent parameters χ_{ARM} versus SIRM (r = 0.94; p <0.001; n = 113) and χ_{ARM} versus $Soft_{IRM40mT}$ (r = 0.97; p <0.001; n = 113). However, the weakest correlation coefficients were associated with $Soft_{\%}$ parameters (r = 0.01; p = 0.727 (NS); n = 113), suggesting although magnetic signal was dominated by soft 'magnetite-type' minerals, the actual percentage of these minerals in a sample was not relevant.

Figure 7.5a shows a strong positive correlation between χ_{LF} versus χ_{ARM} (r = 0.93; p <0.001; n = 113), while Figure 7.5b shows a strong positive correlation between χ_{LF} versus SIRM (r = 0.87; p <0.001; n = 113). These patterns indicate mineral magnetic signals were significantly influenced by ferrimagnetic grains. Figure 7.5c shows a strong positive correlation between χ_{ARM} versus SIRM (r = 0.94; p <0.001; n = 113), further confirming ferrimagnetic grains, but also highlighting the possible influence of ultrafine magnetic domain sizes. The presence of ferrimagnetic grains was also represented by Figure 7.5d, showing a strong negative correlation between ARM/χ versus SIRM/ARM (r = 0.65; p <0.001; n = 113). Figure 7.5e shows a positive correlation between ARM/χ versus SIRM/χ (r = 0.21; p <0.05; n = 113). Samples with low ARM/χ and low SIRM/χ values contain coarse-grained ferrimagnetic grains and samples with high ARM/χ and high SIRM/χ values contain fine-domain ferrimagnetic grains (Booth, 2002). However, the distribution of points around the best-fit line (Figure 7.5e), suggests samples also contained mixed magnetic mineralogies. Figure 7.5f also shows a positive correlation between SIRM/ARM versus SIRM/χ (r = 0.24; p <0.05; n = 113), emphasising that the samples contained mixed mineralogies of various magnetic domain sizes.

7.2.4 Statistical correlation between textural topsoil parameters versus pH, SOM and geochemical topsoil parameters

Table 7.4 shows, with exception of Na, Cl, K and Ca, all geochemical topsoil parameters displayed strong correlations (p <0.05) with at least five textural parameters, with most geochemical parameters exhibiting a stronger association with silt and median particle size. The strongest correlation coefficient was associated with S versus median particle size (r = 0.82; p <0.001; n = 112); whereas, the weakest correlation coefficient was associated with Si versus sorting (r = <0.01; p = 0.991 (NS); n = 112). Figure 7.6a shows a strong negative correlation between pH versus silt (r = 0.61; p <0.001; n = 112), indicating increased acidity was associated with increases in silt-sized particles. The opposite pattern was observed in the positive correlation between SOM versus silt (r = 0.43; p <0.001; n = 112) (Figure 7.6b), where

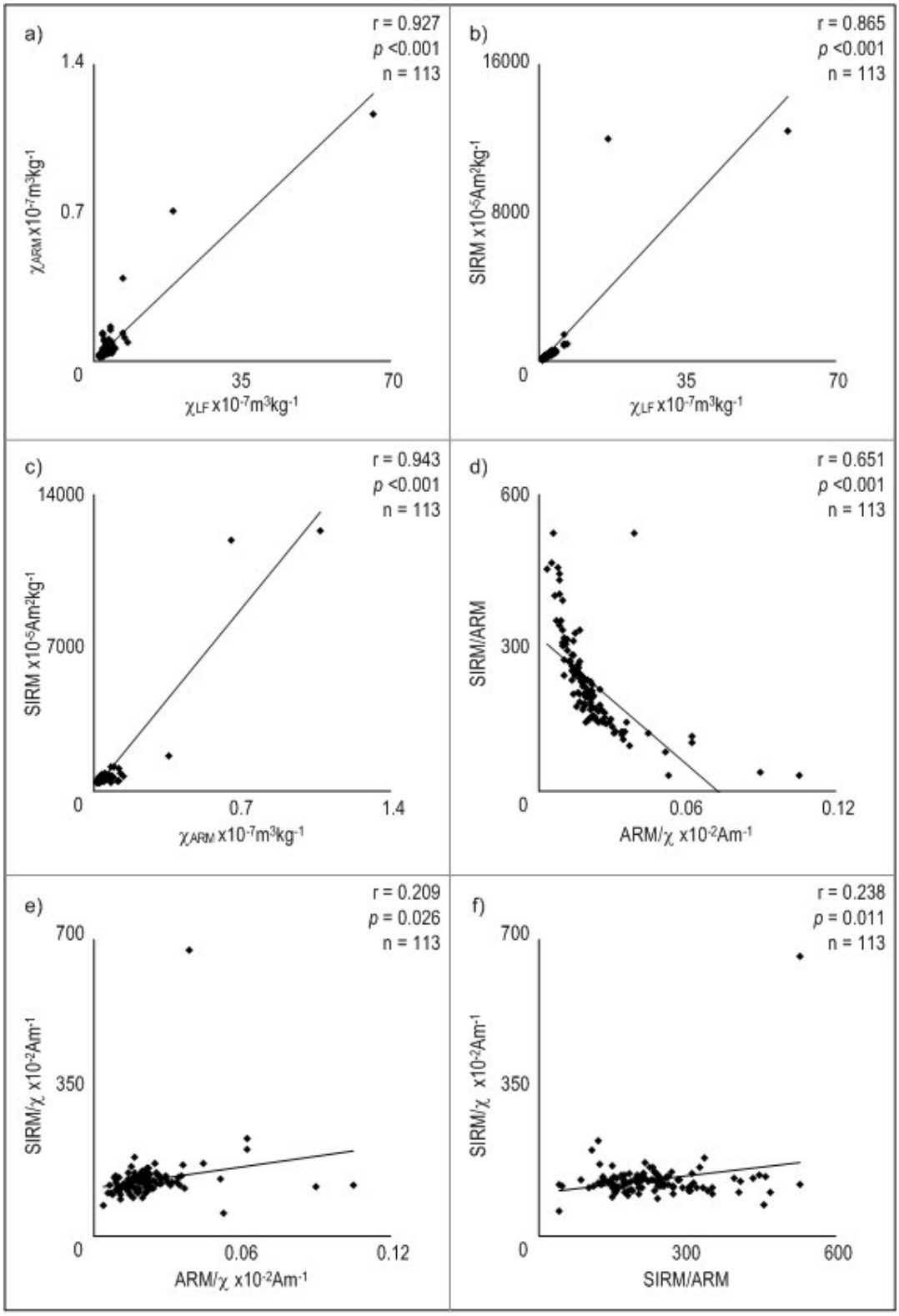

Figure 7.5 Bivariate plots for selected mineral magnetic parameters: a) χ_{LF} versus χ_{ARM}; b) χ_{LF} versus SIRM; c) χ_{ARM} versus SIRM; d) ARM/χ versus SIRM/ARM; e) ARM/χ versus SIRM/χ and f) SIRM/ARM versus SIRM/χ.

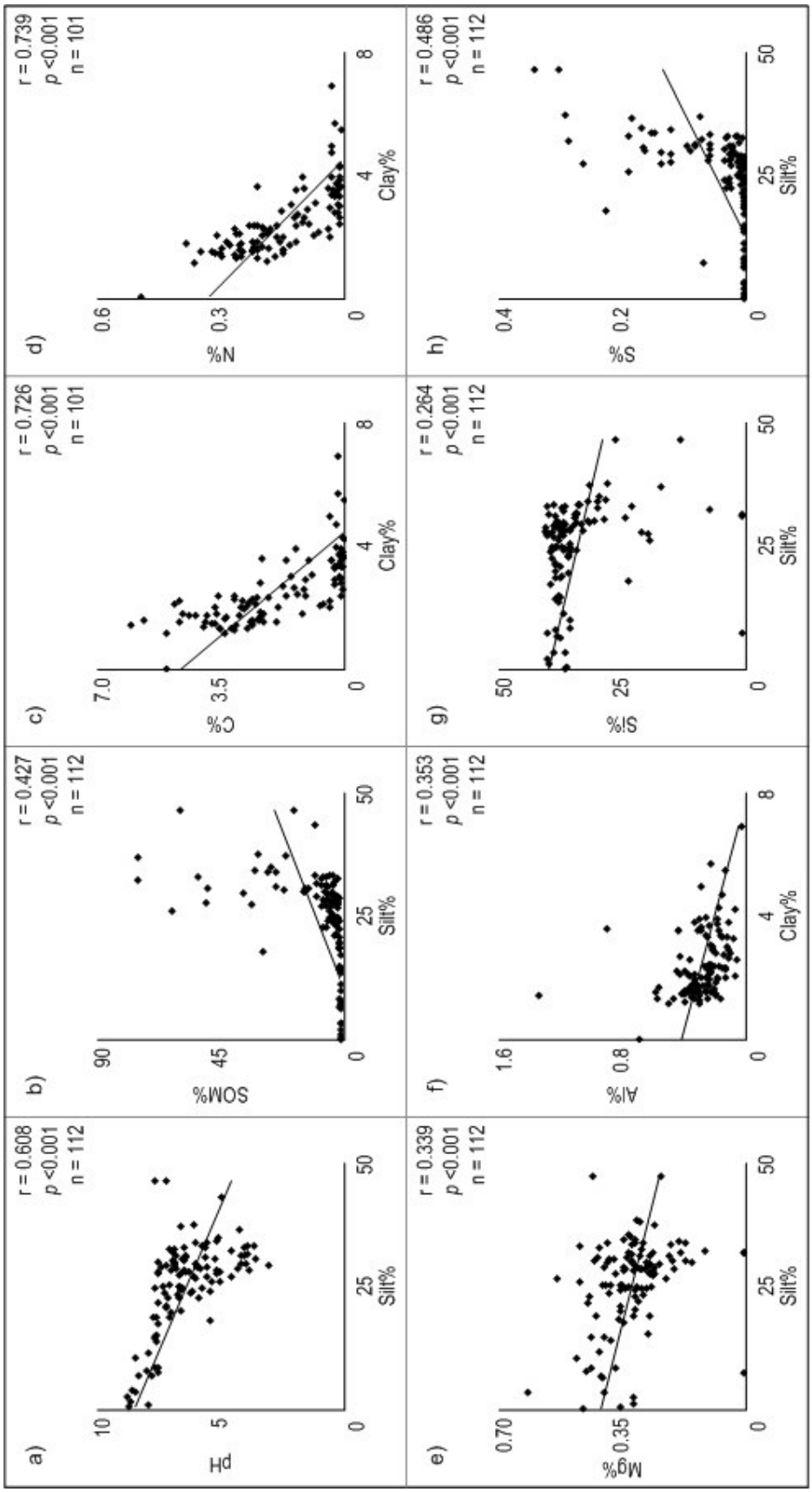

Figure 7.6 Bivariate plots for pH, SOM and selected geochemical parameters versus selected particle size parameters: a) pH versus silt; b) SOM versus silt; c) C versus clay; d) N versus clay; e) Mg versus silt; f) Al versus clay; g) Si versus silt and h) S versus silt.

increases in SOM were associated with increases in the silt-sized fraction. Negative correlations between both C versus clay (r = 0.73; p <0.001; n = 101) (Figure 7.6c) and N versus C (r = 0.74; p <0.001; n = 101) (Figure 7.6d), display a point distribution indicative of highly dependent parameters. Negative correlations between Mg versus silt (r = 0.34; p <0.001; n = 112) (Figure 7.6e), Al versus clay (r = 0.35; p <0.001; n = 112) (Figure 7.6f) and Si versus silt (r = 0.26; p <0.001; n = 112) (Figure 7.6g) show decreases in these oxides were associated with increased particle size. Whereas, a positive correlation between S versus silt (r = 0.49; p <0.001; n = 112) (Figure 7.6h), indicates an increase in non-metal S associated with increases in the silt-sized fraction.

Figure 7.7a shows a strong negative correlation between SOM versus median particle size (r = 0.72; p <0.001; n = 112), indicating that despite SOM correlating negatively with silt, overall trends show general decreased particle size associated with increased SOM. Negative correlations between both C and N with clay were also observed in C versus median particle size (r = 0.61; p <0.001; n = 101) (Figure 7.7b) and N versus median particle size (r = 0.64; p <0.001; n = 101) (Figure 7.7c), suggesting increased C and N were associated with decreased particle size and the silt-sized fraction had no influence. A similar pattern of Al versus clay was observed in a negative correlation between Al versus median particle size (r = 0.45; p <0.001; n = 112) (Figure 7.7d); whereas the pattern of Si versus silt was reversed in a positive correlation between Si versus median particle size (r = 0.49; p <0.001; n = 112) (Figure 7.7e), suggesting although Si decreased as silt percentages increased, overall trends associate increased Si with particle size increases. Negative correlations between P versus median particle size (r = 0.57; p <0.001; n = 112) (Figure 7.7f) and S versus median particle size (r = 0.82; p <0.001; n = 112) (Figure 7.7g), indicate increased particle size associations with decreases in these oxides. Therefore, comparisons with S versus silt, determines that silt has no influence. Figure 7.7h shows a negative correlation between Fe versus median particle size (r = 0.33; p <0.001; n = 112). The point distribution indicates, although there was limited variability in Fe percentages, higher values were associated with finer grain size fractions. General correlation patterns suggest pH, SOM and geochemical parameters were highly dependent upon textural parameters, but patterns were reversed in the silt-sized fraction.

Figure 7.8a shows three topsoil population samples, bare sand community (terrestrial raw sand), heath (micro-podzol) and slack community (groundwater gley), from the 10 original dune environments for pH versus silt correlation. Populations showed evidence of separation, with bare sand in the alkaline division and heath in the acid division. The slack population had samples on either side of the boundary. However, when the data were separated into environment-specific correlations, pH and silt associations were no longer significant. Figure 7.8b also shows bare sand, heath and slack community populations for Mg versus silt, where the association became insignificant after population separation. Figure 7.8c shows the bare sand and fixed dune communities, along with deciduous woodland, for Al versus clay. The

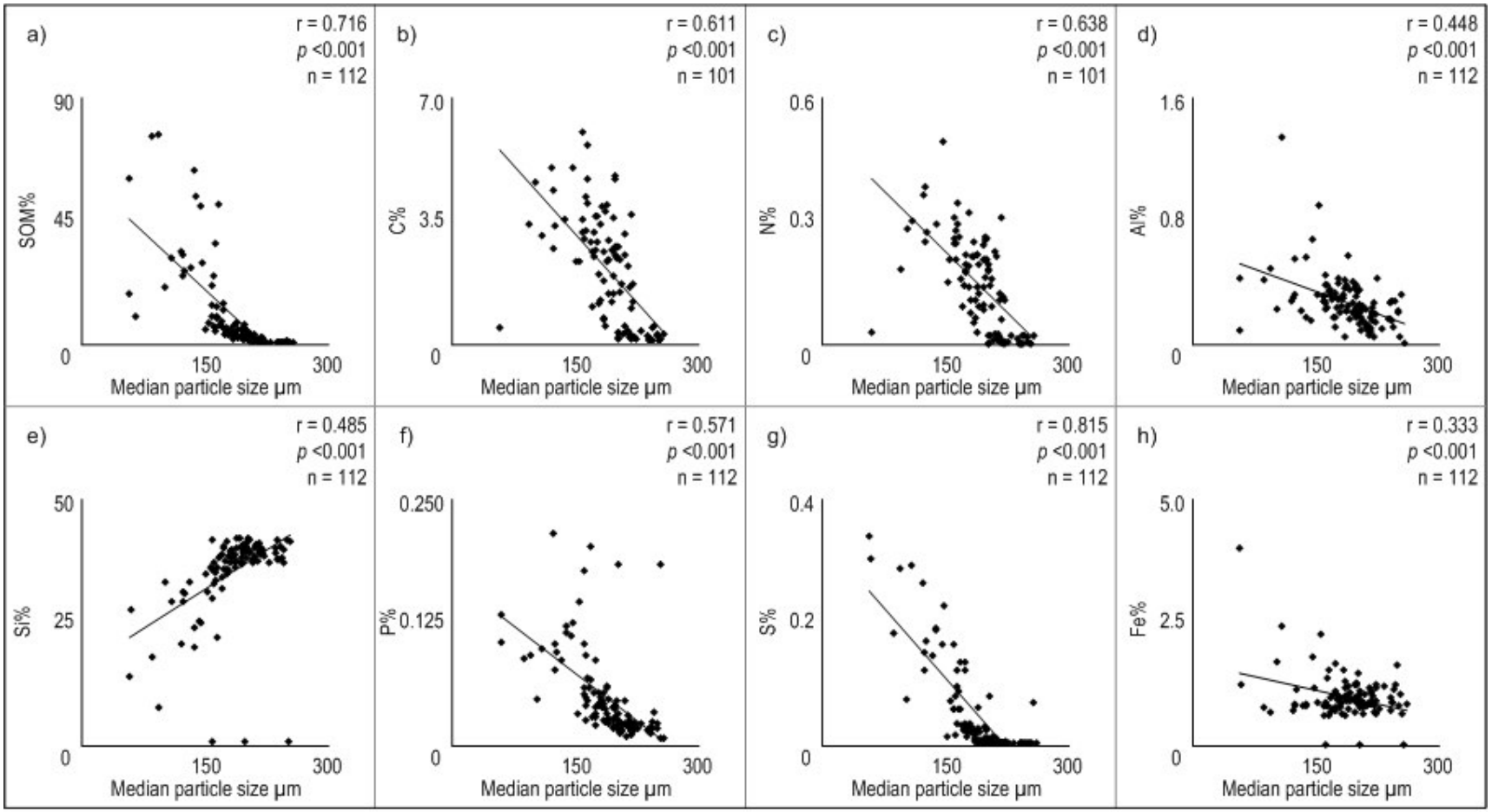

Figure 7.7 Bivariate plots for SOM and selected geochemical parameters versus median particle size distribution: a) SOM versus median particle size; b) C versus median particle size; c) N versus median particle size; d) Al versus median particle size; e) Si versus median particle size; f) P versus median particle size; g) S versus median particle size and h) Fe versus median particle size.

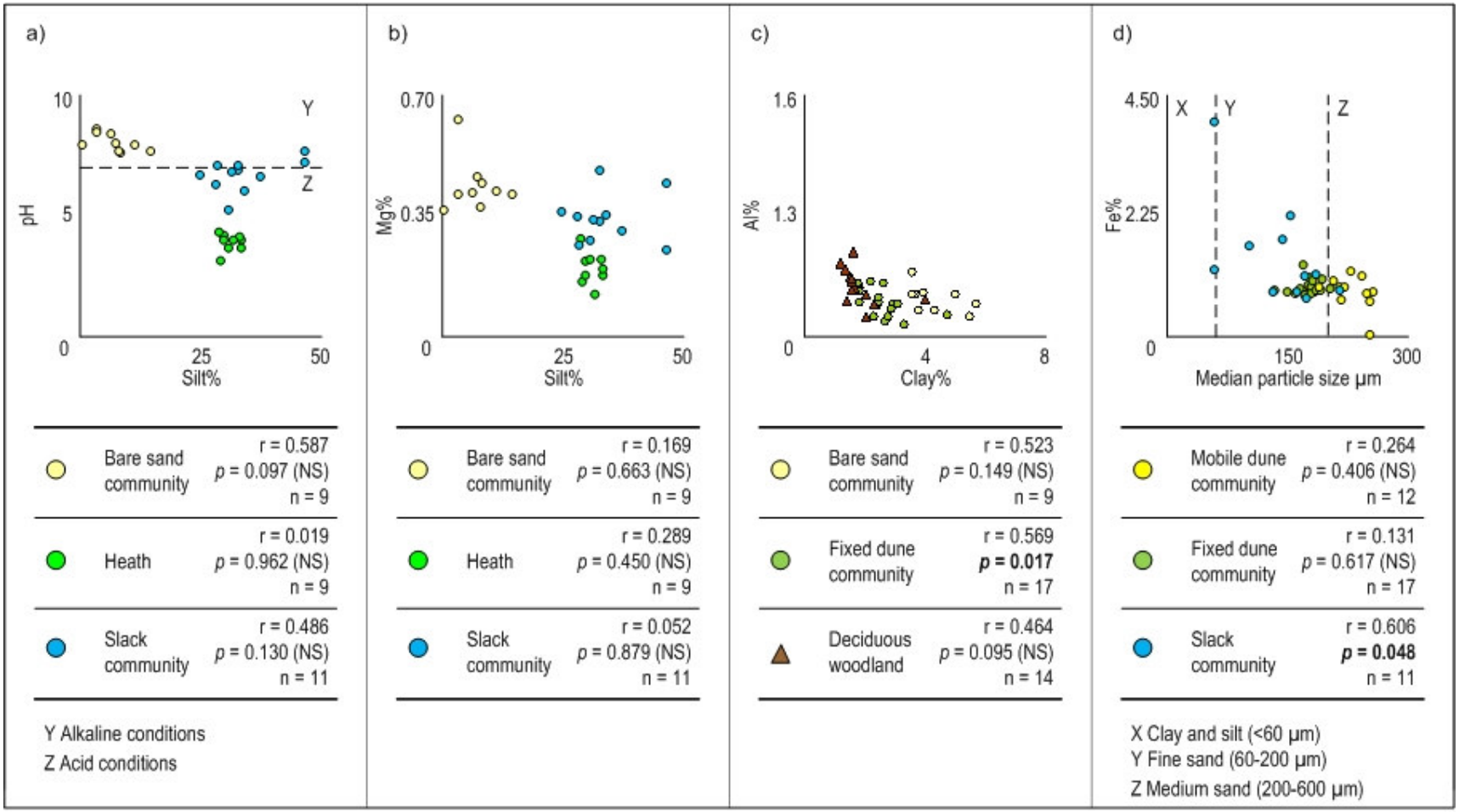

Figure 7.8 Bivariate plots for selected pH and geochemical parameters versus textural parameters for selected dune environments (**bold** text is significant (p <0.05)): a) pH versus silt; b) Mg versus silt; c) Al versus clay and d) Fe versus median particle size.

significance of the association continued to be evident for the fixed dune community topsoils (r = 0.57; p <0.05; n = 17); whereas, the association became insignificant for both bare sand community and deciduous woodland topsoils. Figure 7.8d shows the mobile dune, fixed dune and slack communities for Fe versus median particle size. Populations show evidence of separation, with most mobile dune samples in the medium sand-sized fraction and most fixed dune samples in the fine sand-sized fraction. The slack population had samples throughout the particle size divisions, the significance of which continued to be evident (r = 0.61; p <0.05; n = 11). However, the Fe and median particle size association became insignificant for both mobile and fixed dune community topsoils.

7.2.5 Statistical correlation between textural topsoil parameters versus mineral magnetic topsoil parameters

Table 7.5 shows approximately half of the mineral magnetic and textural topsoil parameters were significantly (p <0.05) inter-correlated. With the exception of $Hard_{IRM}$ and S-ratio, mineral magnetic parameters correlated moderately to at least one of the textural parameters. Strongest correlations were associated with $Hard_{\%500}$ versus silt (r = 0.44; p <0.001; n = 112) and ARM/χ versus median particle size (r = 4.75; p <0.001; n = 112). Clay-sized particles were not significantly correlated to percentages of soft minerals or any of the magnetic domain size parameters.

Figure 7.9 shows the bivariate relationships between magnetic mineralogy dependent parameters $Soft_{\%}$ and $Hard_{\%}$ versus textural parameters sand, silt and clay, all displaying significant correlations (p <0.05). However, despite the strength of these relationships, each bivariate plot, especially plots displaying silt values, show a widespread positioning of the samples around the best-fit line. Figure 7.10 shows bivariate relationships between the magnetic domain size dependent parameters versus the textural parameters, sand, silt and clay. The data points are extremely scattered in each of the plots in relation to the best-fit line.

The only magnetic concentration parameter to have had significant correlations to each of the sand, silt and clay textural parameters was χ_{ARM} (r <0.396; p <0.05; n = 112). Bivariate plots (Figure 7.11) show data points scattered along the textural-axis in relation to the best-fit line, explaining why the relationships had weak correlation coefficients. Figure 7.11d shows three population samples, bare sand, pasture and slack community, from the 10 original dune environments, for silt versus $Hard_{\%300}$ correlation. Populations showed evidence of separation using both textural and mineral magnetic characteristics. However, when the data were separated into environment-specific correlations, the association was no longer significant.

7.2.6 Statistical correlation between pH, SOM and geochemical topsoil parameters versus mineral magnetic parameters

Table 7.6 shows SOM, N, Al, S and Fe correlate (p <0.05) with at least half of the mineral magnetic topsoil parameters; whereas, only $Hard_{\%}$ parameters display significant correlations

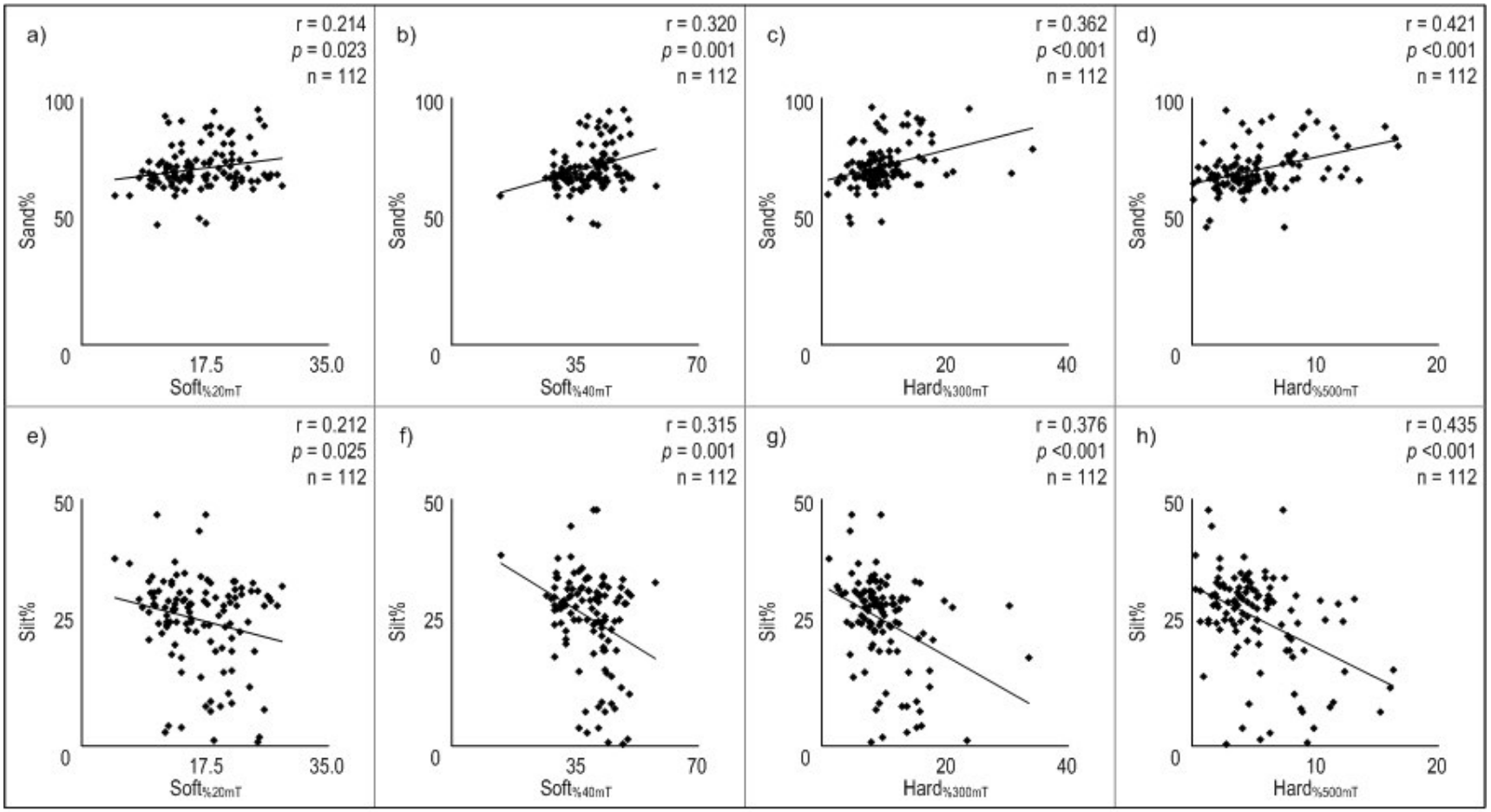

Figure 7.9 Bivariate plots for magnetic mineral percentage parameters: a) $Soft_{\%20}$ versus Sand; b) $Soft_{\%40}$ versus Sand; c) $Hard_{\%300}$ versus Sand; d) $Hard_{\%500}$ versus Sand; e) $Soft_{\%20}$ versus Silt; f) $Soft_{\%40}$ versus Silt; g) $Hard_{\%300}$ versus Silt and h) $Hard_{\%500}$ versus Silt.

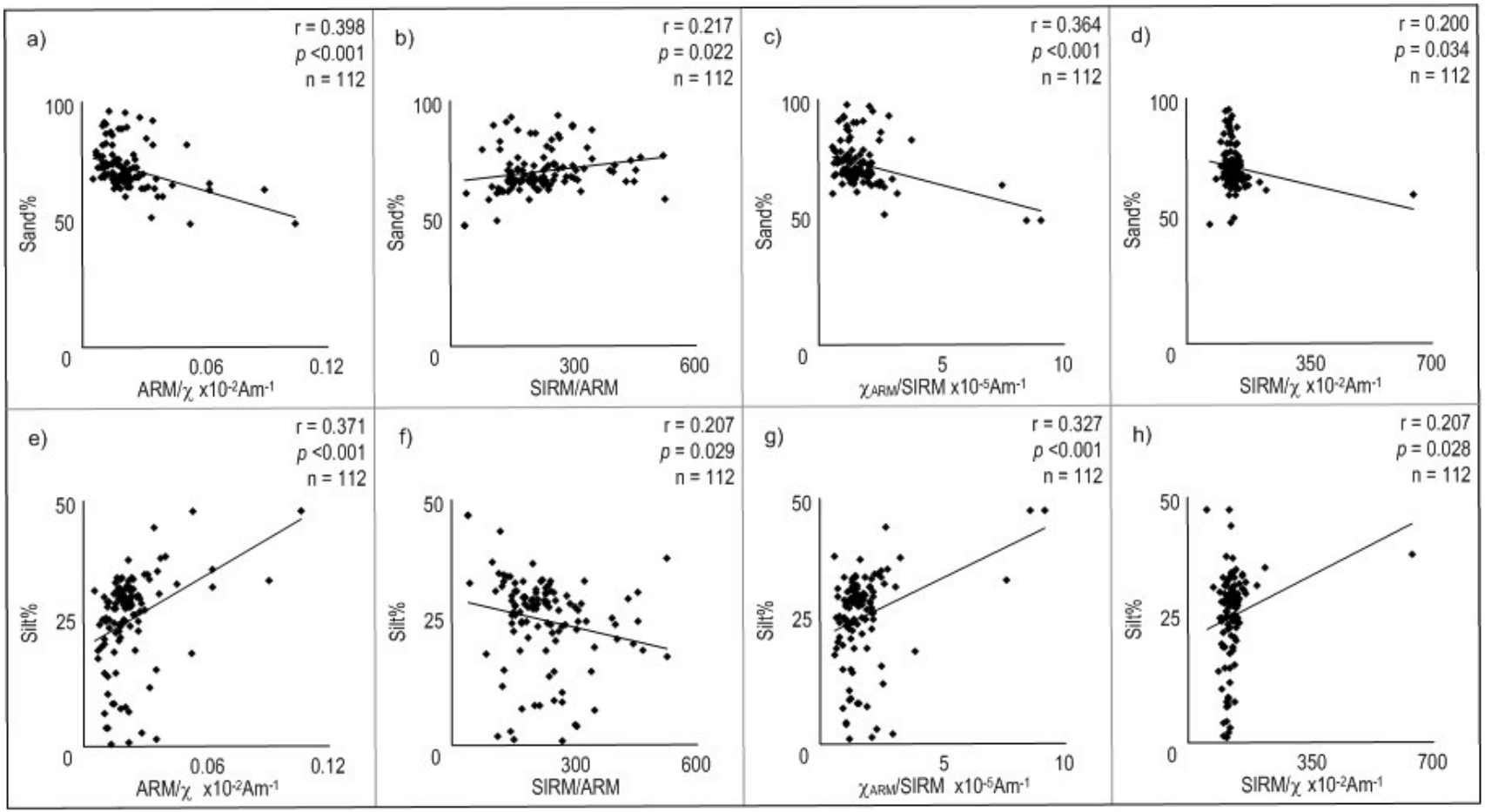

Figure 7.10 Bivariate plots for magnetic grain size parameters: a) ARM/χ versus Sand; b) SIRM/ARM versus Sand; c) χ_{ARM}/SIRM versus Sand; d) SIRM/χ versus Sand; e) ARM/χ versus Silt; f) SIRM/ARM versus Silt; g) χ_{ARM}/SIRM versus Silt and h) SIRM/χ versus Silt.

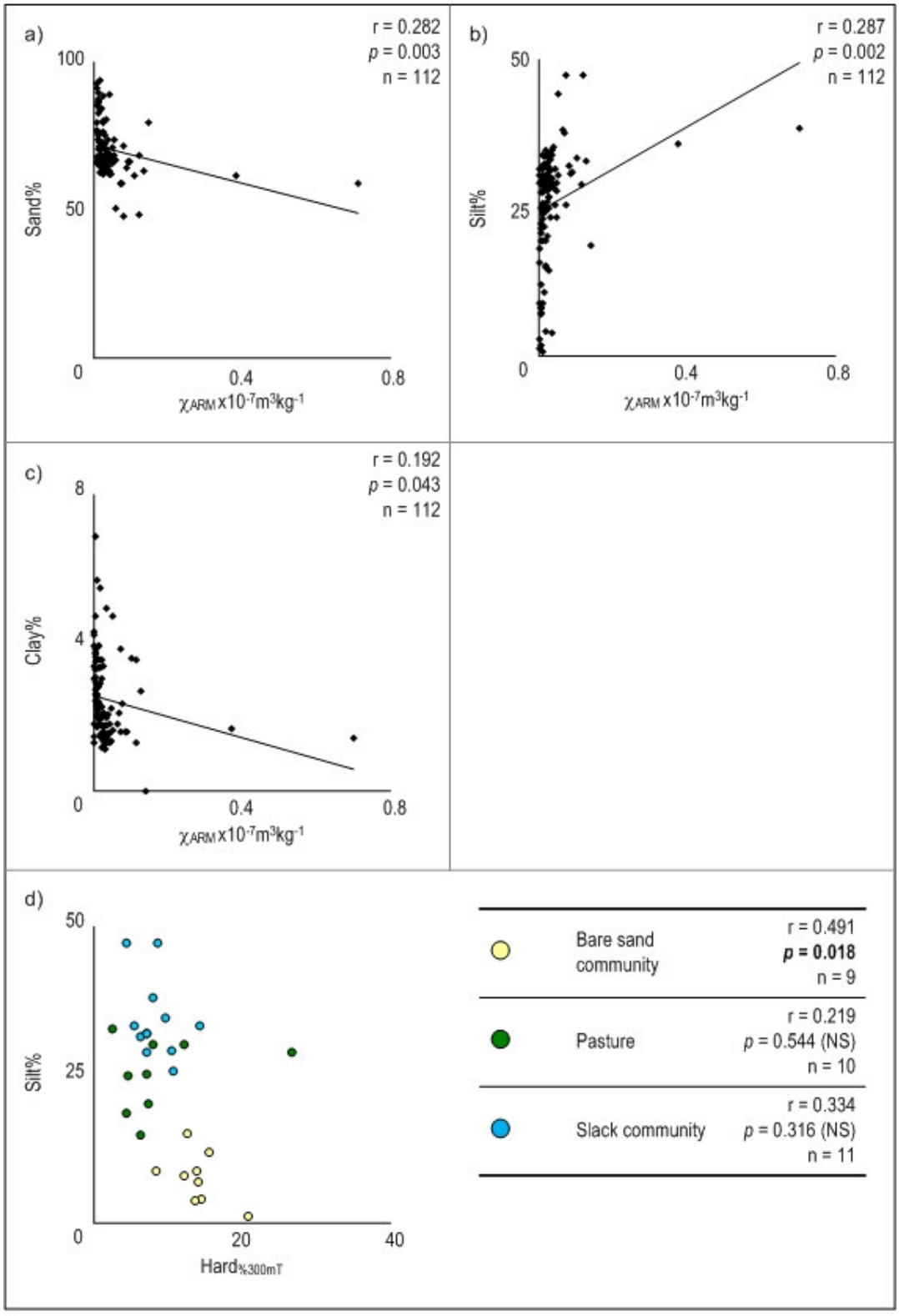

Figure 7.11 Bivariate plots for χ_{ARM} versus particle sizes: a) χ_{ARM} versus sand; b) χ_{ARM} versus silt; c) χ_{ARM} versus clay and bivariate plot for selected dune environments and d) $Hard_{\%300}$ versus the textural parameter silt for selected dune environments (**bold** text is significant (p <0.05)).

(p <0.05) with half of the pH, SOM and geochemical topsoil parameters. Na, Cl and K were not significantly correlated with any of the mineral magnetic parameters. The strongest correlation coefficients were associated with Al versus both χ_{ARM} (r = 0.72; p <0.001; n = 112) and $Soft_{IRM40}$ (r = 0.66; p <0.001; n = 112), suggesting soft 'magnetite-type' minerals were dominated by aluminium. The general weakness of correlations suggests mineral magnetic properties were not dependent upon pH, SOM or geochemical properties.

Figures 7.12a,b show weak positive correlations between SOM versus magnetic concentration dependent parameters χ_{LF} (r = 0.19; p <0.05; n = 113) and χ_{ARM} (r = 0.25; p <0.01; n = 113), respectively, indicating increased influence of ferrimagnetic grains was associated with increased SOM. Positive correlations between SOM versus both ARM/χ (r = 0.21; p <0.05; n = 113) (Figure 7.12c) and χ_{ARM}/SIRM (r = 0.26; p <0.01; n = 113) (Figure 7.12d), confirms influences of ferrimagnetic grains and associates high SOM with increasing magnetic domain size. Figures 7.12e,f show slightly stronger positive correlations between χ_{LF} versus N (r = 0.29; p <0.01; n = 101) and χ_{ARM} versus N (r = 0.31; p <0.01; n = 101), respectively, indicating increased ferrimagnetic grains was associated with increased N. Positive correlations between N versus both SIRM/ARM (r = 0.26; p <0.05; n = 101) (Figure 7.12g) and SIRM/χ (r = 0.22; p <0.05; n = 101) (Figure 7.12h), highlights associations between increased N and increased magnetic domain size.

Figures 7.13a,b show strong positive correlations between χ_{ARM} versus Al (R = 0.72; p <0.001; n = 112) and SIRM versus Al (r = 0.64; p <0.001; n = 112), respectively, suggesting increased magnetic concentrations and Al indicate aluminium contributions towards ferrimagnetism. Positive correlations between $Soft_{IRM20}$ versus Al (r = 0.64; p <0.001; n = 112) (Figure 7.13c) and $Soft_{IRM40}$ versus Al (r = 0.66; p <0.001; n = 112) (Figure 7.13d), suggest magnetic minerals contain soft-metal aluminium. S was positively correlated with both χ_{ARM} (r = 0.47; p <0.001; n = 112) (Figure 7.13e) and χ_{ARM}/SIRM (r = 0.47; p <0.001; n = 112) (Figure 7.13f), indicating both increased magnetic concentrations and domain sizes were associated with increased S. This pattern was similar to Fe versus both χ_{LF} (r = 0.46; p <0.001; n = 112) (Figure 7.13g) and χ_{ARM}/SIRM (r = 0.42; p <0.001; n = 112) (Figure 7.13h), indicating increased magnetic concentrations and domain sizes were also associated with increased Fe. However, distributions of points around the best-fit line suggest variations were minor.

7.2.7 Lateral variations in topsoil pedo-properties

The physio-chemical topsoil data sets have aided the identification of lateral trends within the Sefton dune landscape, through regression of soil properties with distance from mean high water (MHW). This relationship can be used as a surrogate for relative age, assuming that pedogenic processes become more advanced further from the sea (James and Wharfe, 1989). The parameters analysed for lateral variations were chosen for their significant roles in pedogenesis; termed 'key' parameters.

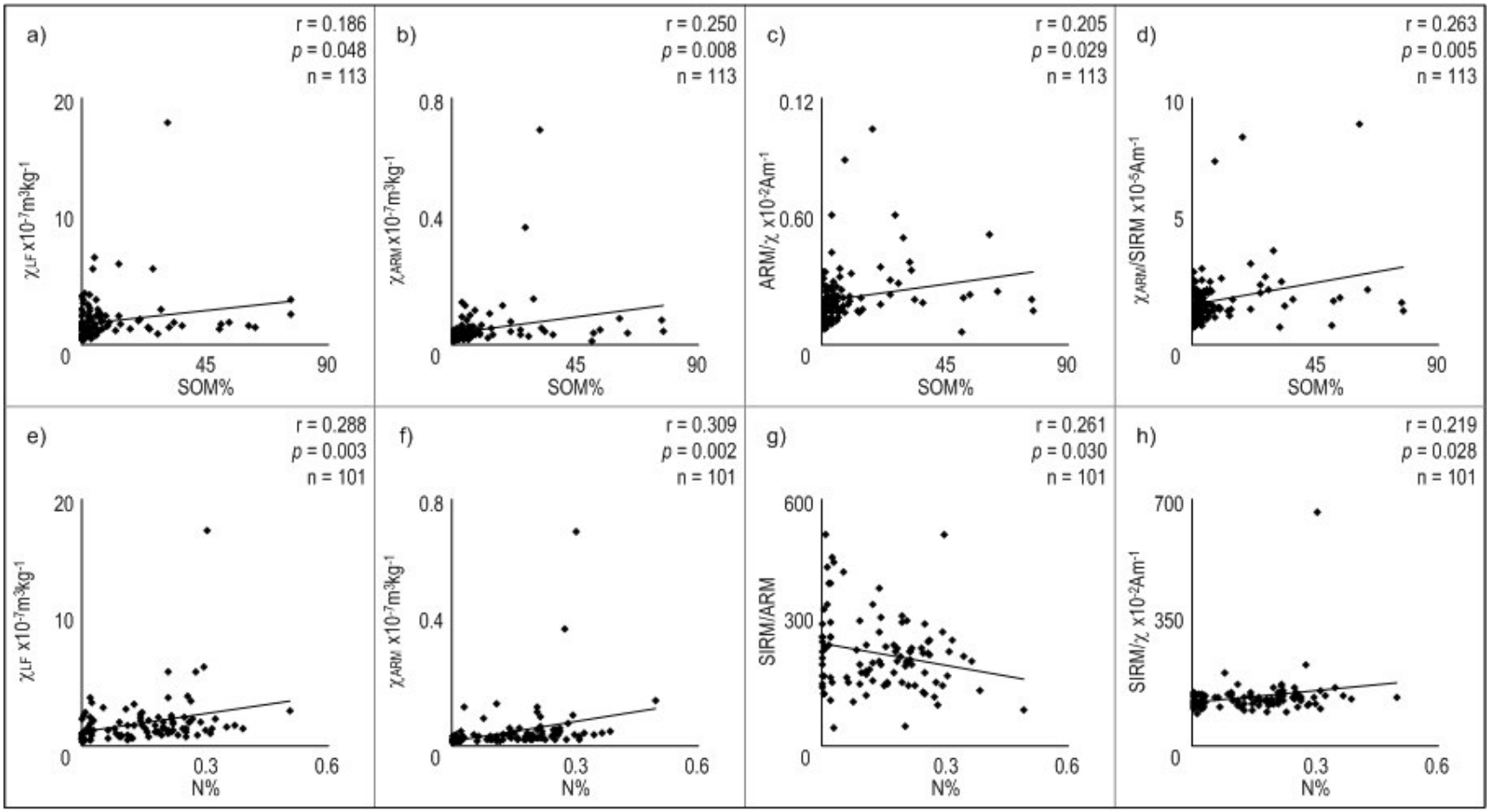

Figure 7.12 Bivariate plots for SOM and N versus selected mineral magnetic parameters: a) SOM versus χ_{LF}; b) SOM versus χ_{ARM}; c) SOM versus ARM/χ; d) SOM versus χ_{ARM}/SIRM; e) N versus χ_{LF}; f) N versus χ_{ARM}; g) N versus SIRM/ARM and h) N versus SIRM/χ.

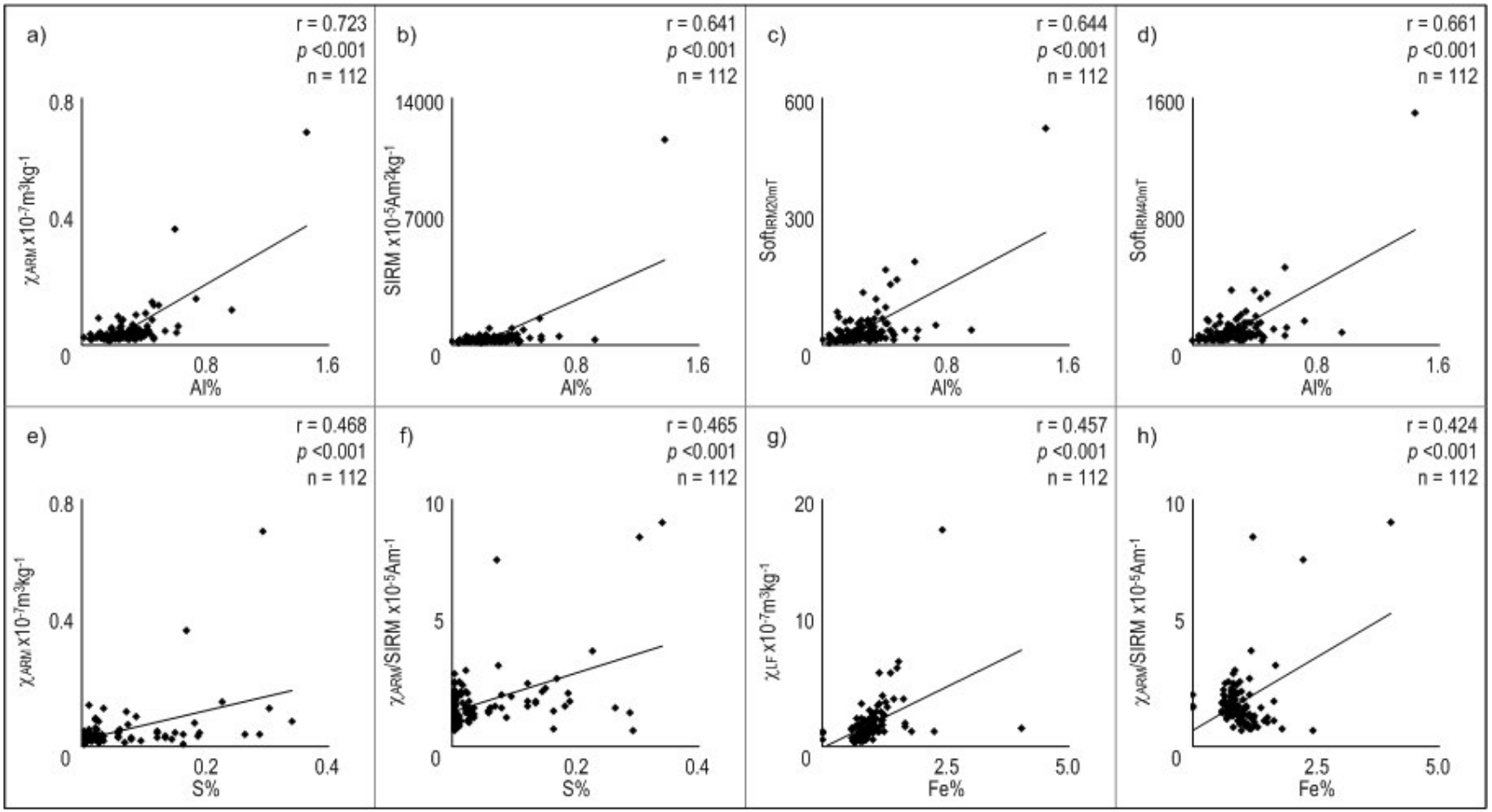

Figure 7.13 Bivariate plots for selected geochemical parameters versus selected mineral magnetic parameters: a) Al versus χ_{ARM}; b) Al versus SIRM; c) Al versus $Soft_{IRM20}$; d) Al versus $Soft_{IRM40}$; e) S versus χ_{ARM}; f) S versus χ_{ARM}/SIRM; g) Fe versus χ_{LF} and h) Fe versus χ_{ARM}/SIRM.

Figure 7.14a shows a strong negative correlation between pH versus distance from MHW (r = 0.81; p <0.001; n = 113), indicating increased acidity was associated with distance from the shoreline. The opposite pattern was observed in the positive correlation between SOM versus distance from MHW (r = 0.25; p <0.01; n = 113) (Figure 7.14b) and silt versus distance from MHW (r = 0.46; p <0.001; n = 112) (Figure 7.14c). Point distributions indicate the strong positive relationship between silt% and distance does not take effect until ~500 m from MHW. Figures 7.14d,f show positive correlations between both C (r = 0.42; p <0.001; n = 112) and Al (r = 0.19; p <0.001; n = 112) with distance from MHW. Negative correlations between distance from MHW versus Mg (r = 0.50; p <0.001; n = 112) (Figure 7.14e), Ca (r = 0.39; p <0.001; n = 112) (Figure 7.14g) and Fe (r = 0.20; p <0.05; n = 112) (Figure 7.14h), display point distributions indicative of highly dependent parameters. The positive correlation between $\chi_{FD\%}$ versus distance from MHW (r = 0.20; p <0.05; n = 113) (Figure 7.14i), alongside the negative correlation between $Soft_{\%40mT}$ versus distance (r = 0.26; p <0.01; n = 113) (Figure 7.14j), indicates decreased presence of SP magnetic domain sizes of soft 'magnetite-type' magnetic mineralogy with distance from the coast.

7.3 Variations in topsoil pedo-properties in erosion/accretion regimes

Two-dimensional analysis of relationships between pedogenic parameters and distance from MHW is not realistic, as it ignores longshore movement and the fact that sediment loss on one stretch of the coast is usually countered by accumulation in another (Carter, 1991). This is evident on the Sefton coast, considering the onset of erosion at Formby Point (Turner, 1984) (refer to Chapter 6, Section 6.2.1). Compositional data can be useful in defining coastal sediment cells (Saye and Pye, 2006), as fluctuations in shoreline position and erosion/accretion regimes will affect the rates and types of pedogenic processes in operation on the dune system. For example, 'coastal squeeze', where natural landward migration is prevented by fixed landward boundaries (Doody, 2001), may prevent soil evolution in an eroding environment. Whereas, in accreting regimes sea level fluctuations may affect groundwater levels and, therefore, base level for deflation (van der Meulen, 1990; Carter, 1991; Noest, 1991; Pye, 2001) and soil development. It is for these reasons that both erosion and accretion zones on the Sefton coast will be analysed individually to identify those pedo-properties affected by such environmental conditions.

In order to determine pedogenic processes of erosion/accretion zones, the topsoil sample population must be divided into such coastal units with established boundaries. These units, termed 'littoral cells', can be marked by several features, usually associated with sediment transport processes, the most obvious being estuaries as rivers supply sediment to the coast (Woodroffe, 2002). However, as the limits of the study area are already determined by the River Ribble in the north and the River Alt in the south, this division technique is not viable. Headlands can also mark divisions between cells (Woodroffe, 2002), which would mean placing the boundary directly through Formby Point. This would result in two units, each experiencing

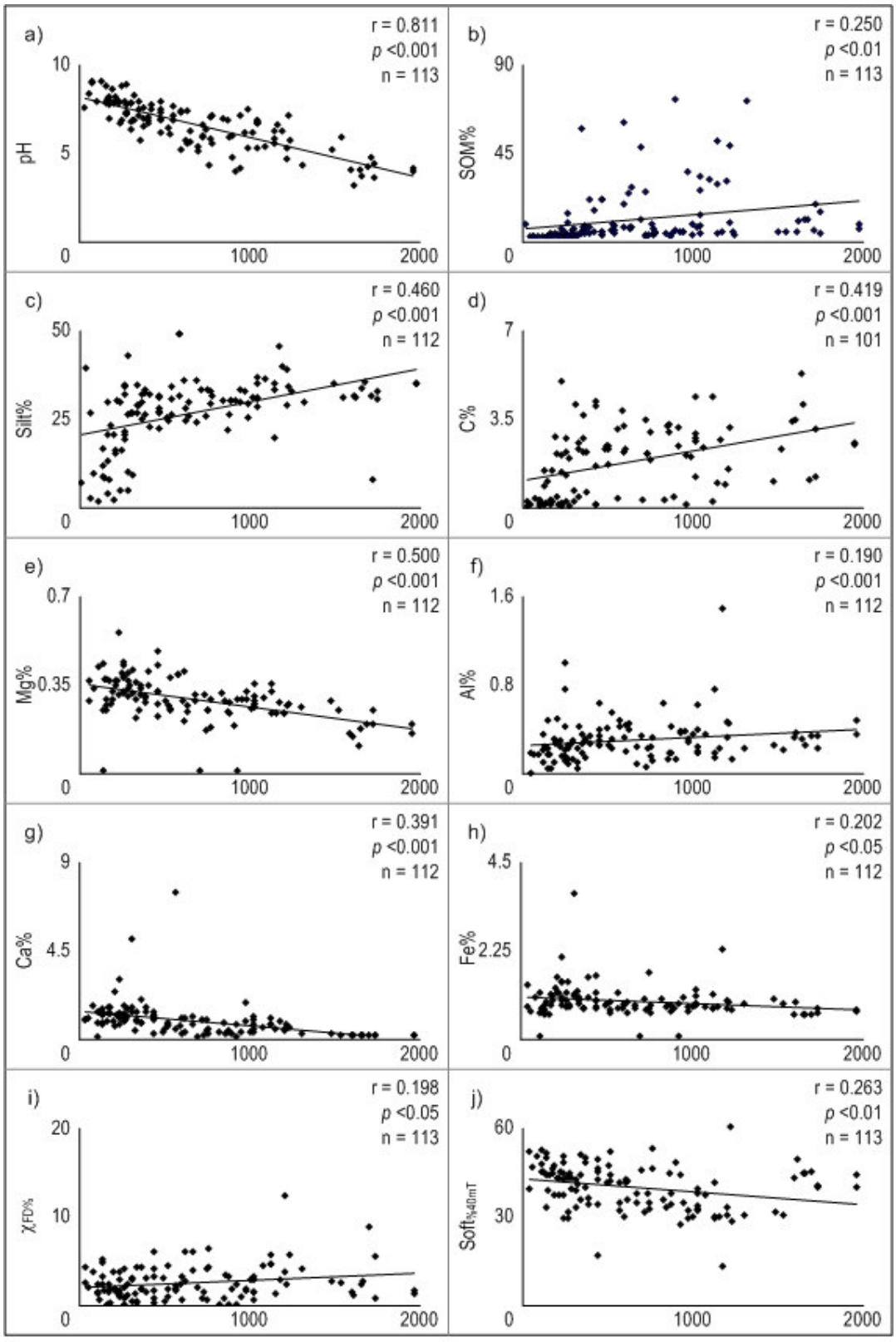

Figure 7.14 Key physio-chemical topsoil pedo-characteristic correlations with distance from mean high water (MHW) (m) (x-axis).

erosion, longshore drift and accretion processes operating to the north and south. This technique is also not viable, as the erosion and accretion zones need to be separated.

Cell boundaries can also occur where wave refraction patterns exist (Woodroffe, 2002), dividing the coast into areas of natural erosion and accretion. The pivot points of erosion/accretion transitions on the Sefton coast have already been identified and mapped (Turner, 1984), consequently, dividing the shoreline into three separate lengths. The location of these pivot points (refer to Chapter 6, Section 6.2.1) are used to divide the entire coast into units for analysis, with the boundaries passing through each point. Figure 7.15 displays the boundary positions, sitting on lines of northings. To place the boundaries perpendicular to the shore would not have accounted for direction of pedogenesis, which is influenced by direction of prevailing wind and aeolian derived sand. However, to place the boundaries parallel to the direction of longshore drift, would not have accounted for the wave refraction influences on erosion and accretion zones. Therefore, placing the boundaries along lines of northings was deemed the most suitable and unbiased technique. The northern zone of accretion (Unit 1) sits ~1 km north of Fisherman's Path (SD 280 099). A zone of erosion (Unit 2) occurs around Formby Point, with a southern accretion zone (Unit 3) south of Alexandra Road (SD 273 057) (refer to Chapter 6, Section 6.2.3).

7.3.1 Alongshore variations in topsoil pedo-properties

Summary data for the topsoil physico-chemical characteristics of each of the coastal units were described and both null (H_0) and alternative (H_1) hypotheses tested. Non-parametric Mann-Whitney U tests compared the differences of the medians of each coastal unit population for each key parameter.

Tested Hypotheses	
Null Hypothesis (H_0)	There was no significant difference between the medians of each of the sample populations compared to each other.
Alternative Hypothesis (H_1)	There was a significant difference between the medians of each of the sample populations compared to each other.

Tables 7.7-9 present summary data for Unit 1 (n = 63), Unit 2 (n = 40) and Unit 3 (n = 10), respectively. The pH of Unit 1 (3.89-8.84) represents a neutral-acidic accreting coastal section, which was significantly different (p <0.01) from Units 1 and 2 (Figure 7.16a). The pH values of Unit 2 (3.10-8.43) were relatively acidic, displaying highly significantly different values (p <0.001) from the relatively alkaline (6.53-8.00) conditions of Unit 3. SOM values of Unit 1 were generally low (mean 8.75%), although some topsoils contained >50%. Unit 1 showed no significant differences in SOM to the other units (Figure 7.16b); whereas, the relatively high SOM of Unit 2 (0.10-77.17%) was significantly different (p <0.05) from the low values of Unit 3 (0.11-21.29%). High acidity and SOM content in Unit 2 was more likely to be indicative of mature hind dune soils, than erosion influences. Levels of silt showed great variability in all units

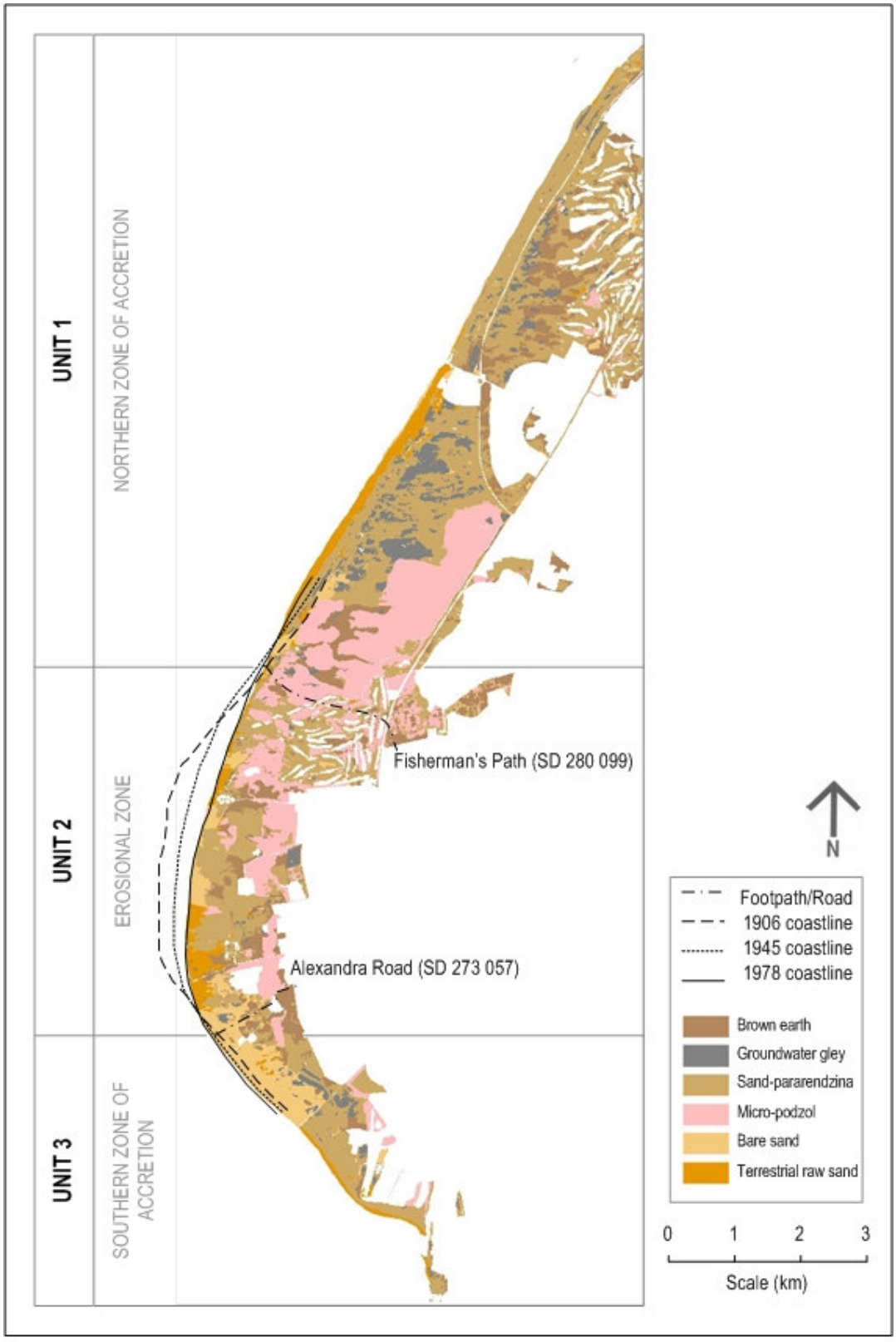

Figure 7.15 GMP map of the Sefton coast, showing erosion and accretion zones under active management. Erosion limits, based on O.S. map evidence, are redrawn from Turner (1984).

Table 7.7 Summary data* for topsoil key physico-chemical characteristics of Unit 1 (n = 63)

Parameters	Units	Mean	SD	CV	Min	Max
pH	mol/ltr	6.628	1.104	16.661	3.890	8.840
SOM	%	8.753	13.745	157.027	0.109	61.244
Silt	%	26.159	10.251	39.189	0.396	47.178
Carbon	%	2.039	1.594	78.192	0.018	5.767
Magnesium	%	0.314	0.101	32.360	0.001	0.625
Aluminium	%	0.245	0.212	86.413	0.000	1.365
Calcium	%	1.008	1.252	124.210	0.033	8.148
Iron	%	1.035	0.571	55.174	0.004	4.030
χ_{FD}	%	2.413	1.633	67.697	0.000	6.122
$Soft_{\%40mT}$	%	38.634	7.624	19.735	12.860	51.266

Table 7.8 Summary data* for topsoil key physico-chemical characteristics of Unit 2 (n = 40)

Parameters	Units	Mean	SD	CV	Min	Max
pH	mol/ltr	5.915	1.546	26.146	3.100	8.430
SOM	%	11.623	20.596	177.198	0.101	77.165
Silt	%	25.589	8.056	31.484	6.621	37.320
Carbon	%	2.096	1.688	80.512	0.056	6.136
Magnesium	%	0.328	0.103	31.578	0.111	0.540
Aluminium	%	0.299	0.111	37.203	0.097	0.578
Calcium	%	0.765	0.583	76.216	0.073	1.961
Iron	%	0.903	0.211	23.327	0.601	1.381
χ_{FD}	%	2.291	2.292	100.043	0.000	12.000
$Soft_{\%40mT}$	%	39.167	6.704	17.116	28.683	58.881

Table 7.9 Summary data* for topsoil key physico-chemical characteristics of Unit 3 (n = 10)

Parameters	Units	Mean	SD	CV	Min	Max
pH	mol/ltr	7.279	0.560	7.688	6.530	8.000
SOM	%	4.948	7.198	145.464	0.105	21.289
Silt	%	20.898	9.670	46.273	0.726	30.817
Carbon	%	1.826	1.559	85.369	0.070	3.688
Magnesium	%	0.352	0.055	15.574	0.275	0.447
Aluminium	%	0.286	0.086	30.132	0.146	0.431
Calcium	%	1.110	0.425	38.263	0.433	1.682
Iron	%	0.933	0.276	29.581	0.665	1.663
χ_{FD}	%	2.547	1.501	58.923	0.591	5.000
$Soft_{\%40mT}$	%	41.837	6.504	15.547	28.741	51.821

**Mean; SD = standard deviation; CV = percentage coefficient of variation; Min = minimum value; Max = maximum value. Values are shown to 3 decimal places for consistency, not accuracy.*

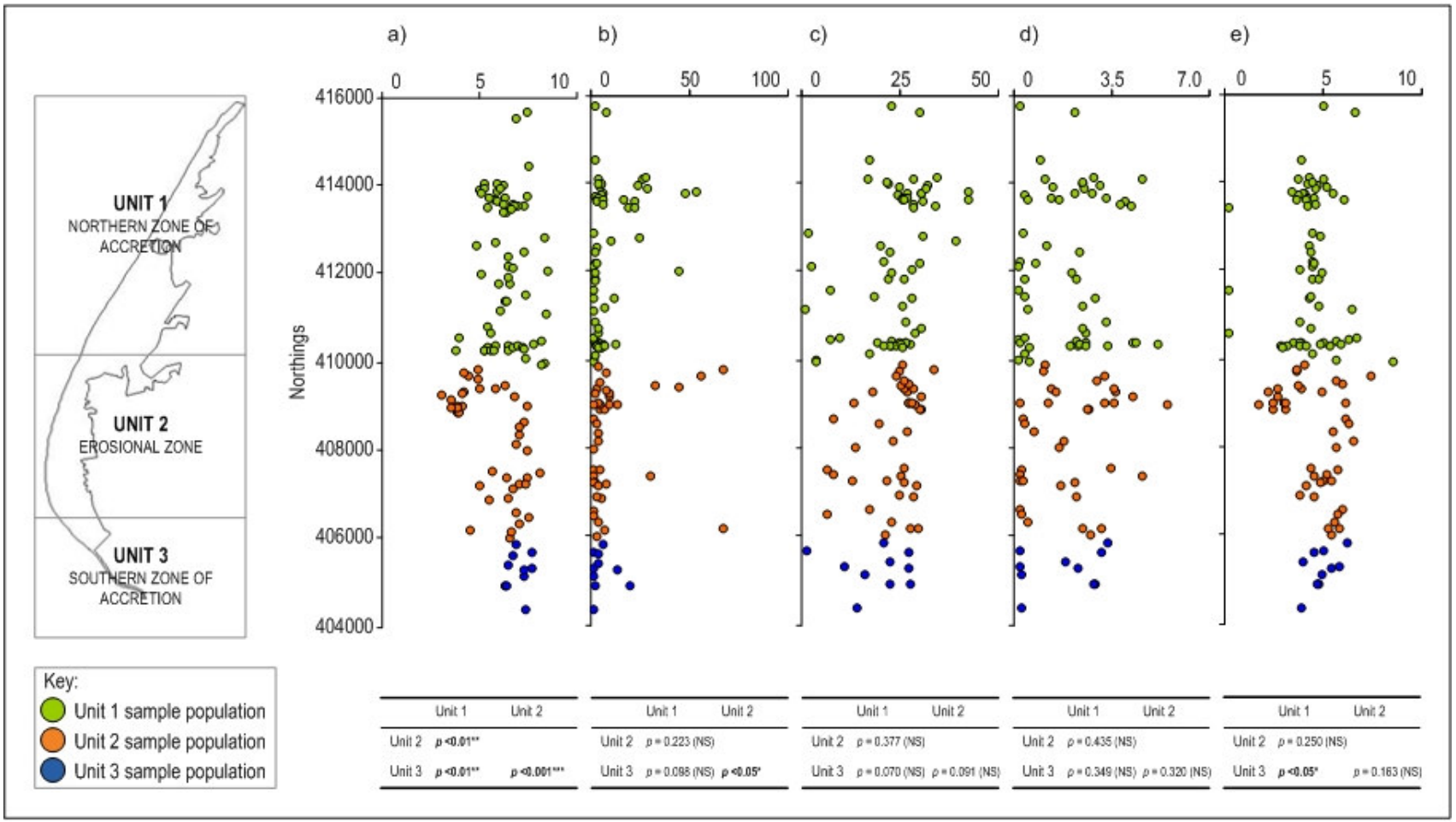

Figure 7.16 Alongshore variations in key physio-chemical topsoil pedo-characteristics with associated Mann-Whitney U test results for; a) pH; b) SOM%; c) Silt%; d) C% and e) Mg%. (**Bold** MINITAB '*p*' value text is significant (**p* <0.05; ***p* <0.01; ****p* <0.001)).

(0.40-47.18%) (Figure 7.16c) and, despite showing no significant differences to each other, silt levels in Unit 1 represented the highest contribution to the textural total (mean 26.16%).

There were no significant differences between C levels within Unit 1 (0.02-5.77%), Unit 2 (0.06-6.14%) and Unit 3 (0.07-3.69%) (Figure 7.16d). Similarly, there were also no significant differences between Mg levels of Unit 1 (<0.01-0.63%) and Unit 2 (0.11-0.54%), although Unit 3 (0.28-0.45%) was significantly different from Unit 1 (p <0.05) (Figure 7.16e), despite both being depositional environments. Levels of Al were significantly higher (p <0.05) in Unit 1 (0.00-1.37%) than Unit 3 (0.10-0.58%) (Figure 7.17a), suggesting Al accumulation was associated with a stable landscape. There was great variability in Ca in Unit 1 (0.03-8.15%), but only values of Units 2 (0.07-1.96%) and 3 (0.43-1.68%) are significantly different (p <0.05) from each other (Figure 7.17b), suggesting that higher percentages of Ca in eroding regimes were possibly derive from increased aeolian sand. Levels of Fe were significantly higher (p <0.05) in Unit 1 (<0.01-6.12) compared to Unit 2 (0.60-1.38%), suggesting Fe accumulation was associated with a stable landscape (Figure 7.17c). However, there were no significant differences between Unit 2 and Unit 3 (0.67-1.66%).

There were no significant differences between $\chi_{FD\%}$ within Unit 1 (0.00-6.12%), Unit 2 (0.00-12.00%) and Unit 3 (0.59-5.00%) (Figure 7.17d). Similarly, there were also no significant differences between $Soft_{\%40mT}$ within Unit 1 (12.86-51.27%), Unit 2 (28.68-58.88%) and Unit 3 (28.74-51.82%) (Figure 7.17e), suggesting magnetic minerals and their domain size are not influenced by erosion/accretion regimes.

These longitudinal variations suggest pedogenic processes operate at different rates and are influenced by different pedo-characteristics, depending on environmental conditions. It is, therefore, necessary to conduct further lateral regressions on each coastal unit to identify varying pedogenic trends.

7.3.2 Lateral variations in Unit 1 topsoil pedo-properties

Figure 7.18a shows a strong negative correlation between pH versus distance from MHW (r = 0.67; p <0.001; n = 63), indicating increased acidity was associated with distance from the shoreline. The opposite pattern was observed in the positive correlation between SOM versus distance from MHW (r = 0.28; p <0.05; n = 63) (Figure 7.18b), which is less significant than the correlation for all units combined. Silt versus distance from MHW (r = 0.41; p <0.01; n = 62) (Figure 7.18c) is also less significant than the correlation for all units combined, although the steeper trend line indicates increased rates of silt input in Unit 1.

Figure 7.18d shows a positive correlation between C (r = 0.32; p <0.05; n = 62) with distance from MHW. Although values appear higher in Unit 1, the correlation significance is less than all units combined. Correlation of Al (r = 0.27; p <0.05; n = 62) with distance from MHW (Figure

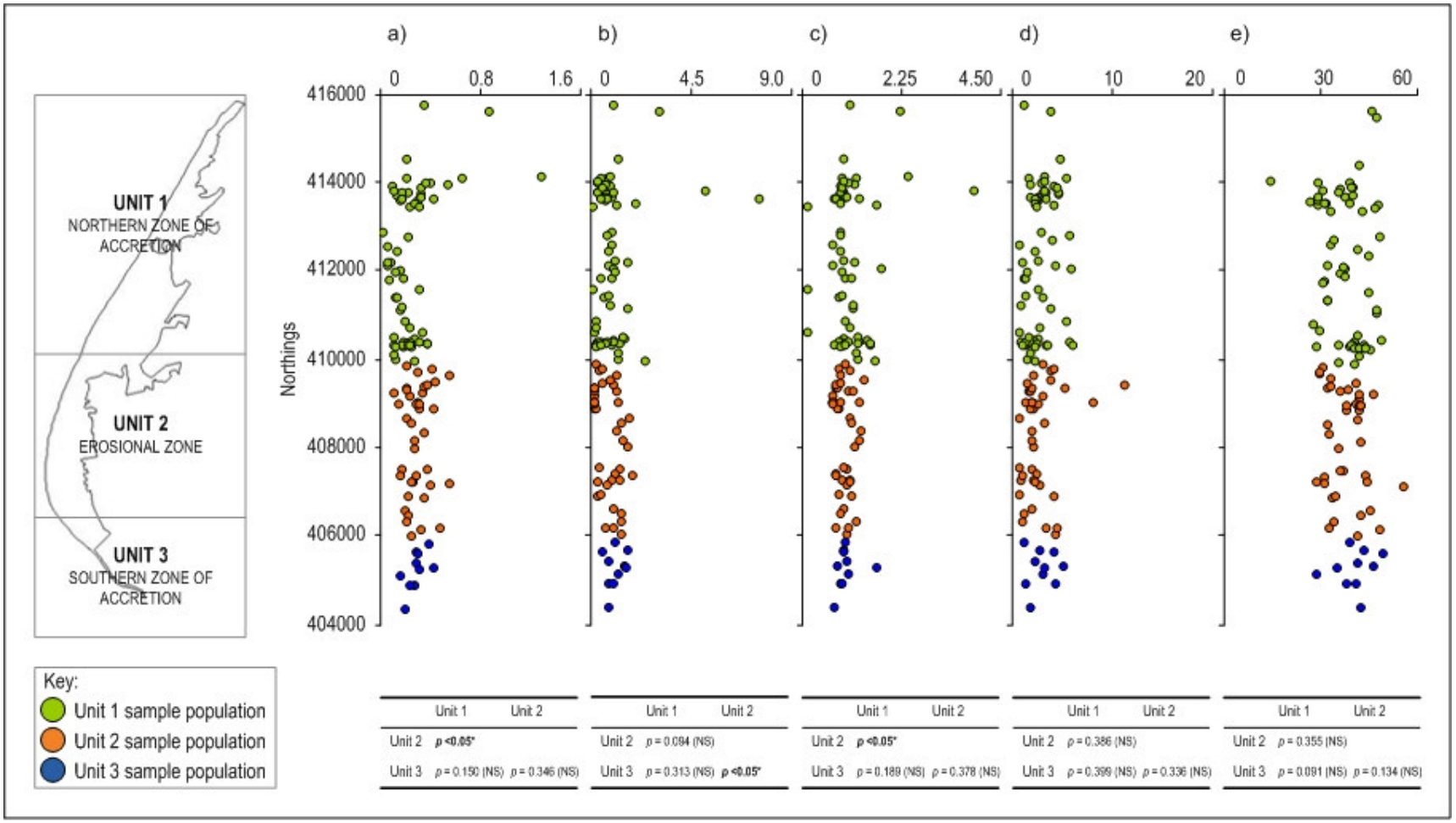

Figure 7.17 Alongshore variations in key physio-chemical topsoil pedo-charcteristics with associated Mann-Whitney U test results for; a) Al%; b) Ca%; c) Fe%; d) $\chi_{FD\%}$ and e) $Soft_{\%40mT}$. (**Bold** MINITAB '*p*' value text is significant (**p* <0.05; ***p* <0.01; ****p* <0.001)).

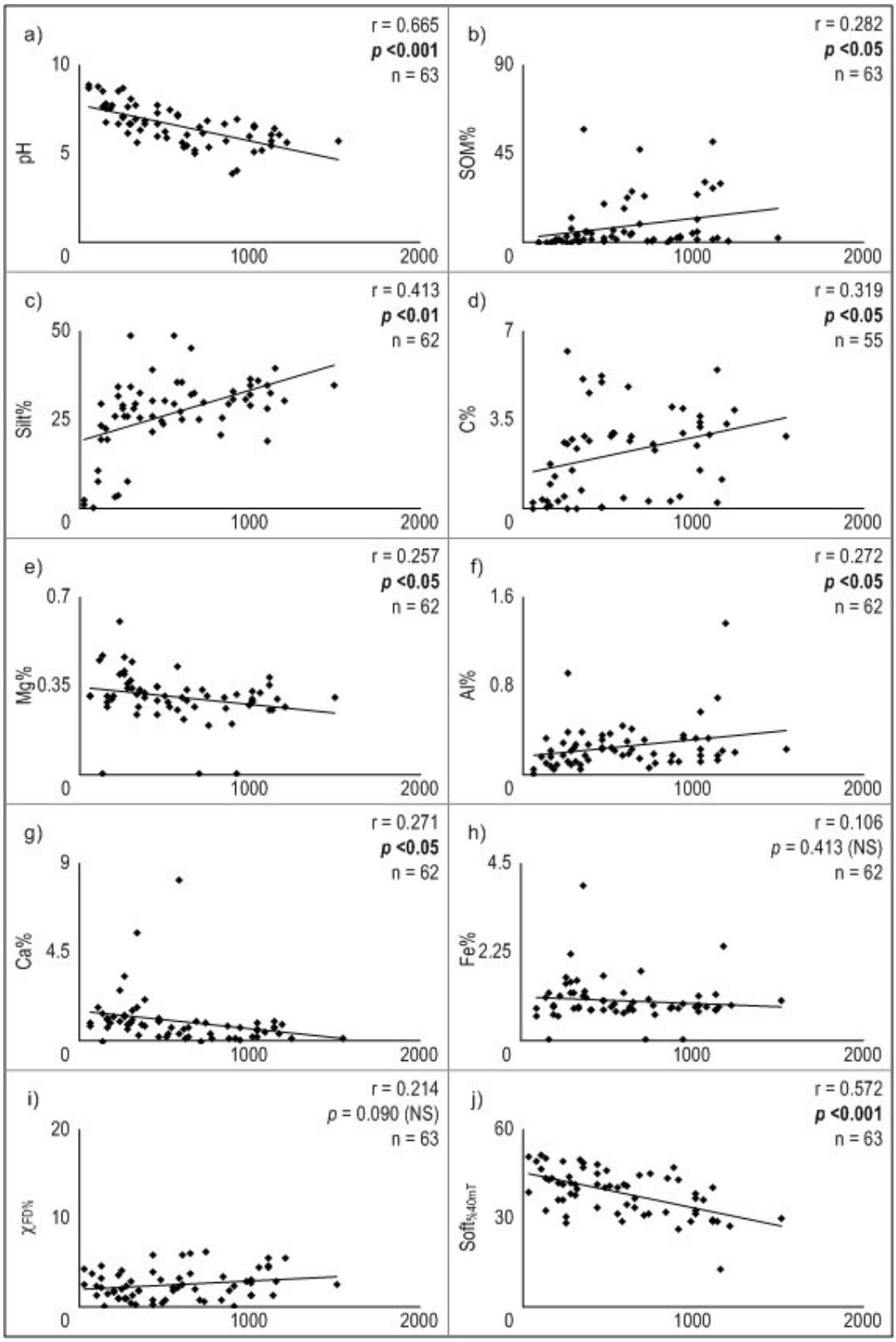

Figure 7.18 Key physio-chemical topsoil pedo-characteristic correlations with distance from mean high water (MHW) (m) (x-axis) for Unit 1 (northern accreting dunes) (**bold** text is significant (p <0.05)).

7.18f), is less significant than all units combined, but the steeper trend line indicates increased rates of Al input. Negative correlations between distance from MHW versus MgO ($r = 0.26$; $p < 0.05$; $n = 62$) (Figure 7.18e) and Ca ($r = 0.27$; $p < 0.05$; $n = 62$) (Figure 7.18g) are less significant in Unit 1 than all units combined. Correlation of Fe ($r = 0.11$; $p = 0.413$ (NS); $n = 62$) (Figure 7.18h) is not significant, suggesting Fe does not have any influence in Unit 1.

The correlation between $\chi_{FD\%}$ versus distance from MHW ($r = 0.21$; $p = 0.09$ (NS); $n = 63$) (Figure 7.18i) is not significant; suggesting the presence of SP magnetic domain sizes does not have any influence in Unit 1. The negative correlation between $Soft_{\%40mT}$ versus distance ($r = 0.57$; $p < 0.001$; $n = 63$) (Figure 7.18j) is more significant than all units combined; indicating decreased content of soft 'magnetite-type' mineralogy is associated with distance from the coast. This may suggest content of hard 'haematite-type' mineralogy increases with distance in Unit 1.

7.3.3 Lateral variations in Unit 2 topsoil pedo-properties

Figure 7.19a shows a strong negative correlation between pH versus distance from MHW ($r = 0.87$; $p < 0.001$; $n = 40$) with a steep trend line indicating rapid acidity associated with distance from the coast. However, the correlation between SOM versus distance from MHW ($r = 0.17$; $p = 0.286$ (NS); $n = 40$) (Figure 7.19b) is not significant. There appears to be limited change in silt versus distance from MHW ($r = 0.72$; $p < 0.001$; $n = 40$) (Figure 7.19c), when compared to all units combined.

Figure 7.19d shows a positive correlation between C ($r = 0.53$; $p < 0.01$; $n = 36$) with distance from MHW. Although this correlation is less significant than when all units are combined, the steeper trend line indicates increased rates of C input in Unit 2. The steeper trend line on the negative correlation between Mg versus distance from MHW ($r = 0.82$; $p < 0.001$; $n = 40$) (Figure 7.19e) is steeper, suggesting rates of Mg input are rapidly decreased in Unit 2. The correlation between Al with distance from MHW ($r = 0.29$; $p = 0.072$ (NS); $n = 40$) (Figure 7.19f), is not significant in Unit 2. There appears to be limited change in Ca versus distance from MHW ($r = 0.79$; $p < 0.001$; $n = 40$) (Figure 7.19g), when compared to all units combined. The negative correlation between Fe versus distance from MHW ($r = 0.61$; $p < 0.001$; $n = 40$) (Figure 7.19h) is more significant for Unit 2, than when all units are combined.

The correlation between $\chi_{FD\%}$ versus distance from MHW ($r = 0.25$; $p = 0.114$ (NS); $n = 40$) (Figure 7.19i), and $Soft_{\%40mT}$ versus distance ($r = 0.06$; $p = 0.711$ (NS); $n = 40$) (Figure 7.19j) are not significant, indicating the presence of SP magnetic domain sizes of soft 'magnetite-type' magnetic mineralogy do not have any detectable influence in Unit 2.

7.3.4 Lateral variations in Unit 3 topsoil pedo-properties

Figures 7.20a,b show no significant correlation between both pH versus distance from MHW

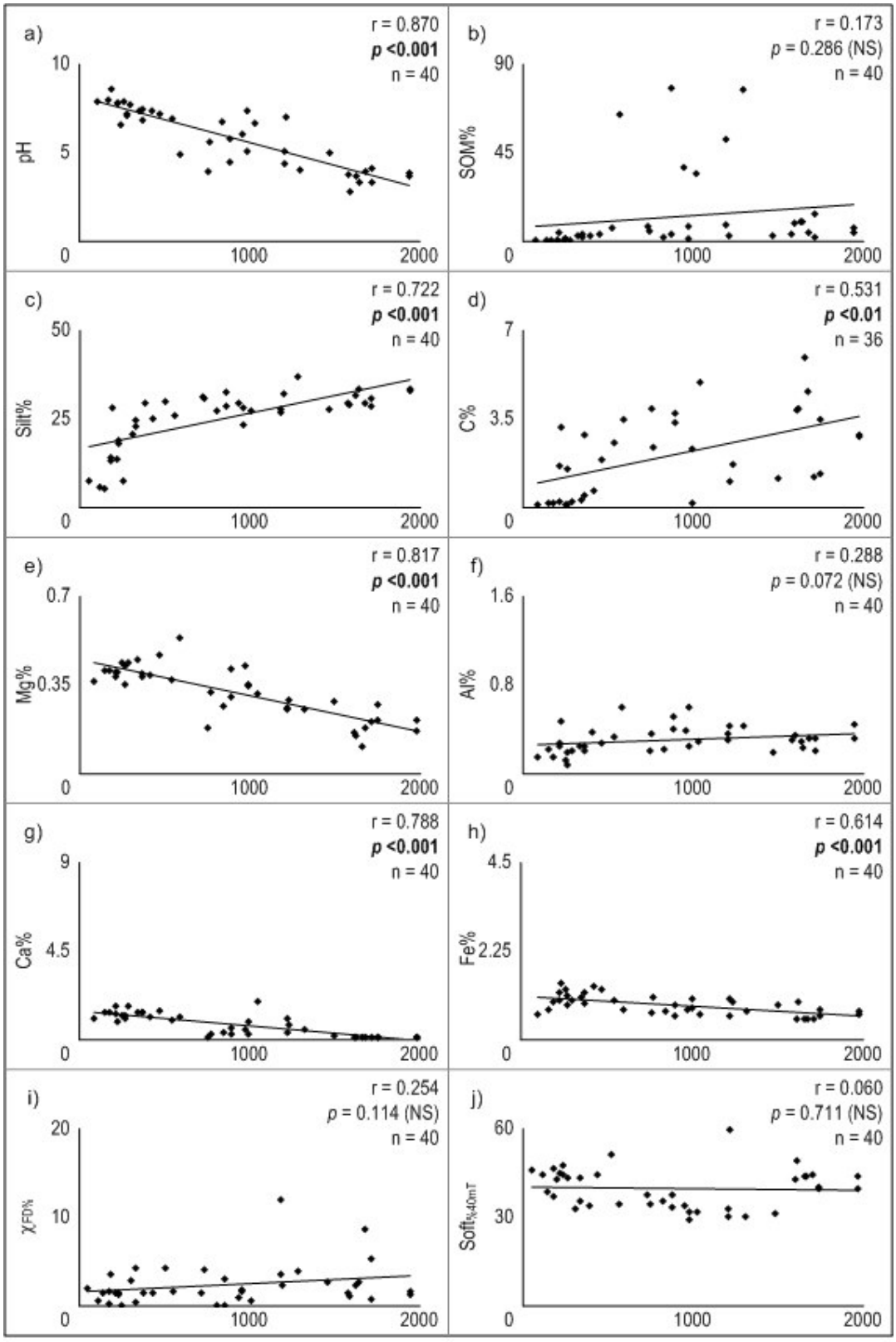

Figure 7.19 Key physio-chemical topsoil pedo-characteristic correlations with distance from mean high water (MHW) (m) (x-axis) for Unit 2 (eroding dunes) (**bold** text is significant (p <0.05)).

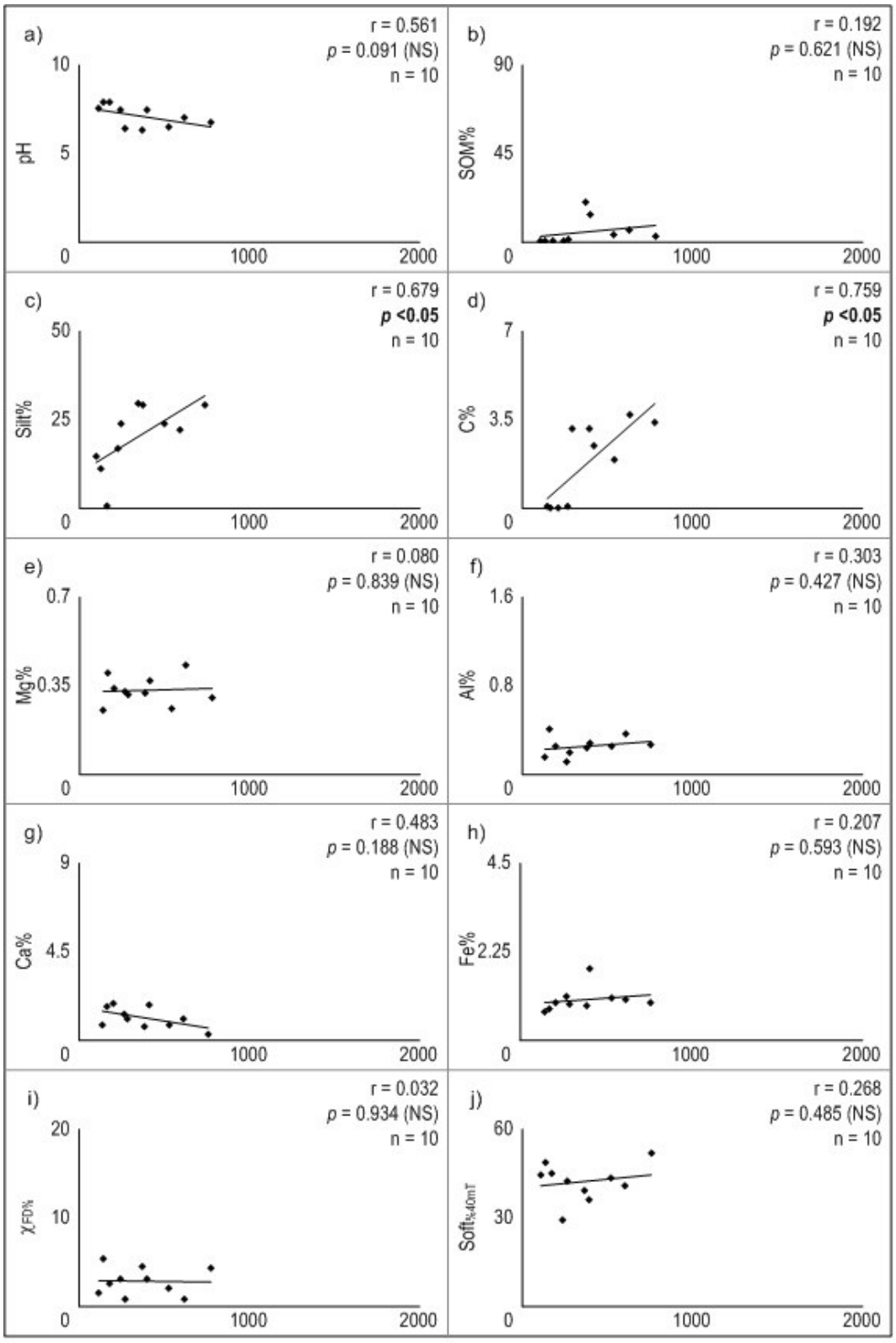

Figure 7.20 Key physio-chemical topsoil pedo-characteristic correlations with distance from mean high water (MHW) (m) (x-axis) for Unit 3 (southern accreting dunes) (**bold** text is significant (p <0.05)).

(r = 0.56; p = 0.091 (NS); n = 10) and SOM versus distance from MHW (r = 0.19; p = 0.621 (NS); n = 10), respectively. The positive correlation between silt versus distance from MHW (r = 0.68; p <0.05; n = 10) (Figure 7.20c) is less significant than when all units are combined, but the increased steepness of the trend line indicates rapid increased silt input in Unit 3 compared to Unit 1.

Figure 7.20d shows a positive correlation between C (r = 0.76; p <0.05; n = 10) and distance from MHW. Although this correlation is less significant than all units combined, the steep trend line indicates rapid increases in C input in Unit 3 compared to Unit 1. The correlation between distance from MHW versus Mg (r = 0.08; p = 0.839 (NS); n = 10) (Figure 7.20e) is not significant, suggesting that Mg influences are stable across Unit 3. Correlations between both Al (r = 0.30; p = 0.427 (NS); n = 10) (Figure 7.20f) and Ca with distance from MHW (r = 0.48; p = 0.188 (NS); n = 10) (Figure 7.20g) are not significant. The correlation between Fe versus distance from MHW (r = 0.21; p = 0.593 (NS); n = 10) (Figure 7.20h) is also not significant. However, the trend line indicates a change to a positive correlation, in comparison to the negative correlation of all units combined, suggesting Fe content is slightly increased with distance.

The correlations between both $\chi_{FD\%}$ versus distance from MHW (r = 0.03; p = 0.934 (NS); n = 10) (Figure 7.20i) and $Soft_{\%40mT}$ versus distance (r = 0.27; p = 0.485 (NS); n = 10) (Figure 7.20j) are not significant. However, the trend line on the $Soft_{\%40mT}$ plot indicates increased a change to a positive regression, compared to the negative regression of all units combined.

7.4 Conceptional pedogenic modelling on the Sefton coast

Macro-scale dune management requires comprehensive consideration of system components and interactions so that appropriate decisions can be made for ecosystem sustainability. Conceptual models provide the necessary framework to represent such multiple, complex system components and to identify function pathways. A conceptual model of pedogenesis on the Sefton coast will provide a tool to graphically represent the structure and function of the relationships between pedo-environments that lead to a pedological target within the dune system as an entirety. Further models, created with the same principles of pedogenesis within each coastal unit, will aid understanding of the response of pedo-environments to localized environmental change or anthropogenic stresses.

7.4.1 Conceptual model of pedogenesis on the Sefton coastal dunes

Based on both topsoil and soil profile pedo-characteristic relationships, Figure 7.21 attempts to conceptually model a two-dimensional pedogenic pathway of classified soil profiles from the active coastline to the stable inland dune landscape. The key geochemical, textural and mineral magnetic parameters are considered, allowing each soil classification to be presented in proposed order of pedogenesis. Lateral correlations are used to decipher ascending order of pedo-characteristic variances against distance from MHW.

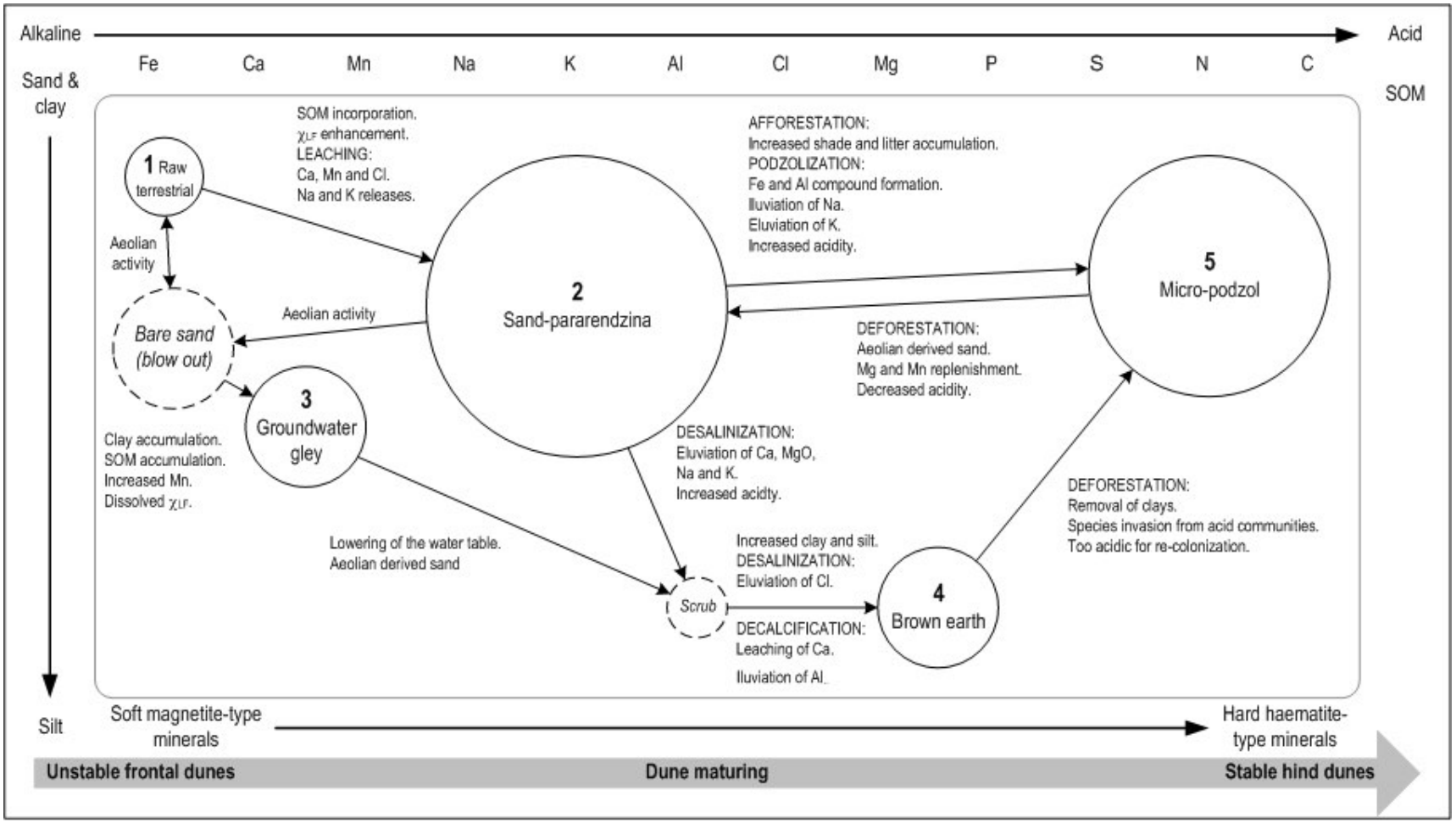

Figure 7.21 Conceptual model of a two-dimensional pedogenic pathway, from the active coastline to the stable inland dune landscape, based on pedo-characteristic correlations (Spearman's Rank) *(size of circles represent relative spatial soil cover, but are not to scale)*.

Pedogenic Stage 1 on the Sefton coast is characterized by terrestrial raw sand, representing a relatively small proportion of total soil cover. These topsoils are highly influenced by sand- and clay-sized particles, alkaline elements Ca and Mn and relatively high percentages of Fe, associated with soft 'magnetite-type' ferrimagnetic minerals. Slight increases in aeolian activity may be sufficient to cause erosion of terrestrial raw soils, resulting in patches of bare sand. However, if environmental conditions remain sufficiently stable, SOM eventually becomes incorporated into the mineral horizon, acting as a sink for magnetic particles. Leaching of Ca, Mn and Cl, alongside illuviation of Na and K, contributes to Stage 2 pedogenesis, where a negative correlation exists in the topsoils between increases in clay-sized particles and decreased Al, leading to sand-pararendzina profile formation; the most abundant soil-type on the Sefton coast. As SOM content also depends on soil particle size distribution (Hagedorn *et al.,* 2001; Jankauskas *et al.,* 2006; Fullen *et al.,* 2006), this correlates positively with increases in silt-sized particles.

Blowout formation, through increased aeolian activity, may cause deflation down to the water table and, subsequent, slack development. This hollow landscape feature provides ideal conditions for accumulation of both SOM and clay-sized particles (Ragg *et al.,* 1984) which, in turn, contribute towards creating pedogenic Stage 3, a waterlogged anaerobic groundwater gley; in which dissolution of magnetic minerals may occur. The negative correlation in the topsoils between decreased mean particle size and increased Fe, alongside increased Mn through sufficient aeration by seasonal waterlogging (James, 1993), places Stage 3 in-between Stages 1 and 2. Drying of the groundwater gley profile, the likely result of afforestation (Gee, 1991), may lead to invasion of scrub species. Otherwise, the likely path towards the optimum Stage 4 brown earth profile is through desalinization and decalcification of the sand-pararendzina, alongside increased silt-sized particles in the topsoils.

Planting of coniferous woodland may result in increased shade and needle litter accumulation, which, subsequently alters sand-pararendzinas through increased acidity and podzolization to create Stage 5 of the conceptual pedogenic model. Topsoils from micro-podzol pedo-environments, representing the second most abundant soil-type on the Sefton coast, are highly influenced by P, S, N and C, with strong positive correlations between acidity and SOM content, similar to Redel *et al.* (2008). Lower profile horizons are influenced by hard 'haematite-type' magnetic minerals. Deforestation creates open expanses, allowing re-deposition of aeolian derived sand and Mg and Mn replenishment. Therefore, reversion to the Stage 2 sand-pararendzina profile is possible. Stage 5 may also be achieved, through deforestation of the brown earth pedo-environment alongside species invasion from acid communities.

7.4.2 Conceptual model of pedogenesis for the northern accreting Sefton coast

Based on both topsoil and soil profile pedo-characteristic relationships from Unit 1, Figure 7.22 presents a conceptual model of a two-dimensional pedogenic pathway of classified soil profiles

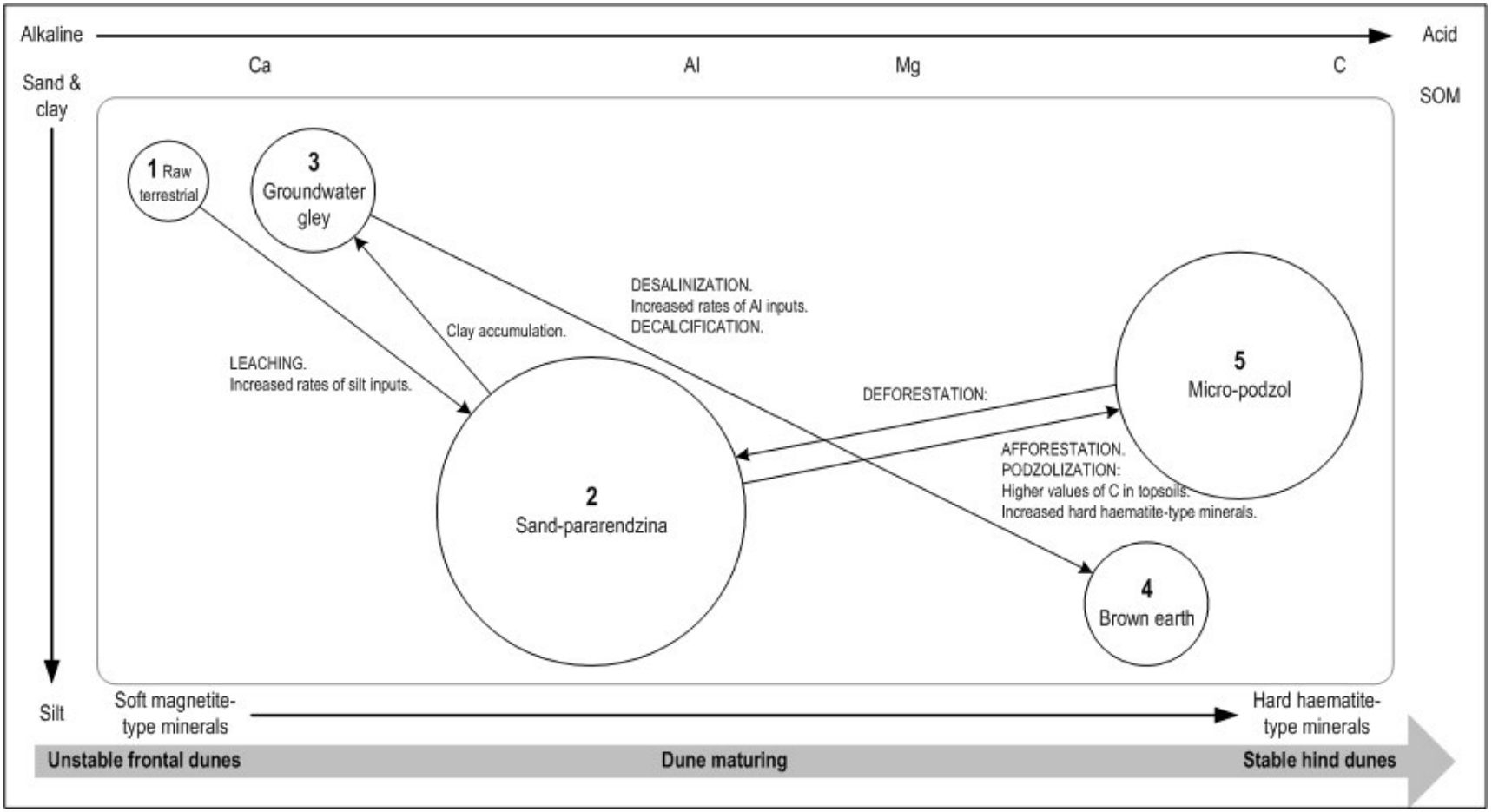

Figure 7.22 Conceptual model of a two-dimensional pedogenic pathway, from the active coastline to the stable inland dune landscape, based on pedo-characteristic correlations (Spearman's Rank) from Unit 1 (northern accreting dune system) *(size of circles represent relevant spatial soil cover, but are not to scale)*.

from the active coastline to the stable inland dune landscape. Ca, Al, Mg and C were significant factors on this coastal section.

Pedogenic Stage 1 in Unit 1 is characterized by terrestrial raw sand, representing only a minor proportion of total soil cover. Similar to the Sefton coast model, these topsoils are highly influenced by sand- and clay-sized particles and alkaline elements, predominantly Ca. Mn and Fe are no longer significant, although associated soft 'magnetite-type' ferrimagnetic minerals are present. The initial difference between the conceptual model of the entire Sefton coast and that of Unit 1 is there is no bare sand representation in the latter. This may be due to insufficient aeolian activity to cause fresh blowouts in a stabilized landscape. Accretion and stabilization of this coastal section may explain the rapid siltation of topsoil properties and account for the lower position of the sand-pararendzina profile, pedogenic Stage 2, along the textural axis of the conceptual model.

It can be assumed, the older, inland groundwater gleys of pedogenic Stage 3 formed through SOM and clay accumulations in relic dune hollows/blowouts. However, immature groundwater gleys, on the seaward margin, are likely to have formed as a response to geomorphic migration of mobile dune ridges from inland (Pethick, 1984). This may explain the decreased significance of Mn in these soils, which is usually associated with a fluctuating water table further inland (van Breemen and Buurman, 2002). Similar to the Sefton coast model, Stage 3 is placed between Stages 1 and 2. Drying of groundwater gley profiles and, subsequent, dissolution of Ca (Dearing, 1999) leads to decalcification and desalinization, alongside increased Al influences, to pedogenic Stage 4, the brown earth profile. Dissimilar to the Sefton coast model, this pedogenic pathway is only achievable from groundwater gley profiles in Unit 1.

Stage 5, the micro-podzol profiles of the conceptual model of Unit 1, represents the second largest percentage total soil cover on this coastal section. However, this is not a natural pedogenic trend as its development is a response to anthropogenic afforestation. The distance of these micro-podzol soils from the coast may explain the decreased influence of sand. Similar to the Sefton coast model, these topsoils have highly significant correlations between acidity, SOM and C, alongside lower horizons influenced by hard 'haematite-type' magnetic minerals. Reversion of the micro-podzol profile back to a Stage 2 sand-pararendzina can be achieved through deforestation and, subsequent, Mg replenishment through deposition of aeolian derived sand.

7.4.3 Conceptual model of pedogenesis for the eroding Sefton coast

Based on both topsoil and soil profile pedo-characteristic relationships from Unit 2, Figure 7.23 conceptually models a two-dimensional pedogenic pathway of classified soil profiles from the active coastline to the stable inland dune landscape. Fe, Ca, Mg and C parameters were significant factors on this coastal section. As both SOM and mineral magnetic parameters were

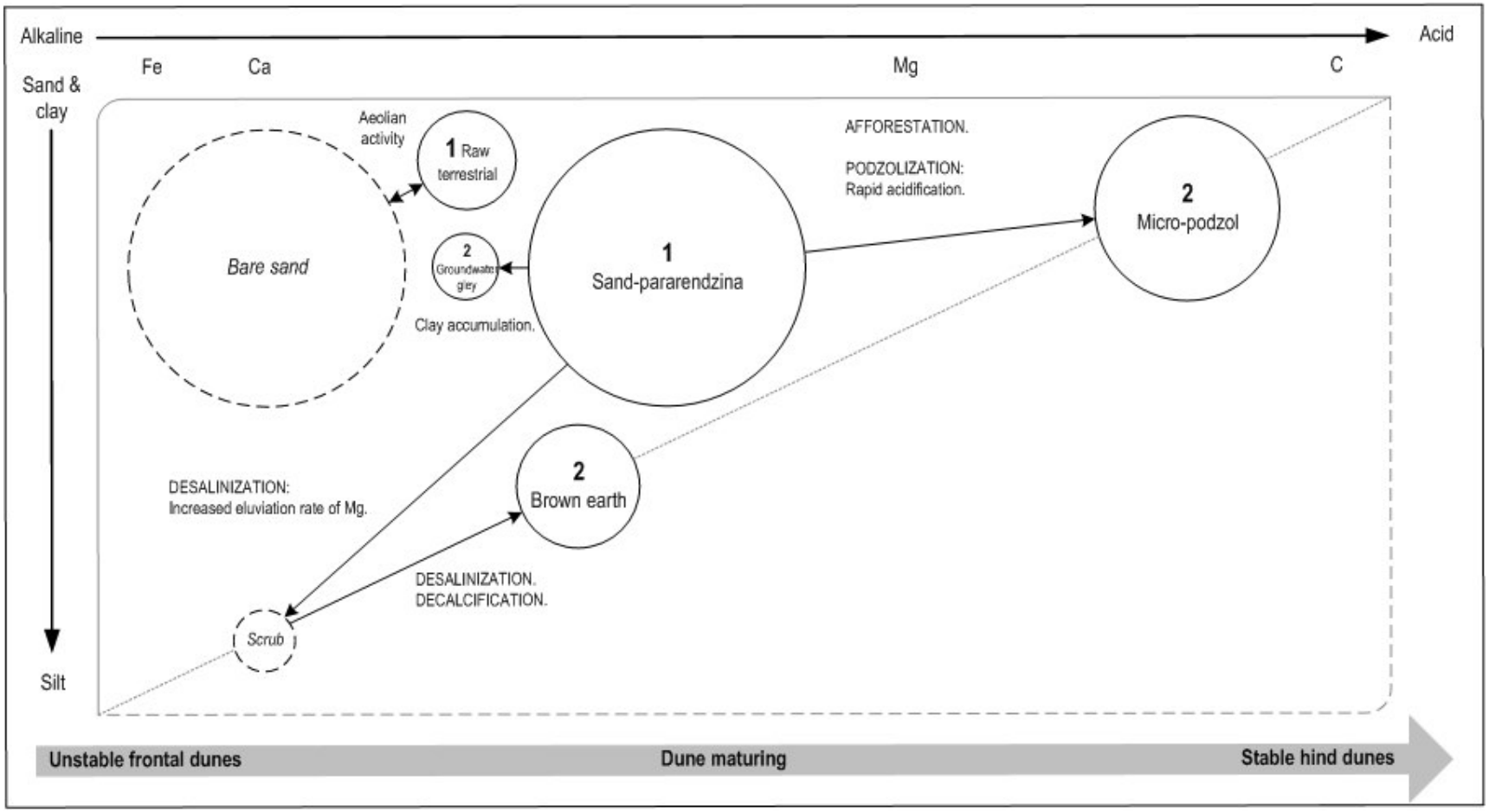

Figure 7.23 Conceptual model of a two-dimensional pedogenic pathway, from the active coastline to the stable inland dune landscape, based on pedo-characteristic correlations (Spearman's Rank) from Unit 2 (eroding dune system) *(size of circles represent relative spatial soil cover, but are not to scale)*.

of no statistical significance they were removed, resulting in a three-sided pedogenic model influenced by texture and geochemical properties.

Increased expanses of aeolian derived sand appear in Unit 2, indicative of unstable, eroding foredunes. This is inhibiting development of terrestrial raw sand (Stage 1), which only represents a small proportion of total soil cover. These soils are not naturally developing into sand-pararendzinas, as conditions are too unstable and, therefore, act as individual models in their own rights. Sand-pararendzinas also represent Stage 1, with high sand- and clay-sized particle contents and Ca and Fe influences, which are similar to those in the entire coast model.

During the second stage of pedogenesis, sand-pararendzinas develop into various soil profiles depending on geomorphic, anthropogenic and natural pedogenic processes. Natural clay accumulation in dune hollows appears to facilitate development of groundwater gley soil profiles. In contrast, desalinization and decalcification on dune ridges appears to facilitate development of scrub environments and, subsequent, brown earth soil profiles. Due to the effects of coastal erosion, the sand-pararendzina and brown earth pedo-environments are both placed at the same distance from the unstable foredunes. Another Stage 2 profile, developed from the anthropogenically altered sand-pararendzina, is the micro-podzol. Dissimilar to the model of the entire Sefton coast, the micro-podzol represents a smaller proportion of the total soil cover in Unit 2. It has also been placed slightly higher on the model's textural axis, displaying increased influences of aeolian derived sand resulting from re-mobilized sand activity. However, despite proposed aeolian-derived sand influences, these topsoils remain highly acidic and heavily influenced by C, similar to the entire Sefton coast model. On this section of coast, no attempts have been made to restore sand-pararendzina environments through deforestation.

7.4.4 Conceptual model of pedogenesis for the southern accreting Sefton coast

Based on both topsoil and soil profile pedo-characteristic relationships from Unit 3, Figure 7.24 conceptually models a two-dimensional pedogenic pathway of classified soil profiles from the active coastline to the stable inland dune landscape. C was a significant factor on this section of the coast. Although not highly significant, Fe was included as a contributing factor, as its reversed lateral regression-correlation indicates that this parameter is of some importance. The pH, SOM, most geochemical parameters and mineral magnetic parameters were insignificant. Therefore, they were removed, resulting in a three-sided pedogenic model. However, due to reversed lateral regression-correlations, mineral magnetic parameters have been included as 'greyed-out' influences, with greater volumes of hard 'haematite-type' minerals on the unstable frontal dunes grading into softer 'magnetite-type' minerals inland. Because the harder magnetic minerals are positively correlated with sand- and clay-sized particles, the position of textural parameters has also been reversed.

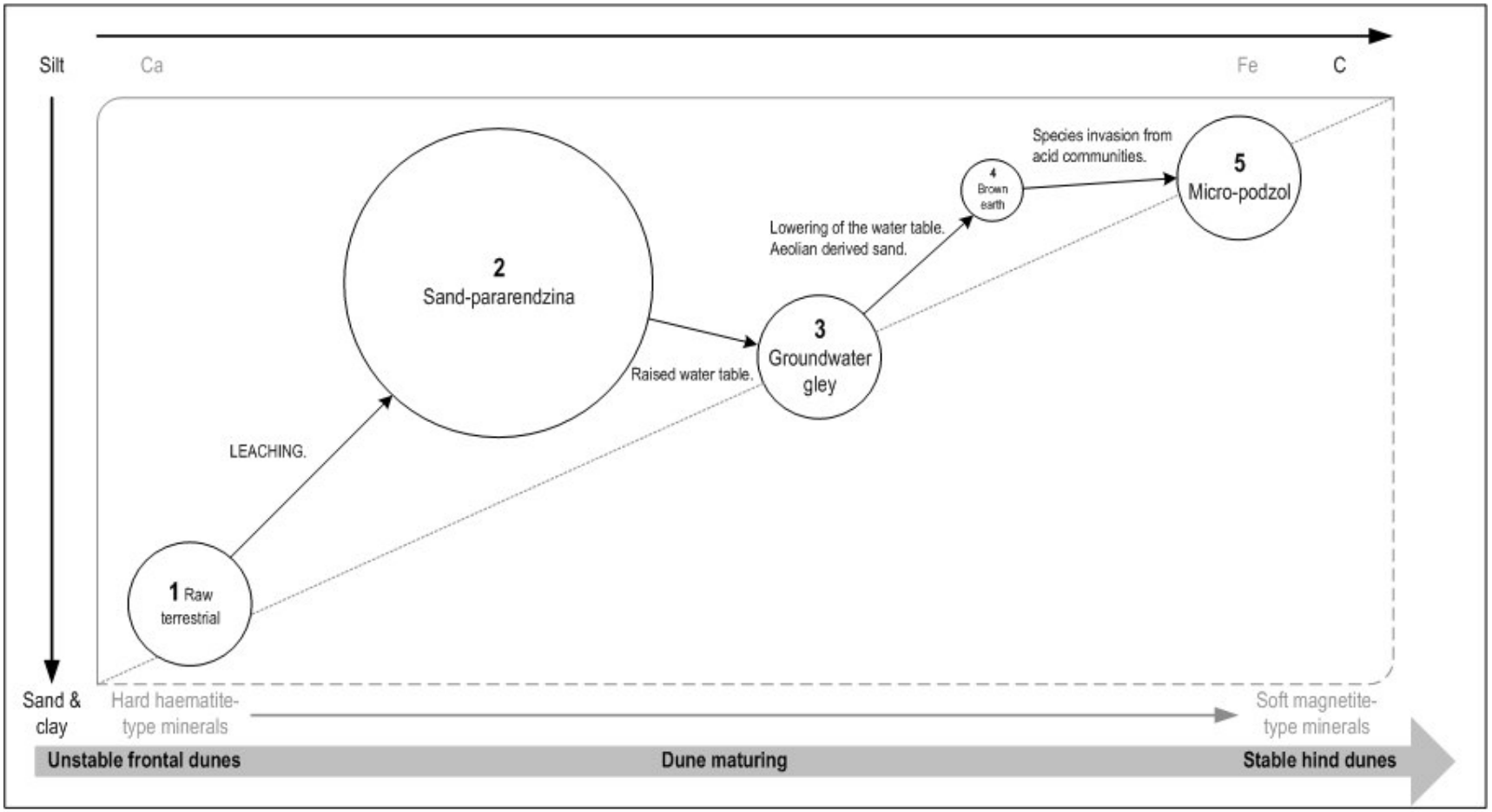

Figure 7.24 Conceptual model of a two-dimensional pedogenic pathway, from the active coastline to the stable inland dune landscape, based on pedo-characteristic correlations (Spearman's Rank) from Unit 3 (southern accreting dune system) *(size of circles represent relative spatial soil cover, but are not to scale)*.

Pedogenic Stage 1 in Unit 3 is characterized by terrestrial raw sand, representing a significant proportion of total soil cover compared to that represented on the entire Sefton coast. These topsoils are highly influenced by sand- and clay-sized particles. Leaching of nutrients leads to pedogenic Stage 2 sand-pararendzina profile formation, which is the most abundant soil in Unit 3. Deflation, down to an already raised water table, allows slack development and, subsequently, a waterlogged anaerobic groundwater gley, representing pedogenic Stage 3. Dissimilar to the model of the entire Sefton coast, the groundwater gley profile in Unit 3 is positioned much further inland due to the accreting nature of this section of coast.

A combination of both increased aeolian derived sand and natural lowering of the water table, as a function of distance from the coast, results in Stage 4 brown earth pedo-environments. Although this pedogenic stage is placed in a similar position to that in the entire Sefton coast model, it only represents a small proportion of the overall total soil cover. The micro-podzol, of pedogenic Stage 5, represents a heath pedo-environment, rather than coniferous plantations and appears to have naturally developed from stage 4 through species invasion from acid communities. Although no longer significant, the positive correlation between soft 'magnetite-type' magnetic minerals and distance from the coast, which is not apparent in any other unit on the Sefton coast, may be attributed to the formation of ferrimagnetic minerals during pedogenesis in mature soils; especially when considering the flat, stabilized topography of the environment and natural species invasion (Turk *et al.,* 2008). On the other hand, hard haematite-type minerals on the seaward edge may represent a different sediment source, possibly sediments obtained from dredging in the Mersey estuary (Smith, 1982).

7.4.5 Review of the conceptual models

Modelling pedogenesis is of great importance in assessing the effects of environmental change on coastal habitats. While other models (e.g. Running and Coughlan, 1988) have been developed to simulate soil processes (eg. carbon allocation, nitrogen mineralization, leaching, clay translocation, podzolization, decalcification, gleying, salinization), few attempts have been made to simulate the processes that progress from the physical and chemical weathering of terrestrial raw sand, to the development of topsoils and, consequently, soil profiles. Most models of pedogenic processes account for chemical reactions and fluxes at the horizon scale and are difficult to extrapolate to the landscape scale (Minasny *et al.,* 2006).

The advantage of this simple *in-situ*, soil model with five major pedogenic characteristics: i) acidity; ii) elemental composition; iii) SOM; iv) particle size distribution; and v) mineral magnetics, is the ability to simulate the formation and process of various soil properties within each classified profile unique to the dune landscape. Therefore, physico-chemical pedo-properties can be tracked laterally through distance from MHW (a surrogate for time). However, the lateral regressions assume a linear soil property evolution from the shoreline and do not easily account for alongshore developments. The rates of soil development are operating on decadal timescales, depending on environmental conditions and stage of pedogenesis, but it is

impossible to decipher these rates of change using the model. These models are not suitable for determining seasonal variations in pedogenesis.

As coastal environmental change problems are generally an issue relevant on all coasts, understanding pedogenic responses is vital for dune management, especially when confronted with issues such as artificial habitat creation/removal or 'coastal squeeze'. Theoretically, these conceptual models can be used to identify both natural and anthropogenic processes operating within other sand dune systems both nationally and internationally. However, it is vital that they are used in conjunction with other dune models, such as geomorphology and sedimentology processes and vegetation data, as issues such as different sediment sources may cause inaccurate interpretations.

7.5 Summary

Correlation analysis has confirmed the significance of topsoil physico-chemical property associations, indicating individual topsoil environments also influence parameter relationships; whereas, lateral regressions have identified varying rates of physio-chemical influences with distance from mean high water (MHW).

Based on topsoil physico-chemical properties, three coastal units were identified on the Sefton coast. The units are influenced by erosion/deposition dynamics, extent of natural vegetation cover and anthropogenic impacts:

- Unit 1 differs from the remaining units by displaying rapid rates of siltation and decreased soft 'magnetite-type' magnetic minerals, interpreted to reflect an actively accreting dune system.
- Unit 2 differs from the remaining units by displaying rapid rates of acidification and C inputs, interpreted as coastal erosion being sufficient to erode the frontal dunes in their entirety to expose mature hind dune soils on the seaward edge.
- Unit 3 differs from the remaining units by having less significant, or no significant, pedo-property associations. This is a relatively stationary dune system, most closely representing natural dune pedo-succession.

Conceptual models of pedogenesis on the Sefton coastal dunes are proposed, accounting for six factors: i) distance from unstable frontal dunes to stable hind dunes; ii) textural content; iii) soil acidity; iv) soil organic matter (SOM); v) geochemical variations; and vi) mineral magnetic influences. These models simulate the formation and various soil processes within each classified profile unique to the dune landscape, by highlighting the impact of geomorphology, soil processes and anthropogenic influences in varying eroding/accreting environments. The physico-chemical pedo-properties can be tracked laterally through distance from MHW (a surrogate for time), which has great implications for dune managers to address soil management problems alongside the effects of coastal and environmental change.

CHAPTER 8

Challenging assumptions of future pedogenesis on sand dune systems

This Chapter outlines some of the strategies and assumptions used to inform coastal management in the UK, by introducing the national Shoreline Management Plan (SMP) policy. Moreover, in raising awareness of pedogenesis as an integral part of nature and associated habitats (Mitchell *et al.,* 2007; van den Ancker and Jungerius, 2007), it also attempts to stimulate discussion on SMP limitations based on the Sefton coast case study.

8.1 Introduction

It is widely believed that climate change and rising sea levels will pose significant challenges, such as flooding and coastal erosion, to the effective management of coastal areas (IPCC, 2007) and associated soils. As coastal areas around the UK are diverse, with shorelines retreating or advancing at various rates, in response to forcing factors, management responses must be appropriate to the area at risk. Therefore, wherever possible, pedogenic sustainability should be achieved by working with coastal processes, rather than against them.

8.1.1 Pedogenic considerations in dune management

There is general agreement that sand dune system responses to climate change and rising sea levels are expected to be dynamic and variable, anticipating future retreating shorelines, raised groundwater and migration of ecological zones (e.g. Hulme *et al.,* 2002; Evans *et al.,* 2004; Orford and Pethick, 2006). According to the final 'England Biodiversity Strategy Report' to DEFRA (Mitchell *et al.,* 2007), one of the underpinning requirements for biodiversity management is data for understanding ecosystem, habitat and species response to climate change. Generally, minimal regard has been shown for the role of pedogenic responses to such environmental change in planning approaches to future dune management.

Concerning the heritage functions of soils, as described by Van den Ancker and Jungerius (2007), the following categories can be recognized on the Sefton dunes; i) 'almost' unaffected soils; ii) agricultural soils in long-term, sustainable use; and iii) soils of special significance for soil science (e.g. palaeosols) and, therefore, are likely to be in existence on other sand dune systems. These all require consideration in dune management and preservation. The underlying principles on which these management practices are based include sufficient understanding of coastal forces, an understanding of the spatial limits of the coastal zone and the capability of the dune system to protect the landscape inland. Each of these issues needs to be readdressed to consider the value of the soil resource.

8.2 Integrated Coastal Zone Management (ICZM)

Integrated Coastal Zone Management (ICZM), at both national and local levels, aims to bring stakeholders together to implement policies that affect the coast, including promoting sustainable economic development, reducing conflict and improving land use management.

One of the key functions of ICZM on the Sefton coast is to develop and implement appropriate coast defence strategies and main sea defence function of beaches, sand dunes and salt marshes consistent with the natural character and conservation importance of the coast. This is to be achieved through the development of Shoreline Management Plans (SMP).

8.2.1 Shoreline Management Plans (SMP)

SMPs are a nationally adopted approach to coastal management that provide large-scale assessments and long-term policy frameworks associated with reducing the risk of the effects of coastal processes on both the natural and developed environment (DEFRA, 2003). However, the risk of coastal processes on pedogenic environments is not included in these management plans.

SMPs incorporate a littoral 'sediment cell' concept to coastal evolution management in England and Wales. An important objective of SMPs is to work in partnership with all interested organizations, such as local councils and the public, to enable sustainable future management decisions and to avoid fragmented attempts to protect one area at the expense of another. Such decisions need to take account of natural coastal processes and the interactions that occur within coastal systems at various temporal and spatial scales (Cooper and Pontec, 2006).

The shoreline of England and Wales was examined by Wallingford (1993) to provide initial guidance on suitable divisions of the coastline into littoral 'sediment cells', within which a strategic framework for the development of sustainable polices for coastal defences could be identified, based on natural process behaviour. Figure 8.1a shows the 11 coastal cells around England and Wales. This first generation of SMPs (1998) was successfully mapped and improved understanding of coastal processes operating on ~6000 km of coastline around England and Wales. SMP documents, applicable for the next 50 years, were put together on the basis of information known and available in 1998 and were designed to evolve as further information became available. Policy options were chosen from five possible alternatives: i) Do not provide any flood or coastal defence; ii) Hold the existing defence line to maintain the shoreline in its present position/location; iii) Advance the existing defence line to relocate the shoreline to seaward of its present position/location; iv) Retreat the existing defence line to allow the shoreline to relocate landward of its present position; and v) Natural Defence Management to work with natural processes to minimize erosion and maximize accretion. The first generation of SMPs are currently under review, accounting for increased awareness and scientific knowledge on future risk management challenges. Outcomes will lead towards producing SMP2s, which must be completed by March 2010 (DEFRA, 2003).

8.2.2 SMPs on the Sefton coast

The coast from Great Orme's Head to the Solway Firth represents cell 11 of the series around England and Wales (Figure 8.1b). Five SMP divisions exist within cell 11, based on natural sediment transfer limits, rather than administrative boundaries (Lymbery, 1999). The Sefton

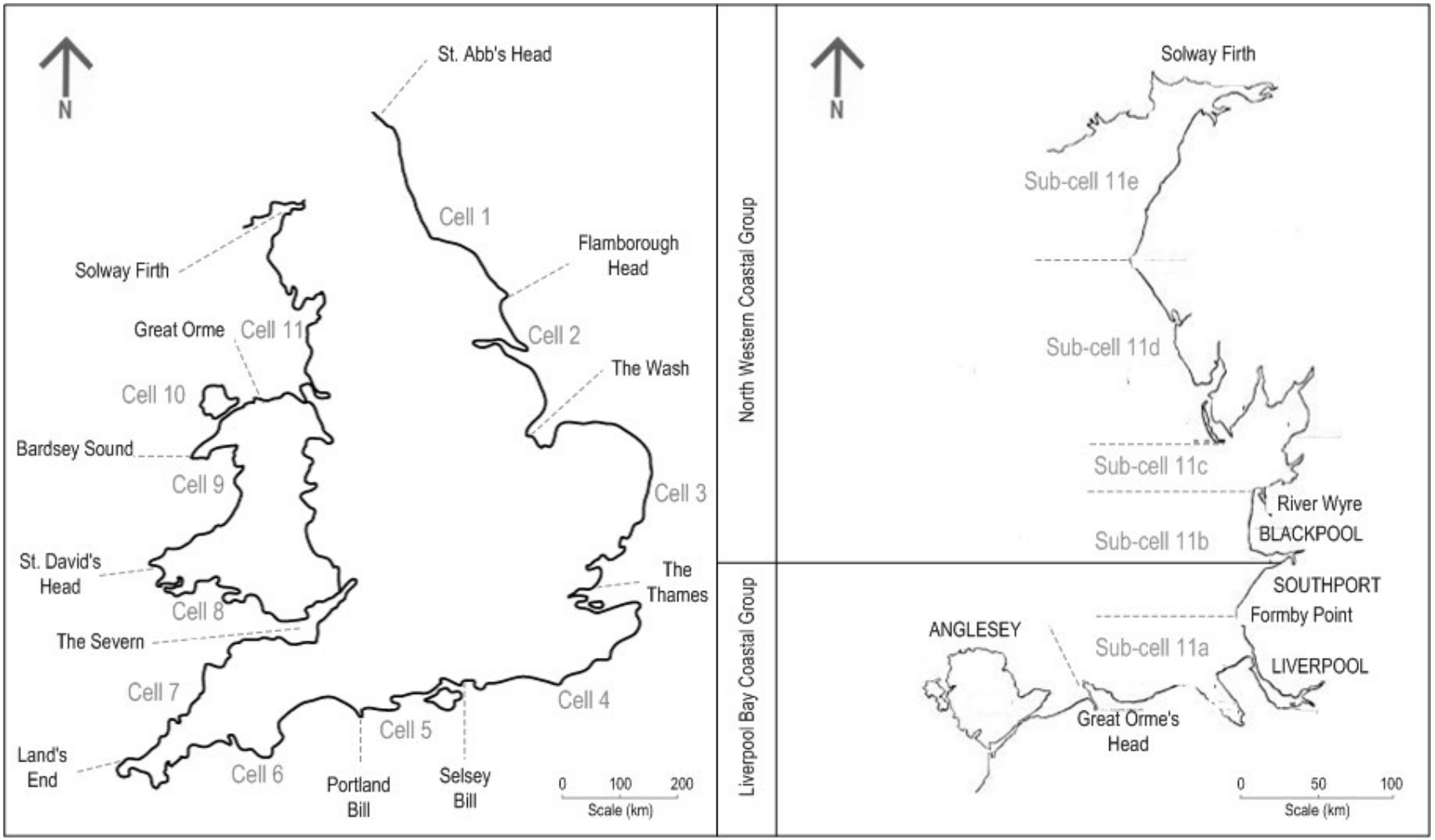

Figure 8.1 Strategic overview of coastal groups: a) coastal cell groups in England and Wales; and b) location of sub-cells 11a and 11b.

coast falls within the two sub-cells, 11a and 11b, each with its own SMP. The Liverpool Bay SMP extends from Great Orme's Head to Formby Point and the Ribble Estuary SMP from Formby Point to the River Wyre.

Stage 1 of the Liverpool Bay SMP preparation identified the primary division of the shoreline into eight coastal process units (CPU) based on coastal process evaluation (Liverpool Bay Shoreline Management Plan, 1993), with CPU8 including part of the Sefton coast from Seaforth Dock to Formby Point. The existing coastal defence policy for CPU8 is 'hold the line', identified by the Liverpool Bay Shoreline Management Plan (1993), which remains the same course of action for future coastal defence policies, for both short-term (<10-15 years) and anticipated long-term (<50 years) management.

Evaluation of coastal process behaviour within sub-cell 11b identified eight CPUs based on coastal process evaluation (Ribble Estuary Shoreline Management Plan, 1999), with both CPU7 and CPU8 including part of the Sefton coast from Southport to Ainsdale and then Ainsdale to Formby Point, respectively. The existing coastal defence policy for CPU7 is 'natural defence management' and 'hold the line', identified by the Ribble Estuary Shoreline Management Plan (1993), which remains the same course of action for short-term (<10-15 years) future coastal defence policies and is just 'hold the line' for anticipated long-term (<50 years) management. The existing coastal defence policy for CPU8 is 'natural defence management', which remains the same course of action for short-term (<10-15 years) future coastal defence policies and is combined with managed 'retreat the line' for anticipated long-term (<50 years) management.

8.3 Effects of current coastal habitat management on pedogenesis

8.3.1 Coastal forcing

Gradual sea level rise is often considered to be the main contributing factor to coastal change (e.g. Hulme *et al.,* 2002; Evans *et al.,* 2004). However, increased storminess is constantly affecting shorelines by destroying essential sediment barriers (Woodroffe, 2002). If climatic changes accompanying sea level rise result in drier and windier conditions (IPCC, 2007), coastal dunes that are presently stable and vegetated may become unstable as vegetation cover is weakened and sand mobilized, and dunes that are already active will become increasingly mobile. However, a wetter or calmer climate could facilitate dune stabilization (Bird, 2000; Pye, 2001).

Initial coastal features to be affected by rising sea level are the beaches, which could be lost if erosion is allowed to prevail. Present management practices aim to avoid loss of beaches to erosion by managing the risk of flooding (North West and North Wales Coastal Group, 2008). However, the long-term effects of this on pedogenesis beyond the foredunes would be a reduction in availability of aeolian derived sand and, subsequent rapid acidification, creating a pedo-environment unsuitable for natural dune habitats. On the other hand, warmer

temperatures may increase evaporation, leading to greater capillary rise of groundwater. This, along with extensive marine inundation and rising soil water tables, could cause increased soil salinization (Fullen and Catt, 2004).

Another loss prevention management practise, adopted during increased storminess, involves dune re-profiling, with minimal regard for barrier width. Re-mobilization, or natural 'dune roll-back' transgression processes, due to overwash and barrier retreat, are often prevented by fixed landward boundaries (artificial or otherwise), termed 'coastal squeeze', causing destabilization of key pedo-environments and direct loss of associated dune habitats (Doody, 2001). This often occurs at a greater rate than simple inundation (Orford and Pethick, 2006), not allowing sufficient time for natural pedogenic recovery. This issue becomes especially complicated when the fixed boundary is a specific habitat valued for biodiversity (Johnston *et al*., 2002). For example, it is recognized that both natural and anthropogenic processes can alter dune habitats, with the latter often regarded as unacceptable (e.g. Atkinson, 1988; Hill and Wallace, 1989). However, conflicts occur when the fixed boundary under preservation (e.g. coniferous plantations) is anthropogenic in origin and publicly perceived as a natural habitat.

8.3.2 Spatial constraints

The effects of vertical variations in sea level are constantly challenged (IPCC, 2007), but horizontal variations and coastal realignment are rarely considered for spatial availability in future absorption of coastal energy. Integrated management practices allow managed realignment for sea-defence purposes (Leggett *et al*., 2004) due to its low cost. According to Orford and Pethick (2006), most UK coastal managers do not perceive shoreline realignments to exceed the current coastal zone limits.

It has been reported on the Sefton coast (e.g. Gresswell, 1953; Turner, 1984; Pye and Neal, 1994; Saye *et al.,* 2005; Pye and Blott, 2008) that erosion of Formby Point is paralleled by increased accretion rates on northern and southern margins, resulting in formation of new stabilized fixed dune habitats (Edmondson *et al.,* 2001) and associated soil profiles. The existing SMP coastal defence policy, for the section of coast within Cell 11a CPU8 (that extends from the River Alt Pumping Station to Formby Point), is 'do nothing' (Liverpool Bay Shoreline Management Plan, 1993). This remains the same course of action for both short-term and anticipated long-term future management. However, if this policy is adopted, as realignment processes continue in order to absorb future coastal energy, new habitats are unlikely to be sustainable. Such formations should be viewed as temporary as the coast is likely to continue retreating with associated pedo-environments continuously taking on new characteristics.

8.3.3 Creation of dune habitats

Dune managers have tried to overcome the potential loss of dune habitats and biodiversity by recreating habitats that cannot easily be maintained in other locations, improving recreation and amenity value. However, these practices have detrimental effects on pedogenic processes, as

new nature areas (i.e. scraped slacks and artificially flattened dune pastures for agriculture) are often created by digging away complete soil profiles. The resultant bare sand sets back ecosystem development by decades (van den Ancker and Jungerius, 2007). Subsequently, poor soil conditions will affect the success of habitat creation schemes, as low soil fertility will prevent species establishment and high fertility may result in a few dominant species and exclusion of others (Fullen and Catt, 2004). There should also be concerns about how permanent these newly created coastal habitats are (refer to Section 8.3.2).

The existing SMP coastal defence policy, for the section of coast within Cell 11b CPU8 that extends from the Ainsdale NNR North boundary to Dale Slack Gutter, is 'natural defence management' (Ribble Estuary Shoreline Management Plan, 1999), which remains the same course of action for short-term future management and is combined with managed 'retreat the line' for anticipated long-term management. Within this SMP policy, the importance of creation and/or maintenance of natural habitat diversity are expressed. Managed retreat of the shoreline includes the use of stabilization techniques, such as artificial planting, in an attempt to control shoreline behaviour. Whilst this allows natural dune processes to continue relatively unhindered, it is also likely to have adverse effects on natural soil development and pedo-properties.

For successful managed retreat, mobile dune widths must be maintained at present levels to encourage dune growth during environmentally stable periods; whilst, allowing for dune erosion under unstable regimes. This will require continued woodland clearing, resulting in subsequent development of natural soil profiles encouraging vegetation succession towards a flora more representative of natural dune landscapes. As soils are an integral part of the coast, soil diversity and responses should be taken into account when managing dune areas.

8.4 A need for revised coastal policies

Policies and actions defined within SMPs are proposed to be implemented at the present time. However, the plans are working documents to be re-evaluated at regular intervals as new information and data become available. For example, the belief that protection provided by contemporary natural dune barriers will not be maintained in future circumstances, due to sea level rise, can be overcome by an increased understanding of the processes that shape and maintain the dune landscape. It is widely accepted that dunes do not 'roll-over' or migrate for any great distance or timescale, as a developing foredune is halted once the stationary vegetated hind dune ridges are met (Doody, 2001). However, it is now known that the cessation of a migrating dune ridge can be overcome by encouragement of grazing or trampling pressure (Pethick, 1984) thereby, retaining a dynamic mobile dune system, rather than adopting stabilization techniques, such as planting.

Expanding knowledge may necessitate a change in coastal defence strategy. Now as the first generation of SMPs are currently under review, these management practices may no longer be adequate given that dunes are recognized to form an active part of the system during storms

(Cooper, 2007) and soils should be regarded as playing a vital role in dune preservation (van den Ancker and Jungerius, 2007). Table 8.1 highlights eight management objectives, initially identified by the Coast Management Scheme Steering Group (1983), which were designed to combat degradation of the Sefton dunes and reduce the threat of marine flooding. Table 8.1 also identifies Cell 11 SMP (1993; 1999) objectives for the same challenges a decade later and, draft broad scale SMP2 actions for the next 100 years. The final column outlines how findings in this research can aid stakeholders to recognize that soils play a vital role in dune systems.

8.4.1 Role of the conceptual pedogenic models in coastal dune management

The conceptual models, presented in Chapter 7 (Figures 7.21-24) should be included in future policies and actions defined within the SMPs, as they contain new information and data for the Sefton coast. The models do not simulate rising sea level, but they do identify the effects of coastal forcing on pedogenic processes, which can inform dune managers of the key geochemical, textural and mineral magnetic parameters that are considered important under varying management techniques.

The conceptual model of the entire Sefton coastal dunes landscape (Chapter 7, Figure 7.21) considers soil development under erosion of Formby Point paralleled by accretion in the north and south. Therefore, this model can be applied to other coasts that are undergoing 'managed realignment' for sea-defence purposes. Managed retreat of the shoreline can include stabilization techniques, such as artificial planting, which have proved detrimental to natural soil characteristics on the Sefton coast. The model suggests that continued deforestation would result in natural soil profile development, encouraging vegetation succession towards a flora more representative of natural dune landscapes. However, if viewed alongside the conceptual model for the eroding coast (Chapter 7, Figure 7.23), dune managers can consider potential implications of the 'do nothing' management policy, which would include rapid loss of fixed dune habitats and cessation of aeolian derived sand, resulting in very acidic dune soils unable to support natural dune flora.

8.5 Summary

An essential requirement to future dune management is to gain an appreciation of the scale of coastal retreat. Ultimately, the responsibility for updating and reviewing the SMP lies with the authorities involved. However, it is also important that this soil information is shared. It should be realized that sustainable pedo-environments and habitats are temporal rather than spatial, and that future pedogenic development should be considered as cyclic. The conceptual models have established that, unlike previous management strategies, in the absence of human interference pedo-environments could either maintain themselves adequately or develop both laterally and spatially in a recognized sequence, depending on erosional/depositional forces. It must be accepted, some natural coastal habitats are going to be 'squeezed' or lost under rapid transgressive conditions and temporary habitats will have to be accepted as substitutes. This expanding knowledge may contribute towards a change in coastal defence strategy.

Table 8.1 Eight management objectives for the Sefton coast identified by the Coast Management Scheme Steering Group (1983), with SMP suggestions alongside revised management techniques, recognizing soils play a vital role in dune systems

Objective	Integrated Coastal Zone Management Plan	Coast Management Scheme Steering Group (1983)	Shoreline Management Plan for Cell 11 (1993-99)	Draft Shoreline Management Plan 2 for Cell 11 (2010-2100)	Proposed revision of future dune management incorporating the role of soils (2009)
1. Dune conservation		To maintain the dune system as a natural sea defence.	To maintain, manage and encourage the development of natural coastal defences and recommend appropriate measures to mitigate against problems from erosion of Formby Point.	Identify opportunities to maintain and improve the environment by managing the risks from floods and coastal erosion.	To encourage a mobile dune system and prevent unnatural vegetation succession, through destabilization techniques such as increased grazing and trampling.
2. Landscape maintenance and renewal	To support development that is coast dependent and sustainable within the coastal zone.	To maintain the quality of the dune landscape and to restore it in those areas where it has been degraded.	To preserve the foreshore and dune areas, in particular designated sites of environmental interest, in a way that is compatible with sea defence and coastal protection considerations.	Inform others so that future land use, planning and development of the shoreline takes account of the risks and the preferred policies.	To allow natural evolution of pedo-environments and habitats and to accept that some habitats may be lost.
3. Woodland management		To maintain the continuity and quality of woodland cover, extending it in some areas to screen unattractive developments.	Woodland clearing for successful managed retreat.		Unchanged from SMP...and to understand that woodland cover is not necessarily a natural dune environment, halts vital sedimentary movement and alters soil characteristics beyond successful reversion.
4. Nature Conservation	Conserve, protect and enhance the landscape character, natural beauty and biodiversity of the coast.	To maintain and where appropriate widen the diversity of habitats and the wildlife they contain.	Implementation of Habitats Directive.	Opportunities exist to create wetland habitat in low-lying parts of the SMP2 area.	To understand that artificially creating habitats destroys pedogenic processes and decreases ecosystem development.
5. Foreshore management	Develop appropriate coast defence strategies, maintaining sea defence of beaches, sand dunes and salt marshes consistent with natural character and conservation importance of the coast.	To improve the appearance of the foreshore through measures such as litter collection.	To realise that beach cleaning affects habitats.	Identify the preferred policies for managing risks from floods and erosion over the next century.	Unchanged from SMP.
6. Visitor management	Develop opportunities for recreation, sporting and tourist activities that are consistent with the natural character and conservation value of the coast.	To deal with recreational demands in such a way as to minimize damage to the dune system and its habitats while continuing to allow public enjoyment of the area.	Improvement of the landscape quality of the area, where necessary, and management of visitor pressure so that the environment is protected and people's enjoyment and understanding of it enhanced.	To minimise coastal flood and erosion risk to key community, recreational and amenity facilities.	To balance anthropogenic utilization with a naturally dynamic system.
7. Interpretation	Facilitate and enhance understanding, enjoyment and appreciation of the coast by creating opportunities for education.	To increase people's understanding of the area, their enjoyment of it and care of it.	To facilitate on-going consultation between those bodies with an interest in the shoreline.	Set out the risks from flooding and erosion to people and the developed, historic and natural environment within the SMP2 area.	Unchanged from SMP...and to increase public awareness of the critical role soils play on the coast.
8. Research	Promote awareness and create opportunities for research including collaborative research activities.	To collect and assess information about changes affecting the area, and to review regularly the effectiveness of management techniques and polices.	To continue and enhance present coastal process monitoring to provide further data from which the scale and magnitude of policy actions can be defined.	Highlight areas where there are gaps in knowledge about the coast and produce an action plan to address these gaps.	Unchanged from SMP.

CHAPTER 9
Conclusions

The conclusions of this research project outline the scientific contribution to understanding pedogenesis on the Sefton coast. The main findings are related back to the original aims and objectives, through applying summary detail from each section into a concise synopsis. Suggestions for further work are proposed.

9.1 Advances to scientific knowledge

This research project stimulates discussion on soil heritage and its role as an integral part of the coastal system, an issue that is generally disregarded in coastal dune management. Scientific advancement is focused on; i) the potential to associate topsoil characteristics with classified soil profiles and ii) the 'fresh' approach to conceptual modelling of pedogenesis on varying coastal dunes.

9.1.1 Soil associations

Distinguishing dune environments' using topsoil pedo-characteristics and, subsequently, associating these pedo-environments with NRSI profile classifications, has proved successful. As, only simple physico-chemical analyses of selected topsoil (0-5 cm) samples are required, this approach provides an alternative to digging soil profiles, which can be detrimental to the environment and is time-consuming. Potentially, the relationship between topsoils and vegetation cover could be applied to any desk-based study of multi-date dune vegetation maps, providing surrogate information on relative proportions of pedo-environments. This would aid the understanding of pedogenic processes involved in dune succession and the prevailing direction, in which, these processes are happening.

9.1.2 Application of the conceptual models

The concept behind the pedogenic models is based on using soil physico-chemical measurements to address coastal environmental change problems; an issue relevant on all coasts. The models identify processes operating within dune habitats that are not necessarily visible on the surface, but are, nevertheless, affected by both natural and anthropogenic influences that alter habitat characteristics. Understanding such pedogenic responses is vital for dune management, especially when confronted with issues such as artificial habitat creation/removal or 'coastal squeeze'. This pedogenic conceptual model technique could be used to validate sand dune succession if utilized in conjunction with other dune models, such as geomorphology and sedimentology processes and vegetation data.

9.1.3 Regional, national and international implications

Given the scientific and public concerns regarding the Sefton coast environment and how it may evolve, the findings of this research project would benefit the next generation of shoreline management plans (SMPs) in this area, by providing evidence that fixed dune topography, by

vegetation, is an inappropriate management technique, as natural soil characteristics are altered, often to an irreversible degree. As the conceptual models aid determining long-term pedogenesis, they can be utilized under DEFRA's recommendation that options should be appraised over a 100-year period, rather than 50 years (DEFRA, 2003), to offer a sustainable vision for the coast. The role of soil was not fully considered in the first generation SMPs; therefore, this project suggests the SMP2 reviews take advantage of these research findings, to aid guidance on the strategic direction for this coastal unit.

Given concerns regarding the effects of rising eustatic sea-level, the conceptual models of pedogenesis in both erosional and depositional regimes could be applied to national and international coastal dune landscapes, where coastal process and historical shoreline change data could be complemented or are unavailable, or where similar chronologies of increasingly acidic soils exist. For example, across the Ayres, northern coast of the Isle of Man, or on dunes on the South Haven peninsula, Dorset, where leaching of carbonates and iron oxides have occurred (Ranwell, 1972). Patterns of soil development on the Sefton coast could also be correlated with chronologies from The Netherlands (e.g. Jelgersma *et al.,* 1970) to aid identification of large scale forcing of dune system evolution. This approach can help the strategies of dune managers, coastal engineers, commercial activities and conservation management plans by offering a means of understanding and determining the rates of past, present and perhaps future pedogenesis of coastal dunes.

9.2 Overall synopsis of research findings relating to original aims and objectives

- Analysis and mapping of topsoil characteristics have defined pedo-environment boundaries, which correspond to existing vegetation habitats. Dune pedo-succession is a combined function of atmospheric inputs, fluctuating leaching rates, translocation rates, eluviation and illuviation. To some extent, the difference between each of these characteristics has shown potential to distinguish ‘frontal dune’ topsoils (i.e. bare sand and mobile dune communities), heath topsoils, slack community topsoils and ‘hind dune’ topsoils (i.e. fixed dune community, pasture, scrub, deciduous woodland and coniferous plantation). However, absolute distinctions are not entirely possible, suggesting dune environments are linked by pedogenic processes.
- National Soil Resources Institute (NSRI) classifications have been identified and assigned to independent dune environments, but are also linked by order of pedo-succession. Pedogenic processes between soil profile horizons have been identified and used to determine both natural and anthropogenically induced soil evolution trends from the shoreline to hind dunes.
- Development of a geomorphopedological (GMP) map illustrates the spatial distribution of NRSI soil profile classifications on the Sefton dunes, based on topsoil characteristics. Soils have been divided into three coastal units, governed by accretion and erosion/deposition regimes. Conceptual models of pedogenesis on the Sefton coastal dunes highlight the

impact of geomorphic and anthropogenic influences on proposed pedogenic pathways within each coastal unit.

- Reconstruction of historic dune environments was achieved through identification and classification of buried soils on the shoreline. This has aided development of a cyclic model, used to graphically represent the recurring cyclic nature of dune mobilization and, subsequent, dune stabilization/soil development phases, as a function of marine regression and transgression.
- Through consideration of shoreline behaviour diversity and changing dune dynamics, three centuries of macro-scale natural and anthropogenic coastal changes have been identified on the Sefton coast, responding to cyclic phases of coastal transgression and regression. Meso-scale dune morphological changes are generally associated with varying erosion and accretion regimes, operating under wave refraction patterns. Fixed Point Photography (FPP) identified erosion and, subsequent, landward migration of the dunes on a micro-scale and seasonal timescale.
- Recommendations for dune management are to allow the Sefton sand dunes to act as a natural dynamic flood defence in response to sea-level rise and shoreline erosion. In the interest of both geomorphological and ecological diversity, permitting these systems to evolve naturally, wherever possible, is preferred. Allowing natural cyclic episodes of fresh bare sand deposition, interspersed with developments of young soil profiles, will retain a healthly, nourished dune landscape. These habitats will be capable of supporting native dune flora and fauna, as opposed to an unnaturally acidic environment, in which a thick layer of pine needles inhibits any future pedogenic evolution for the foreseeable future. Loss of habitat and associated soil profiles is inevitable, but will be compensated by gains in other areas and by the enhanced value of a dynamic landscape.

9.3 Suggestions for future work

The following points highlight possible directions for future work on pedogenesis on the Sefton coastal dunes:

- Continuation of the FPP survey would provide an ongoing monitoring programme of erosion and accretion processes seasonally, annually and possibly decadal, to provide long-term understanding of dune dynamics in response to both internal and external factors. The inclusion of more FPP stations, both alongshore and inland along transects, would provide increased detail on spatial extremity and ‘knock-on’ effects of geomorphic processes. In conjunction with the FPP, annual conductions of the dune toe survey should continue to determine the pivot point between erosion/accretion zones and identify any directional trends. It may prove beneficial to also conduct both photographic surveys after storm events to gain insights into the time-lags involved in dune response.
- Further topsoil sampling would provide more accurate representation of pedo-environment distribution on the Sefton dunes, towards obtaining a higher resolution GMP map. Contemporary topsoil samples collected annually or seasonally would monitor whether physico-chemical soil characteristics, from each pedo-environment, vary over time.

- Seasonal coring at soil profile location sites and physico-chemical analysis would investigate the effects of groundwater fluctuations on pedogenic processes, which subsequently would provide insights into predicting the future response of dune soils to climate change (i.e. increased rainfall/storminess). A soil profile transect analysis, ranging from a dry frontal dune pedo-environments through to a slack and, finally, a hind dune pedo-environment, would determine rates of pedogenesis and dune migration. Depending on the transect location, the effects of plantations on dune hydrology may also be monitored, the results of which would contribute towards future dune stabilization decisions as part of SMP2s.
- The extent of the buried soil on the shoreline could be investigated through coring at regular intervals in both alongshore and seaward directions at low tide, to improve understanding of the historic pedo-environment spatial distribution and sea regression extent. Similar methods could be applied to buried organic layers, exposed in dune cliffs, to determine spatial distributions alongshore and inland. With the exception to the two buried soil profiles already analysed, further buried soils have been identified (n = 12), bulk-sampled and analysed for all physico-chemical parameters across the dunes. Due to time limitations, these soils have not been mapped or discussed. However, soil classification and mapping would, to some extent, identify the spatial distribution of historic pedo-environments and provide an insight into the cyclic nature of dune evolution.
- As buried soils often preserve pollen from the vegetation at the time of stability and associated soil formation, pollen analysis, along with existing sea level and morphological chronology data, would confirm pedo-environment classification and provide evidence for environmental reconstruction. However, preservation of such pollen may be limited and the transport distance of pollen by aeolian processes must be considered in such a relatively small landscape.
- The conceptual models could be updated to incorporate buried soil profile physico-chemical properties to establish relative proportions of historic pedo-environments and the pedogenic processes involved in their alteration. The model could then be employed to both reconstruct and predict environmental change.
- Modelling of pedogenesis on the Sefton coastal dunes could be enhanced further by applying OS contours to a GIS program, creating a three-dimensional computer aided graphics model that could be used to model the effects of existing sea level rise predictions on dune landscapes. Aerial photography, dune environment and GMP map overlays would ascertain the pedo-environments likely to be effected by rising sea-level and groundwater and may even suggest future dune migration and pedogenic pathways.
- Finally, it is necessary to apply this research, along with the updated future work, to other regional, national or international coastal dune systems to investigate the wider applicability of these pedogenic monitoring techniques and conceptual models.

References

Aitkenhead, M.J. and Aalders, I.H. (2009) Predicting land cover using GIS, Bayesian and evolutionary algorithm methods. *Journal of Environmental Management*, **90**, 236-250.

Ampe, C. and Langohr, R. (1993) Distribution and dynamics of shrub roots in recent coastal dune valley ecosystems of Belgium. *Geoderma,* **56**, 37-55.

Ampe, C. and Langohr, R. (2003) Morphological characterisation of humus forms in recent coastal dune ecosystems in Belgium and northern France. *Catena,* **54**, 363-383.

Andrews, B.D., Gares, P.A. and Colby, J.D. (2002) Techniques for GIS modelling of coastal dunes. *Geomorphology,* **48**, 289-308.

Anselin, L. (2000) Computing environments for spatial data analysis. *Journal of Geographical Systems,* **2**, 201-220.

Anthony , E.J., Vanhée, S. and Ruz , M.H. (2006) Embryo dune development on a large, actively accreting macrotidal beach: Calais, North Sea coast of France. *Earth Surface Processes and Landforms,* **32(4)**, 631-636.

Arens, S.M. (1997) Transport rates and volume changes in coastal foredunes on a Dutch Wadden Island. *Journal of Coastal Conservation,* **3**, 49-56.

Ashman, M.R. and Puri, G. (2002) *Essential Soil Science.* Blackwell, Oxford.

Aspinall, R.J., Miller, D.R. and Birnie, R.V. (1993) Geographical information systems for rural land use planning. *Applied Geography,* **13**, 54-66.

Atkinson, D. (1988) The effects of afforestation on a sand dune grassland. *British Ecological Society Bulletin,* **29(2)**, 99-101.

Atkinson, D. and Sturgess, P.W. (1991) Restoration of sand-dune communities following deforestation. *Perturbation and Recovery of Terrestrial and Aquatic Ecosystems.* Ellis Horwood, London.

Avery, B.W. (1980) *Soil Classification for England and Wales (Higher Categories),* Soil Survey Technical Monograph 14. Soil Survey of England and Wales, Harpenden.

Avery, B.W. and Bascomb, C.L. (1982) *Soil Survey Laboratory Methods*. Soil Survey of England and Wales, Harpenden.

Bailey, S.D. and Bristow, C.S. (2004) Migration of parabolic dunes at Aberffraw, Anglesey, north Wales. *Geomorphology,* **59**, 165-174.

Bakker, T.W.M., Jungerius, P.D. and Klijn, J.A. (1990) *European Coastal Dunes.* Catena Supplement, **18**, 31-39.

Ball, D.F. (1964) Loss-on-ignition as an estimate of organic matter and organic carbon in non-calcareous soils. *Journal of Soil Science,* **15**, 84-92.

Banerjee, S.K., King, J., and Marvin, J. (1981) A rapid method for magnetic granulometry with applications to environmental studies. *Geophysical Research Letters*, **8**, 333-336.

Barton, J. (1981) *The taxonomy of* Salix repens *agg. and related ecological aspects at Ainsdale Sand Dunes National Nature Reserve.* Unpublished B.Sc. thesis, University of Liverpool.

Beach Protection Authority (1982) Report No D. 02. 8. *Mulch Trial*. Dune Management Research Papers, Beach Protection Authority, Brisbane, Australia.

Beard, G.R., Thompson, T.R.E. and Lea, J.W. (1987) *Soils of the Liverpool District.* Memoirs of the Soil Survey of England and Wales.
Beltman, B., Kooijman, A.M., Ellers, J. and Oosterbeek, B.J. (1992) Nutrient availability and plant species composition of rich fens in the dune complex at Dooaghtry, Co. Mayo, Ireland. In: R.W.G. Carter, T.G.F. Curtis and M.J. Sheehy-Skeffington (Eds.). *Coastal Dunes.* Balkema, Rotterdam.

Bengtsson, L. and Enell, M. (1986) Chemical analysis. In: B.E. Berglund. *Handbook of Holocene Palaeoecology and Palaeohydrology.* John Wiley, Chichester and New York.

Berendse, F. (1998) Effects of dominant plant species on soils during succession in nutrient-poor ecosystems. *Biogeochemistry,* **42**, 73-88.

Bird, E.C.F. (1985) *Coastline Changes, A Global Review.* Wiley & Sons Ltd., Chichester.

Bird, E.C.F. (1993) *Submerging Coasts: The Effects of a Rising Sea Level on Coastal Environments.* John Wiley & Sons, Chichester.

Bird, E.C.F. (1995) *Geology and Scenery of Dorset.* Ex Libris, Bradford on Avon.

Bird, E.C.F. (1998) *The Coasts of Cornwall.* Alexander, Fowey.

Bird, E.C.F. (2000) *Coastal Geomorphology: An introduction.* John Wiley & Sons Ltd, England.

Bird, E.C.F. and Jones, D.J.B. (1988) The origin of foredunes of the coast of Victoria, Australia. *Journal of Coastal Research,* **4**, 181-192.

Blanchard, B. (1952) *An Ecological Survey of the Sand Dune System of the South West Lancashire Coast, with Special Reference to an Associated Marsh Flora.* Unpublished Ph.D. Thesis, University of Liverpool.

Bloomfield, C. (1951) Experiments on the mechanism of gley formation. *Journal of Soil Science,* **2**, 196-221.

Bock, M.D. and Van Rees, K.C.J. (2002) Forest harvesting impacts on soil properties and vegetation communities in the Northwest Territories. *Canadian Journal of Forest Research,* **32**, 713-724.

Bockheim, J.G., Gennadiyev, A.N., Hammer, R.D. and Tandarich, J.P. (2005) Historical development of key concepts in pedology. *Geoderma,* **124**, 23-36.

Bohren, C.F. and Huffman, D.R. (1998) *Absorption and Scattering of Light by Small Particles*. John Wiley & Sons, New York.

Booth, C.A. (2002) *Sediment-source-linkages in the Gwendraeth Estuary, South Wales, Based on Mineral Magnetic Analyses*. Unpublished Ph.D. Thesis, University of Wolverhampton.

Booth, C.A., Fullen, M.A., Jankauskas, B. and Jankauskiene, G. (2003) International calibration of the textural properties of Lithuanian Eutric Albeluvisols. *Soil Science and Agrochemistry. Journal of the Lithuanian Academy of Sciences,* **4**, 3-10.

Booth, C.A., Fullen, M.A., Smith, J.P., Hallett, M.D., Walden, J., Harris, J. and Holland, K. (2005) Magnetic properties of agricultural topsoils of the Isle of Man: Their characterization and classification by factor analysis. *Communications in Soil Science and Plant Analysis,* **36(9&10)**, 1241-1262.

Booth, C.A., Fullen, M.A., Smith, J.P., Hallett, M.D., Walden, J., Harris, J. and Holland, K. (2006) Factor analysis of particle size specific mineral magnetic measurements on agricultural topsoils from the Isle of Man. *Communications in Soil Science and Plant Analysis,* **37**, 249-273.

Booth, C.A., Walden, J., Neal, A., Smith, J.P. and Morgan E. (2004) A comparison of inter-site, intra-site, intra-sample and instrument variability in environmental magnetic data: an example based on the Gwendraeth Estuary, South Wales, U.K. *Journal of Coastal Research,* **20(3)**, 808-813.
Brady, N.C. and Weil, R.R. (1999) *The Nature and Properties of Soils.* Prentice-Hall, Inc. New Jersey.

Brodie, J. (1996) *The Development of Sand Dunes on the Sefton Coast, Lancashire.* Unpublished B.Sc. thesis, University of Birmingham.

Burkmar, R. (2008) *Revision note for: Sand Dunes HAP for North Merseyside.* Unpublished.

Burrough, P.A. and McDonnell, R.A. (1998) *Principles of Geographical Information Systems*. Clarendon Press, Oxford.

Calder, I., Garratt, J., James, P. and Nash, E. (2008) Models, myths and maps: Development of the Exploratory Climate Land Assessment and Impact Management (EXCLAIM) tool. *Environmental Modelling & Software,* **23**, 650-659.

Carter, R.W.G. (1991) Near-future sea-level impacts on coastal dune landscapes. *Landscape Ecology,* **6**, 9-40.

Carter, R.W.G. and Wilson, P. (1990) The geomorphological, ecological and pedological development of coastal foredunes at Magilligan Point, Northern Ireland. In: K.F. Nordstrom, N. Psuty and R.W.G. Carter (Eds.). *Coastal Dunes: form and process.* John Wiley & Sons, Chichester.

Carter, R.W.G., Hesp, P.A. and Nordstrom, K.F. (1990) Erosional landforms in coastal dunes. In: K.F. Nordstrom, N. Psuty and R.W.G. Carter (Eds.). *Coastal Dunes: Form and Process.* John Wiley & Sons, Chichester.

Carter, R.W.G., Johnston, T.W., McKenna, J. and Orford, J.D. (1987) Sea-level, sediment supply and coastal changes: examples from the coast of Ireland. *Progress in Oceanography,* **18**, 79-101.

Challinor, D. (1968) Alteration of surface soil characteristics by four tree species. *Ecology,* **49**, 286-290.

Chamberlain, E.J. and Butt, K.R. (2008) Distribution of earthworms and influence of soil properties across a successional sand dune ecosystem in NW England. *European Journal of Soil Biology,* **44**, 554-558.

Charlesworth, S.M. and Lees, J.A. (1997) The use of mineral magnetic measurements in polluted urban lakes and deposited dusts, Coventry, UK. Physics and Chemistry of the Earth, **22**, 203-206.

Charlesworth, S.M. and Lees, J.A. (2001) The application of some mineral magnetic measurements and heavy metal analysis for characterizing fine sediments in an urban catchment, Coventry, UK. *Journal of Applied Geophysics,* **48**, 113-125.

Chen, C.R., Condron, L.M. and Xu, Z.H. (2008) Impacts of grassland afforestation with coniferous trees on soil phosphorus dynamics and associated microbial processes: A review. *Forest Ecology and Management,* **255**, 396-409.

Chen, T-H., Chiu, C-Y. and Tian, G. (2005) Seasonal dynamics of soil microbial biomass in coastal sand dune forest. *Pedobiologia,* **49**, 645-653.

Chittleborough, D.J., Tejan-Kelle, M.S. and Fitzpatrick, R.W. (1998) Genesis of podzols on coastal dunes in southern Queensland. V. chemistry and mineralogy of the non-opaque heavy mineral fraction. *Australian Journal of Soil Research,* **36(4)**, 699-714.

Choi, K. (2005) Pedogenesis of Late Quaternary deposits, northern Kyonggi Bay, Korea: Implications for relative sea-level change and regional stratigraphic correlation. *Palaeogeography, Palaeoclimatology, Palaeoecology,* **220**, 387-404.

Christiansen, C. and Bowman, D. (1986) Sea level changes, coastal dune building and sand drift, northwestern Jutland. *Geografisk Tidskrift,* **86**, 28-31.

Christiansen, C., Blæsild, P. and Dalsgaard, K. (1984) Reinterpreting 'segmented' grain-size curves. *Geological Magazine,* **121**, 47-51.

Claydon, B. and Hollis, J.M. (1984) *Criteria for Differentiating Soil Series.* Soil Survey Technical Monograph No.17, Lawes Agricultural Trust, Harpenden.

Coast Management Steering Group (1983) *Coast Management Scheme. Plan for Coastal Management Between Hightown and Birkdale – Metropolitan Borough of Sefton.* Planning Department, Sefton Metropolitan Borough Council, Bootle.

Cooper, A. (2007) Temporal coastal environments. In: C. Perry and K. Taylor (Eds.) *Environmental Sedimentology.* Blackwell Publishing.

Cooper, N.J. and Pontec, N.I. (2006) Appraisal and evolution of the littoral 'sediment cell' concept in applied coastal management: Experiences from England and Wales. *Ocean & Coastal Management,* **49**, 498-510.

CORINE (1991) *Examples of the Use of the Programme 1985-1990*. European Commission.

Cornell, R. and Schwertmann, U. (1996) *The Iron Oxides. Structure, Properties, Reactions, Occurrence and Uses.* VCH Verlagsgesellschaft, Weinham, New York.

Costantini, E.A.C., Fantappiè, M., Bocci, M., Marzocchi, S., Sacchi, G., Paolanti, M., Riveccio, R., Giorgianni, A. and Perciabosco, M. (2007) Monitoring soil erosion and landslides in Sicily by an integrated physiographic and geomorphological GIS. In: C. Dazzi (Ed.) *Changing Soils in a Changing World: the Soils of Tomorrow.* Book of Abstracts. 5th International Congress of the European Society for Soil Conservation. Palermo, Italy.

Crockford, R.H. and Willet, I.R. (2001) Application of mineral magnetism to describe profile development of toposequences of a sedimentary soil in south-eastern Australia. *Australian Journal of Soil Research,* **39**, 927-949.

Cruickshank, J.G. (1972) *Soil Geography.* David & Charles, Newton Abbot.

Crummay, S., Neil, C. and Spalding, A. (2001) Monitoring the changing ecology of sand dunes at Gear Sands SSSI and candidate SAC in conjunction with management of access, recreation and wildlife. In: J.A. Houston, S.E. Edmondson and P.J. Rooney (Eds.). *Coastal Dune Management. Shared Experience of European Conservation Practice.* Liverpool University Press.

Davis, J.C. (1986) *Statistics and Data Analysis in Geology.* 2nd. Edition, John Wiley & Sons, Chichester.

Davis, J.C. (2002) *Statistics and Data Analysis in Geology.* 3rd. Edition, John Wiley & Sons, Chichester.

Dearing, J.A. (1999) Magnetic susceptibility. In: J. Walden., F. Oldfield. and J.P. Smith. (1999) *Environmental Magnetism: A Practical Guide*, Quaternary Research Association, Technical Guide No. 6, Cambridge.

Dearing, J.A., Hay, K.L., Baban, S.M.J., Huddleston, A.S., Wellington, E.M.H. and Loveland, P.J. (1996) Magnetic susceptibility of soil: an evaluation of conflicting theories using a national data set. *Geophysical Journal International,* **127**, 728-734.

Dearing, J.A., Lees, J.A. and White, C. (1995) Mineral magnetic properties of acid gleyed soils under oak and Corsican Pine. *Geoderma,* **68**, 309-319.

Dearing, J.A., Maher, B.A. and Oldfield, F. (1985) Geomorphological linkages between soils and sediments: the role of magnetic measurements. In: R.R. Arnett and S. Ellis (Eds) *Geomorphology and Soils.* George Allen and Unwin, London.

DEFRA (2003). *Shoreline Management Plans.* Available:
http://www.defra.gov.uk/environment/flooding/policy/guidance/smp.htm.
Last accessed 6 November 2009.

de Jong, E., Pennock, D.J. and Nestor, P.A. (2000) Magnetic susceptibility of soils in different slope positions in Saskatchewan, Canada. *Catena,* **40**, 291-305.

de Rance, C.E. (1883) Notes on the Post-glacial geology of the country around Southport. *Nature,* **28**, 490-491.

Dobson, M.R, (1977) The geological structure of the Irish Sea. In: C. Kidson and M.J. Tooley (Eds) *The Quaternary History of the Irish Sea*. Seel House, Liverpool.

Doody, J.P. (1989) Management for nature conservation. *Proceedings of the Royal Society of Edinburgh,* 247-265.

Doody, J.P. (1991) *Sand Dune Inventory of Europe.* Joint Nature Conservation Committee, Peterborough, UK.

Doody, J.P. (2001) *Coastal Conservation and Management: an Ecological Perspective.* Kluwer, Academic Publishers, Boston, USA. Conservation Biology Series, **13**.

Duchaufour, P. (1982) *Pedology* (translated by T.R. Paton). Allen and Unwin, London.

Ebdon, D. (1978) *Statistics in Geography: A Practical Approach*. Basil Blackwell, Oxford.

Edmondson, S.E. (1991) *Temporal and Spatial Variations in Dune Slack Vegetation at Ainsdale, Merseyside.* Unpublished M.Sc. thesis. University of Liverpool.

Edmondson, S.E., Gately, P.S., Rooney, P. and Sturgess, P.W. (1993) Plant communities and succession. In: D. Atkinson, and J. Houston (Eds.). *The Sand Dunes of the Sefton Coast.* Eaton Press Ltd, England.

Edmondson, S.E., Traynor, H. and McKinnell, S. (2001) The development of a green beach on the Sefton Coast, Merseyside, UK. In: J.A. Houston, S.E. Edmondson and P.J. Rooney (Eds.). *Coastal Dune Management. Shared Experience of European Conservation Practice.* Liverpool University Press.

Edelman, T. (1968) Dune erosion during storm conditions. *Proceedings of the 11th Conference on Coastal Engineering.* London. **2**, 719-722.

Ellenberg, H. (1988) *Vegetation ecology of Central Europe*. Cambridge University Press.

Evans, E.P., Ashley, R., Hall, J.W., Penning-Rowsell, E.P., Saul, A., Sayers, P.B., Thorne, C.R. and Watkinson, A. (2004) *Foresight. Future Flooding: Scientific Summary: Volume I, Future Risks and their Drivers.* Office of Science and Technology, London.

Fairbanks, R.G. (1989) A 17,000-year glacio-eustatic sea level record: influence of glacial melting rates on the Younger Dryas event and deep-ocean circulation. *Nature*, **342**, 637-342.

Fairbridge, R.W. (1961) Eustatic changes in sea level. *Physics and Chemistry of the Earth,* **4**, 99-185.

Fassbinder, J.W.E., Stanjek, H. and Vali, H. (1990) Occurrence of magnetic bacteria in soil. *Nature,* **343**, 161-163.

Fialová, H., Maier, G., Petrovskỳ, E., Kapička, A., Boyko, T. and Scholger, R. (2006) Magnetic properties of soils from sites with different geological and environmental settings. *Journal of Applied Geophysics,* **59**, 273-283**.**

Fieller, N.R.J., Gilbertson, D.D. and Olbricht, W. (1984) A new method for environmental analysis of particle size distribution data from shoreline sediments. *Nature,* **311**, 648-651.

Fine, P., Singer, M.J. and Verosub, K. (1992) Use of magnetic-susceptibility measurements in assessing soil uniformity in chronosequence studies. *Soil Science Society of America Journal,* **56**, 1195-1199.

Fine, P., Singer, M.J., La Ven, R., Verosub, K. and Southard, R.J. (1989) Role of pedogenesis in distribution of magnetic susceptibility in two California chronosequences. *Geoderma,* **44**, 287-306.

Fitzpatrick, E.A. (1986) *An Introduction to Soil Science.* Longman, London.

Folk, R.L. (1964) *Petrology of Sedimentary Rocks.* Hemphills, Austin.

French, J.R., Spencer, T. and Reed, D.J. (1995) Editorial – Geomorphic response to sea level rise: Existing evidence and future impacts, *Earth Surface Processes and Landforms,* **20**, 1-6.

Fullen, M.A. (1991) A comparison of runoff and erosion rates on bare and grassed loamy sand soils. *Soil Use and Management,* **7**, 136-139.

Fullen, M.A. (1998) Effects of grass ley set-aside on runoff, erosion and organic matter levels in sandy soils in east Shropshire, UK. *Soil and Tillage Research,* **46**, 41-49.

Fullen, M.A. and Booth, C.A. (2006) Grass ley set-aside and soil organic matter dynamics on sandy soils in Shropshire, UK. *Earth Surface Processes and Landforms,* **31**, 570-578.

Fullen, M.A. and Catt, J.A. (2004) *Soil Management – Problems and Solutions.* Arnold, London.

Fullen, M.A. and Moore, G. (1999) Photographing dune dynamics. *Geography Review,* **November**, 14-17.

Fullen, M.A., Booth, C.A. and Brandsma, R.T. (2006) Long-term effects of grass ley set-aside on erosion rates and soil organic matter on sandy soils in east Shropshire, UK. *Soil & Tillage Research,* **89**, 122-128.

Fullen, M., Harris, J. and Kear, B. (1999) Soil-forming factors on the Isle of Man. *Geography Review,* **September**, 22-26.

Gale, S.J. and Hoare, P.G. (1991) *Quaternary Sediments*. Belhaven Press, London.

Galván, V., Torres Deluigi, M., Mentasty, L., De Vitoc, I. and Riverosa, J.A. (2009) Comparison between XRF and EPMA applied to study the ionic exchange in zeolites. *X-Ray Spectrometry*, **38**, 540-543.

Gares, P.A. (1992) Topographic changes associated with coastal dune blowouts at Island Beach State Park, New Jersey. *Earth Surface Processes and Landforms,* **17**, 589-604.

Gares, P.A. and Nordstrom, K.F. (1990) Topographic changes in a formerly stabilized dune system, in a coastal park. *Proceedings of the Symposium on Coastal Dunes.* National Research Council of Canada, Ottawa, 159-170.

Gee, M. (1991) *The Effect of a Coniferous Plantation upon the Water Table of a Sand Dune System.* Unpublished Postgraduate Diploma Project, Manchester Polytechnic.

Gerrard, J. (2000) *Fundamentals of Soils.* Routledge, London.

Gherardi, M., Lorito, S., Pontalti, F., Vianello, G. and Vittori Antisari, L. (2007) Evolution of soils on sandy formations under the impact of chestnut orchard reconservation. In: C. Dazzi (Ed.) *Changing Soils in a Changing World: the Soils of Tomorrow.* Book of Abstracts. 5th International Congress of the European Society for Soil Conservation. Palermo, Italy.

Gibson, D.J. and Looney, P.B. (1992) Seasonal variation in vegetation classification on Perdido Key, a barrier island off the coast of the Florida Panhandle. *Journal of Coastal Research,* **8(4)**, 943-956.

Goldsmith, V. (1985) Coastal Dunes. In: R.A. Davis, *Coastal Sedimentary Environments.* Springer-Verlag, New York.

Goldsmith, V. (1989) Coastal sand dunes as geomorphological systems. *Proceedings in the Royal Society of Edinburgh,* **96B**, 3-15.

Goodchild, M.F. (2000) Communicating Geographic Information in a Digital Age. *Annals of the Association of American Geographers*, **90(2)**, 344–355.

Green, R.N., Trowbridge, R.L. and Klinka, K. (1993) Towards a Taxonomic Classification of Humus Forms. *Forest Science*, 29, a0001-z0002(2).

Gresswell, R.K. (1953) *Sandy Shores in South Lancashire*. Liverpool University Press, Liverpool.

Guo, L.B., Cowie, A.L., Montagu, K.D. and Gifford, R.M. (2008) Carbon and nitrogen stocks in a native pasture and an adjacent 16-year-old *Pinus radiata* D. Don. plantation in Australia. *Agriculture, Ecosystems & Environment,* **124**, 205-218.

Hagedorn, F., Maurer, S., Egli, P., Bucher, J.B. and Siegwolf, R. (2001) Carbon sequestration in forest soils of soil type, atmospheric CO_2 enrichment and N deposition. *European Journal of Soil Science,* **52**, 619-628.

Hall, B.R. and Folland, C.J. (1967) Soils of the South-West Lancashire Coastal Plain (Sheets 74 and 83). *Memoirs of the Soil Survey of Great Britain England and Wales.* Harpenden.

Hanesch, M. and Petersen, N. (1999) Magnetic properties of a recent parabrown-earth from Southern Germany. *Earth and Planetary Science Letters,* **169**, 85-97.

Hansom, J.D. (2001) Coastal sensitivity to environmental change: a view from the beach. *Catena,* **42**, 291-305.

Hart, R. and Peterson, C. (2006) Late-Holocene buried forests on the Oregon coast. *Earth Surface Processes and Landforms*, **32**, 210-229.

Hendrickson, O.Q., Chatarpaul, L. and Burgess, D. (1989) Nutrient cycling following whole-tree and conventional harvest in northern mixed forest. *Canadian Journal of Forest Research,* **19**, 725-735.

Hentschel, K., Borken, W. and Matzner, E. (2007) Leaching losses of inorganic N and DOC following repeated drying and wetting of a spruce forest soil. *Plant and Soil,* **300**, 21-34.

Hesp, P.A. and Thom, B.G. (1990) Geomorphology and evolution of active transgressive dunefields. In: K.F. Nordstrom, N. Psuty and R.W.G. Carter (Eds.). *Coastal Dunes: Form and Process.* John Wiley & Sons, Chichester.

Hewett, D.G. (1970) The colonisation of sand dunes after stabilisation with marram grass (*Ammophila arenaria*). *Journal of Ecology,* **58**, 653-668.

Hill, M.O. and Wallace, H.L. (1989) Vegetation and environment in afforested sand dunes at Newborough, Anglesey. *Forestry,* **62**, 249-267.

Hodgson, J.M. (1997) *Soil Survey Field Handwork.* Soil Survey and Land Research Centre. Cranfield University, Soil Survey Technical Monograph No.5, Silsoe.

Houghton, J.T., Meira Filho, L.G., Callander, B.A., Harris, N., Kattenberg, A. and Maskell, K. (1996) *Climate Change 1995: The Science of Climate Change.* Cambridge University Press.

Houston, J. (1989) The Sefton coast management scheme in northwest England. In: F. van der Meulen, P.D. Jungerius and J.H. Visser (Eds.). *Perspectives in Coastal Dune Management,* The Hague, The Netherlands.

Houston, J. (1992) Blowing in the wind. *Landscape Design,* December 1991/January 1992.

Houston, J. (1993) Introduction to the Coast. In: D. Atkinson, and J. Houston (Eds.). *The Sand Dunes of the Sefton Coast.* Eaton Press Ltd, England.

Hulme, M., Jenkins, G.J., Lu, X., Turnpenny, J.R., Mitchell, T.D., Jones, R.G., Lowe, J., Murphy, J.M., Hassell, D., Boorman, P., McDonald, R. and Hill, S. (2002) *Climate Change Scenarios for the United Kingdom: the UKCIP02 Scientific Report,* Tyndall Centre for Climate Change Research, University of East Anglia, Norwich.

Hunter, R.E., Richmond, B.M. and Alpha, T.R. (1983) Storm-controlled oblique dunes of the Oregon coast. *Bulletin of the Geological Society of America,* **94**, 1450-1465.

Hutchinson, S.M. (1995) Use of magnetic and radiometric measurements to investigate erosion and sedimentation in a British upland catchment. *Earth Surface Processes and Landforms*, **20**, 293-314.

Innes, J.B. and Frank, R.M. (1988) Palynological evidence for Late Flandrian coastal changes at Druridge Bay, Northumberland. *Scottish Geographical Magazine,* **104(1)**, 12-23.

Innes, J.B. and Tooley, M.J. (1993) The age and vegetational history of the Sefton coast dunes. In: D. Atkinson, and J. Houston (Eds.). *The Sand Dunes of the Sefton Coast.* Eaton Press Ltd, England.

Intergovernmental Panel on Climate Change (IPCC) (2007) *Climate Change 2007: The Scientific Basis,* Cambridge University Press.

James, P.A. (1985) Spatial and temporal aspects of soil chemical change in the Ainsdale National Nature Reserve, Merseyside. In: A.M. Harvey (Ed.). *First International Conference on Geomorphology, Guide to field excursions in Northwest England.* British Geomorphological Research Group.

James, P.A. (1993) Soils and nutrient cycling. In: D. Atkinson, and J. Houston (Eds.). *The Sand Dunes of the Sefton Coast.* Eaton Press Ltd, England.

James, P.A. and Wharfe, A.J. (1989) Timescales of soil development in a coastal sand dune system, Ainsdale, north-west England. In: F. van der Meulen, P.D. Jungerius and J.H. Visser (Eds.). *Perspectives in Coastal Dune Management,* The Hague, The Netherlands.

James, P.A., Wharfe, A.J., Pegg, R.K. and Clarke, D. (1986) A cation budget analysis for a coastal dune system in north-west England. *Catena,* **13**, 1-10.

Jankauskas, B., Jankauskiene, G., Slepetiene, A., Fullen, M.A. and Booth, C.A. (2005) International comparison of analytical protocols for determining soil organic matter content on Lithuanian Albeluvisols. In: *Earth and Environmental Sciences.* Latvijas University.

Jankauskas, B., Slepetiene, A., Jankauskiene, G., Fullen, M.A. and Booth, C.A. (2006) A comparative study of analytical methodologies to determine the soil organic matter content of Lithuanian Eutric Albeluvisols. *Geoderma,* **136**, 763-773.

Jarvis, R.A., Bendelow, V.C., Bradley, R.I., Carroll, D.M., Furness, R.R., Kilgour, I.N.L. and King, S.J. (1984) *Soils and Their Use in Northern England.* Soil Survey of England and Wales. Bulletin 10. Harpenden.

Jelgersma, S., Jong, J. de, Zagwijn, W.H. and Regteren Altena, J. (1970) Holocene sea level changes in The Netherlands. *Mededelingen van de Geologische Stichting,* Serie C. VI 7, 1-100.

Jenkins, R. (1988) *X-ray Fluorescence Spectrometry*. In: I.M. Kolthoff., (Ed.) John Wiley & Sons. Chichester.

Jenny, H. (1941) Factors *of Soil Formation: A System of Quantitative Pedology*, Dover Publications, New York.

Johnson, P.E. (1979) *Nutritional Problems Associated with the Revegetation of Eroded Sand Dunes.* Unnpublished Ph.D. Thesis, University of Liverpool.

Johnston, C.M., Turnbull, C.G. and Tasker, M.L. (2002) *Natura 2000 in UK Offshore Waters*. Joint Nature Conservation Commitee Report 325, ISSN 0963 8091

Jones, C.R., Houston, J.A. and Bateman, D. (1993) A history of human influence on the coastal landscape. In: D. Atkinson, and J. Houston (Eds.). *The Sand Dunes of the Sefton Coast.* Eaton Press Ltd, England.

Jones, J. (1980) *Some Aspects of the Mineral Nutrition of Salix repens, With Reference to Ainsdale.* Unpublished B.Sc. thesis, University of Liverpool.

Jones, M.L.M., Wallace, H.L., Norris, D., Brittain, S.A., Haria, S., Jones, R.E., Rhind, P.M., Reynolds, B.R. and Emmett, B.A. (2004) Changes in vegetation and soil characteristics in coastal sand dunes along a gradient of atmospheric nitrogen deposition. *Plant Biology,* **6**, 1-8.

Jungerius, P.D. (1989) Geomorphology, soils and dune management. In: F. van der Meulen, P.D. Jungerius and J.H. Visser (Eds.). *Perspectives in Coastal Dune Management,* The Hague, The Netherlands, 91-98.

Jungerius, P.D. (1990) The characteristics of dune soils. *Catena Supplement,* **18**, 155-162.

Jungerius, P.D. (2008) Dune development and management, geomorphological and soil processes, responses to sea level rise and climate change. *Baltica,* **21**, 13-23.

Jungerius, P.D. and van der Meulen, F. (1988) Erosion processes in a dune landscape along the Dutch coast. *Catena,* **15**, 217-228.

Jungerius, P.D. and van der Meulen, F. (1989) The development of dune blowouts, as measured with erosion pins and sequential air photographs. *Catena,* **16**, 369-376.

Jungerius, P.D., Verheggen, A.J.T. and Wiggers, A.J. (1981) The development of blowouts in 'De Blink', a coastal dune area near Noordwijkerhout, The Netherlands. *Earth Surface Processes and Landforms*, **6**, 375-396.

Kapička, A., Jordanova, N., Petrovskỳ, E. and Podrázskỳ, V. (2003) Magnetic study of weakly contaminated forest soils. *Water, Air and Soil Pollution,* **148**, 31-44.

Kear, B.S. (1985) Soil development and soil patterns in north-west England. In: R.H. Johnson (Ed.). *The Geomorphology of North-West England.* Manchester University Press.

Kemp, R.A., Jerz, H., Grottenhaler, W. and Preece, R.C. (1994) Pedosedimentary fabrics of soils within loess and colluvium in southern England and southern Germany. In: A.J. Ringrose-Voase and G.S. Humpreys (Eds.). *Soil Micromorphology: Studies in Management and Genesis,* Elsevier, Amsterdam.

Kenna, R.J.B. (1986) The Flandrian sequence of North Wirral (NW England). *Geological Journal,* **21**, 1-27.

King, J., Banerjee, S.K., Marvin, J., and Ozdemir, O. (1982) A comparison of different magnetic methods for determining the relative grain size of magnetite in natural materials: some results from lake sediments. *Earth and Planetary Science Letters*, **59**, 404-419.

Knight, J., Orford, J.D., Wilson, P. and Braley, S.M. (2002) Assessment of temporal changes in coastal sand dune environments using the log-hyperbolic grain-size method. *Sedimentology,* **49**, 1229-1252.

Kovach, W.L. (1995) Multivariate data analysis. In: D. Maddy. and J.S. Brew. (Eds) *Statistical Modelling of Quaternary Science Data*, Technical Guide Series No. 5, Quaternary Research Association, Cambridge.

Kubiena, W.L. (1953) *The Soils of Europe.* Murby, London.

Kundu, S., Bhattacharyya, R., Prakash, V., Ghosh, B.N. and Gupta, H.S. (2007) Carbon sequestration and relationship between carbon addition and storage under rainfed soybean–wheat rotation in a sandy loam soil of the Indian Himalayas. *Soil & Tillage Research*, **92(1-2)**, 87-95.

Kutiel, P., Peled, Y. and Geffen, E. (2000) The effect of removing shrub cover on annual plants and small mammals in a coastal sand dune ecosystem. *Biological Conservation,* **94(2)**, 235-242.

Lal, R. (2003) Soil erosion and the global carbon budget. *Environmental International,* **29**, 437-450.

Lammerts, E.J., Sival, F.P., Grootjans, A.P. and Esselink, H. (1992) Hydrological conditions and soil buffering processes controlling the occurrence of dune slack species on the Dutch Wadden Sea island. In: R.W.G. Carter, T.G.F. Curtis and M.J. Sheehy-Skeffington (Eds.). *Coastal Dunes.* Balkema, Rotterdam.

Leatherman, S.P. (1979) Barrier dune systems: A reassessment. *Sediment Geology,* **24 (1-2)**, 1-16.

Leatherman, S.P. (1990) Modelling shore response to sea level rise on sedimentary coasts. *Progress in Physical Geography,* **14**, 447-464.

Leggett, D.J., Cooper, N. and Harvey, R. (2004) *Coastal and Estuarine Managed Realignment – Design Issues.* Report C628. CIRIA: London.

Lehner, D., Kellner, G., Schnablegger, H. and Glatter, O. (1998) Static light scattering on dense colloidal systems: new instrumentation and experimental results. *Journal of Colloid & Interface Science*, **201**, 34-47.

Lee, E.M. (2008) Coastal cliff behaviour: Observations on the relationship between beach levels and recession rates. *Geomorphology*, **101(4)**, 558-571.

Lees, J.A. (1994) *Modelling the Magnetic Properties of Natural and Environmental Materials.* Unpublished Ph.D. thesis, Coventry University.

Lees, J.A. (1999) Evaluating magnetic parameters for use in source identification, classification and modelling of natural and environmental materials. In: J. Walden., F. Oldfield. And J.P. Smith. (Eds), *Environmental Magnetism: A Practical Guide*, Quaternary Research Association, Technical Guide No. 6.

Lennon, G.W. (1963) The identification of weather conditions associated with the generation of major storm surges along the west coast of the British Isles. *Quaternary Journal of the Royal Meteorological Society,* **89**, 381-394.

Lewis, J. and Cowell, R. (2002) The Archaeology of a changing landscape: the last thousand years in Merseyside. *Journal of the Merseyside Archaeological Society,* Volume **11**.

Liverpool Bay Shoreline Management Plan (1993) *Sub-Cell 11a: Great Orme's Head to Formby Point Plan Document*. Liverpool Bay Coastal Group.

Livingstone, I. and Warren, A. (1996) *Aeolian Geomorphology: An Introduction*. Longman, Harlow.

Lowe, J.J. and Walker, M.J.C. (1997) *Reconstructing Quaternary Environments.* Addison Wesley Longman Limited, London.

Lu, S. (2000) Characterization of subtropical soils by mineral magnetic measurements. *Communications in Soil Science and Plant Analysis,* **31(1&2)**, 1-11.

Lucas, N.S., Shanmugam, S. and Barnsley, M. (2002) Sub-pixel habitat mapping of a coastal dune ecosystem. *Applied Geography,* **22**, 253-270.

Lukshin, A.A., Rumyantseva, T.I. and Kovrigo, V.P. (1968) Magnetic susceptibility of the principal soil in the Udmundt ASSR. *Soviet Soil Science,* **3**, 88-93.

Lymbery, G. (1999). *Shoreline Management Plans, A Partnership for Coastal Defence Management*. Available:
http://www.seftoncoast.org.uk/articles/99winter_shoreline.html.
Last accessed 6 November 2009.

Lyon, T.L. and Buckman, H. O. (1922) *The Nature and Properties of Soils: A Textbook of Edaphology*. Macmillan, New York.

MacDonald, J. (1954) Afforestation of sand dunes. *Advancement of Science,* **11**, 33-37.

Mackay, J.M. (1993) Methods of monitoring land use and condition. In: D. Atkinson, and J. Houston (Eds.). *The Sand Dunes of the Sefton Coast.* Eaton Press Ltd, England.

Mackney, D., Hodgson, J.M., Hollis, J.M. and Staines, S.J. (1983) *Legend for the 1:250,000 Soil Map of England and Wales: A Brief Explanation of the Constituent Soil Associations*. Lawes Agricultural Trust (Soil Survey of England and Wales), Harpenden.

Magiera, T., Strzyszcz, Z., Kapicka, A. and Petrovsky, E. (2006) Discrimination of lithogenic and anthropogenic influences on topsoil magnetic susceptibility in Central Europe. *Geoderma,* **130**, 299-311.

Maher, B.A. (1986) Characterisation of soils by mineral magnetic measurements. *Physics of The Earth and Planetary Interiors,* **42**, 76-92.

Maher, B.A. (1998) Magnetic properties of modern soils and Quaternary loessic palaeosols: Palaeoclimatic implications. *Palaeogeography, Palaeoclimatology, Palaeoecology,* **137**, 25-54.

Maher, B.A., Alekseev, A. and Alekseeva, T. (2002) Variation of soil magnetism across the Russian steppe: its significance for use of soil magnetism as a palaeorainfall proxy. *Quaternary Science Review,* **21**, 1571-1576.

Maher, B.A. and Thompson, R. (1999) *Quaternary Climates, Environments and Magnetism,* Cambridge University Press.

Maier, G., Scholger, R. and Schön, J. (2006) The influence of soil moisture on magnetic susceptibility measurements. *Journal of Applied Geophysics,* **59**, 162-175.

Malloch, A.J.C. (1989) Plant communities of the British sand dunes. *Proceedings of the Royal Society of Edinburgh,* **96B**, 53-74.

Manly, B.F.J. (1994) *Multivariate Statistical Methods: A Primer.* Chapman & Hall, London.

Martini, I.P. and Chesworth, W. (1992) *Weathering, Soils and Palaeosols: Developments in Earth Surface Processes 2,* Elsevier, Amsterdam.

McBride, N. and Wilson, P. (1991) Characteristics and development of soils at Magilligan Foreland, Northern Ireland, with emphasis on dune and beach sand soils. *Catena,* **18**, 367-378.

McKinley, D.C., Rice, C.W. and Blair, J.M. (2008) Conversion of grassland to coniferous woodland has limited effects on soil nitrogen cycle processes. *Soil Biology & Biochemistry,* **40**, 2627-2633.

Meikle, R.D. (1984) *BSBI Handbook No 4. Willows and Poplars of Great Britain and Ireland.* Botanical Society of the British Isles, London.

Merino, A., Fernández-López, A., Solla-Gullón, F. and Edeso, J.M. (2004) Soil changes and tree growth in intensively managed *Pinus radiata* in northern Spain. *Forest Ecology and Management,* **196**, 393-404.

Millington, J.A., Fullen, M.A., Moore, G.M., Booth, C.A., Trueman, I.C., Worsley, A.T. and Richardson, N. (2008) Morphodynamics of the Morfa Dyffryn coastal dunes, mid-Wales: photographic survey 1988–2007. *Environmental Problems in Coastal Regions VII, WIT Transactions on the Built Environment,* **99**, 211-220.

Millington, J.A., Booth, C.A., Fullen, M.A., Moore, G.M., Trueman, I.C., Worsley, A.T., Richardson, N. and Baltrėnaitė, E. (2009) The role of long-term landscape photography as a tool in dune management. *Journal of Environmental Engineering and Landscape Management,* **17**, Ia–Ih.

Minton, C.L. (1985) *The Relative Importance of the Input of Cations into the Ainsdale Sand Dune System from Mineral Weathering.* Unpublished B.Sc. thesis, University of Liverpool.

Mitchell, R.J., Morecroft, M.D., Acreman, M., Crick, H.Q.P., Frost, M., Harley, M., Maclean, I.M.D., Mountford, O., Piper, J., Pontier, H., Rehfisch, M.M., Ross, L.C., Smithers, R.J., Stott, A., Walmsley, C.A., Watts, O. and Wilson, E. (2007) *England Biodiversity Strategy – Towards Adaptation to Climate Change.* Final Report to Defra for contract CRO327.

Moore, P.D., Webb, J.A. and Collinson, M.D. (1991) *Pollen Analysis*. Blackwell, Oxford.

Moriarty, D.E.M. (1978) *Acidification and Podzolization Under Pinewoods on the Sand Dunes at Ainsdale, SW Lancashire.* Unpublished Ph.D. thesis, University of Liverpool.

Morkunaite, R. and Cesnulevicius, A. (2001) Comparative characteristics of old and new generations of Curonian spit dunes. In: J.A. Houston, S.E. Edmondson and P.J. Rooney (Eds.). *Coastal Dune Management. Shared Experience of European Conservation Practice.* Liverpool University Press.

Morton, R.A., Leach, M.P., Paine, J.G. and Cardoza, M.A. (1993) Monitoring beach changes using GPS surveying techniques. *Journal of Coastal Research,* **9**, 702-720.

Mullins, C.E. (1977) Magnetic susceptibility of the soil and its significance in soil science – a review. *Journal of Soil Science,* **28**, 223-246.

Nabel, P.E., Morrás, H.J.M., Petersen, N. and Zech, W. (1999) Correlation of magnetic and lithologic features of soils and Quaternary sediments from the Undulating Pampa, Argentina. *Journal of South American Earth Sciences,* **12**, 311-323.

Natura 2000, (2007) *Interpretation Manual of European Union Habitats*. European Commission DG Environment, Nature and Biodiversity.

Neal, A. (1993) *Sedimentology and Morphodynamics of a Holocene Coastal Dune Barrier Complex, North-West England.* Unpublished PhD Thesis, University of Reading.

Neal, A. and Roberts, C.L. (2000) Applications of ground-penetrating radar (GPR) to sedimentological, geomorphological and geoarchaeological studies in coastal environments. In: K. Pye and J.R.L. Allen (Eds.). *Coastal and Estuarine Environments: Sedimentology, Geomorphology and Geoarchaeology*. Geological Society, London, Special Publications, **175**, 139-171.

Neal, A. and Roberts, C.L. (2001) Internal structure of a trough blowout, determined from migrated ground-penetrating radar profiles. *Sedimentology,* **48**, 791-810.

Nikitin, E.D. (2001) Soil as a bio-abiotic polyfunctional system. *Eurasian Soil Science,* **34**, 6-12.

Minasny, B., Salvador-Blanes, S. and McBratney, A. (2006) Modelling soil profile evolution considering physical and chemical weathering, and incorporating bioturbation processes. *18th World Congress of Soil Science*, July 9-15, 2006 - Philadelphia, Pennsylvania, USA.

Noest, V. (1991) Simulated impact of sea level rise on phreatic level and vegetation of dune slacks in the Voorne area (The Netherlands). *Landscape Ecology,* **6**, 89-97.

North West England and North Wales Coastal Group (2008) *Cell 11 Shoreline Management Plan (SMP2) North West England and North Wales: Draft Issues and Objectives Tables*. Halcrow Group Limited, Wiltshire, UK.

Odum, E.P. (1969) The strategy of ecosystem development. *Science,* **164**, 262-270.

O'Garra, A. (1976) *Dune Slack Systems – Vegetation and Morphological Development at Ainsdale.* Unpublished BSc thesis. Department of Geography, University of Liverpool.

Oldfield, F. (2007) Sources of fine-grained magnetic minerals in sediments: a problem revisited. *The Holocene,* **17(8)**, 1265-1271.

Oldfield, F., Darnley, I., Yates, G., France, D.E. and Hilton, J. (1992) Storage diagenesis versus sulphide authigenesis: possible implications in environmental magnetism, *Journal of Palaeolimnology*, **7**, 179-189.

Olff, H., Huisman, J. and Van Tooren, B.F. (1993) Species dynamics and nutrient accumulation during early primary succession in coastal sand dunes. *Journal of Ecology,* **81**, 693-706.

Olson, C.G. and Nettleton, W.D. (1998) Paleosols and the effects of alteration. *Quaternary International,* **51**/**52**, 185-194.

Olsson, B.A., Lundkvist, H. and Staaf, H. (2000) Nutrient status in needles of Norway spruce and Scots pine following harvesting of logging residues. *Plant and Soil,* **23**, 161-173.

Ordóñez, J.A.B., Jong, B.H.J., García-Oliva., Aviña, F.L., Guerrero, P.G., Martínez, R. and Masera, O. (2008) Carbon content in vegetation, litter, and soil under 10 different land-use and land-cover classes in the Central Highlands of Michoacan, Mexico. *Forest Ecology and Management,* **255**, 2074-2084.

Orford, J.D. and Pethick, J. (2006) Challenging assumptions of future coastal habitat development around the UK. *Earth Surface Processes and Landforms,* **31**, 1625-1642.

Ovington, J.D. (1950) The afforestation of the Culbin sands. *Journal of Ecology,* **38**, 303-319.

Ovington, J.D. (1951) The afforestation of Tentsmuir sands. *Jounal of Ecology,* **39**, 363-375.

Ovington, J.D. (1955) Studies of the development of woodland conditions under different trees. *Ecology,* **43**, 1-21.

Parker, W.R. (1975) Sediment mobility and erosion on a multi-barred foreshore (south-west Lancashire, UK). In: J. Hails, and A. Carr (Eds.). *Nearshore Sediment Dynamics and Sedimentation*. John Wiley and Sons Ltd, Chichester.

Paterson, H. (1997) *Sea Level Rise and Environmental Assessment: The Potential Impact on the Sefton Coast, North-West England.* Unpublished M.Sc. thesis, University of Liverpool.

Payne, K.R. (1983) *The Vegetation of Ainsdale Dunes.* Unpublished report, Nature Conservation Council. NW England.

Pennock, D.J. and Van Kessel, C. (1997) Clear-cut forest harvest impacts on soil quality indicators in the mixed-wood forest of Saskatchewan, Canada. *Geoderma,* **75**, 13-32.

Pethick, J. (1984) *An Introduction to Coastal Geomorphology.* Arnold, London.

Pethick, J. (2001) *Ainsdale Sand Dunes NNR: Assessment of Coastal Defence and Sand Dune Response to Erosion Processes.* Centre for Coastal Management, University of Newcastle.

Picton, J.A. (1849) The changes of sea-levels on the west coast of England during the historic period. *Proceedings of the Literary and Philosophical Society of Liverpool,* **5**, 113-115.

Plater, A.J. Huddart, D. Innes, J.B. Pye, K. Smith, A.J. and Tooley, M.J. (1993) Coastal and Sea-level Changes. In: D. Atkinson, and J. Houston (Eds.). *The Sand Dunes of the Sefton Coast.* Eaton Press Ltd, England.

Pope, R.J.J. (2000) The application of mineral magnetic and extractable iron (Fe_d) analysis for differentiating and relatively dating fan surfaces in central Greece. *Geomorphology,* **32**, 57-67.

Purdie, J. (2002) *A pH survey of Ainsdale Sand Dunes National Nature Reserve, Merseyside.* Unpublished Report conducted on behalf of English Nature. Liverpool Hope University College.

Pye, K. (1984) Models of transgressive dune building episodes and their relationship to Quaternary sea level changes: a discussion with reference to evidence from eastern Australia. In: M. Clark (Ed.). *Coastal Research: UK Perspectives.* Geo Books, Norwich.

Pye, K. (1990) Physical and human influences on coastal dune development between the Ribble and Mersey estuaries, northwest England. In: K.F. Nordstrom., N. Psuty and R.W.G. Carter (Eds.). *Coastal Dunes: Form and Process.* John Wiley & Sons, Chichester.

Pye, K. (1991) Beach deflation and backshore dune formation following erosion under storm surge condition: an example from Northwest England. In: O.E. Bardoff-Nielsen and B.B. Willetts (Eds.). *Sand, Dust and Soil in their Relation to Aeolian and Littoral Processes.* Acta Mechanica, Supplementum 2.

Pye, K. (2001) Long-term geomorphological changes and how they may affect the dune coasts of Europe. In: J.A. Houston, S.E. Edmondson and P.J. Rooney (Eds.). *Coastal Dune Management. Shared Experience of European Conservation Practice.* Liverpool University Press.

Pye, K. and Blott, S.J. (2004a) Comparison of soils and sediment using major and trace element data. In: K. Pye. and D.J. Croft. (Eds.). *Forensic Geoscience: Principles, Techniques and Applications.* Geological Society, London, Special Publication, **232**, 183-196.

Pye, K. and Blott, S.J. (2004b) Particle size analysis of sediments, soils and related particulate materials for forensic purposes using laser granulometry. *Forensic Science International,* **144**, 19-27.

Pye, K. and Blott, S.J. (2008) Decadal-scale variation in dune erosion and accretion rates: An investigation of the significance of changing storm tide frequency and magnitude on the Sefton coast, UK. *Geomorphology,* **102**, 652-666.

Pye, K. and Bowman, G.M. (1984) The Holocene marine transgression as a forcing function in episodic dune activity on the eastern Australian coast. In: B.G. Thom (Ed.). *Coastal Geomorphology in Australia.* Academic Press, Sydney.

Pye, K. and Neal, A. (1993) Late Holocene dune formation on the Sefton Coast, northwest Endland. In: K. Pye (Ed.). *The Dynamics and Environmental Context of Aeolian Sedimentary Systems, Geological Society Special Publication No.72,* Geological Society Publishing House, Bath.

Pye, K. and Neal, A. (1994) Coastal dune erosion at Formby Point, north Merseyside, England: Causes and mechanisms. *Marine Geology,* **119**, 39-56.

Pye, K. and Smith, A.J. (1988) Beach and dune erosion and accretion on the Sefton Coast, Northwest England. *Journal of Coastal Research Special Issue,* **3**, 33-36.

Pye, K. and Tsoar, H. (1990) *Aeolian Sand and Sand Dunes*. Unwin Hyman, London.

Pye, K., Stokes, S. and Neal, A. (1995) Optical dating of aeolian sediments from the Sefton coast, north-west England. *Proceedings of the Geologists' Association,* **106**, 281-292.

Ragg, J.M., Beard, G.R., George, H., Heaven, F.W., Hollis, J.M., Jones, R.J.A., Palmer, R.C., Reeve, M.J., Robson, J.D. and Whitfield, W.A.D. (1984) *Soil Survey of England and Wales, Bulletin No.12: Soils and their use in Midland and Western England*. Harpenden. Lawes Agricultural Trust (Soil Survey of England and Wales), Harpenden.

Ramann, E. (1928) *The Evolution and Classification of Soils* (Translated by C.L. Whittles). W. Heffer & Sons, London.

Rance, C.E. de (1869) The Geology of the country between Liverpool and Southport. Explanation of Quarter Sheet 90SE of the 1 inch Geological Survey Map of England and Wales. *Memoirs of the Geological Survey of the UK,* HMSO, London.

Rance, C.E. de (1872) The Geology of the country around Southport, Lytham Southshore. Explanation of Quarter Sheet 90NE. *Memoirs of the Geological Survey of the UK,* HMSO, London.

Rance, C.E. de (1877) The Superficial Geology of the country adjoining the coast of south-west Lancashire. *Memoirs of the Geological Survey of the UK,* HMSO, London.

Rance, C.E. de (1878) Geology of the country around Preston, Blackburn and Burnley. Explanation of Quarter Sheet 89NW of the 1 inch Geological Survey Map of England and Wales. *Memoirs of the Geological Survey of the UK,* HMSO, London.

Ranwell, D.S. (1959) Newborough Warren, Anglesey. I. The dune system and dune slack habitat. *Journal of Ecology,* **47**, 571-601.

Ranwell, D.S. (1960) Newborough Warren, Anglesey. II. Plant associes and succession cycles of the sand dune and dune slack vegetation. *Journal of Ecology,* **48**, 117-141.

Ranwell, D.S. (1972) *Ecology of Salt Marshes and Sand Dunes.* Chapman & Hall Ltd, London.

Ratcliffe, D.A. (1977) *A Nature Conservation Review Vols 1 & 2.* Cambridge University Press, Cambridge.

Read, D.J. (1989) Mycorrhizas and nutrient cycling in sand dune ecosystems. *Proceedings of the Royal Society of Edinburgh,* **96B**, 89-110.

Reade, T.M. (1871) The geology and physics of the post-glacial period, as shown in deposits and organic remains in Lancashire and Cheshire. *Proceedings of the Liverpool Geological Society,* **2**, 36-88.

Reade, T.M. (1872) The post-glacial geology and physiography of west Lancashire and the Mersey estuary. *Geological Magazine,* **9**(93), 111-119.

Reade, T.M. (1881a) On a section of the Formby and Leasowe marine beds, and superior peat bed, disclosed by cuttings for the outlet sewer at Hightown. *Proceedings of the Liverpool Geological Society,* **4**(4), 269-277.

Reade, T.M. (1881b) The date of the last change of level in Lancashire. *Quarterly Journal of the Geological Society of London,* **37**, 436-439.

Reade, T.M. (1902) Glacial and post-glacial features of the lower valley of the River Lune and its estuary. *Proceedings of the Liverpool Geological Society,* **9**(2), 163-193.

Reade, T.M. (1908) Post-glacial beds at Great Crosby as disclosed by the new outfall sewer. *Proceedings of the Liverpool Geological Society,* **10**(4), 249-261.

Rechinger, K.H. (1964). In: T.G. Tutin, V.H. Heywood, N.A. Burges, D.H. Valentine, S.M. Walters and D.A. Webb. *Salix* L. *Flora Europaea.* Cambridge University Press, Cambridge.

Redel, Y., Rubio, R., Godoy, R. and Borie, F. (2008) Phosphorus fractions and phosphatise activity in an Andisol under different forest ecosystems. *Geoderma,* **145**, 216–221.

Repe, B. (2007) Geographical soil map – a different soil determination approach in Slovenia. In: C. Dazzi (Ed.) *Changing Soils in a Changing World: the Soils of Tomorrow.* Book of Abstracts. 5th International Congress of the European Society for Soil Conservation. Palermo, Italy.

Rhind, P.M., Blackstock, T.H., Hardy, H.S., Jones, R.E. and Sandison, W. (2001) The evolution of Newborough Warren dune system with particular reference to the past four decades. In: J.A. Houston, S.E. Edmondson and P.J. Rooney (Eds.). *Coastal Dune Management. Shared Experience of European Conservation Practice.* Liverpool University Press.

Ribble Estuary Shoreline Management Plan (1999) *Sub-Cell 11b: Formby Point to River Wyre Plan Document*. Ribble Estuary Shoreline Management Plan Partnership.

Rivas, J., Ortega, B., Sedov, S., Solleiro, E. and Sychera, S. (2006) Rock magnetism and pedogenic processes in Luvisol profiles: Examples from Central Russia and Central Mexico. *Quaternary International,* **156**/**157**, 212-223.

Roberts, N. (1998) *The Holocene: An Environmental History*. Blackwell Publishing.

Robinson, N.A. (1989) *Southport Sand Dunes and Foreshore SSSI-Site Quality Monitoring. Air Photo Interpretation: Ainsdale Hills 1988, Birkdale Frontal Dunes 1988.* NCC Reports.

Rodwell, J.S. (2000) *British Plant Communities, Volume 5, Maritime Communities and Vegetation of Open Habitats.* Cambridge University Press.

Rosén, B. (1997) On sampling with probability proportional to size. *Journal of Statistical Planning and Inference*, **62**, 159-191.

Ross, S. (1989) *Soil Processes: A Systematic Approach.* Routledge, London.

Rowell, D.L. (1994) *Soil Science: Methods and Applications*. Longman, London.

Ruhe, R.V. (1965) Quaternary paleopedology. In: H.E. Wright and D.G. Frey (Eds.). *The Quaternary of the United States.* Princeton University Press, Princeton.

Rühl, J. Cullotta, S. Minacapelli, M. and La Mantia, T. (2007) Analysis of renaturation processes using LANDSAT 5 and 7 imagery. In: C. Dazzi (Ed.) *Changing Soils in a Changing World: the Soils of Tomorrow.* Book of Abstracts. 5th International Congress of the European Society for Soil Conservation. Palermo, Italy.

Running, S.W. and Coughlan, J.C. (1988) A general model of forest ecosystem processes for regional applications. I. Hydrologic balance, canopy gas exchange and primary production processes. *Ecological Modelling,* **42**, 125-154.

Salisbury, E.J. (1925) Note on the edaphic succession in some dune soils with special reference to the time factor. *Journal of Ecology,* **13**, 322-328.

Salisbury, E.J. (1952) *Downs and Dunes. Their Plant Life and Its Environment.* G. Bell & Sons, London.

Sandgren, P. and Thompson, R. (1990) Mineral magnetic characteristics of podzolic soils developed on sand dunes in the Lake Gosciaz catchment, central Poland, *Physics of The Earth and Planetary Interiors,* **60**, 297-313.

Saye, S.E. and Pye, K. (2006) Variations in chemical composition and particle size of dune sediments along the west coast of Jutland, Denmark. *Sedimentary Geology,* **183**, 217-242.

Saye, S.E., van der Wal, D., Pye, K. and Blott, S.J. (2005) Beach-dune morphological relationships and erosion/accretion: An investigation at five sites in England and Wales using LIDAR data. *Geomorphology,* **72**, 128-155.

Schneeweiss, H. and Mathes, H. (1995) Factor analysis and principal components. *Journal of Multivariate Analysis*, **55**, 105-124.

Schrijver, A de., Mertens, J., Geudens, G., Staelens, J., Campforts, E., Luyssaert, S., Temmerman, L de., Keersmaeker, L de., Neve, S de. And Verheyen, K. (2006) Acidification of forested podzols in North Belgium during the period 1950-2000. *Science of the Total Environment,* **361**, 189-195.

Sefton Borough Council (1995) *Sefton Unitary Development Plan*.

Sevink, J. (1991) Soil development in the coastal dunes and it's relation to climate. *Landscape Ecology,* **6**, 49-56.

Shackley, S., Wood, R., Hornung, M., Hulme, M., Handley, J., Darier, E. and M. Walsh (1998) *Everybody has an Impact: climate change impacts in the North West of England*. Sustainability North West, Manchester.

Sheail, J. (1976) *Nature in Trust, A History of Nature Conservation in Great Britain.* Blackie, Glasgow.

Sherman, D.J. and Bauer, B.O. (1993) Dynamics of beach-dune systems. *Progress in Physical Geography,* **17**, 413-447.

Shoreline Management Plan (1999) *Shoreline Management Plan, Formby to Fleetwood*, Stage 2, **4**.

Short, A.D. and Hesp, P. (1982) Wave, beach and dune interactions in southeastern Australia. *Marine Geology,* **48**, 259-284.

Simpson, D.E. and Gee, M. (2001) Towards best practice in the sustainable management of sand dune habitats: 1. The restoration of open dune communities at Ainsdale Sand Dunes National Nature Reserve. In: J.A. Houston, S.E. Edmondson and P.J. Rooney (Eds.). *Coastal Dune Management. Shared Experience of European Conservation Practice.* Liverpool University Press.

Skelsey, C., Law, A.N.R., Winter, M. and Lishman, J.R. (2004) Automating the analysis of remotely-sensed data. *Photogrammetric Engineering & Remote Sensing,* **70(3)**, 341-350.

Smith, A.J. (1982) *Guide to the Sefton Coast Data Base.* Sefton Council, Merseyside, UK.

Smith, G. (1987) *Does the Orientation of the Coastline Affect the Nature of the Dunes on the Sefton Coast?* Unpublished report, Homerton College.

Smith, G.L. and Zarillo, G.A. (1990) Calculating long-term shoreline recession rates using aerial photographic and beach profiling techniques. *Journal of Coastal Research,* **6**, 112-120.

Smith, J.P. (1999) An introduction to the magnetic properties of natural materials. In: J. Walden., F. Oldfield. And J.P. Smith. (Eds.) *Environmental Magnetism: A Practical Guide*, Quaternary Research Association, Technical Guide No. 6, 5-25.

Smith, P.H. (1978) *The Ecological Evaluation of Wetland Habitats in the North-Merseyside Sand-dune System.* Report to Merseyside County Council. JCAS database 075 Da 071.

Smithson, P., Addison, K. and Atkinson, K. (2002) *Fundamentals of the Physical Environment.* Routledge, London.

Sokoloff, M. (1881) Dunes and moving sands. *Nature*, **23(598)**, 569.

Staaf, H. and Berg, B. (1982) Accumulation and release of plant nutrients in decomposing Scots Pine needle litter. Long term decomposition in a Scots Pine forest II. *Canadian Journal of Botany,* **60**, 1561-1568.

Stace, C. (1997) *New Flora of the British Isles* (Ed.2). Cambridge University Press, Cambridge.

Stoney, R.E. (1988) *Environmental Change and Coastal Development in South-West Lancashire.* Unpublished BSc thesis. Department of Geography, University of Durham.

Strzyszcz, Z. (1989) Ferromagnetic properties of forest soils being under influence of industrial pollution. *Air Pollution and Forest Decline.* Proceedings of the 14th International Meeting for Specialist in Air Pollution Effects on Forest Ecosystems. IUFRO, Interlaken, Switzerland, 201-207.

Sturgess, P.W. (1991) *Post-Felling Vegetation Changes on Three Afforested Sand Dune Systems.* Unpublished Ph.D. thesis, University of Liverpool.

Sturgess, P. (1992) Clear-felling dune plantations: Studies in vegetation recovery. In: R.W.G. Carter, T.G.F. Curtis and M.J. Sheehy-Skeffington (Eds.). *Coastal Dunes.* Balkema, Rotterdam.

Sturgess, P.W. (1993) Clear-felling dune plantations: Studies in vegetation recovery on the Sefton coast. In: D. Atkinson, and J. Houston (Eds.). *The Sand Dunes of the Sefton Coast.* Eaton Press Ltd, England.

Stuttard, R. (1994) *Data Collection, Presentation, Exploration and Analysis*. Third Edition, Erithacus Press, Wolverhampton.

Stutter, M., Langan, S. and Cresser, M. (2003) Weathering and atmospheric deposition signatures of base cations in upland soils of NE Scotland: their application to critical load assessment. *Geoderma,* **116**, 301-342.

Sutherland, R.A. and Lee, C.-T. (1994) Discrimination between coastal subenvironments using textural characteristics. *Sedimentology,* **41**, 1133-1145.

Syvitski, J.P.M. (1991) *Principles, Methods and Application of Particle Size Analysis.* Cambridge University Press, Cambridge.

Thompson, R. (1990) Mineral magnetic characteristics of podzolic soils developed on sand dunes in the Lake Gosciaz catchment, central Poland. *Physics of The Earth and Planetary Interiors,* **60**, 297-313.

Thompson, R. and Oldfield, F. (1986) *Environmental Magnetism*. Allen & Unwin, London.

Tooley, M.J. (1974) Sea-level changes during the last 9000 years in north-west England. *Geographical Journal,* **140**, 18-42.

Tooley, M.J. (1978) *Sea-Level Changes in North-West England During the Flandrian Stage.* Oxford Research Studies in Geography. Clarendon Press, Oxford.

Tooley, M.J. (1982) Sea-level changes in northern England. *Proceedings of the Geologists' Association,* **93**(1), 43-51.

Tooley, M.J. (1990) The chronology of coastal dune development in the United Kingdom. *Catena Supplement,* **18**, 81-88.

Tooley, M.J. and Jelgersma, S. (1992) *Impacts of Sea-Level Rise on European Coastal Lowlands*. Institute of British Geographers, Special Publication 27. Blackwell, Oxford.

Travis, C.B. (1926) The peat and forest bed of the south-west Lancashire coast. *Proceedings of the Liverpool Geological Society,* **14**, 263-277.

Travis, W.G. (1915) Marram grass and dune formation on the Lancashire Coast. *Lancashire and Cheshire Naturalist,* **8**, 313-320.

Tsoar, H., Blumberg, D.G. and Stoler, Y. (2004) Elongation and migration of sand dunes. *Geomorphology,* **57**, 293-302.

Tsoar, H. (2005) Sand dunes mobility and stability in relation to climate. *Physica A,* **357**, 50-56.

Turk, J.K., Goforth, B.R., Graham, R.C. and Kendrick, K.J. (2008) Soil morphology of a debris flow chronosequence in a coniferous forest, southern California, USA. *Geoderma,* **146**, 157-165.

Turner, D.A. (1984) *A guide to the Sefton Coast Data Base.* Metropolitan Borough of Sefton, Engineer's Department. Sefton Coast Data Base.

Vadyunina, A.F. and Babanin, V.F. (1972) Magnetic susceptibility of some soils in the USSR. *Soviet Soil Science,* **4**, 585-589.

van Breeman, N. and Buurman, P. (2002) *Soil Formation*. Kluwer Academic Publishers, Dordrecht, The Netherlands.

van Dorp, D., Boot, R. and Maarel, E. van der. (1985) Vegetation succession on the dunes near Oostvoorne, The Netherlands, since 1934, interpreted from air photographs and vegetation maps. *Vegetatio*, **58**, 123-126.

van den Ancker, J.A.M. and Jungerius, P.D. (2007) Geoheritage and Geodiversity in soil science. In: C. Dazzi (Ed.) *Changing Soils in a Changing World: the Soils of Tomorrow.* Book of Abstracts. 5th International Congress of the European Society for Soil Conservation. Palermo, Italy.

van der Muelen, F. (1990) European dunes: consequences of climatic changes and sea level rise. *Catena Supplement,* **18**, 51-60.

van Reeuwijk, L.P. (2002) *Procedures For Soil Analysis*, Sixth Edition. International Soil Reference and Information Centre, Wageningen, The Netherlands.

Vestin, J.L.K., Nambu, K., van Hees, P.A.W., Bylund, D. and Lundström, U.S. (2006) The influence of alkaline and non-alkaline parent material on soil chemistry. *Geoderma,* **135**, 97-106.

Walden, J. (1990) *The Use of Magnetic Analysis in the Study of Glacial Diamicts*, Unpublished Ph.D. thesis, University of Wolverhampton.

Walden, J. and Smith, J.P. (1995) Factor analysis: a practical application. In: D. Maddy. and J.S. Brew. (Eds), *Statistical Modelling of Quaternary Science Data*, Technical Guide Series No. 5, Quaternary Research Association, Cambridge.

Walden, J., Oldfield, F. and Smith, J.P. (1999) *Environmental Magnetism: A Practical Guide*, Quaternary Research Association, Technical Guide No. 6, Cambridge.

Walden, J., Smith, J.P. and Dackombe, R.V. (1996) A comparison of mineral magnetic, geochemical and mineralogical techniques for compositional studies of glacial diamictons. *Boreas*, **25**, 115-130.

Wallingford, H.R. (1993) *Coastal Management: Mapping of Littoral Cells.* Report to MAFF. H R Wallingford Report SR328.

Wang, J-S., Grimley, D.A., Xu, C. and Dawson, J.O. (2008) Soil magnetic susceptibility reflects soil moisture regimes and the adaptability of tree species to these regimes. *Forest Ecology and Management,* **255**, 1664-1673.

Warrick, R.A., Barrow, E.M. and Wigley, T.M.L. (1993) *Climate and Sea Level Change.* Cambridge University Press, Cambridge.

Wharfe, A.J. (1984) *Towards a Cation Budget for a Coastal Sand Dune System.* Unpublished Ph.D. thesis, University of Liverpool.

Wheeler, D.J., Simpson, D.E. and Houston, J.A. (1993) Dune use and management. In: D. Atkinson, and J. Houston (Eds.). *The Sand Dunes of the Sefton Coast.* Eaton Press Ltd., England.

Wigley, T.M.L. and Raper, S.C.B. (1993) Thermal expansion of sea water associated with global warming. *Nature,* **330**, 127-131.

Williams, R.D. and Cooper, J.R. (1990) Locating soil boundaries using magnetic susceptibility. *Soil Science,* **150(6)**, 889-895.

Willis, A.J. (1963) Braunton Burrows: the effects on the vegetation of the addition of mineral nutrients to the dune soils. *Journal of Ecology,* **51**, 353-374.

Wilson, K. (1960) The time factor in the development of dune soils at South Haven Peninsula, Dorset. *Journal of Ecology,* **48**, 341-359.

Wilson, P. (1991) Buried soils and coastal aeolian sands at Portstewart, Co. Londonderry, Northern Ireland. *Scottish Geographical Magazine,* **107**, 198-202.

Wilson, P. (1992) Trends and timescales in soil development on coastal dunes in the north of Ireland. In: R.W.G. Carter, T.G.F. Curtis and M.J. Sheehy-Skeffington (Eds.). *Coastal Dunes.* Balkema, Rotterdam.

Wilson, P., Orford, J.D., Knight, J., Braley, S.M. and Wintle, A.G. (2001) Late Holocene (post 4000-years BP) coastal dune development in Northumberland, northeast England. *Holocene,* **11**, 215-229.

Woodroffe, C.D. (2002) *Coasts: Form, Process and Evolution.* Cambridge University Press. Cambridge.

Wright, J.E., Hull, J.H., McQuillin, R. and Arnold, S.E. (1971) Irish Sea Investigations 1969-71. *Institute of Geological Sciences Report 71/19.* HMSO, London.

Wright, T.W. (1955) Profile development in the sand dunes of Culbin Forest, Morayshire I. Physical properties. *Journal of Soil Science,* **6**, 270-283.

Wright, T.W. (1956) Profile development in the sand dunes of Culbin Forest, Morayshire II. Chemical properties. *Journal of Soil Science,* **7**, 33-42.

Yu, L. and Oldfield, F. (1989) A multivariate mixing model for identifying sediment source from magnetic measurements. *Quaternary Research*, **32**, 168-181.

Zier, J.L. and Baker, W.L. (2006) A century of vegetation change in the San Juan Mountains, Colorado: An analysis using repeat photography. *Forest Ecology and Management,* **228**, 251-262.

Appendix 1.1 Explanation of types of magnetic behaviour (after Smith, 1999)

Type of magnetic behaviour	Explanation	Examples of minerals exhibiting behaviour
Diamagnetism	Diamagnetism is exhibited by substances with no unpaired electrons in the various electron shells of their constituent atoms. Diamagnetic behaviour is only exhibited when an external (natural or artificial) magnetic field is applied; under such conditions the electron orbits become aligned so as to oppose the external field. This alignment of orbital planes, which would otherwise cancel, therefore produces a magnetic moment. When the field is removed this induced moment is lost and electron orbits precess, effectively at random, to positions giving no net moment. This type of magnetic behaviour is fundamental to all substances, but is weak and negative (relative to the direction of the applied field), and becomes masked if other types of magnetic behaviour are present.	Quartz, alkali-feldspar, calcite, halite, kaolinite.
Paramagnetism	Paramagnetism is a phenomenon produced where a substance has some atoms with unpaired electrons, so that a net magnetic moment exists (from both the electron spin and orbit). The interaction of these atomic magnetic moments with each other is very small because the distances between atoms with unpaired electrons within the substances are relatively large and, with no externally applied field, the magnetic moment of a paramagnetic substance is zero because of the random orientation of such magnetic moments. Within an applied field, the magnetic moments tend to align in the same direction as the applied field. On removing the field, the alignment disappears and no net moment remains. The paramagnetic effect is generally one or two orders of magnitude greater than the diamagnetic effect, but is still weak by comparison with the magnetic behaviour of an equivalent amount of ferromagnetic substance as described below.	Olivine, ilmenite, siderite, pyroxene, garnet, biotite, chamosite, amphibole, epidote, pyrite, illite, bentonite, smectite, chalcopyrite, dolomite.
Ferromagnetism	Ferromagnetism is a collective term for a group of related magnetic phenomena found in substances with unpaired electrons in atoms that are closely and regularly spaced and where, as a consequence, strong interaction (coupling) between unpaired electron spins occur. These crystalline substances are normally compounds of the transition metals: especially iron, cobalt or nickel. Unlike other forms of magnetic behaviour, the relationship of one atom to another is important and ferromagnetism is therefore a co-operative phenomenon. Because of the interaction of forces between unpaired electrons in adjacent atoms, their spins become aligned even in the absence of an externally applied field. This behaviour is called 'spontaneous magnetisation'. It can occur in a small single ferromagnetic crystal, but would not be measurable in a sediment with randomly orientated grains where the net moment would be zero. In a crystal where atoms are organized in fixed geometrical relationships, the spontaneous magnetisation normally forms in one particular direction with respect to the crystallographic axes; giving the so-called 'easy direction' of magnetisation. This preferred orientation of magnetisation leads to what is called magnetocrystalline anisotropy. The difference between the magnetisation energy of the easy direction and that of the most difficult is known as the magnetocrystalline anisotropy energy. Different forms of ferromagnetic behaviour result from the arrangement of atoms in the crystal lattice and four conditions can be defined. In the case of (ferromagnetic) metals and their alloys, parallel coupling of all unpaired electrons may take place and this results in the development of strong magnetization. Such behaviour is known as 'ferromagnetism' (*senso stricto*).	Iron, cobalt, nickel.
	In the oxides of these metals, because the coupling occurs via an intermediate oxygen atom, alternate layers of the crystal lattice become magnetized in opposite directions (anti-parallel). If these alternate layers or sub-lattices have equal numbers of unpaired electron sites, then the substance has no overall ferromagnetic behaviour. However, if the atomic magnetic moments of the two sub-lattices are unequal, then there is a net spontaneous magnetization. This behaviour is known as 'ferrimagnetism'. For various reasons, the sub-lattices in an otherwise anti-ferromagnetic arrangement may not be perfectly anti-parallel and a small residual spontaneous magnetization exists. This behaviour is called 'canted', 'non-colinear' or 'imperfect' anti-ferromagnetism. These contrasts between the magnetic properties of ferrimagnetic minerals (e.g. magnetite) and canted antiferromagnetc minerals (e.g. haematite) provides one of the key ways in which environmental magnetic measurements can be diagnostic of the iron oxide assemblage within a rock, sediment or soil.	Magnetite, maghaematite, titanomagnetite, pyrrhotite, titanohaematite, greigite.
	When a sample of a ferromagnetic substance, of any type, is placed in, or removed from, an externally applied magnetic field, complex patterns of behaviour are exhibited and these are related to the fact that ferromagnetic behaviour is not just controlled by a crystal form but by the presence of magnetic 'domains'.	Haematite, goethite.

Appendix 1.2 Common magnetic minerals and their associated magnetic state (after Dearing, 1999)

Mineral	Magnetic state
Magnetite	Ferrimagnetic
Maghaemite	Ferrimagnetic
Pyrrhotite	Ferrimagnetic
Greigite	Ferrimagnetic
Haematite	Canted antiferromagnetic
Goethite	Canted antiferromagnetic
Ilmenite	Paramagnetic
Ulvospinel	Paramagnetic
Siderite	Paramagnetic
Pyroxene	Paramagnetic
Pyrite	Paramagnetic
Chalcopyrite	Paramagnetic
Dolomite	Paramagnetic
Calcite	Diamagnetic
Quartz	Diamagnetic
Halite	Diamagnetic

Appendix 1.3 Explanations of the three principal forms of magnetic domains (after Lees, 1994)

Type of magnetic domain	Explanation	Identification
Multidomain	Multidomain behaviour is controlled by the movement of domain walls. On the application of a strong field, the domain with a magnetization in the direction of the field will grow at the expense of other domains. Similarly due to magnetization, initial changes will be reversible, while in stronger field changes in the positions of the domain walls will reach a new equilibrium for that field. On removal of the applied field the domains may remain in their magnetized position thus causing the remanence to be held by the material. The material is 'saturated' when all the domains are aligned in the direction of the applied fields.	Low values of SIRM/χ and ARM/χ ratios, and high values of SIRM/ARM ratio.
Single domain	Single domain behaviour cannot be explained by the movement of domain walls since there are no domain boundaries. The single domain grain has an axis of easy magnetization when a field is applied. The direction of magnetization is forced into alignment with the field. The field required to do this may have to be very strong. The hysteresis properties of the grains will depend on the angle that the axis of easy magnetization makes with the field. Once the field is removed the magnetization returns to its original axis direction. An assemblage of single domain grains will then add or oppose each other in terms of magnetization (for reversible changes at low fields).	High values of SIRM/χ and ARM/χ ratios, and low values of SIRM/ARM ratio.
superparamagnetic	As grains become smaller, their magnetic properties become time dependent and changes in remanence occur in minutes and seconds; these grains are superparamagnetic or viscous. Such small grains have a thermal energy that can be as great as their magnetic energy; they are magnetically unstable and do not exhibit hysteresis or any remanence property. The thermal energy can also overcome an applied magnetic field that causes serious implications for measurements. However, this time-dependency can be used to advantage. Many of the affected grains are of secondary magnetite size and can be detected when making high frequency susceptibility field measurements. Whilst in an applied field the grains exhibit alignment to the field, upon removal thermal agitations destroy this alignment. The property of the grains is similar to the overall property of paramagnetism, but is stronger. Superparamagnetic grains have a greater effect on the magnetic susceptibility of a material than both multidomain and single domain grains. A phenomenon that causes many problems in the interpretation of magnetic results, especially in superparamagnetic grains, is that of magnetostatic interaction. This occurs because of grains lying close to each other may interact leading to demagnetization causing reduction of the overall magnetic moment.	Zero values of SIRM and ARM, with a disproportionately high χ value.

Appendix 2.1 Plant species from the embryo dune community (SD 29333 12242)

Vernacular name	Latin name	DAFOR
Sand couch grass	*Elytrigia juncea*	Dominant/frequent
Prickly saltwort	*Salsola kali*	Occasional
Lyme grass	*Leymus arenarius*	Rare
Marram grass	*Ammophila arenaria*	Rare

Appendix 2.2 Plant species from the felled phase one area (SD 28987 10473)

Vernacular name	Latin name	DAFOR
Sand sedge	*Carex arenaria*	Dominant
Common ragwort	*Senecio jacobaea*	Frequent
Rose-bay willowherb	*Chamerion angustifolium*	Frequent
Field wood rush	*Luzula campestris*	Frequent
Common bent grass	*Agrostis capillaris*	Frequent
Stork's bill	*Erodium cicutarium*	Frequent
Hound's tongue	*Cynoglossum officinale*	Occasional
Creeping thistle	*Cirsium arvense*	Occasional
Nettle	*Urtica dioica*	Rare
Autumn hawkbit	*Leontodon autumnalis*	Rare/occasional

Appendix 3.1 The 2006 dune toe photographic survey of the entire study area coastal margin

Appendix 3.1 *Continued*

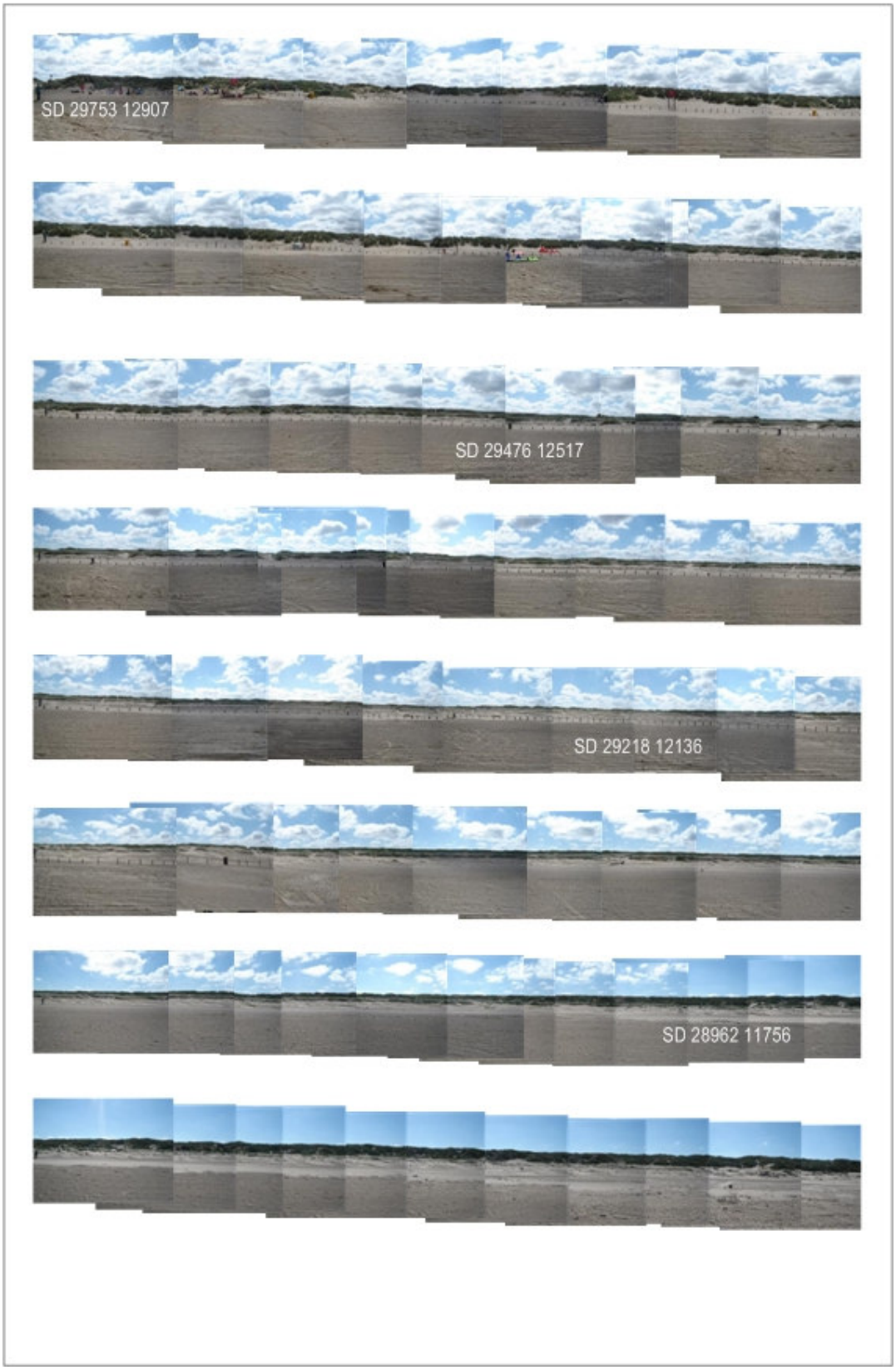

Appendix 3.1 *Continued*

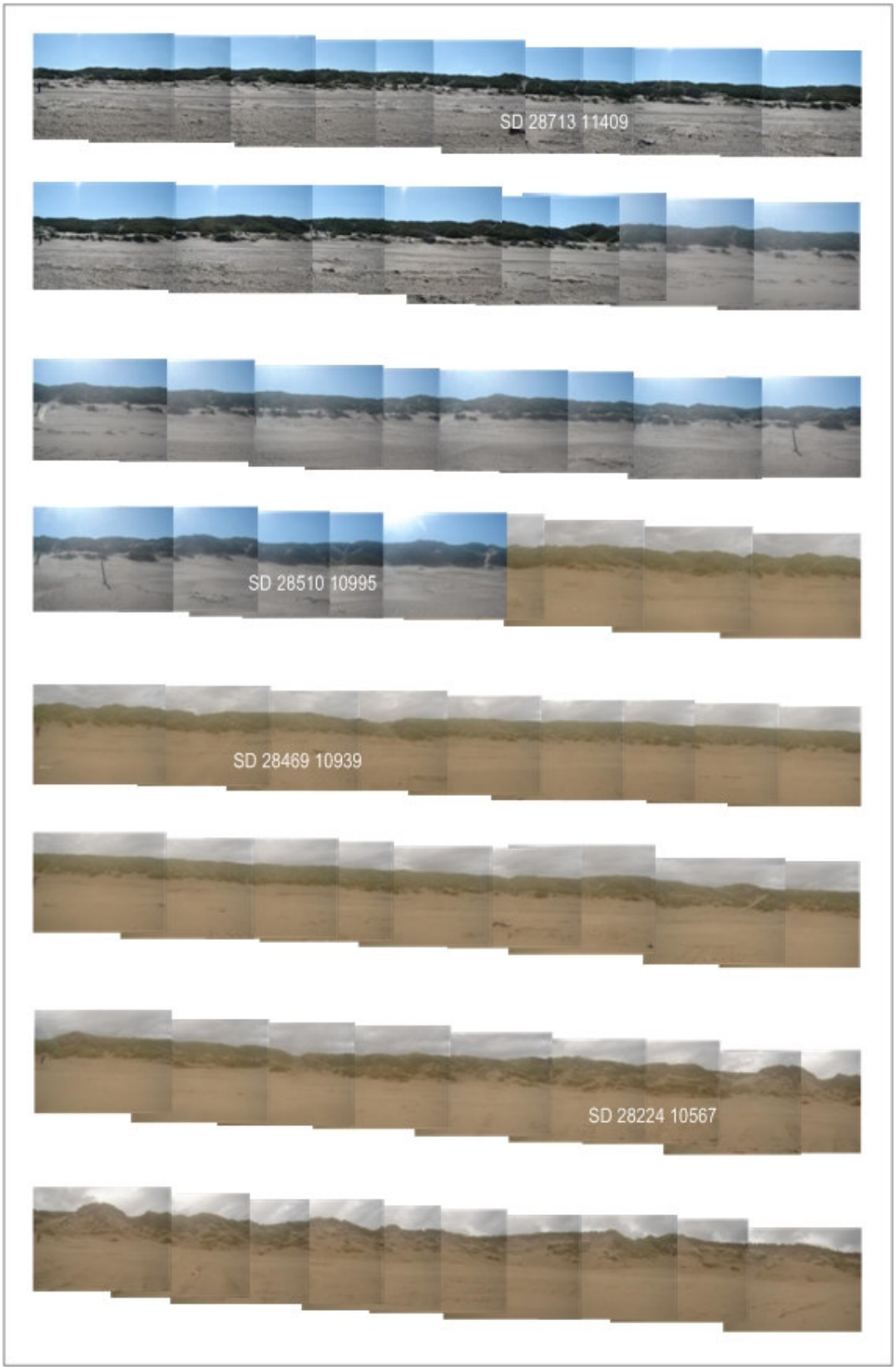

Appendix 3.1 *Continued*

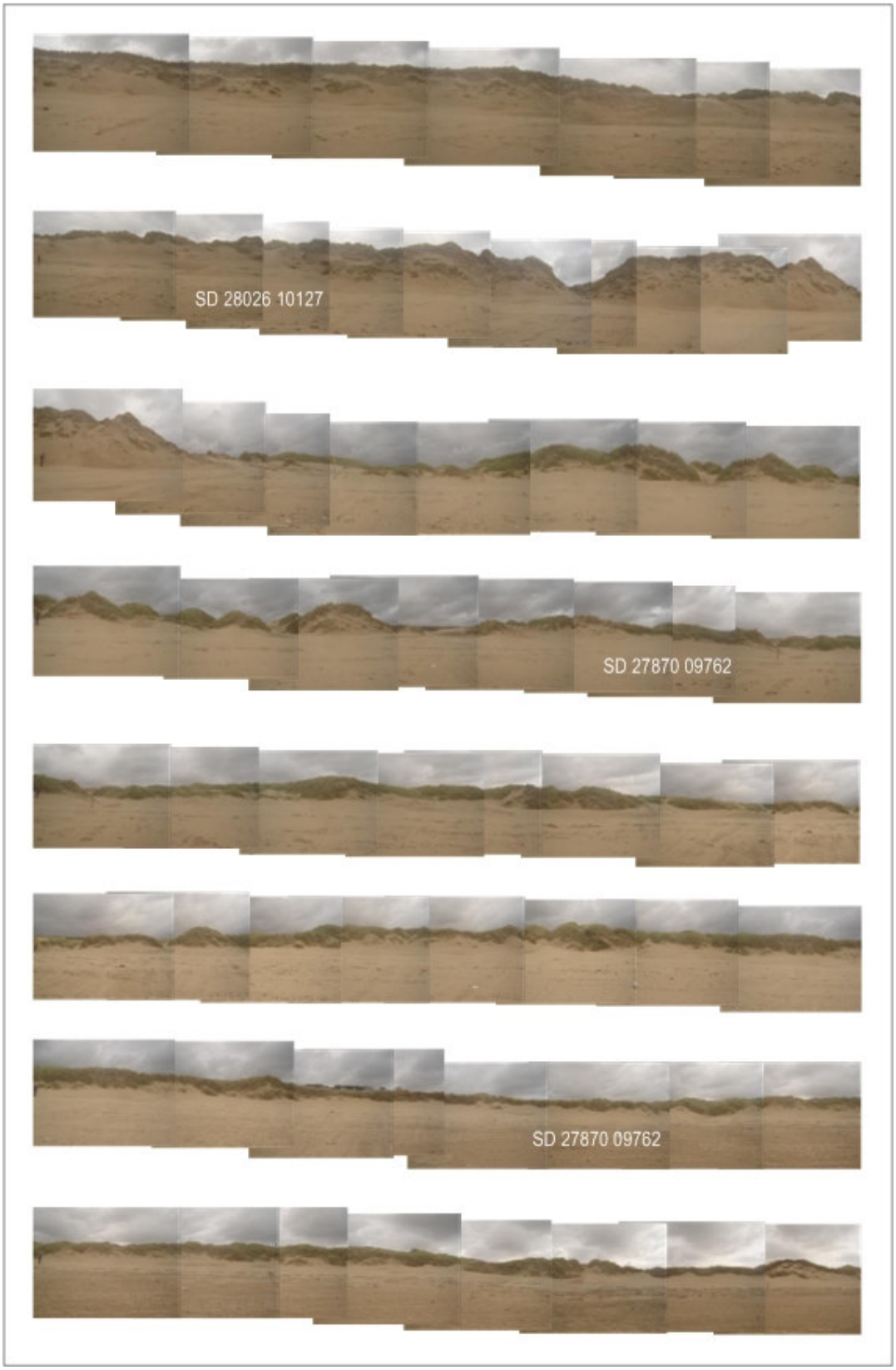

Appendix 3.1 *Continued*

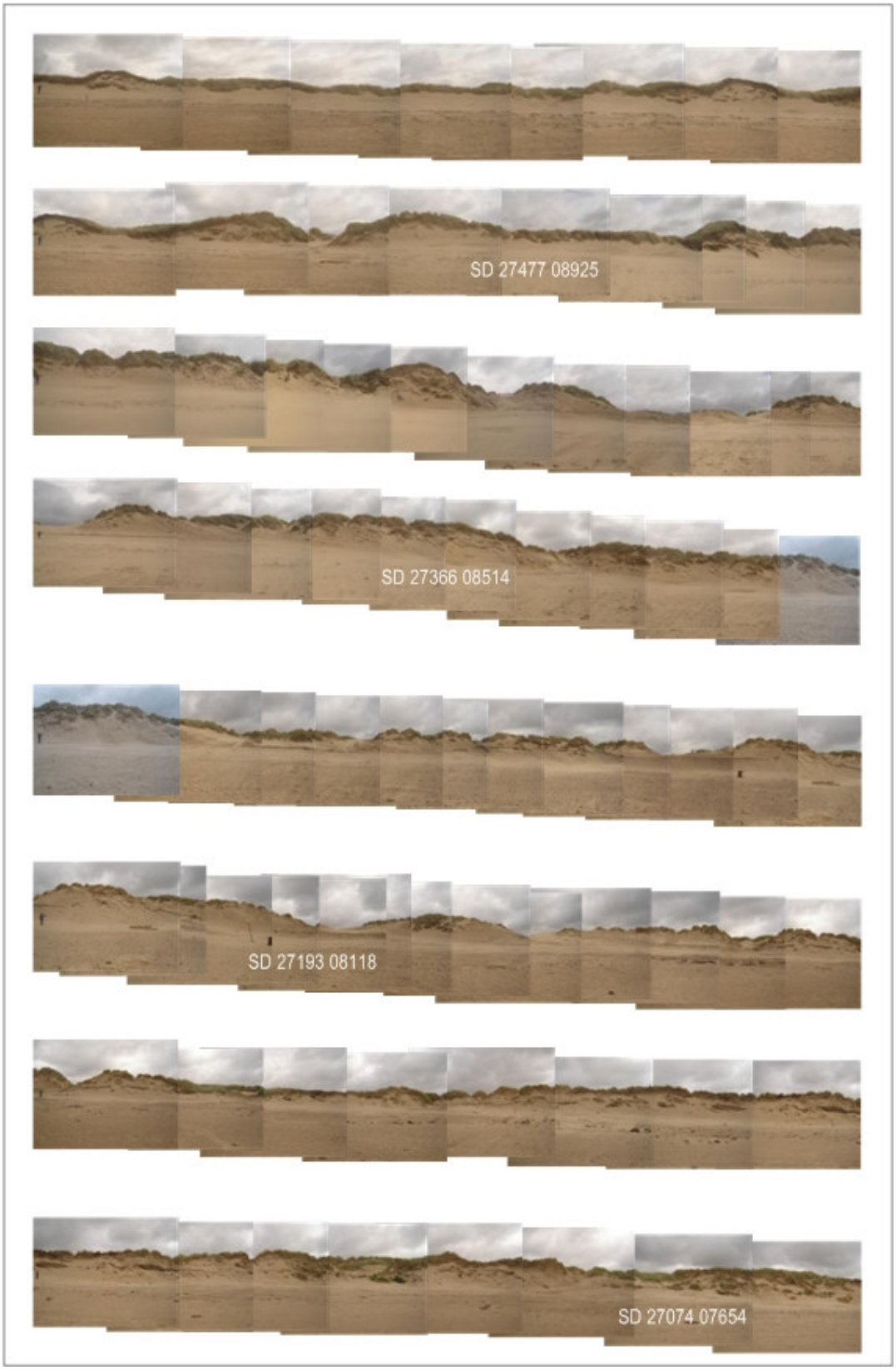

Appendix 3.1 *Continued*

Appendix 3.1 *Continued*

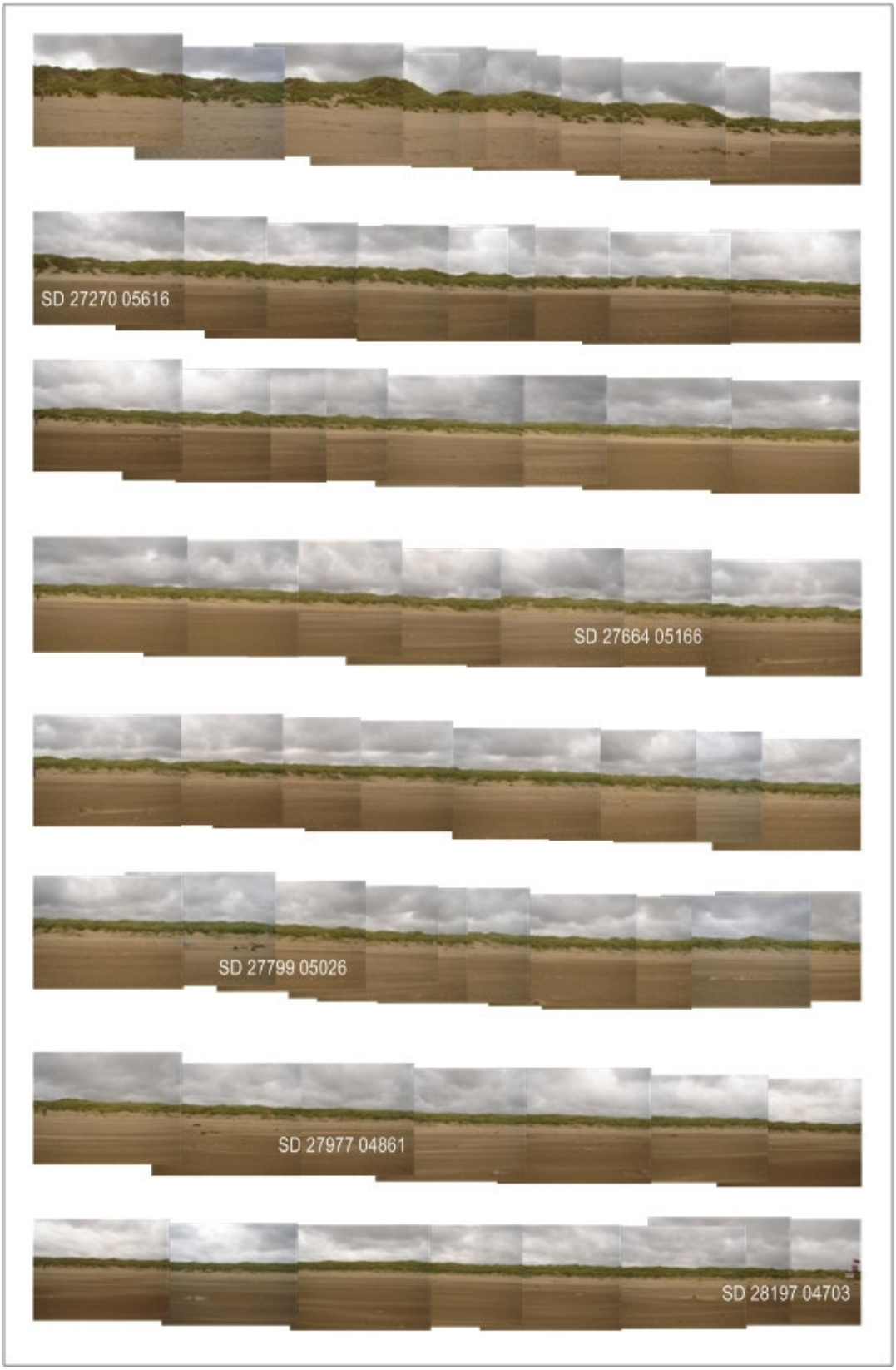

Appendix 3.2.1 Station 1: Birkdale sand dunes (SD 30379 13735)

Season	Facing north (0°)	Facing east (90°)	Facing south (180°)	Facing west (270°)
Season 1 17/11/2006				
Season 2 15/02/2007				
Season 3 24/05/2007				
Season 4 17/08/2007				
Season 5 21/11/2007				
Season 6 12/02/2008				
Season 7 15/05/2008				
Season 8 26/08/2008				
Season 9 27/11/2006				

Appendix 3.2.2 Station 2: Formby Point frontal dunes (SD 28016 09924)

Season	Facing north (0°)	Facing east (90°)	Facing south (180°)	Facing west (270°)
Season 1 17/11/2006				
Season 2 15/02/2007				
Season 3 24/05/2007				
Season 4 17/08/2007				
Season 5 21/11/2007				
Season 6 12/02/2008				
Season 7 15/05/2008				
Season 8 26/08/2008				
Season 9 27/11/2006				

Appendix 3.2.3 Station 3: Raven Meols Hills Nature Reserve (SD 28092 05113)

Season	Facing north (0°)	Facing east (90°)	Facing south (180°)	Facing west (270°)
Season 1 17/11/2006				
Season 2 15/02/2007				
Season 3 24/05/2007				
Season 4 17/08/2007				
Season 5 21/11/2007				
Season 6 12/02/2008				
Season 7 15/05/2008				
Season 8 26/08/2008				
Season 9 27/11/2006